frontiers | Research Topics

Current state of the art of human brain white matter: From structural and functional connectivity to neurosurgical applications

Edited by
Graziano Serrao, Emanuele La Corte, Wellingson Silva Paiva and Jason Michael Johnson

Published in
Frontiers in Neurology

ISSN 1664-8714
ISBN 978-2-83250-950-0
DOI 10.3389/978-2-83250-950-0

About Frontiers

Frontiers is more than just an open access publisher of scholarly articles: it is a pioneering approach to the world of academia, radically improving the way scholarly research is managed. The grand vision of Frontiers is a world where all people have an equal opportunity to seek, share and generate knowledge. Frontiers provides immediate and permanent online open access to all its publications, but this alone is not enough to realize our grand goals.

Frontiers journal series

The Frontiers journal series is a multi-tier and interdisciplinary set of open-access, online journals, promising a paradigm shift from the current review, selection and dissemination processes in academic publishing. All Frontiers journals are driven by researchers for researchers; therefore, they constitute a service to the scholarly community. At the same time, the *Frontiers journal series* operates on a revolutionary invention, the tiered publishing system, initially addressing specific communities of scholars, and gradually climbing up to broader public understanding, thus serving the interests of the lay society, too.

Dedication to quality

Each Frontiers article is a landmark of the highest quality, thanks to genuinely collaborative interactions between authors and review editors, who include some of the world's best academicians. Research must be certified by peers before entering a stream of knowledge that may eventually reach the public - and shape society; therefore, Frontiers only applies the most rigorous and unbiased reviews. Frontiers revolutionizes research publishing by freely delivering the most outstanding research, evaluated with no bias from both the academic and social point of view. By applying the most advanced information technologies, Frontiers is catapulting scholarly publishing into a new generation.

What are Frontiers Research Topics?

Frontiers Research Topics are very popular trademarks of the *Frontiers journals series*: they are collections of at least ten articles, all centered on a particular subject. With their unique mix of varied contributions from Original Research to Review Articles, Frontiers Research Topics unify the most influential researchers, the latest key findings and historical advances in a hot research area.

Find out more on how to host your own Frontiers Research Topic or contribute to one as an author by contacting the Frontiers editorial office: frontiersin.org/about/contact

Current state of the art of human brain white matter: From structural and functional connectivity to neurosurgical applications

Topic editors

Graziano Serrao — University of Milan, Italy

Emanuele La Corte — Neurovascular Neurosurgery Unit, Department of Neurosurgery, IRCCS Carlo Besta Neurological Institute Foundation, Italy

Wellingson Silva Paiva — University of São Paulo, Brazil

Jason Michael Johnson — University of Texas MD Anderson Cancer Center, United States

Citation

Serrao, G., La Corte, E., Paiva, W. S., Johnson, J. M., eds. (2022). *Current state of the art of human brain white matter: From structural and functional connectivity to neurosurgical applications*. Lausanne: Frontiers Media SA. doi: 10.3389/978-2-83250-950-0

Table of contents

frontiers | Frontiers in Neurology

TYPE Editorial
PUBLISHED 22 November 2022
DOI 10.3389/fneur.2022.1068212

OPEN ACCESS

EDITED AND REVIEWED BY
Chase R. Figley,
University of Manitoba, Canada

*CORRESPONDENCE
Emanuele La Corte
emanuele.lacorte2@unibo.it

SPECIALTY SECTION
This article was submitted to Applied Neuroimaging, a section of the journal Frontiers in Neurology

RECEIVED 12 October 2022
ACCEPTED 01 November 2022
PUBLISHED 22 November 2022

CITATION
La Corte E, Ordóñez-Rubiano EG, Paiva WS, Johnson JM and Serrao G (2022) Editorial: Current state of the art of human brain white matter: From structural and functional connectivity to neurosurgical applications. *Front. Neurol.* 13:1068212. doi: 10.3389/fneur.2022.1068212

Editorial: Current state of the art of human brain white matter: From structural and functional connectivity to neurosurgical applications

Emanuele La Corte [1,2]*, Edgar G. Ordóñez-Rubiano[3], Wellingson Silva Paiva[4], Jason Michael Johnson[5] and Graziano Serrao[6]

[1]Department of Neurosurgery, Fondazione IRCCS Istituto Neurologico Carlo Besta, Milan, Italy, [2]Department of Biomedical and Neuromotor Sciences (DIBINEM), Alma Mater Studiorum University of Bologna, Bologna, Italy, [3]Department of Neurological Surgery, Fundación Universitaria de Ciencias de La Salud (FUCS), Hospital de San José, Bogotá, Colombia, [4]Neurosurgery Division, Department of Neurology, Clinical Hospital, Faculdade de Medicina da Universidade de São Paulo (FMUSP), São Paulo, SP, Brazil, [5]Department of Diagnostic Radiology-Neuro Imaging, The University of Texas M.D. Anderson Cancer Center, Houston, TX, United States, [6]San Paolo Medical School, Department of Health Sciences, Università Degli Studi di Milano, Milan, Italy

KEYWORDS

anatomy, central nervous system, connectome, functional mapping, hodology, human brain, meta-network, white matter tracts

Editorial on the Research Topic
Current state of the art of human brain white matter: From structural and functional connectivity to neurosurgical applications

Recent knowledge of brain white matter anatomy represents an important milestone in modern neuroscience and neurosurgery development (1, 2). The human brain anatomy study recently shifted from a grey-matter-centered approach to a more integrative study of functional white matter connections (3–5). Auburtin, Bouillaud, and Broca, as "*localizationists*," based their landmarks physiological studies on specific cortical regions; whereas, Wernicke, Liepmann, and Dejerine, as "*connectionists*," were interested in the analysis of the human brain connections and developed a network theory where multiple and simultaneous transmissions of information could represent the backbone of brain function (6, 7). During recent times, neurosurgery shifted from a traditional planning strategy focused on a purely lesional topography toward a meta-network perspective and evidence of newer network-based circuitopathies (8–10). This paradigmatic shift enhanced neurosurgery to perform extensive resections in supposedly "inoperable" regions and to develop tailored programs of neurological, cognitive, and behavioral rehabilitation, aiming for the preservation of patients' quality of life (8, 11). Complex brain functions are executed through the synchronization between different cortical epicenters ("*nodes*"), which are connected through bundles of white matter

("*edges*"), to ensure a dynamic interaction between parallel delocalized subnetworks (4). The chance to non-invasively examine the human brain connections and the integration of multiple imaging approaches will hopefully provide new metrics about the functional organization of the nervous system to be incorporated into neurosurgical applications (12, 13). These include advanced techniques of brain mapping such as direct cortical and subcortical stimulation and integrative neuropsychology to disclose brain networks in neurosurgical patients; advanced pre- and post-operative neuroimaging (such as DTI, DSI, fMRI, resting-state fMRI, MEG, TMS) and anatomical dissection techniques of human brain white matter (10, 14).

The present Research Topic aims to collect the current advancements in human brain white matter anatomy and function in perioperative stages to tailor cognitive rehabilitation to maximally preserve patient quality of life. Moreover, it will focus on the current state-of-art in brain white matter structural and functional connectivity applied to neurosurgery.

In his opinion paper "*Neural Connectivity: How to Reinforce the Bidirectional Synapse Between Basic Neuroscience and Routine Neurosurgical Practice?,*" Duffau stimulates the future neurosurgical community to augment the synergy between the clinical and basic sciences environments to provide a comprehensive translational view of brain architecture. The extensive application of electrostimulation mapping and accurate neuropsychological assessment in connectome-based surgery, together with a more sophisticated functional neuroimaging, revolutionized the concept of the brain organization from a static and localized system into a more dynamic one constituted by plastic neural pathways acting as a meta-network (15, 16). This translational approach during neurosurgical procedures could also guide the monitoring of high-order cognitive functions such as mentalization. Monticelli et al. provided a narrative review, "*Where We Mentalize: Main Cortical Areas Involved in Mentalization,*" elucidating the fundamental brain cortical areas and connections underpinning mentalization processes that could be assessed and preserved during neuro-oncological surgical procedures. The modern neuro-oncological surgical philosophy relies on preserving the functional and quality of life of patients as much as possible and a connectome-based approach may help to preserve, not only the classical motor and language functions, but also more complex neurocognitive ones. In the article "*Reducing the Cognitive Footprint of Brain Tumor Surgery,*" Dadario et al. provided a case-based review to better understand post-operative cognitive outcomes and to provide a guide on how to use connectomic information to reduce cognitive morbidity following brain surgery and optimize the post-operative neurorehabilitation. Motomura et al., *"Supratotal Resection of Gliomas with Awake Brain Mapping: Maximal Tumor Resection Preserving Motor, Language, and Neurocognitive Functions,*" presented a review on the supra-total resection of gliomas through the integration of intraoperative mapping in awake surgery. To augment the value of pre-operative neuroimaging studies, Tamura et al., *"Combining Pre-operative Diffusion Tensor Images and Intraoperative Magnetic Resonance Images in the Navigation Is Useful for Detecting White Matter Tracts During Glioma Surgery,*" proposed the combination of the pre-operative fractional anisotropy maps and intraoperative MR images into a neuronavigation system to aid in the localization of critical white matter pathways during glioma awake surgery. The continuous study of anatomy through *ex-vivo* dissection, as described by Joseph Klinger, represents a precious activity for the neurosurgeon to improve the knowledge of brain white matter tridimensional structure to provide less morbid surgery (17, 18). Dziedziec et al., *"Cortical and Subcortical Anatomy of the Parietal Lobe From the Neurosurgical Perspective,*" performed an anatomical study based on Klinger's technique on the parietal lobe and provided some neurosurgical perspectives on the different surgical trajectories to approach intra-axial lesion and their relationships to the arcuate and superior longitudinal fascicles. González-López et al., *"Cadaveric White Matter Dissection Study of the Telencephalic Flexure: Surgical Implications,*" performed an anatomical study and a comprehensive embryological review on the telencephalic flexure and provided some case examples of surgery within and around it. The accurate knowledge of subcortical connectivity improved the preservation of cognitive function of patients undergoing neuro-oncological and disconnective epilepsy surgeries. Janelle et al., *"Superior Longitudinal Fasciculus: A Review of the Anatomical Descriptions with Functional Correlates,*" performed a review summary on the different used eponyms of superior longitudinal fasciculus and highlighted the uncertainty, based on the actual technology, to intercept the different components of SLF and differentiate from the arcuate fasciculus. The advancement and the integration of different imaging techniques such as diffusion imaging techniques, and functional MRI in neuroscience applied to senescence and cleft palate surgery have been highlighted in two different studies (Derbie et al., *"Functional and Structural Architectures of Allocentric and Egocentric Spatial Coding in Aging: A Combined DTI and fMRI Study"*; Rao et al., *"Random Network and Non-rich-club Organization Tendency in Children With Non-syndromic Cleft Lip and Palate After Articulation Rehabilitation: A Diffusion Study"*). The cerebellum has been classically involved in movement coordination and its anatomical architecture is sometimes neglected. Recent evidence showed that the cerebellum is also involved in cognitive and behavioral functions. De Benedictis et al., *"Networking of the Human Cerebellum: From Anatomo-Functional Development to Neurosurgical Implications,*" provided a comprehensive review of the current evidence on the anatomical and functional organization of the cerebellar connectome. The knowledge of the involved cerebellar networks in the neurocognitive process could improve the quality of approaches to reduce postoperative

surgical comorbidity such as posterior fossa syndrome. The dynamic nature of reconstructing the neural brain networks resides in its ability to compensate the function in response to some stimuli (19). The presence of neuroplasticity in frontal glioma and after surgery violating the corpus callosum in colloid cyst removal is highlighted in two different studies (Ciavarro et al., "*Structural Brain Network Reorganization Following Anterior Callosotomy for Colloid Cysts: Connectometry and Graph Analysis Results*"; Mitolo et al., "*Neuroplasticity Mechanisms in Frontal Brain Gliomas: A Preliminary Study*").

In conclusion, the present Research Topic includes comprehensive studies summarizing the current state of the art of cortical and subcortical human brain organization applied to neuroscience and neurosurgery. The papers depict the modern knowledge of neuroplasticity mechanisms, white matter anatomical pathways, and functional networks to be incorporated into routine neurosurgical practice. We hope for the future development of new artificial intelligence algorithms that could be able to reduce the subjectivity in the ROIs definition process. This would better qualitatively and quantitively discriminate the contribution of each different source or target structure in the intermingling connection tracts areas (i.e., dentate-rubro-thalamic tract) (20). We also hope this Research Topic will stimulate the neuroscientific and neurosurgical community into a deep and collaborative study of human brain white matter anatomy, to provide high-definition diagnostics and connectome-based neurosurgery oriented to the preservation of networks subserving high-order cognitive functions.

Author contributions

EL, EO-R, WP, JJ, and GS: conceptualization, collection of the data, writing of the draft, and revision of the final manuscript. All authors are accountable for the content of the work.

Conflict of interest

The authors declare that the research was conducted in the absence of any commercial or financial relationships that could be construed as a potential conflict of interest.

Publisher's note

References

1. Duffau H. Stimulation mapping of white matter tracts to study brain functional connectivity. *Nat Rev Neurol.* (2015) 11:255–65. doi: 10.1038/nrneurol.2015.51

2. Sporns O, Tononi G, Kötter R. The human connectome: a structural description of the human brain. *PLoS Comput Biol.* (2005) 1:0245–51. doi: 10.1371/JOURNAL.PCBI.0010042

3. Sarubbo S, De Benedictis A, Merler S, Mandonnet E, Balbi S, Granieri E, et al. Towards a functional atlas of human white matter. *Hum Brain Mapp.* (2015) 36:3117. doi: 10.1002/HBM.22832

4. Bullmore E, Sporns O. Complex brain networks: graph theoretical analysis of structural and functional systems. *Nat Rev Neurosci.* (2009) 10:186–98. doi: 10.1038/nrn2575

5. Fox MD. Mapping symptoms to brain networks with the human connectome. *N Engl J Med.* (2018) 379:2237–45. doi: 10.1056/nejmra1706158

6. De Benedictis A, Duffau H. Brain hodotopy: from esoteric concept to practical surgical applications. *Neurosurgery.* (2011) 68:1703–11. doi: 10.1227/NEU.0b013e3182124690

7. Catani M, Dell'Acqua F, Bizzi A, Forkel SJ, Williams SC, Simmons A, et al. Beyond cortical localization in clinico-anatomical correlation. *Cortex.* (2012) 48:1262–87. doi: 10.1016/j.cortex.2012.07.001

8. Sanai N, Berger MS. Surgical oncology for gliomas: the state of the art. *Nat Rev Clin Oncol.* (2017) 15:112–125. doi: 10.1038/nrclinonc.2017.171

9. Crossley NA, Fox PT, Bullmore ET. Meta-connectomics: human brain network and connectivity meta-analyses. *Psychol Med.* (2016) 46:897–907. doi: 10.1017/S0033291715002895

10. Figley TD, Bhullar N, Courtney SM, Figley CR. Probabilistic atlases of default mode, executive control and salience network white matter tracts: an fMRI-guided diffusion tensor imaging and tractography study. *Front Hum Neurosci.* (2015) 9:585. doi: 10.3389/fnhum.2015.00585

11. Gogos AJ, Young JS, Morshed RA, Hervey-Jumper SL, Berger MS. Awake glioma surgery: technical evolution and nuances. *J Neurooncol.* (2020) 147:515–24. doi: 10.1007/S11060-020-03482-Z

12. La Corte E, Eldahaby D, Greco E, Aquino D, Bertolini G, Levi V, et al. The frontal aslant tract: a systematic review for neurosurgical applications. *Front Neurol.* (2021) 12:1–15. doi: 10.3389/fneur.2021.641586

13. Ottenhausen M, Krieg SM, Meyer B, Ringel F. Functional preoperative and intraoperative mapping and monitoring: increasing safety and efficacy in glioma surgery. *Neurosurg Focus.* (2015) 38:E3. doi: 10.3171/2014.10.FOCUS14611

14. Figley TD, Mortazavi Moghadam B, Bhullar N, Kornelsen J, Courtney SM, Figley CR. Probabilistic white matter atlases of human auditory, basal ganglia, language, precuneus, sensorimotor, visual and visuospatial networks. *Front Hum Neurosci.* (2017) 11:306. doi: 10.3389/fnhum.2017.00306

15. Rossi M, Sciortino T, Nibali MC, Gay L, Viganò L, Puglisi G, et al. Clinical pearls and methods for intraoperative motor mapping. *Neurosurgery.* (2021) 88:457–67. doi: 10.1093/NEUROS/NYAA359

16. Szelényi A, Bello L, Duffau H, Fava E, Feigl GC, Galanda M, Neuloh G, Signorelli F, Sala F. Intraoperative electrical stimulation in awake craniotomy: methodological aspects of current practice. *Neurosurg Focus.* (2010) 28:E7. doi: 10.3171/2009.12.FOCUS09237

17. Bertolini G, La Corte E, Aquino D, Greco E, Rossini Z, Cardia A, et al. Real-time ex-vivo magnetic resonance image—guided dissection of human brain white matter: a proof-of-principle study. *World Neurosurg.* (2019) 125:198–206. doi: 10.1016/j.wneu.2019.01.196

18. Rhoton A. *Rhoton Cranial Anatomy and Surgical Approaches*. Schaumburg, IL: Congress of Neurological Surgeons (2003).

19. Southwell DG, Hervey-Jumper SL, Perry DW, Berger MS. Intraoperative mapping during repeat awake craniotomy reveals the functional plasticity of adult cortex. *J Neurosurg.* (2016) 124:1460–9. doi: 10.3171/2015.5.JNS142833

20. Middlebrooks EH, Tipton P, Okromelidze L, Greco E, Mendez JA, Uitti R, et al. Deep brain stimulation for tremor: direct targeting of a novel imaging biomarker. *Ann Neurol.* (2022) 92:341–2. doi: 10.1002/ana.26422

frontiers in Neurology

OPINION
published: 01 July 2021
doi: 10.3389/fneur.2021.705135

Neural Connectivity: How to Reinforce the Bidirectional Synapse Between Basic Neuroscience and Routine Neurosurgical Practice?

Hugues Duffau [1,2]*

[1] Department of Neurosurgery, Gui de Chauliac Hospital, Montpellier University Medical Center, Montpellier, France, [2] Team "Plasticity of Central Nervous System, Stem Cells and Glial Tumors," National Institute for Health and Medical Research (INSERM), U1191 Laboratory, Institute of Functional Genomics, University of Montpellier, Montpellier, France

Keywords: awake neurosurgery, brain mapping, neural connectivity, neuroscience, neuroplasticity

INTRODUCTION

The quest for all neuroscientists is to better understand neural foundations underpinning human behavior. Neurosurgery offers a unique opportunity to be directly connected to the human connectome, and to provide further findings into brain processes—complementary to current investigations mainly relying on functional neuroimaging (FNI), comprising functional MRI, and diffusion tensor imaging (DTI) (1–4). Especially, awake patients with electrostimulation mapping (ESM) may benefit from an extensive neuropsychological assessment in real-time throughout surgery. This paradigm resulted in the description of the human homunculus by Penfield and Boldrey (5) almost one century ago and in the re-visitation of cortical organization of language by Ojemann (6). However, despite these pioneering works, the contribution of neurosurgery to fundamental neurosciences remains relatively modest, particularly in comparison with the numerous FNI reports (7, 8). Reversely, advances in brain connectomics, which led to new propose-built neurobiological models underlying neurocognition thanks to an improved knowledge of neural connectivity, have not (yet) extensively been incorporated in neurosurgical practice.

Here, the purpose is to consider solutions to reinforce the synapse, which should be bidirectional, between basic neuroscience and routine neurosurgery, in order to bring about synergies across research and clinical worlds based upon a dual vision of scientists and physicians.

CONTRIBUTION OF BRAIN SURGICAL MAPPING TO INVESTIGATE NEURAL CONNECTIVITY

In the emerging field of connectomics, which aims at exploring neural connectivity, brain ESM during awake surgery provides direct insights into the function of both cortical structures and white matter tracts (WMT). Indeed, axonal ESM of the subcortical fibers may elicit a transient disruption of the functional network sub-served by the bundle stimulated, and consequently, may generate a specific behavioral deficit which immediately resolves when ESM stops (9). Beyond a transitory dys-synchronization within a discrete critical circuit, ESM can also disrupt between-network inter-communication, resulting in multi-tasking disorders, e.g., the patient is still able to move or to speak separately, but cannot do both simultaneously (10). Such original anatomo-functional correlations gained from on-line intraoperative cortico-subcortical ESM led researchers to re-visit the functional connectivity mediating neural systems, such as movement execution and control (11), oral and written language (12, 13), semantics (14), executive control (15), self-evaluation (16), or theory of mind (17, 18).

OPEN ACCESS

Edited by:
Emanuele La Corte, University of Bologna, Italy

Reviewed by:
Sandro M. Krieg, Technical University of Munich, Germany

***Correspondence:**
Hugues Duffau
h-duffau@chu-montpellier.fr

Specialty section:
This article was submitted to Applied Neuroimaging, a section of the journal Frontiers in Neurology

Received: *04 May 2021*
Accepted: *10 May 2021*
Published: *01 July 2021*

Citation:
Duffau H (2021) Neural Connectivity: How to Reinforce the Bidirectional Synapse Between Basic Neuroscience and Routine Neurosurgical Practice? Front. Neurol. 12:705135. doi: 10.3389/fneur.2021.705135

Interestingly, this ESM permitted a reappraisal of the model of the human connectome (19), and proposed a new theory relying on a meta-network (network of networks) organization of the brain, i.e., with perpetual changes of intra- and across circuit interactions allowing adapted behavior (20).

Moreover, longitudinal ESM explorations, particularly based upon serial mapping in patients who underwent several awake surgeries because of tumor relapse (21), enabled researchers to better understand mechanisms sustaining neuroplasticity (22). Remarkably, optimal recovery following massive brain resections in tumor patients, with normal scores on objective neuropsychological assessments of conation, cognition, and emotion despite surgery within structures classically deemed "eloquent" according to localizationist dogma, evidenced a considerable potential of neural configuration, higher than previously thought (23, 24). Nonetheless, the limitations of this plastic potential have also been demonstrated, by emphasizing the critical role of the subcortical connectivity (25). Thus, a "minimal common brain" has been suggested, with a low level of inter-individual variability and a low power of functional compensation after cerebral injury (26): such a "cerebral skeleton" is mainly constituted by WMT (27).

Neurosurgery represents a gold mine to develop innovative models in cognitive neurosciences, thanks to the direct information about neural connectivity collected into the operating room (OR) by means of ESM (19). It is regrettable that these original data which challenged the obsolete model of localizationism, e.g., by evidencing that Broca's area was non-critical for speech, were neglected for a long time by neurologists and neuroscientists (28). A solution to reunify learned societies can be to combine findings provided by ESM with those gained from FNI in healthy volunteers as well as before and after surgery in brain-damaged patients (22). Based upon different backgrounds and complementary areas of expertise (neuroanatomy, neuroimaging, awake brain mapping, cognitive neuroscience, neurophysiology, neurocomputational modeling, etc.), speaking a universal language may allow researchers to understand more rapidly and accurately neurobiology-sustaining complex human behavior. Reversely, an improved knowledge of brain circuitry could be helpful in neurosurgical practice, to optimize postoperative outcomes.

HOW TO INTEGRATE A BETTER UNDERSTANDING OF THE CEREBRAL CONNECTOME INTO NEUROSURGICAL PRACTICE?

For many decades, neurosurgeons mainly paid attention to the cortex, with few considerations regarding subcortical connectivity. Beyond research purposes, recent advances in DTI resulted in an improved investigation of WMT for surgical planning (29, 30). Moreover, preoperative tractography data were incorporated into neuronavigational systems to better define surgical approach and limits of resection into the OR (31, 32). However, even though these technological developments played a major role in basic research to explore the connectome (3, 8), and started to bring the gap between neuroscience and clinical applications, the link across both worlds is still weak and superficial. Indeed, the majority of neurosurgeons has no background in FNI methodology and has the wrong belief that DTI is a reliable insight into WMT function. Yet, despite a growing excitement in imaging-guided neurosurgery, these techniques intrinsically suffer from major limitations (from the data acquisition to the statistical models used) (33, 34), the main one being that tractography does not provide any information about the function of subcortical fibers—but is only an indirect reflection of their structures (35). Therefore, an abusive surgical use of these methods whose pitfalls are poorly controlled, even if initially designed to help neurosurgeons, may paradoxically become dangerous. For example, FNI may result in a non-selection for surgery while the tumor could have been removed (with a loss of chance from an oncological perspective), or conversely, may lead to the resection being pushed too far by cutting critical pathways not identified as essential by DTI (with some loss likely from a functional perspective) (36). Furthermore, although FNI is a fantastic didactic tool to help junior neurosurgeons to build an accurate 3D representation of structural and functional connectivity in their own mental imagery, especially when combined with dissection in specimens (37, 38), the overuse of this technology for brain surgery may lead to the opposite effect, i.e., to an addiction to FNI, preventing an optimal surgical act if this tool was unavailable (36).

To reinforce the synapse with fundamental research, neurosurgeons should be neuroscientists, since he/she also has the responsibility to explore the connectome by him/herself, with the ultimate goal of improving postoperative outcomes. Thus, besides a better comprehension of the potentials and drawbacks of FNI for its more appropriate utilization, intraoperative ESM should be used more systematically (39). In addition to cortical mapping, axonal ESM is the sole methodology enabling a direct study of WMT function, concerning one specific bundle and interplay between neural circuits (10). Awake mapping led to a paradigmatic shift from image-guided resection to functional-guided resection, especially in neuro-oncology (40). Remarkably, awake ESM guiding the resection until the individual eloquent cortico-subcortical networks have been encountered resulted in an improvement of both neurological and oncological outcomes (41). Functionally speaking, a connectome-based resection allowed for a significant decrease of neurological morbidity (42–44) with preservation of conation, language, and higher-cognitive functions (e.g., complex movement control, verbal and non-verbal semantics, executive functions, mentalizing or metacognition) (45–48) making it possible to resume a normal life, including return to work in 97% of patients (49)—even for tumors involving areas presumed to be "eloquent" in a rigid localizationist framework (23, 24). Oncologically speaking, functional mapping-guided surgery has enabled a significant increase of extent of resection and overall survival, both in low-grade and high-grade gliomas (50–53). Yet, although ESM is now the gold standard for glioma surgery (39), it is still underused in neurosurgery in general.

This concept of connectome-based surgery represents an actual solution to introduce more robust neuroscience into the

OR. Firstly, beyond its participation in the development of original models of neurocognition (12, 13, 19, 20), awake ESM also enabled the elaboration of a human atlas of neuroplasticity (25) and an atlas of critical cortico-subcortical networks (54–56). This can be helpful for neurosurgeons to predict whether the patient will recover or not according to the extent of resection, especially by highlighting the structures with a low potential of reorganization, such as the subcortical connectivity—the so-called "minimal common brain" mentioned above (27). To facilitate presurgical planning by predicting the distribution of essential neural connections to be preserved, a tool has recently been proposed for a practical use: it allows automated alignment of the cortico-subcortical maps of this probabilistic atlas with T1-weighted MRI of a given patient (57). These data can also be used to estimate before surgery the extent of resection thanks to a probabilistic map of tumor resectability, computed on the basis of postoperative residual glioma voluntarily left because of invading critical structures identified by intraoperative ESM (58).

Secondly, these new cognitive models of meta-networking organization of brain functions (12, 13, 19, 20) and the new atlases built based upon ESM (25, 27, 54–57) represent unmatched educational tools for neurosurgeons to learn 3D neural connectivity. Indeed, they provide real structural-functional information collected intraoperatively in patients who underwent awake surgery, and not virtual data as given by FNI, with different reconstructions according to the biostatistical modeling employed.

Thirdly, besides neuro-oncology, application of the concept of connectome-based resection relying on a better understanding of dynamic interplay within and across neural networks, may be considered in other fields of brain surgery. Surprisingly, although awake ESM was initially developed in epilepsy surgery (5, 6, 59), most of the series dedicated to non-tumoral epilepsy did not use intraoperative mapping in the modern literature. Yet, recent publications supported again the positive role of awake resection for epilepsy, notably with mapping of the subcortical pathways, (such as optic tracts to avoid visual field deficits), in a connectome paradigm of brain processing (60, 61)—knowing that the mechanisms of neuroplasticity are not similar in lesional vs. non-lesional epilepsy (62). An improved exploration of neural connectivity is also valuable for surgical approaches to deep lesions located within hard-to-reach areas. Typically, a trans-cortical approach to have access to the insula should take into account the sub-opercular connectivity, particularly the frontal part of the inferior fronto-occipital fasciculus (IFOF) and of the superior longitudinal fasciculus/arcuate fasciculus (AF) complex (63). Similarly, a transcortico-subcortical approach to the left posterior Medio basal region necessitates the knowledge, detection, and preservation of relevant WMT including the optic pathways, AF, IFOF, and inferior longitudinal fasciculus (64). Also, for deep cavernomas, the best surgical corridor through the subcortical fibers should be defined by validating in real-time that the neural connectivity crossed to reach the lesion was not crucial for brain functions (65). This is especially valuable for lesions involving a neural crossroad, e.g., the ventral precentral fiber intersection area (66) or the temporoparietal fiber intersection area traversed by seven WMT (67). Finally, such a 3D mental representation in the brain's neurosurgeon is also useful for emergent surgery, such as the evacuation of a left deep temporo-insular hematoma under general anesthesia, in an aphasic patient with mass effect. If the patient remained aphasic after surgery, it could be thought that this was related to an irreversible damage generated by the hematoma, whereas in some cases, it might be due to a traumatic surgical corridor through the critical fibers, such as the IFOF—meaning that the patient could have recovered if the approach would have been modified thanks to better knowledge of the connectome, even in asleep patients. To this end, fiber dissection in cadavers to accelerate the learning curve is of utmost importance.

PERSPECTIVES

It is time to overcome the divide between fundamental research in neurosciences, increasing reliance on FNI and neurocomputational modeling which usually do not take into account the structural constraints, and the neurosurgical routine which should preserve the neural connectivity under penalty of no postoperative recovery, but which can also propose new cognitive models based upon direct observation of the connectome into the OR. Dual training for juniors, at the start of their courses, would enhance their chance to create reciprocal connections across basic and clinical neuroscience, and to develop more translational research in their daily practice dedicated to brain understanding and restoration.

AUTHOR CONTRIBUTIONS

The author confirms being the sole contributor of this work and has approved it for publication.

REFERENCES

1. Yeo BT, Krienen FM, Sepulcre J, Sabuncu MR, Lashkari D, Hollinshead M, et al. The organization of the human cerebral cortex estimated by intrinsic functional connectivity. *J Neurophysiol.* (2011) 106:1125–65. doi: 10.1152/jn.00338.2011
2. Sporns O. The human connectome: Origins and challenges. *Neuroimage.* (2013) 80:53–61. doi: 10.1016/j.neuroimage.2013.03.023
3. Van Essen DC, Smith SM, Barch DM, Behrens TE, Yacoub E, Ugurbil K, et al. The WU-Minn human connectome project: an overview *Neuroimage.* (2013) 80:62–79. doi: 10.1016/j.neuroimage.2013.05.041
4. Glasser MF, Coalson TS, Robinson EC, Hacker CD, Harwell J, Yacoub E, et al. A multi-modal parcellation of human cerebral cortex. *Nature.* (2016) 536:171–8. doi: 10.1038/nature18933
5. Penfield W, Boldrey E. Somatic motor and sensory representation in the cerebral cortex of man as studied by electrical stimulation. *Brain.* (1937) 60:389. doi: 10.1093/brain/60.4.389
6. Ojemann GA. Brain organization for language from the perspective of electrical stimulation mapping. *Behav Brain Sci.* (1983) 6:189–206. doi: 10.1017/S0140525X00015491
7. Eickhoff SB, Yeo BTT, Genon S. Imaging-based parcellations of the human brain. *Nat Rev Neurosci.* (2018) 19:672–86. doi: 10.1038/s41583-018-0071-7

8. Jeurissen B, Descoteaux M, Mori S, Leemans A. Diffusion MRI fiber tractography of the brain. *NMR Biomed.* (2019) 32:e3785. doi: 10.1002/nbm.3785
9. Duffau H. Stimulation mapping of myelinated tracts in awake patients. *Brain Plast.* (2016) 2:99–113. doi: 10.3233/BPL-160027
10. Duffau H. What direct electrostimulation of the brain taught us about the human connectome: a three-level model of neural disruption. *Front Hum Neurosci.* (2020) 14:315 doi: 10.3389/fnhum.2020.00315
11. Rech F, Herbet G, Moritz-Gasser S, Duffau H. Somatotopic organization of the white matter tracts underpinning motor control in humans: an electrical stimulation study. *Brain Struct Funct.* (2016) 221:3743–53. doi: 10.1007/s00429-015-1129-1
12. Duffau H, Moritz-Gasser S, Mandonnet E, A. reexamination of neural basis of language processing: proposal of a dynamic hodotopical model from data provided by brain stimulation mapping during picture naming. *Brain Lang.* (2014) 131:1–10. doi: 10.1016/j.bandl.2013.05.011
13. Zemmoura I, Herbet G, Moritz-Gasser S, Duffau H. New insights into the neural network mediating reading processes provided by cortico-subcortical electrical mapping. *Hum Brain Mapp.* (2015) 36:2215–30. doi: 10.1002/hbm.22766
14. Herbet G, Moritz-Gasser S, Duffau H. Direct evidence for the contributive role of the right inferior fronto-occipital fasciculus in non-verbal semantic cognition. *Brain Struct Funct.* (2017) 222:1597–610. doi: 10.1007/s00429-016-1294-x
15. Mandonnet E, Vincent M, Valero-Cabré A, Faque V, Barberis M, Bonnetblanc F, et al. Network-level causal analysis of set-shifting during trail making test part B: A multimodal analysis of a glioma surgery case. *Cortex.* (2020) 132:238–49. doi: 10.1016/j.cortex.2020.08.021
16. Ng S, Herbet G, Lemaitre AL, Moritz-Gasser S, Duffau H. Disrupting self-evaluative processing with electrostimulation mapping during awake brain surgery. *Sci Rep.* (2021) 11:9386. doi: 10.1038/s41598-021-88916-y
17. Herbet G, Duffau H. Awake craniotomy and bedside cognitive mapping in neurosurgery. In: Pearson CM, Ecklund-Johnson E, Gale SD, editors. *Neurosurgical Neuropsychology*. Chennai: Academic Press (2019). p. 113–38.
18. Roux A, Lemaitre AL, Deverdun J, Ng S, Duffau H, Herbet G. Combining electrostimulation with fiber tracking to stratify the inferior fronto-occipital fasciculus. *Front Neurosci.* (2021) 15:683348. doi: 10.3389/fnins.2021.683348 eCollection 2021
19. Duffau H. Stimulation mapping of white matter tracts to study brain functional connectivity. *Nat Rev Neurol.* (2015) 11:255–65. doi: 10.1038/nrneurol.2015.51
20. Herbet G, Duffau H. Revisiting the functional anatomy of the human brain: toward a meta-networking theory of cerebral functions. *Physiol Rev.* (2020) 100:1181–228. doi: 10.1152/physrev.00033.2019
21. Picart T, Herbet G, Moritz-Gasser S, Duffau H. Iterative surgical resections of diffuse glioma with awake mapping: how to deal with cortical plasticity and connectomal constraints? *Neurosurgery.* (2018) 85:105–16. doi: 10.1093/neuros/nyy218
22. Duffau H. Functional mapping before and after low-grade glioma surgery: a new way to decipher various spatiotemporal patterns of individual neuroplastic potential in brain tumor patients. *Cancers.* (2020) 12:2611. doi: 10.3390/cancers12092611
23. Duffau H. Lessons from brain mapping in surgery for low-grade glioma: insights into associations between tumour and brain plasticity. *Lancet Neurol.* (2005) 4:476–86. doi: 10.1016/S1474-4422(05)70140-X
24. Duffau H. The huge plastic potential of adult brain and the role of connectomics: new insights provided by serial mappings in glioma surgery. *Cortex.* (2014) 58:325–37. doi: 10.1016/j.cortex.2013.08.005
25. Herbet G, Maheu M, Costi E, Lafargue G, Duffau H. Mapping neuroplastic potential in brain-damaged patients. *Brain.* (2016) 139:829–44. doi: 10.1093/brain/awv394
26. Duffau H. A two-level model of interindividual anatomofunctional variability of the brain and its implications for neurosurgery. *Cortex.* (2017) 86:303–13. doi: 10.1016/j.cortex.2015.12.009
27. Ius T, Angelini E, Thiebaut de. Schotten M, Mandonnet E, Duffau H. Evidence for potentials and limitations of brain plasticity using an atlas of functional resectability of WHO grade II gliomas: towards a -minimal common brain. *Neuroimage.* (2011) 56:992–1000. doi: 10.1016/j.neuroimage.2011.03.022
28. Mandonnet E, Duffau H. Broca's area: why was neurosurgery neglected for so long when seeking to re-establish the scientific truth? *Brain.* (2021). doi: 10.1093/brain/awab195 [Epub ahead of print].
29. Henderson F, Abdullah KG, Verma R, Brem S. Tractography and the connectome in neurosurgical treatment of gliomas: the premise, the progress, and the potential. *Neurosurg Focus.* (2020) 48:E6. doi: 10.3171/2019.11.FOCUS19785
30. Conti Nibali M, Rossi M, Sciortino T, Riva M, Gay LG, Pessina F, et al. Preoperative surgical planning of glioma: limitations and reliability of fMRI and DTI tractography. *J Neurosurg Sci.* (2019) 63:127–34. doi: 10.23736/S0390-5616.18.04597-6
31. Krivosheya D, Prabhu SS. Combining functional studies with intraoperative MRI in glioma surgery. *Neurosurg Clin N Am.* (2017) 28:487–7. doi: 10.1016/j.nec.2017.05.004
32. Potgieser AR, Wagemakers M, van Hulzen AL, de Jong BM, Hoving EW, Groen RJ. The role of diffusion tensor imaging in brain tumor surgery: a review of the literature. *Clin Neurol Neurosurg.* (2014) 124:51–8. doi: 10.1016/j.clineuro.2014.06.009
33. Pujol S, Wells W, Pierpaoli C, Brun C, Gee J, Cheng G, et al. The DTI challenge: toward standardized evaluation of diffusion tensor imaging tractography for neurosurgery: the DTI challenge on tractography for neurosurgery. *J Neuroimaging.* (2015) 25:875–82. doi: 10.1111/jon.12283
34. Maier-Hein KH, Neher PF, Houde JC, Côté MA, Garyfallidis E, Zhong J, et al. The challenge of mapping the human connectome based on diffusion tractography. *Nat Commun.* (2017) 8:1349. doi: 10.1038/s41467-017-01285-x
35. Azad TD, Duffau H. Limitations of functional neuroimaging for patient selection and surgical planning in glioma surgery. *Neurosurg Rev.* (2020) 48:E12. doi: 10.3171/2019.11.FOCUS19769
36. Duffau H. The dangers of magnetic resonance imaging diffusion tensor tractography in brain surgery. *World Neurosurg.* (2014) 81:56–8. doi: 10.1016/j.wneu.2013.01.116
37. De Benedictis A, Nocerino E, Menna F, Remondino F, Barbareschi M, Rozzanigo U, et al. Photogrammetry of the human brain: a novel method for three-dimensional quantitative exploration of the structural connectivity in neurosurgery and neurosciences. *World Neurosurg.* (2018) 115:e279–91. doi: 10.1016/j.wneu.2018.04.036
38. Panesar SS, Belo JTA, Yeh FC, Fernandez-Miranda JC. Structure, asymmetry, and connectivity of the human temporo-parietal aslant and vertical occipital fasciculi. *Brain Struct Funct.* (2019) 224:907–23. doi: 10.1007/s00429-018-1812-0
39. de Witt Hamer PC, Gil Robles S, Zwinderman A, Duffau H, Berger MS. Impact of intraoperative stimulation brain mapping on glioma surgery outcome: a meta-analysis. *J Clin Oncol.* (2012) 30:2559–65. doi: 10.1200/JCO.2011.38.4818
40. Duffau H. New philosophy, clinical pearls and methods for intraoperative cognition mapping and monitoring "à la carte" in brain tumor patients. *Neurosurgery.* (2021) 88:919–30. doi: 10.1093/neuros/nyaa363
41. Ferracci FX, Duffau H. Improving surgical outcome for gliomas with intraoperative mapping. *Expert Rev Neurother.* (2018) 18:333–41. doi: 10.1080/14737175.2018.1451329
42. Hervey-Jumper SL Li J, Lau D, Molinaro AM, Perry DW, Meng L, et al. Awake craniotomy to maximize glioma resection: methods and technical nuances over a 27-year period. *J Neurosurg.* (2015) 123:325–39. doi: 10.3171/2014.10.JNS141520
43. Boetto J, Bertram L, Moulinié G, Herbet G, Moritz-Gasser S, Duffau H. Low rate of intraoperative seizures during awake craniotomy in a prospective cohort with 374 supratentorial brain lesions: electrocorticography is not mandatory. *World Neurosurg.* (2015) 84:1838–44. doi: 10.1016/j.wneu.2015.07.075
44. Bu LH, Zhang J, Lu JF, Wu JS. Glioma surgery with awake language mapping versus generalized anesthesia: a systematic review. *Neurosurg Rev.* (2020). doi: 10.1007/s10143-020-01418-9 [Epub ahead of print].
45. Mandonnet E, De Witt Hamer P, Poisson I, Whittle I, Bernat AL, Bresson D, et al. Initial experience using awake surgery for glioma: oncological, functional, and employment outcomes in a consecutive series of 25 cases. *Neurosurgery.* (2015) 76:382–9. doi: 10.1227/NEU.0000000000000644

46. Lemaitre AL, Herbet G, Duffau H, Lafargue G. Preserved metacognitive ability despite unilateral or bilateral anterior prefrontal resection. *Brain Cogn.* (2018) 120:48–57. doi: 10.1016/j.bandc.2017.10.004
47. Barzilai O, BenMoshe S, Sitt R, Sela G, Shofty B, Ram Z. Improvement in cognitive function after surgery for low-grade glioma. *J Neurosurg.* (2019) 130:426–34. doi: 10.3171/2017.9.JNS17658
48. Ng S, Herbet G, Lemaitre AL, Cochereau J, Moritz-Gasser S, Duffau H Neuropsychological assessments before and after awake surgery for incidental low-grade gliomas. *J Neurosurg.* (2020) 1–10. doi: 10.3171/2020.7.JNS201507 [Epub ahead of print].
49. Ng S, Herbet G, Moritz-Gasser S, Duffau H. Return to work following surgery for incidental diffuse low-grade glioma: a prospective series with 74 patients. *Neurosurgery.* (2020) 87:720–9. doi: 10.1093/neuros/nyz513
50. Chang EF, Clark A, Smith JS, Polley MY, Chang SM, Barbaro NM, et al. Functional mapping-guided resection of low-grade gliomas in eloquent areas of the brain: improvement of long-term survival. Clinical article. *J Neurosurg.* (2011) 114:566–73. doi: 10.3171/2010.6.JNS091246
51. Duffau H. Long-term outcomes after supratotal resection of diffuse low-grade gliomas: a consecutive series with 11-year follow-up. *Acta Neurochir (Wien).* (2016) 158:51–8. doi: 10.1007/s00701-015-2621-3
52. Rossi M, Gay L, Ambrogi F, Nibali MC, Sciortino T, Puglisi G, et al. Association of supratotal resection with progression-free survival, malignant transformation, and overall survival in lower-grade gliomas. *Neuro Oncol.* (2021) 23:812–26. doi: 10.1093/neuonc/noaa225
53. Zigiotto L, Annicchiarico L, Corsino F, Vitali L, Falchi R, Dalpiaz C, et al. Effects of supra-total resection in neurocognitive and oncological outcome of high-grade gliomas comparing asleep and awake surgery. *J Neurooncol.* (2020) 148:97–108. doi: 10.1007/s11060-020-03494-9
54. Sarubbo S, De Benedictis A, Merler S, Mandonnet E, Balbi S, Granieri E, et al. Towards a functional atlas of human white matter. *Hum Brain Mapp.* (2015) 36:3117–36. doi: 10.1002/hbm.22832
55. Sarubbo S, Tate M, De Benedictis A, Merler S, Moritz-Gasser S, Herbet G, et al. Mapping critical cortical hubs and white matter pathways by direct electrical stimulation: an original functional atlas of the human brain. *Neuroimage.* (2020) 205:116237. doi: 10.1016/j.neuroimage.2019.116237
56. Sarubbo S, Tate M, De Benedictis A, Merler S, Moritz-Gasser S, Herbet G, et al. A normalized dataset of 1821 cortical and subcortical functional responses collected during direct electrical stimulation in patients undergoing awake brain surgery. *Data Brief.* (2019) 28:104892. doi: 10.1016/j.dib.2019.104892
57. Sarubbo S, Annicchiarico L, Corsini F, Zigiotto L, Herbet G, Moritz-Gasser S, et al. Planning brain tumor resection using a probabilistic atlas of cortical and subcortical structures critical for functional processing: a proof of concept. *Oper Neurosurg.* (2021) 20:E175–183. doi: 10.1093/ons/opaa396
58. Mandonnet E, Jbabdi S, Taillandier L, Galanaud D, Benali H, Capelle L, et al. Preoperative estimation of residual volume for WHO grade II glioma resected with intraoperative functional mapping. *Neuro Oncol.* (2007) 9:63–9. doi: 10.1215/15228517-2006-015
59. Rahimpour S, Haglund MM, Friedman AH, Duffau H. History of awake mapping and speech and language localization: from modules to networks. *Neurosurg Focus.* (2019) 47:E4. doi: 10.3171/2019.7.FOCUS 19347
60. Maesawa S, Nakatsubo D, Fujii M, Iijima K, Kato S, Ishizaki T. et al. Application of awake surgery for epilepsy in clinical practice. *Neurol Med Chir.* (2018) 58:442–52. doi: 10.2176/nmc.oa.2018-0122
61. Vigren P, Eriksson M, Duffau H, Wretman A, Lindehammar H, Milos P, et al. Experiences of awake surgery in non-tumoural epilepsy in eloquent localizations. *Clin Neurol Neurosurg.* (2020) 199:106251. doi: 10.1016/j.clineuro.2020.106251
62. Bourdillon P, Apra C, Guénot M, Duffau H. Similarities and differences in neuroplasticity mechanisms between brain gliomas and nonlesional epilepsy. *Epilepsia.* (2017) 58:2038–47. doi: 10.1111/epi.13935
63. Mandonnet E, Martino J, Sarubbo S, Corrivetti F, Bouazza S, Bresson D, et al. Neuronavigated fiber dissection with pial preservation: laboratory model to simulate opercular approaches to insular tumors. *World Neurosurg.* (2017) 98:239–42. doi: 10.1016/j.wneu.2016.10.020
64. Brown DA, Hanalioglu S, Chaichana K, Duffau H. Transcorticosubcortical approach for left posterior mediobasal temporal region gliomas: a case series and anatomic review of relevant white matter tracts. *World Neurosurg.* (2020) 139:e737–47. doi: 10.1016/j.wneu.2020.04.147
65. Matsuda R, Coello AF, De Benedictis A, Martinoni M, Duffau H. Awake mapping for resection of cavernous angioma and surrounding gliosis in the left dominant hemisphere: surgical technique and functional results: clinical article. *J Neurosurg.* (2012) 117:1076–81. doi: 10.3171/2012.9.JNS 12662
66. Gayoso S, Perez-Borreda P, Gutierrez A, García-Porrero JA, Marco de. Lucas E, Martino J. Ventral precentral fiber intersection area: a central hub in the connectivity of perisylvian associative tracts. *Oper Neurosurg.* (2019) 17:182–92. doi: 10.1093/ons/opy331
67. Martino J, da Silva-Freitas R, Caballero H, Marco de Lucas E, García-Porrero JA, Vázquez-Barquero A. Fiber dissection and diffusion tensor imaging tractography study of the temporoparietal fiber intersection area. *Neurosurgery.* (2013) 72(1 Suppl. Operative):87–97. doi: 10.1227/NEU.0b013e318274294b

Conflict of Interest: The author declares that the research was conducted in the absence of any commercial or financial relationships that could be construed as a potential conflict of interest.

frontiers in Neurology

REVIEW
published: 16 August 2021
doi: 10.3389/fneur.2021.711646

Reducing the Cognitive Footprint of Brain Tumor Surgery

Nicholas B. Dadario[1], *Bledi Brahimaj*[2], *Jacky Yeung*[3] *and Michael E. Sughrue*[3]*

[1] *Robert Wood Johnson School of Medicine, Rutgers University, New Brunswick, NJ, United States,* [2] *Department of Neurosurgery, Rush University Medical Center, Chicago, IL, United States,* [3] *Centre for Minimally Invasive Neurosurgery, Prince of Wales Private Hospital, Sydney, NSW, Australia*

The surgical management of brain tumors is based on the principle that the extent of resection improves patient outcomes. Traditionally, neurosurgeons have considered that lesions in "non-eloquent" cerebrum can be more aggressively surgically managed compared to lesions in "eloquent" regions with more known functional relevance. Furthermore, advancements in multimodal imaging technologies have improved our ability to extend the rate of resection while minimizing the risk of inducing new neurologic deficits, together referred to as the "onco-functional balance." However, despite the common utilization of invasive techniques such as cortical mapping to identify eloquent tissue responsible for language and motor functions, glioma patients continue to present post-operatively with poor cognitive morbidity in higher-order functions. Such observations are likely related to the difficulty in interpreting the highly-dimensional information these technologies present to us regarding cognition in addition to our classically poor understanding of the functional and structural neuroanatomy underlying complex higher-order cognitive functions. Furthermore, reduction of the brain into isolated cortical regions without consideration of the complex, interacting brain networks which these regions function within to subserve higher-order cognition inherently prevents our successful navigation of true eloquent and non-eloquent cerebrum. Fortunately, recent large-scale movements in the neuroscience community, such as the Human Connectome Project (HCP), have provided updated neural data detailing the many intricate macroscopic connections between cortical regions which integrate and process the information underlying complex human behavior within a brain "connectome." Connectomic data can provide us better maps on how to understand convoluted cortical and subcortical relationships between tumor and human cerebrum such that neurosurgeons can begin to make more informed decisions during surgery to maximize the onco-functional balance. However, connectome-based neurosurgery and related applications for neurorehabilitation are relatively nascent and require further work moving forward to optimize our ability to add highly valuable connectomic data to our surgical armamentarium. In this manuscript, we review four concepts with detailed examples which will help us better understand post-operative cognitive outcomes and provide a guide for how to utilize connectomics to reduce cognitive morbidity following cerebral surgery.

Keywords: neurosurgery, brain tumor, connectome, cognition, neuroimaging, machine learning, neurorehabilitation

OPEN ACCESS

Edited by:
Emanuele La Corte, University of Bologna, Italy

Reviewed by:
Morgan Broggi, Istituto Neurologico Carlo Besta (IRCCS), Italy
Thomas Picht, Charité – Universitätsmedizin Berlin, Germany

***Correspondence:**
Michael E. Sughrue
sughruevs@gmail.com

Specialty section:
This article was submitted to Applied Neuroimaging, a section of the journal Frontiers in Neurology

Received: *19 May 2021*
Accepted: *12 July 2021*
Published: *16 August 2021*

Citation:
Dadario NB, Brahimaj B, Yeung J and Sughrue ME (2021) Reducing the Cognitive Footprint of Brain Tumor Surgery. Front. Neurol. 12:711646. doi: 10.3389/fneur.2021.711646

INTRODUCTION

Modern glioma surgery has advanced based on the understanding that maximal tumor resection improves overall survival (1). While also considering numerous factors such as patient prognosis, tumor topography relative to "eloquent" or "non-eloquent" cerebrum has generally guided the aggressiveness of surgical cytoreduction in hopes of minimizing the risk of inducing new neurologic deficits (2). Such a balance is often referred to as the patient "onco-functional balance." However, while it is well known that not all cortical tissue is functionally eloquent and the brain is generally resistant to a degree of surgical reduction, glioma patients continue to present post-operatively with poor cognitive functioning limiting social interactions and integration back into the workforce (3–5). If the neurosurgical community is to further consider increasing the extent of resection such as in supramaximal resection, further anatomical and functional information is required to improve our effective navigation of human cerebrum during tumor surgery and to maximize cognitive preservation.

Anatomical familiarity with specific cortical structures and advancements in multimodal imaging have allowed neurosurgeons to minimize surgically induced neurologic deficits related to major functions including language and motor skills. However, such notions are still often unable to explain the subtle deficits seen in patients with higher-order cognitive functions nor can it explain the heterogeneity in cognitive outcomes with lesions located in traditionally "non-eloquent" tissue (3, 5–7). One plausible hypothesis suggests that inter-individual variability in brain network architecture may explain why certain patients cannot safely tolerate resection of tumor in classically non-eloquent tissue that is based on generalized brain atlases (8). As such, awake intraoperative electrical stimulation is often employed on an individual patient basis as a gold standard to identify eloquent cortical regions related language and motor skills and facilitate safe tumor resection (9, 10). However, such methods are still often unable to map more complex cognitive functions, such as cognitive functioning and psychomotor speed, which can involve multiple cortical regions functioning together that are classically less anatomically familiar in the general neurosurgery community. Furthermore, these methods can be invasive, time consuming, and difficult to interpret limiting their widespread adoption and clinical applicability at most centers (11, 12). Similarly, functional and structural neuroimaging data have long provided the medical and scientific community an abundance of highly complex and relevant patient data, but this information too is often highly-dimensional and unable to readily guide clinical decision making (13). Fortunately, recent computational advancements and large scale movements in the neuroscience community have allowed us to take this highly dimensional neuroimaging data and improve previous maps of the human brain in a more digestible framework, offering a unique opportunity to improve neuro-oncological outcomes following cerebral surgery (14–16).

The Human Connectome Project (HCP) recently provided a highly detailed neuroanatomical map of human cerebral cortex allowing a reappraisal of our classical modular maps of the human brain (15). The HCP authors identified 180 unique cortical regions per cerebral hemisphere which are architecturally organized in efficient neural networks within a brain "connectome." Compared to previous *localizationist* views that suggest isolated cortical regions are dedicated to specialized functions, these networks are functionally and structurally organized in a way that minimizes cost while maximizing information transfer between cortical regions to carry out complex human thinking and behavior. Connectomics in turn provides us an improved understanding of the organization and functional relevance of human cortical and subcortical anatomy (15, 17). As the neurosurgeon begins to enter the new era of connectomic-based surgical targeting, further understanding of the structural and functional connectome provides additional information that can allow neurosurgeons to optimize surgical decision making and extend the rate of resection while minimizing new neurologic deficits related to higher-order cognition, among other functions. Furthermore, additional insight may be gained on the potential for functional reallocation during or after cortical insults and on potential targets in brain networks for modulatory treatments and neurorehabilitation (18, 19). However, the ability for this information to readily guide clinical decision making is still relatively nascent and requires further clarification to optimize its clinical applicability.

In the current paper, we discuss and provide evidence for four concepts which we believe can advance the neurosurgical community toward improving patient morbidity and cognitive functioning following cerebral surgery. Furthermore, we review these promising avenues in light of current neurosurgical practices and the current limitations faced. In order to reduce the cognitive footprint of cerebral surgery on the neurosurgical patient, we discuss the following:

Concept 1. Preserve the core of networks whenever possible
Concept 2. Consider the full brain ramifications of the action
Concept 3. Move our thinking toward individual circuits
Concept 4. Consider the possibility that we can change the brain connectome

PRESERVE THE CORE OF NETWORKS WHENEVER POSSIBLE

Difficulty in Anatomic Localization and Outcomes in Supratentorial Neurosurgery

Patients with gliomas experience impairments in executive functioning, speed, and memory prior to any treatment and are inherently at increased risks for further neuropsychological decline after surgery (20). As discussed above, despite the improved ability for neurosurgeons to manage neurologic outcomes related to language and some motor skills, patients with glioblastoma (GBM) exhibit executive functioning decline post-operatively that can lower patient quality of life and prevent re-integration into the workforce (21, 22). Even with mapping during awake craniotomies, perhaps due to the lack of monitoring capable of testing the complexity of executive functioning, both psychomotor speed and visuospatial functioning are especially impacted (6). Furthermore, limited by

TABLE 1 | Seven major brain networks.

1) Central Executive Network

The CEN, in contrast to the DMN, is the external mind that is turned on during active tasks and external thinking involving working memory (39). The CEN works in anticorrelation with the DMN in healthy individuals but works in correlation with the dorsal attention network (DAN) for attention processing, as well as visual spatial planning (40, 41). It comprises regions in the anterior cingulate cortex, the inferior parietal lobe, and the posterior most portions of the middle and inferior temporal gyri (42–44). Aberrations in CEN connectivity with other networks, especially abnormal correlations with DMN, have been implicated in many psychiatric disorders, such as schizophrenia and post-traumatic stress disorder (45, 46).

2) Visual Network

The visual system is situated mostly in the occipital lobe and is comprised of two major pathways, the dorsal and ventral streams (47). The dorsal stream is involved in the guidance of actions and recognition of objects in space and is connected to the parietal lobe (48). The ventral stream is associated with object recognition and form representation (48). It has strong connections to the medial temporal lobe via the basal, tentorial service (49). Although many separate visual functions in spatial and object discrimination are thought to be housed separately in specific parcellations within this network, these two streams are interconnected via the vertical occipital fasciculus and may participate in more interconnected functions than previously understood (49).

3) Default Mode Network

The DMN is the internal mind that is at work when an individual is at a resting state, not actively engaged in *externally* oriented tasks or attentional processing. However, during that time, the DMN is not stagnant but its activity increases for internal thought and passive sensory processing (50). It comprises the retrosplenial cortex, inferior parietal cortex, dorsolateral frontal cortex, inferior frontal cortex, left inferior temporal gyrus, and medial frontal regions (51, 52).

4) Sensorimotor Network

The sensorimotor network enables us to assimilate both external and internal stimuli and produce a motor response to these elements. The senses can range from temperature, pressure, and vibration (external) to balance and coordination (internal). It is one of the most studied networks in history, from initial basic understanding of the motor cortex in dogs to the understanding of perceptual changes that occur in conjunction with motor learning (53, 54). Anatomically it involves the primary motor cortex, cingulate cortex, premotor cortex, supplementary motor area, sensory cortices in the parietal lobe (55).

5) Salience Network

The salience network (SN) serves as an intermediary between the DMN and CEN (56, 57). Independently, the SN is thought to process external stimuli from the outside world and modulates how the different networks view the information (58). The main nodes of the SN are situated in the anterior insula and the dorsal anterior cingulate cortex (58). As the SN is in charge of processing of information from the external world, its hyperactivity can lead to neuroticism or anxiety (heightened sensitivity to outside stimuli) and hypoactivity can be a hallmark of autism (lack of sensitivity to social cues) (19).

6) Limbic Network

The limbic network involves multiple lobes and was initially described to be the central control of emotions (59, 60). Its functions were later found to be much wider in scope, ranging from the memory of olfaction to social recognition (61, 62). The limbic network consists of prefrontal-limbic system, anterior cingulate cortex, medial temporal network, parahippocampal gyrus, olfactory lobe, and the ventral tegmental area (63, 64). Lesions of the limbic system are linked to a variety of psychiatric disorders, including anxiety, bipolar disorder, schizophrenia, and autism (65–68).

7) Dorsal Attention Network

The dorsal attention network (DAN) is an important circuit that governs attention on an object and goal-directed top-down (knowledge derived from previous experience rather than sensory stimulation) processing (69, 70). It comprises bilaterally the intraparietal sulcus and the frontal eye fields of each hemisphere, which are active when attention is overtly or covertly oriented in space (71). Decreased functional connectivity in DAN has been implicated in increased disease severity of dementia (72).

the number of neuropsychological batteries that we currently have and the subsequently limited amount of data reported postoperatively about "non-severe" neurological deficits (i.e., other than aphasia or hemiplegia), it is reasonable to conjecture that declines in neurocognitive functions are vastly underappreciated in this patient population (23).

It is unclear whether anatomical location of the lesion can predict specific neurocognitive deficits. The Glioma Outcome Project showed that functional decline, with the exception of language, is not associated with the dominance of the hemisphere where the tumor is located. This suggests that neurocognitive decline may be based on more complex networks involving both hemispheres as the infiltrative tumor continues to grow (24). Relatedly, there is often conflicting evidence in direct electrical stimulation (DES) treatments due to the arbitrary stimulation paradigm where one cortical region may be stimulated and somehow alter neural activity across multiple, adjacent and long-range brain regions (25). More likely, specific cortical regions act as nodes in a complex neural network system that is connected by distinct white matter pathways in order to transfer information and carry out specialized functions (17). Thus, in order to improve our understanding and treatment of neurologic outcomes, we must contextualize neurosurgery in the setting of brain networks.

Reimagining the Brain as Networks

To understand how to preserve the core of important networks, we must first understand what brain networks are and how function is organized around them. Brain network organization provides a framework to place different cortical regions within that are strongly *functionally* interconnected between time series (26). Functionally connected regions of a network also tend to be *structurally* connected. This idea is supported by a variety of experimental and computational work and has been replicated by our own team in great detail (14, 17, 27–32). In fact, network analyses partly depend on the observations that the *function* of a neural node is in part determined by its *structural* interconnectedness with other nodes in the network (17). Thus, cortical regions in a network represent the nodes of that network and these nodes are connected by edges referred to as white

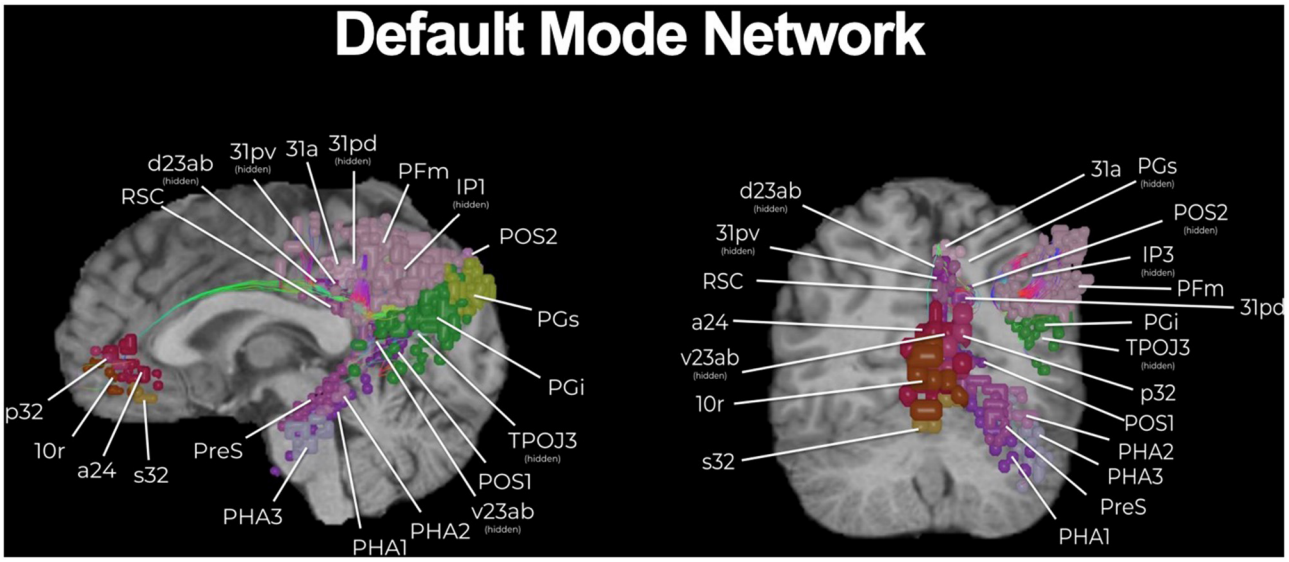

FIGURE 1 | The core of the default mode network (DMN). While a multi-lobar network, the core of the DMN is provided, including its key brain parcellations and connecting structural fibers. Individual regions have been visualized in 3D space and therefore some parcellations have been covered or require multiple views for correct spatial understanding due to parallax. Visualization of tracts have been minimized (thickness and volume) to maximize the visibility of parcellations.

mattery bundles (17). Together, these relationships constitute the *structural* and *functional connectomes*.

Much of how we understand brain circuitry today originates from research based on graph-based network analysis of resting-state functional MRI (33). Resting-state functional MRI (rsMRI) uses low-frequency fluctuations in blood oxygen level-dependent (BOLD) signals to measure endogenous or spontaneous brain activity (34). Early efforts utilized connectivity-based methods to study networks involved in motor, auditory, visual, language, default-mode, and attention systems (34–38). More recently, graph-theory based approaches have allowed for a model of the brain as a complex meta-network and has allowed for us to quantitatively characterize the organization of all brain regions within different, or shared, individual networks. We will not delve into the technical nuances of graph theoretical analyses, but rather briefly describe seven major networks that comprise our current understanding of the brain connectome in **Table 1**, including: central executive network (CEN), default mode network (DMN), salience network (SN), sensorimotor network, dorsal attention network (DAN), limbic network, and visual network. By utilizing combined structural-functional information and meta-analytic processing software, our team has been creating anatomically precise cortical maps of these brain networks describing key regions in precise HCP nomenclature and their major cortico-cortical connections (27, 73, 74).

Each network can be further subdivided based on specialized functions (29, 75, 76). Nonetheless, a few networks which are beneficial to first understand in order to grasp the organizational architecture of neural networks in the human cerebrum and that are especially relevant to neurosurgery in hopes of improving cognitive morbidity can be referred to as the "main cognitive networks" (77). The main cognitive networks refer to the CEN, DMN, and the SN, and provide an axis in which the other networks align (78). The DMN is generally thought to alternate its activity with the CEN in an anticorrelated fashion, in which the DMN activates during passive states of mind while the CEN activates during goal-directed behavior and attentional processing (73). Furthermore, the allocation of resources and switching between these two networks based on stimulus orientation and changes in tasks is thought to be mediated by the SN, a cingulo-opercular network (77). Unsurprisingly, abnormal connectivity or disconnection in these major networks can lead to cognitive depletion and impaired higher-order cognitive abilities, with recent evidence suggesting their dysfunction likely forms the underlying basis of many known neurologic and psychiatric disorders, including schizophrenia, depression, and anxiety (79, 80). Thus, perioperative knowledge of these main cognitive networks is imperative to truly optimize patient cognitive status in cerebral surgery.

Using Brain Network Maps in Surgery

The HCP, as well as many others, have provided a plethora of exciting knowledge about the structural and functional connectome (15). However, the clinical translation of such information is still elusive and transforming such information into clinically actionable anatomic information for neurosurgeons has required further work. In addition to describing individual networks, we have previously published a connectomic atlas of the human cerebrum detailing the anatomy and structural and functional connectivity of all 180 precise cortical parcellations according to the HCP authors (81). Brain network maps add an improved understanding

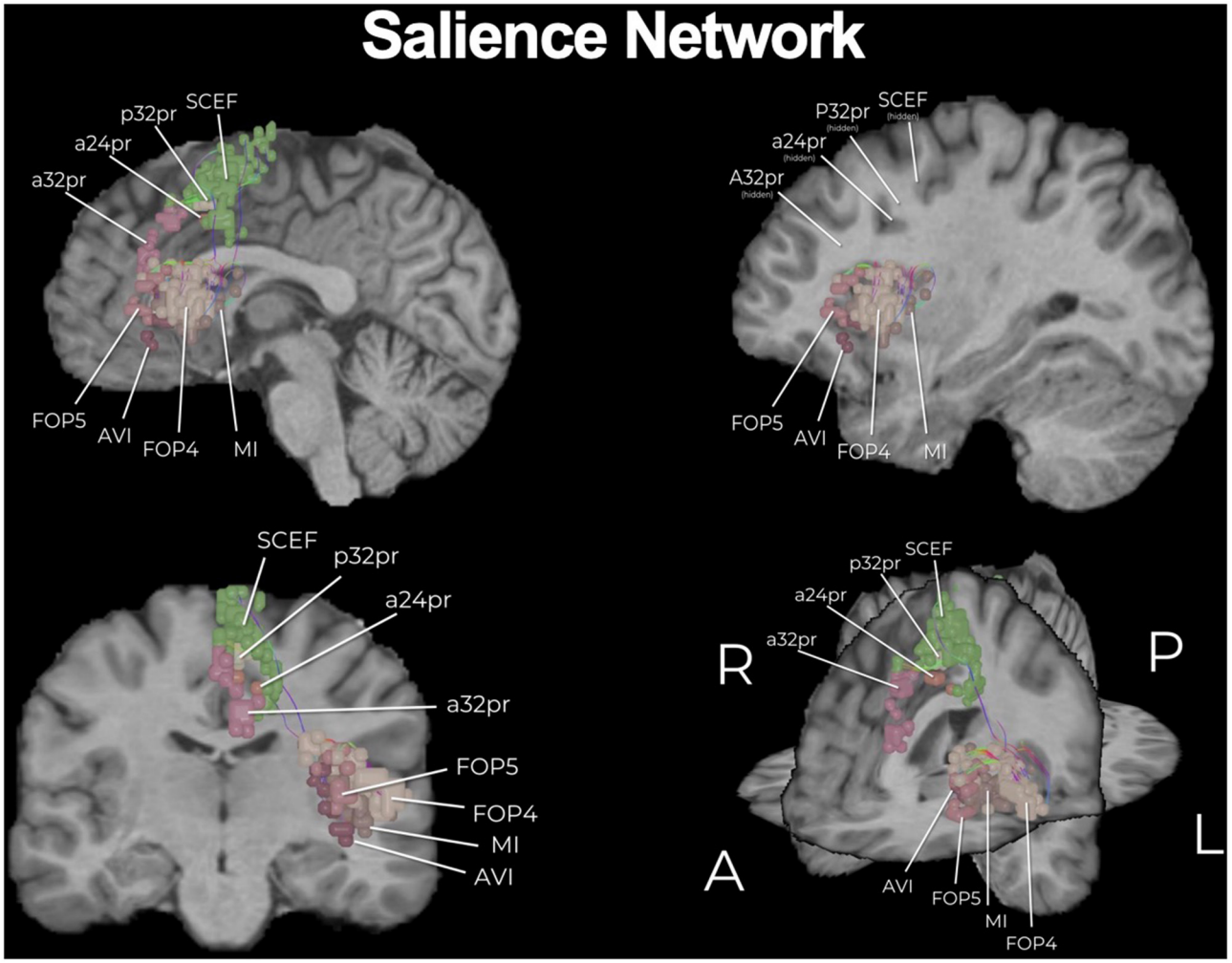

FIGURE 2 | The core of the salience network (SN). Similar to the DMN, the SN is a multi-lobar network and here we show its core. Individual regions have been visualized in 3D space and therefore some parcellations have been covered or require multiple views for correct spatial understanding due to parallax. Visualization of tracts have been minimized (thickness and volume) to maximize the visibility of parcellations.

of the organization of the human cortex and its underlying subcortical anatomy such that we can make more informed surgical decisions and cause fewer neurologic deficits (14, 82). A number of concepts remain unknown, such as how much of the brain networks must actually be preserved and what fibers can be safely disconnected without compromising network communication and subsequent normal functioning. However, what is generally known suggests that cutting though the cores of the main cognitive networks, consisting of the individual parcellations that are fundamental to the network as well as the interconnections between those main parcellations, causes severe cognitive deficits. To support this concept, we provide a number of important examples below that demonstrate the need for neurosurgeons moving forward to preserve the cores of the main cognitive networks whenever it is surgically feasible. The cores of these structures are visualized in **Figures 1**–**3**.

The functional anatomy of the frontal lobe has long been poorly understood, with previous models vaguely suggesting that bifrontal injury causes akinetic mutism and abulia without actually providing a guide on how to avoid such deficits (84). These deficits can generally be thought of as difficulties with the initiation of internally motivated actions, presenting as a lack of self-initiated activity. Fortunately, connectomic data has improved our basis for understanding and avoiding neurologic deficits associated with tumors located along the medial frontal control networks. A model we recently proposed, in what we deemed as the prefrontal cognitive initiation "axis," in brief suggests that the DMN, connected via the cingulum, and the SN, connected via the frontal aslant tract (FAT), create a structural chain that extends up to the SMA in the medial frontal lobe (**Figure 4**) (77). This initiation "axis" is likely responsible for internally modeling goal initiation, such as for

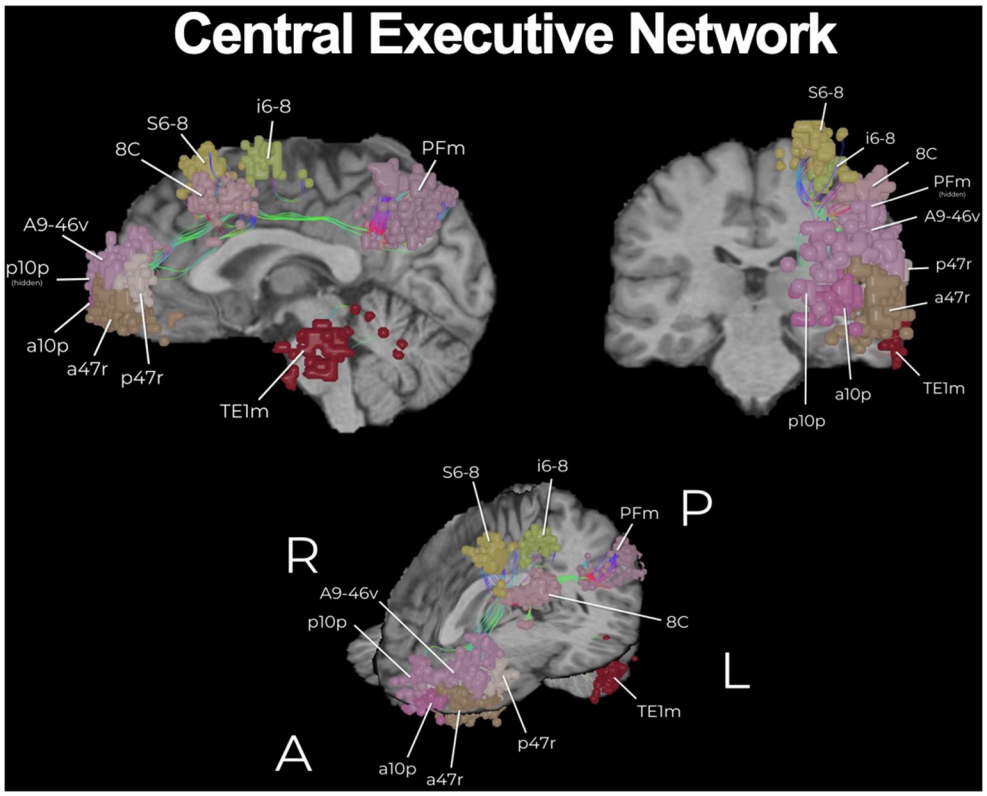

FIGURE 3 | The core of the central executive network (CEN). The CEN is a key multi-lobar control network necessary for effective cognitive functioning and its main core is provided here. Functional regions have been visualized in 3D space and therefore some parcellations have been covered or require multiple views for correct spatial understanding due to parallax. An example of this is the provided with brain parcellation area TE1m (temporal area 1 middle), which is correctly found on the lateral surface of the middle aspect of the middle temporal gyrus (83). Visualization of tracts have been minimized (thickness and volume) to maximize the visibility of parcellations.

the initiation of speech and motor planning, and is supported by multiple lines of evidence providing considerable insight into cognitive outcomes when operating in this area (85). For instance, anecdotal experience has previously suggested that unilateral cingulate transgression is only tolerated by some individuals, while others often develop akinesia or abulia, and that preserving the anterior cingulate can reduce such deficits. Instead, connectomic data provides more clear information on how to avoid these injuries and why they occur. Namely, the DMN contains anterior and posterior cingulate clusters linked via cingulum fibers, and disconnecting this cingulum bundle in the initiation "axis" is what likely causes abulia (73, 86). By applying this tractographic information when operating on anterior butterfly gliomas, a cingulum sparing technique can nearly completely prevent akinesis and abulia compared to not sparing the cingulum fibers (**Figure 1**) (82).

Furthermore, a well known post-operative neurologic deficit when operating in the medial frontal lobe is SMA syndrome, characterized by transient hemiplegia and mutism. Previous localizationist views have suggested that this deficit occurs primarily due to surgical insult in the posteromedial bank of the superior frontal gyrus, yet other patients too demonstrate varying degrees of mutism and hemiplegia when operating outside this canonical SMA (14). Fortunately, further insight on the major connectivity of the medial frontal lobe has revealed that the FAT is the principle pathway linking the SMA to premotor areas and area 44 (Broca's area) and also links hubs of the salience network, supporting a possible role of the FAT in initiating motor or speech activity through its interconnections throughout the initiation axis (87, 88). We have recently shown that by applying this knowledge in patients with gliomas in the SMA, intraoperative identification and subsequent preservation of the FAT can reduce SMA syndrome compared to just "avoiding the posterior bank of the SFG" (**Figure 2**). Thus, connectomic data can provide us helpful information to make more informed decisions during cerebral surgery regarding how to actually avoid causing specific neurologic deficits when considering the underlying network connectivity relative to tumor topography.

Toward "Disconnection Surgery"

Ultimately, it may be best if we begin to move away from the idea of "surgical resections" and instead toward the idea of oncological "disconnection surgery." Such a framework contextualizes tumor surgery as a series of cortical and subcortical disconnections to minimize unnecessary multi-network disturbances based on tumor location and pre-defined patient goals. In addition to the

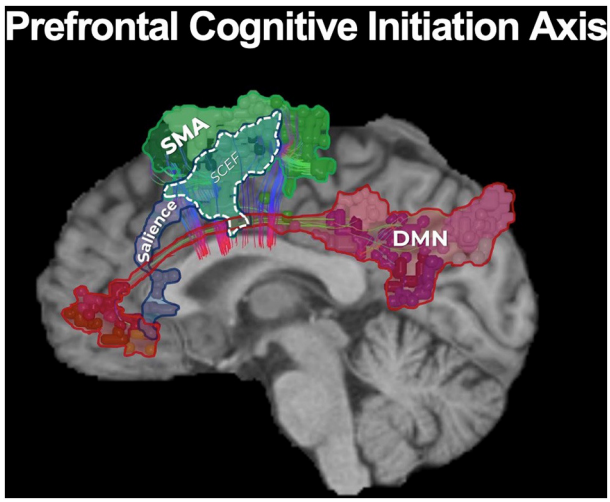

FIGURE 4 | The prefrontal cognitive initiation "axis." Our model of the initiation axis suggests that the DMN, connected via the cingulum, and the SN, connected via the frontal aslant tract (FAT), create a structural chain that extends up to the SMA in the medial frontal lobe (77). In fact, the SMA and salience networks share a node known as SCEF (supplementary and cingulate eye field). The identity and functional relevance of these connections have been supported by multiple lines of evidence (85), together suggesting this initiation "axis" is likely responsible for internally modeling goal initiation, such as with the initiation of speech and motor planning. Unsurprisingly, disruption of the integrity of this "axis" when operating on a tumor in the medial frontal lobe can lead to akinetic mutism and abulia (14, 82, 85).

consequences observed when disrupting the cores of the main cognitive networks as described above, it is likely that similar damage and associated consequences can be scaled to the more subtle networks if their network architecture around a tumor is not considered. **Figure 5** demonstrates a case of a medial anterior, left frontal glioma. One can see that it is a tumor of substantial size, but it also involves complex relationships given it can be seen herniating under the falx cerebri, but also crossing the corpus collosum and also demonstrating an intraventricular portion. It is very easy to think of this as a "ball" of tumor, but in reality it demonstrates important relationships to large scale brain networks. Therefore, instead of thinking of the surgery as a resection, this case can be thought of as a series of disconnections that can be defined against three known brain networks to maximize the extent of resection, to minimize impairments in defined cognitive functions, and to meet patient onco-functional goals (89).

While we suggest preserving the core of the main cognitive networks is of the utmost importance, it must also be known that it may not be surgically feasible nor practical to preserve these networks depending on the tumor location and patient prognosis, a dynamic which inherently represents the concept of optimizing the onco-functional balance. While we may choose to ignore the surrounding networks and focus on the tumor alone, connectomic data still provides valuable data that informs our actual decisions during surgery and the substantial risks associated with certain tumors. Previously, decisions on cognitive preservation during cerebral surgery were being made with incomplete information. Within this concept, future improvements will hopefully clarify our ability to quantitatively measure and understand exactly how much of what specific brain networks can be disconnected without compromising the multi-network communication necessary for effective human functioning.

CONSIDER THE FULL BRAIN RAMIFICATIONS OF THE ACTION

Essentiality and Redundancy in Intracerebral Neurosurgery

Preservation of essential neurocognitive functions that allow for activities of daily living distills into two fundamental principles—essentiality and redundancy. A tremendous amount of time and resources are devoted to preoperative discussions with patients, as are intraoperative maneuvers regarding the need for different types of physiological monitoring. Yet, seldom do we truly challenge what eloquent tissue is worth saving and what we cannot save in given situations. Essentiality, paradoxically may not matter if a patient is already paralyzed from a tumor that has completely infiltrated the motor strip.

The notion of *essentiality* in supratentorial, intracerebral surgeries is based on functions that are needed to maintain a degree of quality of life. A prototypical example of this would be maintaining a functional language network. Language is deemed essential as without it one cannot interpret what is spoken to them or express their wishes, and subsequently interactions with others and the outside world would become limited. In order to preserve language processing and speech functions, the neurosurgeon should not focus on one single anatomical region but rather focus on a network, consisting of high nodal connectivity. Specifically from the inferior frontal gyrus, to the inferior parietal lobule, to the posterior temporal lobe and the fiber tracts (superior longitudinal fasciculus and arcuate fasciculus) that interconnect those anatomical domains (**Figure 6**). The concept of eloquent brain ought to be defined not as a single anatomical region, but to anatomical locations and their interconnected networks and damage should be interpreted accordingly (92, 93). However, an important point we want to bring out is that currently, there are no adequate models or tools that allow us to predict or even visualize "essentiality" or its related networks prior to surgery. Furthermore, as detailed earlier, it is currently unknown the degree to which specific fibers and how much of those specific fibers in such pathways can be safely disconnected without comprising the entire function of a network. We discuss this further in later sections as it remains an important avenue of future research.

When dealing with *redundancy* in neurocognitive functions, we have to take into consideration the laterality of a network and whether there are compensatory mechanisms should an area of the brain be disconnected. A prime example of this is the supplementary motor area as part of the somatosensory network. As previously mentioned, it is well-recognized that disconnection of the core of the SMA can result in hemiparesis, but the

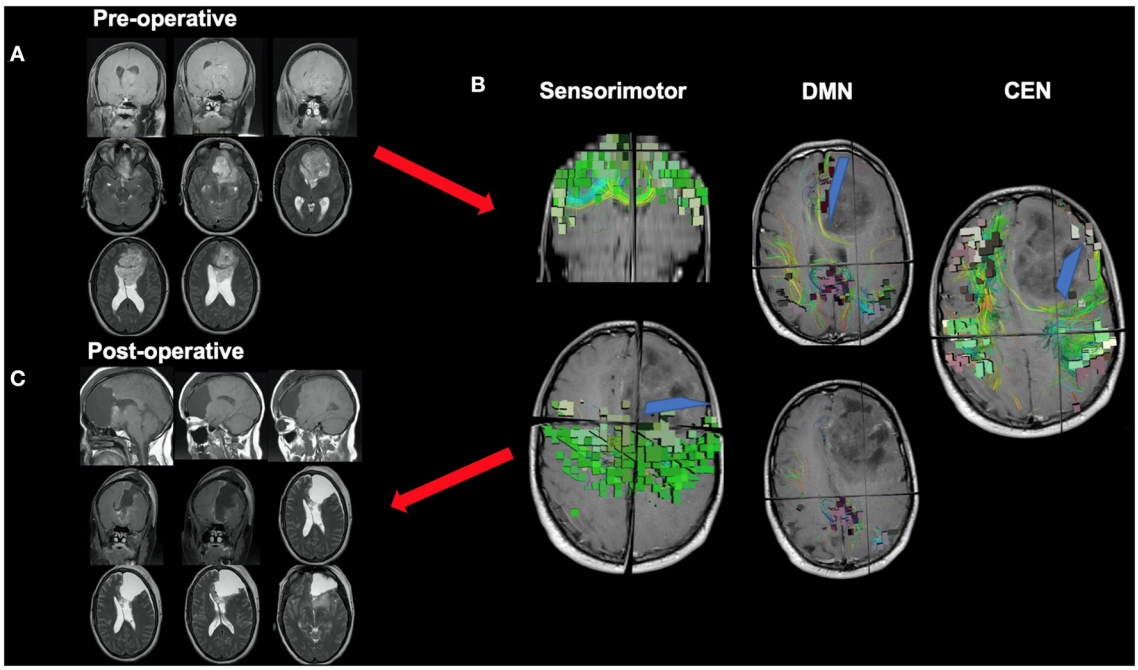

FIGURE 5 | Disconnection surgery. The neurosurgical community should move toward thinking of tumor surgery as a series of cortical and subcortical disconnections to minimize unnecessary network disturbances based on tumor location and patient goals. This figure presents a case of a medial anterior, left frontal glioma which demonstrates complex relationships with adjacent anatomy, such as the corpus collosum and falx cerebri. **(A)** While a complex case, it can be reduced to a series of disconnections that can be defined against three known brain networks: the DMN on medial boundary, the CEN on the lateral boundary, and the sensorimotor network on the posterior boundary. **(B)** Understanding information on the spatial relationship of the tumor to relevant white matter tracts and major networks can allow the neurosurgeon to make more informed decisions during surgery, such as where or how far to disconnect (blue lines) normal tissue infiltrated by a tumor up until certain key fibers or nodes are met. This decision should be made based on patient pre-defined goals and patient prognosis among other factors, and further work will hopefully clarify how much of specific networks can be safely disconnected without compromising certain functions **(C)**.

deficit is often transient in nature (94). One possibility offered through connectomic data is that compensation may occur if transcallosal projections of the FAT fibers ("crossed FAT") are preserved, given their ability to maintain interhemispheric connectivity by connecting the contralateral SMA and premotor area with the ipsilateral motor network (82). This phenomenon is likely dependent on already existing crossing fibers as neuronal regeneration is limited in the adult population (95). In this regard, there is known redundancy in the SMA area that can further guide our surgical decisions, such as to preserve these crossed FAT fibers if possible, and can also inform us about mechanisms of patient recovery post-operatively through specific pathways. In the same manner, we often perform complete right frontal lobectomies especially in light of supramaximal resections. Although the right frontal lobe can harbor important networks, including the DMN and CEN, we know that most patients can go on to live otherwise normal lives. There remains a paucity information in understanding whether a portion of brain can be sacrificed safely due to redundancy in functions.

Hubness Is the New Eloquence

Brain eloquence was traditionally defined as a region that houses a known neurological function, and if injured, results in a disabling neurological deficit (96–98). *How then do we define eloquent brain when planning tumor resection in a connectomics framework*? By utilizing pagerank centrality in graph theory, Ahsan et al. demonstrated that eloquent brain areas can be defined as highly connected brain hubs (93). It turns out that traditional eloquent areas of the brain are regions of high nodal connectedness. When we view the brain as an organ woven together by various networks in a mathematical manner, these hubs coincide with anatomic regions that were described to have high surgical importance by Spetzler and Martin (93, 98). Since graph theory analysis is not limited by physical distortion of the anatomy by mass-occupying pathologies, it may allow for the prediction of eloquence more accurately than anatomical landmarks. This is important given our traditionally better understanding of the general anatomy of regions responsible for language, motor and visual functions compared to that which is responsible for higher-order cognitive functions, like emotion.

Importantly, inter-individual differences exist on a macroscopic brain level in white matter connections as well as all the way down to the genetic makeup of individual cells (99). Fortunately, unique patient hubs can be determined by graph theory utilizing individual neuroimaging data in comparison to group-calculated averages, or probabilistic atlases. Areas of unexpected importance, or unexpected hubs, can be as high as 40% of all parcellations that are independent of gross anatomy

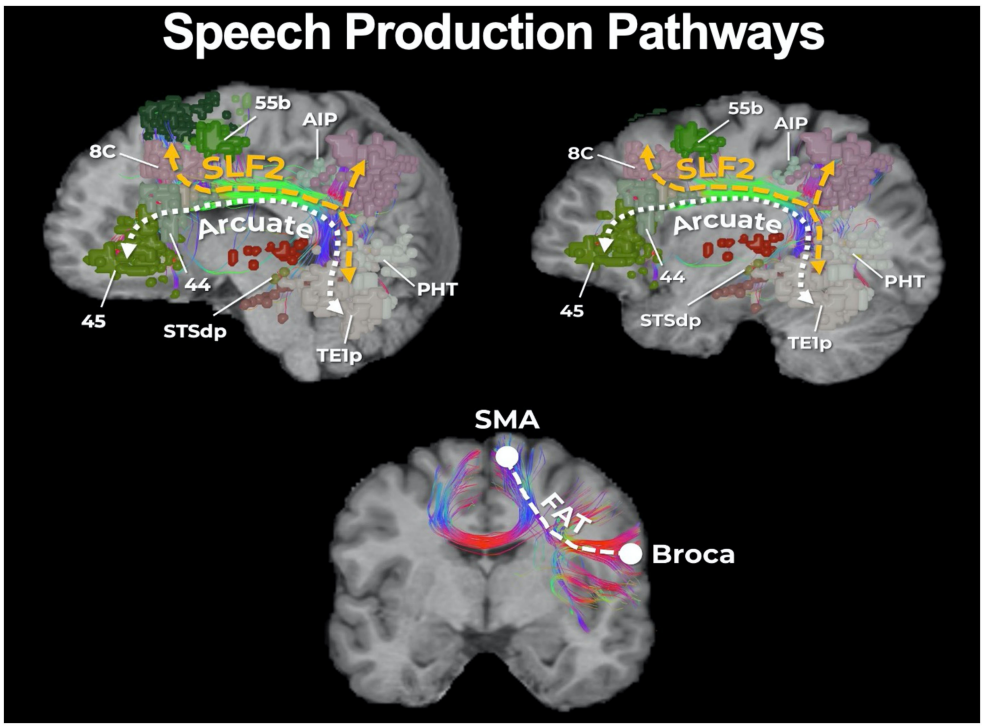

FIGURE 6 | Core parcellations and fibers involved in speech production. It is important to be aware of the core parcellations involved in speech production, as well as the main fibers interconnecting those regions such as the second layer of the superior longitudinal fasciculus (SLF-II), the arcuate fasciculus (AF), and the frontal aslant tract (FAT). For instance, area 55b is a recently discovered region that increasing evidence has suggested is necessary for phonation and motor control of the larynx (90). 55b is connected to the posterior temporal language areas via the SLF-II in the left hemisphere. If unaware of such connections, transgressing 55b leads to apraxia of speech (91).

(100). This is important given that outdated brain atlases based on group-averaged data or single subjects may overlook hubs unique to specific individuals, such as in the temporal pole which is often considered non-eloquent and therefore "safe to resect" (101). Recent improvements in connectomic data has also allowed others to expand the clinical utility of DES in identifying critical hubs on an individualized basis (89, 102). However, similar to graph-theory based analyses, further work is necessary to clarify how complex stimulation effects can allow us to draw stronger and more reliable conclusions about critical brain network functioning for higher-order cognition.

Computational Measures of Cognition and Surgery Can Guide Clinical Decisions

As previously mentioned, localizationists often propose that damage to a single area provides the basis underlying loss of higher-order cognitive functions, whether induced by surgery or by the lesion. However, as described above, connectomic or network-based approaches can instead provide us more accurate models describing this pathophysiology given that a cognitive impairment is often more accurately related to the disconnection of large fiber bundles connecting multiple regions in a network (103). Unsurprisingly, intelligence (i.e., fluid intelligence) does not localize to a single area, but rather involves a series of cortical regions maintained in and interacting between their networks (104). An example of a dynamic, multi-network interaction underlying higher-order cognitive functioning can be seen with complex mathematical thinking. Utilizing meta-analytic software to aggregate task-based fMRI data in the literature concerning mathematical operations, one would identify that mathematical skills implicate a variety of brain regions across visual, semantic, motor, and DAN networks as well as the white matter connections between them. Therefore, in neurosurgery, we must consider the use of advanced computational algorithms to predict how our surgical cuts affect *multiple networks* that function together to facilitate higher-order functions if we are to optimize cognitive morbidity following surgery.

Graph-based network analyses may allow us to better consider these multi-network interactions by measuring the possible effects of lesions or surgical disconnections on general cognitive functioning. *Global efficiency* is one example and it is defined as the average inverse of the shortest distance between two nodes in a brain network, producing a value that represents the capacity for information transfer on a global level (105). The length of a path represents the potential routes of information flow in the brain and therefore it is often considered that the shorter the path, the stronger the potential for functional integration (106). What is particularly advantageous of such data-driven

approaches is that the data can be non-invasively amalgamated from fMRI and DTI techniques. Therefore, patient neuroimaging data can be easily input into these complex algorithms to produce simple, interpretable scores for neurosurgeons to examine (i.e., "a higher global efficiency is better").

Additionally, these analyses provide a safe platform for further surgical decision making as there are computational methods to analyze how resilient an individualized brain network is to a particular insult in the perioperative period. For instance, percolation theory attempts to estimate the minimal set of essential nodes in a brain network to effectively transfer information (106). Therefore, simulated lesions or removal of nodes (*simulated brain surgery*) can be safely performed on patient structural connectivity graphs before or after surgery and then analyzed with measures of global efficiency to understand how a patient might be affected by a specific surgical decision or to understand beneficial avenues for subsequent neurorehabilitation (107). Also, as many neurologic disorders are neurodegenerative occurring throughout a long-term period, such computational analyses can also be applied to gauge a patient's cognitive functioning over time to guide future planning of care. While our team is actively utilizing similar methodology, there is a dearth of research which has yet to link these computational models with clinical outcomes. Given that differences in methodology concerning relatively nascent big data approaches may produce heterogenous results, especially on an individual patient basis, further work must be done to investigate the clinical relevance of such computational models.

MOVE OUR THINKING TOWARD INDIVIDUAL CIRCUITS

The Transdiagnostic Hypothesis

Are there areas in individual human brains that if resected during tumor surgery, can lead to symptoms of anxiety or depression? Such a question must be considered given the severity of post-operative cognitive morbidity which is possible, similar to the observation mentioned above that individual brains may display unique hub areas that if cut can result in unexpected dramatic losses of cognitive functioning (100). However, to answer a complex question such as this, we must strive to get down to the level of individual connectomes and neural microcircuits, and this requires big data that can be best handled with advanced computational algorithms offered with machine learning (ML) (108). In a cohort of patients with Alzheimer's disease who underwent rsfMRI and diffusion tensor imaging, we utilized ML to generate and detect individual-level anomalies in the structural and functional connectome (80). As expected, some similarities were found between patients, namely that there was consistent structural white matter loss focused around the DMN and subcortical structures. However, there was also significant heterogeneity in abnormal functional connectivity between patients, suggesting the opportunity to individualize future therapeutic strategies possibly based on different clinical phenotypes, moving us steps closer to true precision medicine (80). Similar work has been presented by others in a number of disorders with different methodologies (109, 110), however further work is necessary for us to effectively understand and identify abnormal connectivity patterns between different individuals that that relate to specific symptoms.

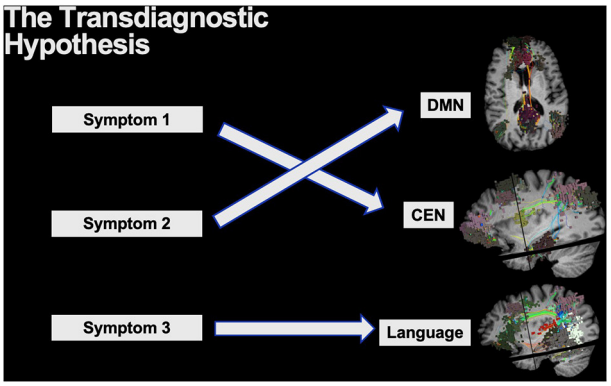

FIGURE 7 | The transdiagnostic hypothesis is often applied to explain the core psychopathological symptoms across a range of psychiatric disorders. Thus, while certain disorders may be clinically grouped together with vague classifications, unique symptoms likely localize to unique brain networks providing the need for addressing them individually.

The *transdiagnostic hypothesis* is often used in psychiatry to describe the core psychopathological symptoms which underlie a range of clinical disorders (18, 111). In the same context, transdiagnostic models can cover both commonalities and differences between clinical disorders or disorder subtypes as it knocks down previous rigid barriers set by vague clinical classifications, such as by the Diagnostic and Statistical Manual of Mental Disorders (DSM). If multiple unique symptoms arise, each can be thought to generally localize to a different brain circuit requiring unique attention despite their rigid DSM clinical classifications (**Figure 7**). For instance, many treatments for major depression disorder (MDD) target the dorsolateral prefrontal cortex (DLPFC) for modulation, yet the responses are highly variable and not all symptoms tend to become resolved (112). While it is known that different disease-subtypes of depression exist which localize to different networks, even the common symptoms across numerous depression subtypes, such as anxiety and anhedonia, also localize to different brain networks and respond to different target selections (18). To add further complexity, while the DLPFC includes core regions of the CEN, it is a functionally heterogenous region that has been characterized into 13 distinct functional regions by the HCP that must all be precisely considered on a patient by patient basis (15). Unsurprisingly, similar complexity can also be seen in other clinically relevant regions such as the precuneus and posterior cingulate cortex which house nodes of the DMN (15, 75). Therefore, to truly understand the connectome of patients presenting with a broad range of symptoms and more effectively target and address their individual symptoms, we must strive to get to the level of microcircuits that are implicated on an individual patient basis.

Incorporating the RDOC Framework into Future Research

If we reimagine surgical anatomy in terms of networks and advance the field with the goal of preserving various domains of neurocognition, it is important to apply a framework as a community in order to identify psychopathology-relevant constructs from the experimental literature. The Research Domain Criteria (RDoC) project was proposed by the US National Institute of Mental Health (NIMH) to classify mental illnesses that are based on dimensions of observable behavioral and neurobiological measures (113). It shifts the focus from clinical descriptions to more squarely examine aberrant mechanisms with the goal of how these mechanistic anomalies drive psychiatric symptoms. It assumes that mental disorders can be explained in terms of brain circuits and that abnormalities of these circuits are identifiable (114).

This tool from the psychiatry world can be leveraged to study neurocognitive changes after craniotomies as the literature in this regard is mostly based on the description of clinical symptoms, such as the DSM criteria for psychiatric illnesses. The application of the RDoC framework will differ in the neurosurgical field in that we can negate more developmental trajectories and environmental influences. The system includes several broad functional domains, such as negative valence, positive valence, cognitive systems, systems for social processes, arousal/modulatory systems, and sensorimotor systems (113). Each relevant domain is studied through queries of genes to circuits to behavior or self-reports, in order to provide an integrative understanding of its functioning (113). In other words, rather than merely reporting neurocognitive outcomes after awake craniotomies, one way to advance the field of research is to investigate changes in a patient's functional connectome and identify how those changes may contribute to and provide an explanation for neurocognitive manifestations after intracerebral surgeries. While these observations suggest a promising future in neuroscience with clinical applicability, there is still currently much to be done and further robust clinical evaluations are necessary to understand how we can better study and treat individualized patient connectomes (115).

THE POSSIBILITY THAT WE CAN CHANGE THE CONNECTOME

The Ability for Neural and Network Plasticity

Tumor resection inherently causes harm in some patients due to the locations of their pathology. If the human brain is composed of networks and each network is composed of various nodes, the question remains*: is there enough plasticity and redundancy in global cerebral networks that abnormal connections can be augmented to reduce neurocognitive or physical deficits*? The answer to this question is a resounding "yes," but with caveats.

The brain can demonstrate a high capacity for cerebral plasticity following a number of cortical and subcortical insults. Although, most of our current understanding of cerebral plasticity comes from stroke patients and less so in glioma patients (116). Following cerebral infarction, primary motor and secondary motor cortices demonstrate functional reorganization to facilitate improved motor functioning (117). However, some computational models argue the capacity for neuroplasticity is dependent on the type of cortical damage which has occurred, especially considering temporal factors (26). For instance, acute brain damage often causes more localized neuronal cell death and may demonstrate less capacity for cerebral plasticity compared to slow growing lesions (i.e., low-grade gliomas), which often disrupt more cerebral cortex and affects more networks, but also provides longer opportunities for functional reorganization due to less abrupt neuronal death. Therefore, it seems unsurprising that patients with slow-growing lesions may demonstrate more capacity for plasticity when targeting their functional connectome compared to patients suffering from acute strokes (26). As such, others have recently extensively detailed possible atlases of neuroplastic potential for diffuse LGGs based on their connectivity (118–120).

However, what about faster growing lesions such as in glioblastoma (GBM)? It is important to note that there exists pathophysiological differences in strokes and gliomas which may explain the ability for cortical reorganization following *acutely* growing GBM lesions in specific instances (121). In a patient presenting with a right frontal GBM with a decreased state of consciousness despite neurosurgical intervention, rsfMRI data demonstrated an absence of the DMN. Remarkably, after five sessions of navigated intermittent theta burst stimulation as an off-label TMS therapy to try to stimulate DMN activity, the patient demonstrated drastic improvements in cognition and alertness with a partial restoration of the DMN in just 2 weeks (121). There exists a number of limitations in this example being a single case. However, this case indeed demonstrates that there is a possibility to actively promote neurorehabilitation with brain stimulation targeted at the DMN in high-grade gliomas as well despite most discussion focusing on LGGs. Individualized connectomic approaches if implemented before any modulatory treatment can identify any network reorganization occurring from the lesion and then these data can subsequently be utilized for effective connectome-based target selection to strengthen previously silent polysynaptic cortical pathways (19). As we improve our understanding of the capacity for neural plasticity in a variety of different brain lesions, we must further link these findings to the structural and functional connectome. Such work will further clarify the opportunities and also limitations in addressing possible network disruptions occurring during the perioperative period.

rTMS for Neurorehabilitation and Restoring Onco-Functional Balance

Repetitive transcranial magnetic stimulation (rTMS) is a form of non-invasive brain stimulation that applies repeated magnetic pulses extracranially to generate an electrical current in the cortex. This in turn provokes electrophysiological changes in the target area and correlated brain networks (122). Given that a cortical insult may disrupt the oscillatory synchrony of the network that the damaged region belongs to, rTMS provides a feasible and safe way to attempt to re-establish this synchronization and reform the network. Currently, it is an evidence-based treatment mainly used for pharmacoresistant

major depressive disorder (MDD), which is thought to be a disorder based on the interplay between the DMN and CEN (123). Repetitive TMS targeting parts of the DLPFC has been shown using rsMRI to selectively modulate functional connectivity both within and between the CEN and DMN (123). In the same manner, rTMS to the primary motor cortex can enhance motor performance by inducing rapid changes in the sensorimotor networks along with activation in the bilateral basal ganglia, left superior frontal gyrus, bilateral pre-SMA, right medial temporal lobe, right inferior parietal lobe, and right cerebellar hemisphere (124). Much of our previous understanding of the benefits of rTMS comes from stroke patients as well (125); however, with concepts of connectomic-based targeting in neuropsychiatric illnesses, more work is needed to be able to apply population averaged connectivity measurements on an individual level.

Importantly, as reiterated throughout the current manuscript, different patients can present with different disease subtypes demonstrating unique clinical symptoms localizing to different brain networks. Despite these complex relationships, fortunately, individualized connectomic-based TMS target selection is possible and provides an important area of future research which has been previously barren. Fox et al. illustrated the feasibility of single-subject, connectivity-guided TMS targeting within regions of the left DLPFC in two patients with depression (19). Furthermore, our team has demonstrated the feasibility of an agile, data-driven, connectomic approach for TMS target selections at the single-subject level based on rsfMRI data for generalized anxiety disorder (GAD). Still, such data-driven, connectomic approaches for rTMS and other modulatory treatments are relatively nascent in the context of individualized treatments. While already demonstrating their safety profile, findings from these studies should be refined in the future to improve and expand their clinical applicability on a larger scale ultimately assessing its reproducibility.

Movements Forward in Connectivity-Based Modulatory Treatments

Examples above for connectome-based neurorehabilitation are mostly focused on rTMS to restore network synchrony; however, similar applications and results have been demonstrated with other modulatory treatments as well. A common method of modulating brain activity is with deep brain stimulation (DBS) of subcortical structures. Unsurprisingly, the most effective DBS subcortical targets demonstrate strong connectivity to the most effective TMS cortical targets for a number of disorders (126). For instance, while parts of the DLPFC are a favorite TMS target to treat symptoms of depression, the most effective subcortical DBS targets for depression resides in the subcallosal cingulate cortex (SCC). Connectomic data suggests these cortical and subcortical targets are strongly connected to each other and both work via modulating the same networks (127). In fact, TMS targets that demonstrate stronger connections to the SCC may demonstrate better clinical improvements in MDD (128); however, the degree to which these relationships expand to other disorders is still uncertain, but likely.

Importantly, similar limitations exist in both modalities in that their current utilization is also hampered by the lack of understanding of brain networks in different disease states and the limited validation of these connectomic-based treatments in individual patients with specific clinical phenotypes. It would be logical to select a node that serves as an important modulatory hub for altering the state of a network. However, what remains to be elucidated is target identification in many of these clinical disorders, and especially in rTMS, if the stimulation should be excitatory or inhibitory. Further, it has to be taken into account that if a crucial fiber tract (i.e., the entire corticospinal tract) is destroyed, no amount of neuromodulation will likely be able to salvage that function. Repetitive TMS, among other modulatory treatments, hold promise for neurorehabilitation, but their application will first require further improvements in our understanding of network disruptions following intracerebral surgeries.

CONCLUSION

Neurocognitive decline is common after intracerebral surgeries. Outside the context of language and motor skills, the mechanisms underlying declines in various neurological domains are not well-studied likely due to our previous lack of understanding of the complete structural and functional brain connectome. It is prudent for neurosurgeons to reimagine the brain as a confluence of networks, rather than an organ comprised of isolated regions dedicated or not dedicated to specialized functions. Brain connectomics provide the neurosurgeon further information on the relationships between tumor, neuroanatomy, and cognitive functions which can be leveraged to maximize our perioperative decisions while minimizing neurocognitive declines following intracerebral surgeries. Furthermore, such connectomic-based decisions provide novel opportunities to optimize post-operative neurorehabilitation via network augmentation, and advance the field using a common research framework that can be refined over time. However, as we appropriately move toward ideas such as "disconnection surgery" and connectome-based neurorehabilitation, further work must be done together in the neuroscience and neurosurgical communities.

AUTHOR CONTRIBUTIONS

ND, BB, and JY: writing—original draft and writing—review and editing. MS: conceptualization, methodology, and supervision. All authors contributed to the article and approved the submitted version.

ACKNOWLEDGMENTS

We would like to thank Omniscient Neurotechnology Pty Ltd (o8t) for the creation of all of the figures utilized in the current manuscript.

REFERENCES

1. Molinaro AM, Hervey-Jumper S, Morshed RA, Young J, Han SJ, Chunduru P, et al. Association of maximal extent of resection of contrast-enhanced and non-contrast-enhanced tumor with survival within molecular subgroups of patients with newly diagnosed glioblastoma. *JAMA Oncol.* (2020) 6:495–503. doi: 10.1001/jamaoncol.2019.6143
2. Yong RL, Lonser RR. Surgery for glioblastoma multiforme: striking a balance. *World Neurosurg.* (2011) 76:528–30. doi: 10.1016/j.wneu.2011.06.053
3. Rijnen SJM, Kaya G, Gehring K, Verheul JB, Wallis OC, Sitskoorn MM, et al. Cognitive functioning in patients with low-grade glioma: effects of hemispheric tumor location and surgical procedure. *J Neurosurg.* (2019) 2019:1–12. doi: 10.3171/2019.8.Jns191667
4. Drewes C, Sagberg LM, Jakola AS, Solheim O. Perioperative and postoperative quality of life in patients with glioma-a longitudinal cohort study. *World Neurosurg.* (2018) 117:e465–74. doi: 10.1016/j.wneu.2018.06.052
5. Herbet G, Moritz-Gasser S. Beyond language: mapping cognition and emotion. *Neurosurg Clin N Am.* (2019) 30:75–83. doi: 10.1016/j.nec.2018.08.004
6. van Kessel E, Snijders TJ, Baumfalk AE, Ruis C, van Baarsen KM, Broekman ML, et al. Neurocognitive changes after awake surgery in glioma patients: a retrospective cohort study. *J Neurooncol.* (2020) 146:97–109. doi: 10.1007/s11060-019-03341-6
7. Brennum J, Engelmann CM, Thomsen JA, Skjoth-Rasmussen J. Glioma surgery with intraoperative mapping-balancing the onco-functional choice. *Acta Neurochir.* (2018) 160:1043–50. doi: 10.1007/s00701-018-3521-0
8. Mandonnet E, Cerliani L, Siuda-Krzywicka K, Poisson I, Zhi N, Volle E, et al. A network-level approach of cognitive flexibility impairment after surgery of a right temporo-parietal glioma. *Neurochirurgie.* (2017) 63:308–13. doi: 10.1016/j.neuchi.2017.03.003
9. Chacko AG, Thomas SG, Babu KS, Daniel RT, Chacko G, Prabhu K, et al. Awake craniotomy and electrophysiological mapping for eloquent area tumours. *Clin Neurol Neurosurg.* (2013) 115:329–34. doi: 10.1016/j.clineuro.2012.10.022
10. Ritaccio AL, Brunner P, Schalk G. Electrical stimulation mapping of the brain: basic principles and emerging alternatives. *J Clin Neurophysiol.* (2018) 35:86–97. doi: 10.1097/WNP.0000000000000440
11. Erez N, Idit M, Tal S, Ori B, Yoni R, Tal G, et al. Failed awake craniotomy: a retrospective analysis in 424 patients undergoing craniotomy for brain tumor. *J Neurosurg.* (2013) 118:243–9. doi: 10.3171/2012.10.JNS12511
12. Ruis C. Monitoring cognition during awake brain surgery in adults: a systematic review. *J Clin Exp Neuropsychol.* (2018) 40:1081–104. doi: 10.1080/13803395.2018.1469602
13. Caras A, Mugge L, Miller WK, Mansour TR, Schroeder J, Medhkour A. Usefulness and impact of intraoperative imaging for glioma resection on patient outcome and extent of resection: a systematic review and meta-analysis. *World Neurosurg.* (2020) 134:98–110. doi: 10.1016/j.wneu.2019.10.072
14. Briggs RG, Allan PG, Poologaindran A, Dadario NB, Young IM, Ahsan SA, et al. The frontal aslant tract and supplementary motor area syndrome: moving towards a connectomic initiation axis. *Cancers (Basel).* (2021). 13:1116. doi: 10.3390/cancers13051116
15. Glasser MF, Coalson TS, Robinson EC, Hacker CD, Harwell J, Yacoub E, et al. A multi-modal parcellation of human cerebral cortex. *Nature.* (2016) 536:171–8. doi: 10.1038/nature18933
16. Brodmann K. *Vergleichende Lokalisationslehre der Grosshirnrinde in ihren Prinzipien dargestellt auf Grund des Zellenbaues von Dr. K Brodmann.* Leipiz: JA Barth. (1909).
17. Bullmore E, Sporns O. The economy of brain network organization. *Nat Rev Neurosci.* (2012) 13:336–49. doi: 10.1038/nrn3214
18. Siddiqi SH, Taylor SF, Cooke D, Pascual-Leone A, George MS, Fox MD. Distinct symptom-specific treatment targets for circuit-based neuromodulation. *Am J Psychiatry.* (2020) 177:435–46. doi: 10.1176/appi.ajp.2019.19090915
19. Fox MD, Liu H, Pascual-Leone A. Identification of reproducible individualized targets for treatment of depression with TMS based on intrinsic connectivity. *Neuroimage.* (2013) 66:151–60. doi: 10.1016/j.neuroimage.2012.10.082
20. van Kessel E, Emons MAC, Wajer IH, van Baarsen KM, Broekman ML, Robe PA, et al. Tumor-related neurocognitive dysfunction in patients with diffuse glioma: a retrospective cohort study prior to antitumor treatment. *Neurooncol Pract.* (2019) 6:463–72. doi: 10.1093/nop/npz008
21. Noll KR, Sullaway CM, Wefel JS. Depressive symptoms and executive function in relation to survival in patients with glioblastoma. *J Neurooncol.* (2019) 142:183–91. doi: 10.1007/s11060-018-03081-z
22. Starnoni D, Berthiller J, Idriceanu TM, Meyronet D. d'Hombres A, Ducray F, et al. Returning to work after multimodal treatment in glioblastoma patients. *Neurosurg Focus.* (2018) 44:E17. doi: 10.3171/2018.3.Focus1819
23. Olson RA, Iverson GL, Carolan H, Parkinson M, Brooks BL, McKenzie M. Prospective comparison of two cognitive screening tests: diagnostic accuracy and correlation with community integration and quality of life. *J Neurooncol.* (2011) 105:337–44. doi: 10.1007/s11060-011-0595-4
24. Polin RS, Marko NF, Ammerman MD, Shaffrey ME, Huang W, Anderson FA Jr, et al. Functional outcomes and survival in patients with high-grade gliomas in dominant and nondominant hemispheres. *J Neurosurg.* (2005) 102:276–83. doi: 10.3171/jns.2005.102.2.0276
25. Stiso J, Khambhati AN, Menara T, Kahn AE, Stein JM, Das SR, et al. White matter network architecture guides direct electrical stimulation through optimal state transitions. *Cell Rep.* (2019). 28:2554.e7–66.e7. doi: 10.1016/j.celrep.2019.08.008
26. Desmurget M, Bonnetblanc F, Duffau H. Contrasting acute and slow-growing lesions: a new door to brain plasticity. *Brain.* (2007). 130(Pt 4):898–914. doi: 10.1093/brain/awl300
27. Allan PG, Briggs RG, Conner AK, O'Neal CM, Bonney PA, Maxwell BD, et al. Parcellation-based tractographic modeling of the dorsal attention network. *Brain Behav.* (2019) 9:e01365. doi: 10.1002/brb3.1365
28. Baum GL, Cui Z, Roalf DR, Ciric R, Betzel RF, Larsen B, et al. Development of structure-function coupling in human brain networks during youth. *Proc Natl Acad Sci USA.* (2020) 117:771–8. doi: 10.1073/pnas.1912034117
29. Sheets JR, Briggs RG, Dadario NB, Young IM, Bai MY, Poologaindran A, et al. A cortical parcellation based analysis of ventral premotor area connectivity. *Neurol Res.* (2021) 2021:595–607. doi: 10.1080/01616412.2021.1902702
30. Honey CJ, Kotter R, Breakspear M, Sporns O. Network structure of cerebral cortex shapes functional connectivity on multiple time scales. *Proc Natl Acad Sci USA.* (2007) 104:10240–5. doi: 10.1073/pnas.0701519104
31. Kaiser M, Hilgetag CC. Nonoptimal component placement, but short processing paths, due to long-distance projections in neural systems. *PLoS Comput Biol.* (2006) 2:e95. doi: 10.1371/journal.pcbi.0020095
32. White JG, Southgate E, Thomson JN, Brenner S. The structure of the nervous system of the nematode *Caenorhabditis elegans. Philos Trans R Soc Lond B Biol Sci.* (1986) 314:1–340. doi: 10.1098/rstb.1986.0056
33. Wang J, Zuo X, He Y. Graph-based network analysis of resting-state functional MRI. *Front Syst Neurosci.* (2010) 4:16. doi: 10.3389/fnsys.2010.00016
34. Biswal B, Yetkin FZ, Haughton VM, Hyde JS. Functional connectivity in the motor cortex of resting human brain using echo-planar MRI. *Magn Reson Med.* (1995) 34:537–41. doi: 10.1002/mrm.1910340409
35. Hampson M, Peterson BS, Skudlarski P, Gatenby JC, Gore JC. Detection of functional connectivity using temporal correlations in MR images. *Hum Brain Mapp.* (2002) 15:247–62. doi: 10.1002/hbm.10022
36. Lowe MJ, Mock BJ, Sorenson JA. Functional connectivity in single and multislice echoplanar imaging using resting-state fluctuations. *Neuroimage.* (1998) 7:119–32. doi: 10.1006/nimg.1997.0315
37. Greicius MD, Krasnow B, Reiss AL, Menon V. Functional connectivity in the resting brain: a network analysis of the default mode hypothesis. *Proc Natl Acad Sci USA.* (2003) 100:253–8. doi: 10.1073/pnas.0135058100
38. Fox MD, Corbetta M, Snyder AZ, Vincent JL, Raichle ME. Spontaneous neuronal activity distinguishes human dorsal and ventral attention systems. *Proc Natl Acad Sci USA.* (2006) 103:10046–51. doi: 10.1073/pnas.0604187103
39. Dosenbach NU, Fair DA, Miezin FM, Cohen AL, Wenger KK, Dosenbach RA, et al. Distinct brain networks for adaptive and

stable task control in humans. *Proc Natl Acad Sci USA*. (2007) 104:11073–8. doi: 10.1073/pnas.0704320104
40. Fox MD, Snyder AZ, Vincent JL, Corbetta M, Van Essen DC, Raichle ME. The human brain is intrinsically organized into dynamic, anticorrelated functional networks. *Proc Natl Acad Sci USA*. (2005) 102:9673–8. doi: 10.1073/pnas.0504136102
41. Niendam TA, Laird AR, Ray KL, Dean YM, Glahn DC, Carter CS. Meta-analytic evidence for a superordinate cognitive control network subserving diverse executive functions. *Cogn Affect Behav Neurosci.* (2012) 12:241–68. doi: 10.3758/s13415-011-0083-5
42. Boschin EA, Piekema C, Buckley MJ. Essential functions of primate frontopolar cortex in cognition. *Proc Natl Acad Sci USA*. (2015) 112:E1020–7. doi: 10.1073/pnas.1419649112
43. Bilevicius E, Kolesar TA, Smith SD, Trapnell PD, Kornelsen J. Trait emotional empathy and resting state functional connectivity in default mode, salience, and central executive networks. *Brain Sci*. (2018). 8:128. doi: 10.3390/brainsci8070128
44. O'Neill A, Mechelli A, Bhattacharyya S. Dysconnectivity of large-scale functional networks in early psychosis: a meta-analysis. *Schizophr Bull.* (2019) 45:579–90. doi: 10.1093/schbul/sby094
45. Dong D, Wang Y, Chang X, Luo C, Yao D. Dysfunction of large-scale brain networks in schizophrenia: a meta-analysis of resting-state functional connectivity. *Schizophr Bull.* (2018) 44:168–81. doi: 10.1093/schbul/sbx034
46. Daniels JK, McFarlane AC, Bluhm RL, Moores KA, Clark CR, Shaw ME, et al. Switching between executive and default mode networks in posttraumatic stress disorder: alterations in functional connectivity. *J Psychiatry Neurosci.* (2010) 35:258–66. doi: 10.1503/jpn.090175
47. Mishkin M, Ungerleider LG. Contribution of striate inputs to the visuospatial functions of parieto-preoccipital cortex in monkeys. *Behav Brain Res.* (1982) 6:57–77. doi: 10.1016/0166-4328(82)90081-x
48. Norman J. Two visual systems and two theories of perception: an attempt to reconcile the constructivist and ecological approaches. *Behav Brain Sci*. (2002). 25:73–96; discussion 96–144. doi: 10.1017/s0140525x020 0002x
49. Baker CM, Burks JD, Briggs RG, Stafford J, Conner AK, Glenn CA, et al. A connectomic atlas of the human cerebrum-chapter 9: the occipital lobe. *Oper Neurosurg*. (2018). 15(Suppl_1):S372–406. doi: 10.1093/ons/o py263
50. Raichle ME, MacLeod AM, Snyder AZ, Powers WJ, Gusnard DA, Shulman GL, et al. default mode of brain function. *Proc Natl Acad Sci USA*. (2001) 98:676–82. doi: 10.1073/pnas.98.2.676
51. Mazoyer B, Zago L, Mellet E, Bricogne S, Etard O, Houde O, et al. Cortical networks for working memory and executive functions sustain the conscious resting state in man. *Brain Res Bull.* (2001) 54:287–98. doi: 10.1016/s0361-9230(00)00437-8
52. Raichle ME, Snyder AZ. A default mode of brain function: a brief history of an evolving idea. *Neuroimage*. (2007). 37:1083–90; discussion 1097–9. doi: 10.1016/j.neuroimage.2007.02.041
53. Carlson C, Devinsky O. The excitable cerebral cortex Fritsch G, Hitzig E. Uber die elektrische Erregbarkeit des Grosshirns. Arch Anat Physiol Wissen (1870). 37:300-32. *Epilepsy Behav*. (2009). 15:131–2. doi: 10.1016/j.yebeh.2009.03.002
54. Vahdat S, Darainy M, Milner TE, Ostry DJ. Functionally specific changes in resting-state sensorimotor networks after motor learning. *J Neurosci.* (2011) 31:16907–15. doi: 10.1523/JNEUROSCI.2737-11.2011
55. Chenji S, Jha S, Lee D, Brown M, Seres P, Mah D, et al. Investigating default mode and sensorimotor network connectivity in amyotrophic lateral sclerosis. *PLoS ONE*. (2016) 11:e0157443. doi: 10.1371/journal.pone.0157443
56. Seeley WW, Menon V, Schatzberg AF, Keller J, Glover GH, Kenna H, et al. Dissociable intrinsic connectivity networks for salience processing and executive control. *J Neurosci.* (2007) 27:2349–56. doi: 10.1523/JNEUROSCI.5587-06.2007
57. Sridharan D, Levitin DJ, Menon V. A critical role for the right fronto-insular cortex in switching between central-executive and default-mode networks. *Proc Natl Acad Sci USA*. (2008) 105:12569–74. doi: 10.1073/pnas.0800005105
58. Menon V, Uddin LQ. Saliency, switching, attention and control: a network model of insula function. *Brain Struct Funct.* (2010) 214:655–67. doi: 10.1007/s00429-010-0262-0
59. Broca P. Anatomie comparée des circonvolutions cérébrales. Le grand lobe limbique et la scissure limbique dans la série des mammifères. *Rev Anthrop.* (1978) 1:385–498.
60. Papez JW. A proposed mechanism of emotion. *Arch. Neurol Psychiatry.* (1937) 38:725–43.
61. Sullivan RM, Wilson DA, Ravel N, Mouly AM. Olfactory memory networks: from emotional learning to social behaviors. *Front Behav Neurosci.* (2015) 9:36. doi: 10.3389/fnbeh.2015.00036
62. Frith C. Brain mechanisms for 'having a theory of mind'. *J Psychopharmacol.* (1996) 10:9–15. doi: 10.1177/026988119601000103
63. Rajmohan V, Mohandas E. The limbic system. *Indian J Psychiatry.* (2007) 49:132–9. doi: 10.4103/0019-5545.33264
64. Rolls ET. The cingulate cortex and limbic systems for emotion, action, and memory. *Brain Struct Funct.* (2019) 224:3001–18. doi: 10.1007/s00429-019-01945-2
65. Cannistraro PA, Rauch SL. Neural circuitry of anxiety: evidence from structural and functional neuroimaging studies. *Psychopharmacol Bull.* (2003) 37:8–25.
66. Brambilla P, Hatch JP, Soares JC. Limbic changes identified by imaging in bipolar patients. *Curr Psychiatry Rep.* (2008) 10:505–9. doi: 10.1007/s11920-008-0080-8
67. Bogerts B, Meertz E, Schonfeldt-Bausch R. Basal ganglia and limbic system pathology in schizophrenia. A morphometric study of brain volume and shrinkage. *Arch Gen Psychiatry.* (1985) 42:784–91. doi: 10.1001/archpsyc.1985.01790310046006
68. Haznedar MM, Buchsbaum MS, Wei TC, Hof PR, Cartwright C, Bienstock CA, et al. Limbic circuitry in patients with autism spectrum disorders studied with positron emission tomography and magnetic resonance imaging. *Am J Psychiatry.* (2000) 157:1994–2001. doi: 10.1176/appi.ajp.157.12.1994
69. Corbetta M, Patel G, Shulman GL. The reorienting system of the human brain: from environment to theory of mind. *Neuron.* (2008) 58:306–24. doi: 10.1016/j.neuron.2008.04.017
70. Hopfinger JB, Buonocore MH, Mangun GR. The neural mechanisms of top-down attentional control. *Nat Neurosci.* (2000) 3:284–91. doi: 10.1038/72999
71. Posner MI. Orienting of attention. *Q J Exp Psychol.* (1980) 32:3–25. doi: 10.1080/00335558008248231
72. Zhang Z, Zheng H, Liang K, Wang H, Kong S, Hu J, et al. Functional degeneration in dorsal and ventral attention systems in amnestic mild cognitive impairment and Alzheimer's disease: an fMRI study. *Neurosci Lett.* (2015) 585:160–5. doi: 10.1016/j.neulet.2014.11.050
73. Sandhu Z, Tanglay O, Young IM, Briggs RG, Bai MY, Larsen ML, et al. Parcellation-based anatomic modeling of the default mode network. *Brain Behav.* (2021) 11:e01976. doi: 10.1002/brb3.1976
74. Briggs RG, Conner AK, Baker CM, Burks JD, Glenn CA, Sali G, et al. A connectomic atlas of the human cerebrum-chapter 18: the connectional anatomy of human brain networks. *Oper Neurosurg (Hagerstown)*. (2018). 15(Suppl_1):S470–80. doi: 10.1093/ons/opy272
75. Buckner RL, Andrews-Hanna JR, Schacter DL. The brain's default network: anatomy, function, and relevance to disease. *Ann N Y Acad Sci.* (2008) 1124:1–38. doi: 10.1196/annals.1440.011
76. Milton CK, Dhanaraj V, Young IM, Taylor HM, Nicholas PJ, Briggs RG, et al. Parcellation-based anatomic model of the semantic network. *Brain Behav*. (2021) 11:e02065. doi: 10.1002/brb3.2065
77. Poologaindran A, Lowe SR, Sughrue ME. The cortical organization of language: distilling human connectome insights for supratentorial neurosurgery. *J Neurosurg*. (2020) 2020:1–8. doi: 10.3171/2020.5.JNS191281
78. Menon V. The triple network model, insight, and large-scale brain organization in autism. *Biol Psychiatry.* (2018) 84:236–8. doi: 10.1016/j.biopsych.2018.06.012
79. Beevers CG. Cognitive vulnerability to depression: a dual process model. *Clin Psychol Rev*. (2005) 25:975–1002. doi: 10.1016/j.cpr.2005.03.003
80. Ren H, Zhu J, Su X, Chen S, Zeng S, Lan X, et al. Application of structural and functional connectome mismatch for classification and individualized therapy in alzheimer disease. *Front Public Health.* (2020) 8:584430. doi: 10.3389/fpubh.2020.584430
81. Baker CM, Burks JD, Briggs RG, Conner AK, Glenn CA, Sali G, et al. A connectomic atlas of the human cerebrum-chapter 1: introduction,

methods, and significance. *Oper Neurosurg.* (2018). 15(Suppl_1):S1–9. doi: 10.1093/ons/opy253
82. Baker CM, Burks JD, Briggs RG, Smitherman AD, Glenn CA, Conner AK, et al. The crossed frontal aslant tract: a possible pathway involved in the recovery of supplementary motor area syndrome. *Brain Behav.* (2018) 8:e00926. doi: 10.1002/brb3.926
83. Baker CM, Burks JD, Briggs RG, Milton CK, Conner AK, Glenn CA, et al. A connectomic atlas of the human cerebrum-chapter 6: the temporal lobe. *Oper Neurosurg*. (2018) 15(Suppl_1):S245–94. doi: 10.1093/ons/opy260
84. Toyoda K. Anterior cerebral artery and Heubner's artery territory infarction. *Front Neurol Neurosci.* (2012) 30:120–2. doi: 10.1159/000333607
85. Darby RR, Joutsa J, Burke MJ, Fox MD. Lesion network localization of free will. *Proc Natl Acad Sci USA*. (2018) 115:10792–7. doi: 10.1073/pnas.1814117115
86. Siegel JS, Snyder AZ, Metcalf NV, Fucetola RP, Hacker CD, Shimony JS, et al. The circuitry of abulia: insights from functional connectivity MRI. *Neuroimage Clin.* (2014) 6:320–6. doi: 10.1016/j.nicl.2014.09.012
87. La Corte E, Eldahaby D, Greco E, Aquino D, Bertolini G, Levi V, et al. The frontal aslant tract: a systematic review for neurosurgical applications. systematic review. *Front Neurol.* (2021) 12:641586. doi: 10.3389/fneur.2021.641586
88. Briggs RG, Conner AK, Rahimi M, Sali G, Baker CM, Burks JD, et al. A connectomic atlas of the human cerebrum-chapter 14: tractographic description of the frontal aslant tract. *Oper Neurosurg*. (2018). 15(Suppl_1):S444–9. doi: 10.1093/ons/opy268
89. Duffau H. New philosophy, clinical pearls, and methods for intraoperative cognition mapping and monitoring "à la carte" in brain tumor patients. *Neurosurgery*. (2021) 88:919–30. doi: 10.1093/neuros/nyaa363
90. Dichter BK, Breshears JD, Leonard MK, Chang EF. The control of vocal pitch in human laryngeal motor cortex. *Cell*. (2018). 174:21.e9–31.e9. doi: 10.1016/j.cell.2018.05.016
91. Chang EF, Kurteff G, Andrews JP, Briggs RG, Conner AK, Battiste JD, et al. Pure apraxia of speech after resection based in the posterior middle frontal gyrus. *Neurosurgery.* (2020) 87:E383–9. doi: 10.1093/neuros/nyaa002
92. Kahn E, Lane M, Sagher O. Eloquent: history of a word's adoption into the neurosurgical lexicon. *J Neurosurg.* (2017) 127:1461–6. doi: 10.3171/2017.3.JNS17659
93. Ahsan SA, Chendeb K, Briggs RG, Fletcher LR, Jones RG, Chakraborty AR, et al. Beyond eloquence and onto centrality: a new paradigm in planning supratentorial neurosurgery. *J Neurooncol.* (2020) 146:229–38. doi: 10.1007/s11060-019-03327-4
94. Oda K, Yamaguchi F, Enomoto H, Higuchi T, Morita A. Prediction of recovery from supplementary motor area syndrome after brain tumor surgery: preoperative diffusion tensor tractography analysis and postoperative neurological clinical course. *Neurosurg Focus.* (2018) 44:E3. doi: 10.3171/2017.12.FOCUS17564
95. Huebner EA, Strittmatter SM. Axon regeneration in the peripheral and central nervous systems. *Results Probl Cell Differ.* (2009) 48:339–51. doi: 10.1007/400_2009_19
96. Chang EF, Clark A, Smith JS, Polley MY, Chang SM, Barbaro NM, et al. Functional mapping-guided resection of low-grade gliomas in eloquent areas of the brain: improvement of long-term survival. *J Neurosurg.* (2011) 114:566–73. doi: 10.3171/2010.6.JNS091246
97. Duffau H, Capelle L, Denvil D, Sichez N, Gatignol P, Taillandier L, et al. Usefulness of intraoperative electrical subcortical mapping during surgery for low-grade gliomas located within eloquent brain regions: functional results in a consecutive series of 103 patients. *J Neurosurg.* (2003) 98:764–78. doi: 10.3171/jns.2003.98.4.0764
98. Spetzler RF, Martin NA. A proposed grading system for arteriovenous malformations. *J Neurosurg.* (1986) 65:476–83. doi: 10.3171/jns.1986.65.4.0476
99. Fornito A, Arnatkevičiute A, Fulcher BD. Bridging the gap between connectome and transcriptome. *Trends Cogn Sci*. (2019). 23:34–50. doi: 10.1016/j.tics.2018.10.005
100. Yeung JT, Taylor HM, Young IM, Nicholas PJ, Doyen S, Sughrue ME. Unexpected hubness: a proof-of-concept study of the human connectome using pagerank centrality and implications for intracerebral neurosurgery. *J Neurooncol.* (2021) 151:249–56. doi: 10.1007/s11060-020-03659-6
101. Briggs RG, Tanglay O, Dadario NB, Young IM, Fonseka RD, Hormovas J, et al. The unique fiber anatomy of middle temporal gyrus default mode connectivity. *Oper Neurosurg.* (2021) 21:E8–14. doi: 10.1093/ons/opab109
102. Sarubbo S, Tate M, De Benedictis A, Merler S, Moritz-Gasser S, Herbet G, et al. Mapping critical cortical hubs and white matter pathways by direct electrical stimulation: an original functional atlas of the human brain. *NeuroImage*. (2020). 205:116237. doi: 10.1016/j.neuroimage.2019.116237
103. O'Neal CM, Ahsan SA, Dadario NB, Fonseka RD, Young IM, Parker A, et al. A connectivity model of the anatomic substrates underlying ideomotor apraxia: a meta-analysis of functional neuroimaging studies. *Clin Neurol Neurosurg*. 2021:106765. doi: 10.1016/j.clineuro.2021.106765
104. Zaidel DW. Overall intelligence and localized brain damage. *Behav Brain Sci.* (2007) 30:173–4. doi: 10.1017/S0140525X07001331
105. Latora V, Marchiori M. Efficient behavior of small-world networks. *Phys Rev Lett.* (2001) 87:198701. doi: 10.1103/PhysRevLett.87.198701
106. Rubinov M, Sporns O. Complex network measures of brain connectivity: uses and interpretations. *Neuroimage.* (2010) 52:1059–69. doi: 10.1016/j.neuroimage.2009.10.003
107. Alstott J, Breakspear M, Hagmann P, Cammoun L, Sporns O. Modeling the impact of lesions in the human brain. *PLoS Comput Biol.* (2009) 5:e1000408. doi: 10.1371/journal.pcbi.1000408
108. Reimann MW, King JG, Muller EB, Ramaswamy S, Markram H. An algorithm to predict the connectome of neural microcircuits. *Front Comput Neurosci.* (2015) 9:120. doi: 10.3389/fncom.2015.00120
109. Ferreira D, Pereira JB, Volpe G, Westman E. Subtypes of Alzheimer's disease display distinct network abnormalities extending beyond their pattern of brain atrophy. *Front Neurol.* (2019). 10:524. doi: 10.3389/fneur.2019.00524
110. Tokuda T, Yoshimoto J, Shimizu Y, Okada G, Takamura M, Okamoto Y, et al. Identification of depression subtypes and relevant brain regions using a data-driven approach. *Scient Rep*. (2018). 8:14082. doi: 10.1038/s41598-018-32521-z
111. Drysdale AT, Grosenick L, Downar J, Dunlop K, Mansouri F, Meng Y, et al. Resting-state connectivity biomarkers define neurophysiological subtypes of depression. *Nat Med.* (2017) 23:28–38. doi: 10.1038/nm.4246
112. Berlim MT, McGirr A, Rodrigues Dos Santos N, Tremblay S, Martins R. Efficacy of theta burst stimulation (TBS) for major depression: an exploratory meta-analysis of randomized and sham-controlled trials. *J Psychiatr Res.* (2017) 90:102–9. doi: 10.1016/j.jpsychires.2017.02.015
113. Sanislow CA, Pine DS, Quinn KJ, Kozak MJ, Garvey MA, Heinssen RK, et al. Developing constructs for psychopathology research: research domain criteria. *J Abnorm Psychol.* (2010) 119:631–9. doi: 10.1037/a0020909
114. Colibazzi T. Journal Watch review of Research domain criteria (RDoC): toward a new classification framework for research on mental disorders. *J Am Psychoanal Assoc.* (2014) 62:709–10. doi: 10.1177/0003065114543185
115. Kelly CJ, Karthikesalingam A, Suleyman M, Corrado G, King D. Key challenges for delivering clinical impact with artificial intelligence. *BMC Med*. (2019). 17:195. doi: 10.1186/s12916-019-1426-2
116. Kong NW, Gibb WR, Tate MC. Neuroplasticity: insights from patients harboring gliomas. *Neural Plast.* (2016) 2016:2365063. doi: 10.1155/2016/2365063
117. Sharma N, Baron J-C, Rowe JB. Motor imagery after stroke: relating outcome to motor network connectivity. *Ann Neurol.* (2009) 66:604–16. doi: 10.1002/ana.21810
118. Duffau HA-O. Functional mapping before and after low-grade glioma surgery: a new way to decipher various spatiotemporal patterns of individual neuroplastic potential in brain tumor patients. Cancers. (2020) 12:2611. doi: 10.3390/cancers12092611
119. Herbet G, Lafargue G, Duffau H. Un atlas du potentiel neuroplastique chez les patients cérébrolésés [An atlas of neuroplastic potential in brain-damaged patients]. *Med Sci (Paris)*. (2017) 33:84–6. French. doi: 10.1051/medsci/20173301014
120. Herbet G, Maheu M, Costi E, Lafargue G, Duffau H. Mapping neuroplastic potential in brain-damaged patients. *Brain*. Mar (2016). 139(Pt 3):829–44. doi: 10.1093/brain/awv394

121. Stephens TM, Young IA-O, O'Neal CA-O, Dadario NB, Briggs RA-O, Teo C, et al. Akinetic mutism reversed by inferior parietal lobule repetitive theta burst stimulation: can we restore default mode network function for therapeutic benefit? *Brain Behav.* (2021) 2021:e02180. doi: 10.1002/brb3.2180
122. Klomjai W, Katz R, Lackmy-Vallee A. Basic principles of transcranial magnetic stimulation (TMS) and repetitive TMS (rTMS). *Ann Phys Rehabil Med.* (2015) 58:208–13. doi: 10.1016/j.rehab.2015.05.005
123. Liston C, Chen AC, Zebley BD, Drysdale AT, Gordon R, Leuchter B, et al. Default mode network mechanisms of transcranial magnetic stimulation in depression. *Biol Psychiatry.* (2014) 76:517–26. doi: 10.1016/j.biopsych.2014.01.023
124. Yoo WK, You SH, Ko MH, Tae Kim S, Park CH, Park JW, et al. High frequency rTMS modulation of the sensorimotor networks: behavioral changes and fMRI correlates. *Neuroimage.* (2008) 39:1886–95. doi: 10.1016/j.neuroimage.2007.10.035
125. Kim YH, You SH, Ko MH, Park JW, Lee KH, Jang SH, et al. Repetitive transcranial magnetic stimulation-induced corticomotor excitability and associated motor skill acquisition in chronic stroke. *Stroke.* (2006) 37:1471–6. doi: 10.1161/01.STR.0000221233.55497.51
126. Horn A, Fox MD. Opportunities of connectomic neuromodulation. *NeuroImage.* (2020) 221:117180. doi: 10.1016/j.neuroimage.2020.117180
127. Fox MD, Buckner RL, White MP, Greicius MD, Pascual-Leone A. Efficacy of transcranial magnetic stimulation targets for depression is related to intrinsic functional connectivity with the subgenual cingulate. *Biol Psychiatry.* (2012) 72:595–603. doi: 10.1016/j.biopsych.2012.04.028
128. Weigand A, Horn A, Caballero R, Cooke D, Stern AP, Taylor SF, et al. Prospective validation that subgenual connectivity predicts antidepressant efficacy of transcranial magnetic stimulation sites. *Biol Psychiatry.* (2018) 84:28–37. doi: 10.1016/j.biopsych.2017.10.028

Conflict of Interest: MS is the Chief Medical Officer of Omniscient Neurotechnology, however this does not pose a conflict of interest in this study.

The remaining authors declare that the research was conducted in the absence of any commercial or financial relationships that could be construed as a potential conflict of interest.

Publisher's Note: All claims expressed in this article are solely those of the authors and do not necessarily represent those of their affiliated organizations, or those of the publisher, the editors and the reviewers. Any product that may be evaluated in this article, or claim that may be made by its manufacturer, is not guaranteed or endorsed by the publisher.

frontiers in Neurology

ORIGINAL RESEARCH
published: 26 August 2021
doi: 10.3389/fneur.2021.727055

Cortical and Subcortical Anatomy of the Parietal Lobe From the Neurosurgical Perspective

Tomasz Andrzej Dziedzic[1]*, *Aleksandra Bala*[1,2] and *Andrzej Marchel*[1]

[1] Department of Neurosurgery, Medical University of Warsaw, Warsaw, Poland, [2] Faculty of Psychology, University of Warsaw, Warsaw, Poland

Introduction: The anatomical structures of the parietal lobe at the cortical and subcortical levels are related mainly to sensory, visuospatial, visual and language function. The aim of this study was to present an intraoperative perspective of these critical structures in terms of the surgical treatment of intra-axial lesions. The study also discusses the results of the technique and the results of direct brain stimulation under awake conditions.

Materials and Methods: Five adult brains were prepared according to the Klingler technique. Cortical assessments and all measurements were performed with the naked eye, while white matter dissection was performed with microscopic magnification.

Results: Intra-axial lesions within the parietal lobe can be approached through a lateral or superior trajectory. This decision is based on the location of the lesions in relation to the arcuate fascicle/superior longitudinal fascicle (AF/SLF) complex and ventricular system. Regardless of the approach, the functional borders of the resection are defined by the postcentral gyrus anteriorly and Wernicke's speech area inferiorly. On the subcortical level, active identification of the AF/SLF complex and of the optic radiation within the sagittal stratum should be performed. The intraparietal sulcus (IPS) is a reliable landmark for the AF/SLF complex in ∼60% of cases.

Conclusion: Knowledge of the cortical and subcortical anatomical and functional borders of the resection is crucial in preoperative planning, prediction of the risk of postoperative deficits, and intraoperative decision making.

Keywords: white matter, anatomy, fiber dissection, tractography, glioma, parietal lobe

OPEN ACCESS

Edited by:
Emanuele La Corte, University of Bologna, Italy

Reviewed by:
Giacomo Bertolini, University of Milan, Italy
Edgar G. Ordóñez-Rubiano, Hospital Infantil Universitario de San José, Colombia

***Correspondence:**
Tomasz Andrzej Dziedzic
tdziedzic@wum.edu.pl
orcid.org/0000-0002-2832-5064

Specialty section:
This article was submitted to Applied Neuroimaging, a section of the journal Frontiers in Neurology

Received: *17 June 2021*
Accepted: *30 July 2021*
Published: *26 August 2021*

Citation:
Dziedzic TA, Bala A and Marchel A (2021) Cortical and Subcortical Anatomy of the Parietal Lobe From the Neurosurgical Perspective. Front. Neurol. 12:727055. doi: 10.3389/fneur.2021.727055

INTRODUCTION

The parietal lobe is the third most common site of glioma incidence in adult patients, following the frontal and temporal lobes (1). In addition to containing cortical regions related to sensory and language function at the subcortical level, the parietal lobe is a crossroads of white matter tracts related to motor, sensory, language, visuospatial, and visual function (2). However, in a study of a large cohort of patients operated on due to parietal lobe gliomas, characteristic parietal lobe syndromes (neglect syndromes; visuospatial dysfunction;

Gerstman's syndrome – agraphia4, acalculia, finger agnosia) were infrequently observed in the long term (3). In contrast to the characteristic parietal lobe syndromes, language and visual field deficits are frequently associated with surgery on the parietal lobe, occurring significantly more often with such procedures than with surgery in other sites, and these deficits negatively impact patients' quality of life. Surgical approaches to the parietal lobe are mainly based on the lesion's localization in relation to the ventricular system and the main white matter tracts of the sagittal stratum (SS) and arcuate fasciculus/superior longitudinal fasciculus complex (AF/SLF complex) (**Figure 1**). From an anatomical perspective, the parietal lobe has four main components: the postcentral gyrus, the inferior parietal lobule (IPL), the superior parietal lobule (SPL), and, on the medial surface, the precuneus, which merges with the SPL on the superior margin of the hemisphere (5) (**Figures 1**, **2**). From a neurosurgical perspective, six different types of tumor infiltration within the parietal lobe have been identified based on the classification proposed by Sanai et al. (3) (**Figure 2**). In the surgical classification, the posterior part of the cingulum, which is anatomically part of the limbic system, is incorporated into the parietal lobe. Tumors within Zones 1 and 3, which correspond to the supramarginal gyrus (SMG) and angular gyrus (AG), are highly related to permanent postoperative language and visual deficits, respectively. In Zones 2 and 4, extensive surgical resections are possible due to a low risk of permanent neurocognitive deficits and are mainly limited anteriorly by the corticospinal and thalamocortical tracts (**Figure 3**). Tumor localization is important in terms of anticipating the risk of the procedure as well as selecting the type of intraoperative mapping and the surgical approach. We studied in detail the cortical anatomy of the parietal lobe as well as of white matter tracts and its relationship to the brain surface, which must be taken into consideration during surgical procedures.

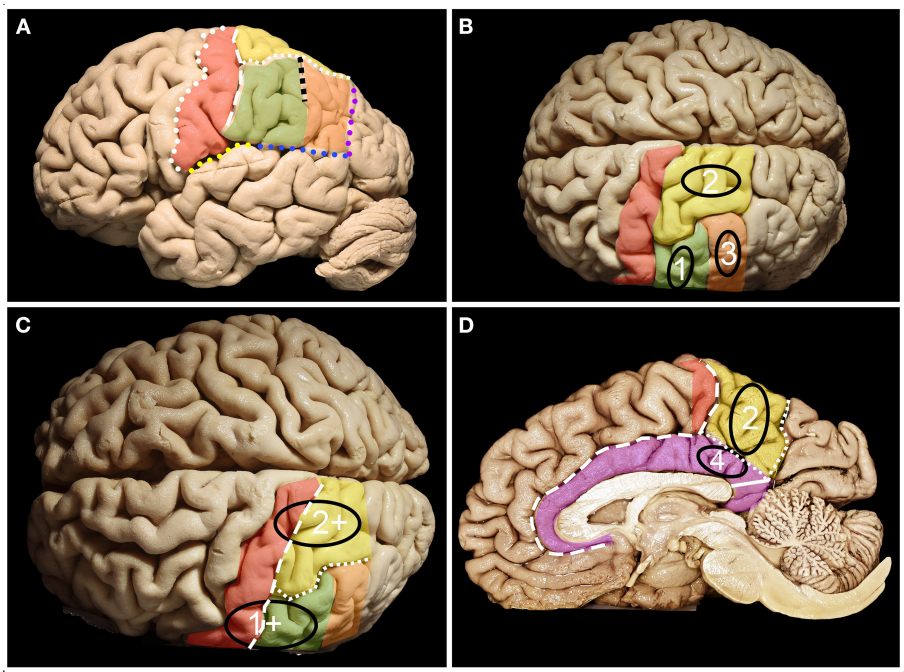

FIGURE 1 | Anatomy of the parietal lobe from lateral, mesial and superior perspectives. **(A)** The parietal lobe is placed posteriorly to the central sulcus (white dots), which is one of the most constant landmarks on the convexity of the brain. The posterior border and inferior border of the parietal lobe on the lateral surface are marked by the temporoparietal line (purple dots) and parieto-occipital line (blue dots) with the posterior ramus of the lateral sulcus (yellow dots), respectively. Running parallel to the central sulcus, the postcentral gyrus (red) can be identified, which is limited posteriorly by the posterior central sulcus (white rectangles). Posterior to the postcentral sulcus, superior (yellow) (SPL) and inferior (green + orange) parietal (IPL) lobules are identified, which are separated by the intraparietal sulcus (white squares) (IPS). The IPS and postcentral sulcus junction patterns can be defined according to the Cunningham into one of the five subtypes: I. postcentral sulcus is divided into superior and inferior portion, IPS separate; II. inferior post-central confluent with IPS, superior postcentral separate; III. superior and inferior post-central confluent, IPS separate; IV. superior and inferior postcentral confluent and unified with IPS; V. IPS confluent with the superior post-central and inferior post-central separate (4). The superior branch of the IPS (the sulcus of Brissaud) is localized within the SPL. The inferior branch of the IPS (black squares) (the sulcus of Jensen) separates the SMG (green) anteriorly from the AG (orange) posteriorly. **(B)** Parietal lobe glioma classification according to Berger et al. distinct three zones 1, 2 and 3 on the lateral brain surface that correspond to SMG, SPL and AG retrospectively. **(C)** Tumors in zones 1 and 2 extending anteriorly beyond the SMG and SPL become tumors within zones 1+ and 2+. **(D)** Zone 2 consists of the mesial surface of the precuneus, while Zone 4 consists of the gyrus cinguli below the precuneus. On the medial surface of the hemisphere. The parietal lobe is defined by the precuneus (yellow) and the posterior part of the paracentral lobule (red). The anterior border of the precuneus is marked by the marginal branch of the cingulate sulcus (white rectangles), posterior by the parieto-occipital sulcus (white squares) and inferior by the subparietal sulcus (white dots). Below which the cingulum (purple) covering the corpus callosum is identified. The isthmus of the cingulum (white continuous line) at the level of the posterior surface of the splenium of the corpus callosum was identified.

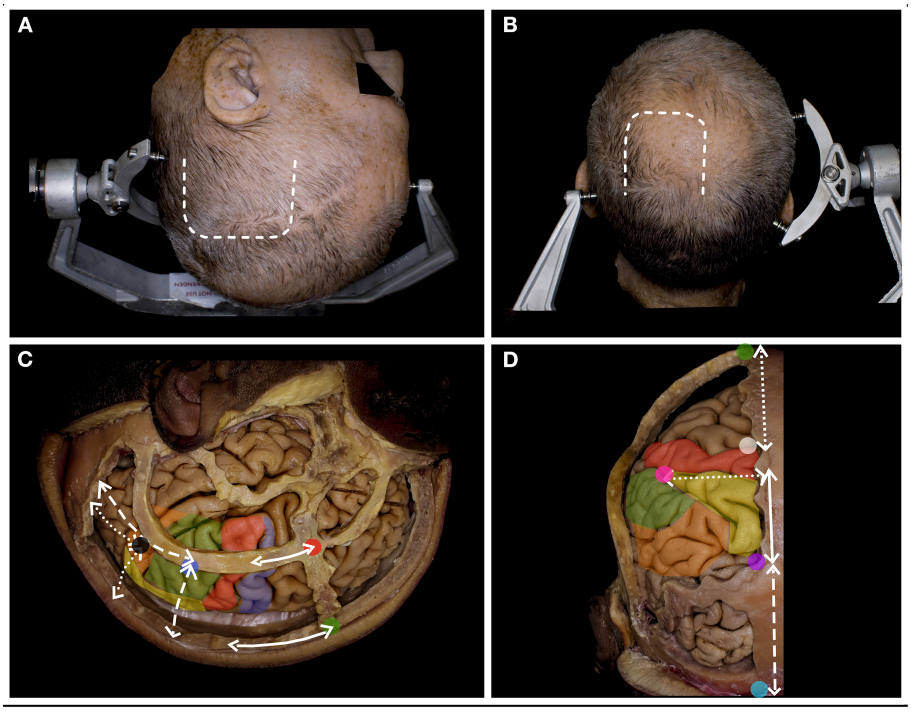

FIGURE 2 | The surgical perspective of the parietal lobe anatomy. **(A)** For the tumors located within Zones 1, 1+ and 3, below the IPS, the lateral trajectory is preferred, and the long axis of the head is rotated to the contralateral side, being almost parallel to the floor. A u-shaped skin incision (white rectangle) based on the skull base is preferred. **(B)** For tumors located above the IPS within Zones 2, 2+, and 4, the superior trajectory is preferred, and the head is positioned in the neutral position. A u-shaped skin incision (white rectangle) with the base at the transverse sinus is preferred. **(C)** The lateral perspective of the parietal lobe in relation to the craniometric points with marked precentral gyrus (blue), the postcentral (red), the SPL (yellow), the SMG (green) and the AG (yellow). The postcentral gyrus (along the continuous white line) is located ∼6.5 cm posterior to bregma (green dot) and 4.1 cm behind stephanion (red dot). The end of the lateral sulcus within the SMG (blue dot) is identified (along the white rectangle line) ∼6.0 cm anterior to the lambdoid suture and 6.4 cm lateral to the sagittal suture. The end of the superior temporal sulcus within the AG (black dot) was identified (along the white dotted line) ∼4.3 cm from the lambdoid and 5.0 cm from the sagittal suture (6). **(D)** The posterior/superior perspective of the parietal lobe in relation to the craniometric points. The superior Rolandic point (white dot) is identified ∼5.0 cm behind bregma, and behind this point, the postcentral gyrus is identified. The parieto-occipital sulcus (purple dot), which marks the posterior border of the parietal lobe, is identified at the level where the lambdoid suture joins the sagittal suture. This point is ∼6 cm anterior to the inion (light blue) along the midline (white rectangle line). Another 6.0 cm anterior to the lambdoid suture along the sagittal suture and 5.0 cm lateral and perpendicular to perpendicular to the midline the point (pink) where IPS joins the postcentral sulcus is identified (7).

MATERIALS AND METHODS

Five adult human cadaveric brains were prepared following the Klingler technique; the details of the technique have been described previously (8). Briefly, the specimens were fixed with 4% formalin for at least 4 weeks, and the arachnoid and vessels were removed; afterwards, each brain was stored dry in a freezer at −15 degrees Celsius for 2 weeks. For thawing and preservation, 4% formalin solution at room temperature was used. The brain was placed in a position simulating an intraoperative scenario. For Zones 2, 2+, and 4, the long axis of the brain was perpendicular (to present perspective from superior trajectory) or parallel (to present perspective from lateral trajectory) to the floor for Zones 1, 1+, and 3 (**Figure 2**). Measurements were made with an electric digital caliper, protractor and measuring tape. Cortical anatomy was assessed with a naked eye and all measurements on the brain surface were performed with a measuring tape and protractor. In the next step, white matter dissection was performed with the aid of surgical microscope. All measurements on the subcortical level were performed with the electric digital caliper and protractor. Each measurement was taken twice by the same observer and the average value was taken for presentation of the results. A digital camera (Nikon D7200 with a Nikon DX 35 mm 1:1.8 G lens) was used for image documentation. The study was approved by the Bioethics Committee of Medical University of Warsaw, approval number AKBE/126/2019.

RESULTS

Lateral Approach

Measurements on the Cortical Level

The postcentral sulcus, which marks the anterior margin of the IPL, was identified 18.1 (ranging from 14 to 22) mm posterior to the inferior Rolandic point (IRP) (**Figure 4**). The inferior border was formed by the occipitotemporal line, which had 41.4 (ranging from 33 to 49) mm. The superior border was formed by the intraparietal sulcus (IPS), which was connected to the postcentral

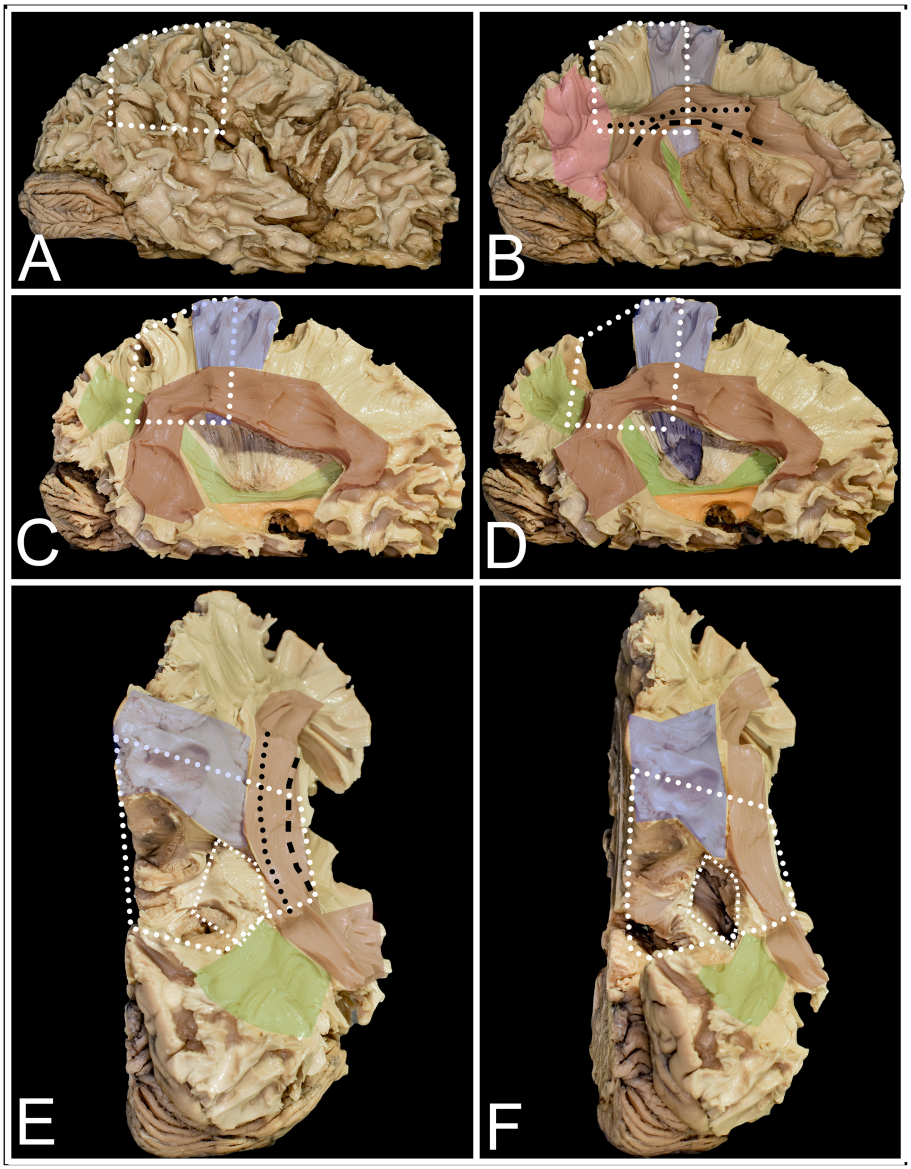

FIGURE 3 | The figure presents the anatomy of white matter tracts within and outside the parietal lobe from lateral **(A–D)** and superior **(E,F)** perspectives. White dots mark the localization of the parietal lobe within the right hemisphere. **(A)** After removal of the cerebral cortex, the short u-fibers connecting neighboring gyri are exposed. **(B)** The most superficial layer of the associated fibers is formed by the AF/SLF complex (burgundy) and by the vertical occipital fasciculus (VOF) (pink). The most superficial layer of the AF/SLF complex is formed by SLF II (black dots), which connects the angular gyrus with the middle frontal gyrus. SLF III (black rectangle) runs inferior to SLF II, without a clear demarcation between them, connecting the SMG with the inferior frontal gyrus. Medial to SLFs II and III, the AF is identified, which is difficult to separate from the SLF complex, as they have the same direction on the horizontal segment of the AF/SLF complex. Under the vertical part of the AF/SLF complex in the anteroposterior direction, the fibers of the sagittal stratum (SS) (green) are exposed. The most superficial layer of the fibers within the SS is formed by the ILF, but they run inferior to the atrium and are not related to parietal lobe surgery. A deeper layer is formed by the IFOF, which covers the whole lateral wall of the atrium. The deepest segment is formed by optic radiation (OR), which at the bottom is fused with the anterior commissure (AC). Deeper to the OR and directed perpendicular to it, the fibers of the tapetum of the lateral ventricle were identified. Mesial to the AF/SLF complex at the level of the paracentral lobule, corticospinal tract (blue) fibers are identified. **(C)** The mean compartment of the SS is formed by the IFOF, which is identified when the cortex of the insula is removed. Ventral to the IFOF, the uncinate fasciculus (UF) (orange), which connects the frontal and temporal lobes, is identified. **(D)** The precuneus was resected to expose the fibers of the paracentral lobule that marked the anterior margin of the resection. The posterior part is formed from thalamocortical fibers, which are sensory fibers. Below the AF/SLF complex, the corticospinal tract forms the posterior limb of the internal capsule, which is covered laterally by the putamen. **(E)** The superior perspective after removal of the precuneus. The surface marked with a line of white squares corresponds to the position of the atrium of the lateral ventricle. **(F)** The atrium of the lateral ventricle was opened from the superior ventricle. Lateral to it, the horizontal segment of the AF/SLF complex is identified, and posteriorly, the superior fibers form the SS.

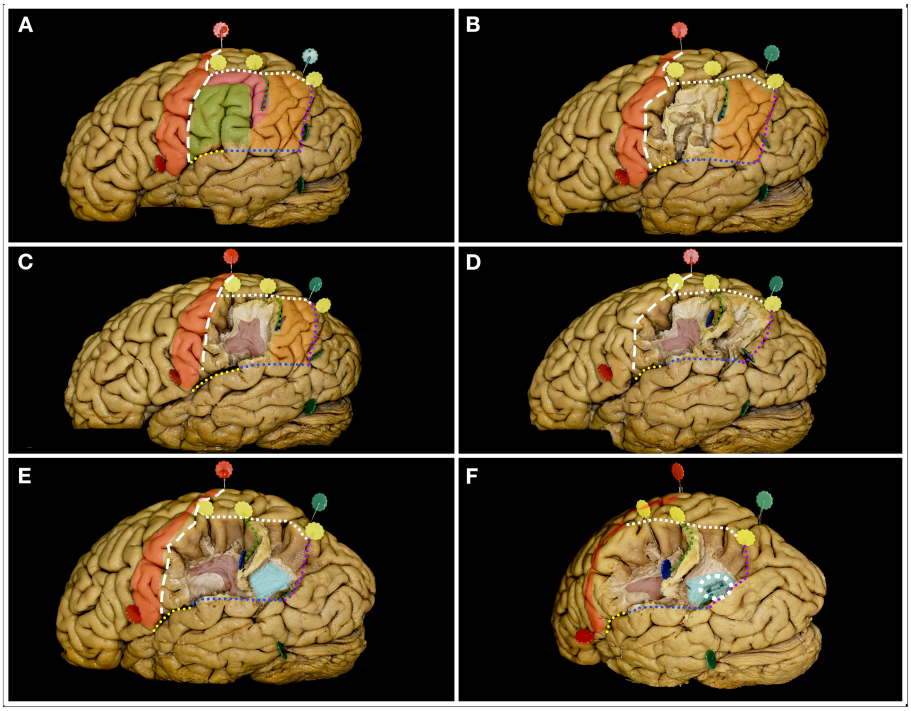

FIGURE 4 | The figure represents the surgical perspective of the surgical field within the inferior parietal lobule from a lateral perspective. **(A)** The IPL is located posterior to the postcentral sulcus (white rectangle line) and to the postcentral gyrus (red), inferior to the intraparietal sulcus (white square line), anterior to the parietotemporal line (purple dots) and superior to the occipitotemporal line (blue dots) posteriorly and the end anteriorly by the posterior ramus of the lateral fissure (yellow dots). Within the IPL, the SMG (green) and AG (orange) are identified. In the typical pattern no additional gyri behind the postcentral sulcus within the IPL can be identified. When additional gyrus is located between the postcentral sulcus and the SMG or between SMG and AG the pattern is defined as PreSMG or PreAG, retrospectively (9). In this case, the additional gyrus (pink) was identified between the AG and SMG, bordering the anterior edge of the AG. The two gyri are separated by the inferior ramus of the IPS, the sulcus of Jensen (green square line). **(B)** Here, the most superficial layer of the fibers within the SMG was constituted by short u-fibers. **(C)** Removal of the u-fiber system reveals the AF/SLF system (burgundy), its genu and posterior segment of the horizontal as well as superior segment of the vertical ramus. The sulcus of Jensen marks the point posterior to the most posterior point of the genu of the AF/SLF complex. **(D)** Posteriorly within the AG, the u-fibers go deeper than anteriorly. **(E)** After removal of these fibers, fibers deeper than the AF/SLF complex within the SMG, the fibers of the sagittal stratum (light blue) running in the anteroposterior direction were identified. **(F)** When the SS fibers were separated, the occipital horn and posterior part of the atrium of the lateral ventricle (white square circle) were identified.

sulcus in all cases. The pattern of confluence of the IPS with the postcentral sulcus was as follows: I (0), II (3), III (0), IV (10), V (1) (descriptions of different patterns of confluence of the IPS with the postcentral sulcus are described in **Figure 1**). The point where the IPS joins the postcentral sulcus was located 40.5 (ranging from 33 to 50) mm and 36.7 (ranging from 28 to 46) mm from the interhemispheric fissure (IHF) and lateral sulcus, respectively. The mean angle where the IPS joined the postcentral sulcus was 114 (ranging from 96 to 155) degrees. The length of the IPS varied from 22 to 47 (mean 36.5) mm. The long axis of the IPS was at 107.4 (varied from 180 - parallel to 110 degrees) angles to the IHF. The posterior end of the IPS was localized 27.4 (varied from 19 to 38) and 59.5 (varied from 48 to 67) mm from the IHF and preoccipital notch, respectively. The inferior branch of the IPS (sulcus of Jensen) was identified in 9/10 cases and measured from 9 to 45 (mean 26.7) mm, while the superior branch (sulcus of Brissaud) was also identified in 9 cases and measured 17.9 (ranging from 4 to 32) mm.

Measurements on the Subcortical Level

Within the SMG, the AF/SLF complex was identified; close to the sulcus of Jensen, the genu of the complex was the horizontal ramus joining the vertical ramus. This point was identified behind the postcentral sulcus at ∼22.4 (ranging from 17 to 35) mm, anterior to the most posterior point of the IPS at ∼24.2 (ranging from 12 to 35) mm at a depth of 22.6 (ranging from 21 to 24) mm from the cortical surface. Posterior to the sulcus of Jensen and in all cases posterior to the artificial line connecting the preoccipital notch with the SRP within the AG, the fibers of the SS at ∼28.6 (ranging from 27 to 30) mm were identified. The SS was ∼5 mm thick, and the lateral ventricle was identified at ∼32.4 (ranging from 29 to 35) mm. The occipitotemporal line started 33.1 (ranging from 23 to 43) mm along the parietotemporal line and had an average of 44.4 (ranging from 32 to 75) mm. From its sylvian end, the IRP was identified in an additional 14.4 (varied from 8 to 23) mm anteriorly (**Table 1**).

Superior Approach

Measurements on the Lateral Surface of the Hemisphere

The superior Rolandic point (SRP) and the parieto-occipital sulcus mark the superior and inferior borders of the superior parietal lobule on the midline (**Figure 5**). The SRP was located 134.9 (ranging from 125 to 140) mm and 104.8 (ranging from 83 to 128) mm from the frontal and occipital bases along the superior margin of the hemisphere, respectively. The long axis of the central sulcus was identified at 109.1 (ranging from 95 to 118) degrees with the IHF and had a length of 85.8 (ranging from 77 to 94) mm. The postcentral sulcus, which defined the posterior border of the primary sensory cortex, was identified 11.2 (ranging from 4 to 23) mm posterior to the SRP. The distances from the SRP and from the postcentral sulcus to the parieto-occipital sulcus were 45.8 (ranging from 36 to 57) mm and 38.7 (ranging from 24 to 47) mm, respectively. The parietotemporal line marks the posterior border of the SPL and its long axis were identified at 73.8 (ranging from 65 to 82) degrees angle to the IHF and had a length of 77.3 (ranging from 70 to 88) mm.

Measurement on the Medial Surface of the Hemisphere

The superior margin of the precuneus had a length of 37 (varying from 31 to 43) mm, while the posterior part of the paracentral lobule was 10.4 (ranging from 4 to 22) mm, and the paracentral lobule was 27.3 (ranging from 19 to 38) mm. The posterior border of the SPL is formed on the medial surface by the parieto-occipital sulcus, which is 24.2 (ranging from 14 to 32) mm and was identified at a 69.2 (ranging from 60 to 85) degree angle to the superior margin of the hemisphere. The marginal branch of the cingulate sulcus stating for the anterior border of the SPL had a length of 21.5 (ranging from 18 to 28) mm and was identified at 99 (ranging from 75 to 130) degrees to the superior margin of the hemisphere. The line connecting the cingulate-marginal sulcus connection point with the parieto-occipital-calcarine connection point (subparietal sulcus), which corresponds to the anatomical inferior border of the SPL on the mesial surface of the hemisphere, had a length of 37.1 (ranging from 32 to 40) mm. The width of the cingulate gyrus below the marginal sulcus was 16.3 (ranging from 11 to 21) mm in the line being extension of the marginal sulcus. Along the same trajectory, the width of the corpus callosum was 6.3 (ranging from 4 to 8) mm. The parieto-occipital-calcarine connection point was located 22 (ranging from 19 to 28) mm posterior to the splenium of the corpus callosum, along the calcarine sulcus through the isthmus.

Measurement on the Subcortical Level

From the lateral perspective, from the superior perspective, the main white matter tracts that are taken into consideration during the procedure are thalamocortical/corticospinal tract anteriorly; AF/SLF complex located lateral and anteriorly; SS located in line with the horizontal segment and behind the previous segment. The most mesial fibers of the AF/SLF complex were identified ∼33.2 (ranging from 27 to 40) mm lateral to the IHF and ∼25.6 (ranging from 23 to 28) mm from the cortical surface. In 60% of patients, the IPS was in line with the horizontal segment of the AF/SLF complex; in rest, its anterior point was located lateral to the genu of the AF/SLF complex. The occipital horn of the lateral ventricle was identified ∼9 (ranging from 2 to 16) mm mesial to the AF/SLF complex at ∼34 (ranging from 32 to 36) mm, measured perpendicular to the brain surface. Resection ended on the inferior anatomical border of the parietal lobe; at the level of the subparietal sulcus, the lateral ventricle should not be encountered (**Table 2**).

TABLE 1 | Measurements related to the lateral approach.

	Average	Range
Superior approach		
Lateral surface		
The inferior Rolandic point to the postcentral sulcus	18.1 mm	14–22 mm
Length of the occipitotemporal line	41.4 mm	33–39 mm
IPS-postcentral sulcus to the IHF	40.5 mm	33–50 mm
IPS-postcentral sulcus to the lateral sulcus	36.7 mm	28–46 mm
IPS-parietotemporal line to the IHF	27.4 mm	19–38 mm
IPS-parietotemporal line to the preoccipital notch	59.5 mm	48–67 mm
Length of the sulcus of Jensen	26.7 mm	9–45 mm
Length of the sulcus of Brissaud	17.9 mm	4–32 mm
Subcortical level		
Genu of the AF/SLF complex to the postcentral sulcus	22.4 mm	17–35 mm
Genu of the AF/SLF complex to the occipitotemporal line	24.2 mm	12–35 mm
Depth to the genu of the AF/SLF complex	22.6 mm	21–24 mm
Depth to the SS complex	28.6 mm	27–30 mm
Depth to the occipital horn	32.4 mm	29–35 mm

ILLUSTRATIVE CASES

Case 1

41-year-old right-handed women presented with a history of seizures without neurological deficit. MRI revealed a lesion characteristic of a low-grade glioma within the non-dominant parietal lobe, being lateral to the SS and AF/SLF complex (**Figure 6**). Patient was operated in the lateral position with the head rotated to the left. Intraoperative electrical stimulation of the cortex anterior to the tumor elicited responses from primary motor and sensory cortex within face and upper extremity. Stimulation of the white matter at the depth of resection elicited flashing within the left visual field and hemineglect syndrome when line bisection task was performed. These areas based on neuronavigation were related to optic radiation and SLF II, respectively. Resection was ended when eloquent structures were encountered. In the postoperative period patient presented mild hemineglect syndrome which improved in long term follow-up. The final neuropathology was WHO grade II astrocytoma.

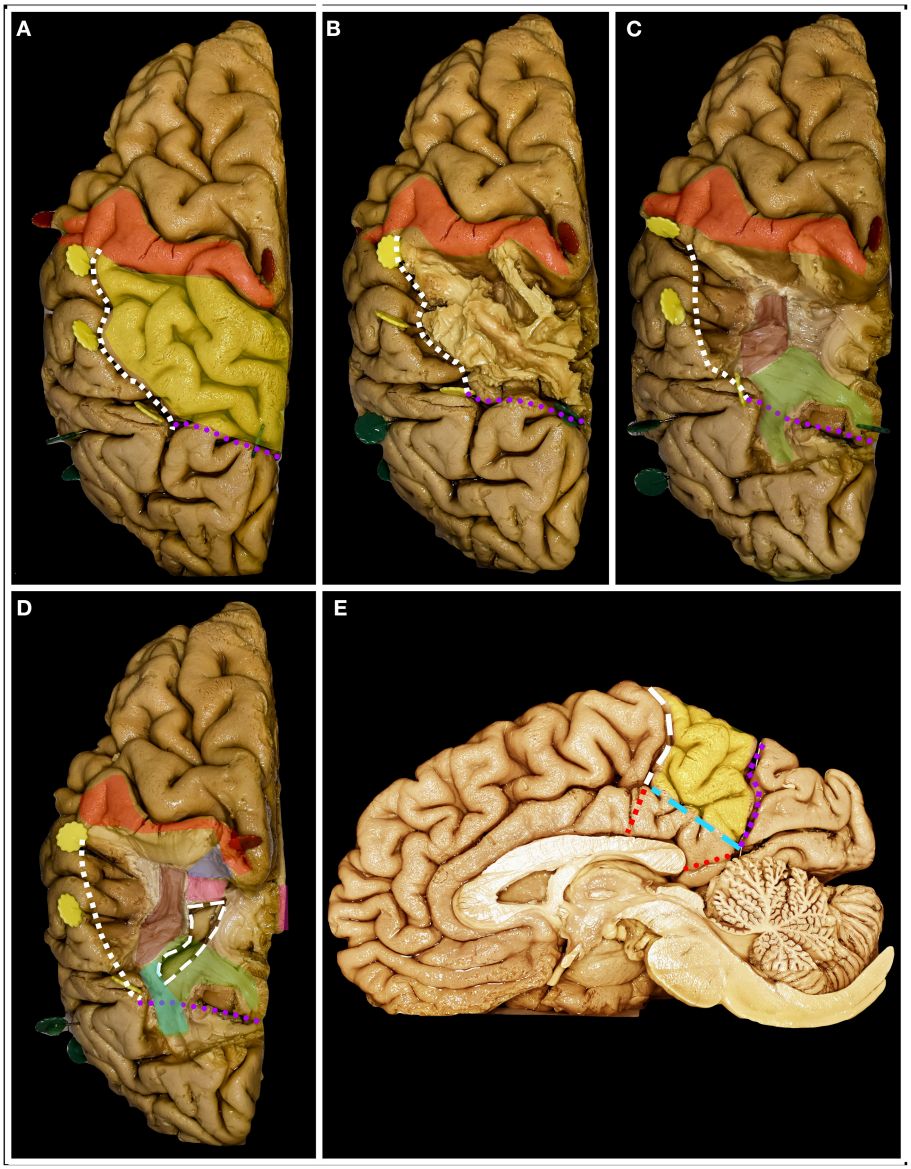

FIGURE 5 | The figure represents the surgical perspective of the surgical field within the superior parietal lobule from a superior perspective. **(A)** The SPL is located posterior to the postcentral gyrus (red), mesial to the intraparietal sulcus (white square outline), anterior to the parietotemporal line (purple dots) and lateral to the interhemispheric fissure. **(B)** The most superficial system of the fibers is constituted by the u-fibers connecting the neighboring gyri going at the bottom of the fissures, which are quite deep in this region, reaching up to the gyrus cinguli. **(C)** Removal of the u-fibers laterally reveals the fibers of the AF/SLF complex (burgundy), which in this case were located mesial to the anterior part of the IPS. Posteriorly and deeper to the AF/SLF fibers of the corona radiata (green) is identified. **(D)** Mesial the most medial fibers of the AF/SLF complex, the atrium and the occipital horn (white rectangular outline) of the lateral ventricle are identified. The lateral ventricle was identified at the level of the corpus callosum (pink). Anteriorly at the level of the postcentral gyrus, the fibers going medial and deeper than the AF/SLF complex are the thalamocortical fibers (blue). Posterior to the vertical segment of the AF/SLF complex, on the lateral wall of the atrium and occipital horn of the lateral ventricle, the SS is identified. **(E)** On the mesial surface, the precuneus (yellow) constitutes the mesial part of the SPL. The resection line can be performed along the well-defined parieto-occipital (purple square outline) sulcus posteriorly and marginal ramus of the cingulate sulcus (white rectangular outline) anteriorly. The anatomical inferior border of the resection is set by the subparietal sulcus (light blue rectangle line) or surgical sulcus on the corpus callosum along the line being extension of the marginal ramus (red square line) and of the calcarine sulcus through the isthmus (red dots).

Case 2

51-year-old right-handed women presented with a history of seizures without neurological deficit. MRI revealed a lesion characteristic of a low-grade glioma within the dominant parietal lobe, being medial to the SS and AF/SLF complex (**Figure 7**). Patient was operated in the semi-sitting position with the head in the neutral position. Intraoperative electrical stimulation of the cortex anterior to the tumor elicited responses from

primary sensory and motor cortex. Stimulation of the white matter at depth of resection elicited movement disturbances on the anterior border of resection and flashing with language disturbances on the lateral/inferior border of resection. These areas based on neuronavigation were related to corticospinal tract, SS and AF/SLF complex, respectively. Resection was ended when eloquent structures were encountered. In the postoperative period patient presented with aphasia which improved in long term follow-up. The final neuropathology was WHO grade II astrocytoma.

DISCUSSION

Cortical and subcortical regions within the parietal lobe are related to core functions such as motor (proprioceptive disturbance), semantic (reading, writing and phonological processing), visuospatial function, and visual fields (2, 10). All of the above factors, except the visual field, cannot be assessed in an unconscious patient; therefore, the functional limits of resection can be identified only based on awake intraoperative brain mapping of the dominant and non-dominant hemispheres (12–15). In terms of the surgical approach to intra-axial lesions, we can distinguish those located medially (Zones 2 and 4) and laterally (Zones 1 and 3) in relation to the IPS and the atrium of the lateral ventricle on the cortical and subcortical levels, respectively. Surgical treatment of tumors within the inferior parietal lobule is related mainly to language and visual field deficits when located within Zone 1 and Zone 3, respectively. The risk of language-related deficits with this tumor is high (8.4%) compared to other locations in proximity to language pathways (3). When the patient undergoing surgery has a tumor in Zone 2 or 4, the main concern is the risk of motor deficits related to motor or sensory impairment. For safe and optimal surgical treatment, the surgeon should be familiar not only with the anatomical aspect of the approach but also with the functional significance of the cortex and white matter tracts that are encountered, in terms of chances of neuronal reorganization at the cortical level and functional restoration (16).

Despite the trajectory of the approach, the anterior border of the resection is constituted by the primary motor cortex within the precentral gyrus and the thalamocortical tract (sensory) at the subcortical level. The SRP can be easily estimated by cranial markers and is identified ∼3.5–4.5 cm behind the coronal suture (5). Posterior to the motor cortex, the primary somatosensory cortex is identified and is marked posteriorly by the postcentral sulcus, which is identified ∼1 and 2 cm posterior to the SRP and IRP, respectively, and runs almost parallel to the long axis of the central sulcus. Intraoperative stimulation of the primary somatosensory cortex and thalamocortical tracts under awake conditions produces different types of paresthesia, dysesthesia, or proprioceptive responses (17). Resection of the primary sensory cortex while preserving the cortex responsible for proprioception and the thalamocortical tract results in immediate postoperative sensory deficits, which will resolve in most cases due to plasticity and recruitment of the secondary somatosensory cortex, posterior parietal cortex, precentral cortex, or contralateral primary somatosensory cortex (2, 18, 19). Only awake conditions allow for an informed decision regarding the end of functional resection on the anterior border at the subcortical level. From an anatomical point of view, the posterior border of the parietal lobe is marked by the parietotemporal line, which measures ∼8 cm and is located at ∼70 degrees to the IHF. The posterior border of the resection despite the operated hemisphere is marked by the tumor, as long as it is above the calcarine sulcus, where the visual cortex can be assessed. The anatomical inferior border of the parietal lobe is constituted by the occipitotemporal line, which measures ∼4 cm and is located ∼8 cm lateral to the IHF. In the dominant hemisphere, the inferior border of the resection due to highly eloquent function should be based on intraoperative brain mapping (3, 12, 20). Wernicke's language area is located mainly within the posterior segment of the STG and SMG and occasionally posteriorly within the AG. These two gyri are separated by the sulcus of Jensen, which is perpendicular to the IPS and has a mean length of 2.5 cm. In some cases, atypical patterns in terms of additional

TABLE 2 | Measurements related to the superior approach.

	Average	Range
Superior approach		
Lateral surface		
The superior Rolandic point to frontal base	134.9 mm	125–140 mm
The superior Rolandic point to occipital base	104.8 mm	83–128 mm
The superior Rolandic point to the parieto-occipital sulcus	45.8 mm	36–57 mm
The superior Rolandic point to postcentral sulcus	11.2 mm	4–23 mm
The long axis of the central sulcus to IHF	109.1 degrees	95–118 degrees
Length of the central sulcus	85.8 mm	77–94 mm
The long axis of the parietotemporal line to IHF	73.8 degrees	65–82 degrees
Length of the parietotemporal line	77.3 mm	70–80 mm
Medial surface		
Width of the paracentral lobule	27.3 mm	19–38 mm
The parieto-occipital sulcus to IHF	69.2 degrees	60–85 degrees
Length of the parieto-occipital sulcus	24.2 mm	14–32 mm
Length of the marginal branch of the cingulate sulcus	21.5 mm	18–28 mm
The marginal branch of the cingulate sulcus to the IHF	99 degrees	75–130 degrees
Length of the subparietal sulcus	37.1 mm	32–40 mm
Subcortical level		
AF/SLF complex from IHF (lateral)	33.2 mm	27–40 mm
Depth to the AF/SLF complex from cortical surface	25.6 mm	23–28 mm
Occipital horn to the mesial surface of the AF/SLF complex	9.0 mm	2–16 mm
Depth to the occipital horn from the cortex	34.0 mm	32–36 mm

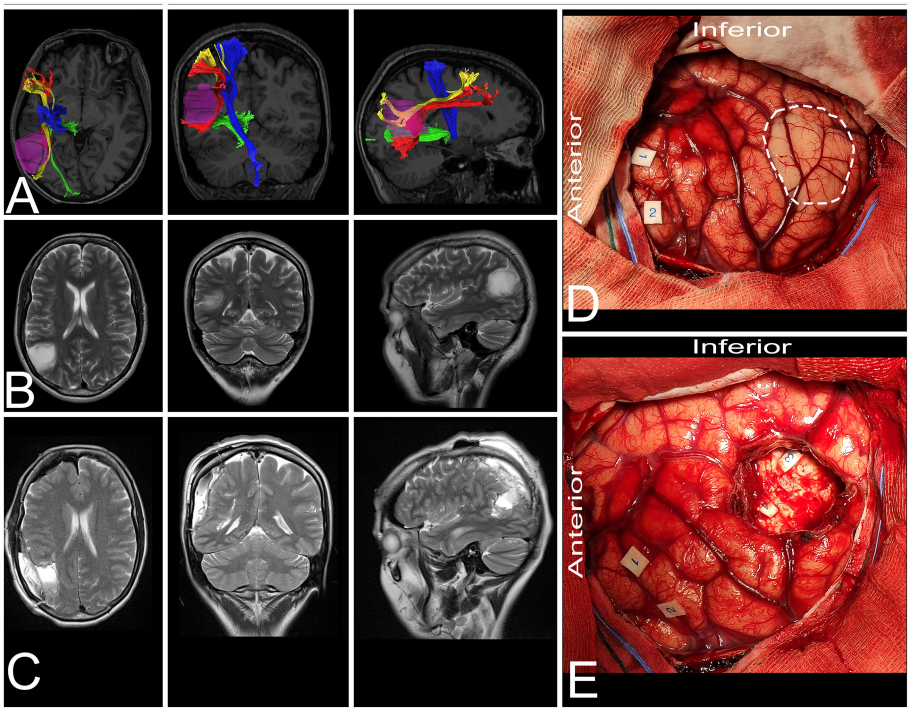

FIGURE 6 | 41-year-old right-handed women with a low-grade glioma within the non-dominant parietal lobe. **(A)** axial, coronal, and sagittal MRIs with diffusion tensor imaging tractography reconstruction of the tracts passing within the parietal lobe. The tumor (purple) is lateral to the AF (red), SLF II (yellow) and optic radiation (green), while posterior to the corticospinal tract (blue). **(B,C)** axial, coronal, and sagittal MRIs with preoperative and postoperative imaging. **(D)** Intraoperative photograph taken before tumor removal, after brain mapping. The tumor (white rectangle) was located posterior to the primary motor (tag 1 and 2) and sensory cortex. **(E)** Intraoperative photograph taken after tumor resection within functional borders, depth of resection is marked with optic radiation (tag 3) and SLF II (tag 4). Patient was operated in the lateral position with the head rotated to the left. DTI were reconstructed in DSI Studio (http://dsi-studio.labsolver.org) (11).

gyri within the IPL should be expected. Mapping of the SMG is performed mainly with the use of picture-naming, and reading tasks are used. Positive language sites are identified when anomia, alexia or phonemic paraphasias are observed (2, 14). To avoid Gerstman syndrome, which is typically related to AG, finger recognition, writing, and calculation tasks are applied in mapping the posterior region of the IPL (2, 21). The resection above the IPS is most commonly negative to mapping, but intraoperative damage of the SPL may result in apraxic dysgraphia (22). One should keep in mind that the IPS, according to our observation, runs parallel to the IHF in only 40% of cases. The anterior end of the IPS was localized ∼4 cm, while the posterior 2.5 cm lateral to the IHF and its long axis formed with the IHF at an angle of ∼115 degrees. This may lead to the wrong assumption that when IPS is identified, the lesion mesial to the IPS is safely resectable. At the subcortical level, the IPS is linked to the AF/SLF complex as well as to the SS complex. From the lateral trajectory within the SMG, the depth border of the resection is marked by the AF/SLF complex, and its horizontal segment transitions into a vertical segment. From a lateral perspective, the complex is identified at a depth of ∼25 mm from the cortical surface. On the dominant side, the main function of the SLF/AF complex is related to language, while on the non-dominant side, it is mainly due to visuospatial function. Intraoperative stimulation of the dominant AF/SLF complex results in expressive aphasia, phonemic paraphasias and repetition disorders (AF) or speech articulation dysfunction (SLF III), which are assessed during the picture naming task. On the non-dominant hemisphere, stimulation of the AF/SLF complex may result in contralateral hemineglect syndrome, which is related to the stimulation of the second compartment of the SLF (SLF II) (23), which is assessed with an intraoperative line bisection task (2, 24). The sagittal stratum is the most superficial fiber system, under the u-fibers posterior to the sulcus of Jensen or posterior half of the IPL. The SS complex is identified at ∼30 mm. Deep to the SS, the lateral ventricle is identified, where distinction of the tracts forming it can be based only on intraoperative mapping. Transgression of the SS most commonly does not cause permanent neurological deficits except visual field deficits. The deep limit of the resection is represented by the visual pathway. Stimulation of the visual pathway may result in flashing, shadowing, or other unexpected visual experiences (25). For optic radiation, a modified picture naming task placed in quadrants is preferable. Laterally to the optic radiation the IFOF, responsible for semantic language processing in the dominant hemisphere with two subcomponents can be identified (26–28). Intraoperative stimulation of the dorsal and superficial subcomponent of the fibers that course in the superior portion of the SS and terminate within the superior

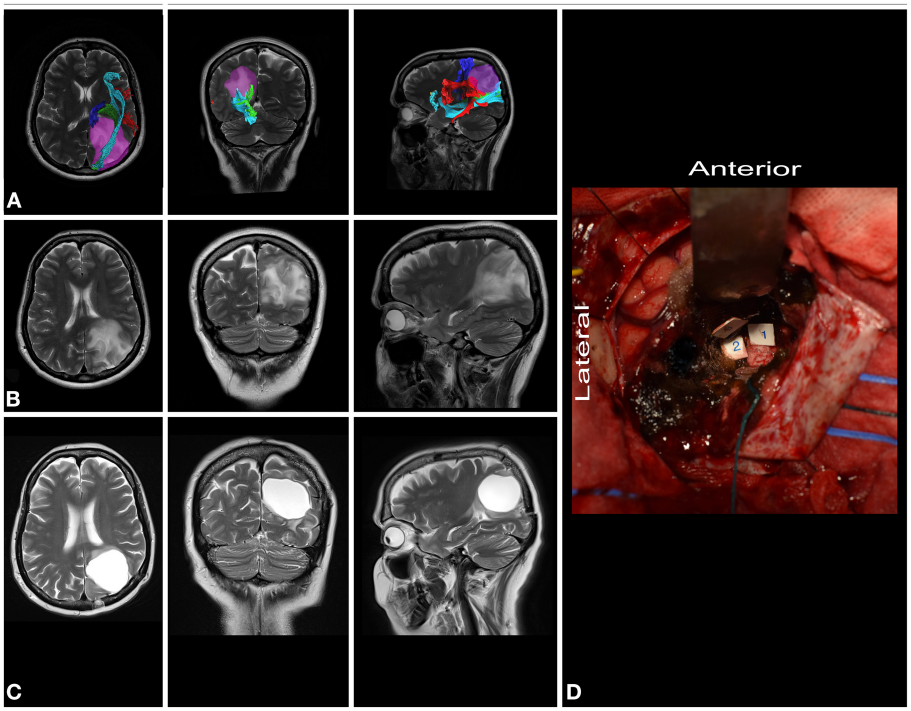

FIGURE 7 | 51-year-old right-handed women with a low-grade glioma within dominant parietal lobe. **(A)** axial, coronal, and sagittal MRIs with diffusion tensor imaging tractography reconstruction of the tracts passing within the parietal lobe. The tumor (purple) is medial to the AF/SLF complex (red), optic radiation (green) and IFOF (light blue), while posterior to the corticospinal tract (blue). **(B,C)** axial, coronal, and sagittal MRIs with preoperative and postoperative imaging. **(D)** Intraoperative photograph taken after tumor resection within functional borders, depth of resection is marked with corticospinal tract (tag 1), AF/SLF complex (tag 3) and the SS (tag 2). Patient was operated on in the semi-sitting position. DTI were reconstructed in DSI Studio (http://dsi-studio.labsolver.org) (11).

parietal lobule may result in disturbances during reading and writing tasks (10, 26, 29). The second subcomponent of the IFOF which connects the frontal lobe with the inferior occipital cortex and posterior temporal-basal regions is located ventrally and deeper to the previous one and has no connections with the parietal lobe. Therefore, if the language pathway is stimulated, naming disturbances will occur without any subjective visual complaint (13, 30). The region superior and medial to the roof of the atrium is free of optic radiation and tracts of the sagittal stratum. The roof of the atrium can be reached through the dissection of the IPS perpendicular to the brain surface, and it marks the lateral border of the superior parietal lobule. The depth of the anterior half of the IPS is located ∼1.25 cm above the atrium, while its posterior half is located above the occipital horn (31). The roof of the ventricular system corresponds to the level of the superior margin of the corpus callosum, and in this case, the trajectory of the dissection should be changed for the midline at the level of the roof of the ventricle. This allows preservation of the optic radiation, which courses on the lateral wall of the ventricle and avoids the eloquent cortical motor and speech areas that are located anteriorly and laterally to the planned corticotomy. Due to anatomical variability of the shape and localization of the IPS, the localization of white matter tracts must in each case be correlated with the sulcal and cortical anatomy. Based on our study and others, the AF/SLF complex might be identified mesial to the IPS, especially on the anterior segment of the IPS, which is why it is safer to start dissection in the middle of the length of the IPS (31). Resection of the mesial part of the parietal lobe also includes resection of the first segment of the SLF (SLF I), but the clinical impact of its damage is not well-described (32).

LIMITATIONS OF THE STUDY

Readers should carefully consider our results, as we were not able to present all anatomical variants due to the limited number of specimens. The anatomical relationship between the structures in patients with gliomas is disturbed by the tumor mass, edema or due to brain shifts related to cerebrospinal fluid loss and tumor debulking. Additionally, the physical parameters of cadaveric brain specimen not exactly present an intraoperative brain structure. Despite the mentioned limitations, knowledge of physiological anatomy is of greatest importance even when the anatomy is disturbed.

DATA AVAILABILITY STATEMENT

The raw data supporting the conclusions of this article will be made available by the authors, without undue reservation.

ETHICS STATEMENT

The studies involving human participants were reviewed and approved by Bioethics Committee of Medical University of Warsaw, approval number AKBE/126/2019. Written informed consent for participation was not required for this study in accordance with the national legislation and the institutional requirements.

AUTHOR CONTRIBUTIONS

TD, AB, and AM: conception/design of the work and final approval of the revision to be published. TD: data collection. TD and AM: data analysis and interpretation. TD and AB: drafting the article. AM: critical revision of the article. All authors contributed to the article and approved the submitted version.

REFERENCES

1. Larjavaara S, Mantyla R, Salminen T, Haapasalo H, Raitanen J, Jaaskelainen J, et al. Incidence of gliomas by anatomic location. *Neuro Oncol.* (2007) 9:319–25. doi: 10.1215/15228517-2007-016
2. Fernandez Coello A, Moritz-Gasser S, Martino J, Martinoni M, Matsuda R, Duffau H. Selection of intraoperative tasks for awake mapping based on relationships between tumor location and functional networks. *J Neurosurg.* (2013) 119:1380–94. doi: 10.3171/2013.6.JNS122470
3. Sanai N, Martino J, Berger MS. Morbidity profile following aggressive resection of parietal lobe gliomas. *J Neurosurg.* (2012) 116:1182–6. doi: 10.3171/2012.2.JNS111228
4. Cunningham DJ. Intraparietal sulcus of the brain. *J Anat Physiol.* (1890) 24:135–55.
5. Rhoton AL Jr. The cerebrum. Anatomy. *Neurosurgery.* (2007) 61 (1 Suppl.):37–118. doi: 10.1227/01.NEU.0000255490.88321.CE
6. Kendir S, Acar HI, Comert A, Ozdemir M, Kahilogullari G, Elhan A, et al. Window anatomy for neurosurgical approaches. Laboratory investigation. *J Neurosurg.* (2009) 111:365–70. doi: 10.3171/2008.10.JNS08159
7. Ribas GC, Yasuda A, Ribas EC, Nishikuni K, Rodrigues AJ Jr. Surgical anatomy of microneurosurgical sulcal key points. *Neurosurgery.* (2006) 59 (4 Suppl. 2):ONS177–210. doi: 10.1227/01.NEU.0000240682.28616.b2
8. Dziedzic TA, Balasa A, Jezewski MP, Michalowski L, Marchel A. White matter dissection with the Klingler technique: a literature review. *Brain Struct Funct.* (2021) 226:13–47. doi: 10.1007/s00429-020-02157-9
9. Kiriyama I, Miki H, Kikuchi K, Ohue S, Matsuda S, Mochizuki T. Topographic analysis of the inferior parietal lobule in high-resolution 3D MR imaging. *AJNR Am J Neuroradiol.* (2009) 30:520–4. doi: 10.3174/ajnr.A1417
10. Burks JD, Boettcher LB, Conner AK, Glenn CA, Bonney PA, Baker CM, et al. White matter connections of the inferior parietal lobule: a study of surgical anatomy. *Brain Behav.* (2017) 7:e00640. doi: 10.1002/brb3.640
11. Yeh FC, Verstynen TD, Wang Y, Fernandez-Miranda JC, Tseng WY. Deterministic diffusion fiber tracking improved by quantitative anisotropy. *PLoS ONE.* (2013) 8:e80713. doi: 10.1371/journal.pone.0080713
12. Maldonado IL, Moritz-Gasser S, de Champfleur NM, Bertram L, Moulinie G, Duffau H. Surgery for gliomas involving the left inferior parietal lobule: new insights into the functional anatomy provided by stimulation mapping in awake patients. *J Neurosurg.* (2011) 115:770–9. doi: 10.3171/2011.5.JNS112
13. Chan-Seng E, Moritz-Gasser S, Duffau H. Awake mapping for low-grade gliomas involving the left sagittal stratum: anatomofunctional and surgical considerations. *J Neurosurg.* (2014) 120:1069–77. doi: 10.3171/2014.1.JNS132015
14. Southwell DG, Riva M, Jordan K, Caverzasi E, Li J, Perry DW, et al. Language outcomes after resection of dominant inferior parietal lobule gliomas. *J Neurosurg.* (2017) 127:781–9. doi: 10.3171/2016.8.JNS16443
15. Rolland A, Herbet G, Duffau H. Awake surgery for gliomas within the right inferior parietal lobule: new insights into the functional connectivity gained from stimulation mapping and surgical implications. *World Neurosurg.* (2018) 112:e393–406. doi: 10.1016/j.wneu.2018.01.053
16. Duffau H, Capelle L, Denvil D, Sichez N, Gatignol P, Lopes M, et al. Functional recovery after surgical resection of low grade gliomas in eloquent brain: hypothesis of brain compensation. *J Neurol Neurosurg Psychiatry.* (2003) 74:901–7. doi: 10.1136/jnnp.74.7.901
17. Berger MS, Hadjipanayis CG. Surgery of intrinsic cerebral tumors. *Neurosurgery.* (2007) 61 (1 Suppl.):279–304. doi: 10.1227/01.NEU.0000255489.88321.18
18. Nii Y, Uematsu S, Lesser RP, Gordon B. Does the central sulcus divide motor and sensory functions? Cortical mapping of human hand areas as revealed by electrical stimulation through subdural grid electrodes. *Neurology.* (1996) 46:360–7. doi: 10.1212/WNL.46.2.360
19. Graveline CJ, Mikulis DJ, Crawley AP, Hwang PA. Regionalized sensorimotor plasticity after hemispherectomy fMRI evaluation. *Pediatr Neurol.* (1998) 19:337–42. doi: 10.1016/S0887-8994(98)00082-4
20. Dziedzic TA, Bala A, Podgorska A, Piwowarska J, Marchel A. Awake intraoperative mapping to identify cortical regions related to music performance: technical note. *J Clin Neurosci.* (2021) 83:64–7. doi: 10.1016/j.jocn.2020.11.027
21. Roux FE, Boetto S, Sacko O, Chollet F, Tremoulet M. Writing, calculating, and finger recognition in the region of the angular gyrus: a cortical stimulation study of Gerstmann syndrome. *J Neurosurg.* (2003) 99:716–27. doi: 10.3171/jns.2003.99.4.0716
22. Shinoura N, Midorikawa A, Onodera T, Yamada R, Tabei Y, Onda Y, et al. The left superior longitudinal fasciculus within the primary sensory area of inferior parietal lobe plays a role in dysgraphia of kana omission within sentences. *Behav Neurol.* (2012) 25:363–8. doi: 10.1155/2012/561427
23. Voets NL, Bartsch A, Plaha P. Brain white matter fibre tracts: a review of functional neuro-oncological relevance. *J Neurol Neurosurg Psychiatry.* (2017) 88:1017–25. doi: 10.1136/jnnp-2017-316170
24. Greene JD. Apraxia, agnosias, and higher visual function abnormalities. *J Neurol Neurosurg Psychiatry.* (2005) 76 (Suppl. 5):v25–34. doi: 10.1136/jnnp.2005.081885
25. Duffau H, Velut S, Mitchell MC, Gatignol P, Capelle L. Intra-operative mapping of the subcortical visual pathways using direct electrical stimulations. *Acta Neurochir.* (2004) 146:265–9. doi: 10.1007/s00701-003-0199-7
26. Martino J, Brogna C, Robles SG, Vergani F, Duffau H. Anatomic dissection of the inferior fronto-occipital fasciculus revisited in the lights of brain stimulation data. *Cortex.* (2010) 46:691–9. doi: 10.1016/j.cortex.2009.07.015
27. Wu Y, Sun D, Wang Y, Wang Y. Subcomponents and connectivity of the inferior fronto-occipital fasciculus revealed by diffusion spectrum imaging fiber tracking. *Front Neuroanat.* (2016) 10:88. doi: 10.3389/fnana.2016.00088
28. Duffau H, Moritz-Gasser S, Mandonnet E. A re-examination of neural basis of language processing: proposal of a dynamic hodotopical model from data provided by brain stimulation mapping during picture naming. *Brain Lang.* (2014) 131:1–10. doi: 10.1016/j.bandl.2013.05.011
29. Martino J, da Silva-Freitas R, Caballero H, Marco de Lucas E, Garcia-Porrero JA, Vazquez-Barquero A. Fiber dissection and diffusion tensor imaging tractography study of the temporoparietal fiber intersection area. *Neurosurgery.* (2013) 72 (1 Suppl. Operative):87–97. doi: 10.1227/NEU.0b013e318274294b
30. Di Carlo DT, Benedetto N, Duffau H, Cagnazzo F, Weiss A, Castagna M, et al. Microsurgical anatomy of the sagittal stratum. *Acta Neurochir.* (2019) 161:2319–27. doi: 10.1007/s00701-019-04019-8

31. Koutsarnakis C, Liakos F, Kalyvas AV, Liouta E, Emelifeonwu J, Kalamatianos T, et al. Approaching the atrium through the intraparietal sulcus: mapping the sulcal morphology and correlating the surgical corridor to underlying fiber tracts. *Oper Neurosurg.* (2017) 13:503–16. doi: 10.1093/ons/opw037
32. Wang X, Pathak S, Stefaneanu L, Yeh FC, Li S, Fernandez-Miranda JC. Subcomponents and connectivity of the superior longitudinal fasciculus in the human brain. *Brain Struct Funct.* (2016) 221:2075–92. doi: 10.1007/s00429-015-1028-5

Conflict of Interest: The authors declare that the research was conducted in the absence of any commercial or financial relationships that could be construed as a potential conflict of interest.

Publisher's Note: All claims expressed in this article are solely those of the authors and do not necessarily represent those of their affiliated organizations, or those of the publisher, the editors and the reviewers. Any product that may be evaluated in this article, or claim that may be made by its manufacturer, is not guaranteed or endorsed by the publisher.

frontiers in Neurology

MINI REVIEW
published: 27 August 2021
doi: 10.3389/fneur.2021.712532

Where We Mentalize: Main Cortical Areas Involved in Mentalization

Matteo Monticelli, Pietro Zeppa, Marco Mammi, Federica Penner, Antonio Melcarne, Francesco Zenga and Diego Garbossa*

Neurosurgery Unit, Department of Neuroscience "Rita Levi Montalcini," Turin University, Turin, Italy

When discussing "mentalization," we refer to a very special ability that only humans and few species of great apes possess: the ability to think about themselves and to represent in their mind their own mental state, attitudes, and beliefs and those of others. In this review, a summary of the main cortical areas involved in mentalization is presented. A thorough literature search using PubMed MEDLINE database was performed. The search terms "cognition," "metacognition," "mentalization," "direct electrical stimulation," "theory of mind," and their synonyms were combined with "prefrontal cortex," "temporo-parietal junction," "parietal cortex," "inferior frontal gyrus," "cingulate gyrus," and the names of other cortical areas to extract relevant published papers. Non-English publications were excluded. Data were extracted and analyzed in a qualitative manner. It is the authors' belief that knowledge of the neural substrate of metacognition is essential not only for the "neuroscientist" but also for the "practical neuroscientist" (i.e., the neurosurgeon), in order to better understand the pathophysiology of mentalizing dysfunctions in brain pathologies, especially those in which integrity of cortical areas or white matter connectivity is compromised. Furthermore, in the context of neuro-oncological surgery, understanding the anatomical structures involved in the theory of mind can help the neurosurgeon obtain a wider and safer resection. Though beyond of the scope of this paper, an important but unresolved issue concerns the long-range white matter connections that unify these cortical areas and that may be themselves involved in neural information processing.

Keywords: mentalization, human brain, cortical areas, functional anatomy, practical neuroscience

OPEN ACCESS

Edited by:
Emanuele La Corte, University of Bologna, Italy

Reviewed by:
Andrey Bykanov, N. N. Burdenko National Scientific and Practical Center for Neurosurgery, Russia
Giacomo Bertolini, University of Milan, Italy

****Correspondence:***
Federica Penner
federica.penner@gmail.com

Specialty section:
This article was submitted to Applied Neuroimaging, a section of the journal Frontiers in Neurology

Received: *20 May 2021*
Accepted: *12 July 2021*
Published: *27 August 2021*

Citation:
Monticelli M, Zeppa P, Mammi M, Penner F, Melcarne A, Zenga F and Garbossa D (2021) Where We Mentalize: Main Cortical Areas Involved in Mentalization. Front. Neurol. 12:712532. doi: 10.3389/fneur.2021.712532

INTRODUCTION

When discussing "mentalization," we refer to a very special ability that only humans and, to the present knowledge, few species of great apes have. It is the ability of thinking about themselves and to represent in their mind their own mental state, attitudes, and beliefs and also those of others (1). Some authors have called this peculiar skill "theory of mind," defined as an awareness of the likely content of other people's minds (2).

It is now well-known that mentalizing is not a unitary process but that it assumes a wide variety of known and unknown, and specific and unspecific subprocesses such as emotions, inferential reasoning, understanding of causality, and the distinction between self and other.

A large number of neuroimaging and lesion studies have attempted to clarify the neural substrate underlying mentalization. Moreover, observations made by numerous authors during intraoperative mapping have been added in the last decades. Awake surgery, with the possibility

of direct electrical stimulation (DES) of the brain, provided neurosurgeons a crucial opportunity to better comprehend and study these networks and areas *in vivo*. Intraoperative DES temporarily alters the function of the stimulated area and thus provides real-time anatomo-functional correlations with high spatial resolution. It has been demonstrated that data acquired through this technique are highly specific and mostly match results gained with other neuroscientific approaches (3). To date, DES is the only technique allowing direct gain of causal information on the functional role of cortical areas as well as white matter tracts in cognition and behavior (4).

Thanks to the observation made with the aforementioned methods, it has been suggested that mentalization is carried out by an extensive network of spatially distributed cortical areas, mainly including the prefrontal cortex (PFC), the inferior frontal gyrus (IFG), the temporo-parietal junction (TPJ), the posterior parietal cortex (PPC), the temporal pole, and the cingulate cortex (4, 5) (**Figure 1**).

In this review, a summary of the main cortical areas involved in the mentalization process is presented. It is the authors' belief that knowledge of the neural substrate of metacognition is essential not only for "pure neuroscientists" but also for "practical neuroscientists" (i.e., neurosurgeons), in order to better understand the pathophysiology of mentalizing dysfunctions in brain pathologies, especially those in which integrity of cortical areas is compromised. Furthermore, in the context of neuro-oncological surgery, understanding the anatomical areas involved in mentalization can help neurosurgeons to obtain a wider and safer resection, avoiding surgical injury to those structures.

Though beyond of the scope of this paper, an important but unresolved issue concerns the long-range white matter connections unifying these cortical areas, that may be themselves involved not only in carrying information but also in processing neural information (6, 7).

MATERIALS AND METHODS

A thorough literature search using PubMed MEDLINE database was performed. The search terms "cognition," "metacognition," "mentalization," "direct electrical stimulation," "theory of mind," and their synonyms were combined with "prefrontal cortex," "temporo-parietal junction," "parietal cortex," "inferior frontal gyrus," "cingulate cortex," and the names of other cortical areas to extract relevant published papers. Initial screening was performed by reading the abstract; only the papers that qualified from this step were analyzed in their entirety. References of extracted papers were screened for other relevant studies to include. All study designs were included in this non-systematic review. Non-English publications were excluded. Data were extracted and analyzed in a qualitative manner.

PREFRONTAL CORTEX

It is well-known, from years of literature about this topic, that the PFC is one of the most involved cortical areas in mentalization. Recent research in cognitive neuroscience has clearly demonstrated how it is implicated in higher cognitive mechanisms (8, 9). These findings are consistent with the hypothesis that the PFC is a key structure, with a crucial role in generating the relevant kind of higher-order cognitive states that underlie phenomenal awareness.

PFC is a generic concept that encloses subregions that are anatomically and functionally different. In 2005 in his *Principles of Brain Evolution*, Striedter proposed that the PFC could be divided into two different regions from a functional

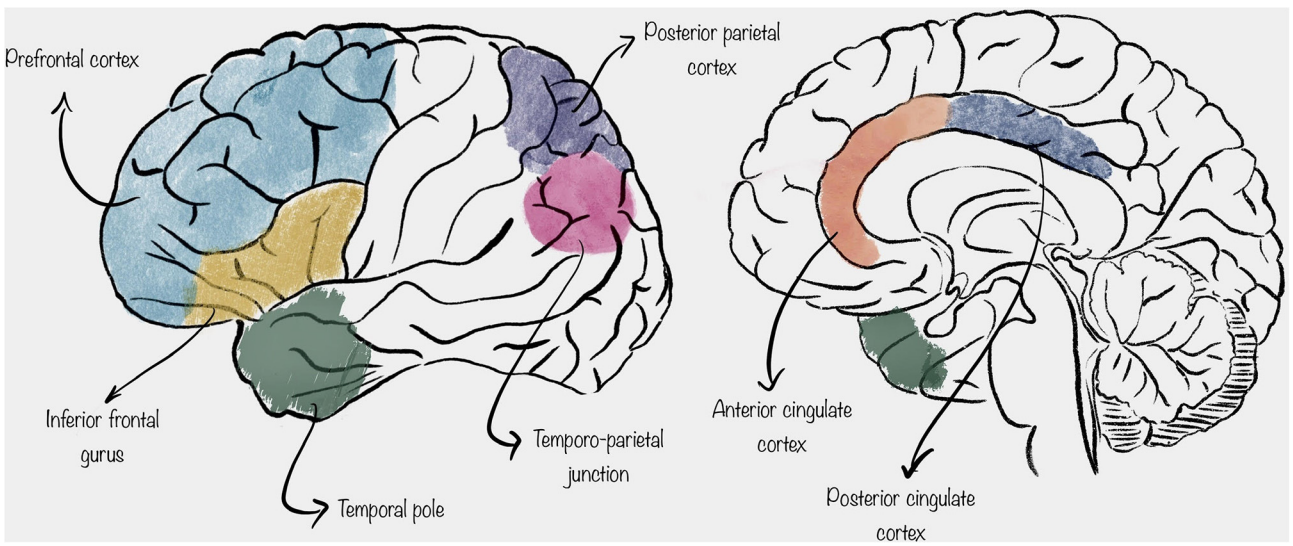

FIGURE 1 | Schematic representation of the location of the cortical areas described in this review.

and anatomic point of view and according to the evolutional development (9). The first region is the ventromedial PFC, which is composed of the ventral PFC and the medial PFC; these cortices are present in all mammals. The second is the lateral PFC, which is composed of the dorsolateral PFC and the ventrolateral PFC, present only in primates. Also at a microscopic level, the PFC has several different subregions with different cytoarchitectonic properties (granular, dysgranular, or agranular); different patterns of connectivity between each other and with sensory, memory, and conceptual processing regions; and different phylogenetic histories (10, 11).

Regarding neurophysiological activity, PFC neurons do not directly discharge an electric impulse responding to constant stimuli; instead, neuronal coding could be complex and involve local and distributed ensembles within and between areas of the PFC (12).

Lau and Rosenthal in their 2011 paper proposed an interesting theory about the higher-order representations in the PFC (13). Their work was primarily about visual perception; however, expanding the discussion to the ventral lateral PFC, they generalized their model to other external senses (14). In this model, different roles for specific areas of the PFC were identified. Specifically, the dorsolateral and the polar regions of the PFC were identified as key areas. The authors suggested that higher-order representations in the prefrontal network are not themselves consciously experienced but facilitate the experience of first-order states. The latter are defined as those states depending on sensory input that allow us to respond meaningfully to the perception of an external object. In their model, conscious experience of the higher-order representation requires an additional level of higher-order representation, whose location was not identified by Lau and Rosenthal.

Other authors suggested that the polar prefrontal region might be responsible for additional higher-order representations (15). For example, medial and insular prefrontal areas receive inputs from conceptual, memory, and subcortical circuits, as well as from sensory and perceptual networks, and, in turn, connect with lateral–polar prefrontal areas. In other words, these prefrontal areas may construct lower-order representations used by the lateral–polar prefrontal areas in the assembly of higher-order representations that are phenomenally experienced. Another possibility is that the higher-order network does not involve a fixed set of prefrontal areas but instead a coalition of areas and connections that are flexibly recruited on a situational basis to meet the needs of the moment.

INFERIOR FRONTAL GYRUS

The IFG is the lowest part of the lateral frontal lobe. From a topographic point of view, it can be divided into three distinct region called the pars opercularis, pars triangularis, and pars orbitalis (16). These three portions are macroscopically divided by two sulci arising from the Sylvian fissure: the ascending ramus separates the pars opercularis and pars triangularis, while the horizontal ramus lies between the pars triangularis and pars orbitalis.

Many functional magnetic resonance imaging (fMRI) studies, as well as DES studies performed during awake craniotomies, indicate that the IFG might be a paramount mentalization site (17, 18). In particular, the lateral part of the pars opercularis has been identified as a key structure in mentalizing accuracy, and some authors proposed that the impairment in mentalizing elicited by DES during awake surgery could be related to the transient inactivation of a mirror system. Mirror systems are, to the present knowledge, the main neuronal substrate underlying the human ability to interact with others and to understand the actions of others without logical inferences (18).

Indeed, the presence of neurons with mirror properties in the pars opercularis is well-established. Most fMRI studies that deal with tasks targeting the mirror system have pointed out this brain region as a central cortical node (19, 20). It is also known that damage to the pars opercularis impairs mirror-related functions, such as emotional empathy and face-based perceptual mentalizing (21). Moreover, abnormal neural activity within the mirror network (and especially within the pars opercularis) is one of the neural bases that characterize some psychopathological conditions (such as autistic spectrum disorders), with huge impairment in social perception and cognition, including mentalizing (22).

As suggested by many papers, while a mirror dysfunction-based mechanism arguably depends on the function of the pars opercularis, the same interpretation becomes less obvious for the adjacent pars triangularis, which is not generally considered to be a mirror area, although several fMRI studies indicate the opposite (19, 20, 23). The reason why the pars triangularis is not considered a mirror area is that its neurons, at least in its dorsal portion, discharge during action and emotional face perception (19), but they do not seem to be activated during execution, a necessary condition for classification as mirror neurons by their original definition provided by Rizzolatti and colleagues (24). To the authors' best knowledge, only one study has currently provided evidence to suggest that imitation and observation of faces expressing emotional states activate the pars triangularis, as well as the classical anterior mirror areas (e.g., the pars opercularis and the ventral premotor cortex) (25).

TEMPORO-PARIETAL JUNCTION

A large body of evidence, mainly from functional neuroimaging studies, highlights that the entire parietal cortex is not equally involved in mentalization processes, which depends on the coordinated interaction between the medial PFC and the posterior temporal gyrus at the junction with the parietal cortex. Because of its anatomical location, this region was termed the TPJ.

Many papers published in the literature, both fMRI studies and "lesion" studies performed during neurosurgical operations using DES have shown that the inferior part of the parietal cortex, more frequently on the right side, at the junction with the posterior temporal cortex, plays a critical role in matching signals arising from self-produced actions with signals from the environment (26, 27).

Intraoperative studies using DES during awake craniotomies once again provided similar results to neuroimaging studies, detecting in the TPJ a key mentalizing structure (28). Such function has usually been located with the "reading the mind in the eyes test" (RME) during awake surgery.

POSTERIOR PARIETAL CORTEX

The PPC is a set of interconnected areas located just rostrally to the TPJ, and it is one of the major associative regions of the mammalian brain, receiving multisensory inputs (visual, auditory, somatosensory, and vestibular) (29). Integration of these multiple perception signals allows a higher-level representation of self and of peripersonal space. Moreover, multisensory input association is the basis of movement-related decision making, which requires rapid integration of sensory stimuli with presumed consequences of actions, based on memory of previous similar situations (30).

Many authors suggest that in non-human primates, the PPC can be divided into distinct subregions. The first is the lateral intraparietal area, which contains high concentrations of neurons responsive to saccades and is involved in perceptual decision making. Others subregions are the parietal reach region, involved in reaching actions, and the anterior intraparietal area, linked to grasping movements (31, 32). Each PPC subregion significantly modulates the encoding and processing of the other subregions (33).

Since making right decisions requires choosing relevant information from competing distractors, it is likely that the PPC benefits from the experience of past decisions. In this regard, there are studies that highlight how lateral intraparietal neurons code the consequences on sensory perceptions produced by a saccade (34, 35). In non-human primates, similar representations for hand-reaching actions were found (36). In humans, a transcranial magnetic stimulation (TMS) study demonstrated that functional inactivation of the right and left PPCs resulted in biased saccades (35).

Taken together, these studies suggest that a fundamental role of the PPC is to filter sensory inputs, focusing attention on behaviorally relevant stimuli in a top-down fashion. The contextual relevance of a given stimulus is determined on the basis of past experience. PPC neural networks therefore constitute a memory substrate for perceptual decision making (37). As in many others cortical networks, PPC neurons show selective tuning, such as a selective response to the direction of saccades in the lateral intraparietal area. It can therefore be assumed that the repeated activation of certain successful response networks may facilitate their subsequent activation and thus constitute the substrate of the experiential component of decision making.

Most research regarding PPC decision making has been related to perceptual decisions. However, it is presumable that this cortical region is also involved in the integration of stimuli and evaluations of non-motor origin, such as emotions and the social context (38). The role of the PPC in the perceptual decision-making processes implies its involvement in the mentalization process, although its role seems to be less relevant than that of other regions considered in this review (39).

TEMPORAL POLE

As for the structures described above, available evidence suggests that damage occurring at the level of temporal poles can impair the ability to mentalize, as described by Funnell (40). Funnell's findings are in agreement with those from Damasio's group that suggested that the temporal poles are convergence zones, where simpler features from different modalities are put together to define, by their conjunction, unique individuals and situation knowledge (41). It seems to be exactly this convergence of information that gives us the ability to understand the function of an object that we are looking at and the chance to infer not only its potential at the moment but also how that object could be modified by the context in which it appears (42). It is therefore clear that these processes generated at the temporal poles have their relevance in the mentalizing mechanism, especially in order to provide the so-called moment-to-moment knowledge about a specific object in a specific condition (43).

Also in this case, DES studies exist with results comparable with the ones obtained by neuroimaging (44).

CINGULATE CORTEX

Anterior Cingulate Cortex

The anterior cingulate cortex (ACC) is located near the medial aspect of the frontal lobe and can be differentiated from the posterior cingulate cortex (PCC) on the basis of cytoarchitecture patterns of projections, as well as function. The anterior portion of cingulate cortex appears to be tasked with executive functions, whereas the posterior part of the cingulum by evaluative functions (43). Several studies based on animal models have shown that ACC lesions resulted in decreased levels of social interaction and decreased preference for social stimuli (45–48). Human fMRI and DES studies have confirmed that ACC activity increased when patients were asked to evaluate others' decisions in a social context and in mentalizing processes in general (49–52).

In addition, the ACC is known for its role, not only in social information coding but also in the processing of information that guides decisions in daily routine (53, 54). Studies based on single-unit recording patterns carried out in non-human primates demonstrated that neuron populations in the ACC were enrolled by a wide range of stimuli, mostly reward related, that led to optimize the decision-making process (55–57).

Matsumoto et al. described that, in addition to all of that above-reported functions, some ACC cell populations showed responses according to errors in the prediction of positive or negative outcomes of some proposed scenarios (58). This was proven to be useful to subjects during the execution of trial-and-error tasks, in order to reach an optimal decision.

Another proposed function that involves the ACC concerns the understanding of others' decision making through simulation. It has been proposed that the neural circuitry used for one's own decision-making process is also used for

the understanding of the decisions of others (59), in a process called embodied simulation, which has been confirmed for the understanding the actions of others (60–63). If understanding others' decisions occurs through simulation, it is possible that the same areas of the ACC may be used to process errors in one's own or another's prediction upon receiving informative feedback.

Posterior Cingulate Cortex

The PCC is located near the medial aspect of the inferior parietal lobe (64). According to Vogt's model, the PCC is composed of Brodmann areas 23 and 31; it is delimited superiorly by the marginal ramus of the cingulate sulcus, inferiorly by the corpus callosum (CC), posteriorly by the parieto-occipital sulcus, and anteriorly by Brodmann area 24, the midcingulate region (65). From a cytoarchitectonic point of view, the PCC contains paralimbic cortex, with transitional features between the typical six layered isocortex and the primitive allocortex of true limbic structures (66).

Much of the information that we have today about structural connectivity and functions of the PCC is assumed from non-human primate studies. However, during the last decades, the continuous improvement of MRI/fMRI techniques has led to a better *in vivo* comprehension of the PCC in humans (67, 68). Diffusor tensor imaging (DTI) tractography, for instance, has confirmed the presence of connections between the ventral part of PCC and the retrosplenial cortex and the medial temporal lobes, as well as connections from the dorsal part of PCC to the ventromedial PFC along the cingulum (69). Some speculations have been made regarding the functions of these connections, but a thorough comprehension of these networks in humans is still elusive. However, it seems that these connections play a key role in information processing and integration (68).

DISCUSSION

Since the beginning of history, human beings have been obsessed with questions about their nature, about their relationship with the world, and of course about consciousness. Consciousness is, as defined by the Oxford Living Dictionary, "the state of being aware of and responsive to one's surroundings," and it is a state that unites in this awareness both humans and many animal species, who are definitely well-aware and responsive to their surrounding environment. However, humans (and very few great apes, to present knowledge) have another very special feature that diversifies them from the majority of other animals: the ability to mentalize, defined as the skill of thinking about themselves and to represent in their mind, not only their own mental state but also the mental state of others. Nowadays, it is well-understood that mentalizing is not a unitary task, but it assumes a wide variety of diverse subprocesses.

It is not trivial to highlight that, when discussing "brain functions," we must not restrict them only to motor and language functions, which are undoubtedly crucial to maintain a good quality of life but are not sufficient. The human being is also made of self-awareness, beliefs, and representation of one's own and others' mental state: in one word, mentalization.

In this brief review, we reported the main cortical areas involved in this fascinating but still widely mysterious process, in order to provide a quite simple but precise idea of their spatial representation for neurosurgical usage.

Knowing that the prefrontal areas, IFG, TPJ, or temporal pole (whatever the side and whatever the so-called "hemispheric dominance") are involved in higher-level processes must lead brain surgeons to be cautious even if, or perhaps mostly when, the so-called "right non-dominant hemisphere" is involved, in order to avoid permanent deficits of the patient's higher-level functions. And that is possible only knowing where and also how to intraoperatively test those functions. The most accurate way to achieve this goal is to create a real-time cortical brain map using DES and appropriate tasks given to the patient who has to be awake before corticectomy is performed. Indeed, nowadays, it is mandatory for brain surgeons to shift the paradigm from "anatomical based resection" to "functional based resection," being aware of functional limits and areas, mastering awake surgery and DES techniques, at least when approaching low-grade tumors or other pathologies with a long survival rate (e.g., cavernomas) and in which, precisely for this reason, postoperative quality of life is crucial.

It is not the purpose of this article to show and explain the indications and technique for awake surgery craniotomy or DES, but we need to underline, once again, how these have contributed to improve our still limited knowledge about brain function. The subject is still largely unknown, and more studies are needed in order to extend our understanding of this remarkable function.

Finally, it must be underlined again that another important but unresolved issue concerning the mentalization process regards the long-range white matter connections, which unify mentioned cortical areas. Such white fibers may be themselves involved in neural information processing; it is an issue of paramount importance, and more studies are needed in a "connectomic" view of a functional and plastic brain.

The main limit of this paper is its non-systematic nature; we tried to be as concise as possible in order to give young neurosurgeons or neurosurgeons who want to approach brain surgery a schematic view and a basic knowledge of which cortical areas are involved in mentalization. Another limitation is that we have, consciously, left out all the world of subcortical white fiber tracts, focusing our work only on gray matter cortical areas.

CONCLUSIONS

The mentalizing process is still a wide and poorly understood field in cognitive neuroscience. A few publications exist concerning this topic applied to neurosurgery. In this brief review, we reported the main cortical areas involved in this peculiar human skill, namely, the PFC, TPJ, PPC, temporal poles, and cingulate cortex.

We strongly believe that brain surgeons cannot ignore this topic especially when the patient's postoperative life expectancy is long and a return to normal life is anticipated: when damaged, these areas could lead to permanent deficits of the patient's higher-level functions, precluding many normal life nuances.

AUTHOR CONTRIBUTIONS

MMo: idea and text writing. PZ and MMa: data collection. FP: text writing. AM: supervision. FZ and DG: manuscript correction. All authors contributed to the article and approved the submitted version.

FUNDING

This study was produced in the Department of Neuroscience Rita Levi Montalcini and was supported by Ministero dell'Istruzione, dell'Università e della Ricerca–MIUR project Dipartimenti di eccellenza 2018–2022.

REFERENCES

1. Gallup GG. Do minds exist in species other than our own? *Neurosci Biobehav Rev.* (1985) 9:631–41. doi: 10.1016/0149-7634(85)90010-7
2. Premack D, Woodruff G. Does the chimpanzee have a theory of mind? *Behav Brain Sci.* (1978) 1:515–26. doi: 10.1017/S0140525X00076512
3. Desmurget M, Song Z, Mottolese C, Sirigu A. Re-establishing the merits of electrical brain stimulation. *Trends Cogn Sci.* (2013) 17:442–9. doi: 10.1016/j.tics.2013.07.002
4. Duffau H. Stimulation mapping of white matter tracts to study brain functional connectivity. *Nat Rev Neurol.* (2015) 11:255–65. doi: 10.1038/nrneurol.2015.51
5. Schurz M, Radua J, Aichhorn M, Richlan F, Perner J. Fractionating theory of mind: a meta-analysis of functional brain imaging studies. *Neurosci Biobehav Rev.* (2014) 42:9–34. doi: 10.1016/j.neubiorev.2014.01.009
6. Herbet G, Lafargue G, Bonnetblanc F, Moritz-Gasser S, Menjot de Champfleur N, Duffau H. Inferring a dual-stream model of mentalizing from associative white matter fibres disconnection. *Brain.* (2014) 137:944–59. doi: 10.1093/brain/awt370
7. Nakajima R, Kinoshita M, Okita H, Yahata T, Matsui M, Nakada M. Neural networks mediating high-level mentalizing in patients with right cerebral hemispheric gliomas. *Front Behav Neurosci.* (2018) 12:33. doi: 10.3389/fnbeh.2018.00033
8. Miller EK, Cohen JD. An integrative theory of prefrontal cortex function. *Annu Rev Neurosci.* (2001) 24:167–202. doi: 10.1146/annurev.neuro.24.1.167
9. Striedter GF. *Principles of Brain Evolution*. Sunderland: Sinauer Associates (2005).
10. Carlén M. What constitutes the prefrontal cortex? *Science.* (2017) 358:478–82. doi: 10.1126/science.aan8868
11. Teffer K, Semendeferi K. Human prefrontal cortex. *Prog Brain Res.* (2012) 195:191–218. doi: 10.1016/B978-0-444-53860-4.00009-X
12. Knotts JD, Odegaard B, Lau H. Neuroscience: the key to consciousness may not be under the streetlight. *Curr Biol.* (2018) 28:R749–52. doi: 10.1016/j.cub.2018.05.033
13. Lau H, Rosenthal D. Empirical support for higher-order theories of conscious awareness. *Trends Cogn Sci.* (2011) 15:365–73. doi: 10.1016/j.tics.2011.05.009
14. Jack A. Introspective physicalism as an approach to the science of consciousness. *Cognition.* (2001) 79:161–96. doi: 10.1016/S0010-0277(00)00128-1
15. Brown R, Lau H, LeDoux JE. Understanding the higher-order approach to consciousness. *Trends Cogn Sci.* (2019) 23:754–68. doi: 10.1016/j.tics.2019.06.009
16. Greenlee JDW, Oya H, Kawasaki H, Volkov IO, Severson MA, Howard MA, et al. Functional connections within the human inferior frontal gyrus. *J Comp Neurol.* (2007) 503:550–9. doi: 10.1002/cne.21405
17. Zaki J, Weber J, Bolger N, Ochsner K. The neural bases of empathic accuracy. *Proc Nat Acad Sci USA*. (2009) 106:11382–7. doi: 10.1073/pnas.0902666106
18. Herbet G, Lafargue G, Moritz-Gasser S, Bonnetblanc F, Duffau H. Interfering with the neural activity of mirror-related frontal areas impairs mentalistic inferences. *Brain Struct Funct.* (2015) 220:2159–69. doi: 10.1007/s00429-014-0777-x
19. Caspers S, Zilles K, Laird AR, Eickhoff SB. ALE meta-analysis of action observation and imitation in the human brain. *Neuroimage.* (2010) 50:1148–67. doi: 10.1016/j.neuroimage.2009.12.112
20. Molenberghs P, Cunnington R, Mattingley JB. Is the mirror neuron system involved in imitation? A short review and meta-analysis. *Neurosci Biobehav Rev.* (2009) 33:975–80. doi: 10.1016/j.neubiorev.2009.03.010
21. Herbet G, Lafargue G, Bonnetblanc F, Moritz-Gasser S, Duffau H. Is the right frontal cortex really crucial in the mentalizing network? A longitudinal study in patients with a slow-growing lesion. *Cortex.* (2013) 49:2711–27. doi: 10.1016/j.cortex.2013.08.003
22. Dapretto M, Davies MS, Pfeifer JH, Scott AA, Sigman M, Bookheimer SY, et al. Understanding emotions in others: mirror neuron dysfunction in children with autism spectrum disorders. *Nat Neurosci.* (2006) 9:28–30. doi: 10.1038/nn1611
23. Molenberghs P, Cunnington R, Mattingley JB. Brain regions with mirror properties: a meta-analysis of 125 human fMRI studies. *Neurosci Biobehav Rev.* (2012) 36:341–9. doi: 10.1016/j.neubiorev.2011.07.004
24. Rizzolatti G, Craighero L. THE mirror-neuron system. *Annu Rev Neurosci.* (2004) 27:169–92. doi: 10.1146/annurev.neuro.27.070203.144230
25. Carr L, Iacoboni M, Dubeau M-C, Mazziotta JC, Lenzi GL. Neural mechanisms of empathy in humans: a relay from neural systems for imitation to limbic areas. *Proc Nat Acad Sci USA.* (2003) 100:5497–502. doi: 10.1073/pnas.0935845100
26. Blakemore S-J, Frith C. Self-awareness and action. *Curr Opin Neurobiol.* (2003) 13:219–24. doi: 10.1016/S0959-4388(03)00043-6
27. Jackson PL, Decety J. Motor cognition: a new paradigm to study self–other interactions. *Curr Opin Neurobiol.* (2004) 14:259–63. doi: 10.1016/j.conb.2004.01.020
28. Yordanova YN, Duffau H, Herbet G. Neural pathways subserving face-based mentalizing. *Brain Struct Funct.* (2017) 222:3087–105. doi: 10.1007/s00429-017-1388-0
29. Whitlock JR. Posterior parietal cortex. *Current Biology.* (2017) 27:R691–5. doi: 10.1016/j.cub.2017.06.007
30. Desmurget M, Sirigu A. A parietal-premotor network for movement intention and motor awareness. *Trends Cogn Sci.* (2009) 13:411–9. doi: 10.1016/j.tics.2009.08.001
31. Murata A, Gallese V, Luppino G, Kaseda M, Sakata H. Selectivity for the shape, size, and orientation of objects for grasping in neurons of monkey parietal area AIP. *J Neurophysiol.* (2000) 83:2580–601. doi: 10.1152/jn.2000.83.5.2580
32. Hwang EJ, Dahlen JE, Mukundan M, Komiyama T. History-based action selection bias in posterior parietal cortex. *Nat Commun.* (2017) 8:1242. doi: 10.1038/s41467-017-01356-z
33. Foley NC, Kelly SP, Mhatre H, Lopes M, Gottlieb J. Parietal neurons encode expected gains in instrumental information. *Proc Natl Acad Sci USA.* (2017) 114:E3315–23. doi: 10.1073/pnas.1613844114
34. Corbetta M, Kincade JM, Ollinger JM, McAvoy MP, Shulman GL. Voluntary orienting is dissociated from target detection in human posterior parietal cortex. *Nat Neurosci.* (2000) 3:292–7. doi: 10.1038/73009
35. Friedman-Hill SR, Robertson LC, Desimone R, Ungerleider LG. Posterior parietal cortex and the filtering of distractors. *Proc Nat Acad Sci USA.* (2003) 100:4263–8. doi: 10.1073/pnas.0730772100
36. Snyder LH, Batista AP, Andersen RA. Coding of intention in the posterior parietal cortex. *Nature.* (1997) 386:167–70. doi: 10.1038/386167a0
37. Morcos AS, Harvey CD. History-dependent variability in population dynamics during evidence accumulation in cortex. *Nat Neurosci.* (2016) 19:1672–81. doi: 10.1038/nn.4403
38. Maddux J-M, Kerfoot EC, Chatterjee S, Holland PC. Dissociation of attention in learning and action: effects of lesions of the amygdala central nucleus, medial prefrontal cortex, and posterior parietal cortex. *Behav Neurosci.* (2007) 121:63–79. doi: 10.1037/0735-7044.121.1.63
39. Campanella F, Shallice T, Ius T, Fabbro F, Skrap M. Impact of brain tumour location on emotion and personality: a voxel-based lesion–symptom mapping study on mentalization processes. *Brain.* (2014) 137:2532–45. doi: 10.1093/brain/awu183

40. Funnell E. Evidence for scripts in semantic dementia: implications for theories of semantic memory. *Cogn Neuropsychol.* (2001) 18:323–41. doi: 10.1080/02643290042000134
41. Damasio H, Tranel D, Grabowski T, Adolphs R, Damasio A. Neural systems behind word and concept retrieval. *Cognition.* (2004) 92:179–229. doi: 10.1016/j.cognition.2002.07.001
42. Ganis G, Kutas M. An electrophysiological study of scene effects on object identification. *Cognitive Brain Research.* (2003) 16:123–44. doi: 10.1016/S0926-6410(02)00244-6
43. Vogt BA, Finch DM, Olson CR. functional heterogeneity in cingulate cortex: the anterior executive and posterior evaluative regions. *Cereb Cortex.* (1992) 2:435–43. doi: 10.1093/cercor/2.6.435-a
44. Herbet G, Moritz-Gasser S. Beyond language. *Neurosurg Clin N Am.* (2019) 30:75–83. doi: 10.1016/j.nec.2018.08.004
45. Rushworth MFS, Hadland KA, Gaffan D, Passingham RE. The effect of cingulate cortex lesions on task switching and working memory. *J Cogn Neurosci.* (2003) 15:338–53. doi: 10.1162/089892903321593072
46. Rudebeck PH, Bannerman DM, Rushworth MFS. The contribution of distinct subregions of the ventromedial frontal cortex to emotion, social behavior, and decision making. *Cogn Affect Behav Neurosci.* (2008) 8:485–97. doi: 10.3758/CABN.8.4.485
47. Rudebeck PH, Behrens TE, Kennerley SW, Baxter MG, Buckley MJ, Walton ME, et al. Frontal cortex subregions play distinct roles in choices between actions and stimuli. *J Neurosci.* (2008) 28:13775–85. doi: 10.1523/JNEUROSCI.3541-08.2008
48. Rudebeck PH. A role for the macaque anterior cingulate gyrus in social valuation. *Science.* (2006) 313:1310–2. doi: 10.1126/science.1128197
49. Behrens TEJ, Hunt LT, Woolrich MW, Rushworth MFS. Associative learning of social value. *Nature.* (2008) 456:245–9. doi: 10.1038/nature07538
50. Hampton AN, Bossaerts P, O'Doherty JP. Neural correlates of mentalizing-related computations during strategic interactions in humans. *Proc Nat Acad Sci USA.* (2008) 105:6741–6. doi: 10.1073/pnas.0711099105
51. Yordanova YN, Cochereau J, Duffau H, Herbet G. Combining resting state functional MRI with intraoperative cortical stimulation to map the mentalizing network. *Neuroimage.* (2019) 186:628–36. doi: 10.1016/j.neuroimage.2018.11.046
52. Herbet G, Duffau H. Chapter 7 - Awake craniotomy and bedside cognitive mapping in neurosurgery. In: Pearson CM, Ecklund-Johnson E, Gale SD, editors. *Neurosurgical Neuropsychology*. Academic Press (2019). p. 113–38. doi: 10.1016/B978-0-12-809961-2.00008-4
53. Rushworth MFS, Behrens TEJ, Rudebeck PH, Walton ME. Contrasting roles for cingulate and orbitofrontal cortex in decisions and social behaviour. *Trends Cogn Sci.* (2007) 11:168–76. doi: 10.1016/j.tics.2007.01.004
54. Walton ME, Mars RB. Probing human and monkey anterior cingulate cortex in variable environments. *Cogn Affect Behav Neurosci.* (2007) 7:413–22. doi: 10.3758/CABN.7.4.413
55. Hayden BY, Platt ML. Neurons in anterior cingulate cortex multiplex information about reward and action. *J Neurosci.* (2010) 30:3339–46. doi: 10.1523/JNEUROSCI.4874-09.2010
56. Kennerley SW, Dahmubed AF, Lara AH, Wallis JD. Neurons in the frontal lobe encode the value of multiple decision variables. *J Cogn Neurosci.* (2009) 21:1162–78. doi: 10.1162/jocn.2009.21100
57. Kennerley SW, Wallis JD. Reward-Dependent modulation of working memory in lateral prefrontal cortex. *J Neurosci.* (2009) 29:3259–70. doi: 10.1523/JNEUROSCI.5353-08.2009
58. Matsumoto M, Matsumoto K, Abe H, Tanaka K. Medial prefrontal cell activity signaling prediction errors of action values. *Nat Neurosci.* (2007) 10:647–56. doi: 10.1038/nn1890
59. Gallese V. Mirror neurons and the simulation theory of mind-reading. *Trends Cogn Sci.* (1998) 2:493–501. doi: 10.1016/S1364-6613(98)01262-5
60. Gallese V. Before and below 'theory of mind': embodied simulation and the neural correlates of social cognition. *Phil Trans R Soc B.* (2007) 362:659–69. doi: 10.1098/rstb.2006.2002
61. Reithler J, van Mier HI, Peters JC, Goebel R. Nonvisual motor learning influences abstract action observation. *Curr Biol.* (2007) 17:1201–7. doi: 10.1016/j.cub.2007.06.019
62. Schubotz RI. Prediction of external events with our motor system: towards a new framework. *Trends Cogn Sci.* (2007) 11:211–8. doi: 10.1016/j.tics.2007.02.006
63. Schubotz RI, von Cramon DY. The case of pretense: observing actions and inferring goals. *J Cogn Neurosci.* (2009) 21:642–53. doi: 10.1162/jocn.2009.21049
64. Parvizi J, Van Hoesen GW, Buckwalter J, Damasio A. Neural connections of the posteromedial cortex in the macaque. *Proc Nat Acad Sci USA.* (2006) 103:1563–8. doi: 10.1073/pnas.0507729103
65. Vogt BA, Laureys S. "osterior cingulate, precuneal and retrosplenial cortices: cytology and components of the neural network correlates of consciousness. *Progr Brain Res.* 150:205–17. doi: 10.1016/S0079-6123(05)50015-3
66. Mesulam M. From sensation to cognition. *Brain.* (1998) 121:1013–52. doi: 10.1093/brain/121.6.1013
67. Concha L, Gross DW, Beaulieu C. Diffusion tensor tractography of the limbic system. *AJNR Am J Neuroradiol.* (2005) 26:2267–74.
68. Hagmann P, Cammoun L, Gigandet X, Meuli R, Honey CJ, Wedeen VJ, et al. Mapping the structural core of human cerebral cortex. *PLoS Biol.* (2008) 6:e159. doi: 10.1371/journal.pbio.0060159
69. Greicius MD, Supekar K, Menon V, Dougherty RF. Resting-State functional connectivity reflects structural connectivity in the default mode network. *Cerebral Cortex.* (2009) 19:72–8. doi: 10.1093/cercor/bhn059

Conflict of Interest: The authors declare that the research was conducted in the absence of any commercial or financial relationships that could be construed as a potential conflict of interest.

frontiers in Neurology

ORIGINAL RESEARCH
published: 20 January 2022
doi: 10.3389/fneur.2021.805952

Combining Pre-operative Diffusion Tensor Images and Intraoperative Magnetic Resonance Images in the Navigation Is Useful for Detecting White Matter Tracts During Glioma Surgery

*Manabu Tamura[1,2], Hiroyuki Kurihara[2], Taiichi Saito[1,2], Masayuki Nitta[1,2], Takashi Maruyama[2], Shunsuke Tsuzuki[1,2], Atsushi Fukui[2], Shunichi Koriyama[2], Takakazu Kawamata[2] and Yoshihiro Muragaki[1,2]**

[1] Faculty of Advanced Techno-Surgery, Institute of Advanced Biomedical Engineering and Science, Tokyo Women's Medical University, Tokyo, Japan, [2] Department of Neurosurgery, Tokyo Women's Medical University, Tokyo, Japan

OPEN ACCESS

Edited by:
Emanuele La Corte,
University of Bologna, Italy

Reviewed by:
Giovanni Raffa,
University of Messina, Italy
Sandrine de Ribaupierre,
Western University, Canada

***Correspondence:**
Yoshihiro Muragaki
ymuragaki@twmu.ac.jp

Specialty section:
This article was submitted to Applied Neuroimaging, a section of the journal Frontiers in Neurology

Received: 31 October 2021
Accepted: 27 December 2021
Published: 20 January 2022

Citation:
Tamura M, Kurihara H, Saito T, Nitta M, Maruyama T, Tsuzuki S, Fukui A, Koriyama S, Kawamata T and Muragaki Y (2022) Combining Pre-operative Diffusion Tensor Images and Intraoperative Magnetic Resonance Images in the Navigation Is Useful for Detecting White Matter Tracts During Glioma Surgery. Front. Neurol. 12:805952. doi: 10.3389/fneur.2021.805952

Purpose: We developed a navigation system that superimposes the fractional anisotropy (FA) color map of pre-operative diffusion tensor imaging (DTI) and intraoperative magnetic resonance imaging (MRI). The current study aimed to investigate the usefulness of this system for neurophysiological monitoring and examination under awake craniotomy during tumor removal.

Method: A total of 10 glioma patients (4 patients with right-side tumors; 5 men and 5 women; average age, 34 years) were evaluated. Among them, the tumor was localized to the frontal lobe, insular cortex, and parietal lobe in 8, 1, and 1 patient, respectively. There were 3 patients who underwent surgery on general anesthesia, while 7 patients underwent awake craniotomy. The index of DTI anisotropy taken pre-operatively (magnetic field: 3 tesla, 6 motion probing gradient directions) was analyzed as a color map (FA color map) and concurrently co-registered in the intraoperative MRI within the navigation. In addition to localization of the bipolar coagulator and the cortical stimulator for brain mapping on intraoperative MRI, the pre-operative FA color map was also concurrently integrated and displayed on the navigation monitor. This white matter nerve functional information was confirmed directly by using neurological examination and referring to the electrophysiological monitoring.

Results: Intraoperative MRI, integrated pre-operative FA color map, and microscopic surgical view were displayed on one screen in all 10 patients, and white matter fibers including the pyramidal tract were displayed as a reference in blue. Regarding motor function, motor-evoked potential was monitored as appropriate in all cases, and removal was possible while directly confirming motor symptoms under awake craniotomy. Furthermore, the white matter fibers including the superior longitudinal fasciculus were displayed in green. Importantly, it was useful not only to localize the resection site, but to identify language-related, eye movement-related, and motor

fibers at the electrical stimulation site. All motor and/or language white matter tracts were identified and visualized with the co-registration and then with an acceptable post-operative neurological outcome.

Conclusion: Co-registering an intraoperative MR images and a pre-operative FA color map is a practical and useful method to predict the localization of critical white matter nerve functions intraoperatively in glioma surgery.

Keywords: diffusion tensor imaging, magnetic resonance imaging, fractional anisotropy, glioma, craniotomy

INTRODUCTION

The usefulness of perioperative magnetic resonance imaging (MRI) in brain tumor resection has attracted research attention recently. In particular, intraoperative MRI for maximal tumor resection is aimed to prolong prognosis and reduce complications, making it an important method (1–5). Further, with the introduction of navigation-based tumor resection, MR images are now taken intraoperatively, and the position of the surgical tool held by the operator can be displayed on the MR image. The usefulness of this system as an intraoperative support device has been established, and it is now increasingly used in clinical practice. Similar MRI-guided navigation systems have been applied in facilities with no MRI systems inside the operating room, using MR images obtained the day before surgery. This system provides more information and allows a more accurate surgery than that performed only based on the anatomical structure on pre-operative MRI, making it an important surgical support strategy (6).

Advances in pre-operative MRI have made it possible to obtain more detailed functional information of brain tumors and surrounding brain tissues. The acquisition of functional information on brain tumors and surrounding brain tissues has recently attracted attention as a possible method for reducing perioperative functional complications. High-field MRI devices have enabled acquisition of pre-operative MRI function images useful for predicting brain function sites during surgery and estimating brain function after tumor resection. Functional images obtained from pre-operative MRI can be broadly divided into (1) functional MRI (fMRI) and (2) diffusion tensor imaging (DTI) (7). In fMRI, language tasks are performed to image language-dominant hemispheres and functional localization (8). Meanwhile, DTI enables imaging of white matter fibers involved in motor and language functions (FA color map) as well as the tractography of white matter tracts (9). However, there have been reports that notable white matter tracts were not visualized (false negatives) on perioperative tractography (10, 11).

We believe that this issue will be resolved by directly confirming brain function during surgery. Functional mapping under awake craniotomy allows the surgeon to clearly define language, positive motor and negative motor areas as well as the positions of white matter fibers connected with speech and motor functions, helping to prevent unexpected neurological deficits. A meta-analysis demonstrated late severe neurological deficit in 3.4% of patients who underwent resection with stimulation mapping, compared to 8.3% of patients who underwent resection without mapping (12). For intraoperative confirmation of brain function, including the white matter of the cerebral cortex, it is important to capture longitudinal changes in motor and language functions before and after the start of tumor resection. Assessing motor-evoked potential (MEP) with the cerebral cortex indwelling strip is also helpful. Brain function during awake craniotomy is more accurate than that determined on pre-operative imaging. However, frequent brain stimulation can cause seizures, and there are issues with the accuracy of MEP measurement.

Therefore, the optimal strategy for achieving maximal tumor resection and reducing neurological complications is needed. We have previously developed a navigation system that superimposes the FA color map of pre-operative DTI and intraoperative MRI (13). In addition to predicting the FA color map display of DTI as a pre-operative white matter functional site, our system can be used to evaluate brain function complementary to neurophysiological examinations and direct neurological function evaluation under awake craniotomy. The current study aimed to investigate the usefulness of this system for neurophysiological monitoring and examination under awake craniotomy during tumor removal.

METHODS

Among patients who underwent brain tumor resections after April 2016, 10 consecutive patients (5 males, 5 females; average age, 34 years) with co-registered pre-operative DTI and intraoperative MRI were evaluated. Among them, 8 and 2 patients underwent their first and second surgeries, respectively (**Table 1**). There were 4 and 6 patients with right- and left-sided tumors. The tumors were located in the frontal lobe in 8 patients; insular cortex, 1 patient; and parietal lobe, 1 patient. Surgery was performed under general anesthesia and awake craniotomy in 3 and 7 patients, respectively.

Pre-operative DT images were used during surgery to focus on motor fibers near the tumor in all 10 patients and to language fibers in 6 patients. Pre-operative DT images were acquired using a 3-Tesla magnetic field MRI (Philips ACHIEVA^{TM}) with 6 directions of diffusion sensitizing gradient and nearly isotropic voxel size. Raw DTI data obtained in the MRI workstation was color mapped (FA color map) *via* RGB conversion for the index of anisotropy. The left and right x directions were displayed in red (R), the front and back y directions were displayed in green (G), and the up and down z directions were

TABLE 1 | Patient characteristics and clinical results with image integration of pre-operative DTI-FA color map and intraoperative MRI.

Case	Age, sex	Pathology, WHO 2016 grade	Initial or additional	Side-location	Anesthesia	Object for DTI fusion	Clinical results (tumor removal rate and symptoms)		
							R. rate	Post-ope within 7 days	Post-ope at 3 months later
1	19, M	AA, 3	Initial	Rt-Insula	General	M	90	None	None
2	36, M	Oligo, 2	Initial	Lt-Frontal	Awake	M, B	98	Paresis (u-l, 4/5), Aphasia	Paresis (u-l, 4/5), Aphasia
3	37, F	AA, 3	Initial	Lt-Frontal	Awake	M, B	94	Paralysis (u, 0/5), Aphasia	Paresis (u, 4/5)
4	43, M	AA, 3	Initial	Rt-Frontal	Awake	M, B	95	Paresis (u, 2–3/5)	Paresis (u, 4/5)
5	37, F	AA, 3	Additional	Lt-Parietal	Awake	M, B, W	95	Mild agnosia	None
6	24, F	GBM, 4	Initial	Rt-Frontal	Awake	M	95	Paresis (u-1/5 and l-3/5)	Paresis (u-l, 4/5)
7	41, F	AA, 3	Additional	Rt-Frontal	General	M	95	Paresis (u-l, 4/5), Dysarthria	Dysarthria
8	29, F	GBM, 4	Initial	Lt-Frontal	General	M	90	Paresis (u-l, 1/5), Aphasia	Paresis (u-2/5 and l-4/5), Aphasia
9	32, M	AA, 3	Initial	Lt-Frontal	Awake	M, B	75	Paresis (u-l, 3–4/5), Aphasia	Paresis (u-l, 4/5)
10	41, M	AO, 3	Initial	Lt-Frontal	Awake	M, B	70	Paresis (u-l, 4/5), Dysarthria	None

AA, Anaplastic astrocytoma; Oligo, Oligodendroglioma; GBM, Glioblastoma; AO, Anaplastic oligodendroglioma; Rt, Right; Lt, Left, Object for DTI fusion (B, frontal language; W, posterior language; M, motor-sensory); R. rate, Tumor removal rate (%).
Motor symptom (paralysis/paresis) was evaluated by Manual Muscle Test (1–5 scale) using u-l (upper limb and lower limb), u (upper limb) and l (lower limb).

displayed in blue (B) according to the same coordinate axes as in normal MRI (see **Figure 1A**). The FA color map images acquired as 70 consecutive DICOM images in the axial plane and 128 consecutive DICOM images in the coronal plane enabled prediction of the relationship between tumor position and white matter fibers as pre-operative DTI.

Intraoperative MR images (magnetic field strength of 0.3 Tesla, Hitachi™), including 100 T1- and T2-weighted images, obtained after craniotomy (**Figure 1B**) was read on a navigation system (BrainLAB™). Next, the DICOM image of the FA color map created from the pre-operative DTI (**Figure 1A**) was read on the same navigation system, and the image is co-registered with the previous intraoperative MRI and displayed concurrently (**Figure 1C**). Finally, a bipolar coagulator and an electrical stimulation probe (manufactured by Unique Medical™) were registered using a sterile antenna device and a skull-fixed marker (14).

With this method, the position information of the bipolar coagulator and the electrical stimulation probe operated by the operator was displayed simultaneously on the intraoperative MRI and the pre-operative DTI (FA color map). For functional evaluation of motor white matter fibers, MEP findings obtained from the scalp indwelling needle and cerebral cortex surface strip prepared at the start of surgery, direct patient movement confirmation (under awake craniotomy), and FA color map display on the navigation system were used. For the functional evaluation of verbal white matter fibers, the language function of awake patients was evaluated using the language function test system [Intraoperative Examination Monitor for Awake Surgery, IEMAS (15, 16)] we developed in 2004. In addition to direct confirmation and video recording, nerve position was confirmed using the FA color map display on the navigation system.

All procedures performed in studies involving patients were in accordance with the ethical standards of the ethics committee of Tokyo Women's Medical University and with the 1964 Declaration of Helsinki, as revised in 2013. Each patient provided informed consent before the surgical procedure.

RESULTS

In all 10 patients, intraoperative MRI, FA color map, and intraoperative field microscope images were displayed in real time along with the position of the bipolar and probe on the same screen of the navigation monitor. Focusing on the white matter fibers represented by the pyramidal tract, the part that can be expected to run the motor nerves of the lower limbs was displayed in real time in blue (vertical direction). Thus, navigation information other than the tumor position was obtained. In addition to navigation information, resection was confirmed with regular MEP monitoring in all 10 patients. In patients under awake craniotomy, efforts were made to reduce complications while directly evaluating motor function. The language-related nerve tract (arcuate fasciculus) was adequately displayed in green (anterior-posterior direction), providing the surgeon real-time navigation information for the monitoring of verbal symptoms.

All 7 patients who underwent awake surgery received IEMAS assessment for confirmation of language function. Six patients developed motor paralysis (Manual Muscle Test evaluation) at 3 months after the tumor resection; of them, 2 patients

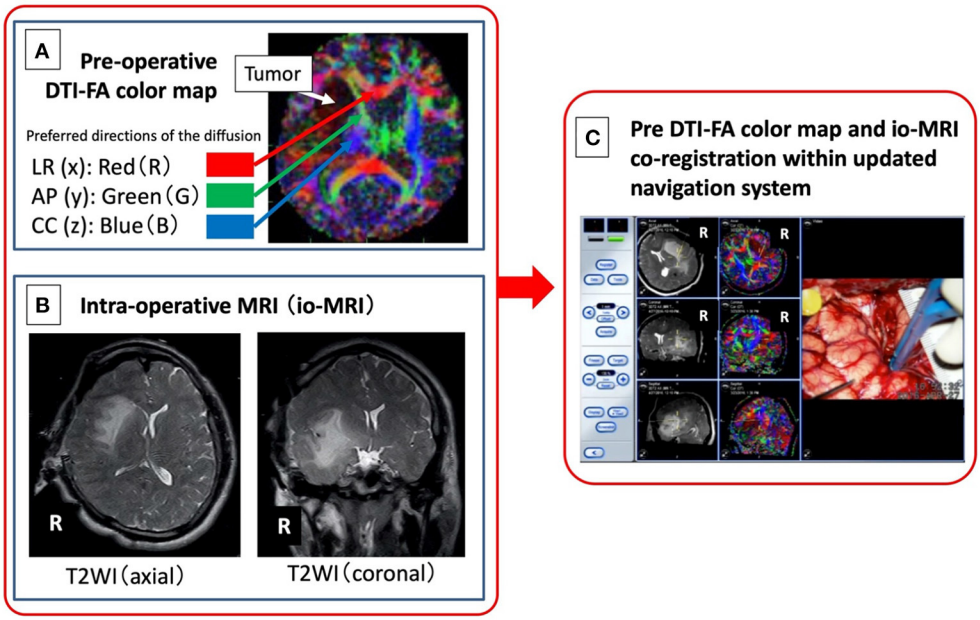

FIGURE 1 | Image integration of pre-operative DTI-FA color map **(A)** and intraoperative MRI **(B)** navigation system. A newly developed system **(C)** in which an FA color map, as an objective measure of neural function, from pre-operative DTI is combined with intraoperative MRI image obtained after craniotomy, is developed.

also developed expressive aphasia. In the 4 patients, 1 and 3 patients had residual dysarthria and no motor/language function complications, respectively. The average tumor resection rate was 89.7% (70–98%). Histopathological findings (World Health Organization grade) were grade 2 in 1 patient, grade 3 in 7 patients, and grade 4 in 2 patients (see **Table 1**).

We present representative cases below. The position of the tumor and surrounding white matter tracts was more accurately indicated by the navigation system. The surgeon can now refer to the pre-operative DTI-FA color map that is displayed in real time in conjunction with the intraoperative MRI image, making it possible to reduce the risk (see **Figures 2**, **3**). Furthermore, when a language function test was performed near the arcuate fasciculus of the white matter of the frontal lobe, a task response was not possible due to joint eye deviation during electrical stimulation mapping, and a false positive mapping condition was confirmed (**Figure 4**). In particular, it was shown that the pre-operative DTI-FA color map provides useful information for identifying motor fibers, language-related fibers, and eye movement-related fibers corresponding to bipolar and electrical stimulation probe positions during awake surgery.

Illustrative Cases

Case 1: General Anesthesia, Confirmation of Motor Nerves

A 19-year-old male underwent tumor resection under general anesthesia for Grade 3 glioma of the right insular cortex. The pre-operative DTI-FA color map indicated that the pyramidal tract (indicated by blue) was close to the tumor. By referring to the FA color map image co-registered with the intraoperative MRI updated after craniotomy, the tumor was successfully resected while visualizing the pyramidal tract in real time (**Figure 2**). Post-operative complications were also avoided while monitoring MEP findings.

Case 2: Awake Craniotomy, Confirmation of Nerve Involved in Joint Eye Movements and Verbal Response

A 36-year-old male underwent tumor resection *via* awake surgery for grade 2 glioma of the left frontal lobe. The pre-operative DTI-FA color map indicated that the pyramidal tract (indicated by blue) and the arcuate fasciculus (superior longitudinal fasciculus) (indicated by green) were close to the tumor. A language function test performed during tumor resection in the deep white matter showed a speech arrest associated with electrical stimulation. This was consistent with the FA color map findings (green) of the white matter fibers predicted to be the superior longitudinal fasciculus (**Figure 3**, positive findings of language mapping). Meanwhile, language function test performed on further tumor resection confirmed that the response to the language task was not possible because joint eye deviation was induced during white matter electrical stimulation (false-positive findings of language mapping, **Figure 4**). We were able to obtain useful findings for anatomical identification of white matter tracts while accurately recording the nerve responses involved in joint eye movement. By referring to the FA color map image co-registered with the intraoperative MRI updated after craniotomy, it was possible to excise the tumor while visualizing the pyramidal tract and arcuate fasciculus (superior longitudinal fasciculus) in real-time during monitoring of MEP and IEMAS findings. This help reduced post-operative complications.

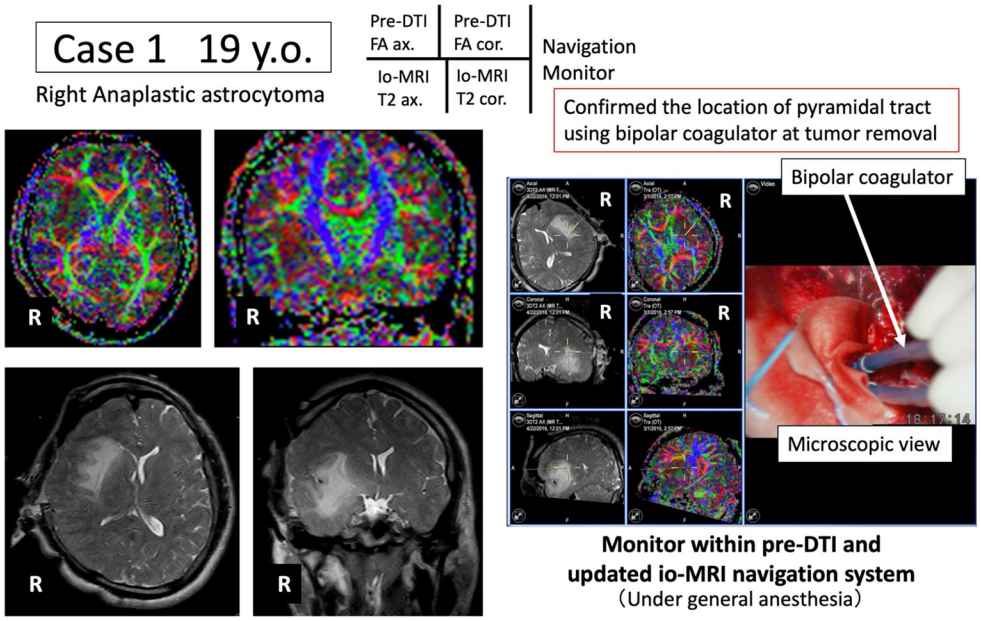

FIGURE 2 | Case 1: navigation based on pre-operative pyramidal tract motor function information. Under general anesthesia, tumor resection is advanced while the pyramidal tract (blue) is monitored in real time using the newly developed navigation system.

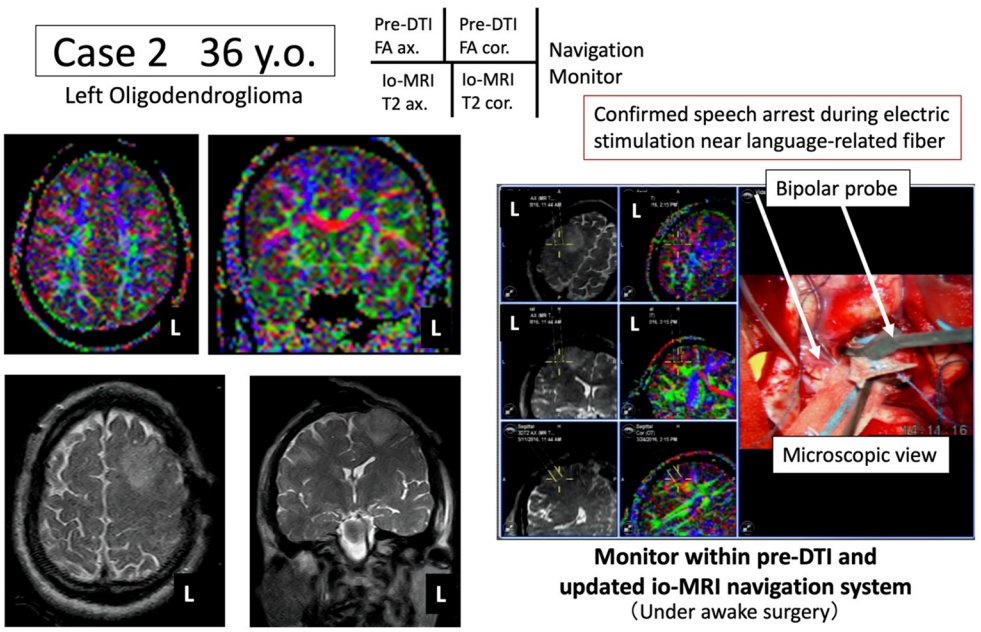

FIGURE 3 | Case 2: navigation based on pre-operative arcuate fasciculus language function information. Under awake craniotomy, tumor resection is performed while the arcuate fasciculus (green) is monitored in real time using the newly developed navigation system.

DISCUSSION

Intraoperative functional evaluation of the brain is important in glioma surgery, but current methods have few information to localize critical white matter nerve with limited accuracy. In this study, a newly developed system in which an FA color map, as an objective measure of neural function, from pre-operative DTI is combined with intraoperative MRI image obtained after craniotomy, is developed and evaluated as a clinical assistance to contribute glioma surgery with an acceptable accuracy.

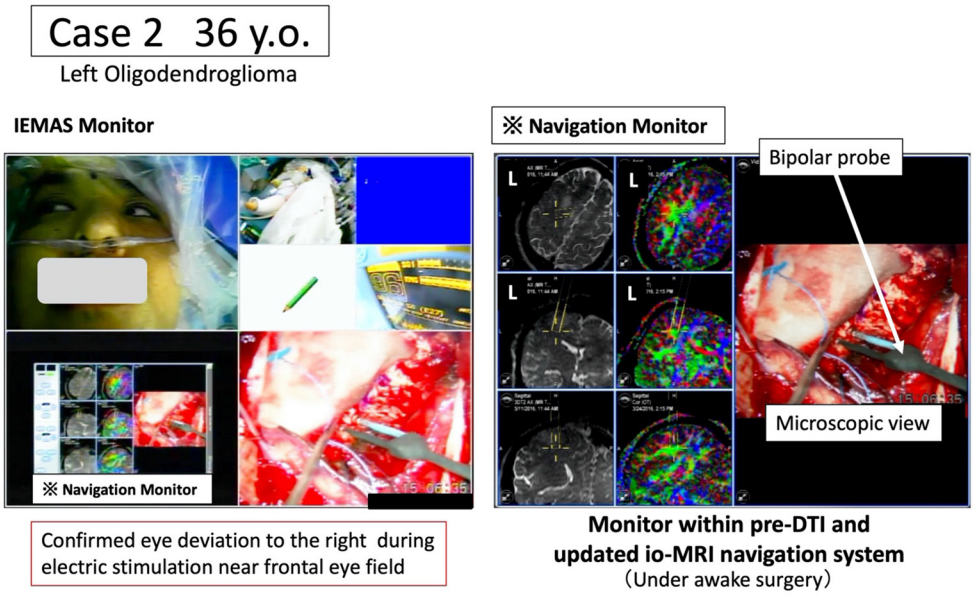

FIGURE 4 | Case 2: pre-operative arcuate fasciculus in which the joint eye movement center is identified based on language function information and language function tests. Under awake craniotomy, the tumor resection is performed while the white matter fiber (green) related to the joint eye movement center is monitored in real time using the newly developed navigation system. The intraoperative language monitoring system (IEMAS) is also used concurrently, and the language reaction associated with the presentation of the language image task is determined by both the surgeon and the examiner, making the system highly useful for awake surgery.

Differences in pre- and intraoperative MRI findings, which mainly occur from mechanical error due to navigation and intraoperative brain shift of post-craniotomy brain tissue, are important factors that need to be considered in brain surgery (17). Particularly, many navigation errors have been evaluated in intraoperative MR images in neurosurgery. For example, in navigating and registering the marker to be attached to the patient during MRI, the skin marker attached to the scalp or face produces an error of 1.5–2 mm (maximum, 4.2 mm) (18). Intraoperatively, driving a marker into the skull after craniotomy (born marker) leads to an error of 0.84–1.4 mm (19). Pre-operative MRI also has issues of position error (brain shift) due to intraoperative changes (20). This is a phenomenon in which the brain including lesions sinks more than before surgery after cerebrospinal fluid outflow or tumor removal (21). Importantly, it is difficult to predict, although it is affected by the size of the craniotomy, tumor histology, patient position, presence/absence of ventricular opening, and amount of excised tumor.

The post method (22) and intraoperative imaging after brain shift are useful methods to address this problem (23, 24). Although navigation errors are difficult to identify intraoperatively, it is possible to infer mechanical errors by confirming the marker position and errors due to brain shift by confirming the position of the brain surface [corresponding to (1) in **Table 2**]. Intraoperative MRI was first performed in 1993 by Black et al. (25) for brain tumor resection in the United States. In Germany, intraoperative imaging is mainly used in neurosurgery. The main purpose of intraoperative MRI is to safely remove lesions in challenging locations, such as tumors existing in parenchymal organs. It can confirm the presence of residual lesions and determine the need to extend the resection, ultimately improving the tumor resection rate.

Intraoperative MR images are usually acquired after craniotomy, and the MRI image is registered in the operating room navigation system. This system can display the position of the surgeon's surgical instrument on the MR image, making it particularly useful. Intraoperative MR images are updated imaged reflecting the brain shift from the parenchymal position of the brain due to craniotomy. They are more accurate for surgical navigation than pre-operative MRI. Although navigation error cannot be avoided, the surgery can perform more quickly and precisely.

This system has been used for 20 years in Japan. Medium-low magnetic field MRI is sufficient to control the removal of brain tumors (particularly gliomas), which is a major role of intraoperative MRI (26, 27). Both the magnetic field strength and the system design and operation are important. Medium magnetic field with enhanced functionality can depict the pyramidal tract using an intraoperative diffusion weighted image (DWI) image (28) [corresponding to (2) in **Table 2**]. We registered 0.3T intraoperative DWI and MRI images in the intraoperative navigation system for functional evaluation of the pyramidal tract nerve, and this allowed us to obtain functional images that minimized the effects of intraoperative brain shift. In addition, we used the FA color maps obtained pre-operatively using DTI [corresponding to (3) in **Table 2**].

There have been profound advances in visualization of brain white matter, but there are also reports that results differ according to the MRI method, software for visualization, and the purpose of the analysis. There are cases where white matter

TABLE 2 | Summary of a combination of image co-registration within navigation system in OR.

	Pre-operative	Intra-operative		DWI or DTI image co-registration	
	DTI	io-DWI	io-DTI	Advantage	Disadvantage
Pre-operative MRI	(1)	–	–	No need for MR in OR	Large brain shift effect
io-MRI (Middle F)	–	(2)	–	Small brain shift effect	Limited to pyramidal tract in DWI
io-MRI (Middle F)	Current study (3)	–	–	Practical, Informative	Middle brain shift effect
io-MRI (High F)	–	–	(4)	Small brain shift effect	Long time for MR scan and setting

Middle F, Middle field magnetic strength (0.3–0.4 Tesla); High F, High field magnetic strength (1.5–3.0 Tesla); io, intra-operative; DTI, Diffusion Tensor Image; DWI, Diffusion Weighted Image; OR, Operation Room.

tracts are not visualized (false negatives) and other excess white matter tracts are visualized (false positives) (11). To solve this problem, we used FA color maps as objective brain function measures and included these in the navigation system along with intraoperative MR images. This enabled real-time and concurrent visualization of the surgery and brain function, providing useful information. It provides the surgeon with real-time information on the white matter tracts related to motor and verbal functions, reducing perioperative complications. Furthermore, false-positive intraoperative language impairments were identified through stimulation of the joint eye movement center, contributing to achieving adequate tumor resection. Collectively, these results support that when pre-operative DTI and intraoperative MRI are combined within an allowable error range, they can be useful as a navigation system and obtain information on white matter function [corresponding to (3) in **Table 2**].

Intraoperative DTI imaging can now be performed simultaneously with intraoperative MRI. fMRI and DTI need to be acquired with a high-magnetic-field MRI device, and brain shift can be minimized by combining intraoperative DTI with intraoperative MRI using a high-magnetic-field MR device [corresponding to (4) in **Table 2**]. Intraoperative MRI is now widely used, and image-guided navigation systems that provide functional information about the brain have become increasingly important and more accurate. These systems improve the safety of surgery by providing reliable and useful information, ultimately improving prognosis by increasing the degree of intraoperative resection. As shown in **Table 2**, between (1) the conventional combination method of image co-registration within navigation system with only pre-operative DTI without intraoperative MRI and (4) the ideal method using intraoperative DTI + intraoperative MRI, there is our new technique (3) pre-operative DTI + intraoperative MRI. This (3) is practical and best choice to use at our operating room with a middle-field MRI device.

This study has some limitations. First, as mentioned in the comparison between (3) and (4) in **Table 2**, DTI imaging that minimizes the effect of brain shift requires high-field MRI in the operating room. Since our environment operated by low-field MRI and the operating room environment are different, it is impossible to evaluate white matter nerve function based on a unified standard. When a high-magnetic-field MRI device is used intraoperatively, it is necessary to examine and verify the improvement of image artifacts and confirm image accuracy, intraoperative acquisition time, and preparation for DTI FA color map creation. Next, the accuracy of the intraoperative MRI images of the high magnetic field and the low magnetic field is compared, and then the co-registration of the high magnetic field MRI and the pre-operative DTI is performed on the navigation to compare the accuracy. Ultimately, we believe that a procedure aiming for clinical application that simultaneously utilizes intraoperative MRI and intraoperative DTI in a high magnetic field is necessary. Third, we do not have the information that can describe the accuracy of this technique, but we are thinking of a method to evaluate the impact of the new method on the conventional method. In other words, a prospective comparative study was conducted between the group that performed the conventional method and the group that added the proposed method to the conventional method. We would like to conduct clinical research with the endpoints of (1) brain function prognosis, degree of rehabilitation, (2) tumor removal rate, and degree of survival prognosis.

CONCLUSION

Co-registering intraoperative MR images with pre-operative FA color maps is a useful and practical method for intraoperative localization of critical white matter nerves and functional assessment in glioma surgery.

DATA AVAILABILITY STATEMENT

The original contributions presented in the study are included in the article/supplementary material, further inquiries can be directed to the corresponding author/s.

ETHICS STATEMENT

The studies involving human participants were reviewed and approved by the Ethics Committee of Tokyo Women's Medical University. The patients/participants provided their written informed consent to participate in this study.

AUTHOR CONTRIBUTIONS

YM, MT, TM, and TK: conception and design. MT, HK, TS, MN, ST, AF, and SK: acquisition of data. YM and MT: analysis and

interpretation of data. MT: drafting the article. YM, MT, HK, TS, MN, TM, ST, AF, SK, and TK: reviewed submitted version of manuscript. YM: approved the final version of the manuscript behalf of all authors. YM and TK: study supervision. All authors contributed to the article and approved the submitted version.

FUNDING

This research was supported by JSPS Grant-in-Aid for Scientific Research (Grant Number C-19K12845), NICT (National Institute of Information and Communications, Grant Number 22009) and AMED (Grant Number JP21he1602003).

ACKNOWLEDGMENTS

The authors are grateful to all staff members of the Department of Neurosurgery and Faculty of Advanced Techno-Surgery (Tokyo Women's Medical University), especially Ms. Kaori Kusuda and Mr. Ken Masamune. We are grateful to Ms. Mana Ohashi for assistance in collecting the neurophysiological data.

REFERENCES

1. Ghinda D, Zhang N, Lu J, Yao CJ, Yuan S, Wu JS. Contribution of combined intraoperative electrophysiological investigation with 3-T intraoperative MRI for awake cerebral glioma surgery: comprehensive review of the clinical implications and radiological outcomes. *Neurosurg Focus.* (2016) 40:E14. doi: 10.3171/2015.12.FOCUS15572
2. Leroy HA, Delmaire C, Le Rhun E, Drumez E, Lejeune JP, Reyns N. High-field intraoperative MRI in glioma surgery: a prospective study with volumetric analysis of extent of resection and functional outcome. *Neurochirurgie.* (2018) 64:155–60. doi: 10.1016/j.neuchi.2018.02.003
3. Karsy M, Akbari SH, Limbrick D, Leuthardt EC, Evans J, Smyth MD, et al. Evaluation of pediatric glioma outcomes using intraoperative MRI: a multicenter cohort study. *J Neurooncol.* (2019) 143:271–80. doi: 10.1007/s11060-019-03154-7
4. Leroy HA, Delmaire C, Le Rhun E, Drumez E, Lejeune JP, Reyns N. High-field intraoperative MRI and glioma surgery: results after the first 100 consecutive patients. *Acta Neurochir.* (2019) 161:1467–74. doi: 10.1007/s00701-019-03920-6
5. Yahanda AT, Chicoine MR. Intraoperative MRI for glioma surgery: present overview and future directions. *World Neurosurg.* (2021) 149:267–8. doi: 10.1016/j.wneu.2021.03.011
6. Muragaki Y, Iseki H, Maruyama T, Nitta M, Yoshimitsu K, Tamura M, et al. Challenges of the workflow during intraoperative MRI-guided surgery for intracranial gliomas. In: Samii A, Nabavi A, Fahlbusch R, editors. *Visualization of the Brain and its Pathologies Technical and Neurosurgical Aspects*. Germany, Der Andere Verlag (2016). p. 195–209.
7. Conti Nibali M, Rossi M, Sciortino T, Riva M, Gay LG, Pessina F, et al. Preoperative surgical planning of glioma: limitations and reliability of fMRI and DTI tractography. *J Neurosurg Sci.* (2019) 63:127–34. doi: 10.23736/S0390-5616.18.04597-6
8. Sakai KL. Language acquisition and brain development. *Science.* (2005) 310:815–9. doi: 10.1126/science.1113530
9. Henderson F, Abdullah KG, Verma R, Brem S. Tractography and the connectome in neurosurgical treatment of gliomas: the premise, the progress, and the potential. *Neurosurg Focus.* (2020) 48:E6. doi: 10.3171/2019.11.FOCUS19785
10. Tamura M, Konishi Y, Tamura N, Hayashi M, Nakao N, Uematsu Y, et al. Usefulness of Leksell GammaPlan for preoperative planning of brain tumor resection: delineation of the cranial nerves and fusion of the neuroimaging data, including diffusion tensor imaging. *Acta Neurochir Suppl.* (2013) 116:179–85. doi: 10.1007/978-3-7091-1376-9_27
11. Tamura M, Muragaki Y, Saito T, Maruyama T, Nitta M, Tsuzuki S, et al. Strategy of surgical resection for glioma based on intraoperative functional mapping and monitoring. *Neurol Med Chir.* (2015) 55:383–98. doi: 10.2176/nmc.ra.2014-0415
12. De Witt Hamer PC, Robles SG, Zwinderman AH, Duffau H, Berger MS. Impact of intraoperative stimulation brain mapping on glioma surgery outcome: a meta-analysis. *J Clin Oncol.* (2012) 30:2559–65. doi: 10.1200/JCO.2011.38.4818
13. Tamura M, Maruyama T, Mangin J-F, Sato I, Nitta M, Takakura T, et al. Role of preoperative DTI tractography for surgical management of gliomas. In: *31th Computer Assisted Radiology and Surgery (CARS)* 2017. Balcelona: Springer. (2017). p. S120–1.
14. Tamura M, Sato I, Maruyama T, Ohshima K, Mangin JF, Nitta M, et al. Integrated datasets of normalized brain with functional localization using intra-operative electrical stimulation. *Int J Comput Assist Radiol Surg.* (2019) 14:2109–22. doi: 10.1007/s11548-019-01957-7
15. Yoshimitsu K, Maruyama T, Muragaki Y, Suzuki T, Saito T, Nitta M, et al. Wireless modification of the intraoperative examination monitor for awake surgery -technical note. *Neurologia Medico Chirurgica.* (2011) 51:472–6. doi: 10.2176/nmc.51.472
16. Fukutomi Y, Yoshimitsu K, Tamura M, Masamune K, Muragaki Y. Quantitative evaluation of efficacy of intraoperative examination monitor for awake surgery (IEMAS). *World Neurosurg.* (2019) 126:e432–38. doi: 10.1016/j.wneu.2019.02.069
17. Muragaki Y, Iseki H, Maruyama T, Nitta M, Saito T, Tamura M, et al. Decision analysis with integration of the intraoperative visible information from multimodal sources for the surgical decision-making. *Jpn J Neurosurg.* (2014) 23:876–86. doi: 10.7887/jcns.23.876
18. Watanabe Y, Fujii M, Hayashi Y, Kimura M, Murai Y, Hata M, et al. Evaluation of errors influencing accuracy in image-guided neurosurgery. *Radiol Phys Technol.* (2009) 2:120–5. doi: 10.1007/s12194-009-0053-6
19. Sugiura M, Muragaki Y, Nakamura R, Hori T, Iseki H. Accuracy evaluation of uptade-navigation system for the resection surgery of brain tumor using intraoperative magnetic resonance imaging. *J JSCAS.* (2005) 7:43–9. doi: 10.5759/jscas1999.7.43
20. Roberts DW, Hartov A, Kennedy FE, Miga MI, Paulsen KD. Intraoperative brain shift and deformation: a quantitative analysis of cortical displacement in 28 cases. *Neurosurgery.* (1998) 43:749–60. doi: 10.1097/00006123-199810000-00010
21. Nimsky C, Ganslandt O, Cerny S, Hastreiter P, Greiner G, Fahlbusch R. Quantification of, visualization, and compensation for brain shift using intraoperative magnetic resonance imaging. *Neurosurgery.* (2000) 47:1070–1080. doi: 10.1097/00006123-200011000-00008
22. Kajiwara K, Yoshikawa K, Ideguchi M, Nomura S, Fujisawa H, Akimura T, et al. Navigation-guided fence-post tube technique for resection of a brain tumor: technical note. *Minim Invasive Neurosurg.* (2010) 53:86–90. doi: 10.1055/s-0030-1249053
23. Wirtz CR, Bonsanto MM, Knauth M, Tronnier VM, Albert FK, Staubert A, et al. Intraoperative magnetic resonance imaging to update interactive navigation in neurosurgery: method and preliminary experience. *Comput Aided Surg.* (1997) 2:172–9. doi: 10.3109/10929089709148110
24. Muragaki Y, Iseki H, Sugiura M, Kawamata T, Ishizaki R, Amano K, et al. Developement of "real-time" navigation system updated with intraoperative MR imaging for total removal of glioma. *J JSCAS.* (2000) 2:213–4. doi: 10.5759/jscas1999.2.209
25. Black PM, Moriarty T, Alexander E, Stieg P, Woodard EJ, Gleason PL, et al. Development and implementation of intraoperative magnetic resonance imaging and its neurosurgical applications. *Neurosurgery.* (1997) 41:831–42. doi: 10.1097/00006123-199710000-00013

26. Senft C, Seifert V, Hermann E, Franz K, Gasser T. Usefulness of intraoperative ultra low-field magnetic resonance imaging in glioma surgery. *Neurosurgery.* (2008) 63:257–66. doi: 10.1227/01.NEU.0000313624.77452.3C
27. Muragaki Y, Iseki H, Maruyama T, Kawamata T, Yamane F, Nakamura R, et al. Usefulness of intraoperative magnetic resonance imaging for glioma surgery. *Acta Neurochir Suppl.* (2006) 98:67–75. doi: 10.1007/978-3-211-33303-7_10
28. Ozawa N, Muragaki Y, Nakamura R, Iseki H. Identification of the pyramidal tract by neuronavigation based on intraoperative diffusion-weighted imaging combined with subcortical stimulation. *Stereotact Funct Neurosurg.* (2009) 87:18–24. doi: 10.1159/000177624

Conflict of Interest: The authors declare that the research was conducted in the absence of any commercial or financial relationships that could be construed as a potential conflict of interest.

frontiers in Neurology

ORIGINAL RESEARCH
published: 28 January 2022
doi: 10.3389/fneur.2021.802975

Functional and Structural Architectures of Allocentric and Egocentric Spatial Coding in Aging: A Combined DTI and fMRI Study

Abiot Y. Derbie[1,2]*, *Bolton K. H. Chau*[1] and *Chetwyn C. H. Chan*[3]

[1] *Applied Cognitive Neuroscience Laboratory, Department of Rehabilitation Sciences, The Hong Kong Polytechnic University, Kowloon, Hong Kong SAR, China,* [2] *Department of Psychology, Bahir Dar University, Bahir Dar, Ethiopia,* [3] *Department of Psychology, The Education University of Hong Kong, Tai Po, Hong Kong SAR, China*

Background: Aging disrupts the optimal balance between neural nodes underlying orienting and attention control functions. Previous studies have suggested that age-related changes in cognitive process are associated to the changes in the myelinated fiber bundles, which affected the speed and actions of the signal propagation across different neural networks. However, whether the age-related difference in allocentric and egocentric spatial coding is accounted by the difference in white-matter integrity is unclear. In this study, using diffusion tensor imaging (DTI) and functional magnetic resonance imaging (fMRI), we sought to elucidate whether age-related differences in white matter integrity accounts for the difference in nodes to the distributed spatial coding-relevant brain networks.

Material and Method: Older ($n = 24$) and younger ($n = 27$) participants completed the structural DTI and fMRI scans during which they engaged in a cue-to-target task to elicit allocentric or egocentric processes.

Results and Conclusion: Efficient modulation of both allocentric and egocentric spatial coding in fronto-parietal attention network (FPAN) requires structure–function interaction. Allocentric task-modulated connectivity of the fronto-parietal network (FPN) and dorsal attention network (DAN) with the temporal lobe was influenced by the aging differences of the white-matter tracts of the posterior and superior corona radiata (PCR and SCR), respectively. On the other hand, aging difference of the superior longitudinal fasciculus mainly influenced the egocentric-task-modulated connections of the DAN and FPN with frontal regions and posterior cingulate cortex. This study suggested that functional connections of the FPAN with near and far task-relevant nodes vary significantly with age and conditions.

Keywords: FPAN, allocentric spatial coding, egocentric spatial coding, spatial representation, frame of reference, white matter integrity, functional magnetic brain imaging (fMRI)

OPEN ACCESS

Edited by:
Graziano Serrao,
University of Milan, Italy

Reviewed by:
Pengfei Xu,
Shenzhen University, China
Domenico Aquino,
IRCCS Carlo Besta Neurological Institute Foundation, Italy

***Correspondence:**
Abiot Y. Derbie
abiot.yenealem@bdu.edu.et

Specialty section:
This article was submitted to Applied Neuroimaging, a section of the journal Frontiers in Neurology

Received: *27 October 2021*
Accepted: *30 December 2021*
Published: *28 January 2022*

Citation:
Derbie AY, Chau BKH and Chan CCH (2022) Functional and Structural Architectures of Allocentric and Egocentric Spatial Coding in Aging: A Combined DTI and fMRI Study. Front. Neurol. 12:802975. doi: 10.3389/fneur.2021.802975

INTRODUCTION

Functional neuroimaging studies demonstrated that the neural substrates mediating allocentric and egocentric spatial coding (aSC and eSC, respectively) are dissociable (1, 2). Age-related differences in the working mechanisms of aSC and eSC have also been observed [for recent review: (3)]. On the other hand, with the absence of any significant disease, aging is characterized by the degeneration of white matter integrity, demyelination, and axonal loss. Alternations of the white matter integrity have been found to alter the transmission of the visuospatial neural signals to the near and far brain regions for information processing (4–6). However, how these age-related alternations would influence the spatial coding corresponding functional networks, and hence the dissociation between the aSC and eSC has not been explored.

Visuospatial attention is subserved by the functional interactions within the fronto-parietal attention network (FPAN) (2, 7, 8). The two subregions, namely the intraparietal sulcus (IPS) and the premotor cortex (PMC) including the frontal eye-fields (FEF) (1, 8) are involved in sensorimotor integration and spatial relationships among objects in space (9–11). The FPAN's subregions of the posterior parietal cortex (PPC) and lateral prefrontal cortex (LPFC) (2, 12) are involved in encoding context dependent and trial-by-trial modulation of attention (such as shifts and reorienting of attention) and response inhibition (10, 13). Common neural substrates have been found between the aSC and eSC along the FPAN. For instance, Szczepanski et al. (2) used a cue-to-target paradigm to elicit the neural related processes of aSC and eSC. The results indicate the supplementary eye-field (SEF) to superior parietal lobule (SPL) as the neural pathway common associated with both the eSC and aSC. The neural pathway of FEF to intraparietal sulcus area two (IPS2) was unique to the eSC. Other studies revealed that aSC tends to demand working memory resources, which involved the MTL (14–16).

The connectivity between the PPC and LPFC is found to be involved in attentional control (7, 17). The fiber tract of the superior longitudinal fasciculus (SLF) has been identified to strengthen the functional connectivity between the near and far neural nodes of the PPC and LPFC (18). Previous studies indicated that functional connectivity within the core nodes of the FPAN influenced participants' reaction times (RT) on visuospatial task (19). In addition, the fractional anisotropy (FA) of the SLF was correlated with the neural activities in the FPAN during visuospatial attention (20). Other correlations between the RTs and the FA values were in the splenium of the corpus callosum (SPN) (5), right posterior thalamic radiation (PTR) (21), bilateral inferior longitudinal fasciculus (ILF) (4), anterior corona radiata (ACR) (22), and posterior corona radiata (PCR) (23). It is noteworthy that the RT–FA relationships are more prominent in the right than the left hemisphere, which is in-line with the right-hemispheric dominance in visuospatial attention (24). Taken together, visuospatial attention is subserved by the FPAN, which involves structure–function interactions.

The intra-parietal lobule (IPL) is a major structural hub with fiber tracts passing through the inferior and middle longitudinal fasciculus (ILF and MLF) (25). The ILF connects the IPL with the middle temporal gyrus (MTG), inferior temporal gyrus (ITG), and superior occipital gyrus (SOG). The inferior occipitofrontal fascicle (IOF) connects the IPL with the precuneus and superior frontal gyrus *via* the caudate, and the SLF connects the IPL with the middle frontal gyrus (MFG) and inferior frontal gyrus (IFG) (25). The left and right IPL are connected *via* the splenium of the corpus callosum (SPN) (26). Disruption of these structural connectivities has been shown to affect the underlying functional mechanisms of aSC and eSC. Complimentary evidence from lesion studies have shown that disruption of the connection of SLF, ILF, and inferior fronto-occipital fasciculus (IFOF) disrupted neural activities of the middle frontal gyrus (MFG), supramarginal gyrus (SMG), and postcentral gyrus (PoCG) during eSC and neural activities of the superior temporal (ST), middle temporal (MT), angular gyrus (AG), and middle occipital gyrus (MOG) during aSC (18, 20, 27).

On the other hand, the caudal part of the IPL (cIPL, known as angular gyrus) projects the signals received to the parieto-premotor and parieto-medial temporal pathways (1). The parieto-premotor pathway is involved in eSC, and its core neural substrates are the cIPL, superior parietal lobule (SPL; including IPS), somatosensory motor area (SMA), and FEF (1, 28, 29). IPS is related to attention and FEF is related to the action template formations (7, 18, 30). The parieto-medial temporal pathway, on the other hand, is involved in aSC (1), and its key neural substrates are the caudal part of IPL (area PG) (31, 32), PCC (33), the retrosplenial cortex (RSC), temproparietal junction (TPJ), and medial temporal lobule (MTL) (34, 35). With strong connections to the PCC and TPJ, the information received by the cIPL is transformed to an aSC representation mediated by the precuneus (14). The precuneus is related to spatial updating (12) and the PCC is related to shifting spatial attention (1, 36). These studies highlighted the important common and distinct roles played by the IPL-related functional and structural connectivity networks, in particular the cIPL, in the eSC and aSC.

Aging disrupts the optimal balance between neural nodes underlying visual attention along the FPAN (34), such as alerting (37), orienting (38), and attention control (39). Such disruption was more prominent in the dorsal parts of FPAN, expressed in decline top–down attentional guidance (5). Age-related changes in orienting attention was associated with the disruption of WM integrity in the SLF and ILF (17). The disrupted WM integrity has been associated to slow down RT among older adults (4). The SLF and ILF fiber tracts influencing the PFC subserve to attentional control, whereas that influencing the PPC subserves orienting attention (40). The WM integrity in the ACR was found related to reduced attentional control in older adults (41) and lowered neural activities in the MT FEF and LPFC (42). Specific to spatial coding, older adults were reported to tend to prefer the egocentric (43) than allocentric orienting (44). Such preference was suggested due to the reduction in functional connectivity between PFC and the parietal regions (40). Subsequently, the eSC to aSC preference is further explained by the latter demands, more visual short-term memory than the former (45). Aging was also suggested to affect the pathway of the PCC (40) and SPL to the LPFC *via* the MT (1, 14, 46), which subserves the retrieval strategy and transformation of visual representation for forming

TABLE 1 | Demographic characteristics of the participants.

	Younger adults (*N* = 27)	Older adults (*N* = 24)
Age	22.37 ± 0.88	68.29 ± 3.59
Sex (m/f)	9/18	11/13
Years in school	14.59 ± 0.50	11.33 ± 2.88
MoCA score	28.25 ± 1.43	26.21 ± 1.68

a mental map in aSC [recent review and metaanalysis: (3, 30)]. The alterations of the structure–function relationships along the SPL, PCC, MTL, and LPFC may lead to the age-related changes in the aSC but not in the eSC.

Previous lesion studies revealed atrophies to the fiber bundles in the SLF, ILF, and IFOF altered the functional connectivity within the FPAN, affecting both the aSC and eSC functions (18, 20, 27). Yet, the underlying mechanism is not well understood. In the present study, we combined structural MRI (diffusion tensor imaging, DTI) and event-related fMRI to investigate how changes in the FPAN's white-mater integrity and brain activations due to old age can explain the unique age-related decline in aSC but not in eSC.

We hypothesized that the aSC task-specific effective connectivities between the fronto-parietal network (FPN) (PPC and LPFC) and the DAN (IPS and FEF) would significantly associate with the FA values of the SLF, PCR, and SCR fiber bundles for both the older and younger groups. In contrast, the eSC task-specific effective connectivities within the FPAN (involving IPS, FEF, PPC, and LPFC) would not significantly associate with the FA values of the SLF, PCR, and SCR tracts.

METHODS

Participants

A total of 51 volunteers participated in the study. Among them were 27 younger (Mean: 22.37 years, SD = 0.88, 18 women) and 24 were older adults (Mean: 68.29 years, SD = 3.59, 13 women). All participants were right-handed and had normal or corrected-to-normal vision. They had normal cognitive functions as screened by the Chinese version of Montreal Cognitive Assessment [MoCA; (47)]. The MoCA scores were not significantly different between the younger and older groups (**Table 1**). The MoCA has been shown to be a reliable measure of cognitive functions in spatial memory (48), attention, and executive functions (49) in aging studies. Ethical approval was obtained from the ethic committees of the Affiliated Rehabilitation Hospital, Fujian University of Traditional Chinese Medicine, where the study was conducted. All participants gave written informed consent prior to engaging in the testing and brain imaging experiment.

Apparatus and Stimuli

Stimuli were displayed on a 30-inch MR-compatible LCD monitor that was placed outside of the MRI brain scanner bore above the head of the participant. Participants viewed the stimuli through a mirror attached to the head coil.

Cueing Paradigm and Procedures

The task used in the fMRI scan involved detection of shapes with a cue-to-target paradigm adapted from Wilson, Woldorff, and Mangun (50). The shape detection task has been used to study attention control networks. Each trial began with the presentation of three stimuli and a cue for 350 ms (**Figure 1**). The three stimuli included a pair of empty squares (subtended 3.75° vertically and horizontally to the center) and one empty rectangle (displayed at 3.75° vertically and 12.2° horizontally to the center). The cue was a Chinese character presented at the center that indicates the type of response required later in the trial. The cue was followed by a stimulus-onset asynchrony (SOA) for a fixed duration of 1,650 ms, in which the Chinese character was replaced by a dot. Next, a new pair of squares appeared inside the two ends of the empty rectangle, i.e., a total of four squares on the screen. One of the four squares showed a "plus" sign that indicates a target and the other three show "asterisks" that indicates distracters. In the eSC condition, the target would appear in one of the squares outside the rectangle and participants had to indicate whether the target was located on the left or right according to their own bodily coordinates by pressing a button using middle or index finger, respectively. In the aSC condition, the target would appear in one of the squares inside the rectangle, and participants had to indicate whether the target was located on the left or right side of the rectangle, regardless of their own bodily coordinates. In the cue phase, at the beginning of the trial, the Chinese character cues the identity of the trial and the position of the target. The font is in italic or a normal format that indicates an egocentric or allocentric type of response, respectively. The character is either 左 (left) or 右 (right) indicating the target would appear on the left or right respectively in its corresponding condition. Finally, an intertrial interval with a varying delay of 500, 2,500, or 4,500 ms is organized in a random order. The combinations of the words and the fonts of the words were counterbalanced across all the participants.

There are four types of trials: valid, invalid, neutral, and cue-only. On the valid trials, the location of the target is consistent with the information provided by the cue. On invalid trials, the location of the target is inconsistent with the information provided by the cue. On cue-only trials, it does not include any target and distracters; rather a dot at the middle of the screen was presented. On the neutral trials, the cue provides no information of the location of the target. A total of 288 trials (144 valid, 48 invalid, 72 cue only, and 24 neutral trials) were presented across three runs, containing 96 trials per run. The distribution of each trial type to the left or right was counter balanced. It took about 30 min to complete all the three runs.

TRAINING SESSION

All participants had to complete a training session to get familiarize with the task before the actual experiment. The trials used for the training and actual experiment were similar,

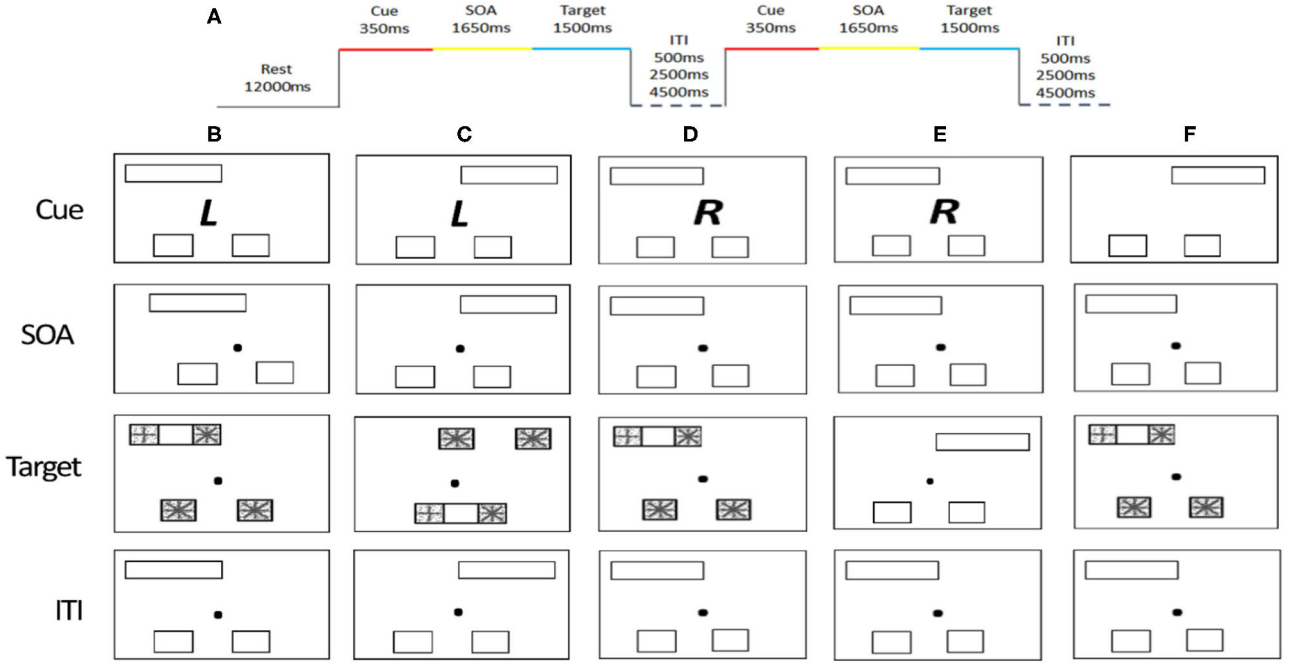

FIGURE 1 | Cue-to-target paradigm and timing parameters. **(A)** Stimulus timing. **(B)** Valid trial for the allocentric condition. **(C)** Valid trial for the egocentric condition. **(D)** Invalid allocentric trial, where the cue does not carry valid information about the probable location of the target stimuli. **(E)** Cue-only trial, where the cue is not followed by a target. **(F)** Neutral trial, where the cue carries no important information. The cue (RandL) is enlarged and the stimuli are displayed here in reverse contrast but appear in a white figure on a black background.

except that in the training session each response was followed by a feedback. All participants were to achieve an accuracy rate of at least 80% of the total trials before engaging in the experiment.

Functional MRI and DTI Image Acquisition and Preprocessing

Image Acquisition and Scanning Parameters

Siemens Prisma 3.0 T MRI system (Germany) with a 64-channel coil was used for the image data acquisition. High-resolution structural T1-weighted images were acquired: echo time (TE) = 2.27 ms, repetition time (TR) = 2,300 ms, field of view (FOV) = 250 × 250 × 240 mm^3, voxel size = 0.98 ×0.98× 1 mm^3, slice thickness = 1.0 mm; image matrix = 256 × 256). Functional images were acquired using a T2-weighted echo planar imaging (EPI) sequence: 37 noncontiguous slices of gradient-echo EPI with TE = 30 ms; TR = 2,000 ms; field of view (FOV) = 230 × 230 × 146 mm^3; voxel size = 3.6 × 3.6 × 3.6 mm^3; slice thickness = 3.6 mm; slice gap = 0.36 mm; image matrix= 64 × 64. Diffusion-weighted spin-echo planar images for diffusion tensor imaging (DTI) were obtained: TR = 5,000 ms, TE = 69 ms; flip angle, 90°; matrix, 96 × 96; 35 sagittal slices with thickness 3.5 mm; FOV = 224 mm; bandwidth = 1,954 Hz/voxel; voxel size = 1.8 × 1.8 × 3.5 mm^3. Diffusion-weighting gradients were applied at a b value of 1,000 s/mm^2. Twelve images with no diffusion gradients (b0) was also acquired for each participant.

Functional MRI Preprocessing and Univariate Analysis

Functional MRI Preprocessing

Preprocessing of the event-related fMRI BOLD signals of the participants was carried out by using FSL version 6.0.0 (FMRIB Software Library; University of Oxford; www.fmrib.ox.ac.uk/fsl) (51). The preprocessing included the removal of non-brain structure using brain extraction tool [BET; (52)], motion correction using MCFLIRT (53), temporal high-pass filtering with 100 s cut-off, slice timing correction, spatial smoothing by a Gaussian kernel with full-width half-maximum of 8 mm. Functional images were, then, registered to its native anatomical image using FMRIB's linear image registration tool (FLIRT) and then linearly registered to the MNI152 high resolution T1 2 mm template brain with 12 degree of freedom affine transformation (53, 54). To allow for signal stabilization, the first two dummy scans of each run were discarded.

Diffusion-Weighted Image Processing

The DTI data of the participants were analyzed using the FMRIB Software Library. The image with no diffusion gradients (b0) from each subject was skull-stripped using FSL's brain extraction tool (52). All diffusion weighted data from all subjects were preprocessed for eddy-current induced distortions and motion correction using the FSL's topup and Eddy tool. After distortions and motion correction, using the FDT toolbox (51),

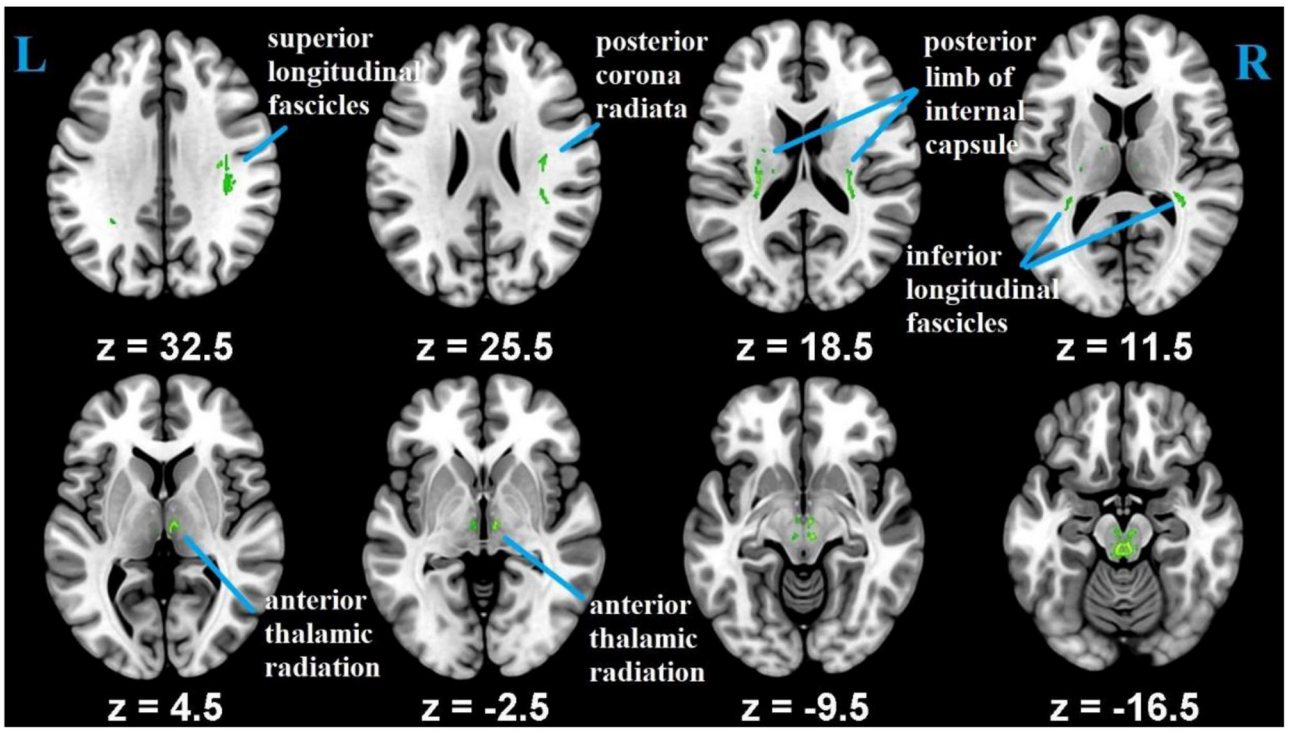

FIGURE 2 | Differences in FA measures between the younger and older groups.

raw DTI data was fit into the diffusion tensor model from which the FA (fractional anisotropy) maps for each participant was generated.

Tract-Based Spatial Statistics

Whole-brain voxel-wise statistical analysis was carried out with the tract-based spatial statistics [TBSS; (55)] parts of the FSL (51). First, all of the participants' FA images were aligned into FMRIB58_FA 1 × 1 × 1 mm standard-space using FNIRT (FMRIB's Non-linear Registration Tool) (56). Second, to achieve skeletization, the aligned FA images were then affine-transformed into 1 x 1 x 1 mm^3 MNI152 space. Third, using the mean FA image, FA skeleton common to crosssubject and crossgroup white-matter tracts was created. This was achieved by thresholding the center of white-matter bundles with a value of 0.2. Each subject's aligned FA maps were then projected onto the mean FA skeletonized map, and the resulting data was subjected for crossgroup voxel-wise statistics. Correction for multiple testing was conducted using threshold-free cluster enhancement (TFCE) method (57) and determined at $p \leq 0.05$. As an additional quality assurance, we tested the difference in FA between young and old, and the results were consistent with previous studies that reported aging difference (4) (**Figure 2**). The mean FA values were, then, extracted from each participant using predefined ROI's as a mask as explained below.

Creation of Functional Networks and White-Matter Region of Interests (ROIs)

To delimit the analysis and reduce the type I error, given the number of voxel to ROI comparisons, two key networks associated with visual attention and top–down attention control, i.e., DAN and FPN were included for the labeling of the functional ROIs according to the anatomical areas derived from the Harvard–Oxford atlas of the CONN (58, 59) (**Figure 3**).

There were two steps for defining the white-matter ROIs. First, we identified published studies on white-matter (particularly FA) in relation with aging and visuospatial attention. Ten key white-matter tracts were selected from five studies (4, 5, 21, 60, 61). The white-matter tracts identified were the anterior and superior corona radiata (SCR) bilaterally, PCR bilaterally, body corpus callosum (BCC), splenium corpus callosum (SPN), SLF bilaterally, and posterior thalamic radiation (PTR) bilaterally. WM labeling and parcellation was done by using the FSL atlas tools provided by Johns Hopkins University ["JHU ICBM-DTI-81"; (62)]. Second, we correlated the FA values and RT of the present data. Three white-matter tracts were correlated in one or more of the RT in older group or younger group in either aSC or eSC condition, and their contributions to the variation of the task-relevant BOLD signal were above and beyond the other white matter tracts. Hierarchical multiple regression was used to test whether one white-matter tract contribution to the variation in the task-relevant BOLD signal is above and beyond the other white-matter tract. They were the right SCR, right PCR, BCC, SPN, and right SLF (**Figure 3**). These tracts were binarized,

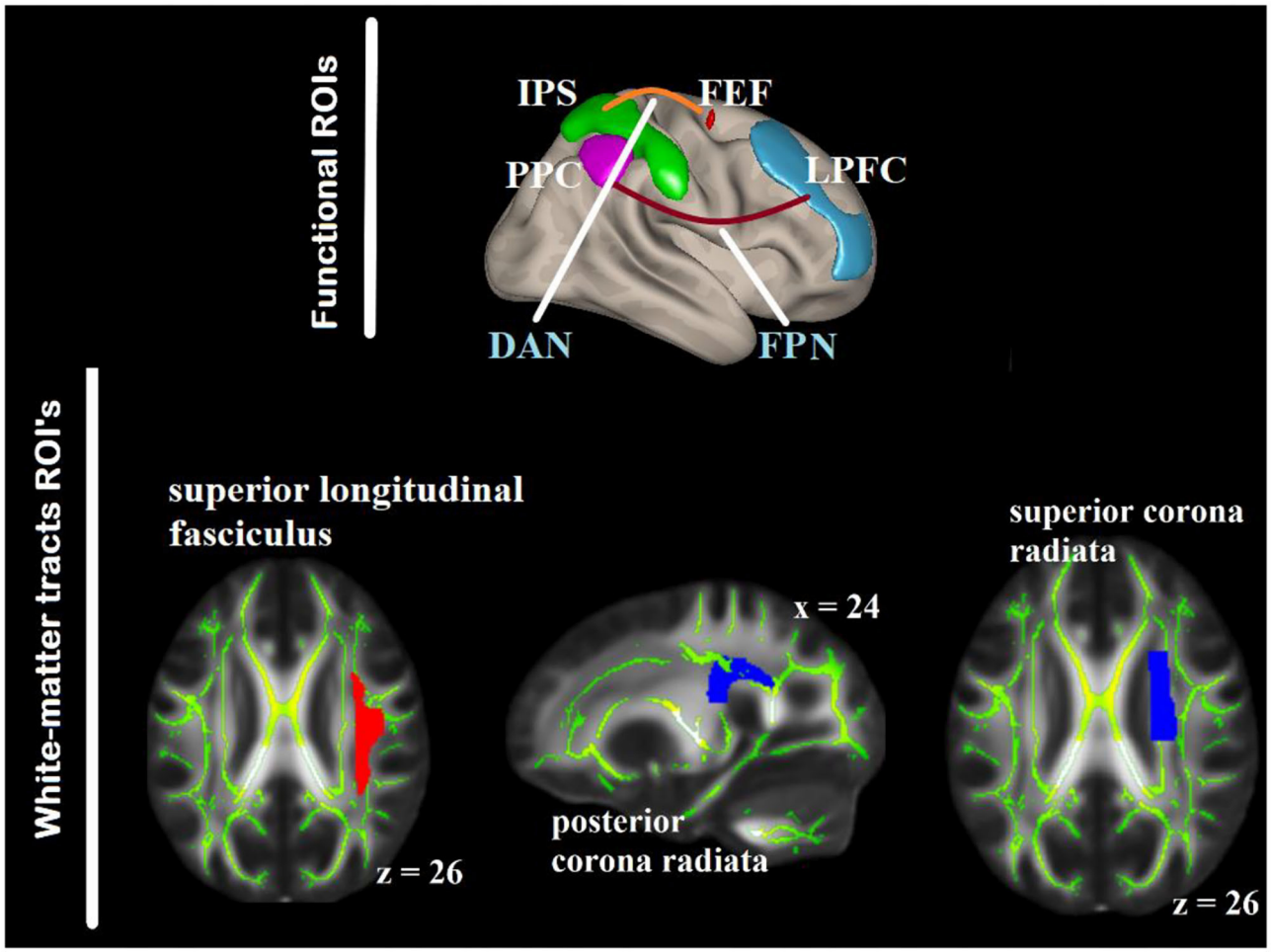

FIGURE 3 | ROIs within the DAN and FPN as seed regions for the gPPI analysis (**top**) defined based on anatomical areas from the Harvard–Oxford atlas included in CONN. The white-matter ROIs are overlaid on the FMRIB58_FA_1-mm standard-space and the mean FA skeleton of both the groups (**bottom**). DAN, dorsal attention networks; FPN, fronto-parietal network; PPC, posterior parietal cortex; IPS, intra-parietal sulcus; FEF, frontal eye-fields, LPFC, lateral prefrontal cortex.

and used as a mask to interrogate the FA values from each participant using "fslmeants" on the all_FA_skeletonized image in FSL. After obtaining the functional and structural ROIs, we tested the relationships between the aSC and eSC task-related effective connectivities within the FPN (cIPL and LPFC) and DAN (IPS and FEF) with the FA values in the PCR, SLF, and SCR. To achieve this, the model for the seed-to-voxel effective functional connectivity analysis contains young FA > old FA as in the between-subject contrasts, aSC > eSC as in the between-condition contrasts, and one seed region in each of the DAN and FPN as in the between source contrasts.

Seed-to-Voxel Connectivity Analysis: Generalized Psycho-Physiological Interaction

The association between functional connectivity and FA during allocentric and egocentric spatial condition along the FPAN was examined using the seed-to-voxel effective functional connectivity analysis of the CONN toolbox (63), following gPPI (64). Using gPPI, we extracted the average BOLD time series from four predefined seed region masks. In our data, both the FA with RT and FA with BOLD relationships were lateralized to the right hemisphere. Studies have also shown that visuospatial attention is mainly maintained by the right hemisphere (1, 65), and thus only the right FPAN seed regions were drawn. The regions were the FEF, IPS, and LPFC. IPS and FEF are parts of the DAN which has been found to relate to object in space (7, 18) and PPC and LPFC are parts the FPN which are related to attentional control (7, 8). The following gPPI regressors were modeled:

1. All of the task effect (allocentric, egocentric, and neutral) convolved with hemodynamic response function (HRF);
2. The seeds (IPS, FEF, LPFC, and PPC) BOLD time series with a task regressors corresponding to the allocentric, egocentric, and neutral; and,
3. The interaction term of those seed regions time series with a task regressor corresponding to the three conditions convolved with HRF.

The aSC, eSC, and neutral-specific connectivity regressors were submitted to a gPPI model to conduct task-modulated seed-to-voxel connectivity analyses. Each seed-to-voxel gPPI map reflecting the regressors above were constructed for each participant. The seed-to-voxel gPPI maps were used to test the effects of between-subject and between-condition contrasts at the group level across each seed.

The gPPI contrast maps for each model were generated, and the results were displayed using the statistical parametric mapping (SPM12). The corresponding group-level beta-weights for each contrast were extracted and plotted along the connectivity brain maps.

RESULTS

The Association Between Functional Connectivity and FA in Aging During Allocentric and Egocentric Spatial Coding

There were associations between FA in the PCR and DAN under the influence of the aSC and eSC task effects (**Figure 4**, **Table 2**). Compared to the older participants, FA values of the PCR for the younger participants showed significant positive association with the connectivity between the right FEF and the anterior temporal fusiform cortex (aTFusC) [$T(47) = 5.05$, $p < 0.01$] and showed negative association with the connectivity between the right FEF and superior division of lateral occipital cortex (sLOC) [$T(47) = -4.62$, $p < 0.001$] and between the right FEF and PaCiG [$T(47) = -5.18$, $p < 0.001$] in the aSC > eSC contrast. Moreover, for the aSC condition, the younger participants showed significant association between connectivity in the right IPS and central opercular cortex [CO: $T(47) = 5.33$, $p < 0.03$] and negative association with connectivity between the right IPS and the caudate [$T(47) = -6.39$, $p < 0.03$].

There were associations between the FA values in the PCR and FPN under the influence of the aSC and eSC task effects (**Figure 4**, **Table 2**). Compared to the older participants, the FA values of the PCR among the younger participants were significantly associated with the connectivity between the right LPFC and LG [$T(47) = 5.73$, $p < 0.02$], right LPFC and pSTG [$T(47) = 4.25$, $p < 0.03$], right LPFC and aMTG [$T(47) = 4.34$, $p < 0.03$], and significantly but negatively associated with the connectivity between the right LPFC and sLOC [$T(47) = -5.77$, $p < 0.03$] in the aSC > eSC contrast. Moreover, for the aSC condition, the FA values of the PCR for the younger participants showed significant association with the connectivity between the right PPC and iLOC [$T(47) = 4.34$, $p < 0.02$] and between right PPC aITG $T(47) = 4.47$, $p < 0.04$).

There were associations between the FA values of the SLF and DAN under the influence of the aSC and eSC task effects (**Figure 5**, **Table 3**). Compared to the older participants, the FA values of the SLF among the younger participants was significantly associated with the connectivity between the right FEF and SFG [$T(47) = 4.37$, $p < 0.001$] and right FEF and Cereb $T(47) = 5.26$, $p < 0.001$), and significantly and negatively associated with the connectivity between the right FEF and precuneus [$T(47) = -4.34$, $p < 0.001$], right FEF and aSMG [$T(47) = -4.91$, $p < 0.001$], and right FEF and SMA $T(47) = -5.89$, $p < 0.001$] for the aSC > eSC contrast. Moreover, for the aSC condition, the FA values for the younger participants showed significantly and negatively association with the connectivity between the right IPS and subcallosal cortex [SUbCal: $T(47) = -5.46$, $p < 0.001$], right IPS and MFG [$T(47) = -4.30$, $p < 0.01$], and right IPS and pITG [$T(47) = -4.80$, $p < 0.01$].

There were associations between the FA values in the SLF and FPN under the influence of the aSC and eSC task effects (**Figure 5**, **Table 3**). Compared to the older participants, the FA values of the SLF for the younger participants was significantly associated with the connectivity between the right LPFC and IC [$T(47) = 4.39$, $p < 0.01$], and significantly and negatively associated with the connectivity between the right LPFC and PCC [$T(47) = -5.03$, $p < 0.001$], right LPFC and sLOC [$T(47) = -4.14$, $p < 0.01$], right LPFC and SFG [$T(47) = -4.15$, $p < 0.04$], and right LPFC and cerebellum (49) $= -5.04$, $p < 0.04$] for the contrast between aSC > 33 eSC. Moreover, for the aSC condition, the FA values for the younger participants showed significant association with the connectivity between the right PPC and medial frontal cortex [$T(47) = 4.99$, $p < 0.001$] and right PPC and TPJ [$T(47) = 4.49$, $p < 0.03$], negatively associated with connectivity between right PPC and PaCiG [$T(47) = -5.49$, $p < 0.001$], right PPC and PO [$T(47) = -4.62$, $p < 0.001$], and right PPC and PoCG [$T(47) = -4.65$, $p < 0.02$].

There were associations between the FA values of the SLF and DAN under the influence of the aSC and eSC task effects (**Figure 6**, **Table 4**). Compared to the older participants, the FA values of the SCR among the younger participants were positively associated with the connectivity between the right FEF and SFG [$T(47) = 5.06$, $p < 0.001$], right FEF and FO [$T(47) = 4.24$, $p < 0.02$], right FEF and forb [$T(47) = 4.16$, $p < 0.02$], and significantly and negatively associated with the connectivity between the right FEF and TO [$T(47) = -3.98$, $p < 0.001$], right FEF and aSMG [$T(47) = -5.59$, $p < 0.001$], right FEF and PoCG [$T(47) = -4.15$, $p < 0.04$] for the aSC > eSC. Moreover, for the allocentric condition, the FA values for the younger participants showed significant association with the connectivity between the right IPS and PaCig [$T(47) = 4.55$, $p < 0.01$], right IPS and Fob [$T(47) = 4.85$, $p < 0.01$], right IPS and PrecG [$T(47) = 4.02$, $p < 0.01$].

There were associations between the FA values of the SCR and DAN under the influence of the allocentric and egocentric task effects (**Figure 6**, **Table 4**). Compared to older participants, the FA values of the SCR among the younger participants were significantly associated with the connectivity between the right FEF and SFG [$T(47) = 5.06$, $p < 0.001$], right FEF and FO [$T(47) = 4.24$, $p < 0.02$], right FEF and forb [$T(47) = 4.16$, $p < 0.02$], and significantly and negatively associated with the connectivity between the right FEF and TO [$T(47) = -3.98$, $p < 0.001$], right FEF and aSMG [$T(47) = -5.59$, $p < 0.001$], right FEF and PoCG [$T(47) = -4.15$, $p < 0.04$] for the aSC > eSC contrast. Moreover, for the allocentric condition, the FA values for the younger participants showed significant association with the connectivity between the right IPS and PaCig [$T(47) = 4.55$, $p < 0.01$], right IPS and Fob [$T(47) = 4.85$, $p < 0.01$], right IPS and PrecG [$T(47) = 4.02$, $p < 0.01$].

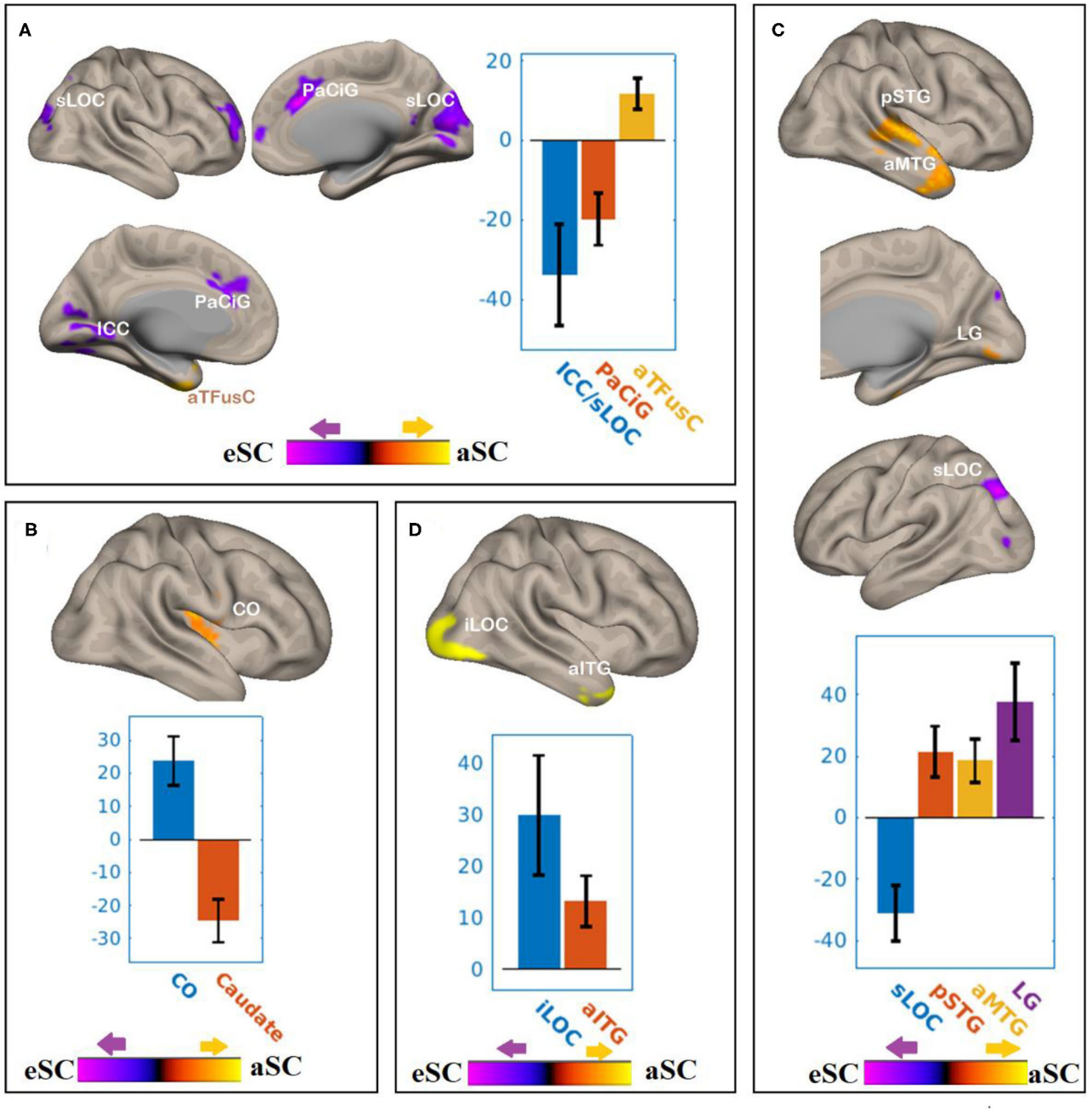

FIGURE 4 | The differences between the younger and older participants in association between the FPN and DAN connectivity the with the FA values of PCR under the influence of the allocentric and egocentric task effects. **(A)** PCR–FEF for aSC > eSC. **(B)** PCR–IPS for aSC > eSC. **(C)** PCR–LPFC for aSC > eSC. **(D)** PCR–PPC for aSC > eSC. The connectivity blobs are thresholded and cluster-level corrected using FDR for multiple comparison at $p = 0.05$. Color bar coding: Violet represents an increased (positive) and reduced (negative) in functional connectivity for the eSC and aSC condition, respectively, whereas the hot represents an increased (positive) and reduced (negative) in functional connectivity for the aSC and eSC condition, respectively. sLOC, superior division of lateral occipital cortex; ICC, intracalcarine cortex; PaCiG, Para-cingulate gyrus; CO, central opercular cortex; pSTG, posterior division of superior temporal gyrus; aMTG, anterior division of middle temporal gyrus; LG, lingual gyrus; iLOC, inferior division of lateral occipital cortex.

DISCUSSION

The gPPI analysis examined the difference between aSC and eSC task-dependent brain network organizations of the DAN and FPAN in aging and delineated its association to the white-matter tracts of the PCR, SCR, and SLF. Efficient modulation of both allocentric and egocentric spatial coding in FPAN requires structure–function interaction. Allocentric

TABLE 2 | Summary on the results based on the seeds constructed within the DAN and FPN for the young_PCR > old_PCR as the between-subject contrast and aSC > eSC as the between-condition contrast.

Seed	Functional connectivity region	K_E	Hemi	Coordinates			P_{FDR}	Peak t
				X	*y*	*Z*		
FEF	Superior lateral occipital cortex	2,254	L	−18	−66	2	<0.001	−4.62
	Paracingulate gyrus	1,492	R	10	28	28	<0.001	−5.18
	Anterior temporal fusiform cortex	650	L	−30	−4	−40	0.01	5.05
IPS	Central opercular cortex	843	R	42	−18	20	0.03	5.33
	Caudate	832	R	2	−20	14	0.03	−6.39
LPFC	Lingual gyrus	885	R	30	−100	−8	0.02	5.73
	Posterior superior temporal gyrus	711	R	62	−20	0	0.03	4.25
	Anterior middle temporal gyrus	680	R	56	14	−32	0.03	4.34
	Superior lateral occipital gyrus	630	L	−18	−78	−40	0.03	−5.77
PPC	Inferior lateral occipital cortex	994	R	38	−84	−10	0.02	4.34
	Anterior inferior temporal gyrus	786	R	36	16	−44	0.04	4.47

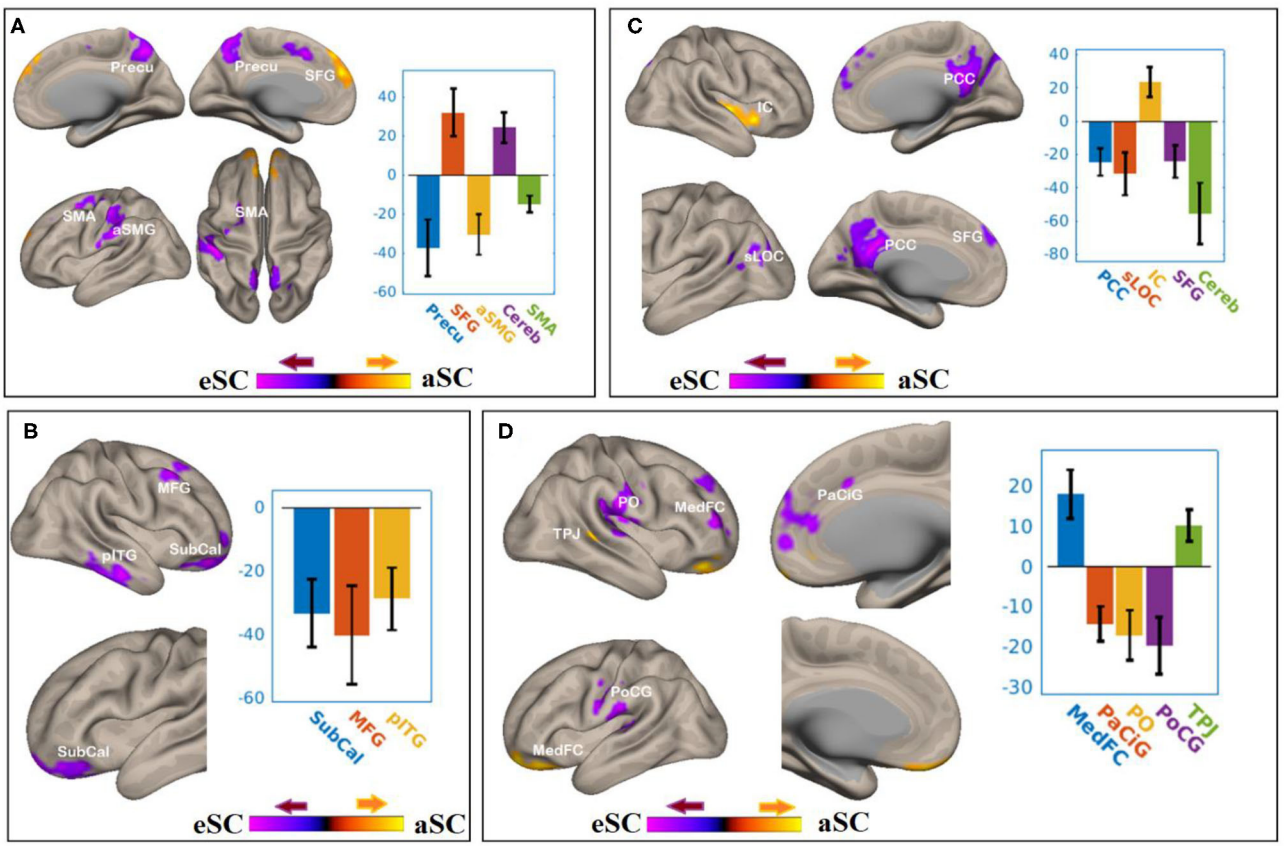

FIGURE 5 | The difference between the younger and older participants in the FPN and DAN connectivity in association ith the FA values of the SLF under the aSC and eSC task effects. **(A)** SLF–FEF for aSC > eSC. **(B)** SLF–IPS for aSC > eSC. **(C)** SLF–LPFC for aSC > eSC. **(D)** SLF–PPC for aSC > eSC. The connectivity blobs are thresholded and cluster-level corrected using FDR for multiple comparison at $p = 0.05$. Color bar coding: violet represents an increased (positive) and reduced (negative) in functional connectivity for the egocentric and aSC condition, respectively, whereas the hot represents an increased (positive) and reduced (negative) in functional connectivity for the aSC and eSC condition, respectively compared to one another. Precu, precuneus; SMA, somatosensory motor area; SMG, supramarginal gyrus; SFG, superior frontal gyrus; MFG, middle frontal gyrus; pITG, posterior division of inferior temporal gyrus; PCC, posterior cingulate cortex; SFG, superior frontal gyrus; sLOC, superior division of lateral occipital cortex; PO, parietal operculum; MedFC, medial prefrontal cortex; PaCiG, paracingulate gyrus; PoCG, postcentyral gyrus; TPJ, temporoparietal junction.

TABLE 3 | Summary on the results for the seeds constructed within the DAN and FPN for the young_SLF > OLD_SLF as the between-subject contrast, aSC > eSC as the between-condition contrast.

Seed	Functional connectivity region	K_E	Hemi	Coordinates			P_{FDR}	Peak t
				x	*y*	*z*		
FEF	Precuneus	1,567	R	0	−60	50	<0.001	−4.34
	Superior frontal gyrus	1,466	R	4	64	28	<0.001	4.37
	Anterior supramarginal gyrus	1,351	L	−46	−30	36	<0.001	−4.91
	Cerebellum	1,257	R	22	−84	−34	<0.001	5.26
	Somatosensory association area	966	L	−16	8	48	<0.001	−5.89
IPS	Subcallosal cortex	2,062	R	20	46	−12	<0.001	−5.46
	Middle frontal gyrus	751	R	34	14	46	0.01	−4.30
	Posterior inferior temporal gyrus	739	R	52	−18	−24	0.01	−4.80
LPFC	Posterior cingulate cortex	3,030	R	2	−46	24	<0.001	−5.03
	Superior lateral occipital cortex	696	L	−54	−66	16	0.01	−4.14
	Insular cortex	616	R	38	−14	0	0.01	4.39
	Superior frontal gyrus	464	R	−6	62	36	0.04	−4.15
	Cerebellum	456	L	−24	−84	−30	0.04	−5.04
PPC	Medial frontal cortex	1,883	L	−18	52	−22	<0.001	4.99
	Para-cingulate gyrus	1,359	R	16	48	16	<0.001	−5.49
	Parietal operculum	1,181	R	62	−20	26	<0.001	−4.62
	Postcentral gyrus	653	L	−46	−16	30	0.02	−4.65
	Temporooccipital area	578	R	22	−30	20	0.03	4.49

task-modulated connectivity of the FPN and DAN with the temporal lobe was influenced by the aging differences of the white-matter tracts of the PCR and SCR, respectively. On the other hand, aging difference of the SLF mainly influenced the egocentric-task modulated connections of the DAN and FPN with frontal regions and posterior cingulate cortex. This study suggested that functional connections of the FPAN with near and far task-relevant nodes vary significantly with age and conditions. Overall, the results showed variability in the magnitude and direction of connectivity changes in association with different white-matter ROIs in to response to aSC and eSC along DAN and FPN. Covarying with aging difference in FA, aSC task-modulated connectivity changes of FEF brought negative connectivity association with sLOC, parietal regions (precuneus, SMG), and frontal regions (SMA, SFG, and paracingulate gyrus) and an increase in connectivity mainly in frontal regions (SFG, fronto-orbital cortex).

Frontal eye-fields connectivity changes could be interpreted in two equally appealing ways that efficient aSC processing in younger adults may have required lesser resources compared to older adults along the interpretation of neural efficiency (66, 67), and that the difference between aSC and eSC processing may have attributed to the nature of FEF connection to near (e.g., SFG and paracingulate gyrus) and far (e.g., sLOC and precuenus) brain regions. FEF connection tends to facilitate an eSC processing in sLOC, precuneus, SMG, and paracingulate gyrus than it facilitates for the aSC. These evidences are consistent to previous studies highlighted the role of FEF in processing top–down content of eSC (1, 7, 8). Ptak and Schnider (18) suggested that FEF holds neurons to encode egocentric associated action template. In addition, using aSC and eSC task requiring top–down attention allocation, the neural pathway of the FEF to IPS was revealed to be unique to the egocentric spatial coding (2), suggesting that compared to younger adults, the slower RT and lesser FC in FEF among older adults may have been accounted for by the difference in connectivity within the DAN (IPS, FEF). However, the FC results shown that a strong preference of FEF during eSC over the IPS was observed. This also tends to supports single cell recording study showing that parietal (PPC) and frontal (FEF) neurons detect target locations at a different pace across paradigms in visual attention in that FEF encode targets requiring top–down allocation earlier than PPC neurons and PPC neurons encodes targets in bottom–up attention processing earlier than the FEF neurons (68).

Allocentric task-modulated connectivity of FEF was also observed with anterior division of temporo-fusiform cortex, consistent to the mainstream hypothesis that aSC subserved by the ventral stream and that the aSC tend to demand working memory resources, which involves the temporal lobe (14–16). From the hierarchical multiple regression results, among older adults, it was shown that the account variance attributed by FA in PCR to the aSC activities of IPL was above and beyond the other WM tracts. Using PCR as a covariate, negative aSC-modulated connectivity exists between FEF and anterior temporal fusiform cortex and FEF and central opercular cortex was shown. These two regions are thought to engage in memory-guided visuospatial attention tasks (69), and thus PCR might mediate between these two neural areas in aSC.

Regarding the FPAN mask in association with WM tract ROIs on aSC and eSC task-modulated FC, the results showed that,

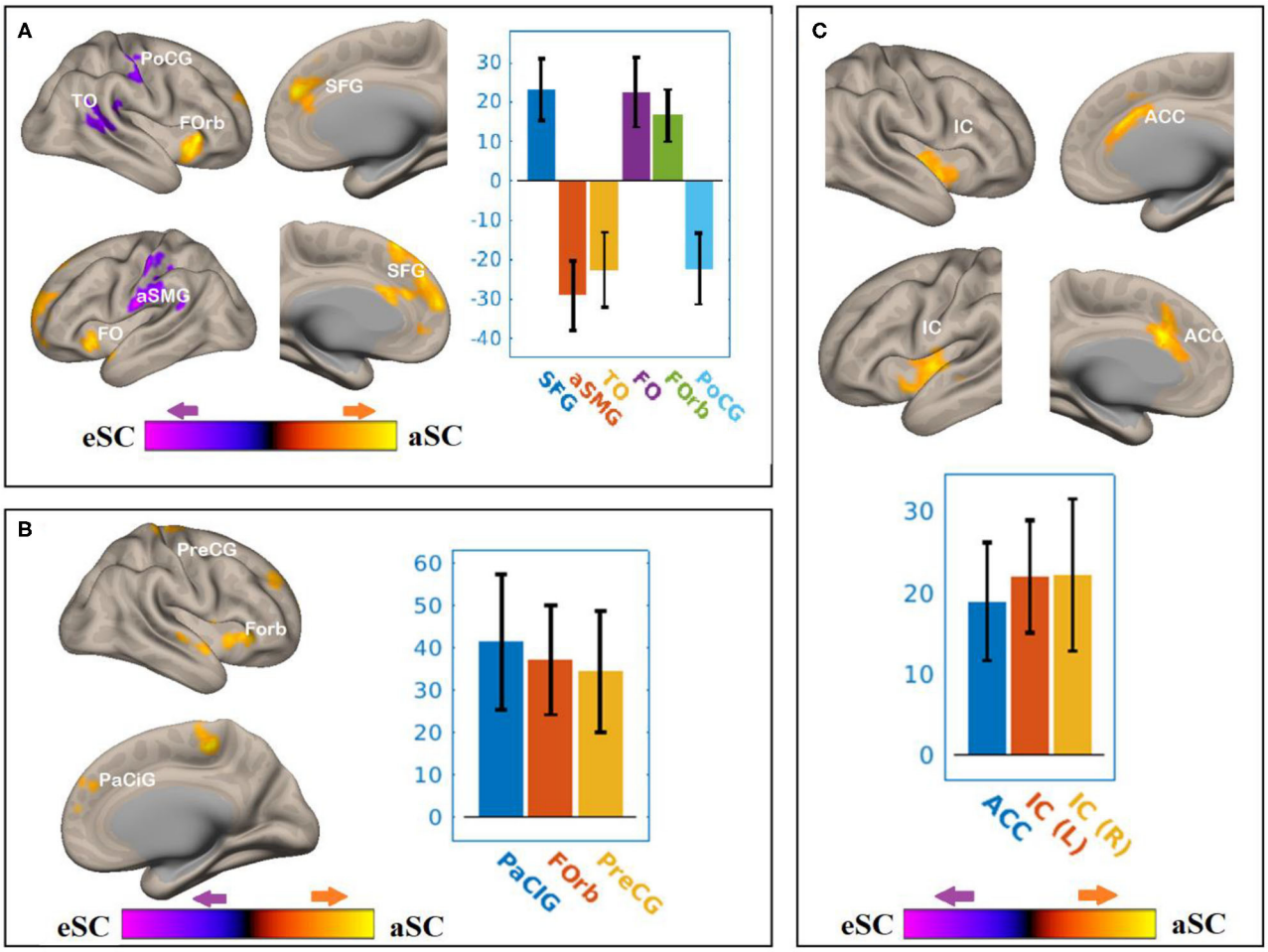

FIGURE 6 | The differences between the younger and older participants in the FPN and DAN connectivity in association with the FA values of the SCR under the influence of the allocentric and egocentric task effects. **(A)** SCR–FEF for aSC > eSC. **(B)** SCR–IPS for aSC > eSC. **(C)** SCR–LPFC for aSC > eSC. The connectivity blobs are thresholded and cluster-level corrected using FDR for multiple comparison at $p = 0.05$. Color bar coding: violet represents an increased (positive) and reduced (negative) in functional connectivity for the egocentric and allocentric condition, respectively, whereas the hot represents an increased (positive) and reduced (negative) in functional connectivity for the allocentric and egocentric condition, respectively. TO, temporo-occipital; PoCG, post central gyrus; Forb, Fronto orbital cortex; SFG, superior frontal gyrus; FO, frontal operculum; aSMG, anterior division of supramarginal gyrus; PaCIG, para-cingulate gyrus; IC, inter-calarine cortex; IC, insular cortex.

compared to eSC, a greater age-related decline of aSC-modulated connectivity of the LPFC with lingual gyrus, posterior STG, anterior ITG, and insular cortex was observed. The connectivity between LPFC and temporal regions is the key in maintaining attention control (41) and encodes in an aSC map (Ref.). Age-related decline of connectivity of LPFC temporal regions was strongly linked to disrupt the feedforward and feedback loop of signals projected to frontal regions for attention execution (42). The results are in agreement with neuroimaging evidence, which showed that older adults tends to rely (preserved) on egocentric orienting (43) alongside specific reduction in aSC orienting (44), which was linked to the alteration of structure–function relationship of the LPFC-MT pathway (1, 14, 46), especially when the task at hand demands visual short-term memory involvement (45). As a consequence of aging effects on the relationship of brain structure and function in orienting and reorienting, differences in the mechanisms underlying spatial representations has been reported (3). The WM nodes in corona radiata was suggested to explain the age-related decline in attention control (41), which the present evidence strongly supports.

The other key region of FPAN examined was the PPC. In association with WM tract of the PCR on aSC and eSC task-modulated FC, the results showed that, compared to eSC, a greater age-related decline of aSC modulated connectivity of the PPC with inferior LOC and anterior ITG was observed. It has been shown that the PPC is a part of the DAN maintaining visuospatial control of the primed action (70), and LOC is parts of ventral parts of the occipito-temporal cortex modulated by long-term representation of objects in the

TABLE 4 | Summary on the results based on the seeds constructed within the DAN and FPN for the young_SCR > old_SCR as the between-subject contrast, and the aSC > eSC as the between-condition contrast.

Seed	Functional connectivity region	K_E	Hemi	Coordinates			P_{FDR}	Peak t
				x	*y*	*z*		
FEF	Superior frontal gyrus	2,479	L	2	44	26	<0.001	5.06
	Anterior supramarginal gyrus	1,339	L	−64	−14	22	<0.001	−5.59
	Temporooccipital gyrus	756	R	50	−38	18	<0.001	−3.98
	Fronto oribital cortex	556	L	−20	22	−4	0.02	4.24
	Fronto orbital cortex	523	R	28	28	−2	0.02	4.16
	Post central gyrus	433	R	58	−18	50	0.04	−4.15
IPS	Para-cingulate gyrus	946	R	0	48	16	0.01	4.55
	Fronto oribital cortex	839	R	34	36	0	0.01	4.85
	Precentral gyrus	748	L	−4	−36	56	0.01	4.02
LPFC	Anterior cingulate	1,091	L	−2	20	32	<0.001	5.58
	Insular cortex	848	L	−60	−10	4	<0.001	4.33
	Insular cortex	557	R	48	−10	0	0.02	4.10

visual-field (71). This implicates that maintenance of aSC may have required both the dorsal (for action control) and ventral stream (for memory-guided object recognition on the visual field) interactions. The WM tract in PCR may have played a greater role in connecting both streams for age-related decline in aSC. Unlike eSC, aSC may have dominated by maintaining visual scene and retrieved the task rule [see (72)]. If eSC is preserved and aSC processing capacity is reduced due to aging (3) on compromise attention control areas (73, 74), then aSC-modulated connectivity of LPFC may have been the hot spot of the functional difference. The results clearly support this premise that compared to older adults, younger adults showed positive (an increase) aSC-modulated connectivity of LPFC with ACC and insular cortex. The fronto-insular cortex and ACC is thought to play a critical role in switching between task-associated rules and executive attention (74–76), suggesting that aging may have altered the switching capabilities between aSC and eSC. The alteration of aSC-modulated connectivity during aSC execution might have linked to the WM nodes of the superior corona radiata.

This study has several limitations, and readers should interpret the results with caution. First, to examine the function–structure interaction, only BOLD signal of the contrast between aSC > eSC was used. Generalization of the results must consider the task-specific differences of the connectivity for aSC > neutral and eSC > neutral. Second, to obtain the FA values, the structural ROI were defined using previous studies on behavior–FA relationships. Readers must consider the reproducibility differences between data-driven and predefined ROI quantifications. Lastly, it is unclear whether age-related differences in WM integrity represent age-related differences in spatial coding with those predefined ROI tracts, or instead are global effects occurring across as age.

DATA AVAILABILITY STATEMENT

The raw data supporting the conclusions of this article will be made available by the authors, without undue reservation.

ETHICS STATEMENT

The studies involving human participants were reviewed and approved by Ethic Committees of the Affiliated Rehabilitation Hospital, Fujian University of Traditional Chinese Medicine and written informed consent was obtained from all participants prior to the experiment. The patients/participants provided their written informed consent to participate in this study.

AUTHOR CONTRIBUTIONS

AD: conceptualization, analysis, investigation, method, writing–original draft, and writing–review and editing. BC: supervision and writing–review and editing. CC: funding acquisition, conceptualization, supervision, validation, writing–original draft, and writing–review and editing. All authors contributed to the article and approved the submitted version.

FUNDING

The General Research Fund of Research Grant Council of Hong Kong (151044) partially supported this study.

ACKNOWLEDGMENTS

The authors thank the University Research Facility in Behavioral and Systems Neuroscience at the Hong Kong Polytechnic University for its support.

REFERENCES

1. Kravitz DJ, Saleem KS, Baker CI, Mishkin M. A new neural framework for visuospatial processing. *Nat Rev Neurosci.* (2011) 12:217–30. doi: 10.1038/nrn3008
2. Szczepanski SM, Pinsk MA, Douglas MM, Kastner S, Saalmann YB. Functional and structural architecture of the human dorsal frontoparietal attention network. *Proc Natl Acad Sci USA.* (2013) 110:15806–11. doi: 10.1073/pnas.1313903110
3. Colombo D, Serino S, Tuena C, Pedroli E, Dakanalis A, Cipresso P, et al. Egocentric and allocentric spatial reference frames in aging: A systematic review. *Neurosci Biobehav Rev.* (2017) 80:605–21. doi: 10.1016/j.neubiorev.2017.07.012
4. Bennett, I. J., Motes, M. A., Rao, N. K., and Rypma, B. (2012). White matter tract integrity predicts visual search performance in young and older adults. *Neurobiol Aging.* 33:433. e421–31. doi: 10.1016/j.neurobiolaging.2011.02.001
5. Madden DJ, Spaniol J, Whiting WL, Bucur B, Provenzale JM, Cabeza R, et al. Adult age differences in the functional neuroanatomy of visual attention: a combined fMRI and DTI study. *Neurobiol Aging.* (2007) 28:459–76. doi: 10.1016/j.neurobiolaging.2006.01.005
6. Sullivan EV, Rohlfing T, Pfefferbaum A. Quantitative fiber tracking of lateral and interhemispheric white matter systems in normal aging: relations to timed performance. *Neurobiol Aging.* (2010) 31:464–81. doi: 10.1016/j.neurobiolaging.2008.04.007
7. Ptak R. The frontoparietal attention network of the human brain: action, saliency, and a priority map of the environment. *Neuroscientist.* (2012) 18:502–15. doi: 10.1177/1073858411409051
8. Vossel S, Geng JJ, Fink GR. Dorsal and ventral attention systems: distinct neural circuits but collaborative roles. *Neuroscientist.* (2014) 20:150–9. doi: 10.1177/1073858413494269
9. Corbetta M, Kincade MJ, Lewis C, Snyder AZ, Sapir A. Neural basis and recovery of spatial attention deficits in spatial neglect. *Nat Neurosci.* (2005) 8:1603–10. doi: 10.1038/nn1574
10. Corbetta M, Patel G, Shulman GL. The reorienting system of the human brain: from environment to theory of mind. *Neuron.* (2008) 58:306–24. doi: 10.1016/j.neuron.2008.04.017
11. Derbie AY, Chau B, Lam B, Fang YH, Ting KH, Wong CYH, Chan, CCH. et al. Cortical hemodynamic response associated with spatial coding: a near-infrared spectroscopy study. *Brain Topogr.* (2021) 34:207–20. doi: 10.1007/s10548-021-00821-9
12. Kravitz DJ, Saleem KS, Baker CI, Ungerleider LG, Mishkin M. The ventral visual pathway: an expanded neural framework for the processing of object quality. *Trends Cogn Sci.* (2013) 17:26–49. doi: 10.1016/j.tics.2012.10.011
13. Cieslik EC, Zilles K, Grefkes C, Eickhoff SB. Dynamic interactions in the fronto-parietal network during a manual stimulus–response compatibility task. *Neuroimage.* (2011) 58:860–9. doi: 10.1016/j.neuroimage.2011.05.089
14. Byrne P, Becker S, Burgess N. Remembering the past and imagining the future: a neural model of spatial memory and imagery. *Psychol Rev.* (2007) 114:340–75. doi: 10.1037/0033-295X.114.2.340
15. Chen Y, Monaco S, Byrne P, Yan X, Henriques DY, Crawford JD. Allocentric versus egocentric representation of remembered reach targets in human cortex. *J Neurosci.* (2014) 34:12515–26. doi: 10.1523/JNEUROSCI.1445-14.2014
16. Milner AD, Goodale MA. Two visual systems re-viewed. *Neuropsychologia.* (2008) 46:774–85. doi: 10.1016/j.neuropsychologia.2007.10.005
17. De Schotten MT, Dell'Acqua F, Forkel SJ, Simmons A, Vergani F, Murphy DG, et al. A lateralized brain network for visuospatial attention. *Nature neuroscience.* (2011) 14:1245. doi: 10.1038/nn.2905
18. Ptak R, Schnider A. The dorsal attention network mediates orienting toward behaviorally relevant stimuli in spatial neglect. *J Neurosci.* (2010) 30:12557–65. doi: 10.1523/JNEUROSCI.2722-10.2010
19. Prado J, Carp J, Weissman DH. Variations of response time in a selective attention task are linked to variations of functional connectivity in the attentional network. *Neuroimage.* (2011) 54:541–9. doi: 10.1016/j.neuroimage.2010.08.022
20. Vaessen MJ, Saj A, Lovblad K-O, Gschwind M, Vuilleumier P. Structural white-matter connections mediating distinct behavioral components of spatial neglect in right brain-damaged patients. *Cortex.* (2016) 77:54–68. doi: 10.1016/j.cortex.2015.12.008
21. Tuch DS, Salat DH, Wisco JJ, Zaleta AK, Hevelone ND, Rosas HD. Choice reaction time performance correlates with diffusion anisotropy in white matter pathways supporting visuospatial attention. *Proc Natl Acad Sci USA.* (2005) 102:12212–7. doi: 10.1073/pnas.0407259102
22. Yin X, Han Y, Ge H, Xu W, Huang R, Zhang D, et al. Inferior frontal white matter asymmetry correlates with executive control of attention. *Hum Brain Mapp.* (2013) 34:796–813. doi: 10.1002/hbm.21477
23. Yin HH, Mulcare SP, Hilario MR, Clouse E, Holloway T, Davis MI, et al. Dynamic reorganization of striatal circuits during the acquisition and consolidation of a skill. *Nat Neurosci.* (2009) 12:333–41. doi: 10.1038/nn.2261
24. Heilman KM, Van Den Abell T. Right hemisphere dominance for attention: the mechanism underlying hemispheric asymmetries of inattention (neglect). *Neurology.* (1980) 30:327–327. doi: 10.1212/WNL.30.3.327
25. Seghier ML. The angular gyrus: multiple functions and multiple subdivisions. *Neuroscientist.* (2013) 19:43–61. doi: 10.1177/1073858412440596
26. Park HJ, Kim JJ, Lee SK, Seok JH, Chun J, Kim DI, et al. Corpus callosal connection mapping using cortical gray matter parcellation and DT-MRI. *Hum Brain Mapp.* (2008) 29:503–16. doi: 10.1002/hbm.20314
27. Chechlacz M, Rotshtein P, Bickerton W-L, Hansen PC, Deb S, Humphreys GW. Separating neural correlates of allocentric and egocentric neglect: distinct cortical sites and common white matter disconnections. *Cogn Neuropsychol.* (2010) 27:277–303. doi: 10.1080/02643294.2010.519699
28. Fattori P, Raos V, Breveglieri R, Bosco A, Marzocchi N, Galletti C. The dorsomedial pathway is not just for reaching: grasping neurons in the medial parieto-occipital cortex of the macaque monkey. *J Neurosci.* (2010) 30:342–9. doi: 10.1523/JNEUROSCI.3800-09.2010
29. Galletti C, Gamberini M, Kutz DF, Fattori P, Luppino G, Matelli M. The cortical connections of area V6: an occipito-parietal network processing visual information. *Eur J Neurosci.* (2001) 13:1572–88. doi: 10.1046/j.0953-816x.2001.01538.x
30. Derbie AY, Chau BKH, Wong CHY, Chen LD, Ting KH, Lam BYH, Smith, Y. et al. Common and distinct neural trends of allocentric and egocentric spatial coding: An ALE meta-analysis. *Eur J Neurosci.* (2021) 53:3672–87. doi: 10.1111/ejn.15240
31. Chafee MV, Averbeck BB, Crowe DA. Representing spatial relationships in posterior parietal cortex: single neurons code object-referenced position. *Cereb Cortex.* (2007) 17:2914–32. doi: 10.1093/cercor/bhm017
32. Crowe DA, Averbeck BB, Chafee MV. Neural ensemble decoding reveals a correlate of viewer-to object-centered spatial transformation in monkey parietal cortex. *J Neurosci.* (2008) 28:5218–28. doi: 10.1523/JNEUROSCI.5105-07.2008
33. Hashimoto R, Tanaka Y, Nakano I. Heading disorientation: a new test and a possible underlying mechanism. *Eur Neurol.* (2010) 63:87–93. doi: 10.1159/000276398
34. Erel H, Levy DA. Orienting of visual attention in aging. *Neurosci Biobehav Rev.* (2016) 69:357–80. doi: 10.1016/j.neubiorev.2016.08.010
35. Vann SD, Aggleton JP, Maguire EA. What does the retrosplenial cortex do? *Nature Reviews Neuroscience.* (2009) 10:792. doi: 10.1038/nrn2733
36. Hopfinger JB, Buonocore MH, Mangun GR. The neural mechanisms of top-down attentional control. *Nat Neurosci.* (2000) 3:284–91. doi: 10.1038/72999
37. Gola M, Kamiński J, Brzezicka A, Wróbel A. Beta band oscillations as a correlate of alertness—changes in aging. *Int J Psychophysiol.* (2012) 85:62–7. doi: 10.1016/j.ijpsycho.2011.09.001
38. Gamboz N, Zamarian S, Cavallero C. Age-related differences in the attention network test (ANT). *Exp Aging Res.* (2010) 36:287–305. doi: 10.1080/0361073X.2010.484729
39. Turner GR, Spreng RN. Executive functions and neurocognitive aging: dissociable patterns of brain activity. *Neurobiol Aging.* (2012) 33:826. e821–13. doi: 10.1016/j.neurobiolaging.2011.06.005
40. Grady C. The cognitive neuroscience of ageing. *Nat Rev Neurosci.* (2012) 13:491–505. doi: 10.1038/nrn3256
41. Niogi SN, Mukherjee P, Ghajar J, Johnson CE, Kolster R, Lee H, et al. Structural dissociation of attentional control and memory in adults with and without mild traumatic brain injury. *Brain.* (2008) 131:3209–21. doi: 10.1093/brain/awn247

42. Amso D, Scerif G. The attentive brain: insights from developmental cognitive neuroscience. *Nat Rev Neurosci.* (2015) 16:606–19. doi: 10.1038/nrn4025
43. Rodgers MK, Sindone JA III, Moffat SD. Effects of age on navigation strategy. *Neurobiol Aging.* (2012) 33:202.e215–22. doi: 10.1016/j.neurobiolaging.2010.07.021
44. Harris MA, Wolbers T. How age-related strategy switching deficits affect wayfinding in complex environments. *Neurobiol Aging.* (2014) 35:1095–102. doi: 10.1016/j.neurobiolaging.2013.10.086
45. Montefinese M, Sulpizio V, Galati G, Committeri G. Age-related effects on spatial memory across viewpoint changes relative to different reference frames. *Psychol Res.* (2015) 79:687–97. doi: 10.1007/s00426-014-0598-9
46. Boccia M, Sulpizio V, Nemmi F, Guariglia C, Galati G. Direct and indirect parieto-medial temporal pathways for spatial navigation in humans: evidence from resting-state functional connectivity. *Brain Struct Funct.* (2017) 222:1945–57. doi: 10.1007/s00429-016-1318-6
47. Lu J, Li D, Li F, Zhou A, Wang F, Zuo X, et al. Montreal cognitive assessment in detecting cognitive impairment in Chinese elderly individuals: a population-based study. *J Geriatr Psychiatry Neurol.* (2011) 24:184–90. doi: 10.1177/0891988711422528
48. Julayanont P, Brousseau M, Chertkow H, Phillips N, Nasreddine ZS. Montreal cognitive assessment memory index score (MoCA-MIS) as a predictor of conversion from mild cognitive impairment to alzheimer's disease. *J Am Geriatr Soc.* (2014) 62:679–84. doi: 10.1111/jgs.12742
49. Julayanont P, Nasreddine ZS. Montreal cognitive assessment (MoCA): concept and clinical review. In: *Cognitive Screening Instruments*: New York, NY, US: Springer (2017). p. 139–95.
50. Wilson KD, Woldorff MG, Mangun GR. Control networks and hemispheric asymmetries in parietal cortex during attentional orienting in different spatial reference frames. *Neuroimage.* (2005) 25:668–83. doi: 10.1016/j.neuroimage.2004.07.075
51. Smith SM, Jenkinson M, Woolrich MW, Beckmann CF, Behrens TE, Johansen-Berg H, et al. Advances in functional and structural MR image analysis and implementation as FSL. *Neuroimage.* (2004) 23 Suppl 1:S208–219. doi: 10.1016/j.neuroimage.2004.07.051
52. Smith SM. Fast robust automated brain extraction. *Hum Brain Mapp.* (2002) 17:143–55. doi: 10.1002/hbm.10062
53. Jenkinson M, Bannister P, Brady M, Smith S. Improved optimization for the robust and accurate linear registration and motion correction of brain images. *Neuroimage.* (2002) 17:825–41. doi: 10.1006/nimg.2002.1132
54. Greve DN, Fischl B. Accurate and Robust Brain Image Alignment using Boundary-based Registration. *Neuroimage.* (2009) 48:63–72. doi: 10.1016/j.neuroimage.2009.06.060
55. Smith SM, Jenkinson M, Johansen-Berg H, Rueckert D, Nichols TE, Mackay CE, et al. Tract-based spatial statistics: voxelwise analysis of multi-subject diffusion data. *Neuroimage.* (2006) 31:1487–505. doi: 10.1016/j.neuroimage.2006.02.024
56. Andersson JL, Jenkinson M, Smith S. Non-linear optimisation. FMRIB technical report TR07JA1. *Practice.* (2007).
57. Smith SM, Nichols TE. Threshold-free cluster enhancement: addressing problems of smoothing, threshold dependence and localisation in cluster inference. *Neuroimage.* (2009) 44:83–98. doi: 10.1016/j.neuroimage.2008.03.061
58. Desikan RS, Segonne F, Fischl B, Quinn BT, Dickerson BC, Blacker D, et al. An automated labeling system for subdividing the human cerebral cortex on MRI scans into gyral based regions of interest. *Neuroimage.* (2006) 31:968–80. doi: 10.1016/j.neuroimage.2006.01.021
59. Fox MD, Corbetta M, Snyder AZ, Vincent JL, Raichle ME. Spontaneous neuronal activity distinguishes human dorsal and ventral attention systems. *Proc Natl Acad Sci USA.* (2006) 103:10046–51. doi: 10.1073/pnas.0604187103
60. Chechlacz M, Humphreys GW, Sotiropoulos SN, Kennard C, Cazzoli D. Structural organization of the corpus callosum predicts attentional shifts after continuous theta burst stimulation. *J Neurosci.* (2015) 35:15353–68. doi: 10.1523/JNEUROSCI.2610-15.2015
61. Voineskos AN, Rajji TK, Lobaugh NJ, Miranda D, Shenton ME, Kennedy JL, et al. Age-related decline in white matter tract integrity and cognitive performance: a DTI tractography and structural equation modeling study. *Neurobiol Aging.* (2012) 33:21–34. doi: 10.1016/j.neurobiolaging.2010.02.009
62. Mori S, Oishi K, Jiang H, Jiang L, Li X, Akhter K, et al. Stereotaxic white matter atlas based on diffusion tensor imaging in an ICBM template. *Neuroimage.* (2008) 40:570–82. doi: 10.1016/j.neuroimage.2007.12.035
63. Whitfield-Gabrieli S, Nieto-Castanon A. Conn: a functional connectivity toolbox for correlated and anticorrelated brain networks. *Brain Connect.* (2012) 2:125–41. doi: 10.1089/brain.2012.0073
64. McLaren DG, Ries ML, Xu G, Johnson SC. A generalized form of context-dependent psychophysiological interactions (gPPI): A comparison to standard approaches. *Neuroimage.* (2012) 61:1277–86. doi: 10.1016/j.neuroimage.2012.03.068
65. Corbetta M, Shulman GL. Control of goal-directed and stimulus-driven attention in the brain. *Nat Rev Neurosci.* (2002) 3:201–15. doi: 10.1038/nrn755
66. Davis KD, Moayedi M. Central mechanisms of pain revealed through functional and structural MRI. *J Neuroimmune Pharmacol.* (2013) 8:518–34. doi: 10.1007/s11481-012-9386-8
67. Haier RJ, Siegel BV, Nuechterlein KH, Hazlett E, Wu JC, Paek J, et al. Cortical glucose metabolic rate correlates of abstract reasoning and attention studied with positron emission tomography. *Intelligence.* (1988) 12:199–217. doi: 10.1016/0160-2896(88)90016-5
68. Buschman TJ, Miller EK. Top-down versus bottom-up control of attention in the prefrontal and posterior parietal cortices. *Science.* (2007) 315:1860–2. doi: 10.1126/science.1138071
69. Goldfarb EV, Chun MM, Phelps EA. Memory-guided attention: independent contributions of the hippocampus and striatum. *Neuron.* (2016) 89:317–24. doi: 10.1016/j.neuron.2015.12.014
70. Goodale MA, Milner AD. Separate visual pathways for perception and action. *Trends Neurosci.* (1992) 15:20–5. doi: 10.1016/0166-2236(92)90344-8
71. James TW, Humphrey GK, Gati JS, Menon RS, Goodale MA. Differential effects of viewpoint on object-driven activation in dorsal and ventral streams. *Neuron.* (2002) 35:793–801. doi: 10.1016/S0896-6273(02)00803-6
72. Committeri G, Galati G, Paradis AL, Pizzamiglio L, Berthoz A, LeBihan D. Reference frames for spatial cognition: different brain areas are involved in viewer-, object-, and landmark-centered judgments about object location. *J Cogn Neurosci.* (2004) 16:1517–35. doi: 10.1162/0898929042568550
73. Boccia M, Nemmi F, Guariglia C. Neuropsychology of environmental navigation in humans: review and meta-analysis of fMRI studies in healthy participants. *Neuropsychol Rev.* (2014) 24:236–51. doi: 10.1007/s11065-014-9247-8
74. Zhu Z, Johnson NF, Kim C, Gold BT. Reduced frontal cortex efficiency is associated with lower white matter integrity in aging. *Cereb Cortex.* (2015) 25:138–46. doi: 10.1093/cercor/bht212
75. Fan J, McCandliss BD, Fossella J, Flombaum JI, Posner MI. The activation of attentional networks. *Neuroimage.* (2005) 26:471–9. doi: 10.1016/j.neuroimage.2005.02.004
76. Sridharan D, Levitin DJ, Menon V. A critical role for the right fronto-insular cortex in switching between central-executive and default-mode networks. *Proc Nat Acad Sci.* (2008) 105:12569–74. doi: 10.1073/pnas.0800005105

Conflict of Interest: The authors declare that the research was conducted in the absence of any commercial or financial relationships that could be construed as a potential conflict of interest.

frontiers | Frontiers in Neurology

TYPE Correction
PUBLISHED 17 August 2022
DOI 10.3389/fneur.2022.1006645

OPEN ACCESS

APPROVED BY
Frontiers Editorial Office,
Frontiers Media SA, Switzerland

*CORRESPONDENCE
Abiot Y. Derbie
abiot.yenealem@bdu.edu.et

SPECIALTY SECTION
This article was submitted to Applied Neuroimaging, a section of the journal Frontiers in Neurology

RECEIVED 29 July 2022
ACCEPTED 02 August 2022
PUBLISHED 17 August 2022

CITATION
Derbie AY, Chau BKH and Chan CCH (2022) Corrigendum: Functional and structural architectures of allocentric and egocentric spatial coding in aging: A combined DTI and fMRI study. *Front. Neurol.* 13:1006645. doi: 10.3389/fneur.2022.1006645

Corrigendum: Functional and structural architectures of allocentric and egocentric spatial coding in aging: A combined DTI and fMRI study

Abiot Y. Derbie[1,2]*, Bolton K. H. Chau[1] and Chetwyn C. H. Chan[3]

[1]Applied Cognitive Neuroscience Laboratory, Department of Rehabilitation Sciences, The Hong Kong Polytechnic University, Kowloon, Hong Kong SAR, China, [2]Department of Psychology, Bahir Dar University, Bahir Dar, Ethiopia, [3]Department of Psychology, The Education University of Hong Kong, Tai Po, Hong Kong SAR, China

KEYWORDS

FPAN, allocentric spatial coding, egocentric spatial coding, spatial representation, frame of reference, white matter integrity, functional magnetic brain imaging (fMRI)

A corrigendum on

Functional and structural architectures of allocentric and egocentric spatial coding in aging: A combined DTI and fMRI study

by Derbie, A. Y., Chau, B. K. H., and Chan, C. C. H. (2022). *Front. Neurol.* 12:802975. doi: 10.3389/fneur.2021.802975

In the published article, there was an error regarding the affiliation for Bolton K. H. Chau. Instead of "Department of Psychology, Bahir Dar University, Bahir Dar, Ethiopia" it should be "Applied Cognitive Neuroscience Laboratory, Department of Rehabilitation Sciences, The Hong Kong Polytechnic University, Kowloon, Hong Kong SAR, China."

The authors apologize for this error and state that this does not change the scientific conclusions of the article in any way. The original article has been updated.

Publisher's note

All claims expressed in this article are solely those of the authors and do not necessarily represent those of their affiliated organizations, or those of the publisher, the editors and the reviewers. Any product that may be evaluated in this article, or claim that may be made by its manufacturer, is not guaranteed or endorsed by the publisher.

frontiers in Neurology

ORIGINAL RESEARCH
published: 02 February 2022
doi: 10.3389/fneur.2022.790607

Random Network and Non-rich-club Organization Tendency in Children With Non-syndromic Cleft Lip and Palate After Articulation Rehabilitation: A Diffusion Study

Bo Rao[1†], *Hua Cheng*[2†], *Haibo Xu*[1*] *and Yun Peng*[2*]

[1] *Department of Radiology, Zhongnan Hospital of Wuhan University, Wuhan University, Wuhan, China,* [2] *Department of Radiology, National Center for Children's Health, Beijing Children's Hospital, Capital Medical University, Beijing, China*

OPEN ACCESS

Edited by:
Graziano Serrao,
University of Milan, Italy

Reviewed by:
Federica Ruggiero,
University of Bologna, Italy
Matteo Figini,
University College London,
United Kingdom

***Correspondence:**
Haibo Xu
xuhaibo1120@hotmail.com
Yun Peng
ppengyun@hotmail.com

†These authors have contributed equally to this work and share first authorship

Specialty section:
This article was submitted to Applied Neuroimaging, a section of the journal Frontiers in Neurology

Received: *07 October 2021*
Accepted: *03 January 2022*
Published: *02 February 2022*

Citation:
Rao B, Cheng H, Xu H and Peng Y (2022) Random Network and Non-rich-club Organization Tendency in Children With Non-syndromic Cleft Lip and Palate After Articulation Rehabilitation: A Diffusion Study. Front. Neurol. 13:790607. doi: 10.3389/fneur.2022.790607

Objective: The neuroimaging pattern in brain networks after articulation rehabilitation can be detected using graph theory and multivariate pattern analysis (MVPA). In this study, we hypothesized that the characteristics of the topology pattern of brain structural network in articulation-rehabilitated children with non-syndromic cleft lip and palate (NSCLP) were similar to that in healthy comparisons.

Methods: A total of 28 children with NSCLP and 28 controls with typical development were scanned for diffusion tensor imaging on a 3T MRI scanner. Structural networks were constructed, and their topological properties were obtained. Besides, the Chinese language clear degree scale (CLCDS) scores were used for correlation analysis with topological features in patients with NSCLP.

Results: The NSCLP group showed a similar rich-club connection pattern, but decreased small-world index, normalized rich-club coefficient, and increased connectivity strength of connections compared to controls. The univariate and multivariate patterns of the structural network in articulation-rehabilitated children were primarily in the feeder and local connections, covering sensorimotor, visual, frontoparietal, default mode, salience, and language networks, and orbitofrontal cortex. In addition, the connections that were significantly correlated with the CLCDS scores, as well as the weighted regions for classification, were chiefly distributed in the dorsal and ventral stream associated with the language networks of the non-dominant hemisphere.

Conclusion: The average level rich-club connection pattern and the compensatory of the feeder and local connections mainly covering language networks may be related to the CLCDS in articulation-rehabilitated children with NSCLP. However, the patterns of small-world and rich-club structural organization in the articulation-rehabilitated children exhibited a random network and non-rich-club organization tendency. These findings enhanced the understanding of neuroimaging patterns in children with NSCLP after articulation rehabilitation.

Keywords: non-syndromic cleft lip and palate, articulation rehabilitation, diffusion tensor imaging, small-worldness, rich-club organization, graph theory

INTRODUCTION

Cleft lip and palate (CLP) is one of the most common craniofacial malformations in infants, and its prevalence has been estimated to be one in 1,000 live births (1). Non-syndromic CLP (NSCLP) is not included in any kind of well-known congenital syndrome and its incidence of articulation disorders ranges from 22 to 92% (2). Even with early surgical treatment, 30–50% of patients with CLP still suffer from cleft palate articulation characterized by hypernasality and/or nasal emissions (3). Articulation therapy is the primary management approach, along with physical management through surgery, combined with motor learning principles by visual, auditory, and touch feedback assistance (4).

Previous studies have found functional and structural changes in the brain in CLP children. The broadly decreased volumes of the subcortical nuclei and the frontal lobe (5), cerebral white matter (6), cerebellum (7), and ventral frontal cortex (8) were found in CLP children. Moreover, adult NSCLP participants after articulation rehabilitation showed increased cortical folding in brain areas related to language, auditory, and execution compared to adults with NSCLP and control participants (9). A subvocalization task performed by adults with CLP during a functional MRI study, although the left hippocampus exhibited increased activation, the rest of the brain regions showed similar brain activity in articulation rehabilitated patients relative to healthy comparison (10). Our recent study based on resting-state functional MRI that detected the increased capability of information transmission and integration involving language and social cognition brain areas in children with CLP after articulation rehabilitation. In addition, we found an increased small-world index in these patients which means optimum equilibrium between local specialization and global integration to process information (11). The structural organization of CLP children in the developing brain after articulation rehabilitation still needs to be investigated.

Graph theory has been broadly used in neuroimaging studies for healthy participants and clinical patients to assess the topological properties of network organizations (12). The graph theory technique can evaluate the small-world properties and rich-club organization of brain networks. There is an optimal balance between global integration and local specialization for information processing in a small-world brain network (13). Rich-club organization is the central hub of a network, exhibiting more density connections than the peripheral regions (14) and can promote neural signaling and integrated information across different brain areas (15). The multivariate pattern analysis (MVPA) is based on a data-driven technique widely used to analyze neuroimaging data. Such a technique could provide not only discriminative spatial patterns but also the quantification of therapy effects at the individual level (16). Additionally, the features contributing most strongly to individual classification could be identified (17). To date, there have been no MVPA studies on CLP children. Therefore, we used the MVPA to explore the structural topology pattern in articulation-rehabilitated children with NSCLP, which might improve our understanding of the recovery mechanism of structural brain networks. We hypothesized the topology pattern of brain structural network in articulation-rehabilitated childrenwith NSCLP was similar to that in healthy comparisons by the MVPA method.

In this study, diffusion tensor imaging (DTI) data were collected and structural brain networks were reconstructed for children with NSCLP after articulation rehabilitation and healthy comparison. We aimed to investigate the pattern of the structural network topology in NSCLP children after articulation rehabilitation with graph theory and the MVPA technique.

MATERIALS AND METHODS

Participants

This study was approved by the Beijing Children's Hospital Ethical Committee and we obtained the informed consent of all the participants. A total of 28 children (mean age 10.0 ± 2.3 years, 21/7 male/female) with NSCLP and 28 typical developing healthy comparisons (age- and sex-matched) were included in this study from January 2016 to September 2017. No NSCLP participants were excluded because of the well-matching. The children with CLP would be excluded when the experienced medical geneticist suspected them within a well-known congenital syndrome by evaluating their medical histories, clinical signs, and genetics files. All the children received a Chinese speech intelligibility test administered by three experienced speech pathologists. The inclusion criteria of children were as follows: (1) aged between 6 and 16 years old; (2) Chinese as the native language; (3) a successful CLP repair for velopharyngeal insufficiency. Speech therapy started 3–6 months after the surgery, 30 min/day, 3 times/week, and lasted for half a year till patients reached a score of 86 points of the CLCDS (full credit was 100 points), which was considered as a clear line of rehabilitation; (4) normal vision and hearing auditory brainstem response (ABR) < 30 dB nHL]; (5) right-handed; and (6) the Chinese Wechsler Intelligence Scale for Children-IV (CWISC-IV) scores ≥ 90, average intelligence). The exclusion criteria were as follows: (1) articulation disorder (the CLCDS scores < 86); (2) dysgnosia; (3) velopharyngeal insufficiency; (4) vision and/or hearing defects; (5) congenital disorders; (6) developmental delays; (7) other chronic health diseases; and (8) other syndromes or possible syndromes.

Image Acquisition

All the participants were scanned on a 3 T GE MRI (750, Discovery) system for DTI and T1-weighted data. For each participant, DTI data were acquired with a single-shot echo-planar imaging (EPI) sequence: matrix: 128×128, time repetition (TR)/time echo (TE) = 7,000/62 ms, slice thickness = 2 mm, field of view (FOV): 256×256, directions = 60, b-value = 0 and 1,000 s/mm^2, and 70 continuous axial slices. The sagittal T1-weighted data were acquired with the magnetization-prepared rapid gradient echo (MPRAGE); sequence: matrix = $256 \times 256 \times 164$, TR/TE = 8.6/3.4 ms, slice thickness = 1 mm, FOV = $240 \times 240 \times 164$, and FA = 12°. All the axial scans were placed parallel to the anterior-posterior commissure line.

Preprocessing

All the DTI data were processed using a pipeline tool, PANDA software (18) based on the FSL toolbox (https://

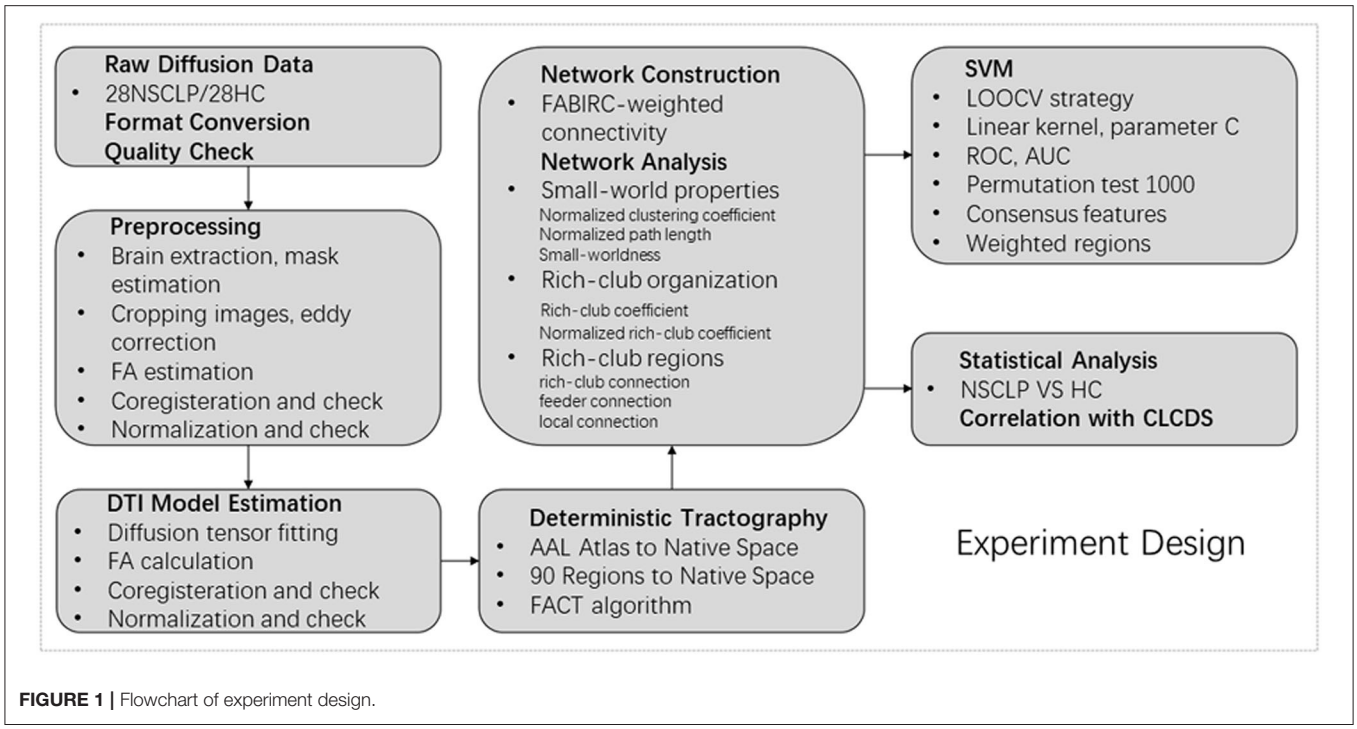

FIGURE 1 | Flowchart of experiment design.

TABLE 1 | Demographic and clinical characteristics.

	Age (years)	Boys/Girls	CLCDS score	CWISC-IV score	Education (years)	
Sample members	**Mean ± SD**	**Median**	**No.**	**Mean ± SD**	**Mean ± SD**	**Mean ± SD**
NSCLP children	10.0 ± 2.3	9.6	21/7	91.6 ± 4.0	97.5 ± 9.5	4.0 ± 2.2
Healthy controls	10.4 ± 2.0	9.5	21/7	–	99.8 ± 6.6	4.7 ± 2.3

NSCLP, non-syndromic cleft lip and palate; CLCDS, Chinese language clear degree scale; CWISC-IV, Chinese Wechsler Intelligence Scale for Children-IV.

fsl.fmrib.ox.ac.uk/fsl/fslwiki/). The main procedure was as follows: (1) format conversion and quality check: conversion from DICOM into NIFTI format and the deletion of poor-quality images. (2) Brain extraction and mask estimation: removal of non-brain tissues and calculation of brain masks. (3) Cropping images and eddy current correction: cropping the redundant parts of scans and correction to remove movements and eddy distortions using FSL FDT. (4) DTI metrics computation: diffusion tensor fitting and diffusion parameter, fractional anisotropy (FA) was calculated using FSL DTIFIT. (5) The FA images were coregistered from the native space to the corresponding T1-weighted images, then tissue borders were checked after coregistration. (6) Non-linear registering of the structural images from native space to the ICBM152 template for an inverse warping transformation and check tissue border after normalization. (7) The automated anatomical labeling (AAL) atlas was applied with the inverse warping transformation to individual native space. (8) The 90 regions of the AAL template inversely transformed were warped to the FA native space of each participant through the nearest neighbor interpolation method. One brain area was considered a node in the AAL atlas. (9) With fiber assignment by a continuous tracking (FACT) algorithm, white matter pathways of each DTI dataset were reconstructed and defined as fibers or tracts with streamlined tractography (19). A streamline was terminated based on its FA value < 0.1 or its turn $> 45°$ (15). Finally, from the original 33 patients, 5 patients were discharged due to poor quality, coregistration, and normalization.

Construction of the Brain Network

We calculated the FA-based interregional connection (FABIRC) as the average of the FA values of all contained streamlines, which formed the interregional connections. The 90×90 FABIRC-weighted connectivity matrices were calculated for all participants. With the GRETNA toolbox (http://www.nitrc.org/projects/gretna/) (20), the topological properties of the brain structural connectivity networks were estimated for all participants. We examined the properties of the structural brain networks and applied a series of threshold values for each graph's same number of edges. In this study, the related graph properties were assessed at threshold values from 0.05 to 0.5 (step 0.01) (21).

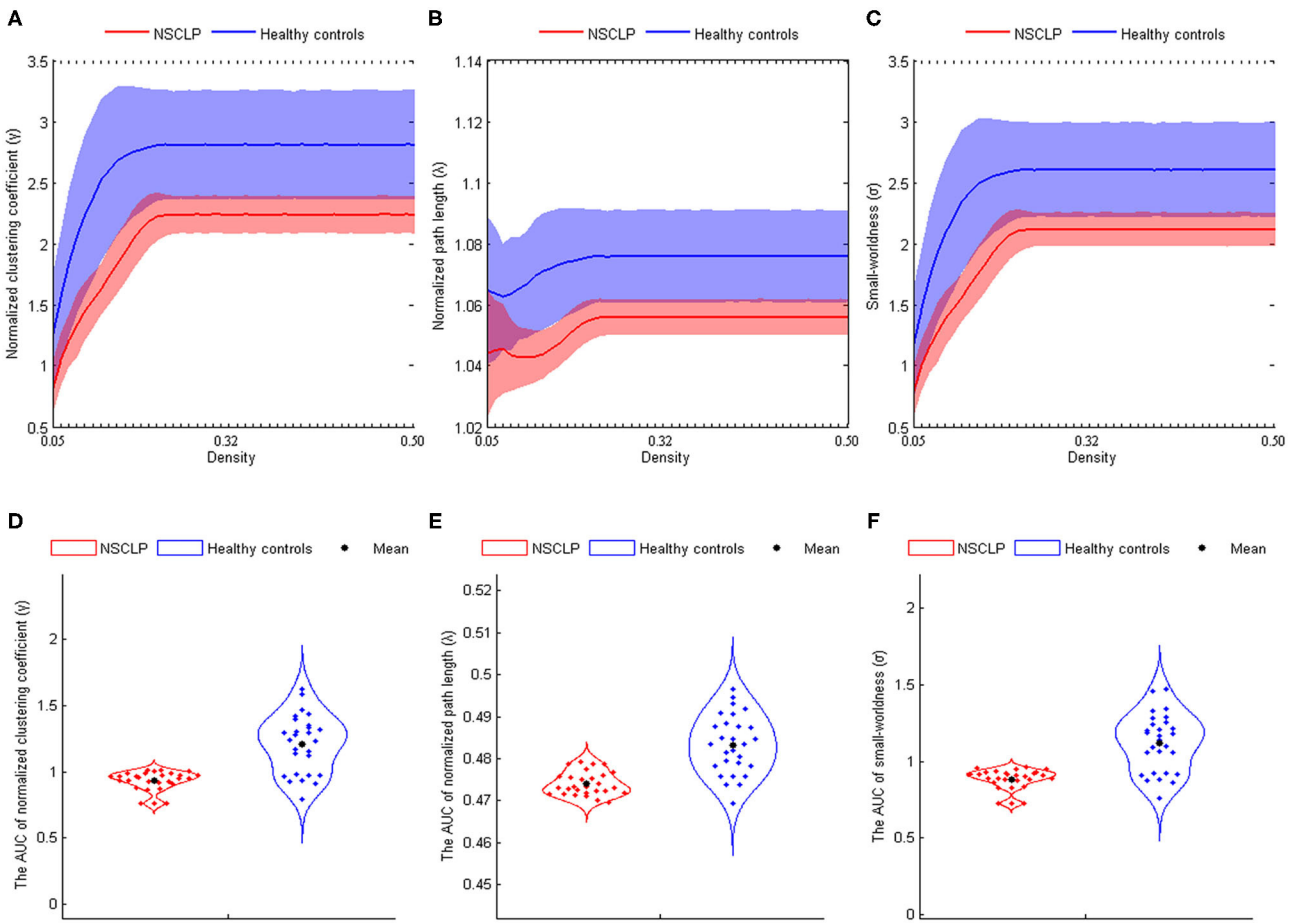

FIGURE 2 | (A–C) The normalized clustering coefficient **(A)**, normalized path length **(B)**, and small-world index **(C)** shown at the whole threshold. Shaded areas represent the standard deviation of the mean. **(D–F)**: Significant differences in the normalized clustering coefficient **(D)**, normalized path length **(E)**, and small-world index **(F)**. Corrected for age and gender. Two-sample two-tailed *t*-test, $p < 0.05$. AUC, area under the curve; NSCLP, non-syndromic cleft lip and palate; HC, healthy comparison.

Network Analysis

Graph theoretical analyses of the weighted structural networks of the patients with NSCLP and controls were estimated with routines by the GRETNA toolbox.

Small-World Properties

The network clustering coefficient (Cp) is the average clustering coefficient of the nodes of the network, representing the network segregation of the brain. The characteristic path length (Lp) is the mean shortest path length through all the possible pairs of network nodes, describing global information integration (22). The Cp was divided by the clustering coefficient of a set of random networks ($n = 5{,}000$) for a normalized clustering coefficient (γ) and the normalized path length (λ) was acquired using the same method (20). Small-worldness (σ) is defined as γ divided by λ and $\sigma > 1$ for small-world networks, characterizing the equilibrium of network segregation and integration (22).

Rich-Club Organization

The ratio of existing connections to full connections of the rich-club is defined as the rich-club coefficient (Φ) (23). Normalized rich-club coefficients (Φ_{norm}) are normalized Φ by a set of 1000 comparable random networks Φ_{rand} ($\Phi_{\text{norm}} = \Phi/\Phi_{\text{rand}}$) (24). $\Phi_{\text{norm}} > 1$ suggests the existence of rich-club organization across ranges of degrees (k) at a density of 16% (15, 25).

Rich-Club Regions

Ranking the brain Regions with the averaged degree across all the groups, the top 13 (15%) nodes were selected as the rich-club regions (25, 26). Based on the rich-club and non-rich-club regions, edges of the network are classified into rich-club connections between the rich-club regions, feeder connections between the rich-club and non-rich-club regions, and local connections between the non-rich-club regions (23). In addition, we calculated the connectivity strength of the three connection classes by summing the edge weights.

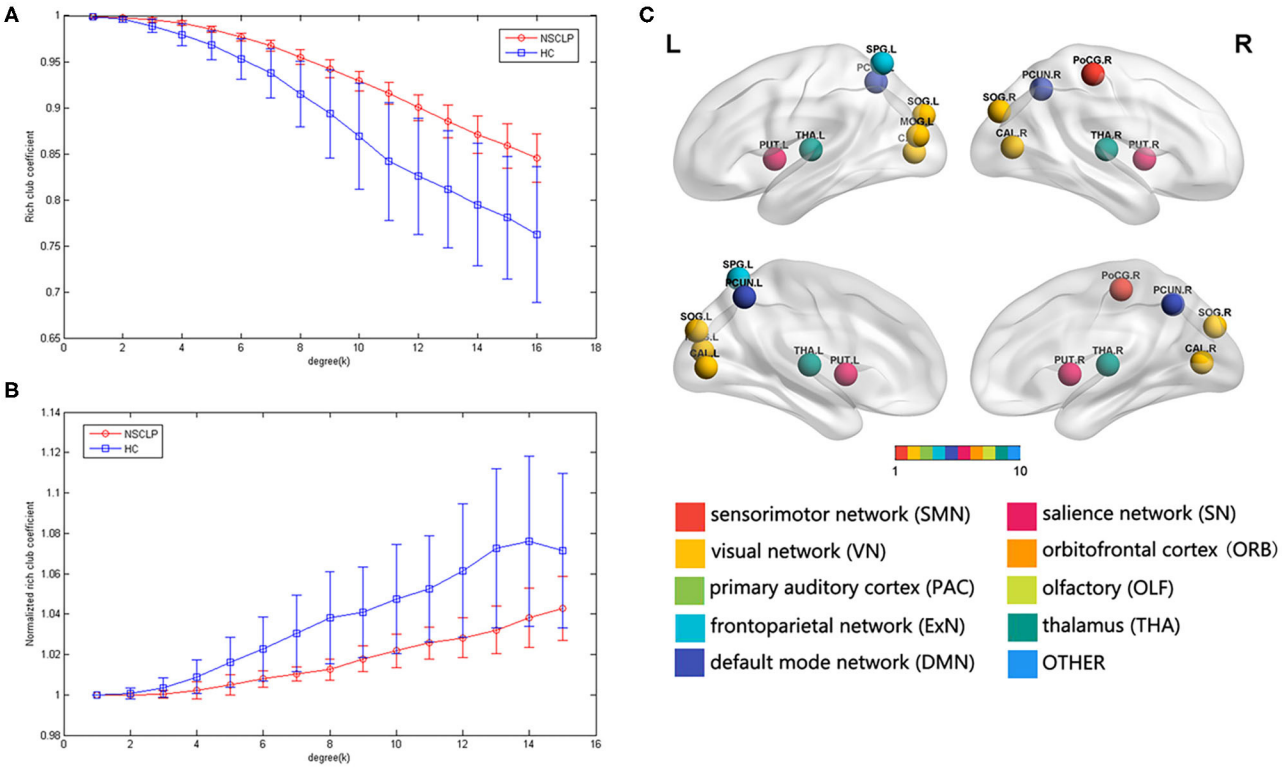

FIGURE 3 | (A,B) Group-averaged rich-club curve and standard error for patients (red) and controls (blue). **(A)**: rich-club coefficient (Φ), **(C)**: normalized rich-club coefficients (Φ_{norm}). **(C)**: rich-club regions across the patients and controls. The color of the balls indicates the intrinsic connectivity networks.

Classification of the Support Vector Machine (SVM)

We applied the F score method for feature selection (27). We used the leave-one-out cross-validation (LOOCV) method to estimate a classifier's performance by the limited number of samples (28). We adopted the linear kernel SVM classifier for classification using the LIBSVM toolbox, with optimized parameter Cs (27). Based on the LOOCV results, we quantified the performance of the classifier by the parameters of accuracy, sensitivity, specificity, and area under the receiver operating characteristic (ROC) curve (AUC). We used a permutation test to correct the classification results (1,000 times) (29). Furthermore, we considered the consensus features as the common features, which were always chosen for the final feature set by every LOOCV iteration. Finally, we defined the weighted regions from the consensus features. The previous literature describes the detailed steps (30).

Statistical Analysis

The statistics module was used to carry out all the statistical analyses in the GRETNA and LIBSVM toolboxes. We calculated the AUCs of small-world parameters over the density range (0.05–0.50). We used the two-sample t-tests to evaluate the intergroup differences in small-world properties, rich-club coefficients, normalized rich-club coefficients, rich-club, feeder and local connections, and three classes of connectivity strengths corrected for age and sex. In addition, the Chinese language clear degree scale (CLCDS) scores were performed for correlation analysis with the significant topological properties and consensus features in NSCLP children after articulation rehabilitation.

The flowchart of the experiment design is shown in **Figure 1**.

RESULTS

In this study, structural networks of the whole brain were constructed and the small-world and rich-club properties of children with NSCLP and healthy comparison were calculated in the density range of 0.05–0.50 (step 0.01).

Demographic Characteristics

The demographic characteristics of children are shown in **Table 1**, **Supplementary Table S1**. The age of children ($t = -0.46$, $p = 0.96$), CWISC-IV scores ($t = -1.19$, $p = 0.24$), and education ($t = -1.10$, $p = 0.28$) showed no significant between-group differences. The number of males was slightly higher than that of females among children with NSCLP and healthy comparison, but the distribution showed no significant differences (chi-squared test, $\chi^2 = 0$, $p = 1$) (see **Table 1**).

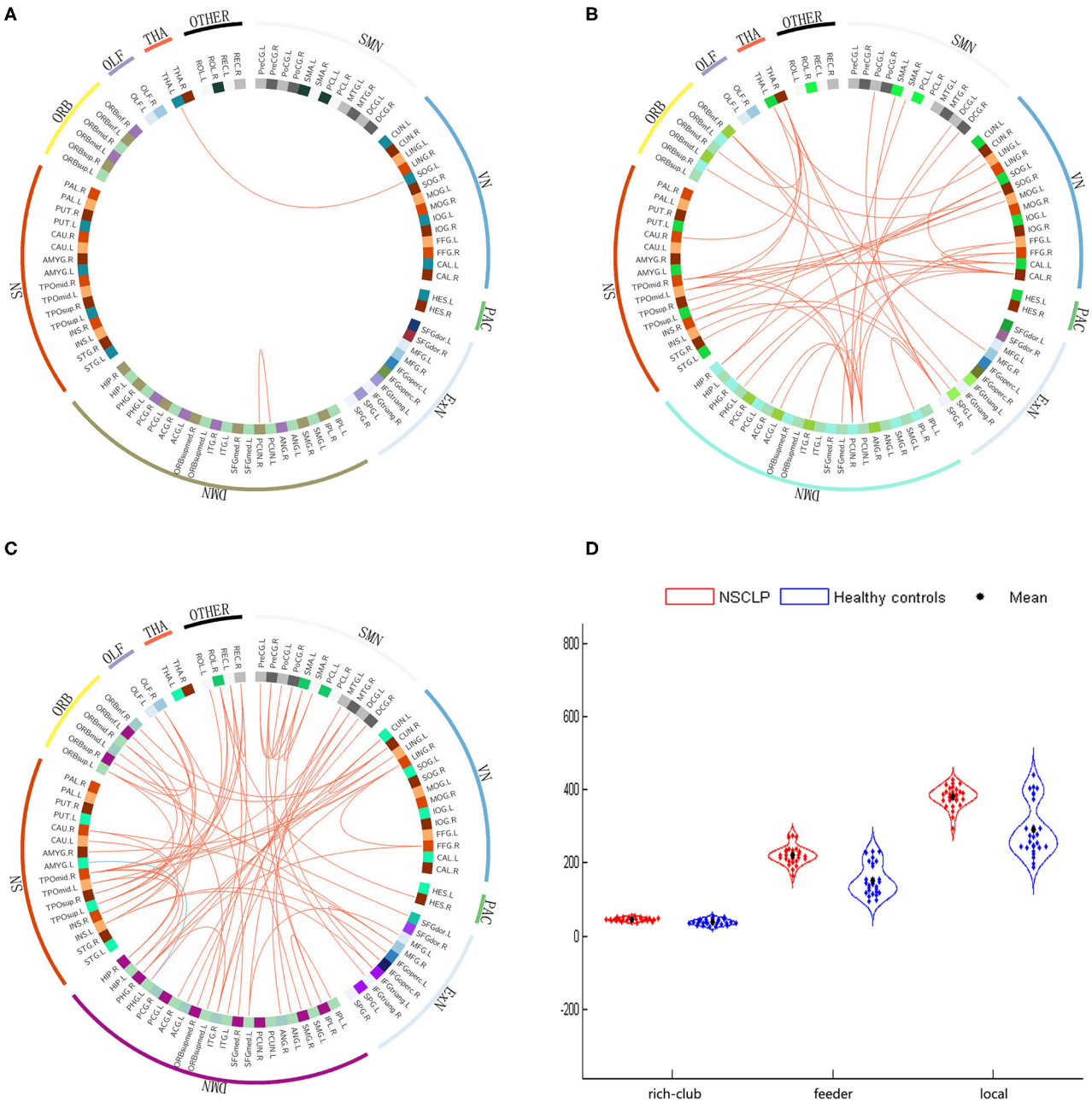

FIGURE 4 | (A–C): The different connections in the NSCLP group relative to healthy comparison. **(A)**: rich-club connections, **(B)**: feeder connections, **(C)**: local connections. Red edges indicate higher connectivity strength in the NSCLP group than in healthy comparison, and blue edges indicate lower connectivity strength. **(D)**: significantly altered between-group connectivity strength illustrated by rich-club, feeder, and local connections. SMN, sensorimotor network; VN, visual network; Exner, external frontoparietal network; DMN, default mode network; SN, salience network; ORB, orbitofrontal cortex; PAC, primary auditory cortex; TAH, thalamus; OLF, olfactory cortex.

Small-World Properties

In both the groups, the structural networks showed a small-world organization in the density of 0.06–0.50 ($\sigma > 1$, see **Figures 2A–C**). Furthermore, there were lower σ^{AUCs} ($t = -6.639$, $p < 0.001$), γ^{AUCs} ($t = -6.752$, $p < 0.001$), and λ^{AUCs} ($t = -7.028$, $p < 0.001$) in articulation-rehabilitated patients with NSCLP (see **Figures 2D,E**).

Rich-Club Organization

We found the rich-club organization and normalized rich-club coefficients $\Phi_{norm} > 1$ in children with NSCLP after articulation rehabilitation and the healthy comparison. A series of two-sample *t*-tests showed significant between-group differences in rich-club coefficients ($k = 4$–16, see **Figure 3A**, **Supplementary Table S2**) and normalized rich-club coefficients

Φ_{norm} (k = 5–15, see **Figure 3B**, **Supplementary Table S2**). The rich-club effects of most participants in each group (90%) were reported. Based on the averaged nodal degree across both groups, we considered the top 13 (15%) highest-degree nodes to be rich-club regions. The rich-club regions are exhibited in **Figure 5**, including 13 areas (in order of degree): the bilateral calcarine fissure and surrounding cortex (CAL), superior occipital gyrus (SOG), superior parietal lobule, precuneus (PCUN), putamen (PUT), thalamus (THA), and left middle occipital gyrus, which is in line with previous rich-club findings (31) (see **Figure 3C**). The remaining 73 regions were identified as peripheral regions.

Rich-Club Connections

We found significantly higher weighted rich-club connections between the left SOG and THA ($t = 2.75$, $p < 0.001$) and the left and right PCUN ($t = 4.57$, $p < 0.001$) in the NSCLP group than in the healthy comparison (see **Figure 4A**).

Feeder Connections

We detected that the values of the 42 feeder connections in the NSCLP group were significantly higher than those in the healthy comparison ($p < 0.001$). These peripheral regions were mostly involved in the sensorimotor network (SMN), visual network (VN), external frontoparietal network (ExN), default mode network (DMN), salience network (SN), and orbitofrontal cortex (ORB) (see **Figure 4B**) (30, 32, 33).

Local Connections

We observed that only one local connection between the left Parahippocampal gyrus (PHG) and amygdala nucleus (AMYG) showed a lower weighted value ($t = -4.12$, $p < 0.001$). In contrast, the other 66 local connections exhibited increased weighted values in the NSCLP children ($p < 0.001$). These peripheral regions extensively affected the SMN, VN, ExN, DMN, SN, and ORB (see **Figure 4C**).

Rich-Club, Feeder, and Local Connectivity Strength

The two-sample t-tests were applied to test for differences in the strength of the rich-club, feeder, and local connections. We discovered that children with NSCLP showed significantly increased strength of rich-club ($t = 4.796$, $p < 0.001$), feeder ($t = 7.324$, $p < 0.001$) and local ($t = 6.173$, $p < 0.001$) connections compared to the healthy comparison (see **Figure 4D**).

Classification of the Support Vector Machine (SVM)

As shown in **Supplementary Figure S1**, the rich-club connections with the 28 highest ranked connections showed an accuracy of 75% (sensitivity 86%, specificity 68%, $p < 0.05$), the local connections with the 2,660 highest ranked connections showed an accuracy of 86% (sensitivity 96%, specificity 75%, $p < 0.001$), and the feeder connections with the 320 highest ranked connections showed an accuracy of 89% (sensitivity 96%, specificity 75%, $p < 0.001$) (see **Figure 5A**). The AUCs of the rich-club, feeder, and local connections were 0.82, 0.96, and 0.83, respectively (see **Figure 5A**).

A total of 22 (rich-club connections), 674 (local connections), and 71 (feeder connections) consensus features were identified in the cross-validation. Consensus structural connectivity was detected primarily in the SMN, VN, ExN, DMN, SN, and ORB (see **Figures 6A–C**).

Among the consensus features, 2 (rich-club), 14 (local), and 6 (feeder) regions were identified as weighted regions (see **Supplementary Figure S2**), which had weights that were at least one standard deviation greater than the average of the weights of all areas. The three types of weighted brains were normalized (see **Figure 6D**) and were mainly distributed in the dorsal stream associated with phonological processing and the ventral stream related to semantic processing (34).

Relationships Between Neuroimaging Properties and the CLCDS

Seven local connections showed a significant correlation with CLCDS and were also consensus features identified in the cross-validation. The connection between the right middle frontal gyrus (MFG), orbital part (ORBmid), and cuneus (CUN) ($r = -0.4388$, $p = 0.0195$ was a negative classification weight. The rest of the connections were positive between the right inferior frontal gyrus, opercular part (IFGoperc) and MFG; the right and left supplementary motor area (SMA), left insula, and olfactory cortex (OLF); the left superior frontal gyrus, medial (SFGmed) and median cingulate and paracingulate gyri (DCG); the right lingual gyrus (LIN) and amygdala (AMYG); and the right middle temporal gyrus (MTG) and angular gyrus (ANG), all mainly involving language-related brain regions (see **Figure 5B**, **Supplementary Figure S3**, **Table 2**).

DISCUSSION

To the best of our knowledge, this diffusion MRI study was the first to explore the topology of white matter structural networks in children with NSCLP after articulation rehabilitation. In this study, the b-values of our diffusion data were relatively low (b = 1,000) and not suitable for the spherical deconvolution or other advanced signal representations/models (35). Multifiber deterministic fiber tract imaging (FACT) is superior to probabilistic fiber tract imaging in connectome mapping (36). Therefore, we used the tensor model and deterministic tractography for the structural network construction. First, compared with the healthy comparison, a lower σ and Φ_{norm} were detected in the structural brain networks of children with NSCLP after articulation rehabilitation. Second, the three types of connectivity strength were higher in the NSCLP group than in the healthy comparison. Additionally, the significant between-group differences in the connections were mainly located in the feeder and local connections. Third, the three types of connections showed a higher classification power, especially for the feeder connections. The consensus features were mostly in the feeder and local connections. Fourth, the local connections and consensus features were significantly correlated with the CLCDS scores, and the weighted regions were distributed in the dorsal and ventral

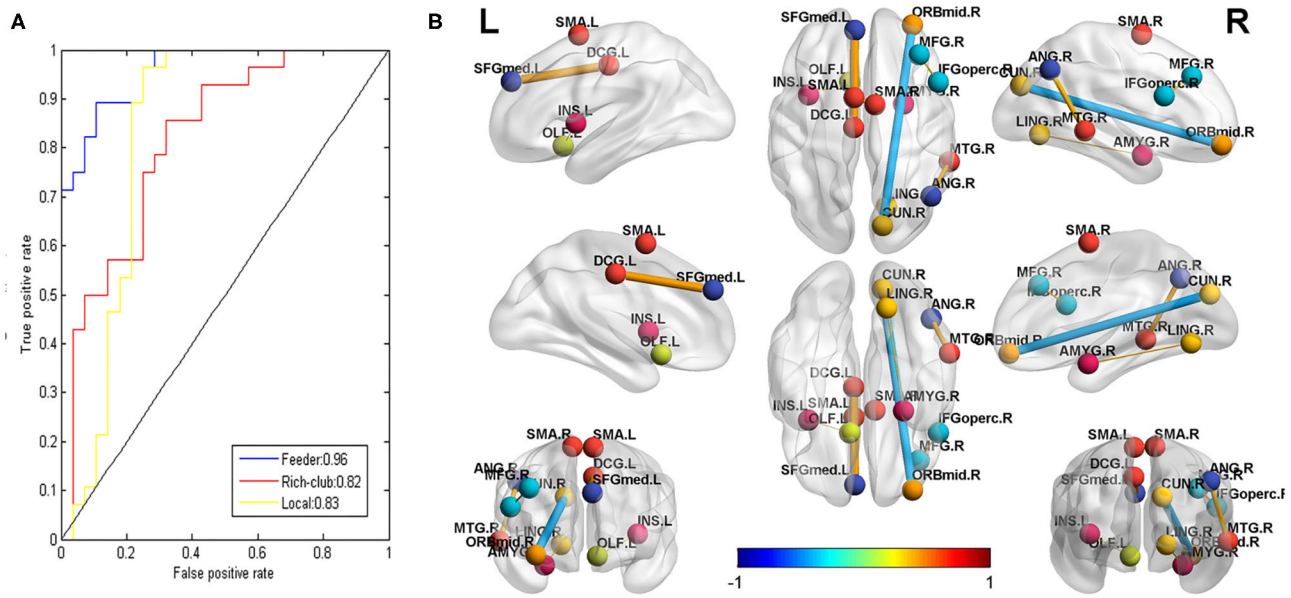

FIGURE 5 | (A): The receiver operating characteristic (ROC) curve of the classifier for rich-club (red, AUC = 0.82), feeder (blue, AUC = 0.96), and local (yellow, AUC = 0.83) connections. AUC: the area under the ROC curve. **(B)**: the connections that were significantly correlated with the CLCDS scores. The balls represent brain areas, and the colors of the balls indicate the intrinsic connectivity networks. The size and color of the lines (connections) represent the *r*-value and correspond to the color bar.

streams related to articulation processing in the non-dominant language hemisphere.

Small-World Properties

We detected small-worldness ($\sigma > 1$, density 0.06–0.50) in both groups, which indicated that articulation-rehabilitated children with NSCLP and healthy comparison showed parallel information transfer at a low cost and an optimal equilibrium of global integration and local specialization (density 0.06–0.50) (37). However, articulation-rehabilitated patients showed the lower AUC values of σ, γ, and λ than healthy comparison. The decreased γ meant reducing the brain's network segregation, and a lower λ represented stronger global information integration (22). The lower σ suggested a disturbance of the average balance and a higher cost for a new equilibrium between weaker local phonologic information transfer and higher global information integration, demonstrating a random network tendency in articulation-rehabilitated children with NSCLP (22). However, our previous study showed that the same participants exhibited a higher σ value of the resting-state functional network in the NSCLP group (11).

We speculated that the neuroplasticity of the structure might occur later than that of the function. The phenotype of the separation between the structural and functional networks was detected in patients with subacute intracerebral hemorrhage (38). In a rehabilitation practice of peripheral nerve-injured rats, rehabilitation therapy of electroacupuncture for 120 days can induce the neuroplasticity of the structural network, but a treatment duration of only 30 days cannot induce the neuroplasticity of the structural network (39). The results of these studies are consistent with our findings.

TABLE 2 | The connection significantly correlated with the CLCDS scores.

	Connections (AAL atlas)						
Brain areas	12	46	20	29	33	48	86
	8	10	19	21	23	42	66
p	0.04	0.02	0.03	0.05	0.02	0.04	0.03
r	0.39	−0.44	0.40	0.38	0.44	0.38	0.41

The number of brain areas corresponds to the code of the automated anatomical labeling (AAL) atlas.
CLCDS, Chinese language clear degree scale.

Rich-Club Organization

Rich-club organization is a basis for efficient global information transfer and complex neurological function in the brain (23). We detected rich-club organizations with an increasing normalized rich-club coefficient ($Ø_{norm} > 1$, $k = 2$–16) across the two groups, representing the existence of a rich-club organization in structural networks (31). Similar results were found in major depressive disorder after selective serotonin reuptake inhibitor treatment in the structural network (40). Compared with the healthy comparison, the $Ø_{norm}$ in the NSCLP group was significantly decreased, mostly in the low-degree regimen ($k < 16$). This finding indicates that connections linked to rich-club regions decrease in the total amount of the strongest connections they could share. This result suggests that the integration of information between peripheral brain regions and

their engagement in various types of cognition measured by the CLCDS scores were weaker in the NSCLP group than in healthy comparison (41). We speculated that although the CLCDS scores reached the average level, the speech errors were not completely corrected (42). The non-rich-club organization of the structural network may be the phenotype of the residual articulation errors in the NSCLP children after speech rehabilitation.

Rich-Club, Feeder, and Local Connections

We found that the connection values in the NSCLP group were significantly higher than those in healthy comparison, mainly located in the feeder and local connections (two rich-club connections); only one connection between the left PHG and AMYG was a lower value compared to controls. A similar network pattern was seen in major depressive disorder after treatment (40). These findings indicate that the significantly different between-group connections after articulation rehabilitation are mostly in the feeder and local connections involved in all of the intrinsic connectivity networks, including the DMN, SMN, SN, VN, primary auditory cortex, ORB, and ExN (30, 32, 33). The special patterns of rich-club organization in NSCLP children after articulation rehabilitation can provide us with a new perspective.

We identified a similar rich-club connection pattern, except two higher strength connections (the left SOG and THA, left PCUN and right PCUN) in articulation-rehabilitated children with NSCLP compared with healthy comparisons. Our results indicated that efficient global information transfer and complex neurological function nearly reached the average level (15), representing average level CLCDS scores. The THA serves as a relay station and applies modulation (43). The SOG and PCUN play a central role in a wide spectrum of highly integrated tasks, including visuospatial imagery, episodic memory retrieval, and self-processing operations (44). We speculated that articulation-rehabilitated NSCLP children might balance residual articulation defectiveness through the increased compensatory function of the modulation and integrated tasks for global information integration of the rehabilitated cognitive functions (CLCDS scores $>$ 90). This result is similar to a subvocalization task functional MRI study in adults after articulation rehabilitation, exhibiting only left hippocampal activation (10).

We detected that the 42 feeder and 66 local connections in the NSCLP group were significantly higher than those in the healthy comparison, covering the peripheral regions involved in the DMN, SMN, SN, VN, PAC, ORB, and ExN. Our results indicated that an increase in structural connectivities induced by speech therapy is mainly located in the peripheral regions. Therefore, the cost of the structural network was increased, which is consistent with the small-worldness alterations of this study. Neuroimaging studies have found that the brain undergoes remodeling induced by short-term training, exhibiting white matter restructuring (45, 46). We speculated that because the NSCLP group imitated the articulation of instructors by visual, auditory, and touch feedback assistance and the white matter connectivities between the affected peripheral regions produced neuroplasticity in the DMN, SMN, SN, VN, PAC, ORB, and ExN.

Only the connection between the left PHG and AMYG was lower in the NSCLP group than in the healthy comparison. The PHG plays a critical role in forming pathological memories (47), and the AMYG is emotionally associated with decision-making (48). This finding suggested that decision-making memory of articulation was impaired, which may be induced by the residual speech errors in the NSCLP group. A pattern of PHG was identified in internet gaming disorder in a resting-state fMRI study (49), which supports our findings.

Connectivity Strength

We found that the rich-club, feeder, and local connection strength were significantly higher in the NSCLP group than in the healthy comparison. Rich-club organization is associated with cognitive performance (50). Our results indicated that the strengths of the rich-club, feeder, and local connections were stronger in the NSCLP group. We conjectured that the stronger connectivity strength might compensate for residual articulation defects measured by the CLCDS scores (42).

SVM Classification

We employed the *F*-score for the feature ranking in the feature selection approach, and an SVM algorithm with a LOOCV strategy showed classification accuracies (75, 86, and 89%) and AUCs (0.82, 0.96, and 0.83) for the rich-club, feeder, and local connections, respectively. Our results indicated that the three types of connections showed good classification ability, especially the feeder connections. Simultaneously, the results suggested that the structural connection pattern in the NSLCP group was specific and different from that in the healthy comparison. We speculated that speech therapy might induce neuroplasticity changes in these connections to improve language function as measured by the CLCDS scores in the NSCLP group, especially the feeder connections. The feeder connections of the structural network showed the most discriminative power in major depressive disorder after treatment (40), which was consistent with our findings.

Consensus Features

The distribution of consensus features was similar to the univariate analysis in the three types of connections, widely involved in the SMN, VN, ExN, DMN, SN, and ORB, which was consistent with a study of the treatment in a major depressive disorder (40). These brain networks are engaged in sensorimotor function, visual processing, executive functioning, auditory processing, language, memory, attention, and/or even consciousness (51, 52). The ORB links subjective values to valuation and choice (53). Our results indicated that articulation rehabilitation resulted from a combination of multiple intrinsic connectivity networks and the cortex. During the speech rehabilitation procedure, the NSCLP group had to comprehend and learn the articulation model, imitate the doctor, and keep repeating speech to achieve a nearly normal vocalization. Therefore, the brain regions associated with sensorimotor, language, visual, auditory, and executive functioning were intensely involved (9).

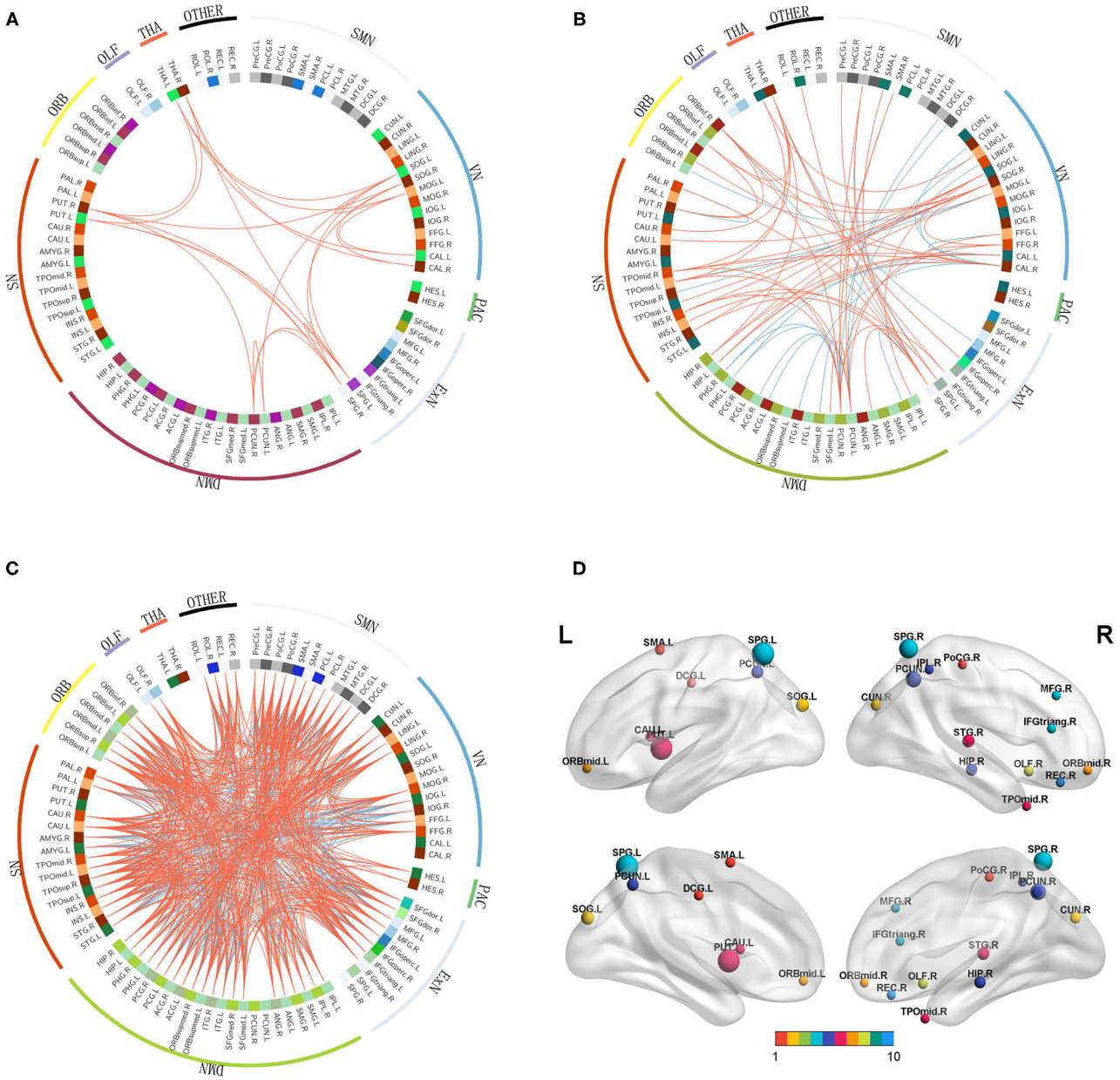

FIGURE 6 | (A–C): Consensus functional connections. The red lines represent positive connections, and the blue lines represent negative connections. **(D)**: The distribution of weighted regions in the NSCLP group. The size of the balls indicates the normalized classification weights, and the color of the balls represents the intrinsic connectivity networks. (1:SMN, sensorimotor network; 2:VN, visual network; 3:ExN, frontoparietal network; 4:DMN, default mode network; 5:SN, salience network; 6:ORB, orbitofrontal cortex; 7:PAC, primary auditory cortex, 8:THA, thalamus; 9:OLF, olfactory cortex; 10 other).

Weighted Regions

We identified the weighted regions that contributed the most to the accurate classification. These regions were mainly distributed in the dorsal stream associated with phonological processing and in the ventral stream related to semantic processing (34, 54, 55), except for the left SOG, PUT, caudate nucleus (CAU), DCG, right CUN, hippocampus (HIP), and OLF. The CUN and SOG are involved in visual processing (56) and integrate the somatosensory information and cognitive processes such as attention, learning, and memory (57). The HIP is related to memory. The PUT and CAU are linked with motor skills and neurofeedback learning (58, 59). The DCG is the key region for proactive rather than reactive action control, indicated by increased neural activity for endogenous action selection (60). Our results showed that the weighted regions were more abundant in the right hemisphere, which suggested that articulation rehabilitation mainly induced neuroplasticity in the brain regions involved in language, memory, vision, and

active learning skills in the non-dominant language hemisphere. Because the impaired brain regions in children with NSCLP with speech therapy were mainly located in the language dominant hemisphere (6), we speculated that the relatively intact non-dominant language hemisphere provided a compensatory function for articulation rehabilitation.

Relationship Between the Connections and the CLCDS

We detected seven local connections, which were also the local connections' consensus features, and showed significant correlations with the CLCDS scores. The brain regions involved in the seven connections showed a similar distribution to the weighted regions, mainly in the dorsal and ventral stream associated with language in the right hemisphere. The language-related connections were between the right MFG and IFGoper, ANG and MTG, LING and AMYG, the left SFG and DCG, left INS and OLF, and the left and right SMA (34, 54, 55). The only negative connection was the one between the right CUN and ORBmid. This finding is similar to that found in a study of stutterers (61). As mentioned above, the CUN is involved in vision, and the ORB links subjective values to valuation and choice (53). We speculated that the increased connectivity of the dorsal and ventral streams caused by the articulation train might promote phonological and semantic processing. The negative correlation with the CLCDS scores implies that the clear articulation may not need to be regulated by high-order brain regions.

Limitations

There were several limitations in this study. First, the sample size in this study was relatively small. Second, more study focused on investigating the structural, topological properties in untreated or non-rehabilitated children with NSCLP should be conducted in the future. Third, multikernel learning based on multimodal features should be applied to a larger sample. Fourth, with age, whether these topological parameters will return to normal levels or complete speech correction is required in further research.

CONCLUSION

The feeder and local connections involving SMN, VN, ExN, DMN, SN, and ORB may perform a compensatory function during articulation rehabilitation. In addition, the language networks may imply a vital role of language processing in articulation rehabilitation. However, articulation-rehabilitated children with NSCLP exhibited a random network and non-rich-club organization tendency. These findings provide a profound understanding of neuroimaging in children with NSCLP after articulation rehabilitation.

DATA AVAILABILITY STATEMENT

The original contributions presented in the study are included in the article/**Supplementary Material**, further inquiries can be directed to the corresponding authors.

ETHICS STATEMENT

The studies involving human participants were reviewed and approved by Beijing Children's Hospital Ethical Committee. Written informed consent to participate in this study was provided by the participants' legal guardian/next of kin.

AUTHOR CONTRIBUTIONS

HC contributed to methodology, software, formal analysis, writing—original draft, and investigation. BR contributed to writing—review and editing, project administration, validation, and data curation. HX contributed to resources and supervision. YP contributed to funding acquisition. All authors contributed to the article and approved the submitted version.

FUNDING

This study was supported in part by the National Natural Science Foundation of China (Grant No. 81671651), the Yang Fan Plan of Beijing Municipal Administration of Hospital Clinical Innovation Project, (Grant No. XMLX201714), and the Cultivate Plan of Beijing Municipal Administration of Hospital (Grant No. PX2018047).

SUPPLEMENTARY MATERIAL

The Supplementary Material for this article can be found online at: https://www.frontiersin.org/articles/10.3389/fneur.2022.790607/full#supplementary-material

REFERENCES

1. Centers for Disease Control and Prevention (CDC). Improved national prevalence estimates for 18 selected major birth defects–United States, 1999-2001. *MMWR Morb Mortal Wkly Rep*. (2006) 54:1301–5.
2. Ruiter J, Korsten-Meijer A, Goorhuis-Brouwer S. Communicative abilities in toddlers and in early school age children with cleft palate. *Int J Pediatr Otorhinolaryngol.* (2009) 73:693–8. doi: 10.1016/j.ijporl.2009.01.006
3. Priester G, Goorhuis-Brouwer S. Speech and language development in toddlers with and without cleft palate. *Int J Pediatric Otorhinolaryngol.* (2008) 72:801–6. doi: 10.1016/j.ijporl.2008.02.004
4. Maas E, Robin D, Austermann Hula S, Freedman S, Wulf G, Ballard K, et al. Principles of motor learning in treatment of motor speech disorders. *Am J Speech Lang Pathol.* (2008) 17:277–98. doi: 10.1044/1058-0360(2008/025)
5. Nopoulos P, Langbehn D, Canady J, Magnotta V, Richman L. Abnormal brain structure in children with isolated clefts of the lip or palate. *Arch Pediatr Adolesc Med.* (2007) 161:753–8. doi: 10.1001/archpedi.161.8.753
6. Adamson C, Anderson V, Nopoulos P, Seal M, Da Costa A. Regional brain morphometric characteristics of nonsyndromic cleft lip and palate. *Dev Neurosci.* (2014) 36:490–8. doi: 10.1159/000365389
7. Conrad A, Richman L, Nopoulos P, Dailey S. Neuropsychological functioning in children with non-syndromic cleft of the lip and/or palate. *Child Neuropsychol.* (2009) 15:471–84. doi: 10.1080/09297040802691120

8. Boes A, Murko V, Wood J, Langbehn D, Canady J, Richman L, et al. Social function in boys with cleft lip and palate: relationship to ventral frontal cortex morphology. *Behav Brain Res.* (2007) 181:224–31. doi: 10.1016/j.bbr.2007.04.009
9. Li Z, Zhang W, Li C, Wang M, Wang S, Chen R, et al. Articulation rehabilitation induces cortical plasticity in adults with non-syndromic cleft lip and palate. *Aging.* (2020) 12:13147–59. doi: 10.18632/aging.103402
10. Zhang W, Li C, Chen L, Xing X, Li X, Yang Z, et al. Increased activation of the hippocampus during a Chinese character subvocalization task in adults with cleft lip and palate palatoplasty and speech therapy. *Neuroreport.* (2017) 28:739–44. doi: 10.1097/WNR.0000000000000832
11. Rao B, Cheng H, Fan Y, Zhang W, Chen R, Peng Y. Topological properties of the resting-state functional network in nonsyndromic cleft lip and palate children after speech rehabilitation. *J Integrat Neurosci.* (2020) 19:285–93. doi: 10.31083/j.jin.2020.02.19
12. Medaglia J. Graph theoretic analysis of resting state functional MR imaging. *Neuroimaging Clin N Am.* (2017) 27:593–607. doi: 10.1016/j.nic.2017.06.008
13. Latora V, Marchiori M. Efficient behavior of small-world networks. *Phys Rev Lett.* (2001) 87:198701. doi: 10.1103/PhysRevLett.87.198701
14. Power JD, Petersen SE. Control-related systems in the human brain. *Curr Opin Neurobiol.* (2013) 23:223–8. doi: 10.1016/j.conb.2012.12.009
15. van den Heuvel MP, Sporns O, Collin G, Scheewe T, Mandl RC, Cahn W, et al. Abnormal rich club organization and functional brain dynamics in schizophrenia. *JAMA Psychiatry.* (2013) 70:783–92. doi: 10.1001/jamapsychiatry.2013.1328
16. Zarogianni E, Moorhead TW, Lawrie SM. Towards the identification of imaging biomarkers in schizophrenia, using multivariate pattern classification at a single-subject level. *Neuroimage Clin.* (2013) 3:279–89. doi: 10.1016/j.nicl.2013.09.003
17. Meier TB, Desphande AS, Vergun S, Nair VA, Song J, Biswal BB, et al. Support vector machine classification and characterization of age-related reorganization of functional brain networks. *Neuroimage.* (2012) 60:601–13. doi: 10.1016/j.neuroimage.2011.12.052
18. Cui Z, Zhong S, Xu P, He Y, Gong G. PANDA: a pipeline toolbox for analyzing brain diffusion images. *Front Hum Neurosci.* (2013) 7:42. doi: 10.3389/fnhum.2013.00042
19. Mori S, van Zijl PC. Fiber tracking: principles and strategies - a technical review. *NMR Biomed.* (2002) 15:468–80. doi: 10.1002/nbm.781
20. Wang J, Wang X, Xia M, Liao X, Evans A, He Y. GRETNA: a graph theoretical network analysis toolbox for imaging connectomics. *Front Hum Neurosci.* (2015) 9:386. doi: 10.3389/fnhum.2015.00386
21. Zhang T, Wang J, Yang Y, Wu Q, Li B, Chen L, et al. Abnormal small-world architecture of top-down control networks in obsessive-compulsive disorder. *J Psychiatry Neurosci.* (2011) 36:23–31. doi: 10.1503/jpn.100006
22. Watts D, Strogatz S. Collective dynamics of 'small-world' networks. *Nature.* (1998) 393:440–2. doi: 10.1038/30918
23. van den Heuvel MP, Kahn RS, Goñi J, Sporns O. High-cost, high-capacity backbone for global brain communication. *Proc Natl Acad Sci USA.* (2012) 109:11372–77. doi: 10.1073/pnas.1203593109
24. Rubinov M, Sporns O. Weight-conserving characterization of complex functional brain networks. *Neuroimage.* (2011) 56:2068–79. doi: 10.1016/j.neuroimage.2011.03.069
25. Yan T, Wang W, Yang L, Chen K, Chen R, Han Y. Rich club disturbances of the human connectome from subjective cognitive decline to Alzheimer's disease. *Theranostics.* (2018) 8:3237–55. doi: 10.7150/thno.23772
26. Daianu M, Mezher A, Mendez MF, Jahanshad N, Jimenez EE, Thompson PM. Disrupted rich club network in behavioral variant frontotemporal dementia and early-onset Alzheimer's disease. *Hum Brain Mapp.* (2016) 37:868–83. doi: 10.1002/hbm.23069
27. Chang CC, Lin CJ. LIBSVM: a library for support vector machines. *ACM Trans Intellig Syst Technol.* (2011) 2:1–27. doi: 10.1145/1961189.1961199
28. Wee CY, Yap PT, Li W, Denny K, Browndyke JN, Potter GG, et al. Enriched white matter connectivity networks for accurate identification of MCI patients. *Neuroimage.* (2011) 54:1812–22. doi: 10.1016/j.neuroimage.2010.10.026
29. Golland P, Fischl B. Permutation tests for classification: towards statistical significance in image-based studies. *Inf Process Med Imaging.* (2003) 18:330–41. doi: 10.1007/978-3-540-45087-0_28
30. Liu F, Guo W, Fouche JP, Wang Y, Wang W, Ding J, et al. Multivariate classification of social anxiety disorder using whole brain functional connectivity. *Brain Struct Funct.* (2015) 220:101–15. doi: 10.1007/s00429-013-0641-4
31. van den Heuvel MP, Sporns O. Rich-club organization of the human connectome. *J Neurosci.* (2011) 31:15775–86. doi: 10.1523/JNEUROSCI.3539-11.2011
32. Allen EA, Erhardt EB, Damaraju E, Gruner W, Segall JM, Silva RF, et al. A baseline for the multivariate comparison of resting-state networks. *Front Syst Neurosci.* (2011) 5:2. doi: 10.3389/fnsys.2011.00002
33. Zhu X, Yuan F, Zhou G, Nie J, Wang D, Hu P, et al. Cross-network interaction for diagnosis of major depressive disorder based on resting state functional connectivity. *Brain Imaging Behav.* (2020) 15:1279–89. doi: 10.1007/s11682-020-00326-2
34. Fujii M, Maesawa S, Ishiai S, Iwami K, Futamura M, Saito K. Neural basis of language: an overview of an evolving model. *Neurol Med Chir.* (2016) 56:379–86. doi: 10.2176/nmc.ra.2016-0014
35. Tournier JD, Calamante F, Connelly A. Determination of the appropriate b value and number of gradient directions for high-angular-resolution diffusion-weighted imaging. *NMR Biomed.* (2013) 26:1775–86. doi: 10.1002/nbm.3017
36. Sarwar T, Ramamohanarao K, Zalesky A. Mapping connectomes with diffusion MRI: deterministic or probabilistic tractography? *Magn Reson Med.* (2019) 81:1368–84. doi: 10.1002/mrm.27471
37. Wang L, Zhu C, He Y, Zang Y, Cao Q, Zhang H, et al. Altered small-world brain functional networks in children with attention-deficit/hyperactivity disorder. *Hum Brain Mapp.* (2009) 30:638–49. doi: 10.1002/hbm.20530
38. Zhang X, Yu X, Bao Q, Yang L, Sun Y, Qi P. Multimodal neuroimaging study reveals dissociable processes between structural and functional networks in patients with subacute intracerebral hemorrhage. *Med Biol Eng Comput.* (2019) 57:1285–95. doi: 10.1007/s11517-019-01953-8
39. Lu YC, Wu JJ, Ma H, Hua XY, Xu JG. Functional organization of brain network in peripheral neural anastomosis rats after electroacupuncture: an ICA and connectome analysis. *Neuroscience.* (2020) 442:216–27. doi: 10.1016/j.neuroscience.2020.06.017
40. Wang X, Qin J, Zhu J, Bi K, Zhang S, Yan R, et al. Rehabilitative compensatory mechanism of hierarchical subnetworks in major depressive disorder: a longitudinal study across multi-sites. *Eur Psychiatry.* (2019) 58:54–62. doi: 10.1016/j.eurpsy.2019.02.004
41. van den Heuvel MP, Stam CJ, Kahn RS, Hulshoff Pol HE. Efficiency of functional brain networks and intellectual performance. *J Neurosci.* (2009) 29:7619–24. doi: 10.1523/JNEUROSCI.1443-09.2009
42. Willadsen E, Lohmander A, Persson C, Lundeborg I, Alaluusua S, Aukner R, et al. Scandcleft randomised trials of primary surgery for unilateral cleft lip and palate: 5. speech outcomes in 5-year-olds - consonant proficiency and errors. *J Plast Surg Hand Surg.* (2017) 51:38–51. doi: 10.1080/2000656X.2016.1254647
43. Moustafa AA, McMullan RD, Rostron B, Hewedi DH, Haladjian HH. The thalamus as a relay station and gatekeeper: relevance to brain disorders. *Rev Neurosci.* (2017) 28:203–18. doi: 10.1515/revneuro-2016-0067
44. Cavanna AE, Trimble MR. The precuneus: a review of its functional anatomy and behavioural correlates. *Brain.* (2006) 129:564–83. doi: 10.1093/brain/awl004
45. May A. Experience-dependent structural plasticity in the adult human brain. *Trends Cogn Sci.* (2011) 15:475–82. doi: 10.1016/j.tics.2011.08.002
46. Voss MW, Vivar C, Kramer AF, van Praag H. Bridging animal and human models of exercise-induced brain plasticity. *Trends Cogn Sci.* (2013) 17:525–44. doi: 10.1016/j.tics.2013.08.001
47. Šlamberová R, Vrajová M, Schutová B, Mertlová M, Macúchová E. Nohejlová K, et al. Prenatal methamphetamine exposure induces long-lasting alterations in memory and development of NMDA receptors in the hippocampus. *Physiol Res.* (2014) 63(Suppl. 4):S547–58. doi: 10.33549/physiolres.932926
48. Dunn BD, Dalgleish T, Lawrence AD. The somatic marker hypothesis: a critical evaluation. *Neurosci Biobehav Rev.* (2006) 30:239–71. doi: 10.1016/j.neubiorev.2005.07.001
49. Wang Z, Dong H, Du X, Zhang JT, Dong GH. Decreased effective connection from the parahippocampal gyrus to the prefrontal cortex in Internet gaming disorder: a MVPA and spDCM study. *J Behav Addict.* (2020) 9:1–11. doi: 10.1556/2006.2020.00012

50. Baggio HC, Segura B, Junque C, de Reus MA, Sala-Llonch R, Van den Heuvel MP. Rich club organization and cognitive performance in healthy older participants. *J Cogn Neurosci.* (2015) 27:1801–10. doi: 10.1162/jocn_a_00821
51. Damoiseaux JS, Rombouts SA, Barkhof F, Scheltens P, Stam CJ, Smith SM, et al. Consistent resting-state networks across healthy subjects. *Proc Natl Acad Sci USA*. (2006) 103:13848–53. doi: 10.1073/pnas.0601417103
52. Smith SM, Fox PT, Miller KL, Glahn DC, Fox PM, Mackay CE, et al. Correspondence of the brain's functional architecture during activation and rest. *Proc Natl Acad Sci USA*. (2009) 106:13040–5. doi: 10.1073/pnas.0905267106
53. Ballesta S, Shi W, Conen KE, Padoa-Schioppa C. Values encoded in orbitofrontal cortex are causally related to economic choices. *Nature.* (2020) 588:450–3. doi: 10.1038/s41586-020-2880-x
54. Friederici AD, Gierhan SM. The language network. *Curr Opin Neurobiol.* (2013) 23:250–4. doi: 10.1016/j.conb.2012.10.002
55. Chang E, Raygor K, Berger M. Contemporary model of language organization: an overview for neurosurgeons. *J Neurosurg.* (2015) 122:250–61. doi: 10.3171/2014.10.JNS132647
56. Rosen ML, Sheridan MA, Sambrook KA, Peverill MR, Meltzoff AN, McLaughlin KA. The role of visual association cortex in associative memory formation across development. *J Cogn Neurosci.* (2018) 30:365–80. doi: 10.1162/jocn_a_01202
57. Price DD. Psychological and neural mechanisms of the affective dimension of pain. *Science.* (2000) 288:1769–72. doi: 10.1126/science.288.5472.1769
58. Choi Y, Shin EY, Kim S. Spatiotemporal dissociation of fMRI activity in the caudate nucleus underlies human de novo motor skill learning. *Proc Natl Acad Sci USA*. (2020) 117:23886–97. doi: 10.1073/pnas.2003963117
59. Zhao Z, Yao S, Zweerings J, Zhou X, Zhou F, Kendrick KM, et al. Putamen volume predicts real-time fMRI neurofeedback learning success across paradigms and neurofeedback target regions. *Hum Brain Mapp*. (2021) 42:1879–87. doi: 10.1002/hbm.25336
60. Aron AR. From reactive to proactive and selective control: developing a richer model for stopping inappropriate responses. *Biol Psychiatry*. (2011) 69:e55–68. doi: 10.1016/j.biopsych.2010.07.024
61. Sitek KR, Cai S, Beal DS, Perkell JS, Guenther FH, Ghosh SS. Decreased cerebellar-orbitofrontal connectivity correlates with stuttering severity: whole-brain functional and structural connectivity associations with persistent developmental stuttering. *Front Hum Neurosci.* (2016) 10:190. doi: 10.3389/fnhum.2016.00190

Conflict of Interest: The authors declare that the research was conducted in the absence of any commercial or financial relationships that could be construed as a potential conflict of interest.

frontiers in Neurology

REVIEW
published: 04 February 2022
doi: 10.3389/fneur.2022.806298

Networking of the Human Cerebellum: From Anatomo-Functional Development to Neurosurgical Implications

Alessandro De Benedictis[1], Maria Camilla Rossi-Espagnet[2], Luca de Palma[3], Andrea Carai[1] and Carlo Efisio Marras[1]*

[1] Neurosurgery Unit, Department of Neurosciences, Bambino Gesù Children's Hospital, Istituto di Ricovero e Cura a Carattere Scientifico, Rome, Italy, [2] Neuroradiology Unit, Imaging Department, Bambino Gesù Children's Hospital, Istituto di Ricovero e Cura a Carattere Scientifico, Rome, Italy, [3] Neurology Unit, Department of Neurosciences, Bambino Gesù Children's Hospital, Istituto di Ricovero e Cura a Carattere Scientifico, Rome, Italy

In the past, the cerebellum was considered to be substantially involved in sensory-motor coordination. However, a growing number of neuroanatomical, neuroimaging, clinical and lesion studies have now provided converging evidence on the implication of the cerebellum in a variety of cognitive, affective, social, and behavioral processes as well. These findings suggest a complex anatomo-functional organization of the cerebellum, involving a dense network of cortical territories and reciprocal connections with many supra-tentorial association areas. The final architecture of cerebellar networks results from a complex, highly protracted, and continuous development from childhood to adulthood, leading to integration between short-distance connections and long-range extra-cerebellar circuits. In this review, we summarize the current evidence on the anatomo-functional organization of the cerebellar connectome. We will focus on the maturation process of afferent and efferent neuronal circuitry, and the involvement of these networks in different aspects of neurocognitive processing. The final section will be devoted to identifying possible implications of this knowledge in neurosurgical practice, especially in the case of posterior fossa tumor resection, and to discuss reliable strategies to improve the quality of approaches while reducing postsurgical morbidity.

Keywords: white matter, cerebellar anatomy, neurosurgery, posterior fossa, structural connectivity

OPEN ACCESS

Edited by:
Emanuele La Corte, University of Bologna, Italy

Reviewed by:
Alberto Cacciola, University of Messina, Italy
Sandrine de Ribaupierre, Western University, Canada

****Correspondence:***
Alessandro De Benedictis
alessandro.debenedictis@opbg.net

Specialty section:
This article was submitted to Applied Neuroimaging, a section of the journal Frontiers in Neurology

Received: *31 October 2021*
Accepted: *13 January 2022*
Published: *04 February 2022*

Citation:
De Benedictis A, Rossi-Espagnet MC, de Palma L, Carai A and Marras CE (2022) Networking of the Human Cerebellum: From Anatomo-Functional Development to Neurosurgical Implications. Front. Neurol. 13:806298. doi: 10.3389/fneur.2022.806298

INTRODUCTION

In the past, the cerebellum was considered to be substantially involved in sensory-motor coordination through a loop circuit between the cerebellar cortex and the motor cortex, passing through the basilar pontine nuclei (descending way) and the thalamus (ascending way) (1, 2).

However, growing evidence coming from neuroanatomic, neuroimaging, physiology, and pathology studies has led to a reassessment of the classic view of a selective cerebro-cerebellar connection system in favor of a more complex organization involving distinct, parallel, and segregated networks constituted by loop-shaped connections between different neuronal subgroups. This structural complexity may explain the role of the cerebellum not only in motor function, but also in a variety of cognitive, affective, social, and behavioral processes as well (3).

As for the supratentorial compartment, cerebellar networks undergo intensive development and rearrangement from childhood to adulthood, allowing for maturation of functional processing (4–6).

This process is strictly dependent on the correct building of white matter (WM) tracts, forming the substrate for structural connectivity and reinforcement of functional interactions. A large variety of pathways are needed to ensure a fast, efficient, multidistance and multidirectional integration between cortical and subcortical regions (2, 7). On the other hand, many diseases may reflect alterations affecting the cerebellar WM architecture (8, 9).

Neurosurgeons are frequently involved in approaching the cerebellum, especially for the management of tumors or vascular malformations. Therefore, an accurate awareness of the anatomo-functional organization of the cerebellum is mandatory to improve the quality of surgical results while minimizing postoperative long-term neurological deficits, which still occur at a not negligible frequency according to recently published series (10).

The aim of this review is to summarize the current scientific evidence covering the anatomo-functional properties of the cerebellar connectome. In the first section, we will focus on the maturation process of afferent and efferent neuronal circuitry, and we will describe the involvement of these networks in different aspects of neurocognitive processing. The second section will be devoted to identifying possible implications of this knowledge in neurosurgical practice, especially in case of posterior fossa tumor resection, and to discuss reliable strategies to improve the quality of approaches.

THE CEREBELLAR CONNECTOME

History

After early pioneering descriptions, a substantial contribution to research on cerebellar anatomy came from Santiago Ramón y Cajal (1854–1934). By adopting the revolutionary method introduced by Camillo Golgi (1843–1926) of nervous tissue fixation in potassium bichromate followed by submersion in a solution of silver nitrate, Cajal identified all the elements constituting the cerebellar cortex. He provided a precise description of avian Purkinje cells, including their axons course, their collaterals, and the spines of their dendrites. Moreover, he showed the reciprocal relationships of Purkinje cells with other cells and the topography of the cellular elements, their dendrites, climbing and mossy fibers in respects to different cortical layers. In this way, he provided evidence for the network anatomo-functional organization of the cerebellar cortex: "the transmission of the nervous impulse is always from the dendritic branches and the cell body to the axon or functional process" (11–13).

Later, the highly homogenous and compartmentalized structure of the cerebellar cortex, and distribution of afferents fields were further highlighted. In 1940, Jansen and Brodal were the first to demonstrate that the cortico-nuclear outputs are organized according to a definite columnar architecture and mediolateral sagittal orientation. The same topography was recognized also for the afferent pathways by following studies (14).

Thanks to methodological advancement for morphological investigation within experimental animals, including histological tract-tracing studies, degeneration techniques, anterograde and retrograde tract-tracing techniques, and transneuronal tracing techniques, the WM architecture of the cerebellum was further characterized, especially regarding the connectivity patterns with the cerebrum. These methods revealed the circuit organization of cerebro-cerebellar networks, consisting of functionally segregated neuronal subgroups interconnected by specific and distinct WM bundles (15–20).

A revolutionary contribution to the exploration of WM anatomy came from Joseph Klingler (1888–1966), who in 1935 introduced an innovative method for the preparation of *post-mortem* human specimens. This approach, based on fiber separation induced by freeze/defrost formalin-fixation process, allowed for easier visualization and dissection of WM fascicles (21, 22). Moreover, development of tractography technique made possible the *in vivo* quantitative and qualitative characterization of both the physiological and pathological pattern of WM connections. The single or combined use of neuroimaging and dissection analysis opened the door to a more accurate and systematic identification of major intra- and inter-hemispheric WM fascicles and reciprocal relationships, for both scientific and therapeutic purposes (23–31).

Even if less frequently reported in comparison with the supratentorial compartment, *in-vivo* and *ex-vivo* methods were also adopted for investigating cerebellar WM anatomy. The most recent available studies reported detailed exposition and three-dimensional representation of different gray and WM structures, focusing on reciprocal relationships and practical surgical implications, mainly concerning the indications, advantages, limitations, and possible risks of specific approaches (32–36).

Maturation

The development of the human cerebellum is a highly protracted and orchestrated process, extending from the early first trimester to the end of the second post-natal year. The cerebellum is a derivative of two rhombomeres respectively located caudally (near the tail) and rostrally (near the front) in the alar plate of the neural tube, which develops along the rhombencephalon of the embryonic brain (6).

Between 20 and 40 weeks of gestation, the morphogenesis of the cerebellar cortex includes neuronal proliferation, migration, differentiation, axon growth, synaptogenesis, and pruning. At birth, the human cerebellar cortex has four layers: the external granular layer (EGL), the molecular layer (ML), the Purkinje cell layer (PL), and the internal granular layer (IGL). In a matter of 12–24 months, the number of layers reduces from four to three, by progressive increasing of the ML and the PL in association with gradual disappearance of the EGL thickness, due to decreased proliferation as well as migration of granule neurons into the IGL (4, 37, 38).

The cerebellar hemispheric WM is among the first region of the brain to myelinate. Available data coming from volumetric, epidemiologic and tractography studies showed that

the myelination process is particularly high during the third trimester and continues, but less drastically, between 2 and 5 years of age (39). Moreover, cerebellar WM does not myelinate uniformly, but along a temporal gradient starting from the archi-cerebellum and followed by the paleo-cerebellum and the neo-cerebellum (40).

Concerning the development of extracerebellar connectivity, over the last decades both post-mortem microdissection and *in-vivo* tractography reconstructions allowed to characterize the maturation process and relationships with the core of the cerebellum, adjacent and distant structures of the three cerebellar peduncles (superior, middle, and inferior). These structures constitute the main connection system between the cerebellum, the brainstem, and the cortex, with 70–80% of fibers providing contralateral connections and the remainder being ipsilateral (34, 41–43).

The superior cerebellar peduncle (SCP) develops between the 28th week and the 6th month and contains fibers converging from the dentate, globose and emboliform nuclei direct to the cerebral cortex *via* the contralateral red nucleus and the thalamus.

The middle cerebellar peduncle (MCP) develops between 42 weeks and 3 years. It consists of afferent fibers traveling from the cerebral cortex to the cerebellum, *via* the pontine nuclei. The pontocerebellar fibers have a transverse orientation in the ventral part of the pons. These fibers run laterally in the cerebello-pontine and in the cerebello-mesencephalic fissures and radiate within the white medullary body terminating in all lobules of the cerebellum, except for the nodulus and the flocculus. Fibers running anterior to the dentate nucleus are divided into a supra-dentate and infra-dentate component, the latter providing connections to the tonsillar peduncle.

The inferior cerebellar peduncle (ICP) is composed of a superficial and a deep component. It carries both afferent and efferent fiber tracts connecting the cerebellum with the vestibular system and the spinal cord, and incoming projections (climbing fibers) to the cerebellum from the inferior olive. Superficial fibers develop between 36 weeks and 4 months (outer part). They run with a centripetal direction from lateral to medial toward the cortex of the vermis. The deep component develops between 26th and 36th weeks of gestational age. These fibers run at the junction of the dentate nucleus with the initial portion of the SCP and direct dorso-laterally to the trigeminal nerve forming the posterior boundary of parabrachial recess between the SCP (medial) and MCP (lateral) (9, 44–51).

It is worth noting that investigation of cerebellar WM maturation has been restricted by methodological constraints, such as the three-dimensional geometry of cerebellar folia and the associated connectivity, the limited resolution of fetal MR imaging, and motion influence on the quality of exam. These barriers mainly reduce the possibility of acquiring accurate quantitative data, limiting the analysis to qualitative observation of indirect inferences from diffusion and anisotropy data. To enhance representation of fiber orientation and distribution in conventional DTI studies, Takahashi et al. applied the high-angular resolution diffusion imaging (HARDI) method to three-dimensional maturation of cerebellar connections from fetal to adult stages cerebrum. This 2014 study demonstrated that, at the earliest gestational age, pathways forming the cerebellar peduncles are already present, but pathways between deep cerebellar nuclei and the cortex are not observed until after the thirty-eighth week (40).

THE CEREBELLAR ANATOMO-FUNCTIONAL NETWORK

Intra-Cerebellar Connectivity

The functional processing of the cerebellum is strictly related to its internal cellular organization. As previously mentioned, from superficial to deep, the cerebellar cortex is arranged into three layers: the molecular layer, the Purkinje cell layer, and the granular layer. These three cortical layers contain five main cell types, including Purkinje cells, stellate cells, basket cells, Golgi cells, and granule cells. Granule cells are excitatory, while the other cells are all inhibitory. Every granule cell receives input from mossy fibers that originate in the pontine nuclei (52).

Granule cell axons ascend to the molecular layer, where they bifurcate to form parallel fibers. Purkinje cells make up the output elements of the cerebellar cortex. Every Purkinje cell receives input from many parallel fibers and from a single climbing fiber that originates in the inferior olive. Purkinje cells provide the sole outflow from the cortex in the form of an inhibitory projection to the cerebellar and vestibular nuclei.

This architecture forms the cerebellar *micro-zones*, which represent the effective functional units. The cerebellar cortex is composed of several thousands of micro-zones. A cortical micro-zone is connected to the inferior olive and the deep cerebellar nuclei to form a cerebellar *micro-complex*. A cerebellar micro-complex can extend to include several micro-zones located in separated cerebellar regions. The micro-complexes correspond to the cerebellar *modules*. Each module is defined by its climbing fiber input coming from a specific subdivision of the inferior olivary complex which targets one or more Purkinje cells, connected to the deep cerebellar nuclei.

This configuration undergoes dramatic changes during the postnatal maturation. In fact, it has been demonstrated that the cerebellar circuit does not simply develop from a rough outline to the adult state but undergoes a series of regulated steps involving transient connections and synaptic components working together to guide the emergence of the mature cerebellar circuit (52).

The Cerebellar Loop-Systems

The complex maturation process described in the previous sections leads to the final setting of the cerebellar circuitry, consisting in a multichannel network of parallel channels, in which signals remain separate throughout the whole circuit, to arrange distinct loop-shaped inputs and outputs pathways (**Figures 1**, **2**). This closed-loop organization represents the fundamental anatomo-functional architecture at the basis of both intracerebellar system and extracerebellar interactions with different cerebral, brainstem, and spinal compartments (2, 53–55) (**Figure 3**).

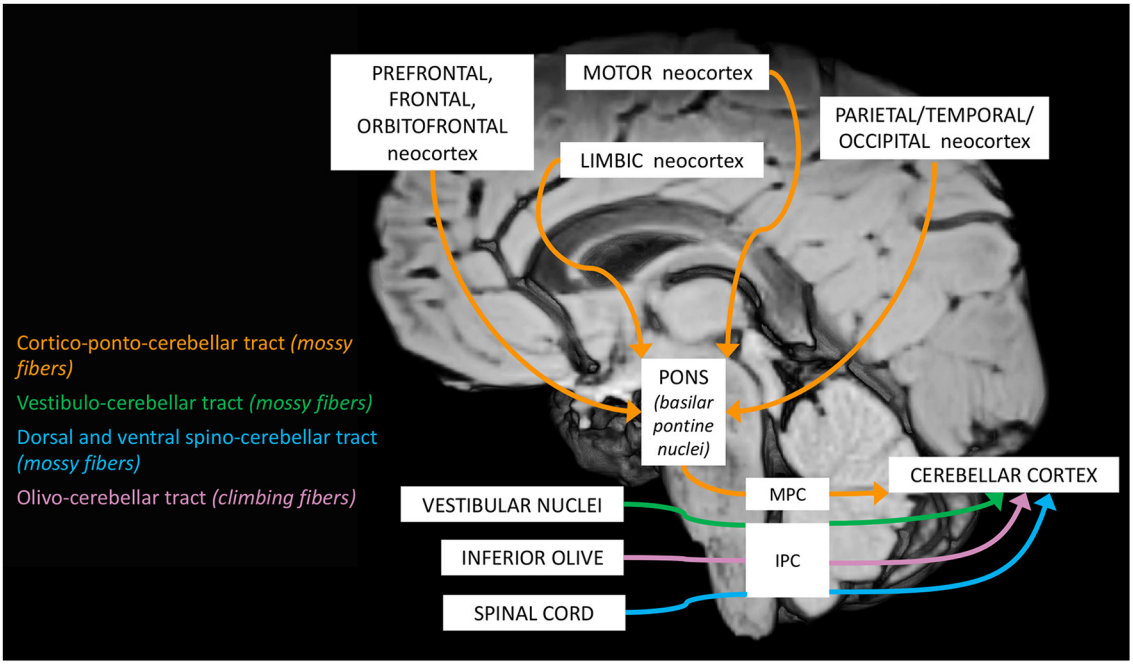

FIGURE 1 | Schematic representation of the main cerebellar afferent pathways.

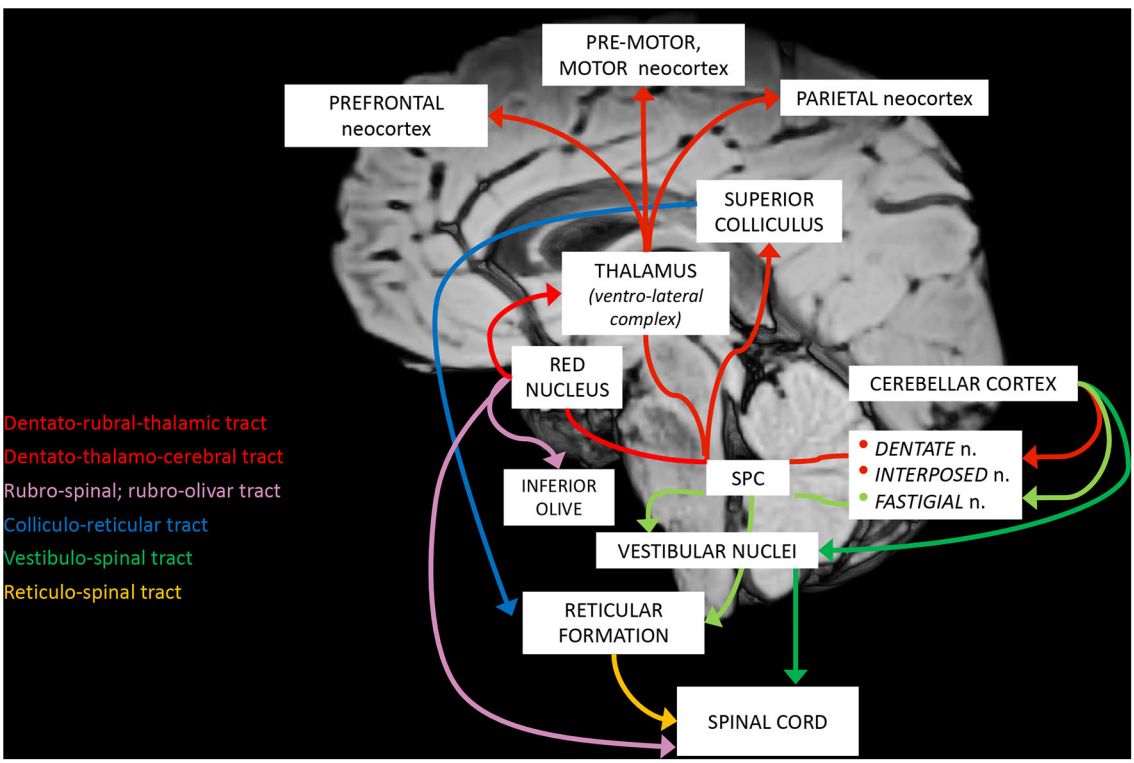

FIGURE 2 | Schematic representation of the main cerebellar efferent pathways.

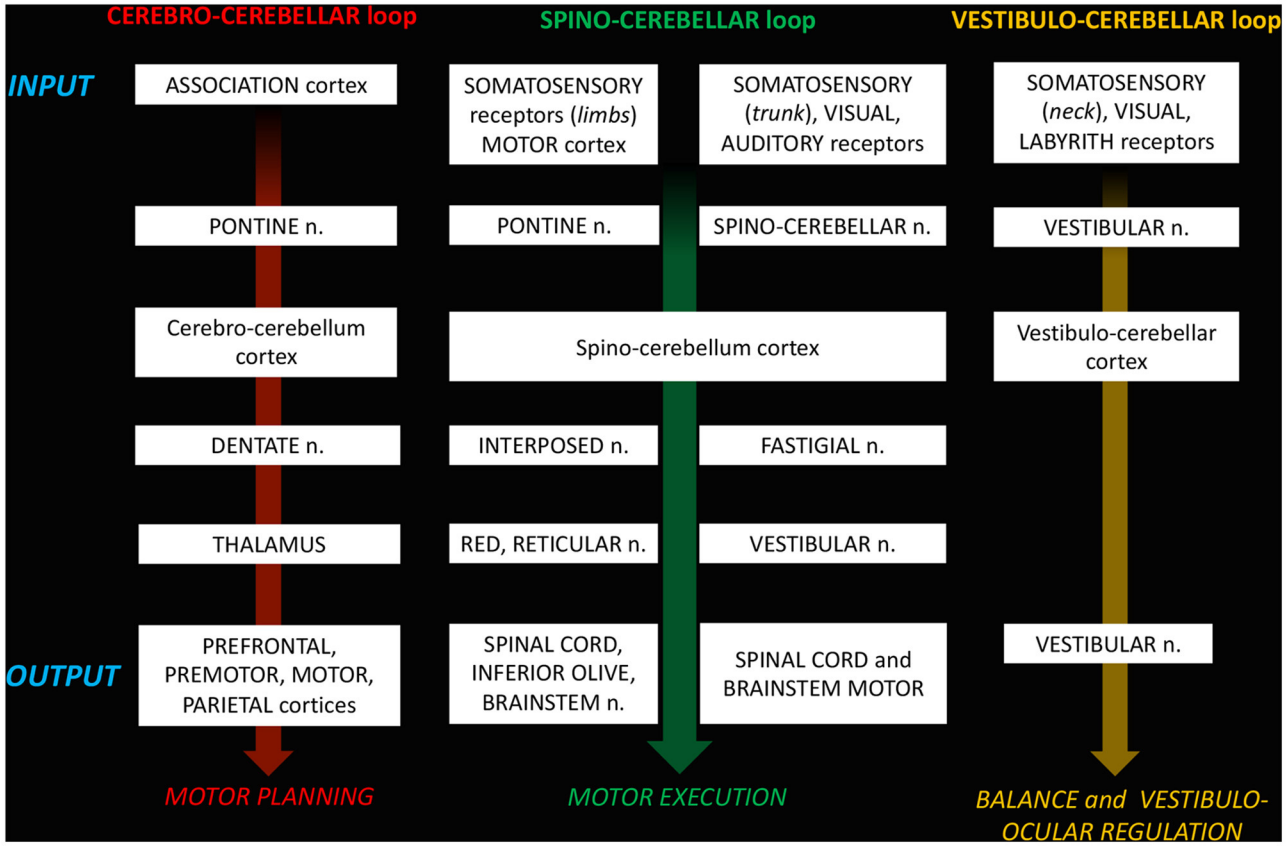

FIGURE 3 | Schematic representation of the loop-organization of cerebellar circuits.

The main loops include (52, 54):

a. The *cerebro-cerebellar loop*, including inputs from frontal, prefrontal, orbitofrontal, premotor, motor cortices. These fibers converge into the pontine nuclei and reach the cerebro-cerebellum cortex, passing through the contralateral MCP. The cerebro-cerebellum is the most *lateral* cortical compartment, involving the cerebellar hemisphere and the *dentate* nucleus. From the dentate nucleus, an ascending way is direct to the contralateral red nucleus within the ventral tegmental area (*dentato-rubro-thalamic* tract) or direct to the cerebral cortex of the primary motor, premotor, supplementary, prefrontal, parietal, limbic, and temporal regions, passing through the ventrolateral nucleus of the thalamus (*dentato-thalamo-cortical* tract). The dentato-rubro-thalamic tract is classically described as a decussating pathway, ascending to the contralateral thalamus. However, recent works applying deterministic fiber tractography in healthy subjects and human brain microdissection has shown the existence of a non-decussating pathway (34). Moreover, a different topography of thalamic terminations has been demonstrated, with contralateral fibers preferentially targeting the anterior and lateral nuclei, and ipsilateral connections reaching more posterior and medial nuclei (42).
b. The *spino-cerebellar loop*, passing through the somatosensory cortex, visual and auditory receptors, the spinal cord, through the dorsal and ventral *spino-cerebellar tracts.* The spino-cerebellum corresponds to the *intermediate* compartment, including the paravermis and the *interposed* nucleus (including the *globose and emboliform nuclei*), and the *medial* compartment, involving the vermis and the *fastigial* nucleus. Efferent connections influence motor neurons and interneurons of the spinal cord and brainstem, *via* the superior colliculus, the red nucleus, the inferior olive, the reticular formation, and the vestibular nuclei.
c. the *vestibulo-cerebellum loop* partially differs from this scheme, since it projects information coming from somatosensory, visual, labyrinths receptors directly to vestibular nuclei located in the brainstem passing through the cerebellar vestibular nuclei, located within the flocculo-nodular lobe.

As a result, since the same cerebral cortical area constitutes the simultaneous target of cerebellar output and the major source of input, the cerebellum respects a strict functional segregation and never contacts the final executive neurons, but rather modulates their activity indirectly (54–56). The continuous differentiation of these cerebellar loops from

childhood and adolescence to adulthood is crucial for healthy brain maturation (57).

On the other side, the same cerebellar structures may be involved in different connectivity patterns. For example, cerebellar nuclei relate to both the ventrolateral motor and non-motor thalamic nuclei. The interpositus and dorsal dentate nuclei project to the motor cortex, and the ventrolateral dentate nucleus projects to the prefrontal cortex. The dorsal part of the dentate nucleus is connected to the supplementary motor area (SMA), which in turn projects to the primary motor cortex and spinal cord. The ventral portion of the dentate nucleus projects to the pre-SMA, which is interconnected with prefrontal regions (3, 52, 58, 59).

CEREBELLUM AND NEUROCOGNITIVE DEVELOPMENT

Functional Anatomy and Topography

Increasing results coming from neuroanatomic, neuroimaging, and clinical investigations conducted over the last three decades have allowed for a revision of the concept of the cerebellum as exclusively involved in motor control. On the contrary, a dense network of reciprocal connections with many supratentorial association areas is involved in many aspects of high-level neurocognitive processing (60–66). Moreover, a high degree of regional specialization of cerebellar functional topography has been demonstrated in both the adult and the pediatric population. According to this evidence, the anterior and inferior posterior cerebellum lobes are predominantly involved in sensory-motor performance. The superior posterior cerebellum is mainly associated with cognitive and social behavior functions. Emotional aspects are potentially related to the vermis (61, 62, 67–71).

Thanks to the loop system organization, the cerebellum plays a crucial modulatory role in the anatomo-functional optimization for both motor and non-motor processing within the developing brain throughout childhood and into adolescence (52).

Interestingly, the microscopic structure of the cerebellar cortex and its basic circuitry do not display significant differences in the various cerebellar lobes and lobules. In other words, the high heterogeneity of cerebellum involvement in functional processing is supported by a relatively constant structural configuration. This might relate to the strategy of improving stability, consistency, regularity, automatization of the regulation and modulation process of the supratentorial compartment, while reducing energy request (2).

MRI studies indicate that the cerebellar structure changes with age, peaking at 12 years of age in females and 15 years in males (72). However, the cerebellar development is not linear, but instead follows an asynchronous sequence. Resting state analysis revealed that more phylogenetically recent regions mature later. In fact, infants have a strong functional connectivity corresponding to the sensory-motor system, while children and adults also have associations with executive control and default mode systems, especially during the middle childhood (73). Moreover, the connectivity between the ipsilateral cerebellum and the contra-lateral primary sensory-motor cortex is stronger in adults than in children and adolescents, and vice-versa for connectivity within the local cerebellum. These findings are in favor of a *local-to-distant* development of cerebellar networks (74).

It is worth noting that several aspects of the cerebellar functional anatomy coming from animal studies need to be further clarified in humans. For example, several Authors discussed about existence and functional role of reciprocal connections between the cerebellum and the hypothalamus. After previous evidence in animal models using track-tracing and electrophysiology methods, direct cerebello-hypothalamic connections passing through the SCP have been recently described also in the human brain using fiber dissection and DTI technique (2, 32, 75, 76). Even if the functional orientation (afferent or efferent) of this pathway needs to be clarified, these results would confirm the effective participation of the cerebellum in typical hypothalamic processing, such as cardiovascular osmolarity regulation, feeding behavior, energy balance, and weight control (77, 78).

Another example concerns the existence of a cerebellar-mammillary network. Afferent connections from the lateral mammillary nucleus to vermis lobule IX (uvula) and the cerebellar anterior lobe in were described exemplars of rodents and primates, while studies performed in monkey reported different possible patterns of ipsilateral and contralateral mainly afferent projections from lateral and medial mammillary, supramammillary, and tuberomammillary nuclei to the deep cerebellar nuclei (75, 79, 80). In humans, more recent tractography analysis in healthy subjects revealed both ipsilateral and contralateral pathways between the mammillary bodies, cerebellar cortex, and dentate nucleus, reinforcing the cerebellum role in several autonomic functions, visuo-spatial orientation, and memory (81).

The Motor Cerebellum

Growing literature, coming from tracer studies in non-human primates, human diffusion tensor imaging and functional connectivity measures, lesion studies, and electrical and magnetic stimulation studies is highlighting the anatomo-functional substrate for the implication of the cerebellum in motor function (82).

Anatomical studies demonstrated that the cerebellum output system projects to all components of the voluntary, balance and postural motor systems, through connections with both homolateral and contralateral agonist, antagonist and synergist muscles which are automatically activated during the motor learning process and most voluntary movements of daily life, including the timing of rhythmic movements (83, 84).

More recently, a strict bidirectional interplay between the cerebellum and the basal ganglia was also demonstrated in animal models. In humans, such interactions were corroborated by neuroimaging and stimulation results in neurological motor diseases associated with basal ganglia disorders, such as Parkinson's disease, writer cramp, and primary dystonia (85, 86).

Based on results of different contribution from clinical and neuroimaging research, Manto et al. summarized in a

consensus paper, the large involvement of the cerebellum in several aspects of sensorimotor control, including oculomotor function, classical conditioning, motor speech, grip strength, voluntary limb movements, timing, sensorimotor synchronization, corticomotor excitability, movement-related sensory data acquisition, and interaction with the cerebrum in visuo-kinesthetic perception of hand movement, functional neuroimaging studies and magnetoencephalographic mapping of cortico-cerebellar dynamics (87).

Further crucial contribution came from clinical ataxiology. In fact, studies performed in both the pediatric and the adult population investigated the role of the cerebellum in three main categories of motor symptoms and signs related to the so-called "cerebellar motor syndrome", including:

(i) speech deficits (dysmetria of speech, impaired motor timing, and abnormal sequencing): ataxic dysarthria, observed in lesions of both hemispheres, with a predominance for lesions on the right side; cerebellar mutism, associated with resection of midline tumor, traumatic events, strokes, or infections;
(ii) impairments of limb movements: hypermetria or hypometria dys-diadochokinesia, cerebellar tremor, isometrataxia, disorders of muscle tone, and impaired check and rebound;
(iii) abnormalities of posture and gait: ataxia of stance (increased body sway with a broad-based stance), irregular and staggering gait (87).

The cerebellar nuclei are key components of this circuitry. Each cerebellar nucleus has a somatotopic representation of the body. For example, two aspects are of special interest. The first one is related to the *interposed nucleus*, which is activated according to temporal patterns, for fine adjustments of the motor output and coordination of both single and multiple muscles. Purkinje neurons receive a massive convergence of inputs from parallel fibers, which allows to integrate the neural information coming from different sources. Their simple spikes modulate weakly during passive movements, but strongly during active movements. The activity of complex spikes following discharges constitutes a teaching signal or a motor clock signal, constituting a synchronization function of the cerebellar cortex.

The other aspect concerns the *dentate nucleus*, that is responsible for the 75% of cerebellar projections to the primary motor cortex, and for the remaining array of connections with the ventral premotor, the supplementary motor area, and with other cognitive prefrontal and posterior parietal areas (52, 88). The functional anatomy and connectivity of this structure has been revisited in a recent study by Tacyldiz et al. Based on their WM dissection technique, a compartmentalization of the DN, including the lateral major, lateral anterosuperior, posteromedial, and anteromedial areas, territorial distribution of WM connections and involvement in the SCP decussation have been carefully characterized. Fiber dissection results were consistent with data from previous functional studies. In fact, the major lateral compartment of the dentate nucleus showed both motor and nonmotor functions, the posteromedial compartment of the dentate nucleus is involved in motor functions, whereas the lateral antero-superior part and non-crossing fibers from the anteromedial compartment are related to nonmotor functions (89).

Dentate nuclear neurons fire at a permanent rate of discharge allowing the sensitivity of target structures to be tuned. This activity increases before the onset of movement and even before the firing of the motor cortex, indicating that the cerebellum is actively involved in the process of movement initiation (52).

Application of non-invasive brain stimulation techniques, such as transcranial magnetic stimulation and transdermal cortical stimulation, in both healthy subjects and cerebellar ataxic patients allowed to evaluate the role of cerebellum in motor control and learning. These functions would depend on connectivity between the cerebellum and the primary motor cortex. Intensity of cerebellar inhibitory output would correlate with quality of movement precision during reaching performance tests, and vice versa (90). On the other hand, results coming from experimental brain stimulation revealed that modulation of cerebellar activity would influence the speed of motor adaptation by decreasing cerebellar-brain inhibition (86, 91, 92).

Two circuits crucially involved in the motor aspects of cerebellum physiology are the olivo-cerebellar and rubro-cerebellar networks. Previous animal and human studies characterized the large connectivity between these structures and several cortical and subcortical areas and highlighted their participation in the extracerebellar connectivity (93).

As resumed in a consensus paper by Lang et al., the olivo-cerebellar circuit is more flexible than traditionally believed. In fact, several experimental findings showed that this system contributes to multiple aspects of the cerebellar motor control function, by generating ongoing motor commands and optimizing future motor performance by gating synaptic plasticity (94). On the other side, inferior olive denervation, associated with lesion of inhibitory projections from deep cerebellar nuclei through the central tegmental tract, would cause hypertrophy and disinhibition, altering the normal tonic firing pattern, thus likely resulting in abnormal olivo-cerebellar feedback manifesting as tremor (95).

Concerning the red nucleus (RN), lesion studies reported that rubro-cebellar circuits are compromised in several motor symptoms, including classic Holmes tremor, oculopalatal tremor, essential tremor, asynergia, adiadochokinesia, dysmetria, and non-motor manifestations, such as memory impairment, decreased verbal fluency, and intellectual fatigability (96).

These data confirmed results coming from both the animal literature and human functional studies, that provided converging evidence on the participation of the RN in planning, initiation and termination of motor tasks, but also in higher functions, such as sensory discrimination, salience detection, and executive functions (86, 97–99). The rich functional implication of the rubro-cerebellar system depends on a complex involvement of the RN in parallel and synergic networks, involving many cortical of cortical and subcortical areas, including basal ganglia, prefrontal cortex, occipital cortex, posterior hippocampus, caudal insula, thalamus, hypothalamus,

left precuneus, superior temporal cortex, presupplementary motor area (preSMA) (100, 101).

Finally, observations in patients affected by the cerebellar motor syndrome indicate that the cerebellum is essential to performing accurate motor predictions and timing commands by generating *internal models,* thanks to its strict integration in large-scale brain networks. In fact, the capacity of the brain to generate predictions by integrating spatial, temporal, and environmental information is critical to performing movements with correct timing and to have adequate perceptual judgments in several tasks of daily life. Childhood is a critical period for the acquisition of this capacity. It has been demonstrated that anticipatory behaviors, especially for grasping, drawing, and postural control, are strictly related to both development of internal models for eye movements, as well as visual and proprioceptive feedback control. Training the accuracy of these internal models starts approximately at the age of 2 years and requires around seven to 10 years to mature to adult levels (102).

The Language Cerebellum

A growing number of neuroimaging and clinical studies are highlighting the cardinal role of the cerebellum in linguistic processing *via* strong cerebello-cerebral interactions.

After the first evidence in healthy subjects in the late 1980s, several positron emission tomography studies confirmed the consistent involvement of the right posterior, lateral and inferior cerebellum during association and word generation tasks (103). A few SPECT perfusion studies highlighted the phenomenon of diaschisis, that is the reciprocal impact by a cerebellar or supratentorial lesion on the distant contralateral cerebral or cerebellar region, respectively, and provided evidence in favor of a "lateralized linguistic cerebellum" (104–110).

Introduction of fMRI technique allowed to better characterize the cerebellar language-specific activations associated with both expressive and receptive tasks, (especially at the level of lobule VI, crus I/II, and midline lobule VII of the right cerebellum), and defined the crossed anatomic interaction with the language association areas within the dominant frontal, parietal, and temporal regions (111, 112).

Moreover, it has been demonstrated that prematurity itself, cerebellar malformations or acquired injuries, involving totally or partially the cerebellar hemispheres, the vermis or the peduncles, may affect speech and language development, with varying degrees of severity, ranging from absence of language to high-level meta-linguistic disorders, according to the site and extent of the defect (113, 114).

Analysis of resting-state fMRI data in unilateral or bilateral malformation patients showed an impairment of the executive-control network involving areas strongly connected with the cerebellum through the fronto-pontine fibers (115, 116).

Lesion studies concerning both children and adult cases reported several different types of motor and non-motor language deficits after cerebellar damage, ranging from pure motor speech disorders (e.g., ataxic dysarthria) or linguistic processing impairments (e.g., mutism, conduction-like aphasia, phonemic, semantic, syntactic, lexical deficits, agrammatism, dysprosody), to high-level metalinguistic disturbances (e.g., sentence construction, word definitions, figurative language, word associations, lexical-semantic manipulation) (117–128).

These data show that the cerebellum is implicated not only in motor and planning aspects of language, but participates also in high-level non-motor linguistic processes, including speech and language perception, verbal working memory, phonological and semantic verbal fluency, syntax processing, grammar processing, as well as reading and writing (110, 129).

Investigation of the neuroanatomical substrate for this functional complexity revealed that a close connection between the cerebellum and the supratentorial motor, paralimbic, and association cortices is established by a dense network of cortico-ponto-cerebellar and cerebello-thalamo-cortical loops. Moreover, functional connectivity analyses demonstrated that, as for motor function, a topographical organization exists also for cognitive and language processing, with representation of the muscles of articulation located in medial lobule VI, whereas conceptual elements of language are mostly represented within the right posterior-lateral regions of lobules VI and VII (3, 61, 71, 128).

As for motor function, the network between the cerebellum and different supratentorial centers reinforces the concept of a regulatory role of the cerebellum in monitoring and coordinating cortical functions. This phenomenon, called "universal cerebellar transform" allows the cerebellum to compare predictions related to internal speech or subvocal rehearsal, neural representation of the external world (called "internal models"), with the incoming feedback from the cerebrum. The internal models are used to create, manipulate, and predict mental representations, by comparing them with the prefrontal and temporo-parietal cortex to optimize cognitive and language performance (71, 110).

The Cognitive, Emotional and Behavior Cerebellum

The third important aspect of cerebellum functional anatomy concerns its contribution to neurocognitive processing. Also in this field, many works provided consistent neuroimaging and clinical data on the strict interactions between the cerebellum and different cortical and subcortical territories involved in cognition, executive, spatial, working memory, emotional, and behavior processing and social domains (61, 71, 109, 129).

The anatomo-functional network related to cognitive and emotional domains develop at a later stage, according to emergence of long-range cerebro-cerebellar connectivity. Moreover, the development of intrinsic connectivity extends beyond the first years of life into late adolescence, consistent with changes in executive function, social interactions, and risk-taking behavior (130, 131).

Clinically, alteration of executive functioning has been associated to different etiologies occurring during both childhood and adulthood, including congenital malformations (cerebellar or vermian hypoplasia, atrophy, or dysplasia), and acquired cerebellar damage, such as viral inflammatory lesion or tumors. These diseases adversely impact the development of both cerebellar gray volume and the integrity of distant projections to basal ganglia and non-motor cortical regions.

Seriousness of clinical consequences depends on both extension of structural defect and timing of lesion event, ranging from mild neuropsychologic delay to severe and long-lasting intellectual disability and neuropsychiatric disorders, such as schizophrenia, Tourette's syndrome, autism, attention deficit disorder, and addiction (132).

Concerning emotional processing, early electrophysiological and anatomical studies in humans and animals that revealed that stimulation of specific cerebellar territories, such as the dentate nucleus and the SCP, evocated different emotional responses or mood modification after chronical stimulation, and demonstrated reciprocal connections with limbic structures (133–137).

Following functional connectivity studies demonstrated that the vermis is a crucial region functionally connected to limbic structures allowing for emotional regulation (through the amygdala), emotional memory (through the hippocampus), and autonomic and cognitive components related to emotional experience. In fact, the vermis has an early-stage pattern of maturation, and it does not show significant changes in volume during childhood and adolescence. This evidence confirms that this phylogenetically "older" part of the cerebellum is recruited during primary emotional processing (138–140).

Social cognition is defined as the set of mental processes required to understand, generate, and regulate social behavior and interpersonal interactions. Social cognition is strictly related to the mentalizing, which consists in the ability to understand the mental state of oneself or others underlying overt behavior (64, 71). Previous researchers identified the brain regions most involved in the "mentalizing network", including the temporoparietal junction, the precuneus, the amygdala, the anterior temporal lobe, the occipital gyrus, the fusiform gyrus, the inferior frontal gyrus, and the medial prefrontal cortex (141–145).

Although participation of the cerebellum to this circuitry received less attention in the past, more recent resting state fMRI studies indicated a functional overlap between the social cognition network of the cerebellum and the mentalizing network of the cerebrum, namely the default-mode network (DMN), which involves a set of brain regions such as the posterior cingulate cortex, the precuneus, the lateral parietal/angular gyrus, the medial prefrontal cortex, the superior frontal gyrus, and the temporoparietal junction (146).

This finding was also reported in clinical studies on diseases typically characterized by an impairment in social mentalizing, such as autism spectrum disorder (147). Otherwise, the possibility that cerebellar damage might cause social cognition or mentalizing deficits would depend on the developmental stage during which the injury occurs, the location of injury, and testing modality (64). According to this model, the role of the cerebellum would be to modulate the activity of default regions by detecting errors between predicted output and current behavior through construction of internal models. In case of mismatch, the feedback error signal would be sent back to the same cerebral regions (146).

Other Authors investigated the specific cerebellar zones mostly implicated in mentalizing processes in association with the human DMN (139, 148–155). For example, a meta-analysis of functional connectivity studies revealed a strong recruitment of posterolateral cerebellar hemisphere corresponding to crus I/II in bilateral mentalizing cerebral regions, such as the left and right temporoparietal junctions, the precuneus, and the medial prefrontal cortex. Within this circuit, the medial prefrontal cortex and the right temporo-parietal junction converge on the right posterior cerebellum and then back to the left temporo-parietal junction, which in turn receives connectivity from the dorsal medial prefrontal cortex and the right temporo-parietal junction. Interestingly, it was shown that cerebello-cerebral connections are not directly linked in both directions, as expected, but have possibly divergent patterns of information communication with other regions during social cognition processing (150).

More recently, Metoki et al. applied a multimodal neuroimaging approach, including functional mapping, effective connectivity, and probabilistic tractography, to investigate the structural and functional role of the cerebellum in the mentalizing network. In addition to confirming that also mentalizing has a domain-specific function, the authors identified stronger effective connections from the left posterior cerebellar hemisphere to the right cerebral mentalizing areas through cerebello-thalamo-cortical and cortico-ponto-cerebellar connections to right cerebral areas mostly involved in mentalizing processing (7, 64, 149).

Finally, electrophysiological, pharmacological and immunohistochemical research studies investigated how different neurotransmitter systems, such as noradrenergic, cholinergic or dopaminergic system, can modulate the synaptic transmission and thereby influence the functional output through activation of specific cerebellar receptor subtypes (156–166).

Norepinephrine responsive cells were identified within both the cerebellar cortex and the cerebellar nuclei (156). Moreover, recent studies in rat have shown that GABAergic synapses of cerebellar interneurons and Purkinje cells are positively regulated by norepinephrine. The overall effect of the noradrenergic afferent input to the cerebellar cortex reinforces GABAergic inhibitory influence from the basket cells to the output signals generated by Purkinje cells. The subsequent modulation of GABAergic transmission at synapses between input and output cells appears to play a critical role in motor coordination associated with the cerebellar connection with the somatosensory cortex (167).

The cholinergic system has been shown to have an important modulatory effect on synaptic transmission, especially at the level of climbing and mossy fibers, and in regulating release of other neurotransmitters. This (plastic) effect would influence the rapid intracerebellar and cerebro-cerebellar causal connectivity, so conditioning the final functional cerebellar outputs during non-motor cognitive task. Moreover, modulation of neuronal excitability and/or synaptic responses would have a significant role during cerebellar development, by facilitating neuronal maturation, differentiation, adaptation, and survival. On the other hand, cholinergic dysfunctions were shown to be involved in the pathogenesis of cognitive impairments and other

neurological disorders, such as cerebellar ataxia, autism, and Parkinsonism (157).

Concerning the dopaminergic system, the cerebellum was traditionally not considered an elective dopaminergic region. However, lesion studies have shown the involvement of cerebellum in dopamine deficit-related neurological and psychiatric disorders, such as Parkinson's disease, schizophrenia, autism spectrum disorders, and drug addiction (158–161). Moreover, data coming from invasive studies in animal and tractography observation in humans revealed relevant patterns of intracerebellar dopaminergic connectivity, such as between the DN and the cerebellar cortex, and extrinsic interconnections between the cerebellum and traditional dopaminergic areas of the brain, including the midbrain, the neostriatum, the neocortex (162–165). These connections could represent part of the cerebellar projective circuits which allow the cerebellum to contribute to motor and cognitive functions (164, 166).

Interestingly, the role of cerebellum in different neurotransmitter systems may have implication for innovative non-invasive treatments (e.g., electrical, or magnetic stimulations) for several neurological and mental disorders (166).

The Visual and Attention Cerebellum

Previous research from animal models and patients with developmental abnormality (e.g., autism) or acquired injury (e.g., tumor and stroke) showed that damage to the cerebellum was associated to slowed spatial attention orienting (168–170).

Following fMRI studies in healthy subjects confirmed these observations and investigated the structural substrate underlying the cerebellum participation to a network of cortical regions, including the posterior parietal cortex, the frontal eye fields, and the dorsolateral prefrontal cortex (the so called, dorsal attention network or fronto-parietal network) that support sustained attention and working memory (171). More specifically, analysis of functional connectivity in intact brains demonstrated that the lobule VI of the left cerebellar hemisphere in both covert attention and saccadic eye movements (172).

Other Authors identified a strong functional correlation between cortical nodes forming the dorsal attention network and cerebellar lobules VIIb and VIIIa within the posterior cerebellum during visual attention and working memory tasks. Moreover, different functional patterns between the dorsomedial and ventrolateral regions of lobule VIIb/VIIIa were also found in relation with visuospatial representations and load-dependent visual working memory processing, respectively (173–175).

More recently, a comprehensive mapping of the cerebellar visuospatial organization based on a retinotopy dataset collected in 181 participants revealed a large distribution of signals involving the vermis and the lobules VIIb and VIIIb. In particular, connections between retinotopically organized cortical regions of lobule VIIb with the intraparietal sulcus confirmed involvement of this structure in spatial cognition, including attention and working-memory-related processes. The lobule VIIIb was found to be related to the dorsal and the ventral attention networks and to the somato-motor network, suggesting an integrative role for this region for both attentional and motor processes. In summary, these data are in favor of participation of the cerebellum in attentional mechanisms by prediction of dynamic perceptual events and integration of visuospatial information for the guidance of effector movements (176).

IMPLICATIONS

The crucial involvement of the cerebellum in sensory-motor and higher cerebral functions may correlate with a variety of clinical consequences in case of pathological processes, including developmental disorders, malformations, stroke, and tumors or iatrogenic causes (10). These conditions may alter the normal anatomo-functional configuration of gray and WM components forming the cerebellar connectome, at both the local and the remote level of the network.

Considering WM structures specifically, direct damage or disconnection of input or output connections with different cerebral supratentorial eloquent regions passing through the cerebellar peduncles should be considered. In fact, anatomo-clinical studies showed that lesions of the SCP cause ipsilateral intention tremor, dysmetria, and decomposition of movement; lesions of the MCP are associated with homolateral hypotonia, ataxia, and dysmetria during voluntary movement; injury to the ICP induces disturbances of equilibrium with truncal ataxia and staggering gait (35, 36, 44).

Concerning neuro-oncology, previous studies indicated that cerebellum undergoes structural and functional alterations, especially concerning language function, induced by supratentorial high-grade and low-grade gliomas, confirming the role of cerebellar system in lesion induced plasticity process (177, 178).

It is worth noting that a majority of previous studies evaluated the local and distant effects of posterior fossa tumors after treatments, especially surgery and radiotherapy, while only a few authors focused on the direct effects of cerebellar tumors on WM structures. Currently, the main evidence on tumor-related alteration of WM integrity concerns the cerebello-thalamo-cerebral tracts. Significant impairment of this pathway was shown, especially in patients with diagnosis of posterior fossa medulloblastoma, large tumors with bilateral extension that cross the midline, and left-handed subjects. In these cases, a significant correlation between the overall damage of the cerebro-cerebellar connectivity and extent of ataxia and fine motor dysfunction has been demonstrated (179).

Regarding the possible effects of surgery and other treatments, a perfect example is posterior fossa syndrome (PFS), which includes ataxia, muscular hypotonia, hemiparesis or tetraparesis, and possible cranial nerve deficits. This condition is frequently associated with cerebellar mutism syndrome, which is characterized by diminished psychological impulsion associated with inhibition of speech output. These well-recognized complications occur at a high rate in children (10 to 40%) who undergo posterior fossa surgery for both malignant and benign tumors (180–185).

In the past, different factors, including brain stem compression, hydrocephalus, and damage to the inferior cerebellar vermis were considered responsible for PFS (183, 186).

More recent large scale-studies revealed that the pathogenesis of PFS depends on a more complex involvement of cerebellar connection systems, including the dentate nucleus and the superior cerebellar peduncle of fronto-cerebellar pathways, independent of chemotherapy or radiation (187–191).

In addition, a significant association between cerebellar tumors and neurocognitive performance, especially working memory, was also demonstrated when a global functional depression of cerebral cortical activity (with a predilection to frontal regions) was found in patients with PFS, related to a decreased integrity of WM pathways and a diaschisis-related mechanism (192–194).

Functional-MRI studies contributed to further characterizing these aspects. A recent study found that cognitive disturbances in pediatric infra-tentorial tumor survivors were related to abnormalities in regional neural synchrony, leading to reorganization of network topology and, consequently, to disconnection of damaged regions and multiple extracerebellar functional brain networks (195). In the largest lesion mapping study to date, the cognitive and affective symptoms following pediatric cerebellar tumor resection were evaluated in 195 pediatric patients. Comparison between resting-state functional connectivity MRI patterns of pathological cases and normal subjects confirmed the role of disrupted cerebro-cerebellar connectivity, particularly involving a network including the fastigial and dentate nuclei, the thalamic mediodorsal nucleus, and projections to the limbic system (anterior cingulate, medial, lateral prefrontal, and orbitofrontal cortices) (196).

Interestingly, it was reported that seriousness of PFS depends also on patient-specific presurgical status. A significant decrease in preoperative neural connectivity involving the corpus callosum, the right cortico-thalamic pathway, and the right cortico-striatal pathway was found in children who developed a post-operative PFS, compared with those who did not (197).

Finally, a positive correlation between the cerebellar volume of output structures and integrity of WM output was shown. Impairment of this correlation, also called trans-neural degeneration, may produce different consequences depending on type of treatment. Without radiation, the primary mechanism of injury is cerebellar tumor growth, resection, and hydrocephalus. Therefore, the lesion involves the most proximal connection (cerebellar-rubral pathway). In contrast, the survivor group treated with radiation may have most extended radiation-induced demyelination of the thalamic-frontal portion of the pathway, based on a strong correlation with volume loss in the cerebellum, the red nucleus, the thalamus, and the frontal lobe (198).

Neurosurgical Implications

Progressive advancement in knowledge on the cerebellar connectome may have important implications for the neurosurgical community, especially regarding management of posterior fossa tumors and vascular malformations (199, 200).

Complexity of the anatomo-functional organization of the intra-cerebellar and the extra-cerebellar circuitry is directly related to the need for careful awareness of surgically related neurological consequences at short and long term. For this reason, the authors of a recent systematic review emphasized that *cerebellar functional anatomy should receive similar awareness during infratentorial surgery as during supratentorial resections* (201).

In this perspective, two aspects might be of special interest to improve the quality of surgical results and functional outputs. First, an accurate understanding of the three-dimensional functional anatomy and topography of cerebellar WM is crucial to select the most appropriate approach, especially in the case of approaches involving the fourth ventricle (44). Fascinating didactic dissection and tractography studies have been devoted to describing the surgical anatomy of the human cerebellum and to discussing implications of main eloquent cerebellar nuclei and cerebellar peduncles in most common surgical routes (192, 202–205).

In fact, dissection studies show that all the cerebellar peduncles converge on the lateral wall and roof of the fourth ventricle. In particular, the ICP and SCP are more likely to be injured during procedures within the fourth ventricle because they abut directly on the ventricular surface. On the other hand, the MCP would be more susceptible to injury when approaching the cerebellopontine angle, where it forms a major part of the cisternal surface of the ventricular wall (36).

In the case of approaches to intrinsic peduncular lesions, it is recommended to perform the incision on the dorsal surface of the MCP following a parallel and longitudinal direction to respect the pontocerebellar fibers. If resection involves deeper ponto-cerebellar fibers, the anatomical boundaries to be respected include the corticospinal tract ventrally, the trigeminal nerve caudally and the medial and lateral lemnisci posteriorly in the tegmental pars of the pons (206). Following these considerations, previous authors have analyzed the main anatomical surgical landmarks to be respected and compared the different possible approaches according to lesion location and extension (192, 203–206).

The second consideration is that development and systematic application of accurate neuromonitoring techniques is of paramount importance for preserving the main components of the network. However, as revealed by a recent review, despite the consolidated experience of intraoperative monitoring during brainstem, fourth ventricle, and skull base surgery, specific neurophysiological data on the cerebellum are lacking, due to the polysynaptic organization of the cerebro-cerebellar circuitry and, in pediatric cases, to the immaturity of nervous structures (88).

Consequently, apart from adoption of basic technical precautions, such as accurate neuronavigation guidance and avoidance of mechanical and thermal injury, for now the possibility of improving safety of intracerebellar surgery seems to rely on the development of other methods able to predict the postoperative outcome (201).

These include, for example: (i) computation of probabilistic connectivity atlas based on segmentation of the cerebellar peduncles, allowing for comparison of WM integrity between patients and controls diffusion maps (207, 208); (ii) application of transcranial magnetic stimulation (TMS) technique to provide either negative or positive inhibitory or facilitatory modulation of the primary motor cortex output using an appropriate

cerebellar stimulus to deduce injury to the dentato-thalamic-cortical circuit and predict postsurgical development of cerebellar mutism (209); (iii) development and validation of reliable procedures for neurophysiological monitoring of the cerebello-cortical connectivity. Preliminary results in this field showed the feasibility of reproducing extra-operative conditioning-test paradigm previously adopted for TMS (210).

CONCLUSIONS

Modern neuroscience has significantly progressed toward a more realistic characterization of cerebellar functional anatomy. A growing number of studies have confirmed that the cerebellum is involved in several networks with both short-range and long-range disposition. This organization results from a continuous process of anatomo-functional refinement continuing from childhood to adulthood, allowing for integration between intra-cerebellar connections and supratentorial circuits.

In parallel with the closed loop structural configuration, the dogma of the cerebellum being merely responsible for motor coordination has been definitively repudiated, in favor of a more complex functional role that also includes emotional and social processing.

This evidence should not be limited just to theoretical speculation, but may have important implications for neurosurgical practice, especially for management of diseases harboring the posterior fossa. In fact, application of multimodal analysis for the pre-operative and post-operative assessment of the cerebello-cerebral networks might provide crucial insights allowing for a better understanding of the effects of a pathological process and of surgery itself and optimizing the quality of intraoperative approaches and rehabilitation strategies.

In this context, some challenging yet promising topics could be mentioned for future research. For example, the role of age, of specific cerebellar sub-regions, and of plasticity mechanisms in normal and pathological motor and cognitive outcomes, especially during critical periods following early life stages should be further highlighted. Moreover, identification of specific biomarkers will allow for the development of reliable probabilistic atlases based on different convergent factors, such as the presurgical cerebellar lesion characteristic, the relationships between the lesion type and location, the cerebellar outflow, the supratentorial cortical activity, and the possible clinical deficits. Finally, all this information might contribute to stratifying the postoperative risk, so improving the quality of communication to patients and families and optimizing both presurgical planning and intraoperative management.

AUTHOR CONTRIBUTIONS

All authors have given substantial contributions to the conception, the draft, and the final approval of the manuscript.

FUNDING

This research was funded by the Ministero della Salute-Ricerca Corrente to Ospedale Pediatrico Bambino Gesu', IRCCS.

ACKNOWLEDGMENTS

The authors acknowledge Mr. Aalap Herur-Raman for the language editing of this manuscript.

REFERENCES

1. Berry MM, Standring SM, Bannister L. "Cerebellum". In Williams PL, editor. *Gray's Anatomy*. New York: Churchill Livingstone. (1995). p. 102765.
2. Benagiano V, Rizzi A, Lorusso L, Flace P, Saccia M, Cagiano R, et al. The functional anatomy of the cerebrocerebellar circuit: a review and new concepts. *J Comp Neurol.* (2018) 526:769–89. doi: 10.1002/cne.24361
3. Stoodley CJ, Schmahmann JD. Functional topography of the human cerebellum. *Handb Clin Neurol.* (2018) 154:59–70. doi: 10.1016/B978-0-444-63956-1.00004-7
4. van Welie I, Smith IT, Watt AJ. The metamorphosis of the developing cerebellar microcircuit. *Curr Opin Neurobiol.* (2011) 21:245–53. doi: 10.1016/j.conb.2011.01.009
5. Brossard-Racine M, Limperopoulos C. Normal Cerebellar Development by Qualitative and Quantitative MR Imaging: From the Fetus to the Adolescent. *Neuroimaging Clin N Am.* (2016) 26:331–9. doi: 10.1016/j.nic.2016.03.004
6. Amore G, Spoto G, Ieni A, Vetri L, Quatrosi G, Di Rosa G, et al. A focus on the cerebellum: from embryogenesis to an age-related clinical perspective. *Front Syst Neurosci.* (2021) 15:646052. doi: 10.3389/fnsys.2021.646052
7. Habas C, Manto M. Probing the neuroanatomy of the cerebellum using tractography. *Handb Clin Neurol.* (2018) 154:235–49. doi: 10.1016/B978-0-444-63956-1.00014-X
8. Koeppen AH. The neuropathology of the adult cerebellum. *Handb Clin Neurol.* (2018) 154:129–49. doi: 10.1016/B978-0-444-63956-1.00008-4
9. Sarnat HB. Cerebellar networks and neuropathology of cerebellar developmental disorders. *Handb Clin Neurol.* (2018) 154:109–28. doi: 10.1016/B978-0-444-63956-1.00007-2
10. Meoded A, Goldenberg NA, Huisman TAGM. Structural connectomics: state of the art and applications in pediatric neurodevelopmental disorders, neuro-oncology, and arterial ischemic stroke. *J Pediatr.* (2020) 221S:S37–42. doi: 10.1016/j.jpeds.2020.01.056
11. Cajal S. *Manual de Histologia Normal y Tecnica Micrografica*. Valencia, Libreria de Pascual Aguilar (1889).
12. De Felipe J. Cajal and the discovery of a new artistic world: the neuronal forest. *Prog Brain Res.* (2013) 203:201–20. doi: 10.1016/B978-0-444-62730-8.00008-6
13. Voogd J, Koehler PJ. Historic notes on anatomic, physiologic, and clinical research on the cerebellum. *Handb Clin Neurol.* (2018) 154:3–26. doi: 10.1016/B978-0-444-63956-1.00001-1
14. Voogd J, Ruigrok TJ. The organization of the corticonuclear and olivocerebellar climbing fiber projections to the rat cerebellar vermis: the congruence of projection zones and the zebrin pattern. *J Neurocytol.* (2004) 33:5–21. doi: 10.1023/B:NEUR.0000029645.72074.2b
15. Schmahmann JD, Pandya DN. Prefrontal cortex projections to the basilar pons in rhesus monkey: Implications for the cerebellar contribution to higher function. *Neuroscience Letters.* (1995) 199:175–8. doi: 10.1016/0304-3940(95)12056-A
16. Brodal P, Bjaalie JG. Salient anatomic features of the cortico-pontocerebellar pathway. *Prog Brain Res.* (1997) 114:227–49. doi: 10.1016/S0079-6123(08)63367-1
17. Ramnani N. The primate cortico-cerebellar system: Anatomy and function. *Nature Reviews Neuroscience.* (2006) 7:511–22. doi: 10.1038/nrn1953

18. Kievit J, Kuypers HG. Organization of the thalamo-cortical connexions to the frontal lobe in the rhesus monkey. *Exp Brain Res.* (1977) 29:299–322. doi: 10.1007/BF00236173
19. Leergaard TB, Bjaalie JB. Topography of the complete cor- ticopontine projection: From experiments to principal maps. *Front Neurosci.* (2007) 1:211–23. doi: 10.3389/neuro.01.1.1.016.2007
20. Suzuki L, Coulon P, Sabel-Goedknegt EH, Ruigrok TJ. Organization of cerebral projections to identified cerebellar zones in the posterior cerebellum of the rat. *J Neurosci.* (2012) 32:10854–69. doi: 10.1523/JNEUROSCI.0857-12.2012
21. Klingler J. Erleichterung der makroskopischen praeparation des gehirns durch den gefrierprozess. *Schweiz Arch Neurol Psychiatr.* (1935) 36:247–56.
22. Zemmoura I, Blanchard E, Raynal PI, Rousselot-Denis C, Destrieux C, Velut S. How Klingler's dissection permits exploration of brain structural connectivity? An electron microscopy study of human white matter. *Brain Struct Funct.* (2016) 221:2477–86. doi: 10.1007/s00429-015-1050-7
23. Agrawal A, Kapfhammer JP, Kress A, Wichers H, Deep A, Feindel W, et al. Josef Klingler's models of white matter tracts: influences on neuroanatomy, neurosurgery, and neuroimaging. *Neurosurgery.* (2011) 69:238–52. doi: 10.1227/NEU.0b013e318214ab79
24. De Benedictis A, Sarubbo S, Duffau H. Subcortical surgical anatomy of the lateral frontal region: Human white matter dissection and correlations with functional insights provided by intraoperative direct brain stimulation: laboratory investigation. *J Neurosurg.* (2012) 117:1053–69. doi: 10.3171/2012.7.JNS12628
25. De Benedictis A, Duffau H, Paradiso B, Grandi E, Balbi S, Granieri E, et al. Anatomo-functional study of the temporo-parieto-occipital region: Dissection, tractographic and brain mapping evidence from a neurosurgical perspective. *J Anat.* (2014) 225:132–51. doi: 10.1111/joa.12204
26. De Benedictis A, Petit L, Descoteaux M, Marras CE, Barbareschi, Corsini F, et al. New insights in the homotopic and heterotopic connectivity of the frontal portion of the human corpus callosum revealed by microdissection and diffusion tractography: homo- and hetero-topic fronto-callosal connectivity. *Hum Brain Mapp.* (2016) 37:4718–35. doi: 10.1002/hbm.23339
27. De Benedictis A, Nocerino E, Menna F, Remondino F, Barbareschi M, Rozzanigo U, et al. Photogrammetry of the human brain: a novel method for three-dimensional quantitative exploration of the structural connectivity in neurosurgery and neurosciences. *World Neurosurg.* (2018) 115:e279–91. doi: 10.1016/j.wneu.2018.04.036
28. De Benedictis A, Marras CE, Petit L, Sarubbo S. The inferior fronto-occipital fascicle: a century of controversies from anatomy theaters to operative neurosurgery. *J Neurosurg Sci.* (2021) 3. doi: 10.23736/S0390-5616.21.05360-1. [Epub ahead of print].
29. Sarubbo S, De Benedictis A, Maldonado IL, Basso G, Duffau H. Frontal terminations for the inferior fronto-occipital fascicle: anatomical dissection, DTI study and functional considerations on a multi-component bundle. *Brain Struct Funct.* (2013) 218:21–37. doi: 10.1007/s00429-011-0372-3
30. Sarubbo S, De Benedictis A, Milani P, Paradiso B, Barbareschi M, Rozzanigo U, et al. The course and the anatomo-functional relationships of the optic radiation: a combined study with 'post mortem' dissections and '*in vivo*' direct electrical mapping. *J Anat.* (2015) 226:47–59. doi: 10.1111/joa.12254
31. Sarubbo S, De Benedictis A, Merler S, Mandonnet E, Barbareschi M, Dallabona M, et al. Structural and functional integration between dorsal and ventral language streams as revealed by blunt dissection and direct electrical stimulation. *Hum Brain Mapp.* (2016) 37:3858–72. doi: 10.1002/hbm.23281
32. Çavdar S, Esen Aydin A, Algin O, Aydogmuş E. Fiber dissection and 3-tesla diffusion tensor tractography of the superior cerebellar peduncle in the human brain: emphasize on the cerebello-hypthalamic fibers. *Brain Struct Funct.* (2020) 225:121–8. doi: 10.1007/s00429-019-01985-8
33. Cacciola A, Bertino S, Basile GA, Di Mauro D, Calamuneri A, Chillemi G, et al. Mapping the structural connectivity between the periaqueductal gray and the cerebellum in humans. *Brain Struct Funct.* (2019) 224:2153–65. doi: 10.1007/s00429-019-01893-x
34. Meola A, Comert A, Yeh FC, Sivakanthan S, Fernandez-Miranda JC. The nondecussating pathway of the dentatorubrothalamic tract in humans: human connectome-based tractographic study and microdissection validation. *J Neurosurg.* (2016) 124:1406–12. doi: 10.3171/2015.4.JNS142741
35. Pruthi N, Kadri PAS, Türe U. Fiber microdissection technique for demonstrating the deep cerebellar nuclei and cerebellar peduncles. *Oper Neurosurg.* (2021) 20:E118–25. doi: 10.1093/ons/opaa318
36. Rhoton AL Jr. Cerebellum and fourth ventricle. *Neurosurgery.* (2000) 47:S7–27. doi: 10.1097/00006123-200009001-00007
37. Haldipur P, Dang D, Millen KJ. Embryology. *Handb Clin Neurol.* (2018) 154:29–44. doi: 10.1016/B978-0-444-63956-1.00002-3
38. Leto K, Arancillo M, Becker EB, Buffo A, Chiang C, Ding B, et al. Consensus paper: cerebellar development. *Cerebellum.* (2016) 15:789–828. doi: 10.1007/s12311-015-0724-2
39. Deoni SC, Catani M. Visualization of the deep cerebellar nuclei using quantitative T1 and rho magnetic resonance imaging at 3 Tesla. *Neuroimage.* (2007) 37:1260–6. doi: 10.1016/j.neuroimage.2007.06.036
40. Takahashi E, Hayashi E, Schmahmann JD, Grant PE. Development of cerebellar connectivity in human fetal brains revealed by high angular resolution diffusion tractography. *Neuroimage.* (2014) 96:326–33. doi: 10.1016/j.neuroimage.2014.03.022
41. Bruckert L, Shpanskaya K, McKenna ES, Borchers LR, Yablonski M, Blecher T, et al. Age-dependent white matter characteristics of the cerebellar peduncles from infancy through adolescence. *Cerebellum.* (2019) 18:372–87. doi: 10.1007/s12311-018-1003-9
42. Petersen KJ, Reid JA, Chakravorti S, Juttukonda MR, Franco G, Trujillo P, et al. Structural and functional connectivity of the nondecussating dentato-rubro-thalamic tract. *Neuroimage.* (2018) 176:364–71. doi: 10.1016/j.neuroimage.2018.04.074
43. Palesi F, Tournier JD, Calamante F, Muhlert N, Castellazzi G, Chard D, et al. Contralateral cerebello-thalamo-cortical pathways with prominent involvement of associative areas in humans in vivo. *Brain Struct Funct.* (2015) 220:3369–84 doi: 10.1007/s00429-014-0861-2
44. Perrini P, Tiezzi G, Castagna M, Vannozzi R. Three-dimensional microsurgical anatomy of cerebellar peduncles. *Neurosurg Rev.* (2013) 36:215–24. doi: 10.1007/s10143-012-0417-y
45. Nagahama H, Wanibuchi M, Hirano T, Nakanishi M, Takashima H. Visualization of cerebellar peduncles using diffusion tensor imaging. *Acta Neurochir.* (2021) 163:619–24. doi: 10.1007/s00701-020-04511-6
46. Salmi J, Pallesen KJ, Neuvonen T, Brattico E, Korvenoja A, Salonen O, et al. Cognitive and motor loops of the human cerebro-cerebellar system. *J Cogn Neurosci.* (2010) 22:2663–76. doi: 10.1162/jocn.2009.21382
47. Sokolov AA, Erb M, Grodd W, Pavlova MA. Structural loop between the cerebellum and the superior temporal sulcus: evidence from diffusion tensor imaging. *Cereb Cortex.* (2014) 24:626–32. doi: 10.1093/cercor/bhs346
48. Karavasilis E, Christidi F, Velonakis G, Giavri Z, Kelekis NL, Efstathopoulos EP, et al. Ipsilateral and contralateral cerebro-cerebellar white matter connections: A diffusion tensor imaging study in healthy adults. *J Neuroradiol.* (2019) 46:52–60. doi: 10.1016/j.neurad.2018.07.004
49. Rorke LB, Riggs HE. *Myelination of the Brain in the Newborn*. Philadelphia, PA: Lippincott (1969).
50. Gilles FH. Myelination in the human brain. *Brain Pathol.* (1976) 7:244–8. doi: 10.1016/S0046-8177(76)80035-4
51. Gilles PI, Lecours A-R. "The myelination cycles of regional maturation of the brain". In: Minkowsky A, editor. *Regional development of the Brain in Early Life*. Philadelphia, PA: Davis. (1967). p. 3–70.
52. D'Angelo E. Physiology of the cerebellum. *Handb Clin Neurol.* (2018) 154:85–108. doi: 10.1016/B978-0-444-63956-1.00006-0
53. Kamali A, Kramer LA, Frye RE, Butler IJ, Hasan KM. Diffusion tensor tractography of the human brain cortico-ponto-cerebellar pathways: a quantitative preliminary study. *J Magn Reson Imag.* (2010) 32:809–17. doi: 10.1002/jmri.22330
54. Ashida R, Cerminara NL, Brooks J, Apps R. Principles of organization of the human cerebellum: macro- and microanatomy. *Handb Clin Neurol.* (2018) 154:45–58. doi: 10.1016/B978-0-444-63956-1.00003-5
55. Apps R, Hawkes R, Aoki S, Bengtsson F, Brown AM, Chen G, et al. Cerebellar modules and their role as operational cerebellar processing units: a consensus paper [corrected]. *Cerebellum.* (2018) 17:654–82. doi: 10.1007/s12311-018-0952-3
56. Strick PL, Dum RP, Fiez JA. Cerebellum and nonmotor function. *Annu Rev Neurosci.* (2009) 32:413–34. doi: 10.1146/annurev.neuro.31.060407.125606

57. Pieterman K, Batalle D, Dudink J, Tournier JD, Hughes EJ, Barnett M, et al. Cerebello-cerebral connectivity in the developing brain. *Brain Struct Funct.* (2017) 222:1625–34. doi: 10.1007/s00429-016-1296-8
58. Dum RP, Strick PL. An unfolded map of the cerebellar dentate nucleus and its projections to the cerebral cortex. *J Neurophysiol.* (2003) 89:634–9. doi: 10.1152/jn.00626.2002
59. Akkal D, Dum RP, Strick PL. Supplementary motor area and presupplementary motor area: targets of basal ganglia and cerebellar output. *J Neurosci.* (2007) 27:10659–73. doi: 10.1523/JNEUROSCI.3134-07.2007
60. Schmahmann JD, Pandya DN. The cerebrocerebellar system. *Int Rev Neurobiol.* (1997) 41:31–60. doi: 10.1016/S0074-7742(08)60346-3
61. Stoodley CJ, Schmahmann JD. Evidence for topographic organization in the cerebellum of motor control versus cognitive and affective processing. *Cortex.* (2010) 46:831–44. doi: 10.1016/j.cortex.2009.11.008
62. Stoodley CJ, Limperopoulos C. Structure-function relationships in the developing cerebellum: Evidence from early-life cerebellar injury and neurodevelopmental disorders. *Semin Fetal Neonatal Med.* (2016) 21:356–64. doi: 10.1016/j.siny.2016.04.010
63. Habas C. Functional connectivity of the cognitive cerebellum. *Front Syst Neurosci.* (2021) 15:642225. doi: 10.3389/fnsys.2021.642225
64. Metoki A, Wang Y, Olson IR. The social cerebellum: a large-scale investigation of functional and structural specificity and connectivity. *Cereb Cortex.* (2021) 25:bhab260. doi: 10.1093/cercor/bhab260
65. Leiner HC, Leiner AL, Dow RS. Does the cerebellum contribute to mental skills? *Behav Neurosci.* (1986) 100:443–54. doi: 10.1037/0735-7044.100.4.443
66. Xue A, Kong R, Yang Q, Eldaief MC, Angeli PA, DiNicola LM. The detailed organization of the human cerebellum estimated by intrinsic functional connectivity within the individual. *J Neurophysiol.* (2021) 125:358–84. doi: 10.1152/jn.00561.2020
67. Schmahmann JD, Pandya DN. Disconnection syndromes of basal ganglia, thalamus, and cerebrocerebellar systems. *Cortex.* (2008) 44:1037–66. doi: 10.1016/j.cortex.2008.04.004
68. Bruckert L, Travis KE, Mezer AA, Ben-Shachar M, Feldman HM. Associations of reading efficiency with white matter properties of the cerebellar peduncles in children. *Cerebellum.* (2020) 19:771–77. doi: 10.1007/s12311-020-01162-2
69. Ashida R, Cerminara NL, Edwards RJ, Apps R, Brooks JCW. Sensorimotor, language, and working memory representation within the human cerebellum. *Hum Brain Mapp.* (2019) 40:4732–47. doi: 10.1002/hbm.24733
70. Guell X, Gabrieli JDE, Schmahmann JD. Triple representation of language, working memory, social and emotion processing in the cerebellum: convergent evidence from task and seed-based resting-state fMRI analyses in a single large cohort. *Neuroimage.* (2018) 172:437–49. doi: 10.1016/j.neuroimage.2018.01.082
71. Schmahmann JD. Emotional disorders and the cerebellum: Neurobiological substrates, neuropsychiatry, and therapeutic implications. *Handb Clin Neurol.* (2021) 183:109–54. doi: 10.1016/B978-0-12-822290-4.00016-5
72. Tiemeier H, Lenroot RK, Greenstein DK, Tran L, Pierson R, Giedd JN. Cerebellum development during childhood and adolescence: a longitudinal morphometric MRI study. *Neuroimage.* (2010) 49:63–70. doi: 10.1016/j.neuroimage.2009.08.016
73. Kipping JA, Tuan TA, Fortier MV, Qiu A. Asynchronous development of cerebellar, cerebello-cortical, and cortico-cortical functional networks in infancy, childhood, and adulthood. *Cereb Cortex.* (2017) 27:5170–84. doi: 10.1093/cercor/bhw298
74. Amemiya K, Morita T, Saito DN, Ban M, Shimada K, Okamoto Y, et al. Local-to-distant development of the cerebrocerebellar sensorimotor network in the typically developing human brain: a functional and diffusion MRI study. *Brain Struct Funct.* (2019) 224:1359–75. doi: 10.1007/s00429-018-01821-5
75. Haines DE, May PJ, Dietrichs E. Neuronal connections between the cerebellar nuclei and hypothalamus in Macaca fascicularis: cerebello-visceral circuits. *J Comp Neurol.* (1990) 299:106–22. doi: 10.1002/cne.902990108
76. Çavdar S, Özgur M, Kuvvet Y, Bay HH. The Cerebello-Hypothalamic and Hypothalamo-Cerebellar Pathways *via* Superior and Middle Cerebellar Peduncle in the Rat. *Cerebellum.* (2018) 17:517–24. doi: 10.1007/s12311-018-0938-1
77. Haines DE, Dietrichs E, Mihailoff GA, McDonald EF. The cerebellar-hypothalamic axis: basic circuits and clinical observations. *Int Rev Neurobiol.* (1997) 41:83–107. doi: 10.1016/S0074-7742(08)60348-7
78. Wen YQ, Zhu JN, Zhang YP, Wang JJ. Cerebellar interpositus nuclear inputs impinge on paraventricular neurons of the hypothalamus in rats. *Neurosci Lett.* (2004) 370:25–9. doi: 10.1016/j.neulet.2004.07.072
79. Dietrichs E, Haines DE. Demonstration of hypothalamo-cerebellar and cerebello-hypothalamic fibres in a prosimian primate (*Galago crassicaudatus*). *Anat Embryol.* (1984) 170:313–8. doi: 10.1007/BF00318735
80. Haines DE, Sowa TE, Dietrichs E. Connections between the cerebellum and hypothalamus in the tree shrew (*Tupaia glis*). *Brain Res.* (1985) 328:367–73. doi: 10.1016/0006-8993(85)91051-0
81. Cacciola A, Milardi D, Calamuneri A, Bonanno L, Marino S, Ciolli P, et al. Constrained spherical deconvolution tractography reveals cerebello-mammillary connections in humans. *Cerebellum.* (2017) 16:483495. doi: 10.1007/s12311-016-0830-9
82. Manto M, Bower JM, Conforto AB, Delgado-García JM, da Guarda SN, Gerwig M, et al. Consensus paper: roles of the cerebellum in motor control—the diversity of ideas on cerebellar involvement in movement. *Cerebellum.* (2012) 11:457–87. doi: 10.1007/s12311-011-0331-9
83. Middleton FA, Strick PL. Cerebellar output channels. *Int Rev Neurobiol.* (1997) 41:61–82. doi: 10.1016/S0074-7742(08)60347-5
84. Kelly RM, Strick PL. Cerebellar loops with motor cortex and prefrontal cortex of a nonhuman primate. *J Neurosci.* (2003) 23:8432–44. doi: 10.1523/JNEUROSCI.23-23-08432.2003
85. Bostan AC, Strick PL. The cerebellum and basal ganglia are interconnected. *Neuropsychol Rev.* (2010) 20:261–70. doi: 10.1007/s11065-010-9143-9
86. Caligiore D, Pezzulo G, Baldassarre G, Bostan AC, Strick PL, Doya K. Consensus paper: towards a systems-level view of cerebellar function: the interplay between cerebellum, basal ganglia, and cortex. *Cerebellum.* (2017) 16:203–29. doi: 10.1007/s12311-016-0763-3
87. Manto M. Cerebellar motor syndrome from children to the elderly. *Handb Clin Neurol.* (2018) 154:151–66. doi: 10.1016/B978-0-444-63956-1.00009-6
88. D'Amico A, Sala F. Intraoperative neurophysiology of the cerebellum: a tabula rasa. *Childs Nerv Syst.* (2020) 36:1181–6. doi: 10.1007/s00381-020-04565-y
89. Tacyildiz AE, Bilgin B, Gungor A, Ucer M, Karadag A, Tanriover N. Dentate nucleus: connectivity-based anatomic parcellation based on superior cerebellar peduncle projections. *World Neurosurg.* (2021) 152:e408–28. doi: 10.1016/j.wneu.2021.05.102
90. Schlerf JE, Galea JM, Spampinato D, Celnik PA. Laterality differences in cerebellar-motor cortex connectivity. *Cereb Cortex.* (2015) 25:1827–34. doi: 10.1093/cercor/bht422
91. Jayaram G, Tang B, Pallegadda R, Vasudevan EV, Celnik P, Bastian A. Modulating locomotor adaptation with cerebellar stimulation. *J Neurophysiol.* (2012) 107:2950–7. doi: 10.1152/jn.00645.2011
92. Haith AM, Krakauer JW. Model-based and model-free mechanisms of human motor learning. *Adv Exp Med Biol.* (2013) 782:1–21. doi: 10.1007/978-1-4614-5465-6_1
93. Schweighofer N, Lang EJ, Kawato M. Role of the olivo-cerebellar complex in motor learning and control. *Front Neural Circuits.* (2013) 28:7:94. doi: 10.3389/fncir.2013.00094
94. Lang EJ, Apps R, Bengtsson F, Cerminara NL, De Zeeuw CI, Ebner TJ, et al. The roles of the olivocerebellar pathway in motor learning and motor control. A consensus paper. *Cerebellum.* (2017) 16:230–52. doi: 10.1007/s12311-016-0787-8
95. Shaikh AG, Hong S, Liao K, Tian J, Solomon D, Zee DS, et al. Oculopalatal tremor explained by a model of inferior olivary hypertrophy and cerebellar plasticity. *Brain.* (2010) 133:923–40. doi: 10.1093/brain/awp323
96. Lefebvre V, Josien E, Pasquier F, Steinling M, Petit H. Infarctus du noyau rouge et diaschisis cérébelleux croisé [Infarction of the red nucleus and crossed cerebellar diaschisis]. *Rev Neurol.* (1993) 149:294–6.
97. Cacciola A, Milardi D, Livrea P, Flace P, Anastasi G, Quartarone A. The known and missing links between the cerebellum, basal ganglia, and cerebral cortex. *Cerebellum.* (2017) 16:753–5. doi: 10.1007/s12311-017-0850-0
98. Milardi D, Quartarone A, Bramanti A, Anastasi G, Bertino S, Basile GA, et al. The cortico-basal ganglia-cerebellar network:

past, present and future perspectives. *Front Syst Neurosci.* (2019) 13:61. doi: 10.3389/fnsys.2019.00061
99. Quartarone A, Cacciola A, Milardi D, Ghilardi MF, Calamuneri A, Chillemi G, et al. New insights into cortico-basal-cerebellar connectome: clinical and physiological considerations. *Brain.* (2020) 143:396–406. doi: 10.1093/brain/awz310
100. Belkhiria C, Mssedi E, Habas C, Driss T, de Marco G. Collaboration of cerebello-rubral and cerebello-striatal loops in a motor preparation task. *Cerebellum.* (2019) 18:203–11. doi: 10.1007/s12311-018-0980-z
101. Basile GA, Quartu M, Bertino S, Serra MP, Boi M, Bramanti A, et al. Red nucleus structure and function: from anatomy to clinical neurosciences. *Brain Struct Funct.* (2021) 226:69–91. doi: 10.1007/s00429-020-02171-x
102. Ego C, Yüksel D, Orban de Xivry JJ, Lefèvre P. Development of internal models and predictive abilities for visual tracking during childhood. *J Neurophysiol.* (2016) 115:301–9. doi: 10.1152/jn.00534.2015
103. Petersen SE, Fox PT, Posner MI, Mintun M, Raichle ME. Positron emission tomographic studies of the processing of singe words. *J Cogn Neurosci.* (1989) 1:153–70. doi: 10.1162/jocn.1989.1.2.153
104. Jansen A, Flöel A, Van Randenborgh J, Konrad C, Rotte M, Förster AF, et al. Crossed cerebro-cerebellar language dominance. *Hum Brain Mapp.* (2005) 24:165–72. doi: 10.1002/hbm.20077
105. Abe K, Ukita H, Yorifuji S, Yanagihara T. Crossed cerebellar diaschisis in chronic Broca's aphasia. *Neuroradiology.* (1997) 39:624–6. doi: 10.1007/s002340050480
106. Marien P, Pickut BA, Engelborghs S, Martin JJ, De Deyn PP. Phonological agraphia following a focal anterior insulo-opercular infarction. *Neuropsychologia.* (2001) 39:845–55. doi: 10.1016/S0028-3932(01)00006-9
107. Mariën P, Saerens J, Nanhoe R, Moens E, Nagels G, Pickut BA, et al. Cerebellar induced aphasia: case report of cerebellar induced prefrontal aphasic language phenomena supported by SPECT findings. *J Neurol Sci.* (1996) 144:34–43. doi: 10.1016/S0022-510X(96)00059-7
108. Mariën P, Baillieux H, De Smet HJ, Engelborghs S, Wilssens I, Paquier P, et al. Cognitive, linguistic and affective disturbances following a right superior cerebellar artery infarction: a case study. *Cortex.* (2009) 45:527–36. doi: 10.1016/j.cortex.2007.12.010
109. De Smet HJ, Paquier P, Verhoeven J, Mariën P. The cerebellum: its role in language and related cognitive and affective functions. *Brain Lang.* (2013) 127:334–42. doi: 10.1016/j.bandl.2012.11.001
110. Mariën P, Ackermann H, Adamaszek M, Barwood CH, Beaton A, Desmond J, et al. Consensus paper: language and the cerebellum: an ongoing enigma. *Cerebellum.* (2014) 13:386–410. doi: 10.1007/s12311-013-0540-5
111. Hubrich-Ungureanu P, Kaemmerer N, Henn FA, Braus DF. Lateralized organization of the cerebellum in a silent verbal fluency task: a functional magnetic resonance imaging study in healthy volunteers. *Neurosci Lett.* (2002) 319:91–4. doi: 10.1016/S0304-3940(01)02566-6
112. E KH, Chen SH, Ho MH, Desmond JE. A meta-analysis of cerebellar contributions to higher cognition from PET and fMRI studies. *Hum Brain Mapp.* (2014) 35:593–615. doi: 10.1002/hbm.22194
113. Tavano A, Grasso R, Gagliardi C, Triulzi F, Bresolin N, Fabbro F, et al. Disorders of cognitive and affective development in cerebellar malformations. *Brain.* (2007) 130:2646–60. doi: 10.1093/brain/awm201
114. Yu F, Jiang QJ, Sun XY, Zhang RW. A new case of complete primary cerebellar agenesis: clinical and imaging findings in a living patient. *Brain.* (2015) 138:e353. doi: 10.1093/brain/awu239
115. Arrigoni F, Romaniello R, Nordio A, Gagliardi C, Borgatti R. Learning to live without the cerebellum. *Neuroreport.* (2015) 26:809–13. doi: 10.1097/WNR.0000000000000428
116. Yu W, Krook-Magnuson E. Cognitive Collaborations: Bidirectional Functional Connectivity Between the Cerebellum and the Hippocampus. *Front Syst Neurosci.* (2015) 22:9:177. doi: 10.3389/fnsys.2015.00177
117. Mariën P, Verhoeven J, Brouns R, De Witte L, Dobbeleir A, De Deyn PP. Apraxic agraphia following a right cerebellar hemorrhage. *Neurology.* (2007) 69:926–9. doi: 10.1212/01.wnl.0000267845.05041.41
118. Spencer KA, Slocomb DL. The neural basis of ataxic dysarthria. *Cerebellum.* (2007) 6:58–65. doi: 10.1080/14734220601145459
119. Murdoch BE, Whelan BM. Language disorders subsequent to left cerebellar lesions: a case for bilateral cerebellar involvement in language? *Folia Phoniatr Logop.* (2007) 59:184–9. doi: 10.1159/000102930
120. Molinari M, Leggio MG, Silveri MC. Verbal fluency and agrammatism. *Int Rev Neurobiol.* (1997) 41:325–39. doi: 10.1016/S0074-7742(08)60358-X
121. Gasparini M, Di Piero V, Ciccarelli O, Cacioppo MM, Pantano P, Lenzi GL. Linguistic impairment after right cerebellar stroke: a case report. *Eur J Neurol.* (1999) 6:353–6. doi: 10.1046/j.1468-1331.1999.630353.x
122. Riva D, Giorgi C. The cerebellum contributes to higher functions during development: evidence from a series of children surgically treated for posterior fossa tumours. *Brain.* (2000) 123:1051–61. doi: 10.1093/brain/123.5.1051
123. Leggio MG, Silveri MC, Petrosini L, Molinari M. Phonological grouping is specifically affected in cerebellar patients: a verbal fluency study. *J Neurol Neurosurg Psychiatry.* (2000) 69:102–6. doi: 10.1136/jnnp.69.1.102
124. Zeffiro T, Eden G. The cerebellum and dyslexia: perpetrator or innocent bystander? *Trends Neurosci.* (2001) 24:512–3. doi: 10.1016/S0166-2236(00)01898-1
125. Whelan B-M, Murdoch BE. Unravelling subcortical linguistic substrates: comparison of thalamic versus cerebellar cognitive-linguistic regulation mechanisms. *Aphasiology.* (2005) 19:1097–106. doi: 10.1080/02687030500174050
126. Baillieux H, Vandervliet EJ, Manto M, Parizel PM, De Deyn PP, Mariën P. Developmental dyslexia and widespread activation across the cerebellar hemispheres. *Brain Lang.* (2009) 108:122–32. doi: 10.1016/j.bandl.2008.10.001
127. Mariën P, de Smet E, de Smet HJ, Wackenier P, Dobbeleir A, Verhoeven J. "Apraxic dysgraphia" in a 15-year-old left-handed patient: disruption of the cerebello-cerebral network involved in the planning and execution of graphomotor movements. *Cerebellum.* (2013) 12:131–9. doi: 10.1007/s12311-012-0395-1
128. Hoche F, Guell X, Vangel MG, Sherman JC, Schmahmann JD. The cerebellar cognitive affective/Schmahmann syndrome scale. *Brain.* (2018) 141:248–70. doi: 10.1093/brain/awx317
129. Timmann D, Daum I. Cerebellar contributions to cognitive functions: a progress report after two decades of research. *Cerebellum.* (2007) 6:159–62. doi: 10.1080/14734220701496448
130. Adamaszek M, D'Agata F, Ferrucci R, Habas C, Keulen S, Kirkby KC. Consensus Paper: Cerebellum and Emotion. *Cerebellum.* (2017) 16:552–76. doi: 10.1007/s12311-016-0815-8
131. Dellatolas G, Câmara-Costa H. The role of cerebellum in the child neuropsychological functioning. *Handb Clin Neurol.* (2020) 173:265–304. doi: 10.1016/B978-0-444-64150-2.00023-X
132. Molinari M, Masciullo M, Bulgheroni S, D'Arrigo S, Riva D. Cognitive aspects: sequencing, behavior, and executive functions. *Handb Clin Neurol.* (2018) 154:167–80. doi: 10.1016/B978-0-444-63956-1.00010-2
133. Heath RG, Harper JW. Ascending projections of the cerebellar fastigial nucleus to the hippocampus, amygdala, and other temporal lobe sites: evoked potential and histological studies in monkeys and cats. *Exp Neurol.* (1974) 45:268–87. doi: 10.1016/0014-4886(74)90118-6
134. Heath RG, Dempesy CW, Fontana CJ, Myers WA. Cerebellar stimulation: effects on septal region, hippocampus, and amygdala of cats and rats. *Biol Psychiatry.* (1978) 13:501–29.
135. Haines DE, Dietrichs E. An HRP study of hypothalamo-cerebellar and cerebello-hypothalamic connections in squirrel monkey (*Saimiri sciureus*). *J Comp Neurol.* (1984) 229:559–75. doi: 10.1002/cne.902290409
136. Nashold BS Jr, Slaughter DG. Effects of stimulating or destroying the deep cerebellar regions in man. *J Neurosurg.* (1969) 31:172–86. doi: 10.3171/jns.1969.31.2.0172
137. Cooper IS, Riklan M, Amin I, Cullinan R. A long-term follow- up study of cerebellar stimulation for the control of epi-lepsy. In: Cooper IS, editor. *Cerebellar Stimulation in Man*. Raven Press, New York (1978). p. 19–38.
138. Sang L, Qin W, Liu Y, Han W, Zhang Y, Jiang T, et al. Resting-state functional connectivity of the vermal and hemispheric subregions of the cerebellum with both the cerebral cortical networks and subcortical structures. *Neuroimage.* (2012) 61:1213–25. doi: 10.1016/j.neuroimage.2012.04.011
139. Habas C, Kamdar N, Nguyen D, Prater K, Beckmann CF, Menon V, et al. Distinct cerebellar contributions to intrinsic connectivity networks. *J Neurosci.* (2009) 29:8586–94. doi: 10.1523/JNEUROSCI.1868-09.2009

140. Baumann O, Mattingley JB. Functional topography of primary emotion processing in the human cerebellum. *Neuroimage.* (2012) 61:805–11. doi: 10.1016/j.neuroimage.2012.03.044
141. Gobbini MI, Koralek AC, Bryan RE, Montgomery KJ, Haxby JV. Two takes on the social brain: a comparison of theory of mind tasks. *J Cogn Neurosci.* (2007) 19:1803–14. doi: 10.1162/jocn.2007.19.11.1803
142. Bzdok D, Langner R, Schilbach L, Jakobs O, Roski C, Caspers S, et al. Characterization of the temporo-parietal junction by combining data-driven parcellation, complementary connectivity analyses, and functional decoding. *Neuroimage.* (2013) 81:381–92. doi: 10.1016/j.neuroimage.2013.05.046
143. Hartwright CE, Hansen PC, Apperly IA. Current knowledge on the role of the inferior frontal gyrus in theory of mind-a commentary on Schurz and Tholen 2016. *Cortex*. (2016) 85:133–6. doi: 10.1016/j.cortex.2016.10.005
144. Lahnakoski JM, Glerean E, Salmi J, Jääskeläinen IP, Sams M, Hari R, et al. Naturalistic FMRI mapping reveals superior temporal sulcus as the hub for the distributed brain network for social perception. *Front Hum Neurosci.* (2012) 6:233. doi: 10.3389/fnhum.2012.00233
145. Wang Y, Metoki A, Xia Y, Zang Y, He Y, Olson IR. A large-scale structural and functional connectome of social mentalizing. *Neuroimage.* (2021) 236:118115. doi: 10.1016/j.neuroimage.2021.118115
146. Leggio M, Olivito G. Topography of the cerebellum in relation to social brain regions and emotions. *Handb Clin Neurol.* (2018) 154:71–84. doi: 10.1016/B978-0-444-63956-1.00005-9
147. Olivito G, Clausi S, Laghi F, Tedesco AM, Baiocco R, Mastropasqua C, et al. Resting-state functional connectivity changes between dentate nucleus and cortical social brain regions in autism spectrum disorders. *Cerebellum.* (2017) 16:283–92. doi: 10.1007/s12311-016-0795-8
148. Olson IR, McCoy D, Klobusicky E, Ross LA. Social cognition and the anterior temporal lobes: a review and theoretical framework. *Soc Cogn Affect Neurosci.* (2013) 8:123–33. doi: 10.1093/scan/nss119
149. Van Overwalle F, D'aes T, Mariën P. Social cognition and the cerebellum: a meta-analytic connectivity analysis. *Hum Brain Mapp.* (2015) 36:5137–54. doi: 10.1002/hbm.23002
150. Van Overwalle F, Mariën P. Functional connectivity between the cerebrum and cerebellum in social cognition: a multi-study analysis. *Neuroimage.* (2016) 124:248–55. doi: 10.1016/j.neuroimage.2015.09.001
151. Van Overwalle F, Manto M, Cattaneo Z, Clausi S, Ferrari C, Gabrieli JDE, et al. Consensus paper: cerebellum and social cognition. *Cerebellum.* (2020) 19:833–68. doi: 10.1007/s12311-020-01155-1
152. Heleven E, van Dun K, De Witte S, Baeken C, Van Overwalle F. The role of the cerebellum in social and non-social action sequences: a preliminary LF-rTMS study. *Front Hum Neurosci.* (2021) 15:593821. doi: 10.3389/fnhum.2021.593821
153. Buckner RL, Krienen FM, Castellanos A, Diaz JC, Yeo BT. The organization of the human cerebellum estimated by intrinsic functional connectivity. *J Neurophysiol.* (2011) 106:2322–45. doi: 10.1152/jn.00339.2011
154. Krienen FM, Buckner RL. Segregated fronto-cerebellar circuits revealed by intrinsic functional connectivity. *Cereb Cortex.* (2009) 19:2485–97. doi: 10.1093/cercor/bhp135
155. O'Reilly JX, Beckmann CF, Tomassini V, Ramnani N, Johansen-Berg H. Distinct and overlapping functional zones in the cerebellum defined by resting state functional connectivity. *Cereb Cortex.* (2010) 20:953–65. doi: 10.1093/cercor/bhp157
156. Gould TJ, Adams CE, Bickford PC. Beta-adrenergic modulation of GABAergic inhibition in the deep cerebellar nuclei of F344 rats. *Neuropharmacology.* (1997) 36:75–81. doi: 10.1016/S0028-3908(96)00148-7
157. Zhang C, Zhou P, Yuan T. The cholinergic system in the cerebellum: from structure to function. *Rev Neurosci.* (2016) 27:769–76. doi: 10.1515/revneuro-2016-0008
158. Wu T, Hallett M. The cerebellum in Parkinson's disease. *Brain.* (2013) 136:696–709. doi: 10.1093/brain/aws360
159. Mittleman G, Goldowitz D, Heck DH, Blaha CD. Cerebellar modulation of frontal cortex dopamine efflux in mice: relevance to autism and schizophrenia. *Synapse.* (2008) 62:544–50. doi: 10.1002/syn.20525
160. O'Halloran CJ, Kinsella GJ, Storey E. The cerebellum and neuropsychological functioning: a critical review. *J Clin Exp Neuropsychol.* (2012) 34:35–56. doi: 10.1080/13803395.2011.614599
161. Miquel M, Gil-Miravet I, Guarque-Chabrera J. The Cerebellum on Cocaine. *Front Syst Neurosci*. (2020) 14:586574. doi: 10.3389/fnsys.2020.586574
162. Perciavalle V, Apps R, Bracha V, Delgado-García JM, Gibson AR, Leggio M, et al. Consensus paper: current views on the role of cerebellar interpositus nucleus in movement control and emotion. *Cerebellum.* (2013) 12:738–57. doi: 10.1007/s12311-013-0464-0
163. Holloway ZR, Paige NB, Comstock JF, Nolen HG, Sable HJ, Lester DB. Cerebellar modulation of mesolimbic dopamine transmission is functionally asymmetrical. *Cerebellum.* (2019) 18:922–31. doi: 10.1007/s12311-019-01074-w
164. Flace P, Livrea P, Galletta D, Gulisano M, Gennarini G. Translational study of the human cerebellar dopaminergic system, its interconnections and role in neurologic and psychiatric disorders. *Eur J Histochem*. (2020) 64(Suppl 3):15. doi: 10.21203/rs.3.rs-30289/v1
165. Coenen VA, Schumacher LV, Kaller C, Schlaepfer TE, Reinacher PC, Egger K, et al. The anatomy of the human medial forebrain bundle: Ventral tegmental area connections to reward-associated subcortical and frontal lobe regions. *Neuroimage Clin.* (2018) 18:770–83. doi: 10.1016/j.nicl.2018.03.019
166. Flace P, Livrea P, Basile GA, Galletta D, Bizzoca A, Gennarini G. The cerebellar dopaminergic system. *Front Syst Neurosci.* (2021) 15:650614. doi: 10.3389/fnsys.2021.650614
167. Saitow F, Satake S, Yamada J, Konishi S. Beta-adrenergic receptor-mediated presynaptic facilitation of inhibitory GABAergic transmission at cerebellar interneuron-Purkinje cell synapses. *J Neurophysiol.* (2000) 84:2016–25. doi: 10.1152/jn.2000.84.4.2016
168. Akshoomoff NA, Courchesne E. A new role for the cerebellum in cognitive operations. *Behav Neurosci.* (1992) 106:731–8. doi: 10.1037/0735-7044.106.5.731
169. Allen G, Buxton RB, Wong EC, Courchesne E. Attentional activation of the cerebellum independent of motor involvement. *Science.* (1997) 275:1940–3. doi: 10.1126/science.275.5308.1940
170. Townsend J, Courchesne E, Covington J, Westerfield M, Harris NS, Lyden P, et al. Spatial attention deficits in patients with acquired or developmental cerebellar abnormality. *J Neurosci.* (1999) 19:5632–43. doi: 10.1523/JNEUROSCI.19-13-05632.1999
171. Kellermann T, Regenbogen C, De Vos M, Mößnang C, Finkelmeyer A, Habel U. Effective connectivity of the human cerebellum during visual attention. *J Neurosci.* (2012) 32:11453–60. doi: 10.1523/JNEUROSCI.0678-12.2012
172. Striemer CL, Chouinard PA, Goodale MA, de Ribaupierre S. Overlapping neural circuits for visual attention and eye movements in the human cerebellum. *Neuropsychologia.* (2015) 69:9–21. doi: 10.1016/j.neuropsychologia.2015.01.024
173. Brissenden JA, Levin EJ, Osher DE, Halko MA, Somers DC. Functional evidence for a cerebellar node of the dorsal attention network. *J Neurosci.* (2016) 36:6083–96. doi: 10.1523/JNEUROSCI.0344-16.2016
174. Brissenden JA, Tobyne SM, Osher DE, Levin EJ, Halko MA, Somers DC. Topographic cortico-cerebellar networks revealed by visual attention and working memory. *Curr Biol.* (2018) 28:3364–72.e5. doi: 10.1016/j.cub.2018.08.059
175. Brissenden JA, Somers DC. Cortico-cerebellar networks for visual attention and working memory. *Curr Opin Psychol.* (2019) 29:239–47. doi: 10.1016/j.copsyc.2019.05.003
176. van Es DM, van der Zwaag W, Knapen T. Topographic maps of visual space in the human cerebellum. *Curr Biol.* (2019) 29:1689–94.e3. doi: 10.1016/j.cub.2019.04.012
177. Zhang N, Xia M, Qiu T, Wang X, Lin CP, Guo Q, et al. Reorganization of cerebro-cerebellar circuit in patients with left hemispheric gliomas involving language network: A combined structural and resting-state functional MRI study. *Hum Brain Mapp.* (2018) 39:4802–19. doi: 10.1002/hbm.24324
178. Cho NS, Peck KK, Gene MN, Jenabi M, Holodny AI. Resting-state functional MRI language network connectivity differences in patients with brain tumors: exploration of the cerebellum and contralesional hemisphere. *Brain Imaging Behav.* (2021) 1. doi: 10.1007/s11682-021-00498-5. [Epub ahead of print].
179. Rueckriegel SM, Bruhn H, Thomale UW, Hernáiz Driever P. Cerebral white matter fractional anisotropy and tract volume as measured by MR imaging are associated with impaired cognitive and motor function in pediatric

posterior fossa tumor survivors. *Pediatr Blood Cancer.* (2015) 62:1252–8. doi: 10.1002/pbc.25485
180. Gomes CA, Steiner KM, Ludolph N, Spisak T, Ernst TM, Mueller O, et al. Resection of cerebellar tumours causes widespread and functionally relevant white matter impairments. *Hum Brain Mapp.* (2021) 42:1641–56. doi: 10.1002/hbm.25317
181. Khan RB, Patay Z, Klimo P, Huang J, Kumar R, Boop FA, et al. Clinical features, neurologic recovery, and risk factors of postoperative posterior fossa syndrome and delayed recovery: a prospective study. *Neuro Oncol.* (2021) 23:1586–96. doi: 10.1093/neuonc/noab030
182. Pollack IF, Polinko P, Albright AL, Towbin R, Fitz C. Mutism and pseudobulbar symptoms after resection of posterior fossa tumors in children: incidence and pathophysiology. *Neurosurgery.* (1995) 37:885–93. doi: 10.1097/00006123-199511000-00006
183. Robertson PL, Muraszko KM, Holmes EJ, Sposto R, Packer RJ, Gajjar A, et al. Incidence and severity of post-operative cerebellar mutism syndrome in children with medulloblastoma: a prospective study by the Children's Oncology Group. *J Neurosurg.* (2006) 105:444–51. doi: 10.3171/ped.2006.105.6.444
184. Gudrunardottir T, Sehested A, Juhler M, Grill J, Schmiegelow K. Cerebellar mutism: definitions, classification and grading of symptoms. *Childs Nerv Syst.* (2011) 27:1361–3. doi: 10.1007/s00381-011-1509-7
185. Catsman-Berrevoets C, Patay Z. Cerebellar mutism syndrome. *Handb Clin Neurol.* (2018) 155:273–88. doi: 10.1016/B978-0-444-64189-2.00018-4
186. Turgut M. Transient "cerebellar" mutism. *Childs Nerv Syst.* (1998) 14:161–6. doi: 10.1007/s003810050204
187. Carr K, Ghamasaee P, Singh A, Tarasiewicz I. Posterior fossa syndrome with delayed MR evidence of unilateral superior cerebellar peduncle (SCP) damage. *Childs Nerv Syst*. (2017) 33:503–7. doi: 10.1007/s00381-016-3287-8
188. Miller NG, Reddick WE, Kocak M, Glass JO, Löbel U, Morris B, et al. Cerebellocerebral diaschisis is the likely mechanism of postsurgical posterior fossa syndrome in pediatric patients with midline cerebellar tumors. *Am J Neuroradiol.* (2010) 31:288–94. doi: 10.3174/ajnr.A1821
189. Schreiber JE, Palmer SL, Conklin HM, Mabbott DJ, Swain MA, Bonner MJ, et al. Posterior fossa syndrome and long-term neuropsychological outcomes among children treated for medulloblastoma on a multi-institutional, prospective study. *Neuro Oncol.* (2017) 19:1673–82. doi: 10.1093/neuonc/nox135
190. Küpeli S, Yalçin B, Bilginer B, Akalan N, Haksal P, Büyükpamuk7u M. Posterior fossa syndrome after posterior fossa surgery in children with brain tumors. *Pediatr Blood Cancer.* (2011) 56:206–10. doi: 10.1002/pbc.22730
191. Law N, Greenberg M, Bouffet E, Taylor MD, Laughlin S, Strother D, et al. Clinical and neuroanatomical predictors of cerebellar mutism syndrome. *Neuro Oncol.* (2012) 14:1294–303. doi: 10.1093/neuonc/nos160
192. Oh ME, Driever PH, Khajuria RK, Rueckriegel SM, Koustenis E, Bruhn H, et al. DTI fiber tractography of cerebro-cerebellar pathways and clinical evaluation of ataxia in childhood posterior fossa tumor survivors. *J Neurooncol.* (2017) 131:267–76. doi: 10.1007/s11060-016-2290-y
193. Soelva V, Hernáiz Driever P, Abbushi A, Rueckriegel S, Bruhn H, Eisner W, et al. Fronto-cerebellar fiber tractography in pediatric patients following posterior fossa tumor surgery. *Childs Nerv Syst.* (2013) 29:597–607. doi: 10.1007/s00381-012-1973-8
194. Law N, Bouffet E, Laughlin S, Laperriere N, Brière ME, Strother D, et al. Cerebello-thalamo-cerebral connections in pediatric brain tumor patients: impact on working memory. *Neuroimage.* (2011) 56:2238–48. doi: 10.1016/j.neuroimage.2011.03.065
195. Gauvreau S, Lefebvre J, Bells S, Laughlin S, Bouffet E, Mabbott DJ. Disrupted network connectivity in pediatric brain tumor survivors is a signature of injury. *J Comp Neurol.* (2019) 527:2896–909. doi: 10.1002/cne.24717
196. Albazron FM, Bruss J, Jones RM, Yock TI, Pulsifer MB, Cohen AL, et al. Pediatric postoperative cerebellar cognitive affective syndrome follows outflow pathway lesions. *Neurology.* (2019) 93:E1561–71. doi: 10.1212/WNL.0000000000008326
197. Meoded A, Jacobson L, Liu A, Bauza C, Huisman TAGM, Goldenberg N, et al. Diffusion tensor imaging connectomics reveals preoperative neural connectivity changes in children with postsurgical posterior fossa syndrome. *J Neuroimaging.* (2020) 30:192–7. doi: 10.1111/jon.12686
198. Ailion AS, Roberts SR, Crosson B, King TZ. Neuroimaging of the component white matter connections and structures within the cerebellar-frontal pathway in posterior fossa tumor survivors. *Neuroimage Clin.* (2019) 23:101894. doi: 10.1016/j.nicl.2019.101894
199. Yasargil MG. *Microneurosurgery: Microsurgical Anatomy of the Basal Cisterns and Vessels of the Brain, Diagnostic Studies, General Operative Techniques and Pathological Considerations of the Intracranial Aneurysms, vol I*. George Thieme-Verlag, Stuttgart (1984).
200. Matsushima T, Inoue T, Inamura T, Natori Y, Ikezaki K, Fukui M. Transcerebellomedullary fissure approach with special reference to methods of dissecting the fissure. *J Neurosurg.* (2001) 94:257–64. doi: 10.3171/jns.2001.94.2.0257
201. Beez T, Munoz-Bendix C, Steiger HJ, Hänggi D. Functional tracts of the cerebellum-essentials for the neurosurgeon. *Neurosurg Rev.* (2021) 44:273–78. doi: 10.1007/s10143-020-01242-1
202. Akakin A, Peris-Celda M, Kilic T, Seker A, Gutierrez-Martin A, Rhoton A. The dentate nucleus and its projection system in the human cerebellum: the dentate nucleus microsurgical anatomical study. *Neurosurgery.* (2014) 74:401–24. doi: 10.1227/NEU.0000000000000293
203. García-Feijoo P, Reghin-Neto M, Holanda V, Rassi MS, Saceda-Gutierrez JM, Carceller-Benito FE, et al. 3-Step didactic white matter dissection of human cerebellum: Micro-neuroanatomical training. *Neurocirugia.* (2021) 3:S1130-1473(20)30137-8. doi: 10.1016/j.neucie.2021.04.003
204. Law N, Smith ML, Greenberg M, Bouffet E, Taylor MD, Laughlin S, et al. Executive function in paediatric medulloblastoma: the role of cerebrocerebellar connections. *J Neuropsychol.* (2017) 11:174–200. doi: 10.1111/jnp.12082
205. Sankey EW, Srinivasan ES, Mehta VA, Bergin SM, Wang TY, Thompson EM. Perioperative assessment of cerebellar masses and the potential for cerebellar cognitive affective syndrome. *World Neurosurg.* (2020) 144:222–30. doi: 10.1016/j.wneu.2020.09.048
206. Ogata N, Yonekawa Y. Paramedian supracerebellar approach to the upper brain stem and peduncolar lesions. *Neurosurgery.* (1997) 40:101–5. doi: 10.1227/00006123-199701000-00023
207. van Baarsen KM, Kleinnijenhuis M, Jbabdi S, Sotiropoulos SN, Grotenhuis JA, van Cappellen van Walsum AM. A probabilistic atlas of the cerebellar white matter. *Neuroimage.* (2016) 124:724–32. doi: 10.1016/j.neuroimage.2015.09.014
208. Grosse F, Rueckriegel SM, Thomale UW, Hernáiz Driever P. Mapping of long-term cognitive and motor deficits in pediatric cerebellar brain tumor survivors into a cerebellar white matter atlas. *Childs Nerv.* (2021) 37:2787–97. doi: 10.1007/s00381-021-05244-2
209. Iwata NK, Ugawa Y. The effects of cerebellar stimulation on the motor cortical excitability in neurological disorders: a review. *Cerebellum.* (2005) 4:2018–23. doi: 10.1080/14734220500277007
210. Giampiccolo D, Basaldella F, Badari A, Squintani GM, Cattaneo L, Sala F. Feasibility of cerebello-cortical stimulation for intraoperative neurophysiological monitoring of cerebellar mutism. *Childs Nerv Syst.* (2021) 37:1505–14. doi: 10.1007/s00381-021-05126-7

Conflict of Interest: The authors declare that the research was conducted in the absence of any commercial or financial relationships that could be construed as a potential conflict of interest.

Publisher's Note: All claims expressed in this article are solely those of the authors and do not necessarily represent those of their affiliated organizations, or those of the publisher, the editors and the reviewers. Any product that may be evaluated in this article, or claim that may be made by its manufacturer, is not guaranteed or endorsed by the publisher.

frontiers in Neurology

ORIGINAL RESEARCH
published: 15 February 2022
doi: 10.3389/fneur.2022.757757

Cadaveric White Matter Dissection Study of the Telencephalic Flexure: Surgical Implications

*Pablo González-López[1], Giulia Cossu[2], Cynthia M. Thomas[3], Jeffery S. Marston[3], Cristina Gómez[1], Etienne Pralong[2], Mahmoud Messerer[2] and Roy T. Daniel[2]**

[1] Hospital General Universitario de Alicante, Alicante, Spain, [2] University Hospital of Lausanne, University of Lausanne, Lausanne, Switzerland, [3] Charles University, Prague, Czechia

Neurosurgery has traditionally been overtly focused on the study of anatomy and functions of cortical areas with microsurgical techniques aimed at preserving eloquent cortices. In the last two decades, there has been ever-increasing data emerging from advances in neuroimaging (principally diffusion tensor imaging) and clinical studies (principally from awake surgeries) that point to the important contribution of white matter tracts (WMT) that influence neurological function as part of a brain network. Major scientific consortiums worldwide, currently working on this human brain connectome, are providing evidence that is dramatically altering the manner in which we view neurosurgical procedures. The development of the telencephalic flexure, a major landmark during the human embryogenesis of the central nervous system (CNS), severely affects the cortical/subcortical anatomy in and around the sylvian fissure and thus the different interacting brain networks. Indeed, the telencephalic flexure modifies the anatomy of the human brain with the more posterior areas becoming ventral and lateral and associative fibers connecting the anterior areas with the previous posterior ones follow the flexure, thus becoming semicircular. In these areas, the projection, association, and commissural fibers intermingle with some WMT remaining curved and others longitudinal. Essentially the ultimate shape and location of these tracts are determined by the development of the telencephalic flexure. Five adult human brains were dissected (medial to lateral and lateral to medial) with a view to describing this intricate anatomy. To better understand the 3D orientation of the WMT of the region we have correlated the cadaveric data with the anatomy presented in the literature of the flexure during human neuro-embryogenesis in addition to cross-species comparisons of the flexure. The precise definition of the connectome of the telencephalic flexure is primordial during glioma surgery and for disconnective epilepsy surgery in this region.

Keywords: brain surgery, disconnective surgery, epilepsy surgery, functional connectome, oncology, telencephalic flexure, sylvian fissure

OPEN ACCESS

Edited by:
Emanuele La Corte, University of Bologna, Italy

Reviewed by:
Harvey B. Sarnat, University of Calgary, Canada
Eduardo Ribas, University of São Paulo, Brazil
Mingchu Li, Capital Medical University, China

***Correspondence:**
Roy T. Daniel
roy.daniel@chuv.ch

Specialty section:
This article was submitted to Applied Neuroimaging, a section of the journal Frontiers in Neurology

Received: *12 August 2021*
Accepted: *05 January 2022*
Published: *15 February 2022*

Citation:
González-López P, Cossu G, Thomas CM, Marston JS, Gómez C, Pralong E, Messerer M and Daniel RT (2022) Cadaveric White Matter Dissection Study of the Telencephalic Flexure: Surgical Implications. Front. Neurol. 13:757757. doi: 10.3389/fneur.2022.757757

INTRODUCTION

Neurosurgical interventions in and around the perisylvian cortices often represent a surgical challenge due to the complexity of the sulcogyral architecture and underlying fiber systems. The capricious anatomy of this region is principally related to the development of the telencephalic flexure, which represents a major landmark during human neuro-embryogenesis (**Figure 1**).

During the early embryonic stages, the telencephalic hemispheres bend caudally in a ventral and rostral direction, resembling a "C-shaped" structure. Therefore, the upcoming temporal lobe derives from the posterior pole of the primitive telencephalon, while the occipital lobe is derived from its dorsal wall. This folding of the telencephalic hemispheres (telencephalic flexure) becomes the operculum and the future Sylvian fissure. Following a complex interaction and excitatory/inhibitory neural signaling, this folding will finally delineate the curved shape of most of the fibers connecting the implicated cortical regions. As a consequence of the folding of the telencephalic hemispheres, the fibers' final shape "suffer" the effects of the aforementioned flexion and the functional neuroanatomy of the connectome in this area may be challenging to understand.

The aim of this study is to illustrate the white matter anatomy around the telencephalic flexure along with a comprehensive review of the mechanisms involved in its embryological development and with the help of a cross-species analysis, and how the understanding of this complex anatomical evolvement might help surgeons to optimize surgical interventions around this region. The subcortical connectivity should be maximally preserved through the performance of selective procedures to preserve the neurological and cognitive functions of our patients.

METHODS

In this study, five cadaveric human brains were prepared following Klingler's technique. The specimens were extracted during the first 12 h postmortem and placed in 10% formalin solution for 8 weeks. The brains were washed under running water and frozen to −15°C for 2 weeks (1). The freezing allowed the expansion of the extracellular water allowing the spreading of the fibers (2). After de-freezing the brains, dissection was carried out in a lateral-to-medial and medial-to-lateral direction. A transventricular dissection was finally carried out, with the aim of a deeper understanding of the aforementioned fibers. The main white matter tracts were identified according to the surface anatomy, and their direction was described in the three planes of the space (3) (**Figure 1**).

In order to better sustain the results based on the brain dissections, as well as the literature review, two surgical cases were discussed to illustrate the importance of this anatomic understanding. Both patients gave their consent to share their clinical records.

RESULTS

Lateral-to-Medial Dissection

Frontal Region

The removal of the cortex and the u-fibers exposed the superior longitudinal fasciculus II (SLF II) connecting parietal and frontal lobes, and the SLF III between the inferior frontal and supramarginal gyri were found running in an anteroposterior linear direction. After removing the insular cortex, extreme and external capsules, the lateral aspect of the putamen was uncovered. Deeper to the lentiform nucleus, the internal capsule (IC) was seen medially and projecting upwards intermingling with the corpus callosum (CC) lateral projections forming together the corona radiata. The anterior limb and genu of the IC were longitudinally oriented into the vertical plane (**Figure 2**).

Parieto-Occipito-Temporal Region

The vertical SLF appeared connecting the supramarginal and angular with the superior and middle temporal gyri. Together with the tapetum, it represents one of the vertically oriented tracts in this area. SLF II-III and arcuate fascicle (AF) were then uncovered. SLF II-III was shown oriented in an anteroposterior linear-direction-traversing the central lobe. The AF was "non-longitudinally oriented" into this area and wrapped around the posterior insular point, connecting the posterior aspect of superior and middle temporal gyri with the central and frontal lobes. This tract is anteroposterior on its frontal aspect, but curves ventrally and laterally on its parietal aspect, thus lining up with the craniocaudal and lateromedial planes. The middle longitudinal fascicle (MLF) was found running anteroposteriorly from the superior temporal gyrus (STG) deep to the AF, curving upwards on the craniocaudal plane toward the superior parietal lobe. The IFOF, connecting the frontal and occipital lobes, followed an anteroposterior direction. However, it moves laterally and basally from the frontal to the temporal aspect. Therefore, it was considered as a curved association tract ventral to the insula. It runs dorsal to the uncinate fasciculus (UF), which courses lateral to the anterior perforated substance. Both converge at the limen insulae, being difficult to be individualized in this area. Removing the putamen allows the identification of the anterior commissure (AC), in which the main axis follows the lateromedial plane by crossing the midline. However, its anterior and posterior-lateral extensions curve into the anteroposterior and craniocaudal planes to reach their respective destinations into the amygdala and temporooccipital cortex. On its posterior projection, the IFOF and AC cover the optic radiations (OR), which remain lateral to the lateral ventricle. Each OR passes below the lentiform as the core of the sublenticular IC and is integrated into the sagittal stratum together with the IFOF and AC. The OR represents a projection system connecting the thalamus and the primary visual area in the ipsilateral occipital lobe following the anteroposterior and lateromedial planes of the space. After removing the sagittal stratum, the tapetum (tap) was shown covering the atrial lateral ependyma running downward and forward. It connects the basal and lateral aspects of both occipital and temporal lobes. As the AC, it is a curved commissural tract aligned into the lateromedial, anteroposterior, and craniocaudal planes. The inferior longitudinal fasciculus (ILF) rests basally connecting the temporal pole to the dorsolateral occipital cortex in the anteroposterior plane (**Figures 3, 4).**

Medial-to-Lateral Dissection

The cingulum, visualized after removing the cortex and u-fibers on the cingulate gyrus, emerges from the subcallosal area and runs posteriorly to join the isthmus. Ventral to the precuneus, some fibers emerge from the cingulum toward the medial aspect of the parietal lobe. The parahippocampal

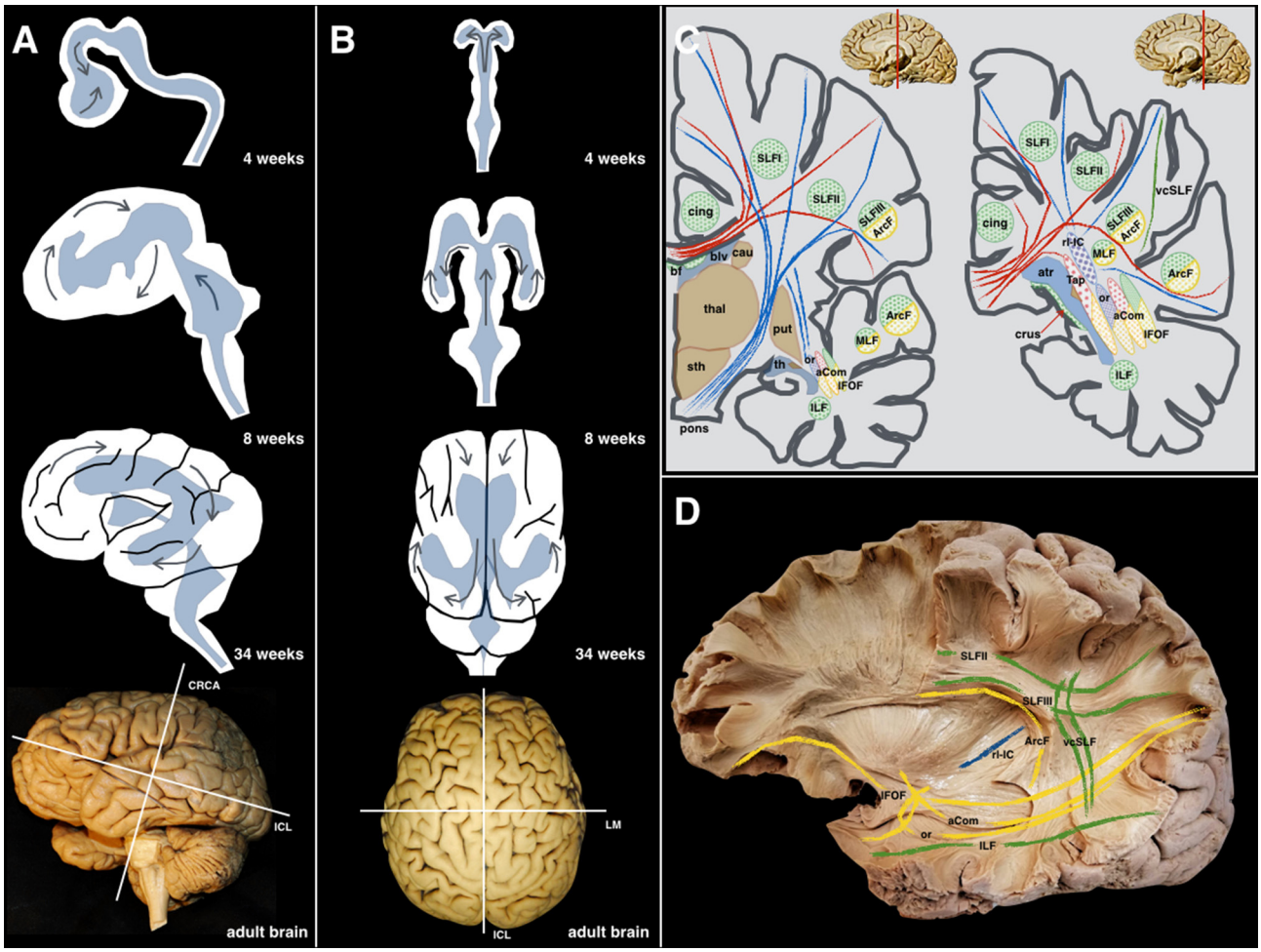

FIGURE 1 | (A) Lateral perspective: The different steps during the embryological development (4, 8, 34 weeks, and adult brain) of the human brain are shown along with the forces that produce morphological stress *(arrows)*. The main internal forces push the occipital lobe from a dorsal to a posterior location resulting in the temporal lobe moving from its posterior and medial location to a more anterior and lateral one. The telencephalic flexure is the result of all these movements happening during the early embryological formation of the CNS. **(B)** Superior perspective: the two telencephalic vesicles are shown as well as the early ventricular cavities. For an accurate understanding of the superficial and deep anatomy, the three planes of the space have been defined according to Talairach's description: the cerebral space is defined by the anteroposterior or intercommissural line *(ICL)* between the anterior and posterior commissures, the craniocaudal *(CRCA)* between vertex and midbrain and perpendicular to the ICL line, and the lateromedial *(LM)* between both hemispheres, and perpendicular to the previous lines. **(C)** As a result of the complex shape acquired by the human brain, and the 3D organization of the ventricular system, most of the association fibers in this area show a curved shape with a specific arrangement pattern. The purely latero-medially oriented fibers are represented in *red*; the craneo-caudal fibers in *blue*; the anteroposterior fibers are *green*; the *yellow* color is employed to represent those fibers that being latero-medial, anteroposterior, or craneo-caudal, that change its direction at some point, becoming curved in shape. **(D)** These anatomical relationships are shown and partially schematized in this left hemisphere showing longitudinally oriented association fibers *(green)*, curved-shape association fibers *(yellow),* and purely longitudinal projection fibers *(blue)*. aCom, anterior commissure; atr, atrium; ArcF, arcuate fascicle; bf, body of fornix; blv, body of the lateral ventricle; cau, caudate nucleus; cing, cingulum; crus, crus of the fornix; IFOF, inferior frontooccipital fascicle; ILF, inferior longitudinal fascicle; MLF, middle longitudinal fascicle; or, optic radiations; pons; brainstem protuberance; put, putamen; rl-IC, retrolenticular component of the Internal Capsule; SLF I, Superior Longitudinal Fascicle I; SLF II, Superior Longitudinal Fascicle II; SLF III, Superior Longitudinal Fascicle III; sth, subthalamic area; Tap, tapetum; th, temporal horn; thal, thalamus; vcSLF, vertical component of the SLF.

fibers represent the continuation of the cingulum toward the temporomesial region. The junction of the cingulum and parahippocampal fibers represents an extraventricular "C" shaped fiber system, belonging to the limbic system. Removing the cingulum and parahippocampal fibers, exposed the medial extension of the CC and the ventral aspect of the dentate gyrus. The lateral longitudinal stria was also seen dorsal to the CC and representing the dorsal remnant of the archicortex of the hippocampus, and fornix, showing connections to the amygdala and induseum griseum. All these limbic systems are represented in the anteroposterior, craniocaudal, and lateromedial planes (**Figure 5**).

Transventricular Dissection

Lateral Aspect

The IC and the corona radiata are in close relationship with the ventricular system. The anterior limb is related to the frontal horn, the genu to the foramen of Monro, the posterior limb to

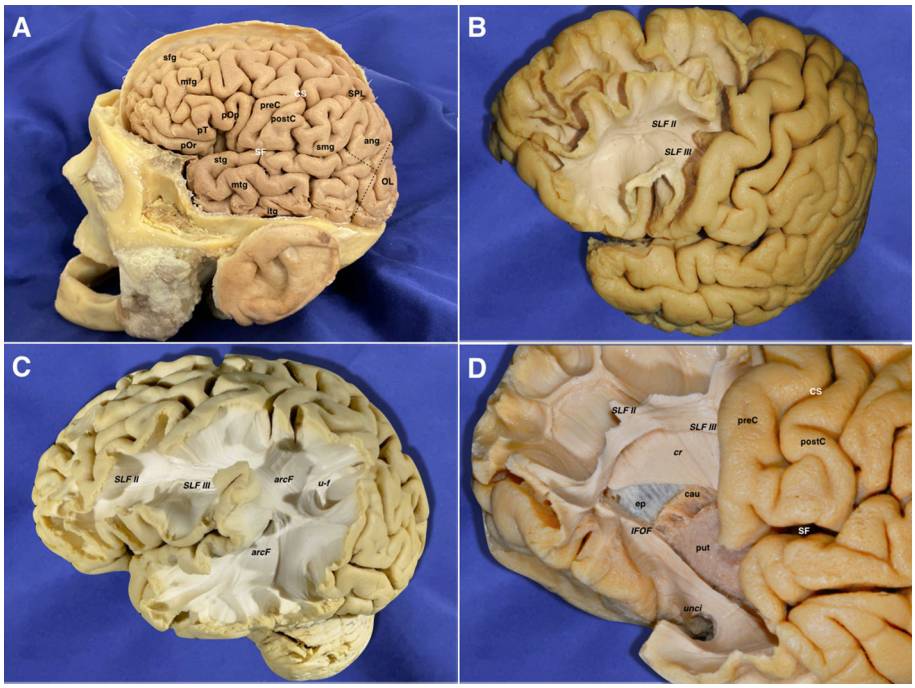

FIGURE 2 | (A) Lateral view of a left hemisphere (before the brain's extraction from the skull). The central lobe represents the boundary between the frontal and parietal areas. The pre-occipital notch and distal end of the sylvian fissure helped to delineate the indistinct border between the temporal, parietal, and occipital lobes. This is the most important pivotal point resulting from the different forces that affect the growth of the human brain during its embryological development. **(B)** The frontal lobe in the left hemisphere has been partially dissected anterior to the precentral sulcus. The gray matter has been scraped away showing the u-fibers in the superior frontal gyrus. The inferior frontal gyrus has been removed along with the underlying u-fibers in this area, showing a clear view of the SLF II & SLF III frontal projections. **(C)** The cortex and u-fibers have been removed showing the SLF II & SLF III and their close relationship with the arcuate fascicle wrapping around the posterior Sylvian point. U-fibers are shown connecting the superior parietal lobe and the angular gyrus. **(D)** A more advanced step in the frontal dissection is shown. The projections of the anterior limb of the internal capsule are arising in between the caudate nucleus and putamen, just lateral to the ependyma of the lateral ventricle frontal horn. The internal capsule cranial projections intermingle with the lateral projections of the corpus callosum at this point, forming a longitudinal layer of tracts, which runs perpendicular in direction to the long association ones (SLF II & III). The temporal pole fibers are also exposed after removing their u-fibers. The inferior fronto-occipital fascicle and uncinate fascicle are also exposed in the temporal aspect. Ang, angular gyrus; arcF, arcuate fascicle; cau, caudate nucleus; cr, corona radiata; CS, central sulcus; ep, ependyma; IFOF, inferior frontooccipital fascicle; itg, inferior temporal gyrus; mfg, middle frontal gyrus; mtg, middle temporal gyrus; OL, occipital lobe; pOp, pars opercularis; pOr, pars orbitalis; postC, postcentral gyrus; preC, precentral gyrus; pT, pars triangularis; put, putamen; SF, sylvian fissure; sfg, superior frontal gyrus; SLF II, superior longitudinal fasciculus II; SLF III, superior longitudinal fasciculus III; smg, supramarginal gyrus; SPL, superior parietal lobe; stg, superior temporal gyrus; u-f, u-fibers; unci, uncinate fasciculus.

the body of the lateral ventricle, while the retro- and sublenticular components are related to the atrium and temporal/occipital horns. The floor of the frontal horn is formed by the rostrum of the CC, and the roof of the frontal horn and body is formed by the body CC. The splenial projections cover the medial wall and roof of the atrium. The head of the hippocampus is seen facing the uncal recess anteriorly and the amygdala superiorly. It runs anteroposteriorly, and the alveus becomes the fimbria of the fornix, which wraps around the pulvinar thalami in a superomedial direction, being thus represented in all three planes (**Figure 6**).

Medial Aspect

The caudate nucleus is seen in the ventricular wall. Scraping it away, allowed us to see the thalamic projections of the IC. The tapetum of the CC was seen covering the roof and lateral wall of the atrium from its medial aspect. The alveus and fimbria continue with the crus fornicis, which runs toward the midline, and then move forward, named body of the fornix, to surround the foramen of Monro and descend toward the mammillary bodies into the hypothalamus through the columns of the fornix.

Cases Illustrations

Intra-axial Tumor Surgery in the Region of the Telencephalic Flexure

One of the more challenging human brain areas to be surgically approached is the dominant fronto-temporoparietal junction. This area shows highly eloquent cortical regions around the terminal part of the Sylvian fissure. Moreover, the underlying white matter fiber tracts connecting these areas and also some other deep fascicles running in between them, make it especially important to understand the 3D architecture of this complex net of tracts. Dealing with an intra-axial tumor as a glioma in this fronto-temporoparietal region requires a strong understanding of its real subcortical origin and the surrounding eloquent areas, as well as the deep relationship of the relevant fiber tracts to

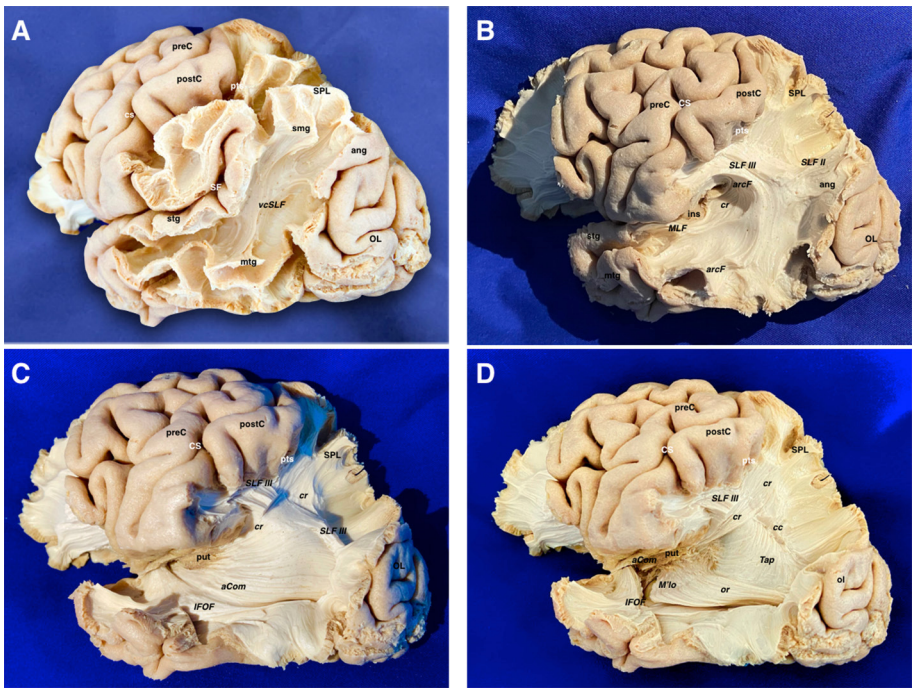

FIGURE 3 | (A) The temporo-parieto-occipital dissection starts by scraping away the cortex exposing the u-fibers and the most superficial long association fiber tract in this region, which is the vertical component of the SLF connecting the superior parietal lobe and supramarginal gyrus with the posterior aspect of the middle and superior temporal gyri. It is interesting to note that this is the only vertically oriented association bundle. **(B)** The vertical component of SLF has been peeled off to expose the next layer of tracts in this area. Thus, the arcuate fascicle is seen wrapping around the posterior insular point. The most posterior part of the SLF II and SLF III are shown just dorsal to the curve of the arcuate fascicle. The middle longitudinal fascicle is shown arising from the middle third of the superior temporal gyrus. Running posteriorly, the MLF is situated just underlying the arcuate. In a deeper location, the retro-lenticular aspect of the internal capsule is shown being part of the corona radiata. **(C)** The AF, SLF II & III, have been cut dorsally at the level of the supramarginal gyrus, uncovering the posterior extension of the IFOF, retro-lenticular fibers of the IC projecting to the parietal and occipital lobes, and the posterior portion of the lateral extension of the anterior commissure (AC) connecting both temporo- occipital basal lobes. The MLF has been removed showing the retro- and sublenticular projections of the IC in relation to the putamen. In the temporal side, the most external layers of the sagittal stratum (anterior commissure and inferior fronto-occipital fascicle) are dissected arising from the ventral aspect of the telencephalic flexure area. **(D)** Scraping away the corona radiata into the posterior part of the flexure has exposed the tapetum just lateral to the ependyma of the lateral ventricle atrium. In the ventral aspect of the telencephalic flexure, the anterior commissure has been cut and the posterior extension of the IFOF is removed. This maneuver allows uncovering the optic radiations, which is the deeper layer of the sagittal stratum. aCom, anterior commissure; ang, angular gyrus; arcF, arcuate fascicle; cr, corona radiata; CS, central sulcus; IFOF, inferior frontooccipital; ins, insula; MLF, middle longitudinal fasciculus; mtg, middle temporal gyrus; OL, occipital lobe; postC, postcentral gyrus; preC, precentral gyrus; pts, postcentral sulcus; put, putamen; SF, Sylvian fissure; SLF II, superior longitudinal fasciculus II; SLF III, superior longitudinal fasciculus III; smg, supra marginal gyrus; SPL, superior parietal lobe; stg, superior temporal gyrus; vcSLF, vertical component of the superior longitudinal fasciculus.

the glioma itself. If we analyze all the fibers that are situated in between the lateral neocortex of the fronto-temporoparietal region and the ependyma of the body, atrium, and temporal horn of the lateral ventricle, several relevant fibers will appear (vertical SLF, arcuate fascicle, MLF, IFOF, anterior commissure, optic radiations, and tapetum). The sagittal stratum deserves a special mention, as a complex anatomical fibers arrangement into this area, mainly composed by the MLF, IFOF, OR, and other posterior thalamic radiations directed to non-visual areas of the cerebral cortex. In addition, small contributions to the sagittal stratum come from the anterior commissure anteriorly and the inferior longitudinal fasciculus inferiorly (4). As previously discussed, some of these fibers show a curved shape as a result of the telencephalic flexure appearing due to the physical and genetic forces that made our brains more functionally advanced. Advances in the field of neuroimaging (DTI, fMRI, neuronavigation, etc.) are helpful technologies in order to understand these fibers and their relationships. However, intraoperative testing and checking the functions of most of these structures is still the gold-standard technique to maximize the tumor resection minimizing postoperative deficits (**Figure 7**).

Disconnective Epilepsy Surgery of the Region

Intractable epilepsy arising from the centro-parieto-occipital lobes is rare and is frequently a disease of childhood. The common etiologies are perinatal ischemic lesions, Sturge Weber syndrome, Rasmussen's encephalitis, and sub-hemispheric cortical dysplasias. When these etiologies involve the entire hemisphere, the surgery indicated is hemispherotomy (5–7). In the presence of normal frontal and temporal lobes, the situation becomes complex for a curative surgical procedure. In situations where the motor function is normal and near normal, investigations to locate the functional primary motor

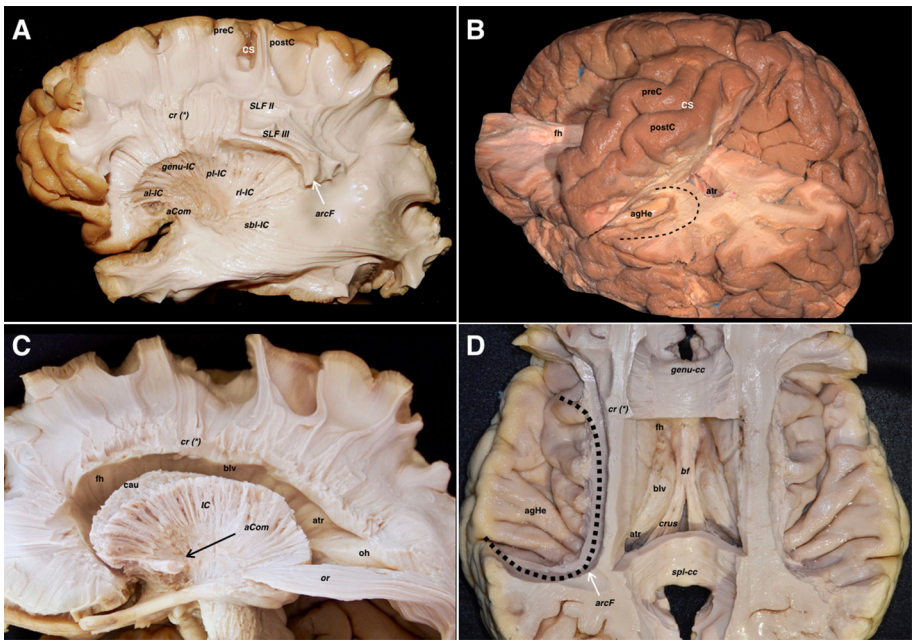

FIGURE 4 | (A) The corona radiata is exposed in relation to the parietal parts of the SLF II, SLF III, and AF. The lateral basal ganglia are removed to show the different components of the IC namely the anterior limb, genu, posterior limb, retro-lenticular and sub-lenticular parts. The asterisk is showing the line where the projection (internal and external capsules) and commissural (corpus callosum) fibers of the corona radiata are intermingling. **(B)** Relationship of the central lobe with the lateral ventricle frontal horn and body. The central lobe fibers are mainly projection descending corticofugal and ascending thalamocortical. The different association tracts traversing the central lobe thickness are horizontally oriented and represented by the SLF I, SLF II, SLF III as well as the AF. The transverse gyrus of Heschl is located hidden in the depth of the sylvian fissure due to the telencephalic flexure and lobar movements. Note how the curve of the AF *(black dotted line)* wraps around the posterior insular point. **(C)** The IC and the corona radiata have been disconnected opening the lateral ventricle. The only projection fibers that have been preserved are the optic radiations. The AC is located ventral to the anterior limb of the IC. Note that the lateral aspect of the frontal horn, body, and atrium of the lateral ventricle has been uncovered to demonstrate the association, commissural, and projection tracts. The shape of most of the association fibers follows somehow the direction of the ventricular system, all influenced by the telencephalic flexure forces and movements. **(D)** An axial cut at the level of the telencephalic flexure has been performed, showing the hidden anatomy of the superior aspect of the temporal lobe. Interestingly, the representation of the AF shape and direction *(black dotted line)*, represents the forces that affect the human brain during its embryological development. In this superior view, a clear boundary in between the ventricular chambers and the lateral aspect of the brain is shown and represented by the corona radiata, at the point where the projection and commissural fibers join together. A wide window along the body of the corpus callosum has been created to show the body of the lateral ventricle from above. In its medial aspect, are shown most of the medial association fibers (mainly related to the limbic system) that assume a curved shape that is determined primarily by the telencephalic flexures. Most of them are connecting temporo-mesial with anterior frontal and septal areas. This fact explains the curved shape of the association fibers of the medial aspect that are found wrapping around the corpus callosum and the diencephalon. aCom, anterior commissure; agHe, anterior transverse gyrus of Heschl; al-ic, anterior limb of the internal capsule; arcF, arcuate fascicle; atr, atrium; bf, body of the fornix; blv, body of the lateral ventricle; cau, caudate nucleus; cr (*), corona radiata and callosal fibers intermingling point; crus, crus fornicis; CS, central sulcus; fh, frontal horn; genu-cc, corpus callosum genu; genu-IC, genu of the internal capsule; IC, internal capsule; oh, occipital horn; or, optic radiations; pl-IC, posterior limb of the internal capsule; postC, postcentral gyrus; preC, precentral gyrus; rl-IC, retrolenticular component of the internal capsule; sbl-IC, sublenticular component of the internal capsule; SLF II, superior longitudinal fasciculus II; SLF III, superior longitudinal fasciculus III; spl-cc, splenium of the corpus callosum.

area needs to be done to ensure that the procedure planned for does not produce an irreversible motor deficit. In the dominant hemisphere, the locations of the speech areas need to be ascertained using fMRI. If then a disconnection of these lobes is deemed possible, a precise knowledge of the tracts that could traverse the lines of disconnection is mandatory. The association fibers as the SLF I, II, and III, IFOF, MLF, cingulum are to be sectioned in addition to disconnecting the occipital lobe from the functional temporal lobe. The corticospinal, thalamocortical, parietopontine, occipitopontine, and optic radiations represent the projection fibers disconnected. The lateral extension of the anterior commissure, tapetum, posterior third of corpus callosum, and splenium are the commissural fibers that are disconnected in this surgery. The arcuate fasciculus can be spared if a posteriorly directed oblique white matter section trajectory can be performed around after the corticectomy at the posterior insular point. An accurate understanding of the 3D anatomical configuration of the telencephalic flexure is primordial to know the distribution of these white matter tracts in order to achieve a total disconnection of the lobes (to achieve seizure freedom) while preserving important adjacent tracts in the frontal and temporal lobes and those tracts that traverse the telencephalic flexure (**Figure 8**).

DISCUSSION

The development of the cerebral cortex takes place predominantly in the fetal period. At approximately 25

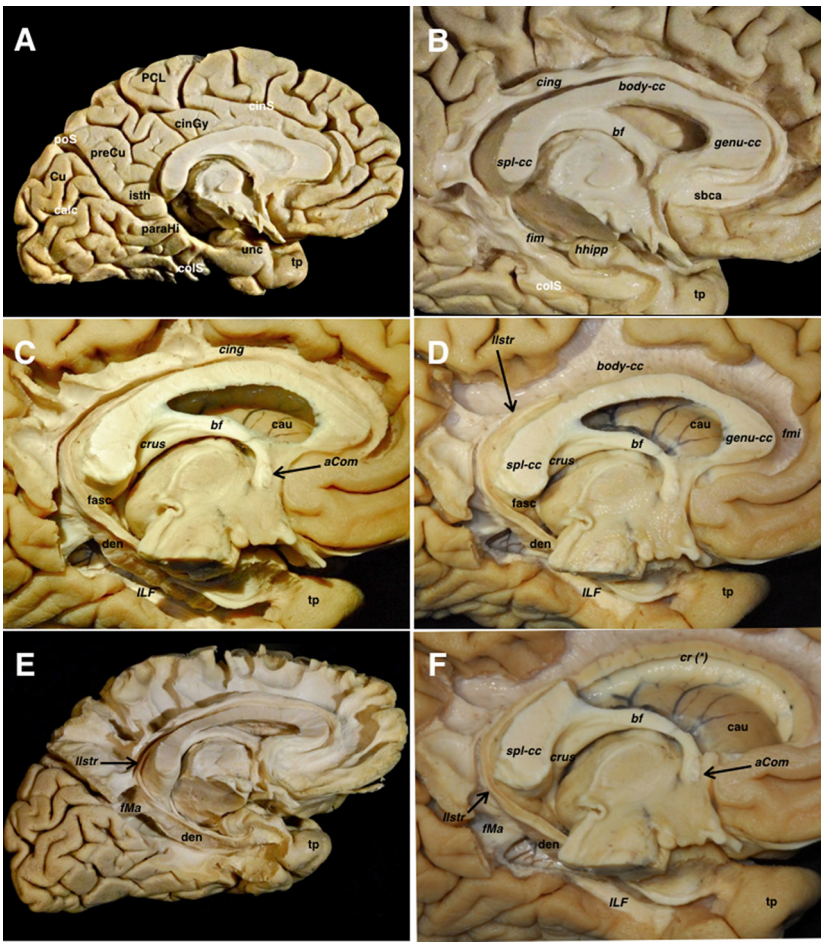

FIGURE 5 | (A) A left hemisphere is viewed from its medial aspect. The telencephalic flexure is responsible for this complex shape of the human brain, where the medial and basal regions of the telencephalic vesicles (hemispheres) are finally covering the diencephalon and upper parts of the brainstem. The basal aspect might be considered part of the medial hemisphere due to its anatomical continuation. Indeed, the temporobasal, temporomesial regions, and temporal pole have reached their final locations due to the influences of the embryonic movements, thus encircling the thalamus and midbrain. This movement is also responsible for the complex orientation of the supratentorial ventricular system, and subsequently the arrangement of the white matter tracts (see also **Figure 1**). From a purely anatomical point of view, important midline surface landmarks are the cingulate sulcus with its marginal ascending ramus, the paracentral lobule and precuneus, the parieto- occipital fissure, the calcarine fissure, the splenium of CC, the parahippocampal gyrus, and the isthmus of the cingulum which is an anatomical key point at the junction of the calcarine and parietooccipital fissures. **(B)** The cortical layer covering the external limbic belt (cingulate and parahippocampal gyrus) has been removed exposing the whole cingulum and parahippocampal bundle. This curved association fiber tract mainly connects the subcallosal area and the mesial temporal pole, with some fibers to the precuneal region arising from the isthmus. Again, the telencephalic flexure is responsible for this curvilinear trajectory as the temporal pole is finally located ventral and anterior. **(C)** The parahippocampal fibers have been completely removed opening the atrium and showing the basal aspect of the dentate gyrus. The inferior longitudinal fascicle connecting the temporal and occipital lobes is shown in the floor of the temporal horn deep to the relative location of the fusiform gyrus. **(D)** The cingulum has been removed showing the callosal fibers from a medial view. The dentate gyrus moves posteriorly and superiorly and continues with the lateral longitudinal striae wrapping around the splenium of the corpus callosum. Note how this thin fiber bundle continues extraventricularly as the fasciola cinerea. This is considered as a rudiment of the hippocampal formation, and follows a curved trajectory around the corpus callosum to connect the fasciola and dentate gyrus with the induseum griseum on the dorsal surface of the callosal body. On the ventral surface of the hippocampus, the alveus continues posteriorly through the crus fornicis. Both crura become close at the midline at the ventral surface of the callosal splenium to run anteriorly through the body of the fornix along the floor of the lateral ventricle body. **(E)** I Once the body of the fornix reaches the foramen of Monro, it changes its direction to go inside the hypothalamic nuclei craneo-caudally to reach its target onto the mammillary body. A few fibers run anterior to the anterior commissure to reach the septal region, and are known as the precommissural part of the fornix. This is considered one of the intraventricular limbic belts, and its characteristic curved shape, is again a consequence of the flexure in the midline region. **(F)** The midline aspect of the rostrum, genu and body of the corpus callosum have been cut through the angle formed by the lateral wall and roof of the lateral ventricle. This is the point where the corona radiata and callosal fibers were seen intermingling in the lateral aspect of the hemisphere (**Figure 4A**). The medial hemispheric region shows a completely different organization compared to the lateral aspect of the hemisphere. The number of fiber systems are much less, and the organization is mainly provided by a wide association fascicle (cingulate- parahippocampal), which turns around the CC and the intraventricular temporomesial structures, and the underlying commissural fibers of the CC projecting toward the medial edge of the hemisphere. aCom, anterior commissure; bf, body of the fornix; body-cc, body of the corpus callosum; calc, calcarine fissure; cau, caudate nucleus; cing, cingulum; cinGy, cingulate gyrus; cinS, cingulate sulcus; colS, collateral sulcus; cr (*), corona radiata and callosal fibers intermingling point; Cu, cuneus; crus, crus fornicis; den, dentate gyrus; fasc, fasciola cinerea; fim, fimbria; fMa, forceps major; fmi, forceps minor; genu-cc, genu of the corpus callosum; hhipp, head of the hippocampus; ILF, inferior longitudinal fasciculus; isth, isthmus of the cingulum; llstr, lateral longitudinal stria; paraHi, parahippocampal gyrus; PCL, paracentral lobe; poS, parietooccipital sulcus; preCu, precuneus; sbca, subcallosal area; spl-cc, splenium of corpus callosum; tp, temporal pole; unc, uncus.

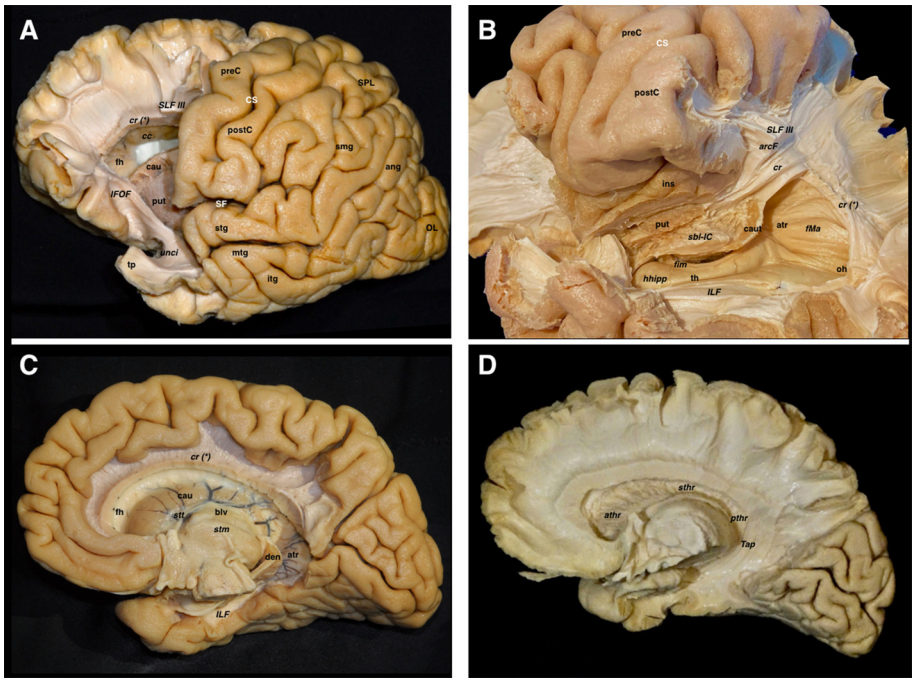

FIGURE 6 | Both lateral and medial dissections end up reaching the last remaining fibers adjoining the walls of the lateral ventricle. **(A)** The frontal horn of the lateral ventricle is seen after opening its lateral wall. Thus, the last layer of fibers cut is the corticostriate and frontopontine descending fibers running to the anterior limb of the internal capsule, as well as the anterior thalamic radiations running from the anterior thalamic nuclei toward the prefrontal and cingular cortex. The SLF II & SLF III have been also cut in a more lateral plane. In the frontal region, the association fibers are purely longitudinal and oriented in the anteroposterior plane, while the projection fibers are also longitudinal but following a craneo-caudal direction. The curvilinear irregular shape of the IFOF and the uncinate are clearly seen in the ventral aspect of the telencephalic flexure. **(B)** In this image, the dissection has progressed into the temporoparietal area, which represents the dorsal and posterior parts of the telencephalic flexure. The vertical component of SLF, arcuate, corona radiate, sagittal stratum, and tapetum fiber bundles, as well as the ependyma of the atrium and temporal horn, have been removed, thereby providing a lateral view of the temporal horn and atrium. The head of the hippocampus is seen in the most anterior aspect of the temporal horn. The fimbria above the hippocampal surface follows a posterior direction in close contact with the choroidal fissure. The tail of the caudate nucleus is located in the temporal horn roof as well as in the anterior wall of the atrium while wrapping around the thalamus. This curved shape to the caudate follows the main dogma of the already discussed flexure. Note how the sub-lenticular component of the internal capsule is located ventral and medial to the putamen, where it runs lateral to the caudate. **(C)** A medial view of the lateral ventricle is shown in this dissection, where the cingulum, parahippocampal and callosal fibers, as well as the fornix have been removed. The curved shape of the caudate nucleus, as well as the stria terminalis connecting the amygdala and the septal area, are shown wrapping around the thalamus. **(D)** The lateral ependymal layer and caudate nucleus gray matter have been removed with the aim of uncovering the medial aspect of the internal capsule, with the anterior, superior, and posterior thalamic radiations, and the tapetum covering the lateral wall of the atrium, occipital and temporal horns. ang, angular gyrus; arcF, arcuate fascicle; athr, anterior thalamic radiation; atr, atrium; blv, body of the lateral ventricle; cau, caudate nucleus; caut, caudate nucleus tail; cc, corpus callosum; cr, corona radiata; cr (*), corona radiata and callosal fibers intermingling point; CS, central sulcus; den, dentate gyrus; fh, frontal horn; fim, fimbria; fMa, forceps major; hhipp, head of the hippocampus; IFOF, inferior frontooccipital fasciculus; ILF, inferior longitudinal fasciculus; ins, insula; itg, inferior temporal gyrus; mtg, middle temporal gyrus; oh, occipital horn; OL, occipital lobe; postC, postcentral gyrus; preC, precentral gyrus; pthr, posterior thalamic radiation; put, putamen; sbl-IC, sublenticular component of the internal capsule; SF, Sylvian fissure; SLF III, superior longitudinal fasciculus III; smg, supramarginal gyrus; SPL, superior parietal lobe; stg, superior temporal gyrus; sthr, superior thalamic radiation; stm, stria medullaris; stt, stria terminalis; Tap, tapetum; th, temporal horn; tp, temporal pole; unci, uncinate fascicle.

days, the cephalic flexure divides the unfused neural folds into prosencephalon, mesencephalon, and rhombencephalon (3). At 4.5 gestational weeks (gw), the prosencephalic vesicle thins in the sagittal midline, growing in a mediolateral direction, resulting in forebrain outpouchings that will form the two telencephalic hemispheres. At 8 gw, the telencephalic hemispheres grow caudally bending in a ventral and rostral direction, best described as "C-shaped" (3). Perhaps counterintuitively, the posterior pole of the primitive telencephalon becomes the temporal lobe, while the occipital lobe is derived from the dorsal wall of this primitive telencephalon. This folding of the telencephalic hemispheres (telencephalic flexure) becomes the operculum and the future Sylvian fissure (8). The frontal and temporal lips of the Sylvian fissure, along with the insula all derive from the ventral margin of the primitive telencephalon (8). The first visualization of a fissure at this level starts at the 13 gw, perpendicular to the ventral surface of the hemisphere. This groove will become the posteroinferior peri-insular sulcus. At 18–19 gw the peri-insular sulcus is completed due to the faster development of the surrounding lobules compared with the growth speed of the insula. Around 20 gw, the opercularization process starts, which will develop into operculi completely covering the insula (9). The opercularization starts in the posterior part of the fissure as the parietotemporal cortex develops earlier than the

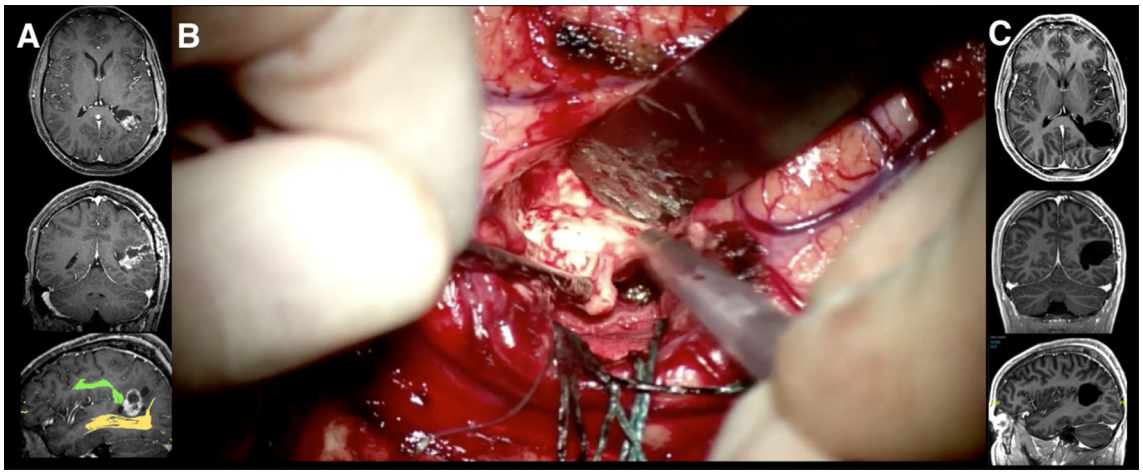

FIGURE 7 | A 33-year-old man who presented with a headache was treated by awake surgery for a Pleomorphic Xanthoastrocytoma after an open biopsy was performed in a referral center. **(A)** The T1 weighted MR images after gadolinium injection in axial, coronal, and sagittal planes are shown. The lesion is located in the left temporoparietal area, just dorsal to the telencephalic flexure. This area shows highly eloquent cortical regions around the terminal part of the Sylvian fissure. The tumor grows from the cortical surface of the angular gyrus toward the ependymal wall of the left atrium. This area presents an underlying complex network of white matter tracts, the intimate relationships of which must be studied preoperatively. Some of these fibers show a curved shape as a result of the telencephalic flexure appearing due to the physical and genetic forces that made our brains more functionally advanced. Thus, the sagittal image shows its close relationship with the fused DTI-tractography images of the arcuate fascicle *(green)* and the optic radiations *(yellow*), which seemed to be displaced by the tumor itself. The neurological examination was completely normal including the visual field campimetry **(B)**. Due to the age of the patient and tumor location, an awake craniotomy was performed with the aim of testing the language and visual function during the tumor resection. The speech was tested to increase the tumor resection anteriorly and no deficit was noted even when reaching the most anterior part. During resection of the deeper parts of the tumor, intra- operative visual tests were performed. Stimulations to different points along the optic radiations evoked reversible scotomas in different portions of the visual field as described by the patient. At the completion of the optic radiation mapping, the resection of the tumor was performed radically in those areas where the vision remained normal despite subcortical stimulation. **(C)** The postoperative MRI at three months revealed a complete resection of the tumor. Postoperative campimetry at three months revealed a minor homonymous deficit in the right inferior quadrant.

frontal. The sylvian fissure completely closes at the end of the first postnatal year. The positional change of the hippocampus starts before the telencephalic flexure begins to form and its position is in part induced by the flexure, with the original dorsal aspect becoming its ventral aspect, and the dorsal area moving to a caudal end as a ventral structure after the "rotation". These rotational movements of the hippocampal rudiment occur due to gradients induced by genetic expression, the fact that is key in some malformations (8). The formation of the forebrain fissures is also impacted by the development of the ventricles, which behaves as an external mechanical force rather than an internal force (8, 10, 11).

The specific developmental patterns happening during its embryological evolution can be extrapolated to the phylogenetic changes of the CNS of different species (12, 13). From a morphological perspective, the evolution of the CNS in different species has gone from very simple tubular longitudinal shapes to more complex, round, and flexed forms in primates (**Figure 1**). A cross-species comparison of neuroembryology **(Figure 9)**, with a particular focus on telencephalic flexure, reveals interesting information. In rodents, there is no formation of a telencephalic flexure, but, as in humans, their primary visual cortex lies on the dorsomedial aspect, rostral to the occipital pole. Furthermore, there is no looping of the stria terminalis, and the hippocampus extends all the way to the posterior hemisphere (14). Animals that do form a telencephalic flexure include all primates, dogs, whales, cats, cows, horses, and pigs (8). The real cause of the telencephalic folding or cortex gyrification has been hypothesized to be due to the lack of space for cortical development or due to differential regional proliferation and mechanical tension along the axons that try to bring together distal structures (15). The hippocampal shift from dorsal to a ventral position, and a reversal in orientation of genetic gradients are partly mediated by the telencephalic flexure (8). Seemingly this occurs at a marginally earlier embryonic stage in humans as compared with non-human primates.

When analyzing the differential proliferation speeds, the diverse origins of the operculum and the insular cortex must be considered. The operculi originate due to the radial migration from the ventricular and subventricular zones while the insula is formed by cells from the pallial/subpallial boundary that migrate around the basal ganglia. At 11–12 gw the Sylvian fossa is identified, and its configuration starts developing thanks to the curvature of the lateral ventricles. Since 13 gw, cells from the subpallial neurons migrate into the insular cortex along the radial glial fascicle reaching the final configuration before birth (16). Mallela et al. (17, 18) found different gene expressions from the opercula to the insula resulting in the highest proliferation of the former allowing their growth over the insula. This different origin might explain the fact that the tracts that developed later

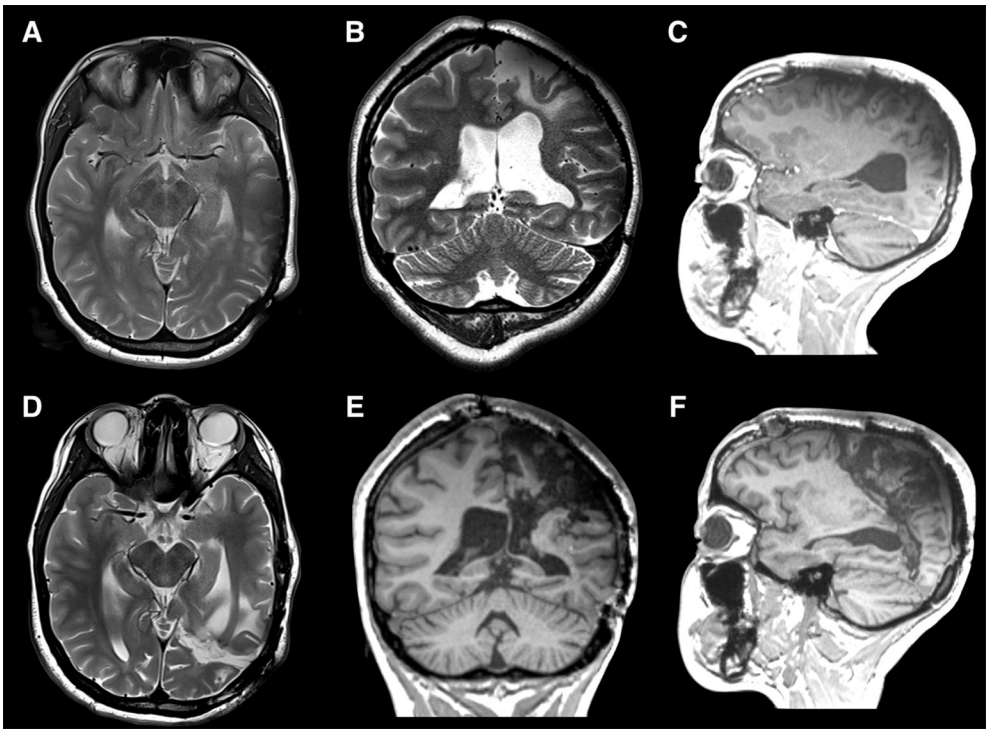

FIGURE 8 | An 18-year-old left-handed girl presented with medically refractory epilepsy that was symptomatic since the age of 3 years due to a perinatal stroke in the territory of the left middle cerebral artery. Cerebral MRI (multiplanar) confirmed the radiological sequelae of an ischemic lesion involving primarily the central, parietal, and occipital lobes **(A–C)**. At the age of 7 years, based on phase II subdural grid evaluation, the majority of the seizures were determined to arise from the supplementary motor area (SMA) on the left side for which she underwent a subpial resection of the SMA. She continued to have an unfavorable seizure outcome and regression of developmental milestones along with a mild right hemiparesis with a limited fine motor movement of the right hand. Phase I and II (SEEG) evaluations showed major epileptogenic foci in the left parasagittal parietal lobe and precentral area. When the centro-parieto-occipital lobes (central quadrant) are involved, in the presence of normal frontal and temporal lobes, the situation becomes complex for a curative surgical procedure. A precise knowledge of the tracts that could traverse the lines of disconnection is mandatory. The association fibers like the SLF I, II, and III, IFOF, MLF, and cingulum are to be sectioned in addition to disconnecting the occipital lobe from the functional temporal lobe. The corticospinal, thalamocortical, parieto-pontine, occipito-pontine and optic radiations represent the projection fibers disconnected. The posterior lateral extension of the anterior commissure, tapetum, posterior third of corpus callosum, and splenium are the commissural fibers that are disconnected in this surgery. In view of the refractory nature of the epileptic illness and progressive cognitive decline, we decided to perform a centro-parieto-occipital lobotomy (central quadrantotomy). During this lobotomy, the arcuate fasciculus was spared, by performing a posteriorly directed oblique white matter section trajectory at the posterior insular point. Indeed, the direction of this disconnective procedure follows the direction of the forces that cause the telencephalic flexure during the early embryological development. The language functions remained unchanged and similar to the pre-operatively acquired language skills. The patient remained in Engel class I at the last follow-up at 10 months after surgery. Postoperative MRI (multiplanar) demonstrated the complete disconnections (arrows) of the central quadrant with preservation of the AF **(D–F)**.

connecting frontal, temporal, and parietooccipital regions 'avoid crossing the insula', thus being located ventral or dorsal to it, and in some cases wrapping around it with specific curved patterns (19–21).

There is still a large gap in understanding the excitatory and inhibitory signals mediating the formation of such a complex net of fibers, which will finally lead to the capricious human subcortical anatomy. In this sense, it has been recently discovered the role of the extracellular proteoglycan molecule keratan sulfate, which surrounds and envelops white matter tracts and fascicles from mid-gestation (much sooner than myelination of axons) and thus preserves the functional and anatomical "purity" of such fascicles, so that axons entering the tracts at one end cannot exist until they reach their destination and that axons from subcortical gray matter or indeed even other regions of cortex cannot enter the en-route tracts (8).

Understanding Evolution of White Matter Tracts

Clear differences are observed when the subcortical architecture in monkeys is compared to the human one. Regarding the frontal connections, most of the studies reveal that monkeys' IFOF lacks the posterior projections to the occipital lobe ending at the temporal lobe level (22). Regarding the human brain's embryological development, the IFOF is one of the latest fascicles to develop, not appearing clearly identifiable till 20 gw (11). This longitudinally oriented tract is located ventral to the telencephalic bending, so it looks like not being too much affected by the flexure. However, the large development of the ventral insula pushed it downwards and maybe thickened its main core, marking its curved shape in this area. Although showing a similar structure to humans, monkeys' SLF cortical connections are slightly different. This fact is especially important for the

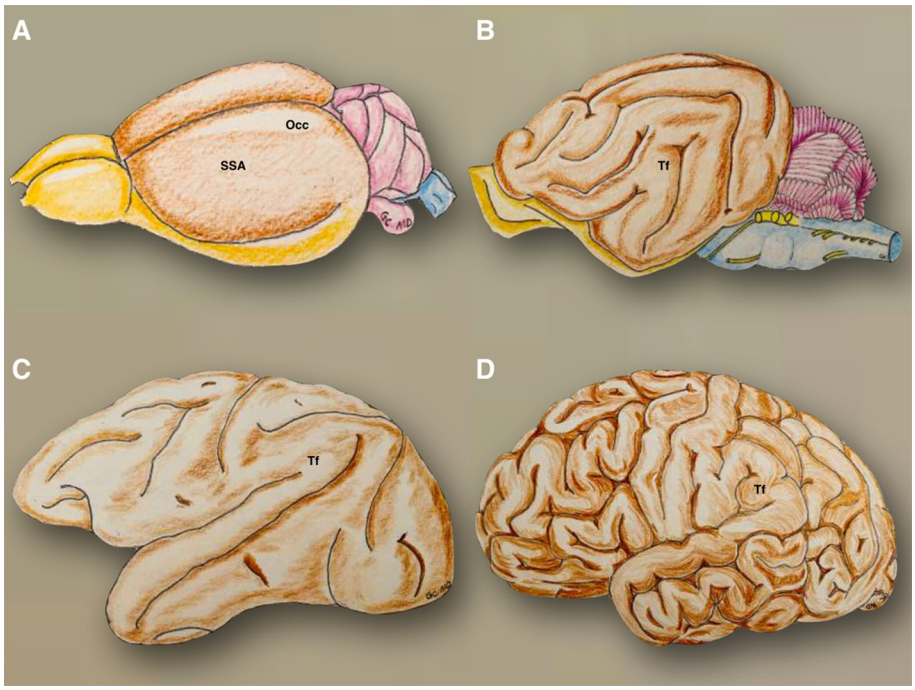

FIGURE 9 | The phylogenetic evolution of the telencephalic flexure is illustrated. In the mouse **(A)**, the olfactory bulbs *(yellow)* are well developed and were continued posteriorly through the olfactory tracts and tubercles, to reach the entorhinal area on the posteroventral side of the hemispheres. The hemispheres are otherwise smooth *(brown)*, with the precentral area situated anteriorly to the somatosensory area, and postcentral region situated dorsally, and the occipital area located on the posterodorsal side. The cerebellum and brainstem are colored in *violet* and *blue*, respectively. In the cat **(B)**, the olfactory bulbs and tracts are situated on the ventral side of the hemispheres and connect posteriorly with the piriform lobe *(yellow)*. The telencephalic flexure is present in a primordial form, along with gyri and sulci *(brown)*. The cerebellum and brainstem are colored in *violet* and *blue*, respectively. In the Rhesus monkey **(C)**, the morphology of the telencephalic flexure is more similar but less pronounced to that of the human brain **(D)**. SSA, somatosensory and postcentral region; Occ, occipital area; Tf, telencephalic flexure.

SLF III, as it has the strongest and more anterior connections in the human inferior frontal gyrus, while the monkey's main connections are centered in the ventral premotor cortex. This is translated into a more important prefrontal connection in humans, especially on the right side. (23). Moreover, and although the horizontal segment is widely similar in humans and monkeys, the vertical segment is missed in the latter. The frontotemporal connections are the first ones to be identified during the embryogenesis (around the 17 gw), while the parietal branches appear a few weeks later during the development (20 gw) (11). SLF II and III posterior extensions to the angular and supramarginal gyri show a slight inferolateral curve, probably given by the inferior parietal lobe ventrolateral movement during the CNS development. The vertical component of SLF joins the superior parietal lobe (dorsal) with the posterior aspect of the superior temporal gyrus, which, in less developed species and the early embryonic stages, are oriented into the same horizontal-longitudinal axes. The ventral movement of the temporal lobe might be responsible for this vertical direction (**Table 1**).

The SLF I anteroposterior longitudinal shape seems not to be affected by the flexure itself as the implicated cortical areas remain dorsal during the telencephalic bending.

The MLF shows a posterior and dorsal curve as joins the superior temporal gyrus with the superior temporal lobe. Before the tremendous telencephalic development happens, the rudimental temporal lobe is situated posterior and lateral to the parietal lobe, so probably, during this early stage these connections would be running horizontally, but anterior and dorsal from the temporal to the parietal rudiments.

Regarding the ILF, and according to the connected cortical areas (temporal pole and occipital lobe), the rudimental axons of this tract should have probably turned 180° as the temporal appears initially dorsal to the occipital lobe.

The human AF shows an increased number of temporal lobe connections, being responsible for a wider language specialization. When compared with macaques, we observe a longitudinal tract without a large number of temporal connections, mainly connecting the frontal and parietal cortices (24, 25). The ventrolateral movement of the neocortex of the temporal lobe is responsible for the C shape of the arcuate fascicle, as it is connecting the inferior frontal and superior temporal gyri, which were previously aligned in the same 'x' horizontal axis. The embryological development of such a highly specialized fiber tract is quite special, as it is not clearly visible until the 30 gw, being fully evident around the second

TABLE 1 | Summary of white matter tracts encountered during the lateral-to-medial and medial-to-lateral dissection.

White matter tract		Type	Shape	Orientation	Connections
Lateral aspect	**SLF I**	Association	Longitudinal	AP	SFG-SPL
	SLF II	Association	Longitudinal	AP	MFG-AG
	SLF III	Association	Longitudinal	AP	IFG-SMG
	vcSLF	Association	Longitudinal	CC	post.1/3 STG-SPL
	Arcuate	Association	Curved	AP/CC/LM	IFG-STG
	MLF	Association	Curved	AP/CC	mid.1/3 STG-SPL
	IFOF	Association	Curved	AP/CC	FBL-OL
	ILF	Association	Longitudinal	AP	TP-OL
	Uncinate	Association	Curved	AP/CC	FBL-TML
	Ant. Commissure	Commissural	Curved	AP/CC/LM	TML-TOL bilat.
	Optic radiations	Projection	Curved	LM/AP	LGB-OL
	IC/cr	Projection	Longitudinal	CC	Cortex-(BG,Tha,Brst,SC)
	Corpus callosum	Commissural	Curved	AP/CC/LM	Both hemispheres
Medial aspect	**Cingulum**	Association	Curved	AP/CC/LM	Subcallosal area -Parahippocampal
	Fornix	Association	Curved	AP/CC/LM	Hippoc.-MB
	Lateral long. stria	Association	Curved	AP/CC/LM	FC-indusium griseum
	Stria terminalis	Association	Curved	AP/CC/LM	Amygdala-septal area
	Stria medularis	Association	Curved	AP/CC	Habenula-septal & hypothal. Nuclei

Their shape (longitudinal/curved), orientation/main axis (antero-posterior, craneo-caudal, latero-medial) and principal connections are detailed. AG, angular gyrus; AP, antero-posterior; BG, basal ganglia; Brst, brainstem; CC, cranio-caudal; cr, corona radiata; FBL, fronto-basal lobe; FC, fasciola cinerea; IC, internal capsule; IFG, inferior frontal gyrus; IFOF, inferior fronto-occipital fascicle; LGB, lateral geniculate body; LM, latero-medial; MB, mammillary body; MFG, middle fontal gyrus; MLF, middle longitudinal fasciculus; OL, occipital lobe; SC, spinal cord; SFG, superior frontal gyrus; SLF I, superior longitudinal fasciculus I; SLF II, superior longitudinal fasciculus II; SLF III, superior longitudinal fasciculus III; SMG, supramarginal gyrus; SPL, superior parietal lobe; STG, superior temporal gyrus; TML, temporomesial lobe; TOL, temporo-occipital lobes; TP, temporal pole; Tha, thalamus; vcSLF, vertical component of SLF.

year of age. Some pathological conditions during the Sylvian fissure development such as lissencephaly, polymicrogyria (26), or Perisylvian Syndrome (27), are related to alterations of development or even the absence of the AF. Most of the aforementioned tracts are located in between interconnected structures that initially were adjacent, becoming more distant as the telencephalic flexure proceeds, requiring their pathways to elongate and curve into a loop (8).

The changes suffered by the uncinate are the same suffered by the arcuate. Indeed, both are connecting temporal and frontal regions, with a big difference, as the uncinate connects the most rudimental areas of the human cortex (frontoorbital and temporomesial), related to the olfactory and mnesic functions, while the arcuate is related to one of the most advanced and complex human functions as speech is. Thus, the bending forces and the intrinsic anatomy of these different archicortical and neocortical areas are progressively separated by the appearance and development of the insular lobe, which will finally be responsible to push the uncinate to a ventral and the arcuate to a dorsal position into the telencephalic flexure.

Most of the relevant fibers in the medial aspect (cingulum, fornix. lateral longitudinal stria, stria terminalis, stria medularis), show a similar "C-shape" wrapping around the corpus callosum, ventricular system, and thalamus. This shape is the result of the telencephalic flexure, as most of these fiber tracts are longitudinally oriented in the first stages of development (11). One illustrative disease is the alobar and semilobar forms of holoprosencephaly where telencephalic fissure is absent due to uncleavage of the interhemisferic fissure. This causes the absence of temporal lobe rotation, becoming the most posterior aspect of the hemispheres, and therefore, the hippocampus does not rotate, having a linear disposition in the medial aspect, as it happens in rodents. This fact could explain a direct relationship between the telencephalic flexure and the curved shape of some of these tracts (8).

The internal capsule, and its cortical ascending and descending projections, are probably the fibers most affected by the telencephalic growth in primates. While the genu, anterior and posterior limbs are somehow oriented in the same sagittal plane, the aforementioned ventrolateral movement of the temporal lobe influences the appearing of the sub- and retrolenticular fibers in a more lateral position, curving its direction posteriorly to the temporal and occipital lobes respectively, and covering the lateral wall of the temporal horn, atrium and occipital horn of the lateral ventricles. Thus, the final shape of the internal capsule is a reminder of a baseball glove hugging the lenticular core.

A relevant part of the internal capsule, regarding these specific changes in shape and direction, is the optic radiations. As thalamic corticopetal fibers, they run from the lateral geniculate toward the occipital lobe in a horizontal longitudinal direction. The visual projection system runs dorsally and superiorly in fishes and even in rodents to reach the dorsally located occipital region regarding the central position of the thalamus (28).

However, and probably due to the expansive lateral growing of the lateral ventricles and the telencephalic bending in primates, the occipital lobe is moved to the posterior pole of the brain. Therefore, the optic radiations are pushed inferiorly and laterally being forced to travel through the depth of the temporal lobe on its way to the visual areas.

Important attention must be given to the commissural fibers. The anterior commissure is the primordial commissural tract, connecting both temporomesial (medial component) and temporo-occipital areas (lateral component). Its posteriorly directed shape might have happened due to the fragmentation of the primordium of the temporo-occipital cortex, the temporal areas moving ventral, anterior, and lateral, and the occipital ones moving dorsally. As the corpus callosum connects the neocortex of both telencephalic hemispheres, it perfectly describes the way in which the wide development of the neocortex has covered the central core. Thus, it shows a lateromedial direction in the coronal plane, as well as an anterior curve (genu-forceps minor) and a posterior one (splenium-forceps major) in the sagittal plane. These two curves contain fibers connecting basal and polar areas of the frontal lobe, as well as the medial and basal aspects of the occipital lobe respectively. A special part of the corpus callosum is the tapetum, which, as connects both temporal lobes, runs in a ventrolateral direction in the lateral wall of the atrium and temporal horn. The corpus callosum is mainly developed once the flexure has happened (8).

Performing the simple exercise of "drawing" these fibers in some animals' brains, one might realize that 'older CNS' (in phylogenetic terms), have more longitudinally oriented tracts (specifically in one plane). However, the primates' CNS evolution added the acquisition of more complex functions. This was the result of evolutional genetic expressions, giving rise to a brain in which the lobes are morphologically located in the three different planes due to the telencephalic movements (**Figures 1, 9**). These growth forces taking place in the human brain during its development, as well as the flexure that will hide the insular lobe, involve important implications for the 3D understanding of the white fibers (**Figure 1**).

Our dissections have shown the complex anatomical arrangement and relationships among the different association, projection, and commissural fiber tracts around the central core. Interestingly, we mainly found anteroposterior longitudinally oriented fibers in the frontal region. However, posteriorly (parietooccipital) and basally (temporal), some fibers appear curving around the flexure, ventrally (IFOF, UF, and AC), and dorsally (MLF, vertical SLF, and AF) **(Figure 4).** Some of those fiber tracts, especially those connecting relatively 'distant' cortical areas (AF, IFOF, UC) show a specific curved shape. Those tracts connecting adjacent lobes, predominantly show a longitudinal direction as the SLF, MLF, and ILF. This pattern of shapes could be related to the fact that the temporal lobe has been pushed laterally, anteriorly, and ventrally from its posterior position, and the occipital lobe has moved posteriorly from a dorsal location during the embryological development. On the other hand, the medial movement of the ventral cortex could be ascribed to the insula being pushed to the depth of the Sylvian fissure, being responsible for the curved shape of the aforementioned fascicles, as well as for the fan-shape radiations of the corona radiata (**Table 1**). Therefore, while there exists a clear relationship between the white matter tracts' disposition and the formation of the Sylvian fissure in humans, it is not yet known if this is the cause or the effect.

Surgical Implications

Oncological surgery for intra-axial lesions deep to the perisylvian cortices, especially for the dominant hemisphere, requires a profound knowledge of the anatomy of the cortex and of the subjacent WMT, some of which are of curvilinear morphology and the others longitudinal. Analysis of pre-operative MR imaging (including DTI and fMRI) and its use for neuronavigation are standard techniques to allow maximal preservation of the WMT connectivity. The 3D anatomical appreciation of this region may be particularly complex and the performance of cadaveric dissection studies as well as case-to-case analysis of preoperative images to evaluate the distortion of the normal anatomy provoked by the tumor are essential to tailor the surgical procedure. To perform a maximally safe resection, intraoperative monitoring through the performance of awake craniotomies is often used to perform a direct study of the WMT and thereby obtain a functionally-guided resection.

The anatomy of this region is also of particular importance for the planning of sub- hemispheric epilepsy surgery (29–33). When dealing with lesions of the centro-parieto-occipital lobes (central quadrant), disconnective surgery implies particular problems because of the necessity to preserve some traversing fibers while selectively disconnecting all afferent and efferent connections of these lobes. White matter areas where the associative fibers are intermingling with projection and commissural fibers should be carefully analyzed to safely perform the disconnective epilepsy surgery in order to obtain a favorable seizure outcome with minimal additional neurological morbidity.

Limitations of the Study and Future Perspectives

This cadaveric study defined the complex orientation of the white matter anatomy of this region in adult human brains. Ongoing development of diffusion tensor imaging techniques in human brains with the surface rendering of these important tracts around the flexure will help improve our understanding of the intimate relationships of the projection, association, and commissural fibers in this region. We have attempted to provide correlations from existing literature using human embryological data and cross-species studies of the region of the telencephalic flexure. However, this can be further enhanced with human embryological studies using histological and/or neuroimaging methods.

CONCLUSIONS

A precise knowledge of the connectome of the region around the telencephalic flexure is crucial to safe surgery for

intra-axial pathologies in the area. A 3D appreciation of the WMT topography allows the identification and preservation of eloquent tracts during the removal of intra-axial tumors in this region. This is also crucial while performing disconnective epilepsy surgery of the centro-parieto-occipital lobes that aim to achieve a complete disconnection while preserving important white matter tracts that adjoin or traverse the telencephalic flexure.

DATA AVAILABILITY STATEMENT

The original contributions presented in the study are included in the article/supplementary material, further inquiries can be directed to the corresponding author/s.

ETHICS STATEMENT

Ethical review and approval was not required for the study on human participants in accordance with the local legislation and institutional requirements. The patients/participants provided their written informed consent to participate in this study.

AUTHOR CONTRIBUTIONS

PG-L and RD conceived the paper. PG-L and CG performed the cadaveric dissection. GC and PG-L analyzed the data and wrote the main body of the text. CT and JM wrote two paragraphs of the paper. EP performed an analysis and revision of the paper. MM and RD supervised the paper and both deserve to be the last authors. All authors revised the last version of the paper.

REFERENCES

1. Ludwig E, Klingler J: Der innere Bau des Gehirns, dargestellt auf Grund makroskopischer Präparate, in Atlas cerebri humani.. Basel: Karger, (1956).
2. Ture U, Yasargil MG, Friedman AH, Al-Mefty O: Fiber dissection technique: lateral aspect of the brain. *Neurosurgery.* (2000) 47:417–26. doi: 10.1097/00006123-200008000-00028
3. O'Rahilly R, Muller F. Developmental stages in human embryos: revised and new measurements. *Cells Tissues Organs.* (2010) 192:73–84. doi: 10.1159/000289817
4. Maldonado IL, Destrieux C, Ribas EC, Guimarães BS, Cruz PP, Duffau H. Composition and organization of the sagittal stratum in the human brain: a fiber dissection study. *J Neurosurg.* (2021) 135:1214–22. doi: 10.3171/2020.7.JNS192846
5. Daniel RT, Joseph TP, Gnanamuthu C, Chandy MJ. Hemispherotomy for paediatric hemispheric epilepsy. *Stereotact Funct Neurosurg.* (2001) 77:219–22. doi: 10.1159/000064609
6. Daniel RT, Villemure JG. Peri-insular hemispherotomy: potential pitfalls and avoidance of complications. *Stereotact Funct Neurosurg.* (2003) 80:22–7. doi: 10.1159/000075155
7. Villemure JG, Daniel RT. Peri-insular hemispherotomy in paediatric epilepsy. *Childs Nerv Syst.* (2006) 22:967–81. doi: 10.1007/s00381-006-0134-3
8. Sarnat HB, Flores-Sarnat L. Telencephalic Flexure and Malformations of the Lateral Cerebral (Sylvian) Fissure. *Pediatr Neurol.* (2016) 63:23–38. doi: 10.1016/j.pediatrneurol.2016.05.005
9. Afif A, Bouvier R, Buenerd A, Trouillas J, Mertens P. Development of the human fetal insular cortex: study of the gyration from 13 to 28 gestational weeks. *Brain Struct Funct.* (2007) 212:335–46. doi: 10.1007/s00429-007-0161-1
10. Gholipour A, Rollins CK, Velasco-Annis C, Ouaalam A, Akhondi-Asl A, Afacan O, et al. A normative spatiotemporal MRI atlas of the fetal brain for automatic segmentation and analysis of early brain growth. *Sci Rep.* (2017) 7:476. doi: 10.1038/s41598-017-00525-w
11. Horgos B, Mecea M, Boer A, Szabo B, Buruiana A, Stamatian F, et al. White Matter Dissection of the Fetal Brain. *Front Neuroanat.* (2020) 14:584266. doi: 10.3389/fnana.2020.584266
12. E. H: Ueber die Entwicklungstheorie Darwin's. In: *Amtlicher Berich ueber die acht und dreissigste Versammlung Deutscher Naturforscher und aerzte.* in Stettin.: Stettin: Hessenland's Buchdruckerei, (1864). pp. 17–30.
13. Hall BK. Ontogeny does not recapitulate phylogeny, it creates phylogeny. In: Robert J. Richards ED e (ed): *A review of The Tragic Sense of Life: Ernst Haeckel and the Struggle over Evolutionary Thought.* (2011). Vol 13, pp 401–4. doi: 10.1111/j.1525-142X.2011.00495.x
14. Basma J, Guley N, Michael Ii LM, Arnautovic K, Boop F, Sorenson J. The Evolutionary Development of the Brain As It Pertains to Neurosurgery. *Cureus.* (2020) 12:e6748. doi: 10.7759/cureus.6748
15. Van Essen DC, Donahue CJ, Glasser MF. Development and evolution of cerebral and cerebellar cortex. *Brain Behav Evol.* (2018) 91:158–69. doi: 10.1159/000489943
16. Gonzalez-Arnay E, Gonzalez-Gomez M, Meyer G. A Radial Glia Fascicle Leads Principal Neurons from the Pallial-Subpallial Boundary into the Developing Human Insula. *Front Neuroanat.* (2017) 11:111. doi: 10.3389/fnana.2017.00111
17. Mallela AN, Deng H, Brisbin AK, Bush A, Goldschmidt E. Sylvian fissure development is linked to differential genetic expression in the pre-folded brain. *Sci Rep.* (2020) 10:14489. doi: 10.1038/s41598-020-71535-4
18. Mallela AN, Deng H, Bush A, Goldschmidt E. Different Principles Govern Different Scales of Brain Folding. *Cereb Cortex.* (2020) 30:4938–48. doi: 10.1093/cercor/bhaa086
19. Choi CY, Han SR, Yee GT, Lee CH. A understanding of the temporal stem. *J Korean Neurosurg Soc.* (2010) 47:365–9. doi: 10.3340/jkns.2010.47.5.365
20. Peltier J, Verclytte S, Delmaire C, Pruvo JP, Godefroy O, Le Gars D. Microsurgical anatomy of the temporal stem: clinical relevance and correlations with diffusion tensor imaging fiber tracking. *J Neurosurg.* (2010) 112:1033–8. doi: 10.3171/2009.6.JNS08132
21. Ribas EC, Yagmurlu K, de Oliveira E, Ribas GC, Rhoton A. Microsurgical anatomy of the central core of the brain. *J Neurosurg.* (2018) 129:752–69. doi: 10.3171/2017.5.JNS162897
22. Thiebaut de. Schotten M, Dell'Acqua F, Valabregue R, Catani M: Monkey to human comparative anatomy of the frontal lobe association tracts. *Cortex.* (2012) 48:82–96. doi: 10.1016/j.cortex.2011.10.001
23. Hecht EE, Gutman DA, Bradley BA, Preuss TM, Stout D. Virtual dissection and comparative connectivity of the superior longitudinal fasciculus in chimpanzees and humans. *Neuroimage.* (2015) 108:124–37. doi: 10.1016/j.neuroimage.2014.12.039
24. Ghazanfar AA. Language evolution: neural differences that make a difference. *Nat Neurosci.* (2008) 11:382–4. doi: 10.1038/nn0408-382
25. Rilling JK, Glasser MF, Preuss TM, Ma X, Zhao T, Hu X, et al. The evolution of the arcuate fasciculus revealed with comparative DTI. *Nat Neurosci.* (2008) 11:426–8. doi: 10.1038/nn2072
26. Andrade CS, Figueiredo KG, Valeriano C, Mendoza M, Valente KD, Otaduy MC, et al. DTI-based tractography of the arcuate fasciculus in patients with polymicrogyria and language disorders. *Eur J Radiol.* (2015) 84:2280–6. doi: 10.1016/j.ejrad.2015.07.014
27. Kilinc O, Ekinci G, Demirkol E, Agan K. Bilateral agenesis of arcuate fasciculus demonstrated by fiber tractography in congenital bilateral perisylvian syndrome. *Brain Dev.* (2015) 37:352–5. doi: 10.1016/j.braindev.2014.05.003
28. Mueller T. What is the thalamus in zebrafish? *Front Neurosci.* (2012) 6:64. doi: 10.3389/fnins.2012.00064

29. Cossu G, Messerer M, Lebon S, Daniel RT. Posterior Peri-insular Quadrantotomy. In: Cataltepe O, Jallo GI. e (ed): *Pediatric Epilepsy Surgery: Preoperative Assessment and Surgical Treatment.* New York: Thieme, (2020). p. 465–71.
30. Cossu G, Gonzalez-Lopez P, Pralong E, Kalser J, Messerer M, Daniel RT. Unilateral prefrontal lobotomy for epilepsy: technique and surgical anatomy. *Neurosurg Focus.* (2020) 48:E10. doi: 10.3171/2020.1.FOCUS19938
31. Cossu G, Messerer M, Lebon S, Pralong E, Seeck M. R.T. D Anterior Peri-insular quadrantotomy. In Cataltepe O, Jallo GI. e (ed): *Pediatric epilepsy Surgery: preoperative Assessment and Surgical Treatment.* ed Second Edition New York: Thieme, (2020)., pp 459-464
32. Daniel RT, Meagher-Villemure K, Farmer JP, Andermann F, Villemure JG. Posterior quadrantic epilepsy surgery: technical variants, surgical anatomy, and case series. *Epilepsia.* (2007) 48:1429–37. doi: 10.1111/j.1528-1167.2007.01095.x
33. Gonzalez-Lopez P, Cossu G, Pralong E, Baldoncini M, Messerer M, Daniel RT. Anterior peri-insular quadrantotomy: a cadaveric white matter dissection study. *J Neurosurg Pediatr.* (2019) 25:331–9. doi: 10.3171/2019.10.PEDS19472

Conflict of Interest: The authors declare that the research was conducted in the absence of any commercial or financial relationships that could be construed as a potential conflict ofinterest.

frontiers | Frontiers in Neurology

REVIEW
published: 27 April 2022
doi: 10.3389/fneur.2022.794618

Superior Longitudinal Fasciculus: A Review of the Anatomical Descriptions With Functional Correlates

*Felix Janelle, Christian Iorio-Morin, Sabrina D'amour and David Fortin**

Division of Neurosurgery, Department of Surgery, Faculty of Medicine and Health Sciences, Université de Sherbrooke, Sherbrooke, QC, Canada

The superior longitudinal fasciculus (SLF) is part of the longitudinal association fiber system, which lays connections between the frontal lobe and other areas of the ipsilateral hemisphere. As a dominant association fiber bundle, it should correspond to a well-defined structure with a clear anatomical definition. However, this is not the case, and a lot of confusion and overlap surrounds this entity. In this review/opinion study, we survey relevant current literature on the topic and try to clarify the definition of SLF in each hemisphere. After a comparison of postmortem dissections and data obtained from diffusion MRI studies, we discuss the specifics of this bundle regarding its anatomical landmarks, differences in lateralization, as well as individual variability. We also discuss the confusion regarding the arcuate fasciculus in relation to the SLF. Finally, we recommend a nomenclature based on the findings exposed in this review and finalize with a discussion on relevant functional correlates of the structure.

Keywords: superior longitudinal fascicle (SLF), association fibers, white matter tracts, diffusion imaging, MRI

OPEN ACCESS

Edited by:
Wellingson Silva Paiva, University of São Paulo, Brazil

Reviewed by:
Ryan P. Cabeen, University of Southern California, United States
Emmanuel Caruyer, UMR6074 Institut de Recherche en Informatique et Systèmes Aléatoires (IRISA), France

****Correspondence:***
David Fortin
David.Fortin@USherbrooke.ca

Specialty section:
This article was submitted to Applied Neuroimaging, a section of the journal Frontiers in Neurology

Received: *13 October 2021*
Accepted: *21 February 2022*
Published: *27 April 2022*

Citation:
Janelle F, Iorio-Morin C, D'amour S and Fortin D (2022) Superior Longitudinal Fasciculus: A Review of the Anatomical Descriptions With Functional Correlates. Front. Neurol. 13:794618. doi: 10.3389/fneur.2022.794618

INTRODUCTION

Although brain surgery for intrinsic glial tumor has greatly evolved in the last decades, progress in this discipline has been hampered by incomplete knowledge of the brain functional anatomy (1). One of the main challenges of glioma brain tumor surgery is to follow the principle of maximal safe resection, which is to remove as much of the tumor as possible while preserving the healthy surrounding tissue to minimize functional loss and preserve the quality of life (2). This is especially challenging for infiltrative or diffuse tumors such as gliomas, which present no clear boundaries between tumor and normal brain parenchyma. To achieve this goal, it is paramount to protect the integrity of relevant cortices as well as intact peritumoral white matter bundles. As such, a pursuit in improving the anatomical and functional knowledge of cortical and subcortical structures is in keeping with this objective.

The superior longitudinal fasciculus (SLF) is considered to be the largest associative fiber bundle system in the brain. The SLF is a part of the longitudinal association fiber system, which lays connections between the frontal lobe and other areas of the ipsilateral hemisphere. To put it simply, it connects the perisylvian areas in the hemisphere (frontal, temporal, and parietal). As such, this fiber bundle is likely to be one of the most affected whenever we undertake a surgery for an intrinsic brain tumor. Although our interest in refining the definition of the SLF stems from our work in infiltrative glial brain tumors, a clearer definition would also benefit all spheres of clinical

neurosciences. Hence, the goal of this study is to review SLF anatomy, nomenclature, and function. Interestingly, one would expect that this fiber bundle would already be thoroughly portrayed and delineated by now, and that this modelization would meet with a large consensus; as we will see, nothing could be further from the truth!

A Brief History of the Birth and Characterization of the SLF Anatomy

Reil and Autenrieth, pioneers of connectional anatomy, identified the SLF using postmortem brain dissections at the beginning of the 19th century. The first description coined it as a group of fibers located in the white matter of the temporal, parietal, and frontal lobes (3). This initial description was further refined by Burdach, a contemporary of Autenrieth, followed by Dejerine in 1895 (3, 4). These authors unveiled a peri-Sylvian arch-shaped fiber tract connecting the posterior temporal lobe with the frontal lobe. They named this bundle the arcuate fasciculus (AF) because of its shape and used the term "superior longitudinal fasciculus" as a synonym, introducing a confusion that still persists today (3, 5). A century later, studying the rhesus monkey by means of autoradiographic technique, Petrides and Pandya divided the SLF into three distinct segments (6, 7). These authors distinguished the SLF and AF as two distinct entities with different pathways, blurring the classical description prevailing at the time (6).

Until the early 1990s and the advent of diffusion magnetic resonance imaging (MRI), the anatomy of the SLF was studied in non-human primates using axonal tracing, a technique considered the "gold standard" in unveiling connectional anatomy of white matter *in vivo* (7, 8). Hence, this led to a paucity in human-derived data for this period (7–10). The arrival of diffusion imaging and fiber tractography changed all that, allowing the study of the human brain connection modelization *in vivo* (11–13). The use of this technology has helped elucidate some controversies regarding the SLF anatomy data derived from postmortem dissection (14, 15).

Anatomical Description Derived From Postmortem Dissections

Martino et al. (16) developed a modification to the classical fiber dissection methodology, initially designed by Klinger (15). The idea was to preserve the cortex by removing minimal tissue during dissection, hence producing a cortex-sparing fiber dissection. In the first step of the cortex-sparing fiber dissection, a wooden spatula is used to remove the cortex within the depth of the sulci only, preserving the cortex of the convexity surface of the gyri. This is crucial as it skeletonizes the stems of the gyri, providing space to dissect the white matter while preserving the cortical anatomical landmarks. This allowed the study of the fiber trajectory and the orientation within the white matter, as well as an estimate of cortical anatomical connectivity that diffusion imaging is still unable to produce. Using this approach, two superficial segments of the SLF were identified: the first, which is horizontally oriented connects the inferior parietal lobe and the posterior portion of the superior temporal gyrus with the frontal operculum. The second component runs along the AF and connects the posterior portion of the middle temporal gyrus with the posterior portion of the inferior parietal lobe (the angular gyrus). A deeper fiber segment that corresponds to the classical AF was also identified (3).

However, not all investigators found evidence of the presence of SLF during their dissection. Studying 10 consecutive cadaveric brains in search of long horizontal fronto-parietal association bundle in the white matter, Maldonado et al. (17) could not identify the SLF after having removed the short "U fibers". This illustrates the limitations of postmortem dissection, a technique fraught by constraints adversely impacting its validity (7). Indeed, this macroscopic dissection can not only resolve fibers crossing or follow fibers for a long distance but is also unable to identify the distal terminations of bundles (3, 7). As the brain commonly used are from elderly subjects, the technique is inherently biased toward old age, and potential effects of exposure to pharmacological treatment, nutritional status, medical condition, and cause of death also represent other potential biases. Postmortem factors, such as the interval between death and fixation, as well as the known effects of the fixative on the tissue can also alter results (18–21). Hence, the necessity to use an *in vivo* method to carry these studies (22, 23). Moreover, it obviously is a macroscopic approach for the resolution of a microscopic architecture!

Anatomical Description Derived From Diffusion MRI Studies

MRI is based on the fact that hydrogen atoms in water molecules act like protons having a spin that can respond to a magnetic field or gradient. Protons align to this external field, and it is possible to assess their spin and their decay back to their relaxed state after having been excited by an RF pulse (24). Investigators are constantly pushing the boundaries of the technique to design new imaging sequences and applications.

What Is Diffusion MRI?

Diffusion MRI is an imaging modality that scrutinizes the diffusion of water in the brain. In a free medium, water molecules normally display Brownian motion, i.e., they diffuse equally in all directions. When these molecules are in and around axons, however, their movement is hindered and restricted by axonal and dendritic membranes, glial cells, and myelin sheaths (25). As a result, their net diffusion is higher in the direction parallel to the fibers. This directional diffusion can be surveyed by the MRI scanner by applying magnetic gradients and taking measurements from different directions. The more structured and organized the axonal tissue is within a voxel, the more it is said to be anisotropic, and the more likely there is a white matter bundle going through this voxel in a singular direction (26–29). Diffusion MRI is classically modeled by a diffusion tensor, which is a single-fiber model per voxel projecting an estimate of the principal direction of diffusion in 3D. This model is at the heart of diffusion tensor imaging (DTI) (28). Classically, fractional anisotropy (FA) map or red–green–blue (RGB) colored directional images are used to represent diffusion data (24, 30) (**Figure 1**). Once the data is acquired, it is processed

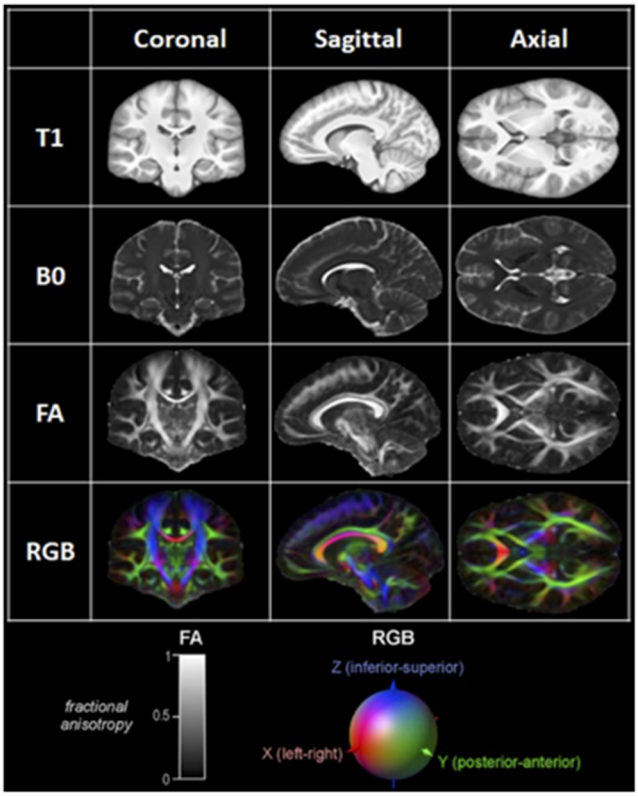

FIGURE 1 | Examples of coronal, sagittal, and axial MRI and DTI images. T1: T1-weighted image. B0: B0 image. FA: Fractionnal anisotropy image; Representation of the level of anisotropy in each voxel on a scale of 0 to 1, as shown in the lower left corner. RGB: Red-Green-Blue Color-coded FA image; Color-coded representation of the main direction of diffusion in each voxel, as shown in the lower right corner.

using mathematical deterministic or probabilistic algorithms to "connect" coherent diffusion tensors from adjacent voxels to produce a simulation of tracts; this process is called tractography.

Since the inception of DTI, newer techniques have emerged (advanced dMRI), refining both the scanning sequences, as well as the tractography algorithms (31, 32). Indeed, increasing the number of directions measured per voxel allowed the creation of high angular resolution diffusion imaging (HARDI), in which the resolution of multiple fiber populations crossing within the same voxel is now possible (33). Other such next-generation of refined techniques are diffusion spectrum imaging (DSI) (34–36), diffusion kurtosis imaging, (37–39) and q-ball imaging (40, 41). These newer approaches were designed to solve the problems generated by cases where fibers are crossing, kissing, fanning, or bending within a singular voxel (42). This is a problem of considerable importance since it is estimated that 63–90% of white matter volume contains crossing fibers (43).

Is DMRI Reliable in Revealing White Matter Anatomical Structures?

To this complex question, we can now safely answer yes, but with a few distinctions. Classical DTI postmortem histological validation studies have shown that fiber orientation is correctly represented in large unidirectional fiber bundles, but fails in complex regions with fiber crossings and low anisotropy (44–46). Newer studies using refinements to dMRI mentioned earlier are promising in solving these complex issues (47).

Fernandez-Mirannda et al. (48) mapped the whole brain using advanced dMRI and validated the tractography findings by dissecting 20 normal brains. Their results showed that advanced dMRI overcame DTI challenges in multiple areas such as the cortical and subcortical termination of fibers, decussation of fibers, zones of triple crossings, high and complex angulations, terminal arborization of fascicules, and cortical connectivity. Various investigators have studied specific white matter bundles with dMRI by comparing and validating results with the anatomy observed by postmortem microdissection (7, 47). Overall, the results were in support of an adequate validity and reproducibility of the technique with some nuances. However, there is one domain where histological postmortem studies have shown a consistent failure of dMRI, which is in regions of transition between white and gray matter, where orientation errors of as much as 90° have been observed (49, 50).

Hence, this imaging technique is greatly evolving and shows great promise (51). However, certain methodological pitfalls remain, and validation with other measures should be encouraged, as the technique is not entirely mature yet. The essence is to distinguish the extent to which these methodological shortcomings impact the validity of the tractography results. As a warning, Maier-Hein et al. (52) reported that this impact could be considerable. Indeed, these authors organized an international tractography competition and drew several striking conclusions. One of them was that current state-of-the-art tractography algorithms do not control for false positives. And false positive there are! Indeed, they found that most tractograms produced in this competition were made up of more invalid than valid bundles (52). Hence, they suggested using brain dissection for validation to avoid anatomy misrepresentation (16). These results instruct us to be cautious about dMRI data interpretation.

In terms of validation, *ex vivo* dMRI in cadaveric samples appears ideally suited to the study of normal anatomy as it can be obtained with maximal quality. There is no movement of artifacts, a very strong magnetic field can be used, and the scan can last many hours, which allows for a very small voxel size and high signal-to-noise ratio compared to clinical scans (53). A potential new method for validation was presented by Zemmoura et al. (54) Fibrascan is an approach designed by the authors allowing 3D white matter tract dissection in the cadaveric brain while using the *ex vivo* MR reference space to allow adequate correspondence.

What Diffusion Imaging Revealed About the SLF

Initial *in vivo* studies in non-human primates concluded that the SLF can structurally be divided into four independent components, the SLF I, SLF II, SLF III, and arcuate fasciculus (15). Yet, as the human brain is significantly different from other primates, especially in the peri-Sylvian areas, this nomenclature should obviously not be extrapolated to humans without confirmation (5, 55, 56).

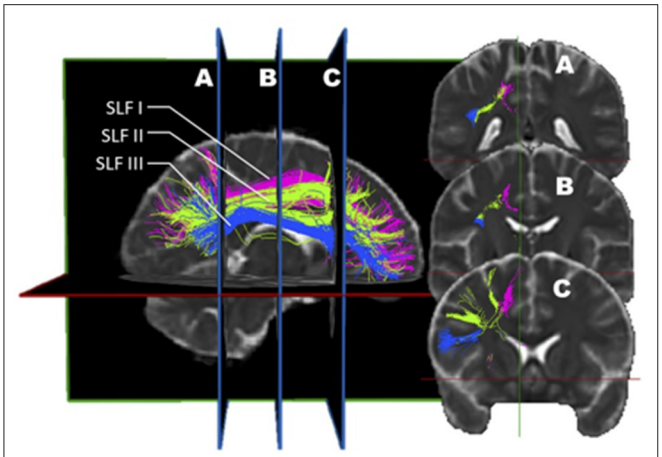

FIGURE 2 | *In vivo* fiber tractography of the right SLF I (pink), SLF II (green), and SLF III (blue). A three-dimensional reconstruction of the three segments of the SLF is displayed at the left of the figure. The coronal sections of it (A, B, and C) are represented on the right. The dorso-ventral as well as medio-lateral localization of each sub-segment can be visualized on the coronal planes.

Hence, the first step in human imaging studies was to survey for the presence of these 4 SLF subdivisions (15). Makris et al. successfully segmented the four SLF subcomponents in humans. In their nomenclature, the SLF I represents the dorsal division. It connects the superior parietal and superior frontal lobes. The SLF II takes its origin from the angular gyrus, passes through the core of the centrum semi-ovale above the insula, and ends in the caudal–lateral prefrontal region. The SLF III extends from the supramarginal gyrus, anterior to the angular gyrus, to the ventral premotor and prefrontal areas. SLF III is the most ventral of these three subdivisions. The fourth subcomponent of the SLF is homologous to the SLF IV described previously in non-human primates and corresponds to the AF. Its trajectory connects the caudal part of the superior temporal gyrus with the lateral prefrontal cortex, passing through the caudal end of the Sylvian fissure (15). Similar parcellation of the SLF that comprises the AF has also been described by subsequent investigators (57, 58). However, the inclusion of the AF as the 4th component of the SLF is far from unanimous and remains a subject of controversy in the nomenclature that is addressed in a later section of this study.

The first three SLF subdivisions are usually reported alike in most studies, except for a few minor differences (**Figure 2**). For example, Cabeen et al. (59) noted that the trajectory of the SLF I passes through the corona radiata and the superior lateral projections of the corpus callosum. Additionally, they found that the SLF II crosses the frontal lateral projections of the corpus callosum. It is as if, in this study, these two subdivisions were more dorsal than in the traditional description. In a distinctive description, Thiebaut de Schotten described the SLF as follows: the SLF I connects the precuneus, the superior parietal lobule, and Brodmann areas (BA) 5 and 7 to the superior frontal and anterior cingulate gyri, BA 8, 9, and 32. The SLF II originates at the angular gyrus and the anterior intraparietal sulcus, BA 39 and 40, and projects toward the posterior portions of the superior and middle frontal gyri, BA 8 and 9. The SLF III connects the temporoparietal junction, BA 40, with the inferior frontal gyrus, BA 44, 45, and 47, where Broca's area is localized (56). According to Schurr et al., SLF 2 and 3 would display different signatures when performing diffusion MRI. This discrepancy would be attributable to the fact that SLF 2 crosses the corona radiata fibers that run caudo-rostrally whereas SLF-3 obviously does not (60). Hence according to these authors, this anatomical divergence can be exploited to reliably identify SLF 2 and SLF3.

However, disparities in the description of this important fasciculus are not limited to these minor discrepancies. Indeed, some studies even describe a fifth division of the SLF comprised of a distinct fasciculus (61–63) that would connect the superior temporal gyrus to the superior parietal. This subdivision has been named "the temporoparietal SLF" (SLF TP) by Kamali (64). The SLF TP represents a distinct subcomponent of the SLF since it has a cranio-caudal orientation and is not in the longitudinal plane.

Furthermore, to emphasize how much this literature is still controversial, Bernal & Altman reported results calling into question much of the anatomical descriptions described above (57). Indeed, their study challenges the anatomical and functional foundation of the SLF. In this diffusion tensor imaging study, the SLF of 12 normal right-handed participants was assessed to find that projection to Broca's area was minimal or absent in the majority of cases. The only rostral endpoint of the SLF in this study was in the precentral gyrus. This finding contradicts the preconceived SLF structure and role, and does not represent the dominant consensus.

The high variability in the definition of the different divisions of the SLF between studies can probably be explained by a number of factors: the high individual variability combined with a limited number of participants accrued in the studies (65–68), as well as extreme variability in tractography algorithms and segmentation technique, leading to many false positives, are probably the major limitations (52). Recently, Schilling et al. studied the variability in results obtained by the segmentation of up to 14 bundles by 42 different groups (69). Even when given the same set of underlying streamlines, variability across protocols for bundle segmentation was found to be greater than all other sources of potential unevenness. The authors concluded that this extreme variance arose because of the poor inter-protocol agreements for the segmentation of many pathways. This is an illustration of the poor consensus on the precise anatomical definition of white matter bundles.

Ultimately, a study combining dMRI and a validation approach such as dissection would be ideal. Wang et al. (7) designed such a study. Before this report, few studies comparing diffusion imaging and postmortem dissection of the SLF had been published. Integrating both dMRI datasets ($n = 10$) and anatomical dissections ($n = 5$), this group analyzed the trajectory, volume, length, asymmetry, and cortical connectivity of the SLF in normal human brains. Their findings are rather provocative, differing from the rest of the literature and challenging the current knowledge on the SLF. The first conclusion is that there is a high discrepancy between the simian and human anatomy; hence, all conclusions derived from the study of the former cannot be applied to the latter. The second conclusion

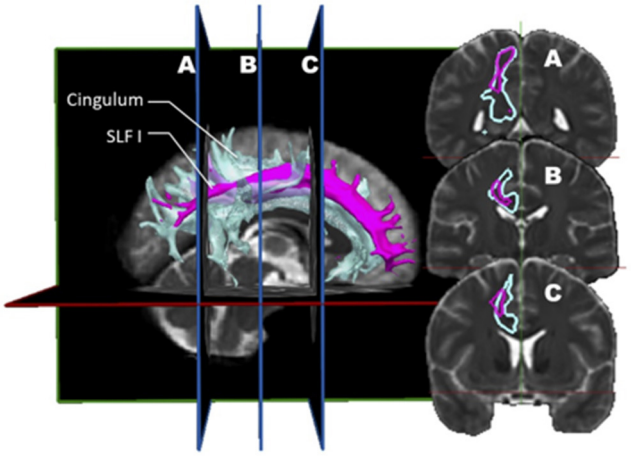

FIGURE 3 | *In vivo* fiber tractography of the right SLF I (pink) and the right cingulum (light blue) represented by volume. A three-dimensional reconstruction of the SLF I and the cingulum is displayed at the left of the figure. The coronal sections of it (A, B and C) are represented on the right. On the coronal planes, it is possible to appreciate the great proximity between the fibers of the SLF I and those of the cingulum.

is more disturbing as it questions the actual nomenclature. In their opinion, the SLF I should no longer be considered as it depicts a spatial relationship so close to the cingulum to be indistinguishable from it (**Figure 3**). The cingulum is described in the literature as being the communication bundle between different regions of the limbic system (7). It forms the main component of the white matter corpus of the cingulate gyrus, running around the medial aspect of the frontal and parietal lobe, just above the corpus callosum. It projects its cingulate gyrus afferences to the entorhinal cortex of the temporal lobe. In a very close anatomical relationship, the SLF1 connects the superior frontal gyrus to the precuneus. Hence, they consider the SLF as only composed of a dorsal (SLF II) and a ventral (SLF III) segment. In this construct, the SLF II represents 66% of the total volume, whereas the SLF III about 33%. Although the SLF was present in both hemispheres, a distinct asymmetry was also observed. This asymmetric pattern affects mostly the SLF II. In the left hemisphere, the connectivity pattern was in keeping with a predominant functional role in speech (connections between the supramarginal gyrus with the dorsal precentral gyrus and caudal middle frontal gyrus). Interestingly, these frontal areas also receive connections from the AF. Hence, this connectivity profile supports the notion that the left SLF II (dorsal) is involved in the motor planning of language and/or syntactic processing during language production, and its role is distinct from the AF.

Interestingly, the connectivity pattern identified on the right was divergent, with the SLF II connecting the angular gyrus and the superior parietal lobe with the caudal and rostral middle frontal gyrus. This anatomical scheme, according to the authors, was congruent with a role in regulating the focus of attention in a spatial orientation. The main contribution of cadaveric dissections in this study was the characterization of the proximity between SLF I, cingulum, and AF, explaining the frequent confusion in the definition of these bundles in prior studies, according to the authors. Finally, when discussing the potential biases and limitations in their study, the authors highlighted the low number of subjects that could not balance the inter-individual variability.

Other authors also support the idea that the SLF is indeed comprised of two main divisions. Martino et al. used dMRI and cortex-sparing fiber dissection and came to the conclusion that there were two segments to the SLF, an anterior and a posterior segment, much like Martino et al. and Wang et al. (3, 7).

A summary of dissection and imaging studies relative to the characteristics of the SLF subdivisions is presented in **Table 1**.

LATERALIZATION

We briefly touched on this aspect in the prior section with the study by Wang et al. But several other studies have investigated this with different conclusions. Let us first consider the non-controversial findings. If we are to still consider the SLF I as part of the SLF, then this trunk appears to be distributed symmetrically between the right and left hemispheres (9). The other finding has to do with the volume of the bundles; overall, the right-sided SLF as a whole appears more voluminous than on the left (3, 55). This is not consensual; however, as other researchers found the SLF II subcomponents' lateralization to be dominant in the left hemisphere (7, 56, 72). This would functionally be related to its role in language. Wang et al., on the other hand, found a slight asymmetric difference in all SLF sub-component with a tendency toward right-hemispheric dominance (7).

It stands to reason that there would be asymmetric findings between both SLF. As there is a clear asymmetry in speech function (left-sided characteristically) and visuospatial functioning (right-sided characteristically), some difference in connectivity is expected. Maybe SLF right and left are two completely different entities.

INDIVIDUAL VARIABILITY

The inherent anatomical variability between an individual's brain cannot be emphasized enough. This variability can be observed at different levels such as in cortical morphology, cytoarchitecture, task-evoked activation, or in dMRI connectivity pattern (65–68). Hence, the idea of a prototypic universal brain blueprint is reductive. Although some areas and connectivity routes are highly conserved amongst individuals (such as primary areas and large projection bundles), others are more variable. This variability is a correlate of the phenotypic variability in general, determined by the genetic substrates and the environmental exposure that shapes this diversity for any trait, including the brain's anatomy, (68) and in fact, it goes even further than interindividual variability, as there is a clear intraindividual variability over time. Indeed, the brain connectivity pattern of an individual is constantly changing, and the density of white matter has been shown to change during the development of the individual. More so, later in life, the degradation of associative

TABLE 1 | A summary of dissection and imaging studies relative to the characteristics of the SLF subdivisions.

Number of SLF divisions	Studies	Technique used	Name of the bundle	Origin	Projection	Potential function
2 or 2 and the AF	Zhang et al. (63)	dMRI	Anterior segment	Medial and inferior frontal lobe	Angular and supramarginal gyri	-
			Posterior segment	Angular and supramarginal gyri	Temporal lobe	-
			Long segment	Medial and inferior frontal lobe	Temporal lobe	-
	Martino et al. (16)	dMRI and dissections	Horizontal segment of the SLF	Inferior parietal lobe and posterior portion of the superior temporal gyrus	Frontal operculum	-
			Vertical segment of the SLF	Posterior portion of the middle temporal gyrus	Angular gyrus	-
			AF	Middle and inferior temporal gyrus	Posterior portion of the frontal operculum	-
	Martino et al. (3)	dMRI and dissections	Anterior segment	Supramarginal and superior temporal gyri	Precentral gyrus	Monitoring of speech articulation
			Posterior segment	Posterior portion of the middle temporal gyrus	Angular gyrus	Language perception (syllabe discrimination and identification)
			AF (long segment)	Middle and inferior temporal gyri	Precentral gyrus and posterior portion of the inferior and middle frontal gyri	Language function
	Zemmoura et al. (54)	dMRI and dissections	Anterior horizontal segment	Ventral premotor cortex	Inferior parietal lobule	-
			Posterior vertical segment	Inferior parietal lobule	Posterior superior and middle temporal gyri	-
			Long segment or AF	Pars opercularis and pars triangularis of the inferior frontal gyrus	Posterior middle temporal gyrus	-
	de Benedictis et al. (58)	dMRI and dissections	SLF II (Anterior component of the indirect component of the SLF)	Inferior frontal gyrus (Broca ‘s territory)	Inferior parietal lobule	-
			SLF III (Posterior component of the indirect component of the SLF)	Inferior parietal lobule	Posterior part of the superior and middle temporal gyrus (Wernicke ‘s territory)	-
			AF (Direct component of the SLF)	Inferior frontal gyrus (Broca ‘s territory)	Posterior part of the superior and middle temporal gyrus (Wernicke ‘s territory)	-
	Wang et al. (7)	dMRI and dissections	Dorsal segment (SLF II) in the left hemisphere	Angular gyrus, Brodmann Areas (BA) 39	Caudal middle frontal gyrus and dorsal precentral gyrus	Motor planning of language function and/or syntactic processing during language production
			Dorsal segment (SLF II) in the right hemisphere	Angular gyrus and the superior parietal lobe	Caudal and rostral middle frontal gyrus	regulating the focusing of attention in spatial orientation
			Ventral segment (SLF III) in the left hemisphere	Supramarginal gyrus (BA 40)	Ventral precentral gyrus and pars opercularis	Language function

(Continued)

TABLE 1 | Continued

Number of SLF divisions	Studies	Technique used	Name of the bundle	Origin	Projection	Potential function
			Ventral segment (SLF III) in the right hemisphere	Supramarginal gyrus (BA 40)	Pars triangularis	Spatial awareness
3	De Schotten et al. (9)	dMRI	SLF I	-	-	-
			SLF II	-	-	Visuospatial for the right SLF II
			SLF III	-	-	-
	Catani and Thiebaut de Schotten (70)	dMRI	SLF I	Parietal precuneus	Medial and superior surface of the superior frontal gyrus	Processes the spatial coordinates of trunk and inferior limbs, movement planning, oculomotor coordination and visual reaching
			SLF II	Posterior region of the inferior parietal lobule	Lateral aspect of the superior and middle frontal gyrus	Processes the spatial coordinates of upper limbs and other functions similar to the SLF I
			SLF III	Supramarginal and anterior angular gyrus	Posterior region of the inferior frontal gyrus	Sensory-motor function or language function
	Thiebaut de Schotten et al. (56) and Lunven and Bartolomeo (71)	dMRI	SLF I	Superior parietal lobule and precuneus (BA 5, 7)	Superior frontal and anterior cingulate areas (BA 8, 9, 32)	-
			SLF II	Angular gyrus and the anterior intraparietal sulcus (BA 39, 40)	Posterior regions of the superior and middle frontal gyri (BA 6, 8, 9)	Visuospatial for the right SLF II
			SLF III	Intraparietal sulcus and inferior parietal lobule (BA 40)	Inferior frontal gyrus (BA 44, 45, 47)	-
	Hecht et al. (55)	dMRI	SLF I	Superior parietal cortex	Superior frontal gyrus	Motor regulation
			SLF II	Posterior inferior parietal cortex	Middle frontal gyrus and dorsolateral prefrontal cortex	Overt and imagined mouvements, spatial orienting and spacial attention
			SLF III	Anterior inferior parietal cortex	Inferior frontal gyrus	Tool use and social learning mainly for the right SLF III
	Cabeen et al. (59)	dMRI	SLF I	Parietal cortex	Superior frontal gyrus	-
			SLF II		Middle frontal gyrus	-
			SLF III		Inferior frontal gyrus	-
	Schurr et al. (60)	dMRI	SLF I	-	-	-
			SLF II	-	-	-
			SLF III	Supramarginal gyrus and angular gyrus	Opecular and triangular parts of the inferior frontal gyrus for the left SLF and inferior frontal gyrus for the right SLF	-
3 and the AF	Makris et al. (15)	dMRI	SLF I	Superior parietal and superior frontal lobes	Dorsal premotor and dorsolateral prefrontal regions	Regulation of higher aspects of motor behavior

(Continued)

TABLE 1 | Continued

Number of SLF divisions	Studies	Technique used	Name of the bundle	Origin	Projection	Potential function
			SLF II	Angular gyrus	Caudal-lateral prefrontal regions	Perception of the visual space
			SLF III	Supramarginal gyrus	Ventral premotor and prefrontal regions	Articulatory component of langage and working memory
			AF	Caudal part of the superior temporal gyrus	Lateral prefrontal cortex	Receive and modulate audiospatial information
	Makris et al. (62)	dMRI	SLF I	-	-	-
			SLF II	-	Anterior part of the angular gyrus	-
			SLF III	-	-	-
			AF	-	Caudal part of the superior and middle temporal gyri	-
	Bernal and Altman (57)	dMRI	SLF I	Posterior temporoparietal area (Posterior langage areas)	Frontal areas (mainly in the precentral gyrus and minimally in Broca's area)	-
			SLF II			-
			SLF III			-
			AF	Temporal lobe		Involved in langage fonction, but not necessary for it.
5	Kamali et al. (64)	dMRI	SLF I	Superior parietal lobule along the cingulate gyri (BA 7, 5, 4)	Dorsal and medial cortex of the frontal lobe and premotor areas (BA 6, 8, 9)	Language
			SLF II	Angular gyrus (BA 39)	Passes through the post central gyrus (BA 3, 1, 2), the precentral gyrus (BA 4), the middle frontal gyrus (BA 6, 46) and terminates in the dorsolateral prefrontal cortex (BA 6, 8, 46)	
			SLF III	Supramarginal gyrus	Ventral premotor and prefrontal cortex (BA 6, 44)	
			AF	Posterior part of the superior temporal gyrus at the temporoparietal junction	Dorsal prefrontal cortex (BA 8, 46)	
			Temporoparietal SLF	Posterior part of the superior temporal gyrus at the temporoparietal junction	Angular gyrus and superior parietal lobule (BA 7)	

pathways due to lesions or neurodegenerative diseases is another cause of intraindividual variability (73).

With regard to the SLF specifically, there is diversity within the population. More precisely, from one individual to another, the volume of the SLF appears different. Fractional anisotropy of SLF also varies between individuals, but less importantly, than volume (67, 68). Hence, we need to apply a precautionary principle to the conclusions from all these anatomical studies, acknowledging the inherent variability from patient to patient. There is no such thing as a singular brain blueprint! Although these efforts to characterize the long associative fibers in the brain are paramount, it must be viewed with humility, considering that these long associative axons comprise only 2% of the total intrahemispheric cortico-cortical fibers and that 98% of the fibers are short U-fibers (74).

IS THE AF PART OF THE SLF?

Sometimes, various descriptions from different authors can give rise to confusion in anatomical classifications and subdivisions. Hence, clarifications in terms are in order. Such appears to be the case for the arcuate fasciculus (AF). As discussed earlier in this study, ever since the term Arcuate Fasciculus (AF) was incepted in the literature, confusion with the SLF was entertained.

However, if we use adequate definition in terms, some clarity emerges. Indeed, the SLF is in its essence a fronto-parietal tract, hence connecting the frontal and parietal cortices, whereas the AF is a fronto-temporal tract that passes through the parietal white matter beneath the SLF (55, 56). As such, the AF is recognized as a distinctive bundle with connection areas and a trajectory different from that of the SLF; if the 2 bundles are sometimes confused as synonyms, it is only because of an outdated nomenclature which should be abandoned. A great many studies clearly distinguish the 2 bundles as distinct entities, both anatomically and functionally (56, 59, 70, 71, 75, 76).

However, this does not entirely solve the controversy. Surveying the literature on the AF with scrutiny, a detailed description emerges where this bundle can be divided into three segments (a long, anterior, and posterior segment), each connecting two regions of either Broca, Wernicke, or the territory of Geschwind (inferior parietal lobule). In this detailed description by Catani and Thiebaut de Schotten (70), the anterior segment of the AF appears to somehow correspond to the SLF III, and the two terms are used interchangeably. Hence, although these 2 bundles are distinct entities, some of their subcomponents appear to overlap as if they each share a subdivision: the SLF III and the anterior segment of the AF (**Figure 4**). This issue will require further insight from anatomico-functional studies.

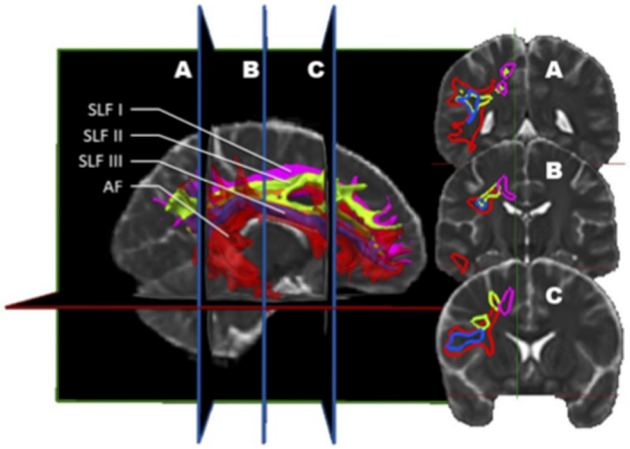

FIGURE 4 | *In vivo* fiber tractography of the right SLF I (pink), SLF II (green), SLF III (blue), and AF (red) represented by volume. A three-dimensional reconstruction of these bundles is displayed at the left of the figure. The AF is slightly transparent to let appear the SLF III, being inside the latter. On the right, the coronal sections (A, B, and C) are represented. This figure confirms that the SLF III also corresponds to a sub-division of the AF. Indeed, throughout its length, the SLF III is located inside the AF.

NOMENCLATURE

Based on all that was discussed in this study, we feel compelled to recommend the adoption of a careful definition in the nomenclature of the SLF. There are clear and obvious reasons as to why the definition of the SLF remains controversial despite numerous studies. The persisting confusion regarding the distinction between the SLF and the AF up to this day is the epitome of this confusion. Moreover, a lot of the prior work which has made its way in the literature and anatomy textbooks is based on non-human primates, which present a rather different connectivity anatomy, thus steering the nomenclature toward a biased pattern (5, 56). Finally, as mentioned before, the individual variability had been underestimated in the past. The recognition of this fact foreshadows a future take on brain study connectivity that will key in this variability in study design and conclusions.

The confusion regarding the actual nomenclature is such that some authors actually suggest erasing the historical connotations and starting from scratch. Recently, Mandonnet et al. (5) suggested the use of anatomical corridors available for the fanning of longitudinal fibers in the brain, in relation to brain landmarks (such as ventricles, grey nuclei, external/extreme capsule) to define a stem-based white-matter nomenclature (**Figure 5**). Hence, they propose seven white matter systems: the superior (SLS), inferior (ILS), and middle longitudinal system MidLS), the basal (BSL) and mesial longitudinal system (MesLS), and the anterior (ATS) and posterior transverse system (PTS). This classification is further complexified by a second level to more precisely identify the cortical areas connected by the fasciculi. As an example, the SLS and the ILS each have 5 divisions. In this scheme, SLS I is equivalent to SLF I, SLS II to SLF II, and SLS III to SLF III. The authors chose to voluntarily ignore historical references by erasing commonly used terms in the literature. Hence, the AF becomes the SLS IV (**Figure 6**), the uncinate fasciculus becomes the ILS IV, the cingulum the MesLS I, and so forth (5). The rationale of defining "anatomical corridors" as a correlate for naming white matter fibers' propagation is

interesting. Now, whether this new classification will succeed in erasing centuries of historical references remains to be seen. However, this might be beneficial, allowing us to redefine better the longitudinal connection pathways in the human using data from recently designed studies, and burying old misconceptions still blurring our literature. Vavassori et al. adopt a similar approach, rewriting the superior longitudinal system in terms of wiring diagram describing the connecting cortices and following a medio-lateral distribution, instead of focusing on specific bundles (77). As an additional distinction, we would also urge investigators to consider the left and right hemispheres as distinct entities in their analyses.

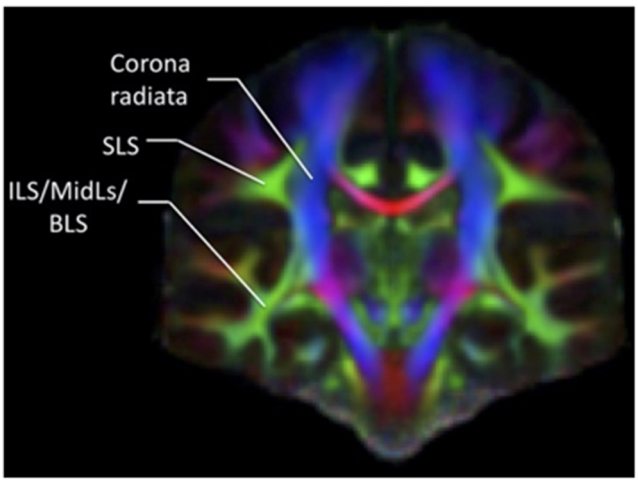

FIGURE 5 | Coronal section of a color-coded FA map. The green associative fibers, representing the fibers perpendicular to the plane, can be grouped into two main systems according to the classification by Mandonnet et al. (5), the SLS and the common stem for the ILS/MidLs and BLS.

FUNCTIONAL CORRELATES OF SLF

The SLF is a massive bundle connecting widespread areas of the frontal and the parietal lobes. As such, it is likely involved in different functional correlates. As the bundle depicts clear asymmetry between both hemispheres, this must translate into obvious functional implications. Hence, although still a controversial matter, the SLF III shares similar connectivity with the AF, linking the inferior frontal gyrus with the ventral pre-central gyrus. This suggests, in the left hemisphere, a role in speech. This view has been confirmed by Maldonado et al. (78) through a brain electrostimulation study. Wang et al. (7) also reported a specific connectivity pattern for the right SLF III terminating at the right pars triangularis. According to some authors, this connectivity pattern is probably involved in spatial awareness functioning (7).

A strong asymmetry also seems to characterize the SLF II. Wang et al. (7) identified a strong bias in leftward connections between the supramarginal gyrus with the dorsal precentral gyrus and the caudal middle frontal gyrus. This would be in keeping with a role for the left SLF II in motor planning of speech and/or syntax processing. In a similar predicament as for the SLF III, the right SLF II preferentially connects the angular gyrus and the superior parietal lobe with the caudal and rostral middle frontal gyrus, respectively. It is presumed that this system plays a role in the regulation of the attention in a spatial orientation. This is in keeping with the fact that the right SLF II is responsible for a faster and preferential visuospatial processing in the right hemisphere (9).

CONCLUSION

"There is no such thing as absolute certainty, but there is assurance sufficient for the purposes of human life" as once said

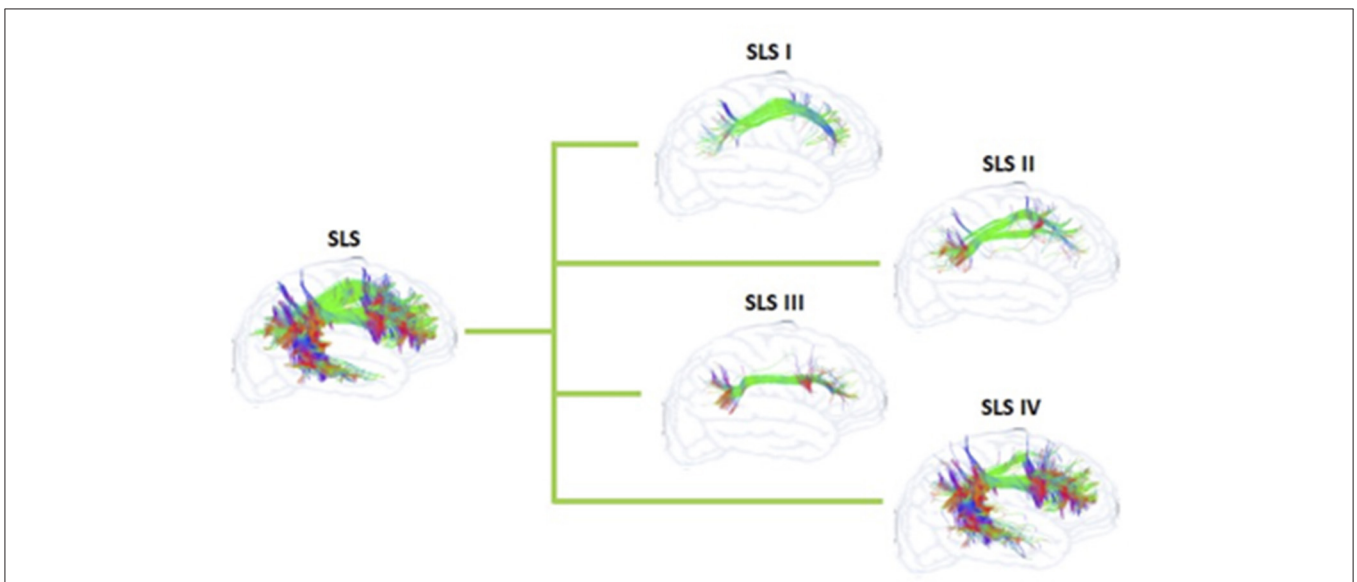

FIGURE 6 | Schematization of the SLS and its sub-systems of the proposed nomenclature by Mandonnet et al. (5) for the human white matter association pathways.

by John Stuart Mill. Through this review and analysis of data regarding the state-of-the-art knowledge on the anatomical and functional correlates of the SLF, we can come to the conclusion that there is only one certainty: we do not know for sure!

Indeed, the SLF itself in its current definition is not a consensual entity. However, we can stand up on some of the groundwork cited in this article, and presumably conclude the following: (1) that the very definition of the SLF, connecting the frontal to the parietal lobe, allows a clear distinction with the AF, connecting the frontal lobe to the temporal lobe. Hence, all classifications including the AF as part of the SLF are misleading. (2) Traditionally, the SLF has been divided into 3 segments. However, the SLF I connecting the parietal precuneus to the superior frontal gyrus appears assimilable to the cingulum. Hence, its existence, as well as its role is unclear at this time. (3) The SLF II and III are clearly defined as distinct entities that are asymmetrical in their function as well as presumably in their role: the left-sided SLF II and III would definitely be involved in speech processing, whereas the right-sided SLF II and III would contribute to visuospatial functioning. (4) The inter as well as intra-individual variability in connectivity is more important than previously suspected. Hence, we need to apply a precautionary principle to the conclusions from the connectivity studies, acknowledging the inherent variability from patient to patient. Mitigation of this limitation can be achieved through the use of larger study cohorts.

AUTHOR'S NOTE

All figures were created using open-source MRI images as well as the whole brain tractogram of the test dataset of Imeka (79). The detailed methodology for Cingulum segmentation was derived from Wakana et al. (80). The detailed methodology for SLF I, II, and III segmentation, as well as AF segmentation, was emulated from Fitzgerald et al. (81).

AUTHOR CONTRIBUTIONS

FJ, CI-M, and DF were responsible for the design of the manuscript. FJ did the literature search. CI-M and DF reviewed and interpreted the data and were responsible for the analysis. DF completed the final version of the manuscript and recommendations about suggested nomenclature. All authors contributed to the article and approved the submitted version.

FUNDING

This work was financed by La fondation coeur en tête on brain tumor research.

REFERENCES

1. Honey CJ, Kötter R, Breakspear M, Sporns O. Network structure of cerebral cortex shapes functional connectivity on multiple time scales. *PNAS.* (2007) 104:10240–5. doi: 10.1073/pnas.0701519104
2. de Benedictis A, Duffau H. Brain hodotopy: from esoteric concept to practical surgical applications. *Neurosurgery*. (2011) 68:1709–23. doi: 10.1227/NEU.0b013e3182124690
3. Martino J, De Witt Hamer P, Berger M, T. Lawton M, Arnold C, et al. Analysis of the subcomponents and cortical terminations of the perisylvian superior longitudinal fasciculus: a fiber dissection and DTI tractography study. *Brain Struct Funct*. (2013) 218:105–21. doi: 10.1007/s00429-012-0386-5
4. Catani M, Dell'acqua F, Bizzi A, Forkel S, Williams S, Simmons A, et al. Beyond cortical localization in clinico-anatomical correlation. *Cortex.* (2012) 48:1262–87. doi: 10.1016/j.cortex.2012.07.001
5. Mandonnet E, Sarubbo S, Petit L. The nomenclature of human white matter association pathways: proposal for a systematic taxonomic anatomical classification. *Front Neuroanat.* (2018) 12:1–14. doi: 10.3389/fnana.2018.00094
6. Petrides M, Pandya DN. Projections to the frontal cortex from the posterior parietal region in the rhesus monkey. *J Comparat Neurol.* (1984) 228:105–16. doi: 10.1002/cne.902280110
7. Wang X, Pathak S, Stefaneanu L, Yeh F-C, Li S, Fernandez-Miranda JC. Subcomponents and connectivity of the superior longitudinal fasciculus in the human brain. *Brain Struct Funct.* (2016) 221:2075–92. doi: 10.1007/s00429-015-1028-5
8. Pandya DN. Kuypers HG. Cortico-cortical connections in the rhesus monkey. *Brain Res*. (1969) 13:13–36. doi: 10.1016/0006-8993(69)90141-3
9. Thiebaut de Schotten M, Dell'Acqua F, Forkel SJ, Simmons A, Vergani F, Murphy DGM, et al. A lateralized brain network for visuospatial attention. *Nat Neurosci.* (2011) 14:1245–6. doi: 10.1038/nn.2905
10. Kawamura K, Naito J. Corticocortical projections to the prefrontal cortex in the rhesus monkey investigated with horseradish peroxidase techniques. *Neurosci Res.* (1984) 1:89–103. doi: 10.1016/S0168-0102(84)80007-3
11. Basser PJ, Pajevic S, Pierpaoli C, Duda J, Aldroubi A. In vivo fiber tractography using DT-MRI data. *Magnetic Resonance in Medicine.* (2000) 44:625–32. doi: 10.1002/1522-2594(200010)44:4<625::AID-MRM17>3.0.CO;2-O
12. Mori S, Crain BJ, Chacko VP, van Zijl PC. Three-dimensional tracking of axonal projections in the brain by magnetic resonance imaging. *Ann Neurol.* (1999) 45:265–9. doi: 10.1002/1531-8249(199902)45:2<265::AID-ANA21>3.0.CO;2-3
13. Mukherjee P, Berman JI, Chung SW, Hess CP, Henry RG. Diffusion tensor MR imaging and fiber tractography: theoretic underpinnings. *AJNR.* (2008) 29:632–41. doi: 10.3174/ajnr.A1051
14. Archip N, Clatz O, Whalen S, Kacher D, Fedorov A, Kot A, et al. Non-rigid alignment of pre-operative MRI, fMRI, and DT-MRI with intra-operative MRI for enhanced visualization and navigation in image-guided neurosurgery. *Neuroimage.* (2007) 35:609–24. doi: 10.1016/j.neuroimage.2006.11.060
15. Makris N, Kennedy DN, McInerney S, Sorensen AG, Wang R, Caviness Jr VS, et al. Segmentation of subcomponents within the superior longitudinal fascicle in humans: a quantitative, in vivo, DT-MRI study. *Cereb Cortex.* (2005) 15:854–69. doi: 10.1093/cercor/bhh186
16. Martino J, De Witt Hamer PC, Vergani F, Brogna C, de Lucas EM, Vázquez-Barquero A, et al. Cortex-sparing fiber dissection: an improved method for the study of white matter anatomy in the human brain. *J Anat.* (2011) 219:531–41. doi: 10.1111/j.1469-7580.2011.01414.x
17. Maldonado IL, Mandonnet E, Duffau H. Dorsal fronto-parietal connections of the human brain: a fiber dissection study of their composition and anatomical relationships. *Anat Rec.* (2012) 295:187–95. doi: 10.1002/ar.22462
18. Chu W-S, Furusato B, Wong K, Sesterhenn IA, Mostofi FK, Wei MQ, et al. Ultrasound-accelerated formalin fixation of tissue improves morphology, antigen and mRNA preservation. *Mod Pathol.* (2005) 18:850–63. doi: 10.1038/modpathol.3800354
19. Schmierer K, Kingshott CAMW, Tozer DJ, Boulby PA, Parkes HG, Yousry TA, et al. Quantitative magnetic resonance of postmortem multiple sclerosis brain before and after fixation. *Magnetic Resonance in Medicine.* (2008) 59:268–77. doi: 10.1002/mrm.21487
20. Stüber C, Morawski M, Schäfer A, Labadie C, Wähnert M, Leuze C, et al. Myelin and iron concentration in the human brain: a

quantitative study of MRI contrast. *NeuroImage*. (2014) 93:95–106. doi: 10.1016/j.neuroimage.2014.02.026
21. van Duijn S, Nabuurs RJA, van Rooden S, Maat-Schieman MLC, van Duinen SG, van Buchem MA, et al. artifacts in human brain tissue after prolonged formalin storage. *Magnetic Resonance in Medicine*. (2011) 65:1750–8. doi: 10.1002/mrm.22758
22. Makris N, Meyer JW, Bates JF, Yeterian EH, Kennedy DN, Caviness VS. MRI-Based topographic parcellation of human cerebral white matter and nuclei II. Rationale and applications with systematics of cerebral connectivity. *NeuroImage*. (1999) 9:18–45. doi: 10.1006/nimg.1998.0384
23. Caviness VS, Meyer JW, Makris N, Bates JF, Yeterian EH, Kennedy DN. MRI-based topographic parcellation of human cerebral white matter and nuclei. *Neuroimage*. (2002).
24. Hagmann P, Jonasson L, Maeder P, Thiran JP, Wedeen VJ, Meuli R. Understanding diffusion MR imaging techniques: from scalar diffusion-weighted imaging to diffusion tensor imaging and beyond. *Radiographics*. (2006) 26:S205–S223. doi: 10.1148/rg.26si065510
25. Alexander DC, Dyrby TB, Nilsson M, Zhang H. Imaging brain microstructure with diffusion MRI: practicality and applications. *NMR Biomed*. (2019) 32:e3841. doi: 10.1002/nbm.3841
26. Beaulieu C. The basis of anisotropic water diffusion in the nervous system - a technical review. *NMR Biomed*. (2002) 15:435–55. doi: 10.1002/nbm.782
27. Leclercq D, Delmaire C, de Champfleur NM, Menjot de Champfleur N, Chiras J, Lehéricy S. Diffusion tractography: methods, validation and applications in patients with neurosurgical lesions. *Neurosurg Clin N Am*. (2011) 22:253–68. doi: 10.1016/j.nec.2010.11.004
28. Pierpaoli C, Jezzard P, Basser PJ, Barnett A, Di Chiro G. Diffusion tensor MR imaging of the human brain. *Radiology*. (1996) 201:637–48. doi: 10.1148/radiology.201.3.8939209
29. Stejskal EO, Tanner JE. Spin diffusion measurements: spin echoes in the presence of a time-dependent field gradient. *J Chem Phys*. (2004) 42:288–92. doi: 10.1063/1.1695690
30. Alexander AL, Lee JE, Lazar M, Field AS. Diffusion tensor imaging of the brain. *Neurotherapeutics*. (2007). doi: 10.1016/j.nurt.2007.05.011
31. Abhinav K, Yeh F-C, Mansouri A, Zadeh G, Fernandez-Miranda JC. High-definition fiber tractography for the evaluation of perilesional white matter tracts in high-grade glioma surgery. *Neuro Oncol*. (2015) 17:1199–209. doi: 10.1093/neuonc/nov113
32. Fernandez-Miranda JC. Editorial: Beyond diffusion tensor imaging. *J Neurosurg*. (2013) 118:1363–5. doi: 10.3171/2012.10.JNS121800
33. Descoteaux M. *High Angular Resolution Diffusion Imaging (HARDI).*Wiley Encyclopedia of Electrical and Electronics Engineering (EEEE). (2015).
34. McDonald CR, White NS, Farid N, Lai G, Kuperman JM, Bartsch H, et al. Recovery of white matter tracts in regions of peritumoral FLAIR hyperintensity with use of restriction spectrum imaging. *American Journal of Neuroradiology*. (2013) 34:1157–63. doi: 10.3174/ajnr.A3372
35. Wedeen VJ, Hagmann P, Tseng WYI, Reese TG, Weisskoff RM. Mapping complex tissue architecture with diffusion spectrum magnetic resonance imaging. *Magn Reson Med*. (2005) 54:1377–86. doi: 10.1002/mrm.20642
36. Wedeen VJ, Wang RP, Schmahmann JD, Benner T, Tseng WYI Dai G, Pandya DN, et al. Diffusion spectrum magnetic resonance imaging (DSI) tractography of crossing fibers. *Neuroimage*. (2008) 41:1267–77. doi: 10.1016/j.neuroimage.2008.03.036
37. Glenn GR, Helpern JA, Tabesh A, Jensen JH. Quantitative assessment of diffusional kurtosis anisotropy. *NMR Biomed*. (2015) 28:448–59. doi: 10.1002/nbm.3271
38. Hui ES, Russell Glenn G, Helpern JA, Jensen JH. Kurtosis analysis of neural diffusion organization. *Neuroimage*. (2015) 106:391–403. doi: 10.1016/j.neuroimage.2014.11.015
39. Jensen JH, Helpern JA, Ramani A, Lu H, Kaczynski K. Diffusional kurtosis imaging: The quantification of non-Gaussian water diffusion by means of magnetic resonance imaging. *Magn Reson Med*. (2005) 53:1432–40. doi: 10.1002/mrm.20508
40. Descoteaux M, Angelino E, Fitzgibbons S, Deriche R. Regularized, fast, and robust analytical Q-ball imaging. *Magn Reson Med*. (2007) 58:497–510. doi: 10.1002/mrm.21277
41. Tuch DS. Q-ball imaging. *Magn Reson Med*. (2004) 52:1358–72. doi: 10.1002/mrm.20279
42. Jbabdi S, Johansen-Berg H. Tractography: where do we go from here? *Brain Connect*. (2011). doi: 10.1089/brain.2011.0033
43. Jeurissen B, Leemans A, Tournier JD, Jones DK, Sijbers J. Investigating the prevalence of complex fiber configurations in white matter tissue with diffusion magnetic resonance imaging. *Hum Brain Mapp*. (2013). doi: 10.1002/hbm.22099
44. Dauguet J, Peled S, Berezovskii V, Delzescaux T, Warfield SK, Born R, et al. Comparison of fiber tracts derived from in-vivo DTI tractography with 3D histological neural tract tracer reconstruction on a macaque brain. *Neuroimage*. (2007) 37:530–8. doi: 10.1016/j.neuroimage.2007.04.067
45. Kaufman JA, Ahrens ET, Laidlaw DH, Zhang S, Allman JM. Anatomical analysis of an aye-aye brain (Daubentonia madagascariensis, primates: prosimii) combining histology, structural magnetic resonance imaging, and diffusion-tensor imaging. *Anat Rec A Discov Mol Cell Evol Biol*. (2005) 1026–37. doi: 10.1002/ar.a.20264
46. Fernandez-Miranda JC, Rhoton AL, Álvarez-Linera J, Kakizawa Y, Choi C, De Oliveira EP. Three-dimensional microsurgical and tractographic anatomy of the white matter of the human brain. *Neurosurgery*. (2008) 62. doi: 10.1227/01.neu.0000333767.05328.49
47. de Benedictis A, Petit L, Descoteaux M, Marras CE, Barbareschi M, Corsini F, et al. New insights in the homotopic and heterotopic connectivity of the frontal portion of the human corpus callosum revealed by microdissection and diffusion tractography. *Hum Brain Mapp*. (2016) 37:4718–35. doi: 10.1002/hbm.23339
48. Fernandez-Miranda JC, Pathak S, Engh J, Jarbo K, Verstynen T, Yeh F, et al. High-definition fiber tractography of the human brain: Neuroanatomical validation and neurosurgical applications. *Neurosurgery*. (2012) 71:430–53. doi: 10.1227/NEU.0b013e3182592faa
49. Dyrby TB, Søgaard LV, Parker GJ, Alexander DC, Lind NM, Baaré WFC, et al. Validation of in vitro probabilistic tractography. *Neuroimage*. (2007) 37:1267–77. doi: 10.1016/j.neuroimage.2007.06.022
50. Seehaus A, Roebroeck A, Bastiani M, Fonseca L, Bratzke H, Lori N, et al. Histological validation of high-resolution DTI in human post mortem tissue. *Front Neuroanat*. (2015) 9. doi: 10.3389/fnana.2015.00098
51. Vanderweyen DC, Theaud G, Sidhu J, Rheault F, Sarubbo S, Descoteaux M, et al. The role of diffusion tractography in refining glial tumor resection. *Brain Struct Funct*. (2020) 34:E1–E24. doi: 10.1007/s00429-020-02056-z
52. Maier-Hein KH, Neher PF, Houde J-C, Côté MA, Garyfallidis E, Chamberland M et al. The challenge of mapping the human connectome based on diffusion tractography. *Nat Commun*. (2017).
53. Takahashi E, Song JW, Folkerth RD, Grant PE, Schmahmann JD. Detection of postmortem human cerebellar cortex and white matter pathways using high angular resolution diffusion tractography: a feasibility study. *Neuroimage*. (2013) 68:105–11. doi: 10.1016/j.neuroimage.2012.11.042
54. Zemmoura, I, Serres B, Andersson F, Barantin F, Tauber C, Filipiak I, Cottier JP, Venturini G, Destrieux C. FIBRASCAN: a novel method for 3D white matter tract reconstruction in MR space from cadaveric dissection. *NeuroImage*. (2014) 103:106–18. doi: 10.1016/j.neuroimage.2014.09.016
55. Hecht EE, Gutman DA, Bradley BA, Preuss TM, Stout D. Virtual dissection and comparative connectivity of the superior longitudinal fasciculus in chimpanzees and humans. *Neuroimage*. (2015). doi: 10.1016/j.neuroimage.2014.12.039
56. Thiebaut de Schotten M, Dell'acqua F, Valabregue R, Catani M. Monkey to human comparative anatomy of the frontal lobe association tracts. *Cortex*. (2011). doi: 10.1016/j.cortex.2011.10.001
57. Bernal B, Altman N. The connectivity of the superior longitudinal fasciculus: A tractography DTI study. *Magn Reson Imaging*. (2010) 28:217–25. doi: 10.1016/j.mri.2009.07.008
58. de Benedictis A, Duffau H, Paradiso B, Grandi E, Balbi S, Granieri E, et al. Anatomo-functional study of the temporo-parieto-occipital region: Dissection, tractographic and brain mapping evidence from a neurosurgical perspective. *J Anat*. (2014). doi: 10.1111/joa.12204
59. Cabeen RP, Bastin ME, Laidlaw DH. Kernel regression estimation of fiber orientation mixtures in diffusion MRI. *Neuroimage*. (2016). doi: 10.1016/j.neuroimage.2015.11.061
60. Schurr R, Zelman A, Mezer A. A subdividing the superior longitudinal fasciculus using local quantitative MRI. *NeuroImage*. (2019) 116439 doi: 10.1016/j.neuroimage.2019.116439

61. Frey S, Campbell JSW, Pike GB, Petrides M. Dissociating the human language pathways with high angular resolution diffusion fiber tractography. *J Neurosci.* (2008) 28:11435–44. doi: 10.1523/JNEUROSCI.2388-08.2008
62. Makris N, Papadimitriou GM, Kaiser JR, Sorg S, Kennedy DN, Pandya DN. Delineation of the middle longitudinal fascicle in humans: A quantitative, in vivo, DT-MRI study. *Cerebral Cortex.* (2009). doi: 10.1093/cercor/bhn124
63. Zhang Y, Zhang J, Oishi K, et al. Atlas-guided tract reconstruction for automated and comprehensive examination of the white matter anatomy. *Neuroimage.* (2010) 52:1289–301. doi: 10.1016/j.neuroimage.2010.05.049
64. Kamali A, Flanders AE, Brody J, Hunter JV, Hasan KM. Tracing superior longitudinal fasciculus connectivity in the human brain using high resolution diffusion tensor tractography. *Brain Struct Funct.* (2014). doi: 10.1007/s00429-012-0498-y
65. Amunts K, Weiss PH, Mohlberg H, Faria AV, Jiang H, Li X, et al. Analysis of neural mechanisms underlying verbal fluency in cytoarchitectonically defined stereotaxic space - The roles of Brodmann areas 44 and 45. *Neuroimage.* (2004) 22:42–56. doi: 10.1016/j.neuroimage.2003.12.031
66. Baldassarre A, Lewis CM, Committeri G, Snyder AZ, Romani GL, Corbetta M. Individual variability in functional connectivity predicts performance of a perceptual task. *Proc Natl Acad Sci U S A.* (2012) 3516–21. doi: 10.1073/pnas.1113148109
67. Good CD, Johnsrude IS, Ashburner J, Henson RN, Friston KJ, Frackowiak RS, et al. voxel-based morphometric study of ageing in 465 normal adult human brains. *Neuroimage.* (2001). doi: 10.1006/nimg.2001.0786
68. Hill J, Inder T, Neil J, Dierker D, Harwell J, Van Essen D. Similar patterns of cortical expansion during human development and evolution. *PNAS.* (2010) 107:13135–40. doi: 10.1073/pnas.1001229107
69. Schilling KG, Rheault F, Petit L, Hansen CB, Nath V, Yeh FC, et al. Tractography dissection variability: what happens when 42 groups dissect 14 white matter bundles on the same dataset? *Neuroimage.* (2021) 243:118502. doi: 10.1016/j.neuroimage.2021.118502
70. Catani M, Thiebaut de Schotten M. Atlas of Human Brain Connections. Oxford: University Press. (2012). doi: 10.1093/med/9780199541164.001.0001
71. Lunven M, Bartolomeo P. Attention and spatial cognition: neural and anatomical substrates of visual neglect. *Ann Phys Rehabil Med.* (2017) 60:124–9. doi: 10.1016/j.rehab.2016.01.004
72. Vernooij MW, Smits M, Wielopolski PA, Houston GC, Krestin GP, van der Lugt A. Fiber density asymmetry of the arcuate fasciculus in relation to functional hemispheric language lateralization in both right- and left-handed healthy subjects: a combined fMRI and DTI study. *Neuroimage.* (2007) 35:1064–76. doi: 10.1016/j.neuroimage.2006.12.041
73. MacDonald SWS, Nyberg L, Bäckman L. Intra-individual variability in behavior: links to brain structure, neurotransmission and neuronal activity. *Trends Neurosci.* (2006) 29:474–80. doi: 10.1016/j.tins.2006.06.011
74. Duffau, H. *Brain Mapping, From Neural Basis of Cognition To Surgical Applications*. Austria: Springer-Verlag/Wien. (2012).
75. Thiebaut de. Schotten M, Ffytche DH, Bizzi A, Dell'Acqua F, Allin M, Walshe M, et al. Atlasing location, asymmetry and inter-subject variability of white matter tracts in the human brain with MR diffusion tractography. *NeuroImage.* (2011) 54:49–59. doi: 10.1016/j.neuroimage.2010.07.055
76. Schmahmann JD, Pandya DN. The complex history of the fronto-occipital fasciculus. *J Hist Neurosci.* (2007). doi: 10.1093/acprof:oso/9780195104233.003.0019
77. Vavassori L, Sarubbo S, Petit L. Hodology of the superior longitudinal system of the human brain: a historical perspective, the current controversies, and a proposal. *Brain Struct Funct*. (2021) 226:1363–84. doi: 10.1007/s00429-021-02265-0
78. Maldonado IL, Moritz-Gasser S, Duffau H. Does the left superior longitudinal fascicle subserve language semantics? A brain electrostimulation study. *Brain Struct Funct.* (2011) 216:263–74. doi: 10.1007/s00429-011-0309-x
79. Rheault FH, Goyette JC, Morency N, Descoteaux FM. *MI-Brain, a Software to Handle Tractograms and Perform Interactive Virtual Dissection*. Lisbon: Breaking the Barriers of Diffusion MRI (ISMRM workshop) (2016).
80. Wakana S, Caprihan A, Panzenboeck MM, Fallon JH, Perry M, Gollub RL, et al. Reproducibility of quantitative tractography methods applied to cerebral white matter. *Neuroimage.* (2007) 36:630–44. doi: 10.1016/j.neuroimage.2007.02.049
81. Fitzgerald J, Leemans A, Kehoe E, O'Hanlon E, Gallagher L, McGrath J. Abnormal fronto-parietal white matter organisation in the superior longitudinal fasciculus branches in autism spectrum disorders. *Eur J Neurosci.* (2018) 47:652–61. doi: 10.1111/ejn.13655

Conflict of Interest: The authors declare that the research was conducted in the absence of any commercial or financial relationships that could be construed as a potential conflict of interest.

frontiers | Frontiers in Neurology

REVIEW
published: 12 May 2022
doi: 10.3389/fneur.2022.874826

Supratotal Resection of Gliomas With Awake Brain Mapping: Maximal Tumor Resection Preserving Motor, Language, and Neurocognitive Functions

Kazuya Motomura, Fumiharu Ohka, Kosuke Aoki and Ryuta Saito*

Department of Neurosurgery, Nagoya University School of Medicine, Nagoya, Japan

Gliomas are a category of infiltrating glial neoplasms that are often located within or near the eloquent areas involved in motor, language, and neurocognitive functions. Surgical resection being the first-line treatment for gliomas, plays a crucial role in patient outcome. The role of the extent of resection (EOR) was evaluated, and we reported significant correlations between a higher EOR and better clinical prognosis of gliomas. However, recurrence is inevitable, even after aggressive tumor removal. Thus, efforts have been made to achieve extended tumor resection beyond contrast-enhanced mass lesions in magnetic resonance imaging (MRI)-defined areas, a process known as supratotal resection. Since it has been reported that tumor cells invade beyond regions visible as abnormal areas on MRI, imaging underestimates the true spatial extent of tumors. Furthermore, tumor cells have the potential to spread 10–20 mm away from the MRI-verified tumor boundary. The primary goal of supratotal resection is to maximize EOR and prolong the progression-free and overall survival of patients with gliomas. The available data, as well as our own work, clearly show that supratotal resection of gliomas is a feasible technique that has improved with the aid of awake functional mapping using intraoperative direct electrical stimulation. Awake brain mapping has enabled neurosurgeons achieve supratotal resection with favorable motor, language, and neurocognitive outcomes, ensuring a better quality of life in patients with gliomas.

Keywords: gliomas, overall survival, progression-free survival, extent of resection, subcortical fiber, supratotal resection, awake brain mapping

OPEN ACCESS

Edited by:
Emanuele La Corte, University of Bologna, Italy

Reviewed by:
Alessandro De Benedictis, Bambino Gesù Children's Hospital (IRCCS), Italy
Jacky Yeung, Yale University, United States

****Correspondence:***
Kazuya Motomura
kmotomura@med.nagoya-u.ac.jp

Specialty section:
This article was submitted to Applied Neuroimaging, a section of the journal Frontiers in Neurology

Received: *13 February 2022*
Accepted: *15 April 2022*
Published: *12 May 2022*

Citation:
Motomura K, Ohka F, Aoki K and Saito R (2022) Supratotal Resection of Gliomas With Awake Brain Mapping: Maximal Tumor Resection Preserving Motor, Language, and Neurocognitive Functions. Front. Neurol. 13:874826. doi: 10.3389/fneur.2022.874826

INTRODUCTION

Gliomas are a heterogeneous population of intrinsic brain tumors of the central nervous system (1–4). Among malignant histological subtypes such as glioblastoma [GBM; World Health Organization (WHO) grade IV], and WHO grade II and III gliomas, GBM is the most aggressive and common form of malignant primary brain tumor. The clinical prognosis of GBM is poor and the median overall survival (OS) is only 12–18 months after diagnosis, even with intensive treatments such as surgery and chemoradiotherapy (5, 6). Surgical intervention plays a crucial role in the treatment of GBM; tumors invariably recur even after aggressive tumor resection and most patients eventually succumb to the disease. The slow-growing primary brain tumors (1, 2),

WHO grade II and III gliomas (hereon, referred to as, lower-grade gliomas) are diagnosed based on molecular features (presence or absence of *IDH*1/2 mutations and 1p/19q co-deletion) (1, 2). Over time, lower-grade gliomas typically undergo malignant transformation to GBMs, and the median survival is only 7.8–31 months, even with intensive treatment including surgery, chemotherapy, and radiotherapy (7, 8).

Several studies have reported a significant relationship between the extent of resection (EOR) in patients with gliomas and survival rate (3, 4, 9–14). Recent studies also provided evidence that increased EOR and decreased postsurgical tumor volume are related to increased progression-free survival (PFS) and OS in diffuse gliomas (4, 14, 15). Therefore, quantifying the EOR is of particular interest for patients with diffuse gliomas. To achieve increased survival rates, an increase in the EOR of tumors has been achieved using modalities such as ultrasound-guided resection (16), neuro-navigation (16), intraoperative magnetic resonance imaging (iMRI) (17, 18), and 5-aminolevulinic acid (5-ALA) (19). Furthermore, Duffau et al. reported that aggressive resection of low-grade gliomas using intraoperative awake mapping to identify functional areas in the brain, can result in supratotal resection and improved patient survival (20–22).

Here, we present a systematic review of the literature on supratotal resection in patients with gliomas with the aim of evaluating the survival benefit of supratotal resection for diffuse gliomas. In particular, we focused on the effects of supratotal resection on glioma survival outcomes.

METHODS

We performed an extensive systematic literature review of the PubMed, Web of Science, and Scopus databases. We used the following keywords: "supratotal resection," "supramarginal resection," "awake brain mapping" for searching original articles, meta-analyses, reviews, clinical series, and case reports.

RESULTS

The literature search yielded 3,341 studies regarding supratotal resection using awake brain mapping. Duplicates were removed from 2301 studies. In total, 21 full texts were reviewed for eligibility. Eleven clinical studies were included in the final review, as shown in the PRISMA flowchart (23) (**Figure 1**).

DISCUSSION

Glioblastomas and EOR

Several studies evaluating the EOR for GBM have shown that maximal tumor removal is significantly associated with better clinical outcomes (3, 24). The correlation between EOR and improved survival is widely agreed upon in the field of surgical neuro-oncology. Many retrospective cohort studies have revealed that increased EOR, ranging from 78 to 98%, improves OS in patients with newly diagnosed GBM (3, 25). Lacroix et al. analyzed 416 consecutive patients with GBM who underwent tumor resection and reported that tumor resection of 98% or more was associated with a survival advantage (25). While they used the outcome scale based on age, Karnofsky Performance Scale (KPS) score, and tumor necrosis on MRI, they concluded that patients with lower scores who underwent aggressive resections were associated with significantly longer survival. Multivariate analysis using a Cox proportional hazards model demonstrated that age (<45, 45–64, >64 years), performance score (<80), necrosis, enhancement, and EOR (≥98%) were significantly related to the survival of GBM patients. Stummer et al. performed a randomized phase III trial of 270 newly diagnosed patients with GBM to evaluate the effect of fluorescence-guided resection with 5-aminolevulinic acid (5-ALA) on clinical outcomes (26). A total of 139 patients were assigned to surgical resection with the fluorescent adjunct 5-ALA and 131 patients were assigned to the white-light control group. The clinical outcome revealed that complete resection was achieved in 65% of 5-ALA cases and 36% of white-light cases. Patients treated with 5-ALA had significantly higher 6-month PFS (41.0%) than in those treated with white light (21.1%).

WHO Grade II Gliomas and EOR

Some studies investigating the role of EOR in gliomas have revealed that extensive surgical resection favors longer survival in WHO grade II gliomas (9–13, 24, 27). A large cohort study including 216 patients with WHO grade II gliomas revealed that patients with an EOR > 90% had 5- and 8-year OS rates of 97 and 91%, respectively, whereas those with an EOR < 90% had 5- and 8-year OS rates of 76 and 60%, respectively (9). Another study in Norway examined survival in population-based cohorts of WHO grade II gliomas from two university hospitals by distinct surgical treatment strategies. Early surgical resection was performed at one university hospital, whereas biopsy and watchful waiting were preferred for WHO grade II gliomas at the other hospital. Notably, this study revealed 5-year OS rates of 60% and 74% in patients in the "biopsy and observation" and "early surgical resection" groups, respectively (12, 13). The survival data of patients treated with biopsy showed significantly better OS than for those treated with early surgical resection. Moreover, another research group reported a significant survival benefit for patients who underwent "early tumor resection" compared to those who underwent only "biopsy" (5-year OS: 82 vs. 54%) at two distinct departments acting independently at the same university medical center (27). These findings suggest that glioma neurosurgeons should attempt to perform maximal safe tumor resection by increasing the EOR to prolong survival in patients with WHO grade II gliomas.

WHO Grade III Gliomas and EOR

Several studies on WHO grade III gliomas have shown that extensive tumor resection affects the OS of patients (28–30). The EOR of tumors had been reported to be significantly related to OS in WHO grade III anaplastic oligodendroglial tumors in a European phase III clinical trial (EORTC-26951) (28). Nomiya et al. evaluated the prognostic parameters of 170 patients with WHO grade III anaplastic astrocytoma (30). Patients who achieved total or subtotal tumor resection showed a significantly more favorable clinical outcome with a median OS of 62.9 months than those patients who underwent partial

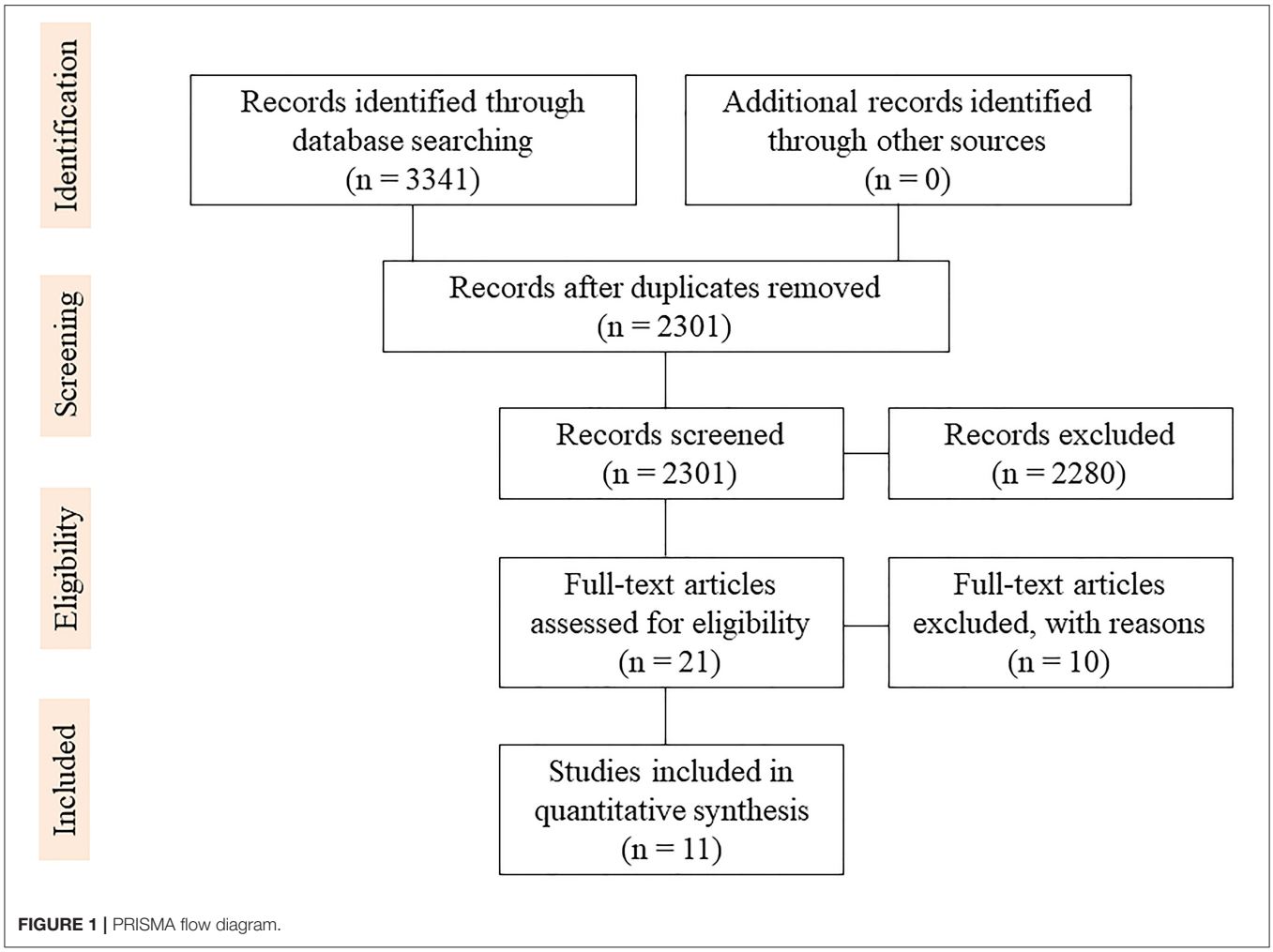

FIGURE 1 | PRISMA flow diagram.

resection or biopsy alone, with a median OS of 22.9 months. The authors emphasized that the EOR of tumors was the most powerful prognostic factor for the treatment of WHO grade III anaplastic astrocytomas in their cohort study. Kawaguchi et al. demonstrated the clinical importance of surgical tumor resection by investigating 124 consecutive patients with WHO grade III gliomas treated at a single institution (29). Among the group with *IDH*1/2 mutations and non-1p/19q co-deletions, survival was significantly longer in those with gross total removal than in those in whom gross total removal was not accomplished (median OS: not reached vs. 77 months). Therefore, extensive surgical tumor removal is essential to improve the prognosis of patients with WHO grade III gliomas, especially for astrocytic tumors with the *IDH*1/2 mutation lacking the 1p/19q co-deletion.

WHO Grade II and III Gliomas and EOR

In this context, surgical tumor resection is considered the first-line treatment for WHO grade II and grade III gliomas. To date, several clinical studies have provided evidence supporting maximum safe tumor resection and early surgical intervention, which prolong survival in patients with WHO grade II and grade III gliomas (9, 11–13, 24, 27, 31, 32). From an ethical perspective, we could not perform randomized controlled trials examining the relationship between a higher EOR and better outcomes of WHO grade II and grade III gliomas, as extensive radiological tumor resection of WHO grade II and grade III gliomas is a better choice.

Supratotal Resection and Awake Brain Mapping

MRI diffusion tractography (DT) is used to estimate subcortical fiber tracts before awake surgery. Voets et al. evaluated DT sensitivity, specificity, and accuracy for five subcortical fiber tracts, including the corticospinal tract (CST), arcuate fasciculus (AF), inferior fronto-occipital fasciculus (IFOF), optic radiation (OR), and inferior longitudinal fasciculus (ILF) (33). The sensitivity and specificity of preoperative DT predictions were very high, at 92.2 and 69.2%, respectively, and it varied across tracts. The authors concluded that preoperative DT of the navigation system is a reliable tool for accurately predicting the spatial location of subcortical fiber tracts in relation to a tumor during awake surgery. However, the information

of some subcortical fiber tracts by DT cannot inform its neurological functions. Moreover, DT does not provide a critical surgical strategy directly during tumor resection in the operating room. Therefore, this technique is difficult to replace intraoperative direct cortical and subcortical stimulation during awake brain mapping.

Considering the infiltrative behavior of gliomas, the goal of maximal tumor removal should be balanced against the risk of neurological dysfunctions such as motor, language, and neurocognitive impairment (34, 35). Awake functional mapping has been proposed as the optimal strategy for patients with gliomas to accomplish maximal safe resection and preservation of neurological functions (36–40). Using awake surgical techniques with both cortical and subcortical functional mapping, a maximum degree of resection is possible while determining the functional boundaries (37, 41). Direct electrical stimulation in glioma patients triggers an increase in the EOR of tumors (42), an improvement in OS and PFS (43), and a significant decrease in the rate of postoperative permanent neurological deficits, including motor, language, and neurocognitive functions (38). When combined with intraoperative tasks for motor and language, awake mapping can detect possible anatomo-functional associations, allowing a deeper understanding of neuroconnectivity in the human brain. In particular, as surgery carries a high risk of injury to subcortical pathways, resulting in permanent neurological impairments, for which functional connectivity is a central limitation of neural regeneration, a better understanding of the connectome is essential for comprehending cortico-subcortical pathways and their relevance to tumor resection during awake surgery.

Although awake brain mapping represents the gold standard technique for identifying and preserving the eloquent areas, it must be acknowledged that awake surgery has some risks and complications. There are some problems regarding the risk of intraoperative seizures (44, 45), variability in anesthetic techniques (46, 47), difficulty in the selection and interpretation of intraoperative tasks (48, 49), and intraoperative pain and discomfort during the procedure (50, 51). In particular, the occurrence of intraoperative seizures is especially crucial, as it is related to procedure failure, reduction of the EOR, and a high incidence of postoperative motor and speech disturbance (52). Furthermore, the risk of intraoperative seizures has been reported to be higher in patients with intra-axial brain tumors during awake surgery (44). Therefore, the decision to perform awake mapping should be considered with caution.

In cases where functional boundaries are detected inside a tumor mass, surgical resection should involve subtotal or partial removal. When functional boundaries are observed outside the tumor mass, gross total or supratotal resection can be performed. Extended resection beyond the tumor margins of abnormalities in MRI-defined areas is termed supratotal resection (20, 53). Supratotal resection of GBM or WHO grade II or grade III gliomas is a newly developed concept that may improve the survival of patients with gliomas. Even with aggressive and intensive tumor surgery, awake brain mapping enables safe maximal resection of language-dominant or non-dominant tumors, preserving both the cortical and subcortical fibers.

A clinical study by Duffau et al. reported that supratotal resection may improve the clinical outcomes of patients with WHO grade II gliomas who underwent awake brain surgery after a long-term period, of a mean follow-up period of 11 years (20). This study demonstrates that supratotal resection, extending beyond the abnormalities detected by T2- or FLAIR-weighted MRI, provides a survival benefit, as tumor cells may be present at a distance of 10–20 mm from the tumor boundaries on MRI (54). As a greater EOR of tumors, including gross total or supratotal removal, could increase PES and OS in patients with WHO grade II gliomas, many neurosurgeons worldwide have recently attempted to perform supratotal resection of tumors whenever possible with the use of awake functional mapping. A conceptual overview of supratotal resection for diffuse gliomas with awake functional mapping is shown in **Figure 2**. To achieve margin removal around MRI-detected abnormalities, performing classical motor and/or language mapping throughout surgical resection is recommended. Furthermore, to evaluate working memory and spatial cognition, stimulation of the fibers associated with cognitive functions has been proposed.

Supratotal Resection and Tumor Location in the Dominant or Non-dominant Hemispheres

When the tumor is located in the non-dominant hemisphere, such as in the frontal and temporal poles, or inside the occipital lobes of patients who already show visual deficits before surgery, supratotal resection via lobectomy can be performed without difficulty. Shah et al. reported that lobectomy for GBM of the non-dominant hemisphere significantly improved PFS and OS, compared to the GTR group (55). Moreover, the authors found no increase in postoperative complications in these patients and concluded that supratotal resection is the best tailored technique for small lesions arising in the non-dominant frontal, temporal, and occipital poles.

In contrast, if the tumor is within the dominant hemisphere for motor and language functions, supratotal resection and gross total removal cannot be accomplished. Yordanova et al. attempted to perform supratotal resection of WHO grade II gliomas within non-eloquent areas of the left language-dominant hemisphere, and reported that four out of 15 patients experienced tumor recurrence without anaplastic transformation, with a mean postoperative follow-up duration of 35.7 months (21). The authors emphasized that it is crucial to delay anaplastic transformation and delay the use of adjuvant therapy, such as chemoradiotherapy, by supratotal resection.

Supratotal Resection and Subcortical Fibers

Our research group assessed the efficacy of awake functional mapping for supratotal resection of frontal WHO grade II and grade III gliomas in both the dominant and non-dominant hemispheres (53). In total, 11 patients with diffuse frontal WHO grade II and grade III gliomas who underwent awake

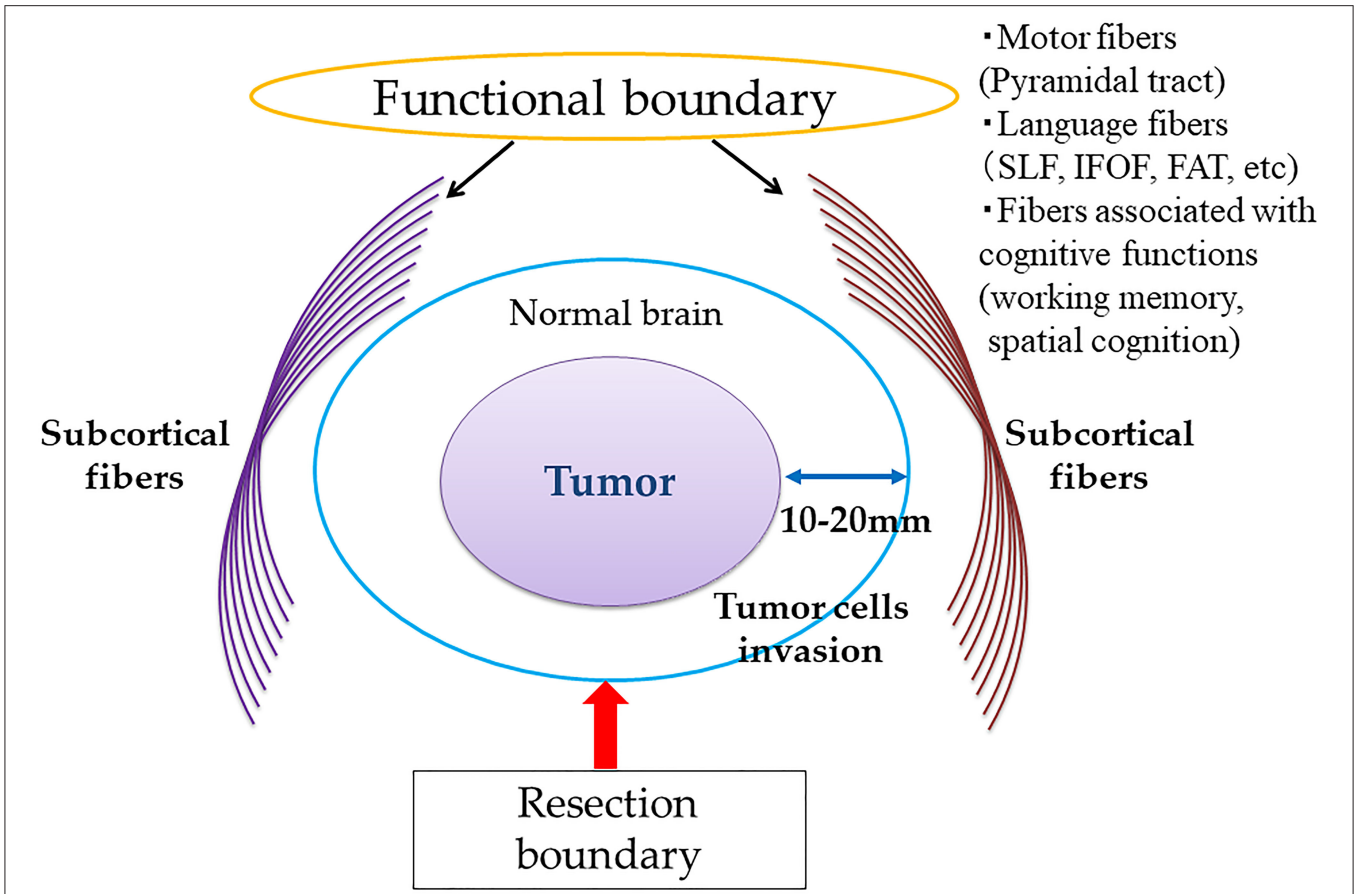

FIGURE 2 | Conceptual diagram of supratotal resection of diffuse gliomas with awake brain mapping.

brain surgery and supratotal resection were analyzed. The oral and written language functions of the tumors in the language-dominant frontal lobe were preserved using counting and picture-naming tasks. Using such intraoperative language tasks, awake functional mapping can detect anatomy-functional associations, which has revealed the "language connectivity" in the human brain. In language-associated subcortical fibers in the frontal lobe, the IFOF is one of the longest association fiber tracts, which constructs a ventral pathway that passes through the deep areas of the temporal lobe and insula, connecting the occipital cortex and posterior temporo-occipitoparietal regions to the orbitofrontal, prefrontal, and dorsolateral prefrontal areas (56). This ventral pathway is related to semantic processing, and stimulation of the IFOF during awake surgery using picture-naming tasks leads to semantic paraphasia (57). Furthermore, the superior longitudinal fasciculus (SLF) connects the inferior frontal gyrus (IFG) and ventral premotor cortex to temporoparietal language regions, which construct a dorsal pathway in the left frontal lobe (58). During awake surgery, phonemic paraphasia and articulatory disorders are elicited during direct stimulation. The frontal aslant tract (FAT), which was discovered only in the last decade, connects the pre-supplementary motor area (pre-SMA) and SMA in the medial frontal areas of the superior frontal gyrus (SFG), and posterior inferior frontal gyrus, which is part of Broca's area in the frontal lobe (59). The FAT is believed to play a role in self-initiated speech, involving the pre-SMA, SMA, and IFG. Our group performed resection extending to the functional boundaries, defined by the white matter fibers FAT, IFOF, and SLF (**Figure 3**), to perform extended resection of a tumor margin beyond MRI abnormalities in left frontal WHO grade II and grade III gliomas.

In contrast, the SLF/arcuate fasciculus complex and the IFOF were mainly associated with parietal tumors when attempting to achieve supratotal resection (**Figure 4**) (60). Subcortical stimulation of the SLF/arcuate fasciculus complex induces disturbances in spatial attention. Furthermore, rightward deviation was generated using a line bisection test. In the deep area of the parietal lobe, semantic paraphasia was induced by stimulating the deep side of the tumor cavity, which was caused by the stimulation of the IFOF.

During awake brain mapping of the temporal tumor for supratotal resection, direct electrical stimulation detects the

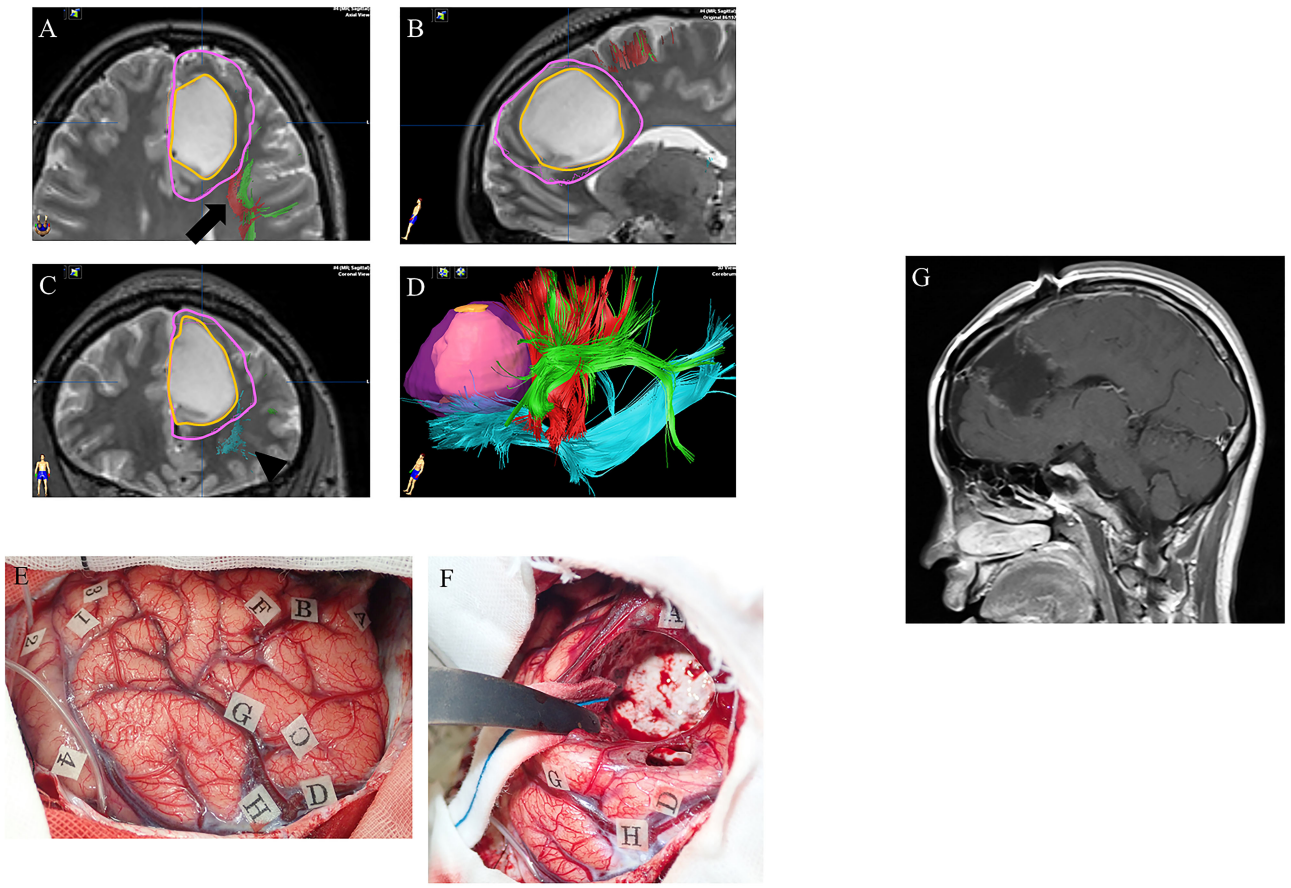

FIGURE 3 | A case of left frontal lower-grade glioma in a 30-year-old right-handed female with no relevant medical history. Preoperative axial **(A)**, sagittal **(B)**, and coronal **(C)** T2-weighted MRI show a high intensity mass in the left frontal lobe. Preoperative three-dimensional tractography **(D)** shows the tumor itself (orange) and the planned resection area (violet; supratotal resection) surrounded by FAT (red; arrow in panel **A**), SLF (green; arrow in panel **A**) and IFOF (blue; arrowhead in panel **C**). Red, FAT; green, SLF; blue, IFOF; FAT, frontal aslant tract; SLF, superior longitudinal fasciculus; IFOF, fronto-occipital fasciculus. Intraoperative photograph prior to resection **(E)**, showing letter tags that indicate tumor boundaries (A–D) and the planned resection area for supratotal resection (E–H). Stimulation over the precentral gyrus induced speech arrest (number tags: 2 and 4), as did stimulation over the opercular part of the inferior frontal gyrus (number tags: 1 and 3). **(F)** Intraoperative photograph obtained after supratotal resection. Stimulation over the IFOF induced semantic paraphasia (number tag: 31), and stimulation over the FAT induced speech arrest (number tags: 33, 34). FAT, frontal anterior tract; IFOF, fronto-occipital fasciculus. Postoperative sagittal T1-weighted MRI with gadolinium enhancement **(G)** showing supratotal resection with awake brain mapping.

IFOF, temporal part of the SLF, inferior longitudinal fascicle, and optic radiation. When the IFOF is stimulated, semantic paraphasia is also induced. Phonological disorders are elicited when the temporal SLF subserves the dorsal stream of the brain. The detection of the inferior longitudinal fascicle generates reading disturbances during stimulation. Optic radiation, which is deeply located, induces transient visual disturbances via stimulation.

Role of Supratotal Resection for Glioblastoma

Several studies have reported that a greater EOR, such as that achieved by supratotal resection, might improve the survival of patients with GBM by decreasing postoperative neurological deficits, while preserving white matter fibers associated with motor, language, and neurocognitive functions (60–66) (**Figure 4**). A systematic review of several clinical studies on the supratotal resection of GBM was therefore conducted (**Table 1**).

Eyüpoglo et al. evaluated the role of supra-complete resection surgery using a dual intraoperative visualization approach combining intraoperative MRI with neuro-navigation and 5-ALA in GBM (61). In this study, 75 patients underwent gross total resection using intraoperative MRI and navigation. Thirty patients underwent supratotal resection using a surgical strategy with 5-aminolevulinic acid (5-ALA) and intraoperative MRI. The median OS of patients treated according to the surgical strategy using intraoperative MRI with navigation was 14 months, whereas those who underwent surgery with 5-ALA and intraoperative MRI had a significantly longer median survival time of 18.5 months. Thus, it was concluded that supra-complete

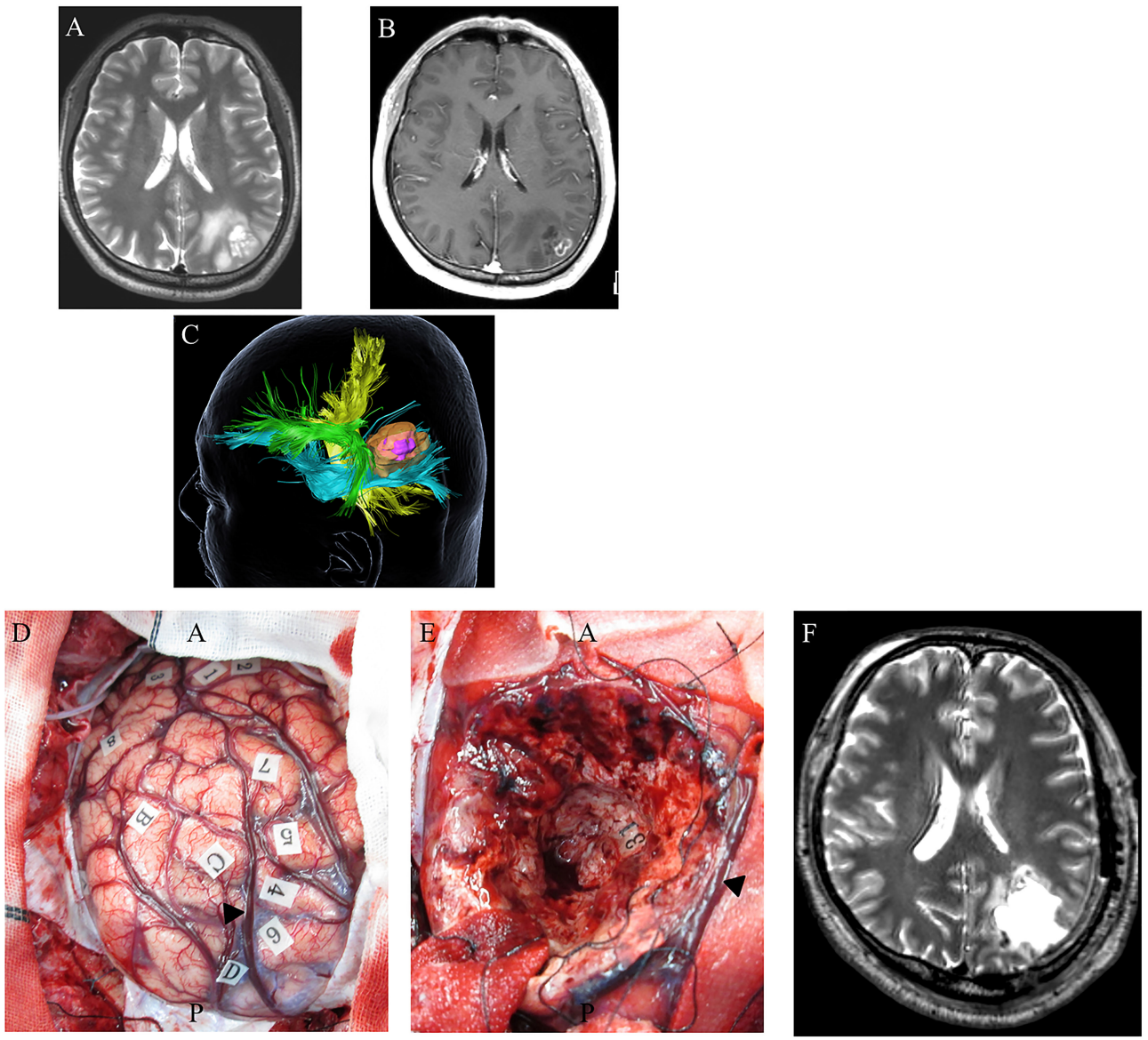

FIGURE 4 | A 48-year-old right-handed male with *IDH*-wildtype glioblastoma (GBM). Preoperative axial T2-weighted **(A)** and axial T1-weighted MRI with gadolinium enhancement **(B)**, showing a high-intensity abnormal area in the left inferior parietal lobule including an enhancing region at the superficial area. Preoperative three-dimensional tractography **(C)** showing a yellow-colored fiber tract bundle showing the corticospinal tract. The green area shows the superior longitudinal fasciculus, the blue fiber tract bundle shows the inferior fronto-occipital fasciculus, and the high-intensity area on T2-weighted MRI is highlighted in orange. The violet-colored lesion in the orange-colored area showed an enhancing mass. **(D)** Intraoperative photograph obtained before tumor resection, with letter tags indicating tumor boundaries **(A–D)**. Stimulation over the postcentral gyrus induced convulsions around the mouth (number tags: 1, 2); stimulation over the left superior parietal lobule induced cessation of right upper limb movement (number tags: 4–7); arrowhead: intraparietal sulcus. **(E)** Intraoperative photograph obtained after supratotal resection. Stimulation over the IFOF induced semantic paraphasia (number tag: 31). Postoperative axial T2-weighted MRI **(F)** revealed no tumor following supratotal resection.

glioma resection leads to significantly prolonged OS in patients with GBM.

Li et al. (62) assessed the role of supratotal resection in 876 GBM patients. In this study, supratotal resection was defined as complete resection of the T1-enhancing regions with a small portion, with additional resection of the surrounding fluid-attenuated inversion recovery (FLAIR) abnormality. The authors showed that resection of $\geq$ 53.21% of the surrounding FLAIR abnormality beyond contrast-enhanced areas was associated with a significant prolongation of survival, compared to less extensive tumor resection (median OS: 20.7 and 15.5 months, respectively). These results suggest that supratotal resection with the resection of the FLAIR abnormality region can lead to longer survival of patients with GBM, without increases in postoperative morbidity.

TABLE 1 | Supratotal resection of glioblastomas (literature review).

	Number of patients	Definition of supratotal resection	Number and rate of supratotal resection cases (%)	OS	PFS	Adjuvant therapy
Eyüpoglu et al. (61)	105	Beyond obvious contrast enhancement using 5-ALA and iMRI	30 (29%)	18.5 vs. 14 months (vs. GTR)	NA	RT + TMZ
Li et al. (62)	643	Resection over 53.21% of FLAIR	159 (25%)	20.7 vs. 15.5 months (vs. <53.21% of FLAIR)	NA	NA
Esquenazi et al. (63)	86	Beyond the zone of enhancement using subpial technique	25 (29%)	54 vs. 16.5 months (vs. GTR)	NA	RT + TMZ ± BCNU wafer
Grossmann et al. (66)	103	≤ 46% of remnant FLAIR (3 months post operation)	NA	26.7 vs. 13.4 months (vs. GTR)	NA	RT + TMZ
Pessina et al. [65)	282	Resection 100% of FLAIR	21 (7%)	28.6 ± 5.2 vs. 16.2 ± 1.2 months (vs. GTR)	24.5 ± 2.4 vs. 11.9 ± 0.6 months (vs. GTR)	TMZ + RT, 6-8 cycles TMZ
Glenn et al. (64)	32	Removal of at least 1 cm of brain tissue surrounding the enhancement	7 (21.9%)	24 vs. 11 months (vs. GTR)	15 vs. 7 months (vs. GTR)	NA

OS, overall survival; PFS, progression free survival; GTR, gross total resection; TMZ, temozolomide; RT, radiotherapy; NA, not available; BCNU, carmustine; 5-ALA. aminolevulinic acid; iMRI, intraoperative magnetic resonance imaging; FLAIR, fluid-attenuated inversion recovery; DC, dendritic cell.

Esquenazi et al. retrospectively evaluated 86 patients with primary GBM with or without carmustine (BCNU) wafer implantation (63). They concluded that the effect of supratotal resection on OS surpassed the effects of tumor volume, age, and KPS score.

Pessina et al. evaluated the role of FLAIR abnormality removal in a retrospective study of 282 newly diagnosed GBM patients. They reported that the median OS for supratotal resection was 28.6 months, compared with a gross total resection OS of 16.2 months. Furthermore, fewer patients showed worsening neurological deficits after supratotal resection (4.8%) than after gross total (13.3%) or subtotal resection (5.6%). This large clinical study suggests that supratotal resection beyond contrast-enhanced boundaries could represent a promising strategy for improving the survival of GBM patients (65).

Glenn et al. reported that patients undergoing supratotal resection for temporal lobe GBM showed a significantly improved median PFS (15 months) compared to those who underwent gross total resection (7 months) (64). Moreover, a median OS advantage was also found in the supratotal resection group at 24 months compared to the gross total resection group at 11 months.

Role of Supratotal Resection in the Treatment of WHO Grade II Gliomas

The first reports on supratotal resection of WHO grade II gliomas were published by Yordanova and Duffau et al. (21) (**Table 2**). Fifteen right-handed patients with 17 tumors underwent the resection of WHO grade II gliomas using intraoperative awake brain mapping. In this series, total resection was accomplished for all 17 tumors, whereas supratotal resection was performed for 15 tumors. Only four of the 15 patients in whom supratotal resection was achieved experienced tumor recurrence without malignant transformation, and the mean time to tumor recurrence was 38 months. The recurrence rate in the control group was 41%, whereas that in the supratotal resection group was 26%.

Duffau et al. analyzed 11 asymptomatic patients with WHO grade II gliomas in the language-dominant hemisphere (67). Supratotal resection was achieved in three patients by intraoperative awake mapping. No mortality or permanent postoperative neurological deficits were observed in any patient. Furthermore, no anaplastic transformation was observed in these cases, with a mean follow-up period of 40 months after tumor resection.

Lima et al. reported the efficacy of supratotal resection based on functional boundaries for incidental WHO grade II gliomas in a group of 19 patients (68, 69). Supratotal resection was achieved in five patients in this study. The PFS rate was significantly higher in patients who underwent total or supratotal resection than in those who underwent partial or subtotal resection (not reached vs. 65 months, respectively). Six months after surgery, all 19 patients were free of permanent neurological disturbances, and 18 had a postoperative KPS of 100.

Role of Supratotal Resection in the Treatment of WHO Grade III Gliomas

Rossi et al. assessed the association between supratotal resection and 319 *IDH*-mutated WHO grade II and grade III gliomas (70) (**Table 3**). This large retrospective study evaluated the relationship between supratotal resection and survival, including PEF and OS, in a series of WHO grade II and grade III gliomas.

TABLE 2 | Supratotal resection of WHO grade II gliomas (literature review).

	Number of patients	Tumor classification (WHO grading)	Definition of supratotal resection	Number of supratotal resection case (%)	Adjuvant therapy	Clinical outcome	Mean follow-up duration and outcomes
Yordanova et al. (21)	15	WHO grade II glioma	Resection extending beyond the area of MRI signal abnormalities	15 (100%)	None after the surgery (1 patient received radiotherapy at the relapse 6 years after the surgery)	Adjuvant treatment, anaplastic transformation, KPS, postop seizures, recurrence rate	35.7 months Average time to recurrence: 38 months
Duffau et al. (67)	11	WHO grade II glioma	A margin of parenchyma was removed around the preoperative FLAIR-weighted signal abnormality with a larger volume of the surgical cavity as compared with the presurgical tumor volume	3 (27.2%)	None after the surgery	Adjuvant treatment, KPS, postop seizures	40.0 months No anaplastic transformation
Duffau et al. (20)	16	WHO grade II glioma	A complete removal of any signal abnormalities with a volume of the postoperative cavity larger than the preoperative tumor volume	16 (100%)	None after the surgery, chemotherapy ($n = 3$), radiotherapy ($n = 2$)	Adjuvant treatment, KPS, malignant transformation, postop seizures, relapse time	132 months Average time to relapse: 70.3 months
Lima et al. (69)	21	WHO grade II glioma	A margin of parenchyma was removed around the preoperative FLAIR or T2-weighted sequence signal abnormality, with a larger volume of the surgical cavity as compared with the presurgical tumor volume	4 (19.0%)	Chemotherapy ($n = 6$), radiotherapy ($n = 1$)	Adjuvant treatment, KPS, postop seizures, tumor regrowth	49 months Alive, enjoy a normal life
Lima et al. (68)	19	WHO grade II glioma	A margin of parenchyma was removed around the preoperative FLAIR or T2-weighted sequence signal abnormality, with a larger volume of the surgical cavity as compared with the presurgical tumor volume	5 (26.3%)	Chemotherapy ($n = 5$), radiotherapy ($n = 2$)	Adjuvant treatment, KPS, postop seizures	62.4 months PFS: not reached

WHO, World Health Organization; KPS, Karnofsky Performance Status; NA, not available; MRI, magnetic resonance imaging; FLAIR, fluid-attenuated inversion recovery.

TABLE 3 | Supratotal resection of WHO grade III gliomas (literature review).

	Number of patients	Tumor classification (WHO grading)	Definition of supratotal resection	Number of supratotal resection case (%)	Adjuvant therapy	Clinical outcome	Mean follow-up duration and outcomes
Motomura et al. (53)	9	WHO grade II glioma, WHO grade III glioma	Tumor resection extending beyond the abnormal MRI-verified area, which indicated that the volume of the postoperative cavity was larger than the preoperative tumor volume	9 (100%)	NA	WMS-R, SLTA, FAB, WAIS-III	NA NA
Rossi et al. (70)	319	WHO grade II glioma, WHO grade III glioma	Complete removal of any signal abnormalities, with the volume of the postoperative cavity larger than preoperative tumor volume	110 (35%)	Chemoradiotherapy (17.6%), chemotherapy only (41.2%)	Adjuvant treatment, anaplastic transformation, postop seizures, recurrence rate, OS, PFS, MPFS	6.8 years PFS at 92 months; 94%

WHO, World Health Organization; WMS-R; Wechsler memory scale revised, SLTA; Standard Language Test of Aphasia, FAB; Frontal Assessment Battery, WAIS-III; the third version of Wechsler adult intelligence score; OS, overall survival; PFS, progression free survival; MPFS, malignant progression free survival, NA, not available.

They showed that PFS was significantly longer in patients with *IDH*-mutated WHO grade II and grade III gliomas, including astrocytomas and oligodendrogliomas, who achieved supratotal resection than in those who underwent gross total resection. Furthermore, supratotal resection was significantly associated with a reduced rate of better OS and malignant transformation (28, 71).

Motomura et al. found that an EOR threshold of 85.3% was beneficial for the treatment of WHO grade II and grade III gliomas. Improved PFS among patients with WHO grade II and grade III gliomas is predicted by a greater EOR (> 85.3%) as a result of aiming for supratotal or gross total resection (72). Their findings also indicated that an EOR of ≥ 100%, including supratotal resection, was significantly correlated with a favorable PFS in patients with WHO grade II and grade III gliomas. Based on these results, maximal safe tumor resection can be considered an important prognostic factor for improving the survival of patients with WHO grade II and grade III gliomas. Moreover, this study also emphasized the efficacy of awake mapping for supratotal resection of frontal WHO grade II and grade III gliomas while preserving motor, language, and neurocognitive functions (53).

Present Issues in Supratotal Resection

In GBM, supratotal resection prolongs OS by 18.5–54 months and PFS by 15–24.5 months (61–66) (**Table 1**). In contrast, several studies have reported that in WHO grade II gliomas, supratotal resection provides a significant increase in PFS with no anaplastic transformation and prolongs the average time to recurrence (20, 21, 67–69) (**Table 2**). Regarding WHO grade II and III gliomas (i.e., lower-grade gliomas), OS, PFS, and malignant progression-free survival (MPFS) were significantly prolonged in a large retrospective study (70). However, several issues to consider regarding the efficacy of supratotal resection of gliomas. First, the definition of supratotal resection remains ambiguous. Although some studies have defined supratotal resection as resection extending beyond the area of MRI signal abnormalities, the extent to which the tumor needs to be resected to achieve supratotal resection and the percentages of tumor resection that are associated with better survival of gliomas is unclear. Second, the tumor location in relation to the eloquent area is a confounder in terms of resectability. In cases where the tumor is within the dominant hemisphere for neurological function, supratotal resection cannot be achieved. Thid, it is essential to consider tumor malignancy during supratotal resection. Tumors with biologically less malignancy may be more amenable to supratotal resection because the cells of such tumors develop relatively locally compared to highly malignant gliomas. Finally, there may be potential for significant bias when selecting only patients eligible for supratotal resection. Such cases feature a relatively small tumor size and location in the non-eloquent area.

CONCLUSIONS

Despite aggressive treatment of GBM and WHO grade II and grade III gliomas, patients are still at a risk of tumor

recurrence. Supratotal resection may improve the survival of patients with GBM and WHO grade II and grade III gliomas without increasing the risk of postoperative neurological deficits, while preserving some subcortical fibers associated with motor, language, and neurocognitive functions. Although several studies have provided novel information regarding the effect of supratotal resection with awake brain mapping on the survival of patients with gliomas, their results are limited compared to those of prospective clinical trials, as retrospective studies may be influenced by unrecognized biases. Therefore, a larger prospective study involving multiple independent research centers is required to establish the role of supratotal resection in awake brain surgery.

AUTHOR CONTRIBUTIONS

KM and RS: experimental design. FO and KA: collection and assembly of data. KM, FO, KA, and RS: analysis and interpretation of the data. KM: manuscript writing. All authors contributed to the article and approved the submitted version.

FUNDING

This work was supported by a Grant-in-Aid for Scientific Research (C) awarded to KM (No. 21K09174) from the Japan Society for the Promotion of Science (JSPS).

REFERENCES

1. Suzuki H, Aoki K, Chiba K, Sato Y, Shiozawa Y, Shiraishi Y, et al. Mutational landscape and clonal architecture in Grade II and III Gliomas. *Nat Genet*. (2015) 47:458–68. doi: 10.1038/ng.3273
2. Aoki K, Nakamura H, Suzuki H, Matsuo K, Kataoka K, Shimamura T, et al. Prognostic relevance of genetic alterations in diffuse lower-grade gliomas. *Neuro Oncol*. (2017) 20:66–77. doi: 10.1093/neuonc/nox132
3. Sanai N, Polley MY, McDermott MW, Parsa AT, Berger MS. An extent of resection threshold for newly diagnosed Glioblastomas. *J Neurosurg*. (2011) 115:3–8. doi: 10.3171/2011.2.JNS10998
4. Brown TJ, Brennan MC, Li M, Church EW, Brandmeir NJ, Rakszawski KL, et al. Association of the extent of resection with survival in Glioblastoma: a systematic review and meta-analysis. *JAMA Oncol*. (2016) 2:1460–9. doi: 10.1001/jamaoncol.2016.1373
5. Omuro A, DeAngelis LM. Glioblastoma and other malignant gliomas: a clinical review. *JAMA*. (2013) 310:1842–50. doi: 10.1001/jama.2013.280319
6. Bryukhovetskii IS, Bryukhovetskii AS, Khotimchenko YS. New biomolecular approaches to the treatment of Glioblastoma Multiforme. *Bull Exp Biol Med*. (2015) 158:794–9. doi: 10.1007/s10517-015-2864-2
7. Ohgaki H, Dessen P, Jourde B, Horstmann S, Nishikawa T, Di Patre PL, et al. Genetic pathways to Glioblastoma: a population-based study. *Cancer Res*. (2004) 64:6892–9. doi: 10.1158/0008-5472.CAN-04-1337
8. Yan H, Parsons DW, Jin G, McLendon R, Rasheed BA, Yuan W, et al. Idh1 and Idh2 mutations in Gliomas. *N Engl J Med*. (2009) 360:765–73. doi: 10.1056/NEJMoa0808710
9. Smith JS, Chang EF, Lamborn KR, Chang SM, Prados MD, Cha S, et al. Role of extent of resection in the long-term outcome of low-grade hemispheric Gliomas. *J Clin Oncol*. (2008) 26:1338–45. doi: 10.1200/JCO.2007.13.9337
10. van Veelen ML, Avezaat CJ, Kros JM, van Putten W, Vecht C. Supratentorial low grade Astrocytoma: prognostic factors, dedifferentiation, and the issue of early versus late surgery. *J Neurol Neurosurg Psychiatry*. (1998) 64:581–7. doi: 10.1136/jnnp.64.5.581
11. Duffau H, Lopes M, Arthuis F, Bitar A, Sichez JP, Van Effenterre R, et al. Contribution of intraoperative electrical stimulations in surgery of low grade Gliomas: a comparative study between two series without (1985–96) and with (1996–2003) functional mapping in the same institution. *J Neurol Neurosurg Psychiatry*. (2005) 76:845–51. doi: 10.1136/jnnp.2004.048520
12. Jakola AS, Myrmel KS, Kloster R, Torp SH, Lindal S, Unsgard G, et al. Comparison of a strategy favoring early surgical resection vs a strategy favoring watchful waiting in low-grade Gliomas. *JAMA*. (2012) 308:1881–8. doi: 10.1001/jama.2012.12807
13. Jakola AS, Skjulsvik AJ, Myrmel KS, Sjavik K, Unsgard G, Torp SH, et al. Surgical resection versus watchful waiting in low-grade gliomas. *Ann Oncol*. (2017) 28:1942–8. doi: 10.1093/annonc/mdx230
14. Molinaro AM, Hervey-Jumper S, Morshed RA, Young J, Han SJ, Chunduru P, et al. Association of maximal extent of resection of contrast-enhanced and non-contrast-enhanced tumor with survival within molecular subgroups of patients with newly diagnosed Glioblastoma. *JAMA Oncol*. (2020) 6:495–503. doi: 10.1001/jamaoncol.2019.6143
15. Wijnenga MMJ, French PJ, Dubbink HJ, Dinjens WNM, Atmodimedjo PN, Kros JM, et al. The impact of surgery in molecularly defined low-grade Glioma: an integrated clinical, radiological, and molecular analysis. *Neuro Oncol*. (2018) 20:103–12. doi: 10.1093/neuonc/nox176
16. Hervey-Jumper SL, Berger MS. Role of surgical resection in low- and high-grade Gliomas. *Curr Treat Options Neurol*. (2014) 16:284. doi: 10.1007/s11940-014-0284-7
17. Leroy HA, Delmaire C, Le Rhun E, Drumez E, Lejeune JP, Reyns N. High-field intraoperative MRI in Glioma surgery: a prospective study with volumetric analysis of extent of resection and functional outcome. *Neurochirurgie*. (2018) 64:155–60. doi: 10.1016/j.neuchi.2018.02.003
18. Motomura K, Natsume A, Iijima K, Kuramitsu S, Fujii M, Yamamoto T, et al. Surgical benefits of combined awake Craniotomy and intraoperative magnetic resonance imaging for Gliomas Associated with Eloquent Areas. *J Neurosurg*. (2017) 127:790–7. doi: 10.3171/2016.9.JNS16152
19. Mansouri A, Mansouri S, Hachem LD, Klironomos G, Vogelbaum MA, Bernstein M, et al. The role of 5-Aminolevulinic acid in enhancing surgery for high-grade Glioma, its current boundaries, and future perspectives: a systematic review. *Cancer*. (2016) 122:2469–78. doi: 10.1002/cncr.30088
20. Duffau H. Long-term outcomes after supratotal resection of diffuse low-grade Gliomas: a consecutive series with 11-year follow-up. *Acta Neurochir*. (2016) 158:51–8. doi: 10.1007/s00701-015-2621-3
21. Yordanova YN, Moritz-Gasser S, Duffau H. Awake surgery for who Grade II Gliomas within "Noneloquent" areas in the left dominant hemisphere: toward a "Supratotal" resection. Clinical Article. *J Neurosurg*. (2011) 115:232–9. doi: 10.3171/2011.3.JNS101333
22. Yordanova YN, Duffau H. Supratotal resection of diffuse Gliomas - An overview of its multifaceted implications. *Neurochirurgie*. (2017) 63:243–9. doi: 10.1016/j.neuchi.2016.09.006
23. Page MJ, McKenzie JE, Bossuyt PM, Boutron I, Hoffmann TC, Mulrow CD, et al. The Prisma 2020 statement: an updated guideline for reporting systematic reviews. *BMJ*. (2021) 372:n71. Epub 20210329. doi: 10.1136/bmj.n71
24. Sanai N, Berger MS. Glioma extent of resection and its impact on patient outcome. *Neurosurgery*. (2008) 62:753–64; discussion 264–6. doi: 10.1227/01.neu.0000318159.21731.cf
25. Lacroix M, Abi-Said D, Fourney DR, Gokaslan ZL, Shi W, DeMonte F, et al. A multivariate analysis of 416 patients with Glioblastoma Multiforme: prognosis, extent of resection, and survival. *J Neurosurg*. (2001) 95:190–8. doi: 10.3171/jns.2001.95.2.0190
26. Stummer W, Pichlmeier U, Meinel T, Wiestler OD, Zanella F, Reulen HJ, et al. Fluorescence-guided surgery with 5-Aminolevulinic acid for resection of Malignant Glioma: a randomised controlled multicentre Phase III trial. *Lancet Oncol*. (2006) 7:392–401. doi: 10.1016/S1470-2045(06)70665-9
27. Roelz R, Strohmaier D, Jabbarli R, Kraeutle R, Egger K, Coenen VA, et al. Residual tumor volume as best outcome predictor in Low Grade Glioma -

A nine-years near-randomized survey of surgery vs. biopsy. *Sci Rep.* (2016) 6:32286. doi: 10.1038/srep32286
28. van den Bent MJ, Carpentier AF, Brandes AA, Sanson M, Taphoorn MJ, Bernsen HJ, et al. Adjuvant Procarbazine, Lomustine, and Vincristine improves progression-free survival but not overall survival in newly diagnosed Anaplastic Oligodendrogliomas and Oligoastrocytomas: a randomized European Organisation for Research and Treatment of Cancer Phase III Trial. *J Clin Oncol.* (2006) 24:2715–22. doi: 10.1200/JCO.2005.04.6078
29. Kawaguchi T, Sonoda Y, Shibahara I, Saito R, Kanamori M, Kumabe T, et al. Impact of gross total resection in patients with who Grade III Glioma harboring the Idh 1/2 mutation without the 1p/19q co-deletion. *J Neurooncol.* (2016) 129:505–14. doi: 10.1007/s11060-016-2201-2
30. Nomiya T, Nemoto K, Kumabe T, Takai Y, Yamada S. Prognostic significance of surgery and radiation therapy in cases of Anaplastic Astrocytoma: retrospective analysis of 170 cases. *J Neurosurg.* (2007) 106:575–81. doi: 10.3171/jns.2007.106.4.575
31. Hervey-Jumper SL, Berger MS. Evidence for improving outcome through extent of resection. *Neurosurg Clin N Am.* (2019) 30:85–93. doi: 10.1016/j.nec.2018.08.005
32. Ius T, Isola M, Budai R, Pauletto G, Tomasino B, Fadiga L, et al. Low-Grade Glioma Surgery in eloquent areas: volumetric analysis of extent of resection and its impact on overall survival. A single-institution experience in 190 patients: Clinical Article. *J Neurosurg.* (2012) 117:1039–52. doi: 10.3171/2012.8.JNS12393
33. Voets NL, Pretorius P, Birch MD, Apostolopoulos V, Stacey R, Plaha P. Diffusion tractography for awake craniotomy: accuracy and factors affecting specificity. *J Neurooncol.* (2021) 153:547–57. doi: 10.1007/s11060-021-03795-7
34. Sawaya R, Hammoud M, Schoppa D, Hess KR, Wu SZ, Shi WM, et al. Neurosurgical outcomes in a modern series of 400 Craniotomies for treatment of Parenchymal Tumors. *Neurosurgery.* (1998) 42:1044–55; discussion 55–6. doi: 10.1097/00006123-199805000-00054
35. Duffau H, Capelle L. Preferential brain locations of Low-Grade Gliomas. *Cancer.* (2004) 100:2622–6. doi: 10.1002/cncr.20297
36. Sanai N, Mirzadeh Z, Berger MS. Functional outcome after language mapping for glioma resection. *N Engl J Med.* (2008) 358:18–27. doi: 10.1056/NEJMoa067819
37. Duffau H, Peggy Gatignol ST, Mandonnet E, Capelle L, Taillandier L. Intraoperative subcortical stimulation mapping of language pathways in a consecutive series of 115 patients with grade Ii glioma in the left dominant hemisphere. *J Neurosurg.* (2008) 109:461–71. doi: 10.3171/JNS/2008/109/9/0461
38. De Witt Hamer PC, Robles SG, Zwinderman AH, Duffau H, Berger MS. Impact of intraoperative stimulation brain mapping on glioma surgery outcome: a meta-analysis. *J Clin Oncol.* (2012) 30:2559–65. doi: 10.1200/JCO.2011.38.4818
39. Aghi MK, Nahed BV, Sloan AE, Ryken TC, Kalkanis SN, Olson JJ. The role of surgery in the management of patients with diffuse low grade glioma: a systematic review and evidence-based clinical practice guideline. *J Neurooncol.* (2015) 125:503–30. doi: 10.1007/s11060-015-1867-1
40. Buckner J, Giannini C, Eckel-Passow J, Lachance D, Parney I, Laack N, et al. Management of diffuse low-grade gliomas in adults - use of molecular diagnostics. *Nat Rev Neurol.* (2017) 13:340–51. doi: 10.1038/nrneurol.2017.54
41. Duffau H. Stimulation mapping of white matter tracts to study brain functional connectivity. *Nat Rev Neurol.* (2015) 11:255–65. doi: 10.1038/nrneurol.2015.51
42. De Benedictis A, Moritz-Gasser S, Duffau H. Awake mapping optimizes the extent of resection for low-grade gliomas in eloquent areas. *Neurosurgery.* (2010) 66:1074–84; discussion 84. doi: 10.1227/01.NEU.0000369514.74284.78
43. Chang EF, Clark A, Smith JS, Polley MY, Chang SM, Barbaro NM, et al. Functional mapping-guided resection of low-grade gliomas in eloquent areas of the brain: improvement of long-term survival. *Clinical Article. J Neurosurg.* (2011) 114:566–73. doi: 10.3171/2010.6.JNS091246
44. Nossek E, Matot I, Shahar T, Barzilai O, Rapoport Y, Gonen T, et al. Intraoperative seizures during awake craniotomy: incidence and consequences: analysis of 477 patients. *Neurosurgery.* (2013) 73:135–40; discussion 40. doi: 10.1227/01.neu.0000429847.91707.97
45. Gonen T, Grossman R, Sitt R, Nossek E, Yanaki R, Cagnano E, et al. Tumor location and Idh1 mutation may predict intraoperative seizures during awake craniotomy. *J Neurosurg.* (2014) 121:1133–8. Epub 20140829. doi: 10.3171/2014.7.JNS132657
46. Stevanovic A, Rossaint R, Veldeman M, Bilotta F, Coburn M. Anaesthesia management for awake craniotomy: systematic review and meta-analysis. *PLoS ONE.* (2016) 11:e0156448. doi: 10.1371/journal.pone.0156448
47. Brown T, Shah AH, Bregy A, Shah NH, Thambuswamy M, Barbarite E, et al. Awake craniotomy for brain tumor resection: the rule rather than the exception? *J Neurosurg Anesthesiol.* (2013) 25:240–7. doi: 10.1097/ANA.0b013e318290c230
48. Mandonnet E, Nouet A, Gatignol P, Capelle L, Duffau H. Does the left inferior longitudinal fasciculus play a role in language? A brain stimulation study. *Brain.* (2007) 130(Pt 3):623–9. doi: 10.1093/brain/awl361
49. Chang EF, Breshears JD, Raygor KP, Lau D, Molinaro AM, Berger MS. Stereotactic probability and variability of speech arrest and anomia sites during stimulation mapping of the language dominant hemisphere. *J Neurosurg.* (2017) 126:114–21. doi: 10.3171/2015.10.JNS151087
50. Whittle IR, Midgley S, Georges H, Pringle AM, Taylor R. Patient perceptions of "Awake" brain tumour surgery. *Acta Neurochir.* (2005) 147:275–7; discussion 7. doi: 10.1007/s00701-004-0445-7
51. Manninen PH, Balki M, Lukitto K, Bernstein M. Patient satisfaction with awake craniotomy for tumor surgery: a comparison of remifentanil and fentanyl in conjunction with propofol. *Anesth Analg.* (2006) 102:237–42. doi: 10.1213/01.ANE.0000181287.86811.5C
52. Nossek E, Matot I, Shahar T, Barzilai O, Rapoport Y, Gonen T, et al. Failed awake craniotomy: a retrospective analysis in 424 patients undergoing craniotomy for brain tumor. *J Neurosurg.* (2013) 118:243–9. doi: 10.3171/2012.10.JNS12511
53. Motomura K, Chalise L, Ohka F, Aoki K, Tanahashi K, Hirano M, et al. Supratotal resection of diffuse frontal lower grade gliomas with awake brain mapping, preserving motor, language, and neurocognitive functions. *World Neurosurg.* (2018) 119:30–9. doi: 10.1016/j.wneu.2018.07.193
54. Pallud J, Varlet P, Devaux B, Geha S, Badoual M, Deroulers C, et al. Diffuse low-grade oligodendrogliomas extend beyond mri-defined abnormalities. *Neurology.* (2010) 74:1724–31. doi: 10.1212/WNL.0b013e3181e04264
55. Shah AH, Mahavadi A, Di L, Sanjurjo A, Eichberg DG, Borowy V, et al. Survival benefit of lobectomy for glioblastoma: moving towards radical supramaximal resection. *J Neurooncol.* (2020) 148:501–8. Epub 20200705. doi: 10.1007/s11060-020-03541-5
56. Sarubbo S, De Benedictis A, Maldonado IL, Basso G, Duffau H. Frontal terminations for the inferior Fronto-occipital fascicle: anatomical dissection, Dti study and functional considerations on a multi-component bundle. *Brain Struct Funct.* (2013) 218:21–37. doi: 10.1007/s00429-011-0372-3
57. Martino J, Brogna C, Robles SG, Vergani F, Duffau H. Anatomic dissection of the inferior fronto-occipital fasciculus revisited in the lights of brain stimulation data. *Cortex.* (2010) 46:691–9. doi: 10.1016/j.cortex.2009.07.015
58. Maldonado IL, Moritz-Gasser S, Duffau H. Does the left superior longitudinal fascicle subserve language semantics? A brain electrostimulation study. *Brain Struct Funct.* (2011) 216:263–74. doi: 10.1007/s00429-011-0309-x
59. Catani M, Robertsson N, Beyh A, Huynh V, de Santiago Requejo F, Howells H, et al. Short parietal lobe connections of the human and monkey brain. *Cortex.* (2017) 97:339–57. doi: 10.1016/j.cortex.2017.10.022
60. Yamaguchi J, Motomura K, Ohka F, Aoki K, Tanahashi K, Hirano M, et al. Survival benefit of supratotal resection in a long-term survivor of IDH-wildtype glioblastoma: a case report and literature review. *NMC Case Rep J.* (2021) 8:747–53. doi: 10.2176/nmccrj.cr.2021-0120
61. Eyupoglu IY, Hore N, Merkel A, Buslei R, Buchfelder M, Savaskan N. Supra-complete surgery via dual intraoperative visualization approach (Diva) prolongs patient survival in glioblastoma. *Oncotarget.* (2016) 7:25755–68. doi: 10.18632/oncotarget.8367
62. Li YM, Suki D, Hess K, Sawaya R. The influence of maximum safe resection of glioblastoma on survival in 1229 Patients: can we do better than gross-total resection? *J Neurosurg.* (2016) 124:977–88. doi: 10.3171/2015.5.JNS142087
63. Esquenazi Y, Friedman E, Liu Z, Zhu JJ, Hsu S, Tandon N. The survival advantage of "supratotal" resection of glioblastoma using selective cortical mapping and the subpial technique. *Neurosurgery.* (2017) 81:275–88. doi: 10.1093/neuros/nyw174
64. Glenn CA, Baker CM, Conner AK, Burks JD, Bonney PA, Briggs RG, et al. An examination of the role of supramaximal resection of

temporal lobe glioblastoma multiforme. *World Neurosurg.* (2018) 114:e747–55. doi: 10.1016/j.wneu.2018.03.072
65. Pessina F, Navarria P, Cozzi L, Ascolese AM, Simonelli M, Santoro A, et al. Maximize surgical resection beyond contrast-enhancing boundaries in newly diagnosed glioblastoma multiforme: is it useful and safe? A single institution retrospective experience. *J Neurooncol.* (2017) 135:129–39. doi: 10.1007/s11060-017-2559-9
66. Grossman R, Shimony N, Shir D, Gonen T, Sitt R, Kimchi TJ, et al. Dynamics of flair volume changes in glioblastoma and prediction of survival. *Ann Surg Oncol.* (2017) 24:794–800. doi: 10.1245/s10434-016-5635-z
67. Duffau H. Awake surgery for incidental who grade II gliomas involving eloquent areas. *Acta Neurochir.* (2012) 154:575–84; discussion 84. doi: 10.1007/s00701-011-1216-x
68. Lima GLO, Dezamis E, Corns R, Rigaux-Viode O, Moritz-Gasser S, Roux A, et al. Surgical resection of incidental diffuse gliomas involving eloquent brain areas. Rationale, functional, epileptological and oncological outcomes. *Neurochirurgie.* (2017) 63:250–8. doi: 10.1016/j.neuchi.2016.08.007
69. Lima GL, Duffau H. Is there a risk of seizures in "preventive" awake surgery for incidental diffuse low-grade gliomas? *J Neurosurg.* (2015) 122:1397–405. doi: 10.3171/2014.9.JNS141396
70. Rossi M, Gay L, Ambrogi F, Nibali MC, Sciortino T, Puglisi G, et al. Association of supratotal resection with progression-free survival, malignant transformation, and overall survival in lower-grade gliomas. *Neuro Oncol.* (2021) 23:812–26. doi: 10.1093/neuonc/noaa225
71. van den Bent MJ, Brandes AA, Taphoorn MJ, Kros JM, Kouwenhoven MC, Delattre JY, et al. Adjuvant procarbazine, lomustine, and vincristine chemotherapy in newly diagnosed anaplastic oligodendroglioma: long-term follow-up of Eortc brain tumor group study 26951. *J Clin Oncol.* (2013) 31:344–50. doi: 10.1200/JCO.2012.43.2229
72. Motomura K, Chalise L, Ohka F, Aoki K, Tanahashi K, Hirano M, et al. Impact of the extent of resection on the survival of patients with grade II and III gliomas using awake brain mapping. *J Neurooncol.* (2021) 153:361–72. doi: 10.1007/s11060-021-03776-w

Conflict of Interest: The authors declare that the research was conducted in the absence of any commercial or financial relationships that could be construed as a potential conflict of interest.

Publisher's Note: All claims expressed in this article are solely those of the authors and do not necessarily represent those of their affiliated organizations, or those of the publisher, the editors and the reviewers. Any product that may be evaluated in this article, or claim that may be made by its manufacturer, is not guaranteed or endorsed by the publisher.

frontiers | Frontiers in Neurology

ORIGINAL RESEARCH
published: 03 June 2022
doi: 10.3389/fneur.2022.867048

Neuroplasticity Mechanisms in Frontal Brain Gliomas: A Preliminary Study

Micaela Mitolo[1,2†], Matteo Zoli[3,4†], Claudia Testa[1,5], Luca Morandi[1,4], Magali Jane Rochat[1], Fulvio Zaccagna[1,4], Matteo Martinoni[6], Francesca Santoro[7], Sofia Asioli[4,8], Filippo Badaloni[6], Alfredo Conti[4,6], Carmelo Sturiale[6], Raffaele Lodi[1,4], Diego Mazzatenta[3,4‡] and Caterina Tonon[1,4‡]*

[1] Functional and Molecular Neuroimaging Unit, IRCCS Istituto delle Scienze Neurologiche di Bologna, Bologna, Italy, [2] Department of Experimental, Diagnostic and Specialty Medicine, University of Bologna, Bologna, Italy, [3] Pituitary Unit, IRCCS Istituto delle Scienze Neurologiche di Bologna, Bologna, Italy, [4] Department of Biomedical and Neuromotor Sciences, University of Bologna, Bologna, Italy, [5] Department of Physics and Astronomy, University of Bologna, Bologna, Italy, [6] Neurosurgery Unit, IRCCS Istituto delle Scienze Neurologiche di Bologna, Bologna, Italy, [7] Neurology Unit, IRCCS Istituto delle Scienze Neurologiche di Bologna, Bologna, Italy, [8] Anatomic Pathology Unit, IRCCS Istituto delle Scienze Neurologiche di Bologna, Bologna, Italy

OPEN ACCESS

Edited by:
Graziano Serrao, University of Milan, Italy

Reviewed by:
Edgar G. Ordóñez-Rubiano, Hospital de San José - Sociedad de Cirugía de Bogotá, Colombia
domenico D'Avella, University of Padua, Italy

***Correspondence:**
Caterina Tonon
caterina.tonon@unibo.it

[†] These authors have contributed equally to this work and share first authorship
[‡] These authors have contributed equally to this work and share last authorship

Specialty section:
This article was submitted to Applied Neuroimaging, a section of the journal Frontiers in Neurology

Received: *31 January 2022*
Accepted: *11 April 2022*
Published: *03 June 2022*

Citation:
Mitolo M, Zoli M, Testa C, Morandi L, Rochat MJ, Zaccagna F, Martinoni M, Santoro F, Asioli S, Badaloni F, Conti A, Sturiale C, Lodi R, Mazzatenta D and Tonon C (2022) Neuroplasticity Mechanisms in Frontal Brain Gliomas: A Preliminary Study. Front. Neurol. 13:867048. doi: 10.3389/fneur.2022.867048

Background: Pathological brain processes may induce adaptive cortical reorganization, however, the mechanisms underlying neuroplasticity that occurs in the presence of lesions in eloquent areas are not fully explained. The aim of this study was to evaluate functional compensatory cortical activations in patients with frontal brain gliomas during a phonemic fluency task and to explore correlations with cognitive performance, white matter tracts microstructural alterations, and tumor histopathological and molecular characterization.

Methods: Fifteen patients with frontal glioma were preoperatively investigated with an MRI study on a 3T scanner and a subgroup underwent an extensive neuropsychological assessment. The hemispheric laterality index (LI) was calculated through phonemic fluency task functional MRI (fMRI) activations in the frontal, parietal, and temporal lobe parcellations. Diffusion-weighted images were acquired for all patients and for a group of 24 matched healthy volunteers. Arcuate Fasciculus (AF) and Frontal Aslant Tract (FAT) tractography was performed using constrained spherical deconvolution diffusivity modeling and probabilistic fiber tracking. All patients were operated on with a resective aim and underwent adjuvant therapies, depending on the final diagnosis.

Results: All patients during the phonemic fluency task fMRI showed left hemispheric dominance in temporal and parietal regions. Regarding frontal regions (i.e., frontal operculum) we found right hemispheric dominance that increases when considering only those patients with tumors located on the left side. These latter activations positively correlate with verbal and visuo-spatial short-term memory, and executive functions. No correlations were found between the left frontal operculum and cognitive performance. Furthermore, patients with *IDH-1* mutation and without *TERT* mutation, showed higher rightward frontal operculum fMRI activations and better cognitive performance in tests measuring general cognitive abilities, semantic fluency, verbal short-term memory, and

executive functions. As for white matter tracts, we found left and right AF and FAT microstructural alterations in patients with, respectively, left-sided and right-side glioma compared to controls.

Conclusions: Compensatory cortical activation of the corresponding region in the non-dominant hemisphere and its association with better cognitive performance and more favorable histopathological and molecular tumor characteristics shed light on the neuroplasticity mechanisms that occur in the presence of a tumor, helping to predict the rate of post-operative deficit, with the final goal of improving patients'quality of life.

Keywords: frontal gliomas, neurosurgery, neuroplasticity, task fMRI, arcuate fasciculus (AF), frontal aslant tract

INTRODUCTION

Neuroplasticity can be defined as the ability of the nervous system to respond to intrinsic or extrinsic stimuli by reorganizing its structure, function, and connections (1). It is a central theme in neuro-oncology and is currently receiving increased attention (2). Several previous studies have suggested that the brain is capable of remodeling itself in the presence of glioma, and it is believed that these changes occur continuously throughout life (3).

Surgery in the proximity of eloquent brain regions for language is burdened by a significant risk of post-operative speech impairment, up to complete aphasia. Therefore, the most accurate pre-operative localization of these areas and their relationship with the tumor is needed to achieve the maximal safe resection, which consists of the removal of the glioma as largest as possible with minimal risks of permanent language deficits in order to ensure a satisfactory patients' quality of life (4, 5).

Although not all brain regions functional for language have been fully delineated and mapped; in the adult healthy brain, hemispheric lateralization and specific eloquent areas have been well-defined (6). Indeed, since the pioneeristic studies by Broca and Wernicke, and afterward confirmed by multiple other investigations, three main brain areas have been identified: the inferior frontal lobe, the superior temporal lobe, and the insula (7–9).

Pathological brain processes, such as intra-axial tumors, may induce cortical reorganization over time, due to plasticity phenomena (10–14). However, these mechanisms are not fully explained. Shedding light on the potential neuroplasticity of a given brain structure or network may be fundamental for the neurosurgical procedure. During the preoperative period, compensatory brain reorganization may limit/delay the severity/onset of functional deficits, and similarly, postoperative plasticity can help recover from potential deficits associated with the possible removal of still-functional brain areas [e.g., (15, 16)]. In this contest, a complete neuropsychological assessment plays an important role, helping to determine the extent of the "initial" neurological deficit and subsequently document the degree of functional recovery (3).

At the molecular level, single-cell genetic and epigenetic analysis, one study (17) revealed that early genetic alterations were associated with DNA methylation modifications which cause altered cellular states that overcome cell stress, increase cellular plasticity, and ultimately enhance treatment resistance.

This study aimed to evaluate functional compensatory cortical activations in patients with frontal brain gliomas during a phonemic fluency task and to explore correlations with cognitive performance, white matter tracts microstructural alterations, and histopathological and molecular characterization with the main goal of defining a surgical paradigm that may maximize the extension of tumor removal when contralateral compensatory mechanism is present.

MATERIALS AND METHODS

Participants

A total of 15 patients (mean age: 46.24 ± 16.37 years; 10 M; 14 right-handed and one ambidextrous, monolingual native speaker Italian) with frontal intra-axial tumors operated in our Institution from September 2019 to June 2021 have been prospectively collected. In all patients with left-sided glioma ($N = 10$), the tumor presented an intimal spatial relationship with the frontal aslant tract (FAT). For six of these patients, the tumor was also in close relationship with the arcuate fasciculus (AF), and for four of them were adjacent to the frontal operculum. Inclusion criteria were as follows: age ≥18 years; the presence of a frontal intra-axial lesion in a language-related area; and planned surgery with resective aim. Exclusion criteria were as follows: absence of histological demonstration of glioma; previous resective brain surgery or radiation or medical oncological treatment; and biopsy (open or stereotactic frameless) not followed by surgery. Demographic and clinical features are reported in **Table 1**; a frequency map of tumor distribution is reported in **Supplementary Materials**.

As controls, a cohort of 24 healthy volunteers (mean age: 46 ± 15.9 years; 12 M; 23 right-handed and one ambidextrous) monolingual native speakers of Italian was also recruited for this study (**Table 2**). Healthy controls were selected from the database of the Neuroimaging Laboratory, designed to collect normative values of quantitative MR parameters for clinical and research purposes.

The study was approved by the Local Ethical Committee (183/2019/OSS/AUSLBO – 19027 (20/03/19), and written informed consent was obtained from all participants.

TABLE 1 | Demographic and clinical features of patients with frontal intra-axial tumor.

Patient	Age (years)	Sex	Education (years)	EHI	Tumor location	Tumor volume (cm^3)	Tumor grade	Histopathology	Genetic analysis	*MGMT* methylation status
F_L_III	58	M	13	0.68	Left -IFG,MFG, SFG	18.08	3	Anaplastic oligodendroglioma	*IDH1 p.R132H; Del1p19q*	Methylated
F_L_IV	40	F	NA	NA	Left -SMA	10.12	4	Glioblastoma	*IDH1-2:WT; TERT C205T*	Unmethylated
F_L_II	30	F	13	1	Left -IFG,MFG, SFG	22.05	2	Diffuse astrocytoma	*IDH1 p.R132H*	Unmethylated
F_L_II	40	M	18	0.89	Left IFG, MFG, Insula	114.09	2	Astrocytoma	*IDH1 p.R132H*	Methylated
F_R_II	38	F	11	1	Right IFG, Insula	29.34	2	Oligodendroglioma	*IDH1 p.R132H; Del1p19q*	Methylated
F_L_IV	41	M	19	0.78	Left -IFG,MFG, SFG	55.85	4	Glioblastoma	*IDH1 p.R132H*	Methylated
F_L_II	38	F	18	0.89	Left- SFG	37.37	2	Diffuse astrocytoma	*IDH1 p.R132H*	Unmethylated
F_L_III	55	M	13	0.84	Left- SMA	46.2	3	Oligodendroglioma	*IDH1 p.R132H; TERT C228T; Del1p19q*	Methylated
F_R_III	54	M	8	0.89	Right- Motor Area	75.66	3	Anaplastic astrocytoma	*IDH1 p.R132H*	Methylated
F_R_IV	47	F	8	0.89	Right- Motor Area (subcortical)	N/A	4	Glioblastoma	*IDH1-2 WT; TERT C205T*	Unmethylated
F_L_II	25	M	11	1	Left- IFG	9.07	2	Diffuse astrocytoma	*IDH1 p.R132H*	Methylated
F_R_III	37	M	18	0.95	Right-SMA	35.92	3	Diffuse astrocytoma	*IDH1 p.R132H*	Methylated
F_L_III	50	M	21	−0.37	Left IFG, Insula	141.47	3	Oligodendroglioma	*IDH1 p.R132H;TERT C228T; Del 1p19q*	Methylated
F_L_IV	65	M	10	1	Left-SMA	37.03	4	Glioblastoma	*IDH1: WT; TERT C228T*	Methylated
F_R_II	76	M	8	0.95	Right IFG, MFG, Insula	116.55	2	Oligodendroglioma	*IDH1 p.R132H; TERT C228T; Del1p19q*	Methylated

In the first column, patients are labeled according to the tumor's (lobe)_(hemisphere)_(grade). NA, not available. EHI, Edinburgh Handedness Inventory (scores between −1 and −0.5 were considered indices of left-handedness; right-handedness was defined by scores between 0.5 and 1; and scores between −0.5 and 0.5 indicated ambidextrousness). IFG, inferior frontal gyrus; MFG, middle frontal gyrus; SFG, superior frontal gyrus; SMA, supplementary motor area.

TABLE 2 | Demographic features of healthy control (HC).

HC	Age (years)	Sex	Education (years)	EHI
$N = 24$	46 ± 16.37	$N = 12$ males $N = 12$ females	19.50 ± 4.49	$N = 23$ left-handedness $N = 1$ ambidextrousness

Mean ± standard deviations are shown. EHI, Edinburgh Handedness Inventory (scores between −1 and −0.5 were considered indices of left-handedness; right-handedness was defined by scores between 0.5 and 1, and scores between −0.5 and 0.5 indicated ambidextrousness).

Pre-surgery Protocol

Neurological and Neurophysiological Evaluation

Initially, the medical history of all 15 patients was collected with specific attention to neurological symptoms and signs, with a focus on possible language impairments, such as aphasia, anomia, paraphasia, or grammatical or syntactic mistakes. In addition, a complete neurophysiological assessment, including somatosensorial, motor, and brainstem auditory evoked responses was performed 24 h before surgery.

Neuropsychological Assessment

Years of education, and handedness dominance using the Edinburgh Handedness Inventory (EHI), were calculated in all patients (18). EHI scores between −1 and 0.5 were considered indices of left-handedness, right-handedness was defined by scores between 0.5 and 1, and scores between −0.5 and 0.5 indicated ambidextrousness.

A subgroup of patients ($N = 10$) also underwent an extensive neuropsychological evaluation with a standardized neuropsychological battery that included the following tests: a general screening test [Mini-Mental State Examination MMSE, (19)] and a non-verbal test of general intelligence [Raven's Colored Progressive Matrices CPM'47, (20)]; language skills were assessed using a naming test [The Boston Naming Test short 30-items version, (21, 22)], a Phonemic Verbal Fluency Test (23) and a Category Fluency Test (24). Short-term verbal memory and episodic memory were assessed using the Digit Span forward test (25) and the immediate and delayed recall of Babcock Story Recall Test (BSRT), (26, 27); instead, visuo-spatial short-term memory span and visuo-spatial long-term memory were investigated using, respectively, the Corsi's Block Test (25) and the delayed recall of the Rey–Osterrieth complex figure [ROCF, (28)]. The copy of ROCF further explored the patients' visuo-constructive and planning abilities. Attention and executive functions were first assessed by a general screening test of frontal functions [i.e., Frontal Assessment Battery, FAB, (29); Italian version (30)], then the Stroop test (31), the Digit Span Backward (32), and The Trail Making Test A and B (TMT) (33) were also administrated (**Table 3**).

Furthermore, the severity of depression and anxiety symptoms were evaluated using Beck Depression Inventory (BDI-II, (37) and the State-Trait Anxiety Inventory [STAI-Y, (38)]. Finally, the Cognitive Reserve Index [CRI, (39)] and The Short Form (39) Health Survey [Sf-36, (40)] were also administrated.

Brain MRI Acquisition Protocol

The MRI protocol was performed in all patients within 20 ± 22 days (mean ± standard deviation) from surgery using a high-field Siemens MAGNETOM Skyra 3T MRI scanner equipped with a head–neck high-density (64 channels) array coil.

The MRI protocol included T1-weighted 3D Magnetization-Prepared Rapid Gradient-Echo Imaging sequence [MPRAGE, 176 continuous sagittal slices, 1-mm isotropic voxel, no slice gap, echo time (TE) = 2.98 ms, repetition time (TR) = 2,300 ms, Inversion Time (IT) = 900 ms, flip angle = 9°, acquisition matrix = 256 × 256, pixel bandwidth = 240 Hz, in-plane acceleration factor = 2, duration ∼5 min] and T2-weighted 3D fluid-attenuated inversion recovery (FLAIR) sequence (SPACE, 176 sagittal acquisition slices, 1-mm isotropic voxel, no slice gap, TE = 428 ms, TR = 5,000 ms, IT = 1,800 ms, flip angle = 120°, acquisition matrix = 256 × 256, pixel bandwidth = 780 Hz, in-plane acceleration factor = 2, duration ∼5 min). In patients, 3D T1-weighted MPRAGE images were also acquired after gadolinium administration (0.1 mmol/kg).

Functional MRI (fMRI)

In order to assess hemispheric language laterality, the neural correlates of verbal fluency were elicited via a phonemic fluency task with a block design. In order to ensure good understanding and performance of the required task, all patients underwent, before the MRI exam, a training session to familiarize themselves with the same neuropsychologists (MM and MJR) that administrated the neuropsychological battery.

Functional MRI was based on a 2D T2*-weighted gradient echo-planar imaging (EPI) sequence sensitive to blood oxygenation level-dependent contrast. Single-shot EPI sequence (56 continuous axial slices, 2.5-mm isotropic voxel, no slice gap, TE = 37 ms, TR = 735 ms, flip angle = 53°, acquisition matrix = 94 × 94, pixel bandwidth = 2,130 Hz, no in-plane acceleration, multiband acceleration factor = 8, phase encoding AP, duration ∼5 min). The block design consisted of alternated resting and active blocks, each lasting 30 s, starting and ending with the resting condition (five resting blocks and four active task blocks in total). The active task blocks were composed of acoustic cues delivered at 5-s intervals through MR-compatible earphones that isolated the background MRI noise. During active cycles of phonemic fluency, the acoustic cue stimulus was a letter of the alphabet, delivered every 5 s. After the presentation of the cue, subjects were prompted to covertly generate (i.e., think about) a noun starting with the given letter. Subjects were previously instructed to generate as many nouns as possible within the time lapse between stimuli but not to generate proper names or names of places (cities/lands/continents). During resting blocks, continuous white noise was delivered, and patients were instructed to lie quietly during the scan without active thinking (41).

Diffusion Tensor Imaging (DTI)

For tractography analyses a high angular resolution diffusion imaging protocol was acquired with b-value = 2.000 s/mm^2 along 64 diffusion gradient directions, and five volumes without diffusion weighting, based on a 2D single-shot EPI sequence [87

TABLE 3 | Neuropsychological corrected scores and correlations with cortical fMRI activations and DTI measures.

		Patients							*N*	Score (mean)	Sd	Normal values cut offs	% pathological scores	Correlations with right frontal operculum		Correlations with left DTI measures	
		F_L_III	F_L_II	F_L_II	F_L_III	F_L_II	F_L_III	F_L_IV	7					*P-value*	*r*	*P-value*	*r*
	Age (years)	58	30	40	55	25	50	65		46	15.03						
	Education (years)	13	13	18	13	11	21	10		14	3.93						
	Sex	M	F	M	M	M	M	M									
	Clinical tests																
Cognitive screening	MMSE score	28.14	30	26.99	30	30	30	22.11	7	28.18	2.93	≥23.8 (34)	14%				
Non-verbal Intelligence	CPM-47	28.6	36	36	30.3	27.53	36	NA	6	32.41	4.04	≥18.96 (23)	0%				
Executive functions	FAB	NA	NA	NA	18	16.08	18	14.12	4	16.55	1.86	≥13.5 (30)	0%				
	Digit Span Backward	NA	NA	5	NA	5	3	3	4	4.00	1.15	≥3	0%	0.074*	0.902		
	Stroop test (RT-sec)	32.28	5.5	14	10.66	14.59	19.55	121.7	7	31.18	40.79	≤36.91 (31)	14%	0.074*	−0.910		
Verbal memory	BSRT_total items recalled	12.8	14.1	5.13	12.45	12.21	16	7.9	7	11.51	3.73	≥4.75 (26)	0%				
	Digit span forward	5.75	5.5	6.19	6.75	5.6	4.13	4.05	7	5.42	1.00	≥3.75 (35)	0%				
Visuo-spatial memory	Corsi's block test	3.75	5.75	5.5	5.75	4.5	3.5	3	7	4.54	1.15	≥3.75 (26)	29%	0.017*	0.954	0.043* (AF)	0.899
	ROCF_delayed recall	12.85	19	NA	18.25	2.42	20.56	19.1	6	15.36	6.88	≥9.47 (31)	17%				
Language	Associative fluency test	37.1	25.8	26.25	42.8	47.92	25.18	19.68	7	32.10	10.53	≥17.35 (23)	0%				
	Category words fluency test	51.6	47.5	35.88	63	33.5	31.38	17.4	7	40.04	15.08	≥25 (24)	14%				
	BNT-short version	30	30	NA	30		30	28	5	29.60	0.89	≥21	0%				
Attention	Trail making test_A	19.2	40	NA	10	28.92	38.5	146.8	6	47.24	50.10	≤93 s (36)	17%				
	Trail making test_B	58.22	82	NA	46	93.2	125.25	484.4	6	148.18	167.04	≤282 s (36)	17%				
	Trail making test_B-A	39.02	42	NA	36	63.8	86.75	337.6	6	100.86	117.57	≤186 s (36)	17%				
Visuoconstructional abilities	ROCF_copy	36	36	NA	36	36	30.38	35.2	6	34.93	2.25	≥ 28,88 (31)	0%			0.944* (FAT)	0.037

*NA, not available; MMSE, Mini-Mental State Examination; FAB, Frontal Assessment Battery; RT-sec, Reaction time, seconds; BSRT, Babcock Story Recall Test; ROCF, Rey-Osterrieth complex figure; BNT-short version, The Boston Naming Test short 30-items version; *p < 0.05, (FDR) < 1.*

continuous axial slices, 2-mm isotropic voxel, no slice gap, TE = 98 ms, TR = 4,300 ms, flip angle = 90°, acquisition matrix = 110 × 110, pixel bandwidth = 1,820 Hz, in-plane acceleration factor = 2, multiband acceleration factor = 3, phase encoding anterior–posterior (AP), duration ∼8 min]. To correct EPI distortion artifacts in the diffusion-weighted scan, an additional sequence of three null b-value volumes was acquired immediately prior to the full diffusion data set, with the same acquisition geometry and timing parameters but inverted phase encoding [posterior–anterior (PA)].

Brain MRI Analysis Protocol

Functional MRI

The fMRI processing pipeline was created using FSL software (https://fsl.fmrib.ox.ac.uk/fsl/fslwiki) (42). Images were skull-stripped using the FSL-bet function and motion correction was performed with the tool "motion correction of functional images using the linear image registration" (FSL-MCFLIRT). Using the output of FSL-MCFLIRT, an automatic pipeline has been developed for quality control of fMRI images: GE-EPI volumes that are displaced more than 1.5 mm in one of the three spatial directions and rotated more than 1.5° around the three spatial axes with respect to the central volume of the temporal fMRI series, are detected. A successive visual inspection was performed to define the number of volumes and the number of contiguous volumes characterized by this motion. Spatial smoothing was performed using a full width at half maximum (FWHM) Gaussian kernel of 5 mm. High-pass filtering of task-based fMRI time series was performed with a threshold of 60 s. FSL-epi_reg permitted registration between structural and functional images. Language-based fMRI data were processed using the FSL-FEAT GUI (FMRI Expert Analysis Tool) (43). Task and rest cycles in block conditions were convolved with the hemodynamic response function to generate the general linear model (GLM). For each subject, fixed-effect GLM was performed using a threshold of $z \geq 3.1$, and then cluster-extent-based thresholding was used, setting $p < 0.05$.

In order to evaluate a hemispheric laterality index (LI), the fMRI activation regions obtained were masked with bilateral ROIs to evaluate activations in selected language areas. Frontal, parietal, and temporal Regions of Interest (ROIs) were extracted from the cortical Harvard–Oxford atlas: frontal ROIs included the inferior frontal gyrus, pars triangularis, pars opercularis, and the frontal operculum; parietal ROIs included the angular gyrus and the posterior supramarginal gyrus; temporal ROIs included the posterior portion of both superior and medial temporal gyri. fMRI activations were non-linearly registered to the MNI-152 space, using the warp field defined by FSL-FEAT. FMRI activation maps registered to the MNI-152 space were thresholded at $Z > 3.1$ and then masked for each subject using the previously defined bilateral frontal, parietal, and temporal areas. The number of activated fMRI voxels was evaluated within each area. The LI was calculated according to the following formula: LI = (Left – Right)/(Left + Right), where "Left" and "Right" indicate the number of voxels activated within the left and right homologous areas, respectively.

These ROIs were investigated on the basis of previous studies (44, 45), and this analysis aims to robustly extract a laterality activation index in each lobe and quantify the reorganization of brain activity in the presence of tumors.

Tractography

Diffusion-weighted images were skull-stripped using the FSL-bet function, image denoising was performed with the MRtrix3-dwidenoise function (https://www.mrtrix.org), using a principal component analysis approach. Susceptibility-related distortions in the EPI acquisition were estimated using the FSL-topup function; subsequently, a combined correction for susceptibility, eddy-current effects, and signal dropout, most commonly induced by subject movement, was performed for the FSL-topup estimates. The FSL-dtifit function was used to model diffusivity along the spatial eigenvectors using the tensor model, obtaining the fractional anisotropy (FA) and mean diffusivity (MD) maps. The tractography pipeline was fully automatized. High-order fiber modeling was used to evaluate crossing fibers, and a probabilistic streamline propagation approach was adopted. ROIs defined in the Montreal Neurological Institute (MNI)-152 space were non-linearly registered (FSL-fnirt function) for subject T1-weighted images. The T1-weighted images were then registered to the diffusion-weighted images using the FSL-epi_reg function, which aligns images, simultaneously correcting for distortions using gray–white intensity contrast. To bilaterally reconstruct the arcuate fasciculus (AF) a previously validated seed target approach was used (46); the same approach was used for the frontal aslant tract, (FAT) considering the Supplementary Motor Area (SMA) as seed mask according to the Harvard–Oxford probabilistic atlas and the Brodmann's area 44 (BA 44) as target mask both thresholded at 25% of subject probability. A midsagittal exclusion ROI was defined at MNI-152 space X = 0.

Constrained spherical deconvolution diffusion modeling and probabilistic tractography were performed (tckgen ifod2- Mrtrix3) in native diffusion space, into which the tractography ROIs defined in MNI-152 space were non-linearly registered. Tractography results were thresholded at 10% of the maximum connectivity within each voxel, to reduce false-positive artifactual reconstructions. Subsequently, along-tract mapping and statistical calculations were performed in MNI-152 space. AF and FAT tractographic reconstructions and DTI maps were linearly aligned to the MNI-152 space (FSL-flirt, allowing 12 degrees of freedom). A linear registration approach was preferred to preserve the native tract bundle geometry, allowing comparisons of patients and healthy controls in a common space. The SurfIce software (https://www.nitrc.org/plugins/mwiki/index.php/surfice:MainPage) was used for the projection of voxel-wise data onto a surface mesh and to display the reconstruction of tracts and the segmentation of tumor volume in three dimensions (i.e., see an example of one patient with left frontal glioblastoma grade IV) (**Figure 1**).

Tumor Segmentation

A neuroradiologist (FZ, with 10 years of experience in neuroimaging) who was blind to the history of each patient and tumor final diagnosis outlined the ROIs on the unenhanced 3D

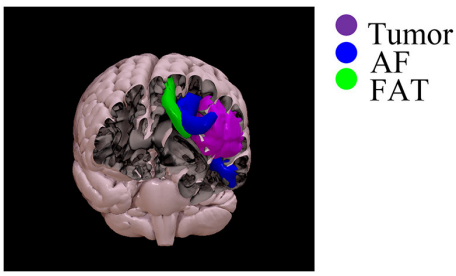

FIGURE 1 | Three-dimensional rendering of the reconstruction of the AF (blue), FAT (green), and tumor segmentation (violet) in the same patient with left frontal glioblastoma grade 4.

T2- weighted FLAIR sequence using an open-source dedicated software (ITK-SNAP v3.6; www.itksnap.org). 3D T1-weighted Fast Spoiled Gradient echo acquisition (FSPGR) acquired before and after gadolinium administration, when available, were also displayed alongside FLAIR images to facilitate the segmentation. 3D manual segmentation of the lesions was performed using the three planes at the same time (axial, coronal, and sagittal). Lesions' boundaries were defined according to the extent of the hyperintensity on FLAIR images; inclusion of the enhancing lesion, if present, was confirmed by overlaying the ROIs on the corresponding FSPGR obtained after gadolinium administration.

For subsequent analysis, the segmentation masks were saved in nifti format and the volumes exported in an excel spreadsheet (**Table 1**).

Brain Tumor Surgery

Surgery was performed with a resective aim through a craniotomy targeted at the tumor extension. Intraoperative neurophysiological monitoring was used in all cases, and, when indicated, an awake setting using specific language tests [i.e., Boston Naming Test (21) and selected items of the Aachen Apahsia test (AAT) (47) chosen case-by-case] was adopted (we opted for the sleeping-awake-sleeping technique). Anesthesia was performed consequently, avoiding the use of myorelaxant.

All surgeries were performed with neuronavigational guidance (StealthStation S8 Surgical Navigation System, MEDTRONIC, Louisville, CO, USA) provided by the co-registered data sets of morphological MRI, tractography reconstructions, and phonemic task activations.

Operative and peri-operative complications were considered.

Post-operative Course and Follow-Up

Neurological examination, with particular regard to language deficits, was performed at patients' awakening and regularly during hospitalization. An early post-operative brain MRI before and after gadolinium administration (0.1 mmoli/Kg) was performed within 3 days after surgery to assess the extension of tumor removal.

Gross total resection (GTR) was considered if no remnants of the tumor could be detected compared with preoperative MRI scans (i.e., with respect to any residual enhancement), otherwise, resection was considered as subtotal resection, when the residual tumor is <10% of initial mass; and partial when it is larger than 10% of pre-operative volume.

After a case-by-case discussion at the Tumor Board multidisciplinary meeting, adjuvant treatments (radio and chemo-therapies) were started 1 month after surgery, based on the final diagnosis.

Neurological examination was repeated at 15 and 30 days and every 3 months from the discharge; neuroradiological follow-up consisting of a morphological MRI scan was performed every 3–6 months.

Tumor Histopathological and Molecular Characterization

Surgical specimens were formalin-fixed and paraffin-embedded (FFPE) according to routine procedures. The diagnosis was assessed by one neuropathologist (S.A) according to 2016 WHO classification of tumors of the central nervous system (48).

Immunohistochemistry was performed in an automated stainer (Ventana, Tucson, AZ, using Ventana purchased pre-diluted antibodies): antibodies anti-GFAP (clone EP672Y, Cell-Marquez), anti-Olig2 (clone EP112, Cell-Marquez), anti-synaptophysin (clone MRQ-40, Cell-Marquez), anti-BRAF V600E (clone VE1, Roche), anti-CD34 (clone QBEnd/10, Roche), anti-IDH1 R132H (Clone H09, Dianova), anti-ATRX (polyclonal, Sigma), anti-p53 (clone DO-7, Roche) were used. Ki67 labeling index (clone 30–9, Ventana Medical Systems Inc, Tucson, AZ, US) was evaluated by counting at least 1,000 neoplastic cells.

DNA from FFPE tissues was purified by the NucleoSpin Tissue kit (Macherey-Nagel, Germany), following the instruction of the provider. Mutational analysis of *IDH1* (exon 4), *IDH2* (exon 4), *H3-3A* (exon 1), and *TERT* (promoter) was performed using locus-specific amplicon libraries with tagged primers based on Nextera™ sequence as previously described (49, 50). Each Next Generation Sequencings (NGS) experiment on MiSEQ (Illumina, San Diego, CA) was designed to obtain a depth of coverage $\geq$1,000×. FASTQ files were processed in a Galaxy Project environment (51), with hg38 as a human reference genome, and mutations were visualized using BWA (Burrows-Wheeler Aligner) and IGV (Integrative Genomics Viewer). *MGMT* DNA Methylation analysis was performed by treating the genomic DNA (50–500 ng) with sodium bisulfite using the EZ DNA Methylation-Lightning Kit (Zymo Research Europe, Freiberg, Germany) according to the manufacturer's protocol. DNA methylation was evaluated using targeted bisulfite NGS for *MGMT* promoter (coordinates on chromosome 10: 129466810-129467529, reference hg38), generating libraries with the same approach for mutation analysis. FASTQ files were processed in a Galaxy Project environment using BWAmeth and MethylDackel, taking the human GRCh38/hg38 as the reference genome (52).

Identification of the 1p/19q allelic status was obtained using a dual-color FISH analysis and an Olympus BX61 epifluorescence microscope: for each case, at least 100 neoplastic nuclei were counted, and the copy numbers of 1p36/1q25 and 19q13/19p25 were recorded for each nucleus.

Statistical Analyses

Paired sample *T*-Tests or independent sample *T*-Tests were used to compare, respectively, measurements are taken from the same group of cases (i.e., right *vs* left fMRI activations) or to compare data (i.e., DTI and histopathological and molecular data) between groups. An adaptive significance threshold was applied using the Benjamini–Hochberg false discovery rate (FDR) procedure to account for multiple comparisons (53).

In addition, correlations between fMRI activations, neuropsychological data, DTI measures (i.e., for the AF and FAT), volume, and histopathological and molecular data were calculated using the Pearson correlation coefficient, again accounting for multiple comparisons using the Benjamini–Hochberg false discovery rate, setting the FDR to 0.1 since in our study the number of subjects was <20 (54). All statistical analyses were performed using IBM SPSS vs.27 and Matlab 2021b Bioinformatics Toolbox functions.

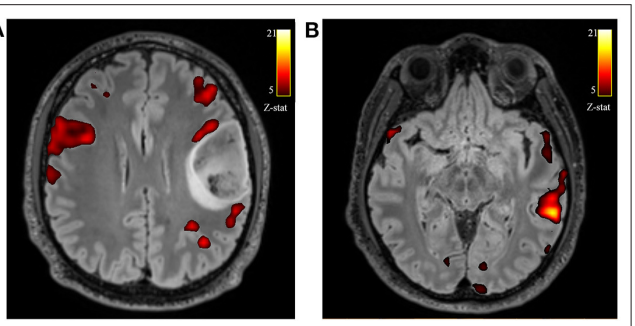

FIGURE 2 | Axial views of the T2-w FLAIR image superimposed the fMRI phonemic fluency fMRI activation. Example of one patient with left frontal glioblastoma grade 4, showing the recruitment of contralateral compensatory activation of right frontal operculum **(A)** and canonical temporal activation on the left hemisphere **(B)**.

RESULTS

Ten patients presented seizures, followed by language impairment and one with transitory mild aphasia, while the remaining were incidental findings in three asymptomatic patients and in one with gait disturbances. Surgery was performed in an awake setting in eight cases and was uneventful for all but three patients. One developed a surgical field hematoma, causing hemiparesis, which required a re-intervention with the prompt recovery of neurological deficit in the following days. Another presented a post-operative seizure, that was controlled with anti-epileptic pharmacological treatment. The last had a transitory hemineglect of the contralateral side, which spontaneously recovered in a few weeks. GTR was achieved in 11 cases and in 4 a remnant inferior to 20% of the initial volume was detected at post-operative MRI. No patients developed language deficits in the post-operative time, and the one with pre-operative transitory aphasia improved after surgery.

Cortical Activation Patterns at Functional MRI

All patients during phonemic fluency task fMRI showed left hemispheric dominance in temporal regions (mean voxel on the left = 3835.08 ± 2624.22; mean voxel on the right = 3243.08 ± 2526.33; LI = 0.13) and parietal regions (mean voxel on the left = 3643.69 ± 2956.89; mean voxel on the right = 3164.92 ± 2874.19; LI = 0.09). On the other hand, we found a slightly right hemispheric dominance in frontal regions, specifically in the frontal operculum (mean voxel on the left = 1321.85 ± 961.12; mean voxel on the right = 1552.62 ± 707.99; LI = −0.16), although not significant, when considering the whole group of patients. Instead, when considering only those patients with tumors located on the left side (N = 10) this difference increases, showing significantly higher activation on the right frontal operculum compared to the left (mean voxel on the left = 1097.78 ± 974.29; mean voxel on the right = 1479.11 ± 682.19; LI = −0.27; FDR adjusted $p < 0.1$) (**Figure 2**). No significant differences were found when considering only those patients with tumors located on the right side ($N = 5$).

Moreover, right frontal operculum activations for left-sided glioma showed significant correlation with neuropsychological performance, specifically with verbal memory (i.e., Digit Span Forward Test, $p = 0.074$; $r = 0.902$), visuo-spatial short-term memory (i.e., Corsi's Block Test, $p = 0.017$; $r = 0.954$) and executive functions (i.e., Stroop Test – time-, $p = 0.074$; $r = -0.910$).

No correlations were found between the left frontal operculum and cognitive performance.

White Matter Fiber Tracts' Microstructural Features

In order to evaluate to which extents frontal gliomas affect the surrounding neural fibers' integrity, patients' microstructural parameters (MD and FA) of AF and FAT were compared to those of healthy controls. Statistical analyses were conducted by subdividing the patients' samples into two subgroups according to the glioma's localization (left hemisphere, $N = 10$; right hemisphere, $N = 5$).

Independent samples *T*-test (FDR correction, adjusted < 0.1) comparing patients with left-sided glioma with controls, showed alterations of left AF microstructural parameters: FA (patients' mean = 0.424 ± 0.019; healthy controls = 0.450 ± 0.024; $p = 0.021$) and MD [patients' mean = $(0.607 \pm 0.019)\ 10^{-3}\ mm^2\ s^{-1}$; healthy controls = $(0.586 \pm 0.019)\ 10^{-3}\ mm^2\ s^{-1}$; $p = 0.021$] values. Similarly, MD values of the patients' left FAT showed higher values compared to controls ($p = 0.021$).

In addition, comparing the subgroup of patients with right-sided glioma to the controls, a reduction of FA and an increase of MD values were detected (all FDR adjusted $p < 0.1$) in right AF and in right FAT ($p = 0.027$ and $p = 0.001$, respectively) (**Table 4** and **Figure 3**).

Correlation analyses were successively conducted between left/right AF and FAT microstructural parameters with neuropsychological data, and significant correlations were only found in the subgroup of patients with left-sided gliomas. Specifically, FA reduction in the left AF was associated with

TABLE 4 | Comparison of DTI parameters between patients and healthy controls.

DTI features		HC ($N = 24$)		LG patients ($N = 10$)		LG patients vs. HC	RG patients ($N = 5$)		RG patients vs. HC
		Mean	**Sd**	**Mean**	**Sd**	***P-value***	**Mean**	**Sd**	***p-value***
Left FAT	*MD*	0.594	0.020	0.637	0.072	0.021*	0.598	0.038	*NS*
	FA	0.404	0.025	0.385	0.053	*NS*	0.404	0.034	*NS*
Left AF	*MD*	0.586	0.019	0.607	0.019	0.021*	0.595	0.030	*NS*
	FA	0.450	0.024	0.424	0.019	0.021*	0.427	0.037	*NS*
Right FAT	*MD*	0.593	0.022	0.602	0.014	*NS*	0.668	0.076	0.001*
	FA	0.405	0.023	0.389	0.027	*NS*	0.340	0.050	*NS*
Right AF	*MD*	0.586	0.020	0.589	0.016	*NS*	0.671	0.106	0.027*
	FA	0.433	0.033	0.415	0.030	*NS*	0.385	0.075	*NS*

*FAT, frontal aslant tract; AF, arcuate fasciculus; MD, mean diffusivity values (10^{-3} mm^2 s^{-1}); FA, fractional anisotropy values; HC, healthy controls; LG, left glioma; RG, right glioma; sd, standard deviation; *p < 0.05, (FDR) < 1. NS, non-significant.*

FAT, left and right frontal aslant tract; AF, arcuate fasciculus; LG, microstructural features of patient with left glioma; RG, patients with right glioma; HC, healthy controls.

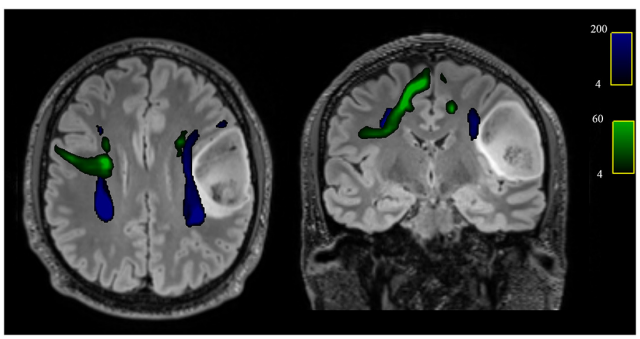

FIGURE 3 | Axial and coronal views of the T2-w FLAIR image with superimposed the reconstruction of the AF (blue) and FAT (green) of one patient with left frontal glioblastoma grade 4, showing the spatial relationship between the tumor and tracts and in particular the displacement of both left AF and FAT.

worse visuospatial short-term memory (Corsi Block Test, $p = 0.04$, $3r = 0.899$), and FA reduction in the left FAT was associated with worse performance in visuo-constructional and planning abilities (ROCF copy, $r = 0.944$, $p = 0.037$).

Histopathological and Molecular Characterization

Histopathological and molecular characterization of tumors was achieved considering tumor grade according to 2016 WHO (48) and several biomarkers (i.e., *IDH-1, TERT, MGMT*, DEL1p/19q, Ki-67). Six tumors confirmed to be grade II according to WHO, five were grade III, and four were grade IV, histological diagnosis was astrocytoma in four cases, oligodendroglioma in two, anaplastic astrocytoma in two, anaplastic oligodendroglioma in three and the remaining were glioblastomas. Molecular characterization is reported in **Table 1**.

Independent sample *t*-tests were run to explore the influence of these parameters on the frontal operculum compensatory mechanisms, white matter tracts integrity, and neuropsychological performance. Results showed that compensatory activations of the right frontal operculum were significantly higher in patient with *IDH-1* mutation (1,704 ± 577,897) compared to wild-type (720 ± 1018.234) (FDR adjusted $p = 0.067$), instead, no association was found with DTI microstructural parameters. A similar difference in the right frontal operculum activation was found between patients with *TERT* mutation in comparison to wild-type (FDR adjusted $p = 0.031$) and in those with deletion of 1p19q (FDR adjusted $p = 0.008$).

No differences in cortical fMRI activation were observed in patients with *MGMT* methylation, Ki-67 values, or different tumor grades, as well as between all these parameters of histopathological and molecular characterization and DTI microstructural alterations.

Significant differences in neuropsychological performance were observed between patients with *IDH-1* mutated gliomas and wild-type. Specifically, patients with *IDH-1* mutation showed better performance in tests that measure general cognitive abilities (i.e., MMSE, FDR adjusted $p = 0.007$), semantic fluency (Category Fluency Test, FDR adjusted $p = 0.093$), verbal short-term memory (Span forward, FDR adjusted $p = 0.037$), and executive functions (FAB, FDR adjusted $p = 0.037$; TMT-B, FDR adjusted $p = 0.093$).

Instead, no significant correlations were found between tumor volumes and right frontal operculum activations, neuropsychological performance or DTI microstructural parameters.

DISCUSSION

Phonemic fluency is the conventional test used for the detection of frontal lobe dysfunction (55). Converging findings from healthy controls and lesion studies using functional fMRI demonstrate that fluency tasks activate a left-lateralized network of cortical regions (56). In this preliminary study, we demonstrate that patients with frontal brain gliomas during a phonemic fluency task showed compensatory cortical activations of the corresponding regions in the non-dominant hemisphere. In

particular, we found that patients with left-sided frontal gliomas, albeit right-handed, showed significantly higher activation of the right frontal operculum compared to the left. This emphasizes the possible pivotal role that the contralateral frontal operculum could play in the neurocognitive adaptive reorganization in patients with brain gliomas. Indeed, our study shows that the results were associated with improved neuropsychological performance in the domains of verbal and visuo-spatial memory and executive functions, while ipsilateral frontal operculum presented no significant association with cognitive performance. This is in line with the suggestions that the frontal operculum, which contains Broca's area, is essential for language and general cognitive functions, and previous studies that examined patients with lesions of the frontal operculum showed a specific association with clinical aphasias (57, 58).

Surgery of gliomas of eloquent areas is challenging for the double aims that it poses to the surgeon. Although its goal should be complete tumor removal, it should avoid neurological deficits to preserve the patient's quality of life. Particularly, frontal gliomas, involving the dominant operculum areas (usually left-sided), are often considered at high risk for resection. It has been argued that compensatory plasticity mechanisms of the brain may help the surgeon to reduce the risk of post-operative deficit, possibly tailoring the surgical resection or, as proposed by some authors, favoring the implementation of these processes by means of specific stimulations also pre- or post-operatively (59).

Besides functional compensatory mechanisms, white matter tracts (i.e., AF and FAT) play also a crucial role in language and general cognitive processing. In this study we found that the presence of microstructural alterations, i.e., reduction of FA values of the FAT, is associated with worse performance in the Rey–Osterrieth complex figure (ROCF), a test that measure visuo-constructive and planning abilities. This result is in line with a recent systematic review that showed the role of the FAT in the visuo-motor process that supports movement planning (60).

Nowadays, histopathological and molecular characterizations are gaining a crucial role in gliomas. Indeed, many glioma entities are defined on the basis of genetic alterations in various driver genes such as *IDH1-2, ATRX, TP53, CDKN2A/B, TERT,* and *H3 K27* (61). Interestingly, we observed that the contralateral compensatory activation of the operculum region was mostly dependent on some molecular parameters of the tumors, such as *IDH-1* mutation, *TERT* mutation, and deletion of 1p19q, instead of the pathological grade of the tumor. This could suggest that those tumors, with a longer natural history and, at least an initial slower growth, could induce more effectively a contralateral cortical compensation, favoring better neuropsychological performances, as we observed for patients with *IDH-1* mutations. The demonstration of such compensatory cortical activation and the association with better cognitive performance would help to clarify neuroplasticity mechanisms that occur in the presence of a tumor and thus predict the rate of post-operative deficit, with the final goal of improving patients' quality of life. One of the main limitations of this study is related to the number of patients enrolled; therefore, inductive statistical techniques (i.e., multivariate analyses and prediction models) are not suitable. In addition, an *ad hoc* pipeline to perform multiparametric advanced analyses that fuse fMRI and DTI data is not available for a small sample size (62). Further studies with a larger sample and follow-ups are needed to complement these encouraging preliminary results and to confirm our 'proof of concept' study. If confirmed, the present results enhance the role of presurgical fMRI in guiding a more aggressive surgery of frontal lobe gliomas when a contralateral compensation is evident.

DATA AVAILABILITY STATEMENT

The data presented in this study are deposited in the online repositories and are accessible with the following link: https://www.ncbi.nlm.nih.gov/sra/PRJNA804145.

ETHICS STATEMENT

The studies involving human participants were reviewed and approved by the Local Ethical Committee AVEC (Area Vasta Emilia Centro) 183/2019/OSS/AUSLBO – 19027 (20/03/19). The patients/ participants provided their written informed consent to participate in this study.

AUTHOR CONTRIBUTIONS

MMi, MZ, and CTo contributed to conception and design of the study. MMi, MR, and MZ organized the database. MMi and CTe performed the statistical analysis. MMi wrote the first draft of the manuscript. MMi, MZ, CTe, LM, MR, and FZ wrote sections of the manuscript. All authors contributed to manuscript revision, read, and approved the submitted version.

ACKNOWLEDGMENTS

The authors would like to acknowledge the radiographers and nursing staff (Head: Maria Grazia Crepaldi), the clerical team (Head: Adele Lodi), and IRCCS Istituto delle Scienze Neurologiche di Bologna, Bellaria Hospital who contributed to the success of this study.

SUPPLEMENTARY MATERIAL

The Supplementary Material for this article can be found online at: https://www.frontiersin.org/articles/10.3389/fneur.2022.867048/full#supplementary-material

Supplementary Figure 1 | Frequency map of tumor distribution. **(A)** the percentage of tumor localization is shown at level of the basal ganglia. **(B)** the percentage of tumor localization is shown at level of the motor areas. Axial T1 images are displayed in the radiological convention orientation.

REFERENCES

1. Cramer SC, Sur M, Dobkin BH, O'Brien C, Sanger TD, Trojanowski JQ, et al. Harnessing neuroplasticity for clinical applications. *Brain.* (2011) 134:1591–609. doi: 10.1093/brain/awr039
2. Cargnelutti E, Ius T, Skrap M, Tomasino B. What do we know about pre- and postoperative plasticity in patients with glioma? A review of neuroimaging and intraoperative mapping studies. *NeuroImage Clinical.* (2020) 28:102435. doi: 10.1016/j.nicl.2020.102435
3. Kong NW, Gibb WR, Tate MC. Neuroplasticity: insights from patients harboring Gliomas. *Neural Plasticity.* (2016) 2016:5063; 2365063. doi: 10.1155/2016/2365063
4. Eyüpoglu I, Buchfelder M, Savaskan N. Surgical resection of malignant gliomas—role in optimizing patient outcome. *Nat Rev Neurol.* (2013) 9:141–51. doi: 10.1038/nrneurol.2012.279
5. Zimmermann M, Rössler K, Kaltenhäuser M, Grummich P, Yang B, Buchfelder M, et al. Refined functional magnetic resonance imaging and magnetoencephalography mapping reveals reorganization in language-relevant areas of lesioned brains. *World Neurosurg.* (2020) 136:e41–59. doi: 10.1016/j.wneu.2019.10.014
6. O'Regan L, Serrien DJ. Individual differences and hemispheric asymmetries for language and spatial attention. *Front Hum Neurosci.* (2018) 12:380. doi: 10.3389/fnhum.2018.00380
7. Broca PP. Remarques sur le siége de la faculté du langage articulé, suivies d'une observation d'aphémie (perte de la parole). *Bull Soc Anat Paris.* (1861) 6:330–57.
8. Wernicke C. *Deraphasische Symptomen Complex*. Breslau: M.Cohn & Weigert. (1970) 1874:1. Auflage.
9. Geschwind N. The organization of language and the brain. *Science.* (1970) 170:940–4.
10. Duffau H, Denvil D, Capelle L. Long term reshaping of language, sensory, and motor maps after glioma resection: a new parameter to integrate in the surgical strategy. *J Neurol Neurosurg Psych.* (2002) 72:511–6. doi: 10.1136/jnnp.72.4.511
11. Grummich P, Nimsky C, Fahlbusch R, Ganslandt O. Observation of unaveraged giant MEG activity from language areas during speech tasks in patients harboring brain lesions very close to essential language areas: expression of brain plasticity in language processing networks? *Neurosci Lett.* (2005) 380:143–8. doi: 10.1016/J.Neulet.2005.01.045
12. Grummich P, Nimsky C, Pauli E, Buchfelder M, Ganslandt O. Combining fMRI and MEG increases the reliability of presurgical language localization: a clinical study on the difference between and congruence of both modalities. *Neuroimage.* (2006) 32:1793–803. doi: 10.1016/j.neuroimage.2006.05.034
13. Lazar RM, Marshall RS, Prell GD, Pile-Spellman J. The experience of Wernicke's aphasia. *Neurology.* (2000) 55:1222–24. doi: 10.1212/wnl.55.8.1222
14. Thiel A, Herholz K, Koyuncu A, Ghaemi M, Kracht LW, Habedank B, et al. Plasticity of language networks in patients with brain tumors: a positron emission tomography activation study. *Ann Neurol.* (2001) 50:620–9. doi: 10.1002/ana.1253
15. Krainik A, Lehéricy S, Duffau H, Capelle L, Chainay H, Cornu P, et al. Postoperative speech disorder after medial frontal surgery: role of the supplementary motor area. *Neurology.* (2003) 25:60:587–94. doi: 10.1212/01.wnl.0000048206.07837.59
16. Kristo G, Raemaekers M, Rutten GJ, de Gelder B, Ramsey NF. Inter-hemispheric language functional reorganization in low-grade glioma patients after tumour surgery. *Cortex.* (2015) 64:235–48. doi: 10.1016/j.cortex.2014.11.002
17. Johnson KC, Anderson KJ, Courtois ET, Gujar AD, Barthel FP, Varn FS, et al. Single-cell multimodal glioma analyses identify epigenetic regulators of cellular plasticity and environmental stress response. *Nat Genet.* (2021) 53:1456–68. doi: 10.1038/s41588-021-00926-8
18. Oldfield RC. The assessment and analysis of handedness: the Edinburgh inventory. *Neuropsychologia.* (1971) 9:97–113. doi: 10.1016/0028-3932(71)90067-4
19. Folstein MF, Folstein SE, Mchugh PR. "Mini-Mental State". A practical method for grading the cognitive state of patients for the clinician. *J Psychiatr Res.* (1975) 12:189–98. doi: 10.1016/0022-3956(75)90026-6
20. Raven JC. Matrix tests. *Ment Health*. (1940) 1:10–8.
21. Kaplan E, Goodglass H, Weintraub S. *Boston Naming Test Philadelphia*, Pennsylvania, PA: Lea & Febiger. (1983).
22. Mack WJ, Freed DM, Williams BW, Henderson VW. Boston naming test: shortened versions for use in Alzheimer's disease. *J Gerontol.* (1992) 47:154–8. doi: 10.1093/geronj/47.3.p154
23. Carlesimo GA, Caltagirone C, Gainotti G, Fadda L, Gallassi R, Lorusso S, et al. The mental deterioration battery: normative data, diagnostic reliability and qualitative analyses of cognitive impairment. *Eur. Neurol.* (1996) 36:378–84. doi: 10.1159/000117297
24. Novelli G, Papagno C, Capitani E, Laiacona N, Vallar G, et al. Tre test clinici di ricerca e produzione lessicale. *Taratura su soggetti normali. Archivio di Psicologia, Neurologia e Psichiatria.* (1986) 47:477–506.
25. Milner B. Interhemispheric differences in the localization of psychological processes in man. *Br Med Bull.* (1971) 27:272–7. doi: 10.1093/oxfordjournals.bmb.a070866
26. Spinnler H, Tognoni G. Standardizzazione e taratura italiana di test neuropsicologici. *Ital J Neurol Sci.* (1987) 8:1–120.
27. Carlesimo GA, Buccione I, Fadda L, Graceffa A, Mauri M, Lorusso S, et al. Standardizzazione di due test di memoria per uso clinico: Breve Racconto e Figura di Rey. *Nuova Rivista di Neurologia.* (2002) 12: 1–13.
28. Caffarra P, Vezzadini G, Dieci F, Zonato F, Venneri A. Rey-Osterrieth complex figure: normative values in an Italian population sample. *Neurol. Sci.* 22 (2002) 6:443–447. doi: 10.1007/s100720200003
29. Dubois B, Slachevsky A, Litvan I, Pillon B. The FAB: a frontal assessment battery at bedside. *Neurology.* (2000) 55:1621–6. doi: 10.1212/wnl.55.11.1621
30. Appollonio I, Piamarta F, Isella V, Leone M, Consoli T, Nichelli P. Strumenti di lavoro: la Frontal assessment battery (FAB). *Demenze.* (2004) 7:28–33.
31. Caffarra P, Vezzadini G, Dieci F, Zonato F, Venneri A. Una versione abbreviata del test di Stroop: Dati normativi nella popolazione Italiana. *Nuova Rivista di Neurologia.* (2002) 12:111–5.
32. Orsini A, Laicardi C. *WAIS-R Contributo alla Taratura Italiana*. Firenze: Giunti Organizzazioni Speciali Editore (1998).
33. Reitan RM, Wolfson D. *The Halstead–Reitan Neuropsycholgical Test Battery: Therapy and Clinical Interpretation*. Tucson, AZ: Neuropsychological Press (1985).
34. Measso G, Cavarzeran F, Zappalà G, Lebowitz BD, Crook TH, Pirozzolo FJ, et al. The mini-mental state examination: Normative study of an Italian random sample. *Dev Neuropsychol.* (1993) 9:77–85. doi: 10.1080/87565649109540545
35. Orsini A, Grossi D, Capitani E, Laiacona M, Papagno C, Vallar G. Verbal and spatial immediate memory span: normative data from 1355 adults and 1112 children. *Ital J Neurol Sci.* (1987) 8:539–48. doi: 10.1007/BF02333660
36. Giovagnoli AR, Del Pesce M, Mascheroni S, Simoncelli M, Laiacona M, Capitani E. Trail making test: normative values from 287 normal adult controls. *Ital J Neurol Sci.* (1996) 17:305–9. doi: 10.1007/BF01997792
37. Beck AT, Steer RA, Brown GK. *BDI-II: Beck Depression Inventory Manual. 2nd ed*. San Antonio: Psychological Corporation (1996).
38. Spielberger CD. *Manual for the State-Trait Anxiety Inventory (Form Y)*. Palo Alto: Consulting Psychologist Press (1983).
39. Nucci M, Mapelli D, Mondini S. The cognitive Reserve Questionnaire (CRIq): a new instrument for measuring the cognitive reserve. *Aging Clin Exp Res.* (2012) 24:218–126. doi: 10.3275/7800
40. Apolone G, Mosconi P. The Italian SF-36 health survey: translation, validation, and norming. *J Clin Epidemiol.* (1998) 51:1025–36. doi: 10.1016/s0895-4356(98)00094-8
41. Black DF, Vachha B, Mian A, Faro SH, Maheshwari M, Sair HI, et al. American society of functional neuroradiology–recommended fMRI paradigm algorithms for presurgical language assessment. *Am J Neuroradiol.* (2017) 38:1789–93. doi: 10.3174/ajnr.A5289
42. Jenkinson M, Bannister P, Brady M, Smith S. Improved optimization for the robust and accurate linear registration and motion correction of brain images. *Neuroimage.* (2002) 17:825–84. doi: 10.1006/nimg.2002.1132
43. Smith SM, Jenkinson M, Woolrich MW, Beckmann CF, Behrens TEJ, Johansen-Berg H, et al. Advances in functional and structural MR

image analysis and implementation as FSL. *Neuroimage.* (2004) 23:S208–19. doi: 10.1016/j.neuroimage.2004.07.051
44. Forkel SJ, Rogalski E, Sancho ND, D'Anna L, Laguna PL, Sridhar J, et al. Anatomical evidence of an indirect pathway for word repetition. *Neurology.* (2020) 94:e594–606. doi: 10.1212/WNL.0000000000008746
45. Zoli M, Talozzi L, Martinoni M, Manners DN, Badaloni F, Testa C, et al. From neurosurgical planning to histopathological brain tumor characterization: potentialities of arcuate fasciculus along-tract diffusion tensor imaging tractography measures. *Front Neurol.* (2021) 12:175. doi: 10.3389/fneur.2021.633209
46. Talozzi L, Testa C, Evangelisti S, Cirignotta L, Bianchini C, Ratti S, et al. Along-tract analysis of the arcuate fasciculus using the Laplacian operator to evaluate different tractography methods. *Magn Reson Imaging.* (2018) 54:183–93. doi: 10.1016/j.mri.2018.08.013
47. Luzzati C, Wilmes K, Bleser, D.. *AAT Aachner Aphasie Test (Edizione italiana).* Firenze: Giunti OS (1996).
48. Louis DN, Perry A, Reifenberger G, von Deimling A, Figarella-Branger D, Cavenee WK, et al. The 2016 world health organization classification of tumors of the central nervous system: a summary. *Acta Neuropathol.* (2016) 131:803–20. doi: 10.1007/s00401-016-1545-1
49. Gabusi A, Gissi DB, Montebugnoli L, Asioli S, Tarsitano A, Marchetti C, et al. Prognostic impact of intra-field heterogeneity in oral squamous cell carcinoma. *Virchows Arch.* (2020) 476:585–95. doi: 10.1007/s00428-019-02656-z
50. Marvi MV, Mongiorgi S, Ramazzotti G, Follo MY, Billi AM, Zoli M, et al. Role of PLCγ1 in the modulation of cell migration and cell invasion in glioblastoma. *Adv Biol Regul.* (2021) 19:100838. doi: 10.1016/j.jbior.2021.100838
51. Afgan E, Baker D, Batut B, van den Beek M, Bouvier D, Cech M, et al. The galaxy platform for accessible, reproducible and collaborative biomedical analyses: 2018 update. *Nucleic Acids Res.* (2018) 2:W537–44. doi: 10.1093/nar/gky379
52. Tresch NS, Fuchs D, Morandi L, Tonon C, Rohrer Bley C, Nytko KJ. Temozolomide is additive with cytotoxic effect of irradiation in canine glioma cell lines. *Vet Med Sci.* (2021) 7:2124–34. doi: 10.1002/vms3.620
53. Benjamini Y, Hochberg Y. Controlling the false discovery rate: a practical and powerful approach to multiple testing. *J Royal Stat Soc Series B.* (1995) 57:289–300. doi: 10.2307/2346101
54. Frommlet F. Bogdan, M. Some optimality properties of FDR controlling rules under sparsity. *Electron J Stat.* (2013) 7:1328–68. doi: 10.1214/13-EJS808
55. Cipolotti L, Xu T, Harry B, Mole J, Lakey G, Shallice T, et al. Multi-model mapping of phonemic fluency. *Brain Commun.* (2021) 3:fcab232. doi: 10.1093/braincomms/fcab232
56. Birn RM, Kenworthy L, Case L, Caravella R, Jones TB, Bandettini PA, et al. Neural systems supporting lexical search guided by letter and semantic category cues: a self-paced overt response fMRI study of verbal fluency. *Neuroimage.* (2010) 49:1099–107. doi: 10.1016/j.neuroimage.2009.07.036
57. Alexander MP, Naeser MA, Palumbo C. Broca's area aphasias Aphasia after lesions including the frontal operculum. *Neurology.* (1990) 40:353. doi: 10.1212/WNL.40.2.353
58. Burns MS, Fahy J. Broca's area: rethinking classical concepts from a neuroscience perspective. *Top Stroke Rehabil.* (2010) 17:401–10. doi: 10.1310/tsr1706-401
59. Raffa G, Conti A, Scibilia A, Cardali SM, Esposito F, Angileri FF, et al. The impact of diffusion tensor imaging fiber tracking of the corticospinal tract based on navigated transcranial magnetic stimulation on surgery of motor-eloquent brain lesions. *Neurosurgery.* (2018) 83:768–82. doi: 10.1093/neuros/nyx554
60. La Corte E, Eldahaby D, Greco E, Aquino D, Bertolini G, Levi V, et al. The frontal aslant tract: a systematic review for neurosurgical applications. *Front Neurol.* (2021) 12:641586. doi: 10.3389/fneur.2021.641586
61. Louis DN, Perry A, Wesseling P, Brat DJ, Cree IA, Figarella-Branger D, et al. The 2021 WHO classification of tumors of the central nervous system: a summary. *Neuro Oncol.* (2021) 23:1231–51. doi: 10.1093/neuonc/noab106
62. Zhu D, Zhang T, Jiang X, Hu X, Chen H, Yang N, et al. Fusing DTI and fMRI data: a survey of methods and applications. *Neuroimage.* (2014) 102:184–91. doi: 10.1016/j.neuroimage.2013.09.071

Conflict of Interest: The authors declare that the research was conducted in the absence of any commercial or financial relationships that could be construed as a potential conflict of interest.

Publisher's Note: All claims expressed in this article are solely those of the authors and do not necessarily represent those of their affiliated organizations, or those of the publisher, the editors and the reviewers. Any product that may be evaluated in this article, or claim that may be made by its manufacturer, is not guaranteed or endorsed by the publisher.

frontiers | Frontiers in Neurology

BRIEF RESEARCH REPORT
published: 18 July 2022
doi: 10.3389/fneur.2022.894157

Structural Brain Network Reorganization Following Anterior Callosotomy for Colloid Cysts: Connectometry and Graph Analysis Results

Marco Ciavarro[1]*, *Eleonora Grande*[2], *Giuseppina Bevacqua*[3], *Roberta Morace*[1], *Ettore Ambrosini*[4,5,6], *Luigi Pavone*[1], *Giovanni Grillea*[1], *Tommaso Vangelista*[1] and *Vincenzo Esposito*[1,7]

[1] Mediterranean Neurological Institute Neuromed (IRCCS) Neuromed, Pozzilli, Italy, [2] Department of Neuroscience, Imaging and Clinical Sciences, Gabriele d'Annunzio University, Chieti, Italy, [3] Department of Translational Medicine, Ferrara University, Ferrara, Italy, [4] Department of General Psychology, University of Padua, Padua, Italy, [5] Department of Neuroscience, University of Padua, Padua, Italy, [6] Padua Neuroscience Center, University of Padua, Padua, Italy, [7] Department of Human Neurosciences, Sapienza University of Rome, Rome, Italy

OPEN ACCESS

Edited by:
Emanuele La Corte,
University of Bologna, Italy

Reviewed by:
Giacomo Bertolini,
University of Bologna, Italy
Edgar G. Ordóñez-Rubiano,
Hospital de San José - Sociedad de Cirugía de Bogotá, Colombia

***Correspondence:**
Marco Ciavarro
marcociavarro@gmail.com

Specialty section:
This article was submitted to Applied Neuroimaging, a section of the journal Frontiers in Neurology

Received: 11 March 2022
Accepted: 03 June 2022
Published: 18 July 2022

Citation:
Ciavarro M, Grande E, Bevacqua G, Morace R, Ambrosini E, Pavone L, Grillea G, Vangelista T and Esposito V (2022) Structural Brain Network Reorganization Following Anterior Callosotomy for Colloid Cysts: Connectometry and Graph Analysis Results. Front. Neurol. 13:894157. doi: 10.3389/fneur.2022.894157

Introduction: The plasticity of the neural circuits after injuries has been extensively investigated over the last decades. Transcallosal microsurgery for lesions affecting the third ventricle offers an interesting opportunity to investigate the whole-brain white matter reorganization occurring after a selective resection of the genu of the corpus callosum (CC).

Method: Diffusion MRI (dMRI) data and neuropsychological testing were collected pre- and postoperatively in six patients with colloid cysts, surgically treated with a transcallosal-transgenual approach. Longitudinal connectometry analysis on dMRI data and graph analysis on structural connectivity matrix were implemented to analyze how white matter pathways and structural network topology reorganize after surgery.

Results: Although a significant worsening in cognitive functions (e.g., executive and memory functioning) at early postoperative, a recovery to the preoperative status was observed at 6 months. Connectometry analysis, beyond the decrease of quantitative anisotropy (QA) near the resection cavity, showed an increase of QA in the body and forceps major CC subregions, as well as in the left intra-hemispheric corticocortical associative fibers. Accordingly, a reorganization of structural network topology was observed between centrality increasing in the left hemisphere nodes together with a rise in connectivity strength among mid and posterior CC subregions and cortical nodes.

Conclusion: A structural reorganization of intra- and inter-hemispheric connective fibers and structural network topology were observed following the resection of the genu of the CC. Beyond the postoperative transient cognitive impairment, it could be argued anterior CC resection does not preclude neural plasticity and may subserve the long-term postoperative cognitive recovery.

Keywords: diffusion MRI, anterior callosotomy, white matter, structural connectivity, network topology, graph analysis, colloid cyst

INTRODUCTION

Lesions invading the third ventricle include a wide variety of neoplasms and cysts formation typically not affecting the brain parenchyma. Colloid cysts are rare and slow-growing benign lesions, most frequently located in the anterior part of the third ventricle. Due to the increased risk of acute obstructive hydrocephalus, or the development of chronic hydrocephalus-related symptoms (i.e., headache, gait disturbance, and cognitive impairment), surgical excision of these lesions is required in symptomatic cases (1–3). The standard surgical procedures include transcortical, transcallosal, or endoscopic surgical approaches (4). However, when the lesion is close to the neurovascular structures such as bringing veins, arteries, fornix, hypothalamus, or cingulate gyrus, surgical procedures are critical, since healthy brain tissue could be damaged (5) with a high risk for postsurgical cognitive sequelae (6–9). In particular, corticocortical connections such as the corpus callosum (CC) may be damaged in the transcallosal approach as a result of surgical access (9, 10), whereas cortico-subcortical structures, i.e., the fornix, may be affected in all the available surgical approaches as result of surgical manipulation due to the close spatial relation with the lesions (11). Damages to the fornix structures have been widely associated with memory dysfunctions (6, 12–14), caused by the disconnection occurring within the limbic system itself (hippocampus and mammillary bodies) and the connection between the frontal lobes (cingulate gyrus) and the limbic system (thalamus, hippocampus). Otherwise, although the more common cognitive deficits after anterior callosotomy are related to long-term memory impairment, executive dysfunctions, and information exchange between the cerebral hemispheres (e.g., the interhemispheric transfer of motor learning and, to a lesser extent, processing speed) (15), there is still a lack of consensus about permanent cognitive deterioration after anterior body callosal resection (16, 17). Here, we aim at investigating the clinical outcome and the brain functional and structural reorganization after a selective resection of the anterior part of the CC in a cohort of patients who underwent colloidal cyst removal through a new interhemispheric transcallosal surgical approach based on a parallel incision on the genu of CC (18). This surgical approach offers some technical advantages: increasing the line of sight along the anteroposterior axis of the third ventricle, allowing a good exposure and bimanual dissection of the lesion, and facilitating complete lesion removal, but even ensuring a better visualization of the closest crucial anatomical healthy structures.

Diffusion Tensor Imaging (DTI) together with neuropsychological data, were collected pre- and postoperatively to study the clinical outcome and the whole-brain structural reorganization, investigating quantitative anisotropy (QA) index, and also changes in the network topology reorganization after the resection of the anterior CC.

MATERIALS AND METHODS

Study Design and Patient Selection

The study protocol was in accordance with the current STROBE guidelines for cohort studies. A series of six consecutive patients (4 F) were recruited at Neuromed Institute (Pozzilli, Is) during the period between September 2019 and June 2021. Eligible patients were those with a characteristic radiological feature of a cystic lesion in the anterior roof of the third ventricle, confirmed by histological findings, who completed the neuropsychological and radiological follow-up. All the surgical procedures have been performed by the last author (V.E.). All the patients gave their informed consent at the moment of the hospitalization. Data were treated in accordance with the Helsinki declaration.

MRI Acquisition and Surgical Procedure

All the patients underwent MRI examinations by using a 3-Tesla scanner (GE SignaHDxt, GE Medical Systems, Milwaukee, USA). A 3D T1-weighted (SPGR) structural scan with voxel size = $1 \times 1 \times 1$ mm^3, repetition time = 7,272 ms, echo time = 300 ms and flip angle = 13° was acquired. dMRI data were collected using a spin-echo echo-planar imaging sequence with 30 diffusion encoding directions with repetition time = 12,200 ms, echo time = 91 ms, slice thickness 3 mm, flip angle 90°, b = 0 and 1,000 s/mm^2. Both the MRI acquisitions were performed during the week before the surgery and repeated 6 months after surgery (postoperative).

In all the cases, the cyst was located in the anterior part of the third ventricle. The surgical technique requires the access through the non-dominant dura mater, incision in performed on the genu of the CC is and runs parallel to the commissural fibers between the two pericallosal arteries, until the frontal horn of the lateral ventricle is accessed and the right foramen of Monro is identified [see Esposito et al., (18) for details on the surgical procedure].

Neuropsychological Evaluation

An extensive cognitive evaluation assessing several cognitive domains (i.e., short-term/working memory, long-term memory, attention, praxis abilities, language, abstract reasoning, and executive/frontal cognitive functions) was collected 3 days before the surgery and in two follow-ups: 1 and 6 months after surgery.

The neuropsychological battery included the Mini-Mental State Examination (MMSE); the Frontal Assessment Battery (FAB) for executive functions (both repeated at the second follow-up only); a task of verbal episodic long-term memory (Rey's Auditory Verbal Learning Test, RAVLT and Babcock Story Recall test, BSRT); tasks of spatial (forward Corsi Block-Tapping Test) and verbal (forward and backward Digit Span) short-term/working memory; a task for long-term visuospatial memory (Rey figure recall); abstract reasoning test (Raven's Progressive Matrices ′47, RPM ′47); phonological and semantic verbal fluency; response inhibition (Stroop interference test,

SCWT); a task of divided visual attention (Trail Making Test A-B); and constructional praxis (Copy of Rey figures).

Data were corrected for age and educational level and tests parallel versions were adopted to minimize practice effects. Differences among baseline vs. 1 month, 1 vs. 6 months, and baseline vs. 6 months evaluations were analyzed by the Wilcoxon's test for non-parametric testing. The statistical analysis was performed using R studio software 1.3.1. The alpha level was set at 0.05 for statistical significance.

Image Processing

Volumetric Data Segmentation for Ventricular Volume

To establish the presence of ventriculomegaly, a volumetric analysis was performed. The volumes of each brain structure were extracted from 3D T1 scan by using a well-established online software pipeline (http://volbrain.upv.es). This pipeline allows to first improve the quality of the images and analyze and locate them in a common geometric and intensity space and then to perform segmentation at several anatomical levels (19). Each subcortical structure volume was extracted as a relative value, measured in relation to the Intracranial Volume (ICV). The pre- and postoperative volumes of both lateral ventriculi were extracted and analyzed using the Wilcoxon's test.

Diffusion MRI Data Processing

The dMRI data were analyzed in DSI Studio software (http://dsi-studio.labsolver.org/). First, the DICOM data of each participant were loaded and renamed to generate the "SRC.gz", a DSI owner file format containing the raw diffusion weighted images and the metadata associated, namely, image dimension, voxel size and b-table, that are used for reconstruction. DTI were corrected for subject motion and the SRC file was checked to ensure its integrity and quality (20). For each patient and scan (pre- and postoperative), the DTI were reconstructed in a common stereotaxic space by applying the q-space diffeomorphic reconstruction (QSDR) algorithm (21) on the HCP-1021 young adult template, selecting the orientation distribution function (ODF), i.e., the marginal probability of diffusion in a given direction, for mapping the orientation architecture of the tissue. The diffusion sampling length ratio was set to 1.25. The goodness-of-fit was evaluated using the R2 between the warped image and template image. All the patients in this study had $R^2 > 0.67$. The vector field (fiber orientations) and anisotropy information (the magnitude; "FIB.gz" file) from all the participants were included in the connectometry database and used to conduct fiber tracking analysis. Finally, the patients' scans were paired between baseline scan and follow-up scan for each patient by using the function "Modify a Connectometry Database."

Group Connectometry Analysis

Using the DSI studio software, the dMRI connectometry protocol (22) was adopted to identify tracts with significant differences in QA between longitudinal scans, by checking "intercept" as study variables. We tested different levels of *T*-score (2; 2.5; 3) at different significance levels (FDR: 0.05, 0.075 and 0.1) (23) and we found that the results were consistent. Then, by using a deterministic fiber tracking algorithm (24), a *T*-score threshold of 2 was chosen to obtain correlational tractography. The QA values were normalized. We used as terminative region left- and right-cerebellum-white matter and cortex using Freesurfer atlas and as seeding region the whole brain. The tracks were filtered by topology-informed pruning (20) with 1 iteration. A length threshold of 20 voxel distances was used to select tracks. Finally, to estimate the false discovery rate, a total of 2,500 randomized permutations were applied to the group label to obtain the null distribution of the track length.

Graph Theory: Reorganization in Network Topology

In order to investigate how reorganizations in the tracts drive changes in the network topology, we extracted graph theory measures to estimate changes between pre- and postoperative dMRI scans, by using DSI studio software. Using the "FIB.gz" file for each patient, two different databases were created, specifically for pre- and postoperative scans. The whole-brain fiber tracking of the population average for each database was calculated (10,000,000 seeds). A connectivity matrix was generated using FreesurferSeg atlas (25) with pass region as nodes, the number of fibers passing through a region (i.e., *count*) as metric and a threshold of 0.001. The (weighted) between centrality (BC) metric, a network property considered as an index of the short pathways passing through a specific node, was extracted and computed between scans, by subtracting the preoperative value from the postoperative value as proposed by Taylor et al. (26).

In order to evaluate whether the strength of connection varies between the CC and the nodes of cortical parcellation, a connectivity matrix of connectivity strength was computed. The five subdivisions of CC (posterior, mid-posterior, central, mid-anterior, and anterior, following the DSI studio built-in parcellation on the FreesurferSeg atlas) were considered as nodes and the cortical sites that show changes between pre- and postoperative scans (55 regions for the left hemisphere and 23 regions for the right hemisphere) were extracted by subtracting the preoperative strength value from the postoperative strength value. Then, a 3D graph presentation was obtained from .mat file in DSI Studio and the connectogram was generated with CIRCOS software package (https://mkweb.bcgsc.ca/tableviewer/).

RESULTS

A total of six consecutive patients (4F; mean age 39.9 years, ranging from 19 to 52 years, mean education was 13.6 years, ranging 8–18 years) who completed neuropsychological and radiological follow-up took part in the study. The transagenual transacallosal surgical approach (18) allowed the gross total resection of colloidal cists in the whole sample. The callosotomy mean was 1.17 ± 0.42 mm (measured on anterior–posterior axis) in all the patients. No disconnection syndrome was registered, and no permanent deficit was reported in all the patients. Although still persisting a post-surgery ventriculomegaly, the volumetric analysis suggested a spontaneous reduction of the preoperative hydrocephalus in five over six patients. In particular,

the preoperative lateral ventricle mean value was 6.24% of the total brain volume (±3.21), while the postoperative lateral ventricle mean value was 3.68% (±1.92; $p > 0.05$ between pre- and postventricular volume). No permanent CSF diversion was required.

Neuropsychological Outcome

Cognitive domains such as working memory, spatial memory, abstract reasoning test, response inhibition, divided visual attention, and constructional praxis showed a slightly worsening 1 month after surgery, with a recovery to the baseline at the second follow-up (**Table 1**). The screening evaluation and executive function battery (MMSE, FAB) remained stable between the baseline and the follow-up evaluation ($p > 0.05$), suggesting no global cognitive deterioration after surgery. Interestingly, memory performance at RAVLT immediate recall showed a significant improvement between the first and the second follow-up ($p = 0.031$), with a recovery in the short-term memory performance. Although not reaching statistical significance, the post-operative evaluation of RAVLT delayed recall was considerably worse compared to the baseline and the 6-month follow-up evaluation ($p = 0.062$; $p = 0.059$, respectively). Similarly, the BSRT median score collected at 1 month was significantly worse compared with the baseline and the second follow-up ($p = 0.035$; $p = 0.035$, respectively). Moreover, fluency test scores (i.e., phonological and semantic verbal fluency) showed a postoperative recovery: semantic fluency performance at early post-operative was significantly worse than the baseline and the second follow-up ($p = 0.036$; $p = 0.030$, respectively). Finally, the verbal fluency score was significantly worse at 1 month, compared with the 6-month follow-up ($p = 0.035$). Thus, beyond the strong impact of the surgery on the episodic memory and executive functions performances at the early postoperative (<1 month), a cognitive functions recovery was registered at 6 months.

Postoperative Microstructural White Matter Reorganization and Network Topology

We characterized surgery-induced microstructural changes in white matter and network topology in colloidal cysts patients considering the longitudinal acquisition of dMRI. The results of connectometry analysis showed a significant variation in QA value (FDR < 0.05) between the baseline dMRI and the postoperative scans. **Figure 1** showed the subsections of white matter tracts with significant changes in negative and positive QA (FDR < 0.05; T-score = 2). First, connectometry study detected widespread surgery-induced changes corresponding to the surgical access (i.e., the genu of CC) and in subsections of the tracts located in the frontal areas of the right hemisphere (reticular tract, anterior thalamic radiation Cingulum Parolfactory, FDR = 0.011). In addition to the previously expected QA reductions, we found QA increased (FDR = 0.071) in the body, forceps major anterior tapetum of CC and in associative bundles of the left hemisphere (frontal Aslant tract, optic radiation and superior longitudinal fasciculus III).

Finally, in order to evaluate whether these changes within the white matter bundle influence the whole-brain network topology, a graph analysis was implemented. Results showed significant changes in BC values in the left hemisphere globally. In particular, BC rises in the left precentral and frontal opercular gyri. It indicates how important the left hemisphere regions are by virtue of being on the shortest paths between other regions, due to the information integrations across the network. By contrast, a decrease in BC was found in the middle and superior frontal gyri bilaterally, with a reduction of their role in passing shortest paths.

Using the connectivity matrix, indicating the connection strength between these nodes and the five sections of CC, we found a postoperative redistribution of fibers connection of middle and superior frontal gyri from anterior CC toward the middle and mid-posterior CC section. On the other hand, considering the connection between the CC and the left precentral region, in which an increase of BC was found, results showed a global increase of these fibers bundles (**Figure 2**). Notably, we found a global increase of fiber bundles in the mid-anterior and central CC, whereas at the same time a reduction was found in the anterior CC (where callosotomy occurs) as well as in the mid-posterior and posterior CC. Importantly, considering the connection strength between the CC subdivision and the cortical nodes, we found an increase in the number of connections between the mid-anterior and central CC and the cortical nodes, especially the middle and superior frontal gyrus bilaterally. Otherwise, considering the anterior CC, we found a decrease in connection with the right frontomarginal gyrus, whereas the connection with the left frontomarginal gyrus increased considerably. In addition, we found a postoperative reduction of strength between the superior frontal gyrus and anterior CC. Considering the connection between the CC central and mid posterior, we found a postoperative increase of connection between the precentral gyrus, in particular in the right hemisphere. Finally, considering the CC posterior, we found a postoperative increase in connections with the superior parietal and occipital region bilaterally and with the left precuneus.

Taken together, beyond the change in connection strength in the resected area, many regions have a substantial increase in their BC and connectivity strength. It shows a postoperative widely distributed redirection of shortest paths in the network suggesting the existence of many alternative pathways in the brain.

DISCUSSION

Measures derived from the whole-brain tractography are increasingly being used to characterize the structural connectome of the brain (27–31). This global tractography approach is complementary to the functional connectivity between cortical regions (i.e., resting-state functional connectivity; rsFC) and was used in a growing number of studies investigating the structure-cognition associations in the healthy subjects (32), in developmental and aging studies (33, 34), and also in a range of clinical populations (35–37). The microsurgical removal

TABLE 1 | Neuropsychological evaluations: number of patients with out of normal range (ONR) scores and mean scores among the three evaluations are showed.

Cognitive domain	Neuropsychological test	Cut-off	Evaluation	ONR score (*N*)	Mean score	1 vs. 6 months ($p < 0.05$)
Screening	MMSE	23.38	Baseline	0/6	28.37	
				0/6	–	
			6 months	0/6	28.95	
	FAB	13.5	Baseline	1/6	15.64	
				0/6	–	
			6 months	0/6	16.50	
Episodic memory	RAVLT immediate recall	28.5	Baseline	2/6	29.00	
			1 month	4/6	21.63	
			6 months	2/6	31.79	*
	RAVLT delayed recall	4.6	Baseline	2/6	5.04	
			1 month	5/6	2.19	
			6 months	3/6	5.26	
	BSRT	8	Baseline	0/6	13.03	
			1 month	3/6	9.01	
			6 months	0/6	16.78	*
Working memory	DSF	4.26	Baseline	3/6	4.48	
			1 month	4/6	4.63	
			6 months	2/6	4.64	
	DSB	2.65	Baseline	1/6	3.37	
			1 month	0/6	3.40	
			6 months	0/6	4.35	
Spatial working memory	Corsi block-tapping test	3.5	Baseline	1/6	4.53	
			1 month	2/6	3.87	
			6 months	2/6	4.50	
Visuo-spatial memory	Rey-figure delayed recall	9.47	Baseline	1/6	15.28	
			1 month	0/6	14.48	
			6 months	0/6	19.77	
Abstract reasoning	RPM '47	18.96	Baseline	0/6	28.77	
			1 month	0/6	26.18	
			6 months	0/6	30.65	
Language fluency	Semantic verbal fluency	7.25	Baseline	0/6	14.10	
			1 month	0/6	7.12	
			6 months	0/6	15.52	*
	Phonological verbal fluency	10.69	Baseline	1/6	26.73	
			1 month	1/6	20.42	
			6 months	0/6	29.16	*
Attention	TMT A	93	Baseline	0/6	37.33	
			1 month	0/6	45.67	
			6 months	0/6	33.00	
	TMT B	282	Baseline	1/6	107.11	
			1 month	0/6	130.44	
			6 months	0/6	103.10	
	TMT B-A	186	Baseline	0/6	69.93	
			1 month	0/6	85.41	
			6 months	0/6	70.24	
Inibhition	SCWT interference time	36.9	Baseline	1/6	36.84	
			1 month	2/6	36.33	
			6 months	1/6	26.80	
	SCWT interference errors	4.2	Baseline	1/6	1.46	
			1 month	1/6	1.80	
			6 months	1/6	1.57	
Constructive apraxia	Rey-figure copy	28.8	Baseline	1/6	32.47	
			1 month	0/6	33.07	
			6 months	0/6	35.48	

Significative differences were found in: RAVLT immediate recall 1 month vs. 6 months; BSRT baseline vs. 1 month and baseline vs. 6 months; Semantic fluency 1 month vs. baseline and 1 month vs. 6 months; Phonological fluency 1 month vs. 6 months. Out fo Normal Range (ONR).

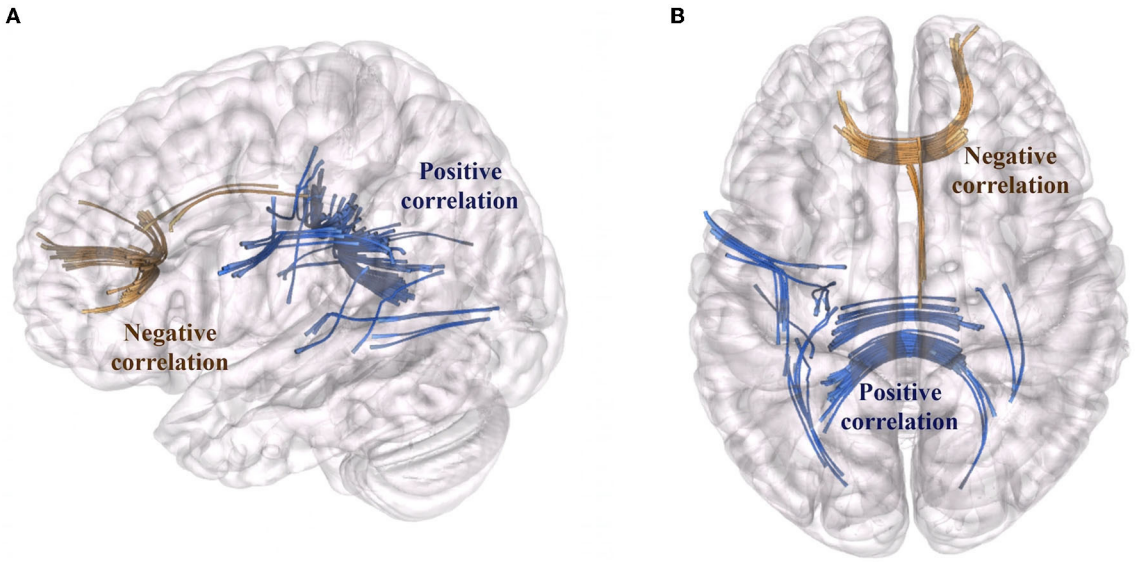

FIGURE 1 | Tract sections with QA changes associated with surgery. Fiber bundles that showed a QA reduction are marked in brown (reticular tract, anterior thalamic radiation, cingulum parolfactory; FDR = 0.011). Fiber bundles that showed an increase of QA (FDR = 0.071) are marked in blue: body, forceps major anterior tapetum of CC and associative bundles of the left hemisphere (frontal aslant tract, optic radiation and superior longitudinal fasciculus). **(A)** Sagittal view, **(B)** Axial view of the brain.

of lesions affecting the third ventricles (e.g., colloid cysts), although rare, offers a unique opportunity to study how brain plasticity occurs as a consequence of targeted lesioning of CC, and, secondarily, how the structure-cognition relationship could be affected.

Corpus callosum is the major commissural association pathway in the brain, subserving the highest and most complex cognitive functions. It exhibits a topographically functional specialization with different callosal subregions connecting a set of cortical areas: the genu, with small unmyelinated fibers, connects the orbitofrontal and medial prefrontal cortices, whereas mid and posterior regions, with large diameter fibers, connects the temporal, parietal, and occipital regions (38, 39). Although the different origin of the anterior and posterior CC portions seems to correlate with different functional properties, the resection gives rise to different effects with the splenium excision that elicit disconnection syndrome (40), whereas resection of the anterior CC may do not (41). Therefore, the influence of CC lesions on clinical outcome and whether or not the vulnerability of each region of the CC surgical resection impacts the cognitive functions remain unclear.

Here, we investigated the cognitive functions and the structural changes of white matter pathways in a small cohort of patients treated with a recently proposed surgical technique, called the transcallosal transgenual approach (18), which requires the incision of the anterior part of the CC to surgically access the lesion.

To this aim, we performed two complementary analyses to study the whole-brain postoperative white matter reorganization that occurs after a selective resection of the CC. dMRI connectometry analysis based on the QA index and graph analysis of brain structural connectivity was used to identify the specific microstructural and structural changes within subsections of fibers that may subserve the brain connectivity or network topology reorganization (22, 42). Alongside the cognitive recovery registered at the second neuropsychological follow-up, the connectometry analysis of dMRI showed significant changes in white matter structural connectivity. Beyond the loss of fibers close to the resection cavity, an increment in QA was registered in the region of the CC close to the lesion, but not affected by the surgery, as well as in long associative bundles such as Frontal Aslant Tract, Superior Longitudinal Fasciculus and Optic Radiation in the left hemisphere. Accordingly, a considerable change in the structural network connectivity was registered, with an increase of centrality in the left hemisphere nodes, particularly the precentral and the fronto opercular gyrus, suggesting these nodes become more important in the information flow at the whole-brain level.

When occurring a lesion, the shortest path between nodes can change by traversing other areas. Thus, the BC in this region can either increase or decrease following surgery (26). Accordingly, with the significant QA increase in the white matter tracts, most of the regions show a BC increase involving the left hemisphere.

Even the connectivity matrix highlights a new network topology following the surgery, with a strengthening toward the middle and mid-posterior CC section, complementary to the loss of strength in the anterior regions. It could be argued that the selective lesion of the genu of the CC could allow for a brain plastic reorganization at the structural network connectivity level. With the disconnection of some tracts, the shortest paths redirect, leading to an increase in BC in specific left hemisphere nodes.

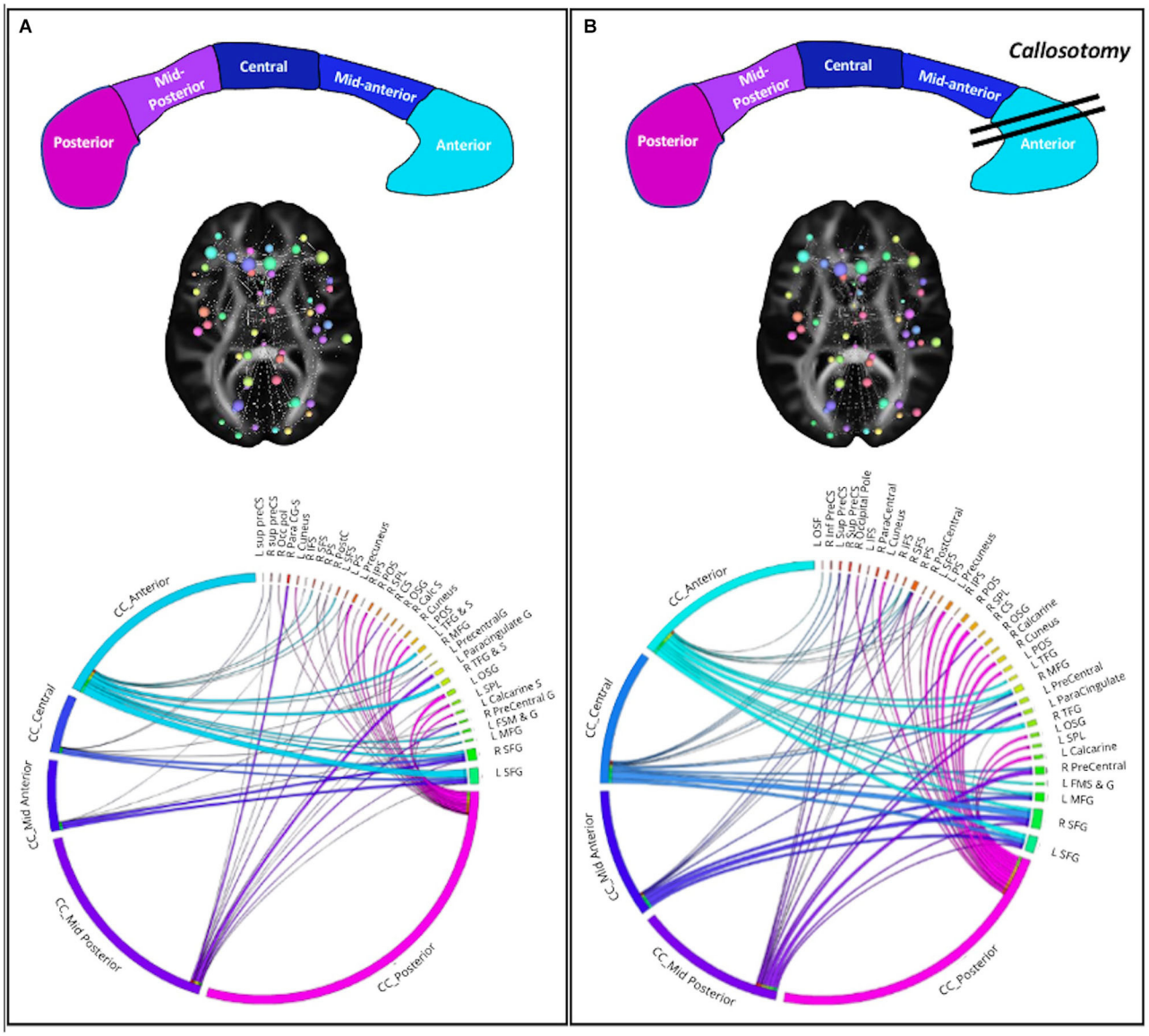

FIGURE 2 | Structural network connectivity changes. **(A)** Preoperative plots; **(B)** postoperative plots. On the top the corpus callosum subsections and surgery. CC subsections are colored as in the CC figure. On the middle the 3D graph visualization of plot connectogram. The cerebral plot shows the brain areas involved in the structural network connectivity changes. On the bottom the Circos plot shows the strength of connectivity among CC subsections and cortical nodes.

Moreover, the evidence on the structural white matter and network reorganization after the resection of the genu of the CC might drive brain plasticity and subserve the cognitive recovery to the baseline.

Few publications deal with the neuropsychological outcomes following colloidal cist removal and the role of the surgical excision in the clinical conditions is still debated (43). Here, no sign of disconnection nor attention impairment were registered, neither at early stage, suggesting that the transgenual approach could be safer than other transcallosal approaches. However, tumors involving deep regions, such as the third ventricle, are frequently associated with memory impairment. The critical role of the fornix has been proposed in several researches, suggesting that the more the severity of fornix damage, the more the severity of memory impairment (7, 13, 14, 44). Notably, here no differences in the fornix micro-structures have been reported by the connectometry analysis between pre- and postoperative DTI scans, indicating the integrity of these structures and suggesting transgenual opening is fornix-sparing. Moreover, we registered a good recovery of verbal memory functions at the second follow-up. Although we found a worsening in-memory performance at early postoperative, in line with the literature demonstrating that nearly half of the patients exhibited reduced performance in verbal recall 4 weeks postoperatively (45–50),

longer follow-up reported an improvement in cognition (51), as occurred in our patients. Our data can help explain the structural basis of this established cognitive recovery, showing that the microstructural white matter pathway and network topology clearly reorganize following the surgery, and, at the same time, the lesion of the genu of the CC does not prevent this reorganization.

It is important to note that even ventriculomegaly might influence the neuropsychological performance (43, 52), although no patients need CSF diversion, ventriculomegaly was still reported and might be associated with poor cognitive performance still registered at the follow-up.

The present study has some limitations. The small size of the sample and the patients' heterogeneity (e.g., age, ventriculomegaly) reduce its statistical power. Nevertheless, colloid cysts are a rare clinical condition making it hard to reach a homogeneous population. Moreover, despite using other processing methods (i.e., macrostructural changes) [i.e., pre- and postoperative functional connectivity investigation of neuropsychological outcomes (53, 54)] may help explain how callosotomy affects brain reorganization and cognition, actually, pre- and postoperative data collection including both radiological and neuropsychological data are very infrequent in the literature. Finally, we highlight the microstructural changes and structural connectivity graph topology, however, other structural connectivity metrics may play a role in the cognitive recovery, such as fibers' volume.

Further detailed pre- and postoperative neuropsychological studies, or experimental studies investigating more cognitive aspects of interhemispheric transfer of information (e.g., tachistoscopic presentation of stimuli) are required to get deeper on how the surgical approaches, tumor location, and the associated ventriculomegaly affect the cognitive function or structural and functional reorganization. As well, here preliminary results are reported suggesting the importance of safer surgery on patients recovery (55). More researches are necessary to further explain how the white matter reorganization occurs and from which factors are driven.

DATA AVAILABILITY STATEMENT

The original contributions presented in the study are included in the article/supplementary material, further inquiries can be directed to the corresponding author/s.

ETHICS STATEMENT

The studies involving human participants were reviewed and approved by IRCCS Neuromed (Ethical Approval Code: 11/17 21-12-17). The patients/participants provided their written informed consent to participate in this study.

AUTHOR CONTRIBUTIONS

MC and VE: design and conceptualize the study. MC, LP, and GG: data acquisition. MC, EG, GB, and EA: major role in formal analysis. RM, TV, EA, and GB: data curation. MC, EG, and GB: wrote the paper. LP, EA, and VE: revised the manuscript. All authors contributed to the article and approved the submitted version.

FUNDING

This work was founded by Neuromed IRCCS, Current Research, by the Italian Ministry of Health.

REFERENCES

1. Beaumont TL, Limbrick DDJ, Rich KM, Wippold FJ II, Dacey RGJ. Natural history of colloid cysts of the third ventricle. *J Neurosurg.* (2016) 125:1420–30. doi: 10.3171/2015.11.JNS151396
2. Musa G, Simfukwe K, Gots A, Chmutin G, Chmutin E, Chaurasia B. Clinical and radiological characteristics in fatal third ventricle colloid cyst. Literature review. *J Clin Neurosci.* (2020) 82(Pt A):52–5. doi: 10.1016/j.jocn.2020.10.032
3. de Witt Hamer PC, Verstegen MJ, De Haan RJ, et al. High risk of acute deterioration in patients harboring symptomatic colloid cysts of the third ventricle. *J Neurosurg.* (2002) 6:1041–5. doi: 10.3171/jns.2002.96.6.1041
4. Elshamy W, Burkard J, Gerges M, Erginoglu U, Aycan A, Ozaydin B, et al. Surgical approaches for resection of third ventricle colloid cysts: meta-analysis. *Neurosurg Rev.* (2021) 44:3029–38. doi: 10.1007/s10143-021-01486-5
5. Little JR, MacCarty CS. Colloid cysts of the third ventricle. *J Neurosurg.* (1974) 40:230–5. doi: 10.3171/jns.1974.40.2.0230
6. Aggleton JP, McMackin D, Carpenter K, Hornak J, Kapur N, Halpin S, et al. Differential cognitive effects of colloid cysts in the third ventricle that spare or compromise the fornix. *Brain.* (2000) 123(Pt 4):800–15. doi: 10.1093/brain/123.4.800
7. Roth J, Sela G, Andelman F, Nossek E, Elran H. Ram Z. The impact of colloid cyst treatment on neurocognition. *World Neurosurg.* (2019) 125:e372–7. doi: 10.1016/j.wneu.2019.01.079
8. Nakajo K, Uda T, Goto T, Morisako H, Nishijima S, Kawashima T, et al. Changes in cognitive function after resection of lesions in the anterior part of the lateral ventricle *via* an interhemispheric transcallosal approach. *J Clin Neurosci.* (2020) 79:39–44. doi: 10.1016/j.jocn.2020.07.026
9. Hutter BO, Spetzger U, Bertalanffy H, Gilsbach JM. Cognition and quality of life in patients after transcallosal microsurgery for midline tumors. *J Neurosurg Sci.* (1997) 41:123–9.
10. Apuzzo ML, Chikovani OK, Gott PS, Teng EL, Zee CS, Giannotta SL, et al. Transcallosal, interfornicial approaches for lesions affecting the third ventricle: surgical considerations and consequences. *Neurosurgery.* (1982) 10:547–54. doi: 10.1227/00006123-198205000-00001
11. Decq P, Le Guerinel C, Brugieres P, Djindjian M, Silva D, Kéravel Y, et al. Endoscopic management of colloid cysts. *Neurosurgery.* (1998) 42:1288–94. doi: 10.1097/00006123-199806000-00051
12. Tsivilis D, Vann SD, Denby C, Djindjian M, Silva D, Kéravel Y, et al. A disproportionate role for the fornix and mammillary bodies in recall versus recognition memory. *Nat Neurosci.* (2008) 7:834–42. doi: 10.1038/nn.2149
13. Garcia-Bengochea F, Friedman WA. Persistent memory loss following section of the anterior fornix in humans. A historical review. *Surg Neurol.* (1987) 4:361–4. doi: 10.1016/0090-3019(87)90012-7
14. Hodges JR, Carpenter K. Anterograde amnesia with fornix damage following removal of IIIrd ventricle colloid cyst. *J Neurol Neurosurg Psychiatry.* (1991) 7:633–8. doi: 10.1136/jnnp.54.7.633
15. Peltier J, Roussel M, Gerard Y, Lassonde M, Deramond H, Le Gars D, et al. Functional consequences of a section of the anterior part of the body of the

corpus callosum: evidence from an interhemispheric transcallosal approach. *J Neurol.* (2012) 259:1860–7. doi: 10.1007/s00415-012-6421-x
16. He J, Li Z, Yu Y, Lu Z, Li Z, Gong J. Cognitive function assessment and comparison on lateral ventricular tumors resection by the frontal transcortical approach and anterior transcallosal approach respectively in children. *Neurosurg Rev.* (2020) 43:619–32. doi: 10.1007/s10143-019-01088-2
17. Alkhaibary A, Baydhi L, Alharbi A, Alshaikh AA, Khairy S, Abbas M, et al. Endoscopic versus open microsurgical excision of colloid cysts: a comparative analysis and state-of-the-art review of neurosurgical techniques. *World Neurosurg.* (2021) 149:e298–308. doi: 10.1016/j.wneu.2021.02.032
18. Esposito V, di Russo P, Del Maestro M, Ciavarro M, Vangelista T, De Angelis M, et al. The interhemispheric transgenual approach for microsurgical removal of third ventricle colloid cysts. *Technical Note World Neurosurg.* (2020) 142:197–205. doi: 10.1016/j.wneu.2020.06.222
19. Manjón JV, Coupé P. VolBrain: an online MRI brain volumetry system. *Front Neuroinform.* (2016) 10:30. doi: 10.3389/fninf.2016.00030
20. Yeh FC, Zaydan IM, Suski VR, Lacomis D, Richardson RM, Maroon JC, et al. Differential tractography as a track-based biomarker for neuronal injury. *Neuroimage.* (2019) 202:116131. doi: 10.1016/j.neuroimage.2019.116131
21. Yeh FC, Tseng WY. NTU-90: a high angular resolution brain atlas constructed by q-space diffeomorphic reconstruction. *Neuroimage.* (2011) 58:91–9. doi: 10.1016/j.neuroimage.2011.06.021
22. Yeh FC, Badre D, Verstynen T. Connectometry: a statistical approach harnessing the analytical potential of the local connectome. *Neuroimage.* (2016) 125:162–71. doi: 10.1016/j.neuroimage.2015.10.053
23. Yeh FC, Verstynen TD, Wang Y, Fernandez-Miranda JC, Tseng WY. Deterministic diffusion fiber tracking improved by quantitative anisotropy. *PLoS ONE.* (2013) 8:e80713. doi: 10.1371/journal.pone.0080713
24. Yeh F-C, Panesar S, Barrios J, Fernandes D, Abhinav K, Meola A, et al. Automatic removal of false connections in diffusion MRI tractography using topology-informed pruning (TIP). *Neurotherapeutics.* (2019) 16:52–8. doi: 10.1007/s13311-018-0663-y
25. Destrieux C, Fischl B, Dale A, Halgren E. Automatic parcellation of human cortical gyri and sulci using standard anatomical nomenclature. *Neuroimage.* (2010) 53:1–15. doi: 10.1016/j.neuroimage.2010.06.010
26. Taylor PN, Sinha N, Wang Y, Vos SB, de Tisi J, Miserocchi A et al. The impact of epilepsy surgery on the structural connectome and its relation to outcome. *Neuroimage Clin.* (2018) 18:202–14. doi: 10.1016/j.nicl.2018.01.028
27. Bastiani M, Roebroeck A. Unraveling the multiscale structural organization and connectivity of the human brain: the role of diffusion MRI. *Front Neuroanat.* (2015) 9:77. doi: 10.3389/fnana.2015.00077
28. Craddock RC, Jbabdi S, Yan CG, Vogelstein JT, Castellanos FX, Di Martino A, et al. Imaging human connectomes at the macroscale. *Nat Methods.* (2013) 10:524–39. doi: 10.1038/nmeth.2482
29. Pandit AS, Robinson E, Aljabar P, Ball G, Gousias IS, Wang Z, et al. Whole-brain mapping of structural connectivity in infants reveals altered connection strength associated with growth and preterm birth. *Cereb Cortex.* (2014) 24:2324–33. doi: 10.1093/cercor/bht086
30. Le Bihan D, Johansen-Berg H. Diffusion MRI at 25: exploring brain tissue structure and function. *Neuroimage.* (2012) 61:324–41. doi: 10.1016/j.neuroimage.2011.11.006
31. van den Heuvel MP, Sporns O. Network hubs in the human brain. *Trends Cogn Sci.* (2013) 17:683–96. doi: 10.1016/j.tics.2013.09.012
32. Schumacher LV, Reisert M, Nitschke K, Egger K, Urbach H, Hennig J, et al. Probing the reproducibility of quantitative estimates of structural connectivity derived from global tractography. *Neuroimage.* (2018) 175:215–29. doi: 10.1016/j.neuroimage.2018.01.086
33. Gong G, Rosa-Neto P, Carbonell F, Chen ZJ, He Y, Evans AC. Age- and gender-related differences in the cortical anatomical network. *J Neurosci.* (2009) 29:15684–93. doi: 10.1523/JNEUROSCI.2308-09.2009
34. Hagmann P, Sporns O, Madan N, Cammoun L, Pienaar R, Wedeen VJ, et al. White matter maturation reshapes structural connectivity in the late developing human brain. *Proc Natl Acad Sci USA.* (2010) 107:19067–72. doi: 10.1073/pnas.1009073107
35. Bonilha L, Jensen JH, Baker N, Breedlove J, Nesland T, Lin JJ, et al. The brain connectome as a personalized biomarker of seizure outcomes after temporal lobectomy. *Neurology.* (2015) 84:1846–53. doi: 10.1212/WNL.0000000000001548
36. Jütten K, Weninger L, Mainz V, Gauggel S, Binkofski F, Wiesmann M, et al. Dissociation of structural and functional connectomic coherence in glioma patients. *Sci Rep.* (2021) 11:16790. doi: 10.1038/s41598-021-95932-5
37. Ortiz A, Munilla J, Álvarez-Illán I, Górriz JM, Ramírez J. Alzheimer's disease neuroimaging initiative. Exploratory graphical models of functional and structural connectivity patterns for Alzheimer's disease diagnosis. *Front Comput Neurosci.* (2015) 9:132. doi: 10.3389/fncom.2015.00132
38. Hofer S, Frahm J. Topography of the human corpus callosum revisited-comprehensive fiber tractography using diffusion tensor magnetic resonance imaging. *Neuroimage.* (2006) 32:989–94. doi: 10.1016/j.neuroimage.2006.05.044
39. Fabri M, Pierpaoli C, Barbaresi P, Polonara G. Functional topography of the corpus callosum investigated by DTI and fMRI. *World J Radiol.* (2014) 6:895–906. doi: 10.4329/wjr.v6.i12.895
40. Berlucchi G. Frontal callosal disconnection syndromes. *Cortex.* (2012) 48:36–45. doi: 10.1016/j.cortex.2011.04.008
41. Purves SJ, Wada JA, Woodhurst WB, Moyes PD, Strauss E, Kosaka B, et al. Results of anterior corpus callosum section in 24 patients with medically intractable seizures. *Neurology.* (1988) 38:1194–201. doi: 10.1212/WNL.38.8.1194
42. Yeh FC, Panesar S, Fernandes D, Meola A, Yoshino M, Fernandez-Miranda JC, et al. Population-averaged atlas of the macroscale human structural connectome and its network topology. *Neuroimage.* (2018) 178:57–68. doi: 10.1016/j.neuroimage.2018.05.027
43. Buhl R, Huang H, Gottwald B, Mihajlovic Z, Mehdorn HM. Neuropsychological findings in patients with intraventricular tumors. *Surg Neurol.* (2005) 64:500–3. doi: 10.1016/j.surneu.2005.04.040
44. McMackin D, Cockburn J, Anslow P, Gaffan D. Correlation of fornix damage with memory impairment in six cases of colloid cyst removal. *Acta Neurochir.* (1995) 1–2:12–8. doi: 10.1007/BF02307408
45. Villani R, Papagno C, Tomei G, Grimoldi N, Spagnoli D, Bello L. Transcallosal approach to tumors of the third ventricle. Surgical results and neuropsychological evaluation. *J Neurosurg Sci.* (1997) 41:41–50.
46. Hellwig D, Bauer BL, Schulte M, Gatscher S, Riegel T, Bertalanffy H. Neuroendoscopic treat- ment for colloid cysts of the third ventricle: the experience of a decade. *Neurosurgery.* (2003) 3:525–33. discussion 532-523. doi: 10.1227/01.NEU.0000047671.27057.55
47. Shapiro S, Rodgers R, Shah M, Fulkerson D, Campbell RL. Interhemispheric transcallosal subchoroidal fornix-sparing craniotomy for total resection of colloid cysts of the third ventricle. *J Neurosurg.* (2009) 1:112–5. doi: 10.3171/2008.4.17495
48. Levine NB, Miller MN, Crone KR. Endoscopic resection of colloid cysts: indications, technique, and results during a 13-year period. *Minim Invasive Neurosurg.* (2007) 6:313–7. doi: 10.1055/s-2007-993215
49. Horn EM, Feiz-Erfan I, Bristol RE, et al. Treat- ment options for third ventricular colloid cysts: comparison of open microsurgical versus endo- scopic resection. *Neurosurgery.* (2007) 4:613–8. discussion 618–620. doi: 10.1227/01.NEU.0000255409.61398.EA
50. Poreh A, Winocur G, Moscovitch M ackon M, Goshen E, Ram Z, et al. Anterograde and retrograde amnesia in a person with bilateral fornix lesions following removal of a colloid cyst. *Neuropsychologia.* (2006) 12:2241–8. doi: 10.1016/j.neuropsychologia.2006.05.020
51. Winkler PA, Ilmberger J, Krishnan KG, Reulen HJ. Transcallosal interforniceal-transforaminal approach for removing lesions occupying the third ventricular space: clinical and neuropsychological results. *Neurosurgery.* (2000) 46:879–88. discussion 888-90 doi: 10.1227/00006123-200004000-00020

52. Peterson KA, Savulich G, Jackson D, Killikelly C, Pickard JD, Sahakian BJ. The effect of shunt sur- gery on neuropsychological performance in normal pressure hydrocephalus: a systematic re- view and meta-analysis. *J Neurol.* (2016) 8:1669–77. doi: 10.1007/s00415-016-8097-0
53. Yeung JT, Taylor HM, Nicholas PJ, Young IM, Jiang I, Doyen S, et al. Using quicktome for intracerebral surgery: early retrospective study and proof of concept. *World Neurosurg.* (2021) 154:e734–42. doi: 10.1016/j.wneu.2021.07.127
54. Ciavarro M, Grande E, Pavone L, Bevacqua G, De Angelis M, di Russo P, et al. Pre-surgical fMRI localization of the hand motor cortex in brain tumors: Comparison between finger tapping task and a new visual-triggered finger movement task. *Front Neurol.* (2021) 12:658025. doi: 10.3389/fneur.2021.658025
55. Paolini S, Severino R, Mancarella C, Cardarelli G, Ciavarro M, Di Castelnuovo A, et al. Mini-craniotomy for intra-axial brain tumors: a comparison with conventional craniotomy in 306 patients harboring non-dural based lesions. *Neurosurg Rev.* (2022). doi: 10.1007/s10143-022-01811-6. [Epub ahead of print].

Conflict of Interest: The authors declare that the research was conducted in the absence of any commercial or financial relationships that could be construed as a potential conflict of interest.

Publisher's Note: All claims expressed in this article are solely those of the authors and do not necessarily represent those of their affiliated organizations, or those of the publisher, the editors and the reviewers. Any product that may be evaluated in this article, or claim that may be made by its manufacturer, is not guaranteed or endorsed by the publisher.

Frontiers in Neurology

Explores neurological illness to improve patient care

The third most-cited clinical neurology journal explores the diagnosis, causes, treatment, and public health aspects of neurological illnesses. Its ultimate aim is to inform improvements in patient care.

Discover the latest Research Topics

See more →

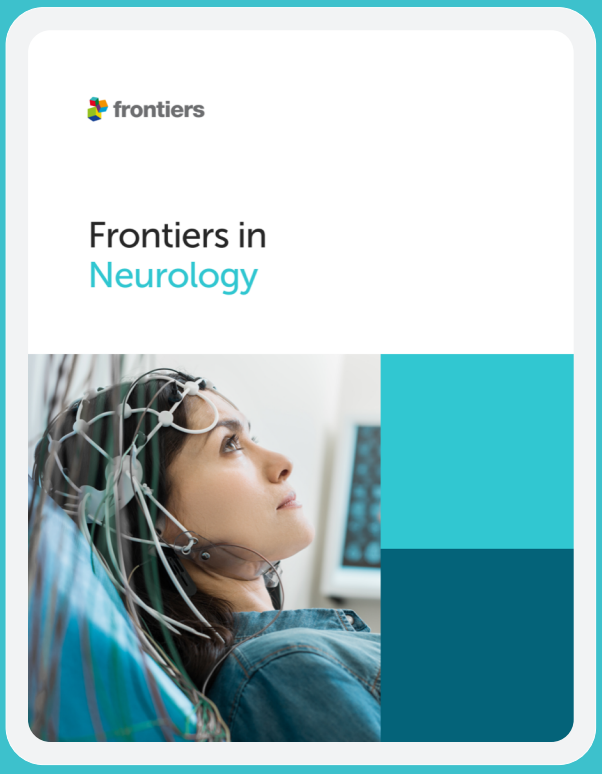

Frontiers

Avenue du Tribunal-Fédéral 34
1005 Lausanne, Switzerland
frontiersin.org

Contact us

+41 (0)21 510 17 00
frontiersin.org/about/contact